

# UBIQUITIN CODE: FROM CELL BIOLOGY TO TRANSLATIONAL MEDICINE

EDITED BY: Lingqiang Zhang, Yu Rao, Cui Hua Liu, Daming Gao and  
Lixin Wan

PUBLISHED IN: Frontiers in Cell and Developmental Biology



# frontiers

## Frontiers eBook Copyright Statement

The copyright in the text of individual articles in this eBook is the property of their respective authors or their respective institutions or funders. The copyright in graphics and images within each article may be subject to copyright of other parties. In both cases this is subject to a license granted to Frontiers.

The compilation of articles constituting this eBook is the property of Frontiers.

Each article within this eBook, and the eBook itself, are published under the most recent version of the Creative Commons CC-BY licence.

The version current at the date of publication of this eBook is CC-BY 4.0. If the CC-BY licence is updated, the licence granted by Frontiers is automatically updated to the new version.

When exercising any right under the CC-BY licence, Frontiers must be attributed as the original publisher of the article or eBook, as applicable.

Authors have the responsibility of ensuring that any graphics or other materials which are the property of others may be included in the CC-BY licence, but this should be checked before relying on the CC-BY licence to reproduce those materials. Any copyright notices relating to those materials must be complied with.

Copyright and source acknowledgement notices may not be removed and must be displayed in any copy, derivative work or partial copy which includes the elements in question.

All copyright, and all rights therein, are protected by national and international copyright laws. The above represents a summary only. For further information please read Frontiers' Conditions for Website Use and Copyright Statement, and the applicable CC-BY licence.

ISSN 1664-8714

ISBN 978-2-88971-899-3

DOI 10.3389/978-2-88971-899-3

## About Frontiers

Frontiers is more than just an open-access publisher of scholarly articles: it is a pioneering approach to the world of academia, radically improving the way scholarly research is managed. The grand vision of Frontiers is a world where all people have an equal opportunity to seek, share and generate knowledge. Frontiers provides immediate and permanent online open access to all its publications, but this alone is not enough to realize our grand goals.

## Frontiers Journal Series

The Frontiers Journal Series is a multi-tier and interdisciplinary set of open-access, online journals, promising a paradigm shift from the current review, selection and dissemination processes in academic publishing. All Frontiers journals are driven by researchers for researchers; therefore, they constitute a service to the scholarly community. At the same time, the Frontiers Journal Series operates on a revolutionary invention, the tiered publishing system, initially addressing specific communities of scholars, and gradually climbing up to broader public understanding, thus serving the interests of the lay society, too.

## Dedication to Quality

Each Frontiers article is a landmark of the highest quality, thanks to genuinely collaborative interactions between authors and review editors, who include some of the world's best academicians. Research must be certified by peers before entering a stream of knowledge that may eventually reach the public - and shape society; therefore, Frontiers only applies the most rigorous and unbiased reviews. Frontiers revolutionizes research publishing by freely delivering the most outstanding research, evaluated with no bias from both the academic and social point of view. By applying the most advanced information technologies, Frontiers is catapulting scholarly publishing into a new generation.

## What are Frontiers Research Topics?

Frontiers Research Topics are very popular trademarks of the Frontiers Journals Series: they are collections of at least ten articles, all centered on a particular subject. With their unique mix of varied contributions from Original Research to Review Articles, Frontiers Research Topics unify the most influential researchers, the latest key findings and historical advances in a hot research area! Find out more on how to host your own Frontiers Research Topic or contribute to one as an author by contacting the Frontiers Editorial Office: [frontiersin.org/about/contact](https://frontiersin.org/about/contact)



# UBIQUITIN CODE: FROM CELL BIOLOGY TO TRANSLATIONAL MEDICINE

Topic Editors:

**Lingqiang Zhang**, National Center of Protein Sciences, China

**Yu Rao**, Tsinghua University, China

**Cui Hua Liu**, Institute of Microbiology, Chinese Academy of Sciences, China

**Daming Gao**, Shanghai Institute of Biochemistry and Cell Biology, Chinese Academy of Sciences (CAS), China

**Lixin Wan**, Moffitt Cancer Center, United States

**Citation:** Zhang, L., Rao, Y., Liu, C. H., Gao, D., Wan, L., eds. (2021). Ubiquitin Code: From Cell Biology to Translational Medicine. Lausanne: Frontiers Media SA. doi: 10.3389/978-2-88971-899-3

# Table of Contents

- 05 Editorial: Ubiquitin Code: From Cell Biology to Translational Medicine**  
Cui Hua Liu, Yu Rao, Daming Gao, Lixin Wan and Lingqiang Zhang
- 09 Caspase-8 Inhibition Prevents the Cleavage and Degradation of E3 Ligase Substrate Receptor Cereblon and Potentiates Its Biological Function**  
Liang Zhou, Wenjun Yu, David S. Jayabalan, Ruben Niesvizky, Samie R. Jaffrey, Xiangao Huang and Guoqiang Xu
- 20 OTUB1 Promotes Progression and Proliferation of Prostate Cancer via Deubiquitinating and Stabbing Cyclin E1**  
Yihao Liao, Ning Wu, Keke Wang, Miaomiao Wang, Youzhi Wang, Jie Gao, Boqiang Zhong, Fuling Ma, Yudong Wu and Ning Jiang
- 33 Cullin3-TNFAIP1 E3 Ligase Controls Inflammatory Response in Hepatocellular Carcinoma Cells via Ubiquitination of RhoB**  
Yue Liu, Wenjuan Zhang, Shiwen Wang, Lili Cai, Yanyu Jiang, Yongfu Pan, Yupei Liang, Jingrong Xian, Lijun Jia, Lihui Li, Hu Zhao and Yanmei Zhang
- 44 Low-Dose Decitabine Augments the Activation and Anti-Tumor Immune Response of IFN- $\gamma$ <sup>+</sup> CD4<sup>+</sup> T Cells Through Enhancing I $\kappa$ B $\alpha$  Degradation and NF- $\kappa$ B Activation**  
Xiang Li, Liang Dong, Jiejie Liu, Chunmeng Wang, Yan Zhang, Qian Mei, Weidong Han, Ping Xie and Jing Nie
- 57 Advances in Cancer Treatment by Targeting the Neddylation Pathway**  
Wenbin Gai, Zhiqiang Peng, Cui Hua Liu, Lingqiang Zhang and Hong Jiang
- 67 Targeting RFWD2 as an Effective Strategy to Inhibit Cellular Proliferation and Overcome Drug Resistance to Proteasome Inhibitor in Multiple Myeloma**  
Mengjie Guo, Pinggang Ding, Zhen Zhu, Lu Fan, Yanyan Zhou, Shu Yang, Ye Yang and Chunyan Gu
- 79 The Absence of PTEN in Breast Cancer Is a Driver of MLN4924 Resistance**  
Meng-ge Du, Zhi-qiang Peng, Wen-bin Gai, Fan Liu, Wei Liu, Yu-jiao Chen, Hong-chang Li, Xin Zhang, Cui Hua Liu, Ling-qiang Zhang, Hong Jiang and Ping Xie
- 93 Ubiquitin Modification Patterns of Clear Cell Renal Cell Carcinoma and the Ubiquitin Score to Aid Immunotherapy and Targeted Therapy**  
Peng Zhou, Yuchao Lu, Yang Xun, Jinzhou Xu, Chenqian Liu, Qidong Xia, Junlin Lu, Shaogang Wang and Jia Hu
- 107 Intricate Regulatory Mechanisms of the Anaphase-Promoting Complex/Cyclosome and Its Role in Chromatin Regulation**  
Tatyana Bodrug, Kaeli A. Welsh, Megan Hinkle, Michael J. Emanuele and Nicholas G. Brown
- 125 CUL5–ASB6 Complex Promotes p62/SQSTM1 Ubiquitination and Degradation to Regulate Cell Proliferation and Autophagy**  
Liyang Gong, Kaihua Wang, Mengcheng Wang, Ronggui Hu, Huaguang Li, Daming Gao and Moubin Lin
- 137 Neddylation Regulates Macrophages and Implications for Cancer Therapy**  
Yanyu Jiang, Lihui Li, Yan Li, Guangwei Liu, Robert M. Hoffman and Lijun Jia

- 147** *Development of an Individualized Ubiquitin Prognostic Signature for Clear Cell Renal Cell Carcinoma*  
Yue Wu, Xi Zhang, Xian Wei, Huan Feng, Binta Hu, Zhiyao Deng, Bo Liu, Yang Luan, Yajun Ruan, Xiaming Liu, Zhuo Liu, Jihong Liu and Tao Wang
- 161** *Global Screening of LUBAC and OTULIN Interacting Proteins by Human Proteome Microarray*  
Lijie Zhou, Yingwei Ge, Yesheng Fu, Bo Wu, Yong Zhang, Lei Li, Chun-Ping Cui, Siying Wang and Lingqiang Zhang
- 174** *Ubiquitination-Dependent Regulation of Small GTPases in Membrane Trafficking: From Cell Biology to Human Diseases*  
Zehui Lei, Jing Wang, Lingqiang Zhang and Cui Hua Liu
- 189** *Light-Controllable PROTACs for Temporospatial Control of Protein Degradation*  
Jing Liu, Yunhua Peng and Wenyi Wei
- 201** *Regulation of Ferroptosis Pathway by Ubiquitination*  
Xinbo Wang, Yanjin Wang, Zan Li, Jieliang Qin and Ping Wang
- 216** *Functions and Molecular Mechanisms of Deltex Family Ubiquitin E3 Ligases in Development and Disease*  
Lidong Wang, Xiaodan Sun, Jingni He and Zhen Liu
- 234** *Tumor Suppressor FBXW7 and Its Regulation of DNA Damage Response and Repair*  
Huiyin Lan and Yi Sun



# Editorial: Ubiquitin Code: From Cell Biology to Translational Medicine

Cui Hua Liu<sup>1,2\*</sup>, Yu Rao<sup>3\*</sup>, Daming Gao<sup>4\*</sup>, Lixin Wan<sup>5\*</sup> and Lingqiang Zhang<sup>6\*</sup>

<sup>1</sup> CAS Key Laboratory of Pathogenic Microbiology and Immunology, Institute of Microbiology, Center for Biosafety Mega-Science, Chinese Academy of Sciences, Beijing, China, <sup>2</sup> Savaid Medical School, University of Chinese Academy of Sciences, Beijing, China, <sup>3</sup> Ministry of Education Key Laboratory of Protein Sciences, Ministry of Education Key Laboratory of Bioorganic Phosphorus Chemistry and Chemical Biology, School of Pharmaceutical Sciences, Tsinghua University, Beijing, China, <sup>4</sup> State Key Laboratory of Cell Biology, Shanghai Institute of Biochemistry and Cell Biology, Center for Excellence in Molecular Cell Science, Chinese Academy of Sciences, Shanghai, China, <sup>5</sup> Department of Molecular Oncology, H. Lee Moffitt Cancer Center and Research Institute, Tampa, FL, United States, <sup>6</sup> State Key Laboratory of Proteomics, Beijing Proteome Research Center, National Center for Protein Sciences (Beijing), Beijing Institute of Lifeomics, Beijing, China

## OPEN ACCESS

### Edited and reviewed by:

Philipp Kaldis,  
Lund University, Sweden

### \*Correspondence:

Cui Hua Liu  
liucuihua@im.ac.cn  
Yu Rao  
yrao@tsinghua.edu.cn  
Daming Gao  
dgao@sibcb.ac.cn  
Lixin Wan  
lixin.wan@moffitt.org  
Lingqiang Zhang  
zhanglq@nic.bmi.ac.cn

### Specialty section:

This article was submitted to  
Cell Growth and Division,  
a section of the journal  
Frontiers in Cell and Developmental  
Biology

**Received:** 09 October 2021

**Accepted:** 12 October 2021

**Published:** 28 October 2021

### Citation:

Liu CH, Rao Y, Gao D, Wan L and  
Zhang L (2021) Editorial: Ubiquitin  
Code: From Cell Biology to  
Translational Medicine.  
Front. Cell Dev. Biol. 9:791967.  
doi: 10.3389/fcell.2021.791967

**Keywords:** ubiquitin code, ubiquitination, deubiquitination, disease, PROTAC technology

## Editorial on the Research Topic

## Ubiquitin Code: From Cell Biology to Translational Medicine

## INTRODUCTION

Ubiquitination is an important post-translational modification that involves the reversible conjugation of single ubiquitin (Ub) or various kinds of poly-ubiquitin chains (polyUb). Ubiquitination is carried out by the sequential actions of three enzymes including Ub-activating enzyme (E1), Ub-conjugating enzyme (E2) and Ub ligase (E3) to covalently link Ub to target protein. Ubiquitination can be classified as monoubiquitination, multi-monoubiquitination, and polyubiquitination according to the number and topology of ubiquitin molecules that are conjugated to the substrate. When polyUb chains are assembled, all seven lysine residues (K6, K11, K27, K29, K33, K48, and K63) and the N-terminal methionine residue on the proximal Ub are accessible by the distal Ub, allowing the assembly of eight homotypic and multiple-mixed conjugates. On top of these, the Ub moiety is often subjected to post-translational modifications. Hence, such three-layered construction of the ubiquitination modification is featured with great complexity and versatility, which is referred to as the ubiquitin code. Ubiquitination is carried out upon substrate proteins by E2/E3 ligase complexes (corresponding to “writers”) and removed from substrates by deubiquitinating enzymes (DUBs) (corresponding to “erasers”). The accurate assembly and interpretation of ubiquitin code is vital to protein homeostasis such as protein turnover, subcellular localization, interactions and activities. Therefore, ubiquitination is involved in all cellular processes and the deregulation of ubiquitination and deubiquitination is linked to the pathogenesis of a number of human diseases, such as cancer, neurodegenerative, infectious, inflammatory and metabolic disorders (Deng et al., 2020; Mulder et al., 2020).

Recently, the in-depth mechanistic studies of several key E3s or DUBs in conjunction with the emergence of high-throughput and novel technologies such as proteome microarray and PROteolysis-Targeting Chimeras (PROTACs) have shed light on the underlying biochemical

mechanisms as well as physiological and pathological functions of ubiquitination (Hu and Crews, 2021; Ramachandran and Ciulli, 2021). This Frontiers Research Topic comprises a series of reviews and original research articles highlighting the current understanding on the functions and mechanisms involved in protein de/ubiquitination and human diseases.

## REGULATORY ROLES OF UBIQUITINATION IN PHYSIOLOGICAL AND PATHOLOGICAL PROCESSES

The majority of the research articles in this Research Topic addresses the regulatory functions and mechanisms of a number of E3s and DUBs during physiological and pathological processes. The study by Gong et al. demonstrates that the CUL5-ASB6 E3 ligase complex that promotes p62/SQSTM1 ubiquitination and degradation to regulate cell proliferation and autophagy. Their study identified a new molecular mechanism regulating p62 stability, which may provide new insights into the delicate control of cell proliferation-autophagy in physiological and pathological settings. The study by Liao et al. aimed to investigate the regulatory effect and the underlying mechanisms of OTUB1, a deubiquitinating enzyme, on prostate cancer (PrCa) cell proliferation. They demonstrate that OTUB1 promotes the proliferation and progression of PrCa via deubiquitinating and stabilizing Cyclin E1. When blocking OTUB1/Cyclin E1 axis or applying the CDK1 inhibitor RO-3306, the occurrence and development of PrCa were significantly repressed. This finding indicates that OTUB1/Cyclin E1 axis might provide a new and potential therapeutic target for PrCa. In another study, Liu Y. et al. discovered that TNFAIP1, an adaptor protein of Cullin3 E3 ubiquitin ligases, coordinates with Cullin3 to mediate RhoB degradation through the ubiquitin proteasome system. They further show that Cullin3-TNFAIP1 E3 ligase controls inflammatory response in hepatocellular carcinoma cells via ubiquitination of RhoB. Their findings reveal a novel mechanism of RhoB degradation and provide a potential strategy for anti-inflammatory intervention of tumors by targeting TNFAIP1-RhoB axis. Another study by Guo et al. unveils that targeting the E3 ubiquitin ligase RFWD2 (also named COP1) could be an effective strategy to inhibit cellular proliferation and overcome drug resistance to proteasome inhibitor in multiple myeloma (MM).

Dysregulation of the ubiquitin-proteasome system itself could influence its function and be associated with multiple cellular homeostasis and disease progress signatures. In a study by Zhou, Yu et al. the authors addressed the question whether the stability and its biological function of Cereblon (CRBN), a substrate receptor of cullin 4-RING E3 ligase (CRL4), could be modulated by caspases. They found that Caspase-8 inhibition prevents the cleavage and degradation of CRBN and potentiates its biological function, suggesting that administration of Caspase-8 inhibitors might enhance the overall effectiveness of Len-based combination therapy in myeloma. With an aim to explore the ubiquitin modification features of clear cell renal cell carcinoma (ccRCC) and to elucidate the role of such ubiquitin

modifications in shaping anti-tumor immunity and individual benefits from immune checkpoint blockade (ICB), Zhou, Lu et al. conducted RNA-seq analysis to elucidate the potential link between ubiquitin modification and immune infiltration landscape of ccRCC. Their study provides a new assessment protocol for the precise selection of treatment strategies for patients with advanced ccRCC through constructing a ubiquitin score to evaluate individual patients' ubiquitination outcome. Similarly, another original research by Wu et al. also addresses the molecular characteristics and prognostic value of ubiquitin in ccRCC, and they developed an individualized ubiquitin prognostic signature for ccRCC and confirmed that the signature is an independent prognostic factor related to the prognosis of ccRCC patients, which may help to reveal the molecular mechanism of ccRCC and provide potential diagnostic and prognostic markers for ccRCC. In the study by Li et al. low-dose DNA demethylating agent decitabine was found to enhance the expression of  $\beta$ -TrCP, a substrate recruiting subunit of the Skp1, Cullin 1, F-box-containing complex (SCF complex). Elevated  $\beta$ -TrCP in turn promotes the proteolysis of I $\kappa$ B $\alpha$  and subsequent NF- $\kappa$ B activation in IFN- $\gamma$ <sup>+</sup> CD4<sup>+</sup> T cells, which improves anti-tumor immunity.

Except for the above original research papers, there are also a few review articles that summarize recent progress in the regulatory function of several important E3s or their components. For example, Wang L. et al. reviewed the function and molecular mechanisms of Deltex family ubiquitin E3 ligases in development and disease, providing insights into future research directions and potential strategies in disease diagnosis and therapy. Another review by Bodrug et al. summarized the intricate regulatory mechanisms of the Anaphase-Promoting Complex/Cyclosome (APC/C) and its role in chromatin regulation. In a comprehensive review, Sun et al. summarize the molecular characteristics of FBXW7, an F-box protein serving as the substrate recognition component of SCF E3 ubiquitin ligase. They also provided future perspectives to further elucidate the role of FBXW7 in the regulation of a variety of biological processes and tumorigenesis, and to design a number of approaches for FBXW7 reactivation in a subset of human cancers for effective anticancer therapy.

Instead of focusing on the regulatory mechanisms of individual ubiquitination-regulating enzymes, there are several review articles addressing the regulation of cellular functions by the ubiquitination process as a whole. For example, in a review article, Lei et al. provided an in-depth understanding of the molecular mechanisms by which ubiquitination regulates small GTPases, thus revealing novel insights into the membrane trafficking process. In another review, Wang X. et al. summarized the current findings of ferroptosis surrounding the viewpoint of ubiquitination regulation, highlighting the potential effect of ubiquitination modulation on the perspective of ferroptosis-targeted cancer therapy.

Although this collection centers on ubiquitination, neddylation, a ubiquitin-like modification that earmarks substrate proteins with the small ubiquitin-like protein NEDD8, is also part of this Research Topic due to its roles in controlling the Cullin-RING and Smurf1 ubiquitin E3 ligases.

Jiang et al. updated our current understand of neddylation in tumor-associated macrophages, and Gai et al. summarized the approaches developed to target the neddylation pathway. The study by Du et al. reported *PTEN* deficiency as a key mechanism that contributes to the neddylation inhibitor MLN4924 resistance in breast cancer cells.

## APPLICATION OF PROTEIN MICROARRAY IN DECIPHERING UBIQUITIN CODE

Linear ubiquitin chain assembly complex (LUBAC) catalyzes linear ubiquitination, while the deubiquitinase OTULIN exclusively cleaves the linear ubiquitin chains (Oikawa et al., 2020). To expand understanding of the substrates and pathways of linear ubiquitination, Zhou, Ge et al. used a human proteome microarray (a high-throughput technology that allows systematically screening up to 20,000 proteins) to conduct global screening of LUBAC- and OTULIN- interacting proteins. They identified many potential new interacting proteins of LUBAC and OTULIN, which may function as novel regulators or substrates of linear ubiquitination. Their results suggest that linear ubiquitination may have broad cellular functions and is associated with diverse signaling pathways, and provide accessible data for the interacting proteins of LUBAC and OTULIN, which helps guide further studies to broaden our understanding on linear ubiquitination.

## DEGRADATION OF TARGET PROTEINS AND RELATED DRUG RESEARCH BY PROTAC TECHNOLOGY

PROTACs is an emerging and promising approach to target intracellular proteins for ubiquitination-mediated degradation, including previously undruggable protein targets, such as transcriptional factors and scaffold proteins. To date, plenty of PROTACs have been developed to degrade various disease-relevant proteins, such as estrogen receptor (ER), androgen receptor (AR), BTK, RTK, and CDKs, etc. Notably, ER and AR targeting PROTAC molecules have entered phase II clinical studies. More recently, the third generation light-controllable PROTACs have been developed to overcome the limitation of the on-target off-tissue and off-target effect of this technology (Hu and Crews, 2021; Ramachandran and Ciulli, 2021). A review by Liu J. et al. summarized the emerging light-controllable

PROTACs and the prospective for other potential ways to achieve temporospatial control of PROTACs.

## CONCLUSIONS

The collection of articles in this Research Topic provides a number of key findings on the regulatory functions and mechanisms of ubiquitination system in recent years, presenting compelling evidence for a critical role of ubiquitination in cell biology and human diseases and suggesting that targeting the ubiquitination machinery could be an effective strategy for treating certain diseases. It should be pointed out that the coverage is far from complete in this Research Topic, and there are some other equally important questions that are not covered in this issue but warrant future in-depth investigation. For example, how the ubiquitin code is dynamically edited and precisely interpreted in different cellular microenvironment? What are the writers, readers and erasers of each type of the polyUb chains as well as the branched ubiquitin chains in cells? What are the new modifications, linkages and targets of ubiquitin molecule? What are the novel host-regulating functions and unique biochemical mechanisms of bacterial/viral ubiquitin ligases and deubiquitinases? Hence, it is clear that ubiquitination remains a dynamic field, and we will see many more exciting discoveries of how ubiquitination is assembled and dis-assembled to dynamically fine-tune normal cellular functions and thus affects multiple disease progress in the near future.

## AUTHOR CONTRIBUTIONS

CL and LZ wrote the original manuscript. All authors reviewed, edited the manuscript, and approved the submitted version.

## FUNDING

CL was supported by National Key Research and Development Program of China (2017YFA0505900) and National Natural Science Foundation of China (Grant Nos. 81825014 and 31830003).

## ACKNOWLEDGMENTS

We greatly thank all authors and reviewers for their contributions to this Research Topic as well as the editorial office for their kind support.

## REFERENCES

- Deng, L., Meng, T., Chen, L., Wei, W., and Wang, P. (2020). The role of ubiquitination in tumorigenesis and targeted drug discovery. *Signal Transduct. Target Ther.* 5:11. doi: 10.1038/s41392-020-0107-0
- Hu, Z., and Crews, C. M. (2021). Recent developments in PROTAC-mediated protein degradation: from bench to clinic. *Chembiochem.* 22, 1–23. doi: 10.1002/cbic.202100270
- Mulder, M. P. C., Witting, K. F., and Ovaa, H. (2020). Cracking the ubiquitin code: the ubiquitin toolbox. *Curr. Issues Mol. Biol.* 37, 1–20. doi: 10.21775/cimb.037.001
- Oikawa, D., Sato, Y., Ito, H., and Tokunaga, F. (2020). Linear ubiquitin code: its writer, erasers, decoders, inhibitors, and implications in disorders. *Int. J. Mol. Sci.* 21:3381. doi: 10.3390/ijms21093381
- Ramachandran, S., and Ciulli, A. (2021). Building ubiquitination machineries: E3 ligase multi-subunit assembly and substrate targeting



by PROTACs and molecular glues. *Curr. Opin. Struct. Biol.* 67, 110–119. doi: 10.1016/j.sbi.2020.10.009

**Conflict of Interest:** The authors declare that the research was conducted in the absence of any commercial or financial relationships that could be construed as a potential conflict of interest.

**Publisher's Note:** All claims expressed in this article are solely those of the authors and do not necessarily represent those of their affiliated organizations, or those of the publisher, the editors and the reviewers. Any product that may be evaluated in

this article, or claim that may be made by its manufacturer, is not guaranteed or endorsed by the publisher.

*Copyright © 2021 Liu, Rao, Gao, Wan and Zhang. This is an open-access article distributed under the terms of the Creative Commons Attribution License (CC BY). The use, distribution or reproduction in other forums is permitted, provided the original author(s) and the copyright owner(s) are credited and that the original publication in this journal is cited, in accordance with accepted academic practice. No use, distribution or reproduction is permitted which does not comply with these terms.*



# Caspase-8 Inhibition Prevents the Cleavage and Degradation of E3 Ligase Substrate Receptor Cereblon and Potentiates Its Biological Function

## OPEN ACCESS

### Edited by:

Cui Hua Liu,  
Institute of Microbiology, Chinese  
Academy of Sciences, China

### Reviewed by:

Yi Sun,  
Zhejiang University, China  
Kwang Chul Chung,  
Yonsei University, South Korea

### \*Correspondence:

Guoqiang Xu  
gux2002@suda.edu.cn  
orcid.org/0000-0002-4753-4769  
Xiangao Huang  
xih2004@med.cornell.edu

### Specialty section:

This article was submitted to  
Cell Growth and Division,  
a section of the journal  
Frontiers in Cell and Developmental  
Biology

**Received:** 14 September 2020

**Accepted:** 20 November 2020

**Published:** 17 December 2020

### Citation:

Zhou L, Yu W, Jayabalan DS,  
Niesvizky R, Jaffrey SR, Huang X and  
Xu G (2020) Caspase-8 Inhibition  
Prevents the Cleavage  
and Degradation of E3 Ligase  
Substrate Receptor Cereblon  
and Potentiates Its Biological  
Function.  
Front. Cell Dev. Biol. 8:605989.  
doi: 10.3389/fcell.2020.605989

**Liang Zhou<sup>1</sup>, Wenjun Yu<sup>1</sup>, David S. Jayabalan<sup>2</sup>, Ruben Niesvizky<sup>2</sup>, Samie R. Jaffrey<sup>3</sup>,  
Xiangao Huang<sup>4\*</sup> and Guoqiang Xu<sup>1\*</sup>**

<sup>1</sup> Jiangsu Key Laboratory of Neuropsychiatric Diseases, Jiangsu Key Laboratory of Preventive and Translational Medicine for Geriatric Diseases, College of Pharmaceutical Sciences, Soochow University, Suzhou, China, <sup>2</sup> Department of Medicine, Weill Cornell Medicine, New York, NY, United States, <sup>3</sup> Department of Pharmacology, Weill Cornell Medicine, New York, NY, United States, <sup>4</sup> Department of Pathology and Laboratory Medicine, Weill Cornell Medicine, New York, NY, United States

Cereblon (CRBN), a substrate receptor of cullin 4-RING E3 ligase (CRL4), mediates the ubiquitination and degradation of constitutive substrates and immunomodulatory drug-induced neo-substrates including MEIS2, c-Jun, CLC1, IKZF1/3, CK1 $\alpha$ , and SALL4. It has been reported that CRBN itself could be degraded through the ubiquitin-proteasome system by its associated or other cullin-RING E3 ligases, thus influencing its biological functions. However, it is unknown whether the CRBN stability and its biological function could be modulated by caspases. In this study, using model cell lines, we found that activation of the death receptor using tumor necrosis factor-related apoptosis-inducing ligand (TRAIL) leads to the decreased CRBN protein level. Through pharmacological inhibition and activation of caspase-8 (CASP-8), we disclosed that CASP-8 regulates CRBN cleavage in cell lines. Site mapping experiments revealed that CRBN is cleaved after Asp9 upon CASP-8 activation, resulting in the reduced stability. Using myeloma as a model system, we further revealed that either inhibition or genetic depletion of CASP-8 enhances the anti-myeloma activity of lenalidomide (Len) by impairing CRBN cleavage, leading to the attenuated IKZF1 and IKZF3 protein levels and the reduced viability of myeloma cell lines and primary myeloma cells from patients. The present study discovered that the stability of the substrate receptor of an E3 ligase can be modulated by CASP-8 and suggested that administration of CASP-8 inhibitors enhances the overall effectiveness of Len-based combination therapy in myeloma.

**Keywords: cereblon, caspase-8, cleavage, TRAIL, multiple myeloma, lenalidomide, anti-myeloma activity, cell viability**

## INTRODUCTION

Cereblon (CRBN) interacts with damage-specific DNA-binding protein 1 (DDB1) and thus forms a cullin 4-RING E3 ligase (CRL4<sup>CRBN</sup>) with cullin 4A/B and RING-box protein ROC1 (Angers et al., 2006; Jackson and Xiong, 2009; Ito et al., 2010; Xu et al., 2013). Therefore, CRBN functions as a substrate receptor and recruits proteins for ubiquitination and their subsequent proteasomal degradation. It has been discovered that the primary target of immunomodulatory drug thalidomide (Thal) is CRBN (Ito et al., 2010). Thal and its structural analogs lenalidomide (Len) and pomalidomide (Pom) bind to CRBN and thus recruit new substrates that would otherwise not bind to CRBN. These substrates, termed as “neo-substrates,” are ubiquitinated by the CRL4<sup>CRBN</sup> E3 ligase leading to their degradation. Two of the most studied neo-substrates of this E3 ligase are transcription factors IKZF1 (Ikaros) and IKZF3 (Aiolos). Their degradation suppresses the proliferation of myeloma cells (Krönke et al., 2014; Lu et al., 2014). This is regarded as the major mechanism by which Len is used to treat myeloma patients.

Low CRBN expression is associated with the Len resistance of myeloma cells, suggesting that high CRBN protein level is required for the anti-myeloma activity of IMiDs (Zhu et al., 2011). After 2–6 months of Len treatment, drug resistance frequently develops as a result of down-regulation of CRBN mRNA and protein levels (Lopez-Girona et al., 2012; Gandhi et al., 2014), which also indicates that CRBN protein levels regulate the sensitivity of myeloma cells to IMiDs. CRBN is targeted for ubiquitination-mediated degradation by SCF<sup>Fbxo7</sup> ubiquitin ligase (Song et al., 2018). CSN9 signalosome inhibits SCF<sup>Fbxo7</sup>-mediated CRBN degradation, thereby promoting the sensitivity of myeloma cells to IMiDs (Sievers et al., 2018; Liu et al., 2019). Several caspases are activated when myeloma cells are treated with proteasomal inhibitor bortezomib (Btz) (Hideshima et al., 2003). However, it is largely unknown whether CRBN stability and its functions are affected by caspase activity.

Tumor necrosis factor-related apoptosis-inducing ligand (TRAIL) is an inducer of apoptosis through binding to death receptor 4/5 (Gazitt, 1999), which results in the cleavage and activation of caspase-8 (CASP-8), a caspase in the extrinsic apoptotic pathway (Galluzzi et al., 2018). Because activated CASP-8 could cleave BID (Li et al., 1998; Luo et al., 1998), BID cleavage or reduction could serve as an indicator to demonstrate the activation of death receptor and CASP-8 (Chou et al., 1999). In our previous study, we found that CRBN inhibits the etoposide-induced intrinsic apoptosis (Zhou and Xu, 2019). However, it is unknown whether CRBN is involved in the death receptor-induced extrinsic apoptotic pathway and whether modulation of caspase activity could regulate the biological function of CRBN.

In this work, we examined CRBN stability in cervical cancer cell line HeLa and small cell lung cancer cell line NCI-H1688 upon the activation of the death receptor by TRAIL. Surprisingly, we discovered that TRAIL down-regulates CRBN protein level. The combination treatment of HeLa and NCI-H1688 cells with TRAIL and Btz results in the observation of the cleaved CRBN. This CRBN cleavage could be blocked by

CASP-8 inhibition. Interestingly, CASP-8 activation by TRAIL and Btz also leads to CRBN cleavage in myeloma cells. Using myeloma as a model system, we further demonstrated that blockage of the CRBN cleavage by pharmacological inhibition or genetic depletion of CASP-8 potentiates the anti-myeloma activity of Len in both myeloma cell lines and bone marrow primary myeloma cells. Database analysis showed that CASP-8 mRNA expression is inversely correlated with the overall survival rate of myeloma patients. Therefore, this work reveals a novel molecular mechanism by which the CRBN cleavage and stability is modulated. Using this discovery, we further disclosed that the anti-myeloma activity of IMiDs can be augmented by inhibiting the CASP-8 activation and suggests a potential new combination therapy that might benefit myeloma patients.

## MATERIALS AND METHODS

### Materials

Bortezomib (S1013), CASP-3 inhibitor z-DEVD-fmk (S7312), CASP-8 inhibitor z-IETD-fmk (S7314), Len (CC-5013), MG132 (S8410), MLN4924 (S7109), and Pom (S1567) were purchased from Selleck; TRAIL (abs04233) was obtained from Absin; pan-caspase inhibitor z-VAD-fmk (C1202) was ordered from Beyotime Biotechnology; and cycloheximide (CHX, C104450) was obtained from Sigma.

The antibodies used in this work were purchased from the following companies: anti-CASP-8 antibody (BA2143) was purchased from Boster Biological Technology; anti-ubiquitin (Ub, sc-8017) and anti-HA (sc-7392) antibodies were from Santa Cruz Biotechnology; anti-Flag (0912-1) and anti-GST (ET1611-47) antibodies were from HuaAn Biotechnology; anti-PARP1 (9532S), anti-CRBN (71810S), and anti-cleaved CASP-8 (9496T) antibodies were from Cell Signaling Technology; anti-GAPDH (60004-1-Ig) and anti-IKZF3 (13561-1-AP) antibodies were from ProteinTech Group; anti-BID (CPA4351) antibody was from Cohesion Biosciences; and anti-IKZF1 (YM1278) antibody was from Immunoway. Mouse anti-CRBN antibody (Xu et al., 2016) was a kind gift from Dr. Xiu-Bao Chang (Mayo Clinic College of Medicine, United States). Secondary antibodies (sheep anti-mouse IgG-HRP and anti-rabbit IgG-HRP) were from Thermo Fisher.

### shRNA and CRBN Plasmids

To make CASP-8 shRNA (shCASP-8), CASP-8 forward oligonucleotide (5'-CCGGCACCAGGCAGGGCTCAAATTTCTGC AGAAATTTGAGCCCTGCCTGGTGTGTTTTTG-3') and CASP-8 reverse complementary oligonucleotide (5'-AATTCAAAAACA CCAGGCAGGGCTCAAATTTCTGCAGAAATTTGAGCCCT GCCTGGTG-3') were annealed and ligated to the pLKO.1 TRC cloning vector (a gift from David Root, Addgene plasmid #10878) using a published procedure (Moffat et al., 2006). A digestion with *Pst*I and *Bam*HI was performed to identify the positive clone, which was further validated by Sanger sequencing.

shNC or shCRBN lentiviruses were purchased from GeneChem (Shanghai, China). The target sequence of shNC

was TTCTCCGAACGTGTCACGT, and the target sequence of shCRBN was CCCAGACACTGAAGATGAAAT.

Plasmids for CRBN-Flag, D-to-A, and Del9 mutants were subcloned or constructed using standard point mutagenesis.

## Generation of Stable Knockdown Cells

The sh*LacZ* (The RNAi Consortium), shCRBN, and shCASP-8 lentiviruses were produced as described in a previous publication (Moffat et al., 2006). Myeloma cells MM1.S and CAG were infected with lentiviruses and selected with puromycin (1  $\mu$ g/ml) for 2 weeks to generate stable knockdown cells.

## Cell Culture

Cervical cancer cell line HeLa, human embryonic kidney cell line HEK293T, multiple myeloma cell lines MM1.S and RPMI8226, and small cell lung cancer cell line NCI-H1688 were obtained from American Type Culture Collection (ATCC). Multiple myeloma CAG cells (Borset et al., 2000) were a kind gift from Dr. Joshua Epstein (University of Arkansas for Medical Sciences, Little Rock, AK, United States). MM1.S, RPMI8226, CAG, and NCI-H1688 cells were cultured in Roswell Park Memorial Institute (RPMI) 1640 medium. HeLa and HEK293T cells were cultured in Dulbecco's Modified Eagle's Medium (DMEM; HyClone). Growth medium was supplemented with 10% fetal bovine serum (FBS; Gibco and Lonsera), 100 U/ml penicillin, and 100  $\mu$ g/ml streptomycin (Gibco).

Bone marrow specimens were obtained from deidentified multiple myeloma patients at the Weill Cornell Medicine under informed consent as part of an Institutional Review Board approved study. CD138<sup>+</sup> primary myeloma cells were isolated from bone marrow and co-cultured with a layer of HS-5 cells and cytokines as previously described (Huang et al., 2012).

## Western Blotting Analysis

Cell lysates or immunoprecipitates were analyzed by Western blotting according to a previously described method (Hou et al., 2015) using NcmECL Ultra substrate (NCM Biotech) for visualization (Tao et al., 2018).

## Affinity Purification

The HEK293T cell lysates were incubated with the anti-Flag affinity gel (Sigma) at 4°C for 3–4 h. The gel was then washed three times with TBST (TBS with 0.1% Tween 20). The Flag-tagged proteins were eluted with the 2 $\times$  sample loading buffer for Western blotting analysis.

## CASP-8 Activity Assay

RPMI8226 cells were first treated with DMSO or 40  $\mu$ M CASP-8 inhibitor z-IETD-fmk for 30 min and then treated with DMSO or 10  $\mu$ M Len for another 24 h. CASP-8 activity was measured using a CASP-8 fluorometric assay (Beyotime Biotechnology) according to the manufacturer's instruction.

## Flow Cytometry Analysis

Myeloma cells expressing sh*LacZ* or shCASP-8 were cultured and treated with DMSO or Len (10  $\mu$ M) for 4 days. Cells were stained

with ToPro-3 (Life Technologies, United States) and analyzed in a BD flow cytometry according to a previously used method (Liu et al., 2015). The data were processed with FlowJo.

## Cell Viability Measurement

Cells were treated with DMSO or the indicated compounds and stained with trypan blue (Beyotime Biotechnology) or analyzed with cell counting kit-8 assay (CCK-8, Beyotime Biotechnology). Live cells were counted under the microscope, and optical density at 460 nm was measured. The percentage of live cells was calculated.

## Analysis of CASP-8 mRNA and Patient Overall Survival Rate

Kaplan–Meier plot of overall survival rate in patients with low (<20 FPKM, Fragments Per Kilobase of exon model per Million mapped fragments) and high (>20 FPKM) CASP-8 mRNA expression levels in the CoMMpass trial (IA14) of single Len or combination of Btz, Len, and dexamethasone (Dex) was generated, and statistical analysis for the pairwise comparison was performed using log-rank test integrated with the tool available at Multiple Myeloma Research Foundation (MMRF) Researcher Gateway<sup>1</sup>.

## RESULTS

### CRBN Is Decreased in HeLa and NCI-H1688 Cells Upon TRAIL Treatment

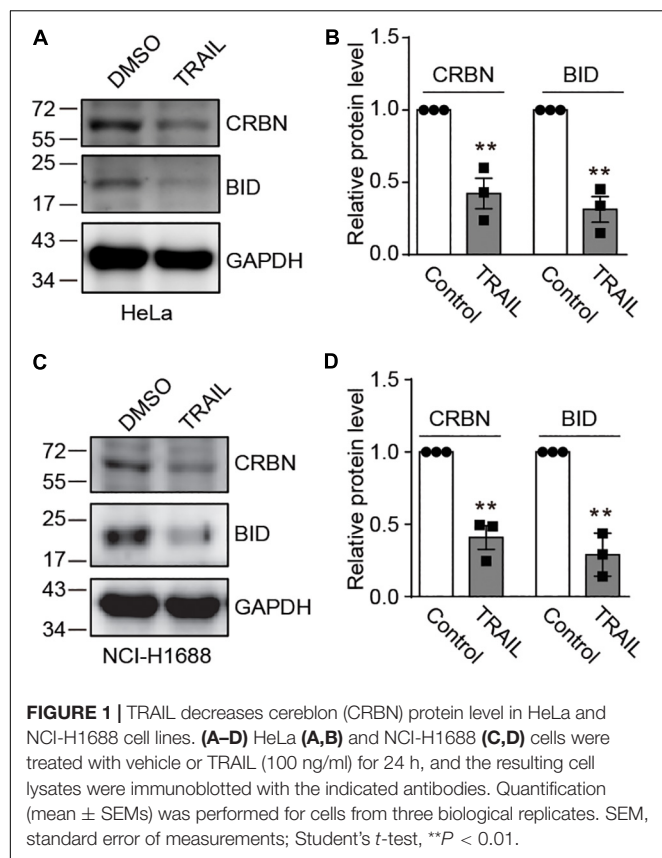
Recently, it has been discovered that CRBN inhibits DNA damage-induced apoptosis (Zhou and Xu, 2019). However, it is unknown whether and how death receptors regulate CRBN and its function. To explore this possibility, we treated HeLa cells with TRAIL to activate the death receptor, which was confirmed by immunoblotting for a death receptor-related biomarker BID (Figures 1A,B). We further discovered that TRAIL clearly led to the down-regulation of CRBN (Figures 1A,B). Similar results were also observed in NCI-H1688 cells (Figures 1C,D), indicating that CRBN reduction upon the activation of death receptor may be a general phenomenon.

### CRBN Is Cleaved Upon TRAIL and Btz Co-treatment

We next sought to investigate the possible molecular mechanisms underlying TRAIL-induced down-regulation of CRBN. Since CRBN undergoes proteasomal degradation, we used the proteasome inhibitors Btz and MG132 to treat HeLa and NCI-H1688 cells in the presence of TRAIL (Figures 2A–D). Surprisingly, immunoblotting of CRBN showed that the band for the full length CRBN disappeared, whereas a new band appeared at about 1–5 kDa below the full length CRBN. This result indicates that CRBN is cleaved and the cleaved fragment is stable in HeLa and NCI-H1688 cells after TRAIL-Btz and TRAIL-MG132 treatment (Figures 2A–D). Similar results were

<sup>1</sup>www.themmr.org

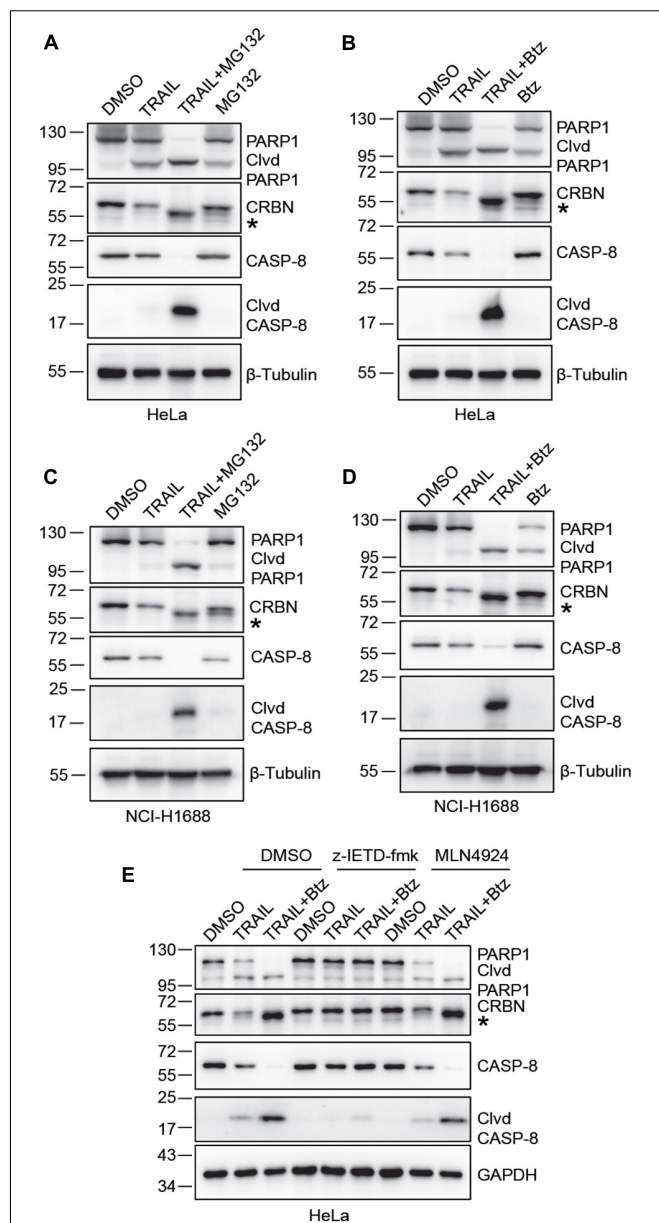




found in MM1.S myeloma cells (Supplementary Figure 1). These data suggested that the cleaved CRBN is most probably degraded through the ubiquitin-proteasome system. The previous study demonstrated that combination use of TRAIL and Btz could dramatically activate CASP-8 and cause apoptosis in the lung cancer cell line through enhancing the surface expression of TRAIL receptor (Voortman et al., 2007). We then examine whether CASP-8 is responsible for the CRBN cleavage. Pharmacological inhibition experiments demonstrated that the CASP-8 inhibitor z-IETD-fmk but not the CASP-3 specific inhibitor z-DEVD-fmk and the NEDD8-activating enzyme inhibitor MLN4924 block synergistic TRAIL-Btz-induced CRBN cleavage in HeLa cells (Figure 2E and Supplementary Figure 2), indicating that CASP-8 is required for the cleavage of CRBN upon TRAIL-Btz treatment.

## CASP-8 Activation Cleaves CRBN at Asp9 and This Cleavage Reduces CRBN Stability

Next, we sought to determine the cleavage site in CRBN upon CASP-8 activation. To do so, we first constructed a CRBN-Flag plasmid and transfected this plasmid into HeLa cells, which were further treated with TRAIL and Btz. Immunoblotting of cell lysates with both anti-Flag and anti-CRBN antibodies resulted in two bands, the full length CRBN and the cleaved CRBN in HeLa cells upon CASP-8 activation (Figure 3A). This



result indicates that the cleavage site on CRBN is located at its N-terminus because the Flag tag is fused to the CRBN C-terminus. Sequence alignment analysis of CRBN indicates that the Asp (D) residues at N-termini are highly conserved

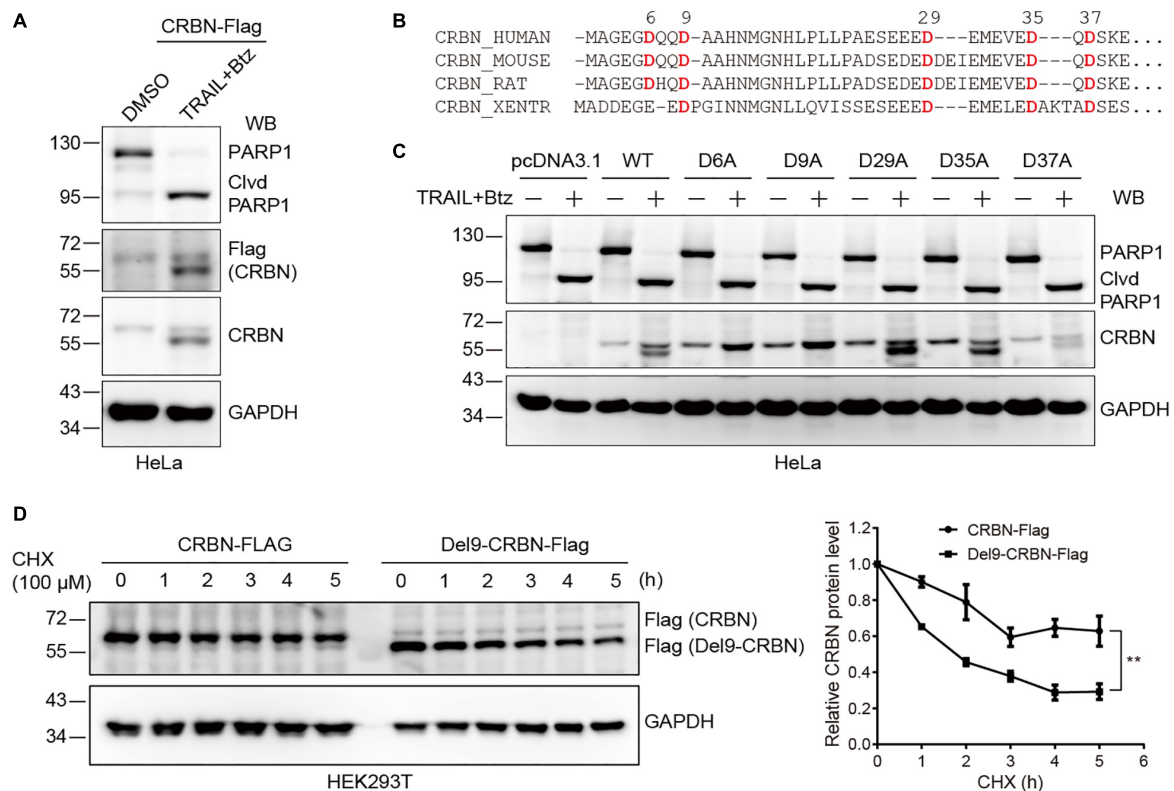


**FIGURE 3 |** Cleavage of CRBN at Asp9 (D9) reduces its stability. **(A)** CRBN is cleaved at the N-terminus upon CASP-8 activation. HeLa cells were transfected with CRBN-Flag plasmid for 48 h and treated with DMSO or TRAIL (100 ng/ml) and Btz (0.5  $\mu$ M) for 24 h. The resulting cell lysates were subjected to immunoblotting analysis. **(B)** Amino acid sequence alignment for CRBN from human, mouse, rat, and western clawed frog (Xentr). Conserved Asp (D) residues were indicated in red. **(C)** CRBN is cleaved at Asp9 (D9) upon CASP-8 activation. HeLa cells were transfected with the WT and CRBN Asp (D) to Ala (A) mutants for 48 h and then treated with DMSO or TRAIL (100 ng/ml) and Btz (0.5  $\mu$ M) for 24 h. Cell lysates were used for immunoblotting. **(D)** Deletion of the N-terminal nine amino acids in CRBN reduces its stability. WT CRBN and Del9-CRBN mutants were expressed in HEK293T cells and split to 24-well plates. At 48 h post-transfection, cells were further treated with cycloheximide (CHX, 100  $\mu$ M) for the indicated time. The cell lysates were immunoblotted with the indicated antibodies. Mean  $\pm$  SEMs were from three independent biological replicates. Two-way ANOVA, \*\* $P < 0.01$ ; Clvd, cleaved.

among human, mouse, rat, and western clawed frog (Figure 3B). To further determine the exact cleavage site, we mutated five Asp residues at the N-terminus to Ala, one at a time, and carried out the same experiment. Immunoblotting of cell lysates demonstrated that CASP-8 activation resulted in the cleavage of the WT, D29A, D35A, and D37A CRBN mutants but not the D6A and D9A mutants (Figure 3C). The sequence of the 6–10 amino acids in CRBN (DQQDA) is the CASP-8 preferred cleavage sequence (L/D/V)XXD(G/S/A) (Stennicke et al., 2000), and the D6A mutation disrupts this sequence. Therefore, these data demonstrate that CRBN is cleaved by CASP-8 after Asp9. This cleavage site was also detected previously by a quantitative N-terminomics (Shimbo et al., 2012).

These results demonstrated that treatment of HeLa and NCI-H1688 cells with TRAIL and Btz led to CRBN cleavage. However, we only observed reduced CRBN levels but not the cleaved fragments in these cells upon the activation of CASP-8 by TRAIL, suggesting that the stability of CRBN might be reduced after cleavage. To test this hypothesis, we measured the stability of the WT and Del9 CRBN in HEK293T cells treated with a protein synthesis inhibitor CHX. Immunoblotting of cell lysates showed

that Del9 CRBN was diminished at a much faster rate than the WT counterpart upon CHX treatment (Figure 3D), confirming its reduced stability. Inhibition of neddylation by MLN4924 significantly increased the WT and Del9 CRBN protein levels (Supplementary Figure 3), indicating that they are ubiquitinated by the cullin RING E3 ligases and subsequently degraded by the proteasome. This is in concert with the fact that the cleaved CRBN was observed in HeLa cells only in the presence of proteasome inhibitor (Figure 2). Furthermore, we found that TRAIL-induced apoptosis was not affected in the CRBN deficient HeLa cells (Supplementary Figure 4), suggesting that the cleavage of CRBN did not regulate CASP-8-dependent apoptosis.

## CASP-8 Inhibition Enhances the Anti-myeloma Activity of Len in Cell Lines

After the discovery of CRBN cleavage by CASP-8, we thought to investigate how this cleavage affects its biological function. It has been reported that IMiDs can activate CASP-8 (Mitsiades et al., 2002; Chauhan and Anderson, 2003; Martiniani et al., 2012).



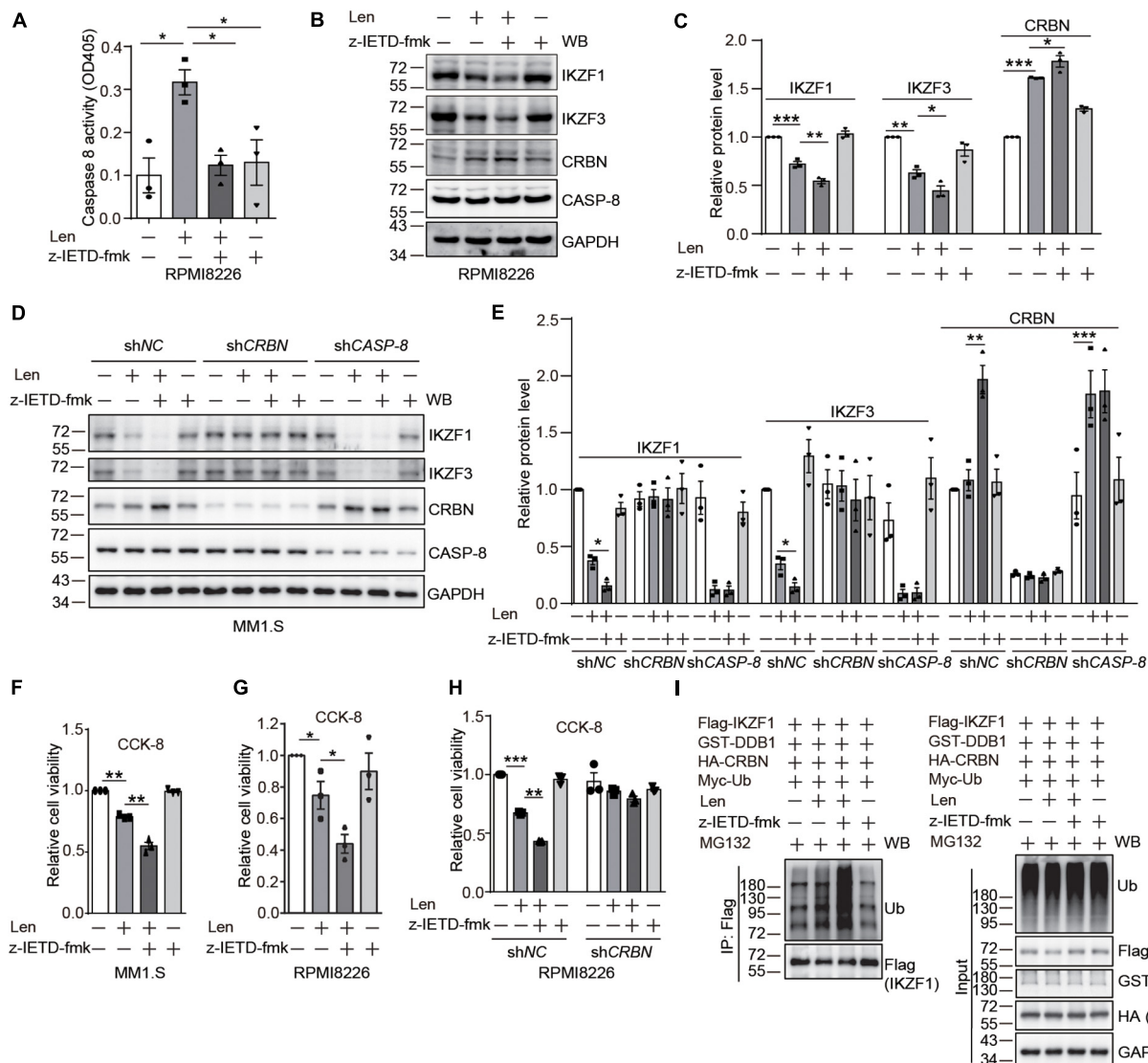


**FIGURE 4 |** CASP-8 inhibition potentiates the anti-myeloma activity of Len. **(A)** Len enhances CASP-8 activity. RPMI8226 cells were pretreated with DMSO or z-IETD-fmk (40  $\mu$ M) for 30 min and then treated with DMSO or Len (10  $\mu$ M) for 24 h. CASP-8 activity was measured using a CASP-8 fluorometric assay kit. Mean  $\pm$  SEMs from three independent biological replicates were plotted. Student's *t*-test, \**P* < 0.05. **(B)** CASP-8 inhibitor z-IETD-fmk enhances the Len-mediated reduction of transcription factors IKZF1 and IKZF3 in RPMI8226 cells. RPMI8226 cells were pretreated with DMSO or CASP-8 inhibitor z-IETD-fmk (40  $\mu$ M) for 30 min and then treated with DMSO or Len (10  $\mu$ M) for 24 h. The resulting cell lysates were immunoblotted with the indicated antibodies. **(C)** Quantitative data (mean  $\pm$  SEMs) for **(B)** were from three independent biological replicates. Student's *t*-test, \**P* < 0.05, \*\**P* < 0.01, \*\*\**P* < 0.001. **(D)** CASP-8 inhibitor z-IETD-fmk enhances the Len-mediated reduction of transcription factors IKZF1 and IKZF3 in stable MM1.S knockdown cell lines. The stable shNC, shCRBN, and shCASP-8 MM1.S cell lines were pretreated with DMSO or CASP-8 inhibitor z-IETD-fmk (40  $\mu$ M) for 30 min and then treated with DMSO or Len (10  $\mu$ M) for 3 h. The resulting cell lysates were immunoblotted with the indicated antibodies. **(E)** Quantitative data (mean  $\pm$  SEMs) for **(D)** were from three independent biological replicates. Student's *t*-test, \**P* < 0.05, \*\**P* < 0.01, \*\*\**P* < 0.001. **(F)** CASP-8 inhibitor enhances Len-mediated reduction of cell viability in MM1.S cell line. MM1.S cells were pretreated with DMSO or z-IETD-fmk (40  $\mu$ M) for 30 min and then treated with DMSO or Len (10  $\mu$ M) for 48 h. The relative cell viability was measured with CCK-8 assay. Mean  $\pm$  SEMs from three independent biological replicates. Student's *t*-test, \*\**P* < 0.01. **(G)** CASP-8 inhibitor enhances Len-mediated reduction of cell viability in RPMI8226 cell line. RPMI8226 cells were pretreated with DMSO or z-IETD-fmk (40  $\mu$ M) for 30 min and then treated with DMSO or Len (10  $\mu$ M) for 48 h. The relative cell viability was measured with CCK-8 assay. Mean  $\pm$  SEMs from three independent biological replicates. Student's *t*-test, \**P* < 0.05. **(H)** CASP-8 inhibitor enhances Len-mediated reduction of cell viability in a CRBN-dependent manner. RPMI8226 cells were infected with shNC or shCRBN lentiviruses for 16 h and then treated as described in **(G)**. Student's *t*-test, \*\**P* < 0.01, \*\*\**P* < 0.001. **(I)** CASP-8 inhibitor z-IETD-fmk enhances the Len-mediated ubiquitination of IKZF1. HEK293T cells were transfected with Flag-IKZF1, HA-CRBN, GST-DDB1, and Myc-Ub and split to four 6-cm plates. At 48 h post-transfection, cells were pretreated with DMSO or z-IETD-fmk (40  $\mu$ M) for 30 min, then with DMSO or Len (10  $\mu$ M) for 1 h, and again with MG132 (10  $\mu$ M) for 12 h. The Flag tagged IKZF1 was purified with anti-Flag affinity gel, and the purified samples and whole cell lysates were immunoblotted with the indicated antibodies.

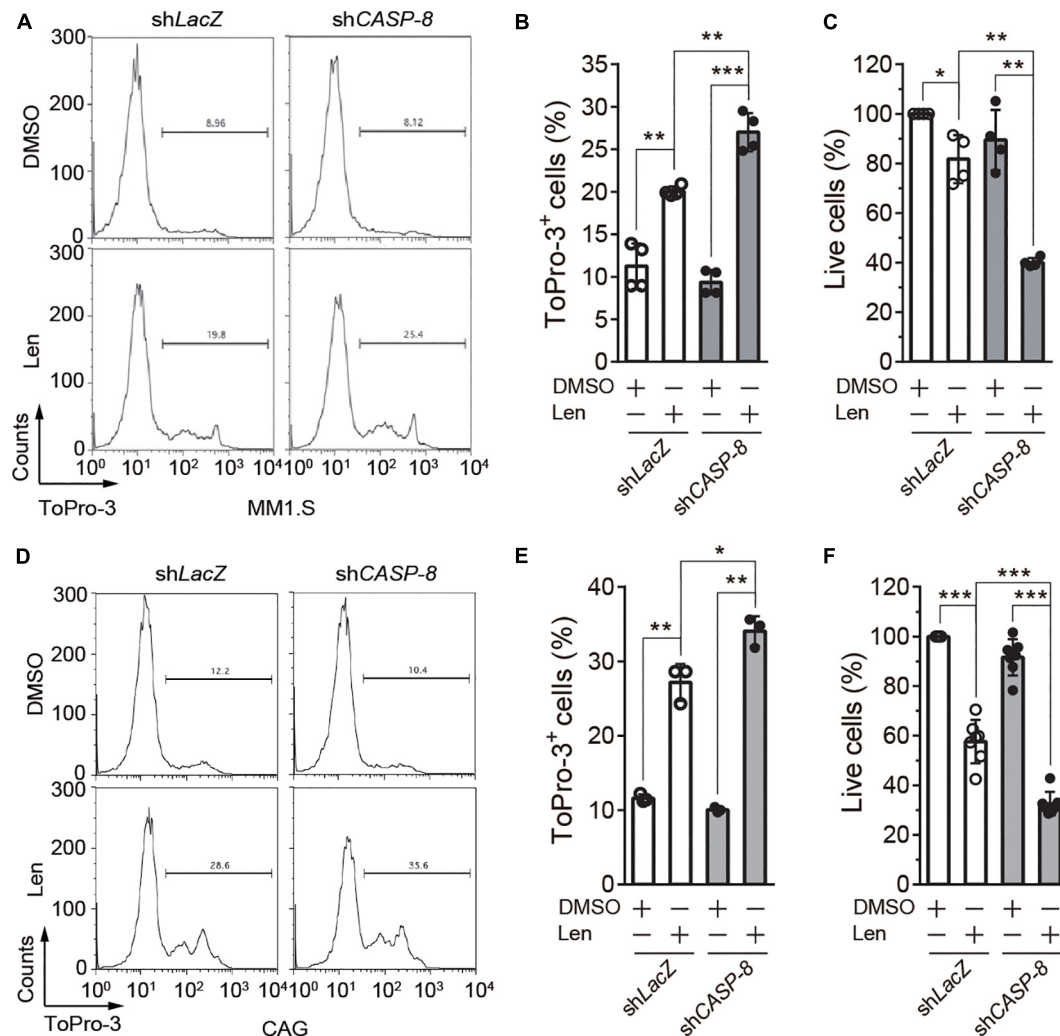


**FIGURE 5 | CASP-8 knockdown enhances the anti-myeloma activity of Len in myeloma cell lines. (A,B)** CASP-8 knockdown increases Len-induced ToPro3<sup>+</sup> cells. MM1.S cells with *LacZ* (mock) or *CASP-8* knockdown were treated with DMSO or Len (10  $\mu$ M) for 4 days and stained with ToPro-3. Cells were analyzed with flow cytometry, and ToPro-3<sup>+</sup> cells (mean  $\pm$  SEMs) were quantified from four biological replicates. Student's *t*-test, \*\**P* < 0.01, \*\*\**P* < 0.001. **(C)** CASP-8 knockdown potentiates the anti-myeloma activity of Len. MM1.S cells stably expressing sh*LacZ* or sh*CASP-8* were treated with DMSO or Len (10  $\mu$ M) for 4 days. Live cells were stained with trypan blue and counted under the microscope. Quantification was performed for cells (mean  $\pm$  SEMs) from four biological replicates and normalized to the DMSO treated sample. Student's *t*-test, \**P* < 0.05, \*\**P* < 0.01. **(D-F)** Same experiments as **(A-C)** were performed for CAG myeloma cells. In **(E,F)**, the numbers of biological replicates were three and seven, respectively. Mean  $\pm$  SEMs, Student's *t*-test, \**P* < 0.05, \*\**P* < 0.01, \*\*\**P* < 0.001.

Therefore, we thought to use myeloma cells as a model system to explore whether CASP-8 regulates CRBN levels after addition of Len. We found that CASP-8 activity is increased upon Len treatment in RPMI8226 cells (Figure 4A). Immunoblotting of CRBN showed that Len increases CRBN protein level at 24 h, which is consistent with previous studies (Liu et al., 2015). CASP-8 inhibitor z-IETD-fmk further increases CRBN protein levels (Figures 4B,C). These results suggest that the effect of Len and CASP-8 inhibitors on CRBN protein levels might be additive. Consequently, z-IETD-fmk further down-regulates the IKZF1 and IKZF3 protein levels mediated by Len (Figures 4B,C). To further investigate the effect of CRBN and CASP-8 on the IKZF1 and IKZF3 upon Len treatment, we obtained the stable

shNC, shCRBN, and shCASP-8 knockdown MM1.S cell lines. We found the same results that CASP-8 inhibitor z-IETD-fmk could further down-regulate IKZF1 and IKZF3 upon Len treatment, which was mediated by CRBN (Figures 4D,E). Furthermore, the CRBN protein level was increased in the CASP-8 deficient cells (Figures 4D,E).

It has been demonstrated that high CRBN protein levels enhance the anti-myeloma activity of Len (Zhu et al., 2011; Liu et al., 2015). Therefore, we examined whether z-IETD-fmk increases the anti-myeloma activity of Len. Results from trypan blue staining and cell counting kit-8 (CCK-8) assay indicated that treatment with Len and z-IETD-fmk indeed further suppresses the viability of myeloma cells compared with Len treatment alone

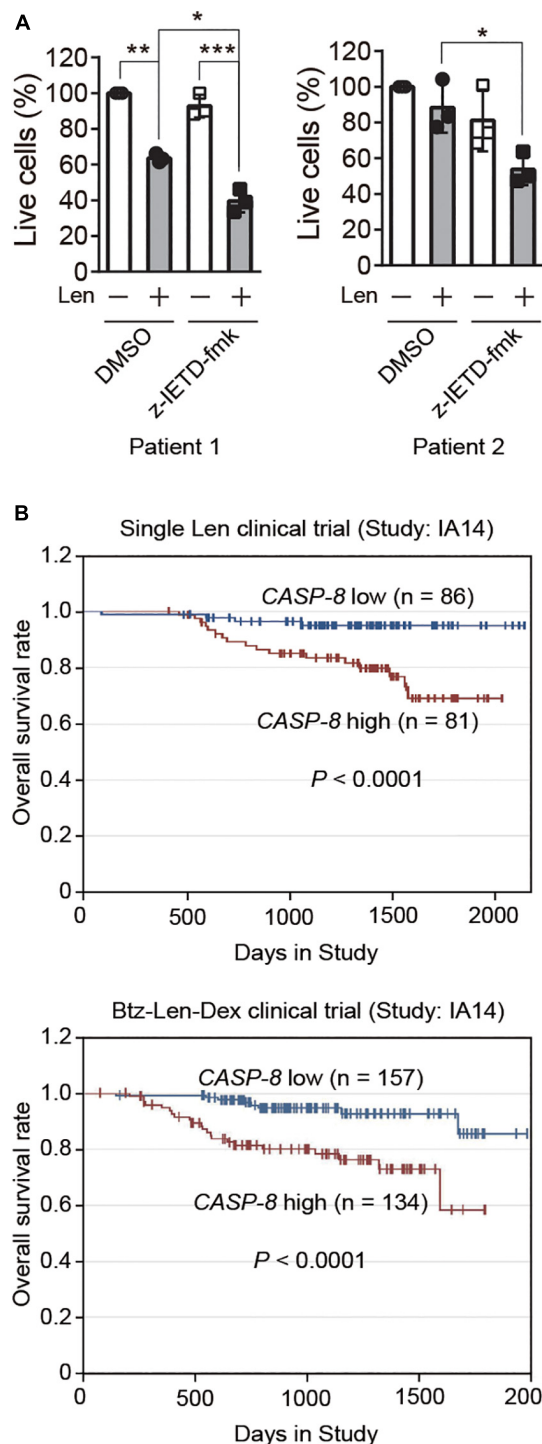


**FIGURE 6 |** CASP-8 inhibition enhances the anti-myeloma activity of Len in primary myeloma cells, and low CASP-8 mRNA level increases the survival rate of myeloma patients. **(A)** CASP-8 inhibitor augments the anti-myeloma effect of Len in primary myeloma cells. CD138<sup>+</sup> primary cells were isolated from myeloma Patient 1 and Patient 2, co-cultured with HS-5 cells, pretreated with DMSO or z-IETD-fmk (40  $\mu$ M) for 1 h, and then treated with DMSO or Len (10  $\mu$ M) for 4 and 5 days, respectively. The percentage of live cells was determined by staining with trypan blue and examined under the microscope. (Continued)

#### FIGURE 6 | Continued

Experiments were carried out in triplicates, and pairwise Student's *t*-test was used to obtain the *P*-value (mean  $\pm$  SEMs). \**P* < 0.05, \*\**P* < 0.01, \*\*\**P* < 0.001. **(B)** Low gene expression of CASP-8 increases the overall survival rate of myeloma patients. The data were obtained from patients in the MMRF CoMMpass trial (IA14) of combination therapy with Btz (Velcade), Len (Revlimid), and Dex (VRd). The numbers of patients for low (<20 FPKM) and high (>20 FPKM) CASP-8 mRNA levels were indicated in the images.

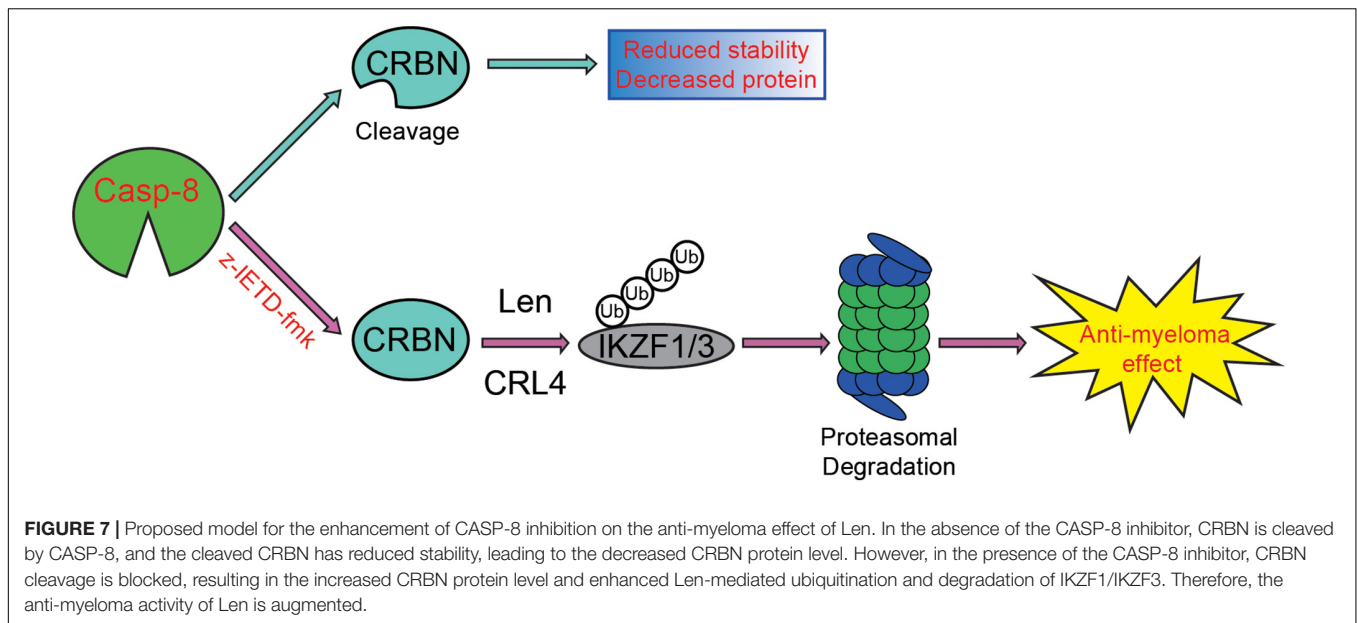
(Figures 4F,G and Supplementary Figures 5, 6). We further knocked down *CRBN* in RPMI8226 cells with lentivirus and treated the cells with z-IETD-fmk to investigate the anti-myeloma activity of Len. The data showed that z-IETD-fmk potentiated the anti-myeloma activity of Len in the mock knockdown and this effect disappeared when *CRBN* was knocked down (Figure 4H and Supplementary Figure 7). We also purified the Flag tagged IKZF1 and determined its ubiquitination upon z-IETD-fmk and Len treatment. We found that z-IETD-fmk could enhance the ubiquitination of IKZF1 upon Len treatment (Figure 4I), which further supported our conclusion that CASP-8 inhibition promotes their degradation through upregulating *CRBN*. This indicates that *CRBN* is required for the enhanced anti-myeloma activity of Len upon CASP-8 inhibition.

### CASP-8 Knockdown Potentiates the Anti-myeloma Activity of Len in Cell Lines

To further determine the role of CASP-8 on the anti-myeloma activity of Len, we established MM1.S and CAG cell lines stably expressing control *shLacZ* or *shCASP-8*. The flow cytometry analysis demonstrated that ToPro-3<sup>+</sup> dead cells are significantly increased upon Len treatment in the *CASP-8* knockdown cells (Figures 5A,B). Consistent with this, the percentage of live cells determined by trypan blue exclusion in the *CASP-8* knockdown cells is markedly reduced upon Len treatment (Figure 5C). Similar results were obtained for CAG myeloma cells (Figures 5D–F). Taken together, our results demonstrated that both inhibition and knockdown of *CASP-8* enhance the anti-myeloma activity of Len in cell lines.

### CASP-8 Inhibition Enhances the Therapeutic Effect of Len in Primary Myeloma Cells

To further validate whether CASP-8 modulates the anti-myeloma activity of Len in primary cells, we cultured CD138<sup>+</sup> primary myeloma cells from bone marrow of two patients and treated them with CASP-8 inhibitor z-IETD-fmk and/or Len. Trypan blue staining and cell counting analyses demonstrated that z-IETD-fmk reduces the percentage of live cells upon Len treatment, whereas z-IETD-fmk alone does not affect the cell viability in both primary myeloma cells (Figure 6A). It should be noted that Len alone exhibited different effects in two primary patient samples. The viability of primary myeloma cells from Patient 1 but not from Patient 2 was significantly reduced by Len treatment. This result suggests that the genetic backgrounds of these two patients might be different, resulting in different



sensitivities to Len. Nevertheless, CASP-8 inhibition enhances the anti-myeloma activity of Len in both cases.

### High CASP-8 Gene Expression Correlates With Poor Overall Survival in Myeloma Patients

Next, we would like to test whether the gene expression of *CASP-8* is associated with the clinical outcome of myeloma patients. To do this, we analyzed the *CASP-8* mRNA level and the overall survival rate of patients participating in a clinical trial of single Len or Btz, Len, and Dex combination therapy obtained from the datasets in MMRF. The result showed that those with lower *CASP-8* mRNA levels exhibited a higher overall survival rate (Figure 6B), suggesting that *CASP-8* expression may be an important factor in determining the clinical response to Len-based therapies likely through the regulation of CRBN protein level in myeloma. This result is also in concert with the data obtained from myeloma cell lines where *CASP-8* inhibition or depletion further reduces the Len-mediated viability of myeloma cells (Figures 4–5).

## DISCUSSION

As a substrate receptor, CRBN mediates the ubiquitination and degradation of constitutive substrates and neo-substrates upon IMiD treatment (Krönke et al., 2014, 2015; An et al., 2017; Donovan et al., 2018; Matyskiela et al., 2018). CRBN can be regulated by SCF<sup>Fbox7</sup> and its associated E3 ligase CRL4<sup>CRBN</sup>, thus modulating its biological function. CRBN is a key modulator in the treatment of myeloma cells with Len and its structural analogs. However, whether CRBN and its function can be regulated by caspases was not explored. In this study, using three different types of cell lines (HeLa, NCI-H1688, and MM1.S cells), we discovered that CRBN can be cleaved upon TRAIL and

Btz treatment (Figures 1, 2, and Supplementary Figure 1) and further demonstrated that this cleavage is blocked by CASP-8 inhibition (Figure 2).

Transcription factors IKZF1 and IKZF3 are required for myeloma cells to undergo proliferation. IMiDs bind to CRBN and recruit IKZF1 and IKZF3 for their ubiquitination and degradation, leading to the reduced proliferation of myeloma cells. This is the recently discovered major mechanism of action of IMiDs for the treatment of myeloma cells (Krönke et al., 2014; Lu et al., 2014). Using this model system, we showed that both pharmacological inhibition and genetic depletion of CASP-8 increase the level of full length CRBN, enhance the degradation of IKZF1 and IKZF3, and then suppress the proliferation of myeloma cells when treated with Len, which is consistent with the previous studies that CRBN protein levels control the sensitivity to IMiDs (Zhu et al., 2011; Liu et al., 2019). Two molecular mechanisms were discovered for the regulation of CRBN by Len. On the one hand, CRBN is required for the anti-myeloma activity of Len. However, the cleavage of CRBN can be induced by CASP-8 activation, which could be mediated by Len in myeloma cells, and the stability of the cleaved CRBN is reduced. On the other hand, our previous experiments detected the increase of CRBN protein level after 3 days treatment of myeloma cell lines with IMiDs (Liu et al., 2015). In that work, we also revealed that IMiDs can prevent CRBN from ubiquitination and subsequent degradation, leading to the increased CRBN protein level and enhanced CRL4<sup>CRBN</sup> E3 ligase activity, contributing to the anti-myeloma effect of IMiDs. In this work, we also observed the increase of CRBN protein level upon Len treatment. These two mechanisms of action of Len possibly result in two opposite effects, increase and decrease, on the CRBN protein level. Nevertheless, both mechanisms support the idea that inhibiting CASP-8 activity increases CRBN protein level and benefits to the therapeutic effect of Len for the treatment of myeloma. Therefore, combination of CASP-8 inhibitor with Len would most likely



benefit to the treatment of myeloma, which was indeed confirmed in myeloma cell lines and primary myeloma cells.

On the one hand, we discovered that the viability of myeloma cells is reduced by the addition of CASP-8 inhibitor during the Len treatment (Figures 4–6). On the other hand, PARP1 cleavage is not significantly altered by the addition of CASP-8 inhibitor. These phenomena suggest that CASP-8 inhibition might affect the proliferation of myeloma cells. This is in accordance with the fact that Len reduces the proliferation of myeloma cells (Krönke et al., 2014; Lu et al., 2014). Using a CASP-8 fluorometric assay, a previous study demonstrated that Len and Pom activate CASP-8 (Mitsiades et al., 2002; Das et al., 2015), although no apparent CASP-8 cleavage was observed in the immunoblotting analysis (Chauhan et al., 2010; Das et al., 2015). Using HeLa cells as a model system, we discovered that CRBN is cleaved at Asp9 upon CASP-8 activation (Figure 3C). However, the cleaved CRBN has much lower stability (Figure 3D), which could reduce the CRL4<sup>CRBN</sup> E3 ligase activity. In combination with CASP-8 inhibitor, Len further elevates the CRBN protein level, resulting in the enhanced degradation of IKZF1 and IKZF3 and enhanced anti-myeloma activity (Figures 4–7). Therefore, a strategy could be an alternative treatment of myeloma with the combination of IMiDs and CASP-8 inhibitors, which suppresses the proliferation of myeloma cells.

It should be noted that different myeloma cell lines and primary myeloma cells may have distinct genetic backgrounds, such as mutations and expression level of genes including *CRBN*, *CASP-8*, and *DDI1*, which affect cell proliferation and regulate cell death pathways. Indeed, truncation and point mutations in *CRBN* and *DDI1* were discovered in myeloma cells and patient samples despite the fact that these mutations were rare (Thakurta et al., 2014). Although our conclusion was obtained from multiple cell lines and two primary patient samples, we cannot completely rule out the possibility that CASP-8 inhibition might not have a significant influence on the treatment of certain myeloma cell lines or some patient samples when CASP-8, CRBN, or other component of the CRL4<sup>CRBN</sup> E3 ligase is not expressed or is mutated.

## DATA AVAILABILITY STATEMENT

The raw data supporting the conclusions of this article will be made available by the authors, without undue reservation.

## REFERENCES

- An, J., Ponthier, C. M., Sack, R., Seebacher, J., Stadler, M. B., Donovan, K. A., et al. (2017). pSILAC mass spectrometry reveals ZFP91 as IMiD-dependent substrate of the CRL4<sup>CRBN</sup> ubiquitin ligase. *Nat. Commun.* 8:15398. doi: 10.1038/ncomms15398
- Angers, S., Li, T., Yi, X., MacCoss, M. J., Moon, R. T., and Zheng, N. (2006). Molecular architecture and assembly of the DDB1–CUL4A ubiquitin ligase machinery. *Nature* 443:590. doi: 10.1038/nature05175
- Borset, M., Hjertner, O., Yaccoby, S., Epstein, J., and Sanderson, R. D. (2000). Syndecan-1 is targeted to the uropods of polarized myeloma cells where it promotes adhesion and sequesters heparin-binding proteins. *Blood* 96, 2528–2536.
- Chauhan, D., and Anderson, K. C. (2003). Mechanisms of cell death and survival in multiple myeloma (MM): therapeutic implications. *Apoptosis* 8, 337–343.
- Chauhan, D., Singh, A. V., Ciccarelli, B., Richardson, P. G., Palladino, M. A., and Anderson, K. C. (2010). Combination of novel proteasome inhibitor NPI-0052 and lenalidomide trigger in vitro and in vivo synergistic cytotoxicity in multiple myeloma. *Blood* 115, 834–845. doi: 10.1182/blood-2009-03-213009
- Chou, J. J., Li, H., Salvesen, G. S., Yuan, J., and Wagner, G. (1999). Solution structure of BID, an intracellular amplifier of apoptotic signaling. *Cell* 96, 615–624. doi: 10.1016/s0092-8674(00)80572-3

## ETHICS STATEMENT

The studies involving human participants were reviewed and approved by an Institutional Review Board of Weill Cornell Medicine. The patients/participants provided their written informed consent to participate in this study.

## AUTHOR CONTRIBUTIONS

LZ, XH, SJ, and GX designed the research. LZ, WY, and XH performed the research. LZ, WY, XH, and GX analyzed the data. DJ and RN provided the patient samples. LZ, XH, and GX wrote the manuscript. WY, DJ, RN, and SJ reviewed the manuscript. All authors contributed to the article and approved the submitted version.

## FUNDING

This work was supported by the National Key R&D Program of China (2019YFA0802400), National Natural Science Foundation of China (31670833 and 81703535), National Institutes of Health (NIH R01 CA186702), Open Project Program of the State Key Laboratory of Proteomics (SKLP-O201905), Jiangsu Key Laboratory of Neuropsychiatric Diseases (BM2013003), National Center for International Research (2017B01012), Suzhou Science and Technology Project (SYS2020093), and a project funded by the Priority Academic Program Development (PAPD) of Jiangsu Higher Education Institutions.

## ACKNOWLEDGMENTS

We thank Dr. Selina Chen-Kiang from Weill Medical College for kind support in experiments and fruitful discussion, Dr. Xiu-Bao Chang from the Mayo Clinic College of Medicine (United States) for generously providing the mouse anti-CRBN antibody, and Dr. Joshua Epstein from the University of Arkansas for Medical Sciences (United States) for kindly providing CAG cells.

## SUPPLEMENTARY MATERIAL

The Supplementary Material for this article can be found online at: <https://www.frontiersin.org/articles/10.3389/fcell.2020.605989/full#supplementary-material>

- Das, D. S., Ray, A., Song, Y., Richardson, P., Trikha, M., Chauhan, D., et al. (2015). Synergistic anti-myeloma activity of the proteasome inhibitor marizomib and the IMiD® immunomodulatory drug pomalidomide. *Br. J. Haematol.* 171, 798–812. doi: 10.1111/bjh.13780
- Donovan, K. A., An, J., Nowak, R. P., Yuan, J. C., Fink, E. C., Berry, B. C., et al. (2018). Thalidomide promotes degradation of SALL4, a transcription factor implicated in Duane Radial Ray syndrome. *eLife* 7:e38430. doi: 10.7554/eLife.38430
- Galluzzi, L., Vitale, I., Aaronson, S. A., Abrams, J. M., Adam, D., Agostinis, P., et al. (2018). Molecular mechanisms of cell death: recommendations of the Nomenclature Committee on Cell Death 2018. *Cell Death Differ.* 25, 486–541. doi: 10.1038/s41418-017-0012-4
- Gandhi, A. K., Mendy, D., Waldman, M., Chen, G., Rychak, E., Miller, K., et al. (2014). Measuring cereblon as a biomarker of response or resistance to lenalidomide and pomalidomide requires use of standardized reagents and understanding of gene complexity. *Br. J. Haematol.* 164, 233–244. doi: 10.1111/bjh.12622
- Gazit, Y. (1999). TRAIL is a potent inducer of apoptosis in myeloma cells derived from multiple myeloma patients and is not cytotoxic to hematopoietic stem cells. *Leukemia* 13, 1817–1824. doi: 10.1038/sj.leu.2401501
- Hideshima, T., Mitsiades, C., Akiyama, M., Hayashi, T., Chauhan, D., Richardson, P., et al. (2003). Molecular mechanisms mediating antimyeloma activity of proteasome inhibitor PS-341. *Blood* 101, 1530–1534. doi: 10.1182/blood-2002-08-2543
- Hou, X., Si, J., Ren, H., Chen, D., Wang, H., Ying, Z., et al. (2015). Parkin represses 6-hydroxydopamine-induced apoptosis via stabilizing scaffold protein p62 in PC12 cells. *Acta Pharmacol. Sin.* 36, 1300–1307. doi: 10.1038/aps.2015.54
- Huang, X., Di Liberto, M., Jayabalan, D., Liang, J., Ely, S., Bretz, J., et al. (2012). Prolonged early G1 arrest by selective CDK4/CDK6 inhibition sensitizes myeloma cells to cytotoxic killing through cell cycle-coupled loss of IRF4. *Blood* 120, 1095–1106. doi: 10.1182/blood-2012-03-415984
- Ito, T., Ando, H., Suzuki, T., Ogura, T., Hotta, K., Imamura, Y., et al. (2010). Identification of a primary target of thalidomide teratogenicity. *Science* 327, 1345–1350. doi: 10.1126/science.1177319
- Jackson, S., and Xiong, Y. (2009). CRL4s: the CUL4-RING E3 ubiquitin ligases. *Trends Biochem. Sci.* 34, 562–570. doi: 10.1016/j.tibs.2009.07.002
- Krönke, J., Fink, E. C., Hollenbach, P. W., MacBeth, K. J., Hurst, S. N., Udeshi, N. D., et al. (2015). Lenalidomide induces ubiquitination and degradation of CK1α in del(5q) MDS. *Nature* 523, 183–188. doi: 10.1038/nature14610
- Krönke, J., Udeshi, N. D., Narla, A., Grauman, P., Hurst, S. N., McConkey, M., et al. (2014). Lenalidomide causes selective degradation of IKZF1 and IKZF3 in multiple myeloma cells. *Science* 343, 301–305. doi: 10.1126/science.1244851
- Li, H., Zhu, H., Xu, C.-J., and Yuan, J. (1998). Cleavage of BID by caspase 8 mediates the mitochondrial damage in the Fas pathway of apoptosis. *Cell* 94, 491–501. doi: 10.1016/s0092-8674(00)81590-1
- Liu, J., Song, T., Zhou, W., Xing, L., Wang, S., Ho, M., et al. (2019). A genome-scale CRISPR-Cas9 screening in myeloma cells identifies regulators of immunomodulatory drug sensitivity. *Leukemia* 33, 171–180. doi: 10.1038/s41375-018-0205-y
- Liu, Y., Huang, X., He, X., Zhou, Y., Jiang, X., Chen-Kiang, S., et al. (2015). A novel effect of thalidomide and its analogs: suppression of cereblon ubiquitination enhances ubiquitin ligase function. *FASEB J.* 29, 4829–4839. doi: 10.1096/fj.15-274050
- Lopez-Girona, A., Mendy, D., Ito, T., Miller, K., Gandhi, A. K., Kang, J., et al. (2012). Cereblon is a direct protein target for immunomodulatory and antiproliferative activities of lenalidomide and pomalidomide. *Leukemia* 26, 2326–2335. doi: 10.1038/leu.2012.119
- Lu, G., Middleton, R. E., Sun, H., Naniong, M., Ott, C. J., Mitsiades, C. S., et al. (2014). The myeloma drug lenalidomide promotes the cereblon-dependent destruction of ikaros proteins. *Science* 343, 305–309. doi: 10.1126/science.1244917
- Luo, X., Budihardjo, I., Zou, H., Slaughter, C., and Wang, X. (1998). Bid, a Bcl2 interacting protein, mediates cytochrome c release from mitochondria in response to activation of cell surface death receptors. *Cell* 94, 481–490. doi: 10.1016/s0092-8674(00)81589-5
- Martiniani, R., Di Loreto, V., Di Sano, C., Lombardo, A., and Liberati, A. M. (2012). Biological activity of lenalidomide and its underlying therapeutic effects in multiple myeloma. *Adv. Hematol.* 2012:842945. doi: 10.1155/2012/842945
- Matyskiela, M. E., Couto, S., Zheng, X., Lu, G., Hui, J., Stamp, K., et al. (2018). SALL4 mediates teratogenicity as a thalidomide-dependent cereblon substrate. *Nat. Chem. Biol.* 14, 981–987. doi: 10.1038/s41589-018-0129-x
- Mitsiades, N., Mitsiades, C. S., Poulaki, V., Chauhan, D., Richardson, P. G., Hideshima, T., et al. (2002). Apoptotic signaling induced by immunomodulatory thalidomide analogs in human multiple myeloma cells: therapeutic implications. *Blood* 99, 4525–4530. doi: 10.1182/blood.V99.12.4525
- Moffat, J., Grueneberg, D. A., Yang, X., Kim, S. Y., Kloepper, A. M., Hinkle, G., et al. (2006). A lentiviral RNAi library for human and mouse genes applied to an arrayed viral high-content screen. *Cell* 124, 1283–1298. doi: 10.1016/j.cell.2006.01.040
- Shimbo, K., Hsu, G. W., Nguyen, H., Mahrus, S., Trinidad, J. C., Burlingame, A. L., et al. (2012). Quantitative profiling of caspase-cleaved substrates reveals different drug-induced and cell-type patterns in apoptosis. *Proc. Natl. Acad. Sci. U.S.A.* 109, 12432–12437. doi: 10.1073/pnas.1208616109
- Sievers, Q. L., Gasser, J. A., Cowley, G. S., Fischer, E. S., and Ebert, B. L. (2018). Genome-wide screen identifies cullin-RING ligase machinery required for lenalidomide-dependent CRL4<sup>CRBN</sup> activity. *Blood* 132, 1293–1303. doi: 10.1182/blood-2018-01-821769
- Song, T., Liang, S., Liu, J., Zhang, T., Yin, Y., Geng, C., et al. (2018). CRL4 antagonizes SCFFbxo7-mediated turnover of cereblon and BK channel to regulate learning and memory. *PLoS Genet.* 14:e1007165. doi: 10.1371/journal.pgen.1007165
- Stennicke, H. R., Renatus, M., Meldal, M., and Salvesen, G. S. (2000). Internally quenched fluorescent peptide substrates disclose the subsite preferences of human caspases 1, 3, 6, 7 and 8. *Biochem. J.* 350, 563–568.
- Tao, J., Yang, J., and Xu, G. (2018). The interacting domains in cereblon differentially modulate the immunomodulatory drug-mediated ubiquitination and degradation of its binding partners. *Biochem. Biophys. Res. Commun.* 507, 443–449.
- Thakurta, A., Gandhi, A. K., Waldman, M. F., Bjorklund, C., Ning, Y., Mendy, D., et al. (2014). Absence of mutations in cereblon (CRBN) and DNA damage-binding protein 1 (DDB1) genes and significance for IMiD therapy. *Leukemia* 28, 1129–1131. doi: 10.1038/leu.2013.315
- Voortman, J., Resende, T. P., Abou El Hassan, M. A. I., Giaccone, G., and Kruyt, F. A. E. (2007). TRAIL therapy in non-small cell lung cancer cells: sensitization to death receptor-mediated apoptosis by proteasome inhibitor bortezomib. *Mol. Cancer Ther.* 6, 2103–2112. doi: 10.1158/1535-7163.mct-07-0167
- Xu, G., Jiang, X., and Jaffrey, S. R. (2013). A mental retardation-linked nonsense mutation in cereblon is rescued by proteasome inhibition. *J. Biol. Chem.* 288, 29573–29585. doi: 10.1074/jbc.M113.472092
- Xu, Q., Hou, Y., Langlais, P., Erickson, P., Zhu, J., Shi, C., et al. (2016). Expression of the cereblon binding protein argonaute 2 plays an important role for multiple myeloma cell growth and survival. *BMC Cancer* 16:297. doi: 10.1186/s12885-016-2331-0
- Zhou, L., and Xu, G. (2019). Cereblon attenuates DNA damage-induced apoptosis by regulating the transcription-independent function of p53. *Cell Death Dis.* 10:69. doi: 10.1038/s41419-019-1317-7
- Zhu, Y. X., Braggio, E., Shi, C.-X., Bruins, L. A., Schmidt, J. E., Van Wier, S., et al. (2011). Cereblon expression is required for the antimyeloma activity of lenalidomide and pomalidomide. *Blood* 118, 4771–4779. doi: 10.1182/blood-2011-05356063

**Conflict of Interest:** The authors declare that the research was conducted in the absence of any commercial or financial relationships that could be construed as a potential conflict of interest.

Copyright © 2020 Zhou, Yu, Jayabalan, Niesvizky, Jaffrey, Huang and Xu. This is an open-access article distributed under the terms of the Creative Commons Attribution License (CC BY). The use, distribution or reproduction in other forums is permitted, provided the original author(s) and the copyright owner(s) are credited and that the original publication in this journal is cited, in accordance with accepted academic practice. No use, distribution or reproduction is permitted which does not comply with these terms.





# OTUB1 Promotes Progression and Proliferation of Prostate Cancer via Deubiquitinating and Stabilizing Cyclin E1

Yihao Liao<sup>1</sup>, Ning Wu<sup>2,3</sup>, Keke Wang<sup>1</sup>, Miaomiao Wang<sup>1</sup>, Youzhi Wang<sup>1</sup>, Jie Gao<sup>1</sup>, Boqiang Zhong<sup>1</sup>, Fuling Ma<sup>1</sup>, Yudong Wu<sup>4</sup> and Ning Jiang<sup>1\*</sup>

<sup>1</sup> Tianjin Institute of Urology, The Second Hospital of Tianjin Medical University, Tianjin Medical University, Tianjin, China, <sup>2</sup> Key Laboratory of Breast Cancer Prevention and Therapy, State Ministry of Education, National Clinical Research Center for Cancer, Tianjin Medical University Cancer Hospital and Institute, Tianjin, China, <sup>3</sup> Key Laboratory of Cancer Prevention and Therapy, Tianjin Clinical Research Center for Cancer, Tianjin Medical University Cancer Hospital and Institute, Tianjin, China, <sup>4</sup> Department of Urology, The First Affiliated Hospital of Zhengzhou University, Zhengzhou, China

## OPEN ACCESS

### Edited by:

Lixin Wan,  
Moffitt Cancer Center, United States

### Reviewed by:

Xiaowei Zhang,  
Peking University Health Science  
Centre, China  
Ming Chen,  
Duke University, United States

### \*Correspondence:

Ning Jiang  
jiangning@tmu.edu.cn

### Specialty section:

This article was submitted to  
Cell Growth and Division,  
a section of the journal  
Frontiers in Cell and Developmental  
Biology

**Received:** 15 October 2020

**Accepted:** 15 December 2020

**Published:** 18 January 2021

### Citation:

Liao Y, Wu N, Wang K, Wang M, Wang Y, Gao J, Zhong B, Ma F, Wu Y and Jiang N (2021) OTUB1 Promotes Progression and Proliferation of Prostate Cancer via Deubiquitinating and Stabilizing Cyclin E1. *Front. Cell Dev. Biol.* 8:617758. doi: 10.3389/fcell.2020.617758

**Background:** Prostate cancer (PCa) is currently the most common cancer among males worldwide. It has been reported that OTUB1 plays a critical role in a variety of tumors and is strongly related to tumor proliferation, migration, and clinical prognosis. The aim of this research is to investigate the regulatory effect of OTUB1 on PCa proliferation and the underlying mechanism.

**Methods:** Using the TCGA database, we identified that OTUB1 was up-regulated in PCa, and observed severe functional changes in PC3 and C4-2 cells through overexpression or knock down OTUB1. Heterotopic tumors were implanted subcutaneously in nude mice and IHC staining was performed on tumor tissues. The relationship between OTUB1 and cyclin E1 was identified via Western blotting and immunoprecipitations assays.

**Results:** We found that the expression of OTUB1 in PCa was significantly higher than that in Benign Prostatic Hyperplasia (BPH). Overexpression OTUB1 obviously promoted the proliferation and migration of PC3 and C4-2 cells via mediating the deubiquitinated Cyclin E1, while OTUB1 knockout has the opposite effect. The nude mice experiment further explained the above conclusions. We finally determined that OTUB1 promotes the proliferation and progression of PCa via deubiquitinating and stabilizing Cyclin E1.

**Conclusions:** Our findings reveal the critical role of OTUB1 in PCa, and OTUB1 promotes the proliferation and progression of PCa via deubiquitinating and stabilizing Cyclin E1. Blocking OTUB1/Cyclin E1 axis or applying RO-3306 could significantly repress the occurrence and development of PCa. OTUB1/Cyclin E1 axis might provide a new and potential therapeutic target for PCa.

**Keywords:** cyclin E1, OTUB1, prostate cancer, progression, proliferation

## INTRODUCTION

Prostate cancer (PCa) is the most common malignant tumor in the United States. The prevalence of PCa approximately accounts for 20% of all types of cancers. In 2019, there were 174,650 new cases and 31,620 deaths from PCa (Siegel et al., 2019). If detected early and treated aggressively, the 5-year survival rate of PCa will almost reach 100%. However, many patients with PCa are diagnosed in the late stage, and their survival rate declines drastically because PCa has no obvious symptoms except urinary tract infection (Nguyen-Nielsen and Borre, 2016). Due to the irreplaceable role of androgen receptor (AR) in the development of PCa, the most important and standard treatment is androgen deprivation therapy (ADT) (Murillo-Garzón and Kypta, 2017; Bastos and Antonarakis, 2018). ADT mainly includes drug castration and surgical castration, but most patients eventually develop to castration-resistant prostate cancer (CRPC), even metastasis castration resistant prostate cancer (mCRPC), without effective treatment (Gasnier and Parvizi, 2017; Hossain et al., 2018). CRPC and mCRPC still are the most difficult problems during the diagnosis and treatment of prostate cancer. In recent years, with the development of urology, chemotherapy, radiotherapy, target therapy, and immunotherapy have emerged, and the overall survival rate has been prominently improved (Sebesta and Anderson, 2017; Altwaijry et al., 2018; Komura et al., 2018). At present, there is still a lack of effective and sensitive drugs for prostate cancer, especially the urgent demand for new drugs to treat CRPC (Smolle et al., 2017).

Ubiquitination is a vital pathway for protein degradation and conducts a crucial regulatory factor in many cellular signal pathways (Popovic et al., 2014). As a member of the deproteinized cysteine protease subfamily of the ovarian tumor domain (OTU) (Sivakumar et al., 2020), OTUB1 could stabilize the expression level of target protein and maintain its function by inhibiting ubiquitination degradation (Wiener et al., 2012). Many researchers have demonstrated that OTUB1 regulates lots of important cellular processes, such as DNA-repair, cell signaling transduction, proliferation, and apoptosis (Nakada et al., 2010; Liu et al., 2019). Furthermore, OTUB1 plays an increasingly important and irreplaceable role in the field of cancer. For example, OTUB1 is found to be up-regulated in colorectal cancer (Zhou et al., 2014), gastric adenocarcinoma (Weng et al., 2016), esophageal cancer (Sun et al., 2020), ovarian cancer (Wang et al., 2016), human glioma (Xu et al., 2017), and hepatocellular carcinoma (Ni et al., 2017), which could promote tumor invasion and predict a poor prognosis. OTUB1 promotes tumor progression in two ways: to stabilize the expression of oncogenic genes by inhibiting the ubiquitination of target protein, and the other mode does not depend on the deproteinization manner (Saldana et al., 2019) but directly interacts with E2 ubiquitin ligase. These results imply that

OTUB1 might provide a tumor associated biomarker and candidate target for PCa treatment. Currently, the relationship between OTUB1 and PCa has been preliminarily researched. Previous research verified that OTUB1 promotes prostate cancer invasion *in vitro* and aggravates tumorigenesis *in vivo* via regulating RhoA activity and p53 expression (Iglesias-Gato et al., 2015). The cyclin/Cdk complexes involved in cell cycle are the primary regulators during the various stages of mitosis, which could influence the conversion within different cell phases through the phosphorylation of cell phase-specific substrate proteins (Malumbres and Barbacid, 2009; Wei et al., 2020). Cyclin E1 is known to be a conserved protein and its essential function is to promote G1/S conversion. In previous studies, Cyclin E1/Cdk2 axis has been associated with the proliferation of various cancers in previous studies (Geng et al., 2003; Masaki et al., 2003). The anticancer effect of Cyclin E1/Cdk2 complexes has been extensively concerned in a variety of tumors, including ovarian cancer (Kanska et al., 2016), liver cancer (Bisteau et al., 2014; Ehedego et al., 2018), and so on (Fang et al., 2016).

In this study, we focus on the characteristics of OTUB1 involved in the process of cell cycle, and we investigate the specific mechanism of OTUB1 promoting tumor progression. Further experiments were performed to explore the possibility OTUB1 serves as a potential therapeutic target and diagnostic biomarker for PCa.

## METHODS

### Clinical Samples

Clinical tissue samples were acquired from patients undergoing transurethral resection of the prostate in the Second Affiliated Hospital of Tianjin Medical University (Tianjin, China) and examined by a professional pathologist in order to obtain Gleason grade. This study was approved by the Ethics Committee of the Tianjin Medical University and strictly complied with the Helsinki Declaration of Human Rights.

### Prostate Cancer Cell Lines

Human prostate cancer cell lines (PC3 and C4-2) were obtained from ATCC cell bank. The cells were cultured with RPMI 1640 medium supplemented with 10% fetal bovine serum and 1% penicillin/streptomycin in a humidified environment containing 5% CO<sub>2</sub> at 37°C.

### Cell Transfection and Inhibitor

A total of  $6 \times 10^5$  PC3 and C4-2 cells were seeded in 6-well plates. After 24 h, the cells were transfected with 2 µg plasmid or 100-nM siRNA with Lipofectamine™ 2000 (Invitrogen) according to the manufacturer's protocol. The FLAG-OTUB1 plasmid and pcDNA3.1-OTUB1C91S plasmid was transfected into PC3 cell and C42 cell. The knockdown of OTUB1 and Cyclin E1 was generated by transient transfecting with RNA (OTUB1 siRNA and Cyclin E1 siRNA). After 48 h, the cells were collected for western blotting, MTT, transwell, and migration assays. The relative siRNA primers are showed in **Supplementary Table 1**. The cell cycle inhibitor RO-3306 was purchased from MCE,

**Abbreviations:** OTUB1, ovarian tumor domain deubiquitination 1; PCa, prostate cancer; CCNE1, Cyclin E1; AR, Androgen receptor; BPH, Benign prostate hyperplasia; IP, Immunoprecipitation; UB, Ubiquitination; DUB, Deubiquitination; ADT, androgen deprivation therapy; CRPC, castration-resistant prostate cancer; mCRPC, metastasis castration resistant prostate cancer.

and different doses of RO-3306 were added into the 6-well plate respectively.

## Immunoprecipitation and Western Blot Analysis

Total protein was extracted from PC3, C4-2 cell lines, and tumor tissues using RIPA (Biosharp) and PMSF, and the BCA kit was used to determine the protein concentration. In the 10% acrylamide gels, an equal amount of protein sample (40 µg per channel) was separated by SDS-polyacrylamide gel electrophoresis (PAGE) and transferred to the poly vinylidene difluoride (PVDF) membrane (Millipore, Billerica, MA). The membrane was blocked in 5% fat-free milk and incubated overnight with the following primary antibodies: rabbit anti-OTUB1 (1:1,000 dilution; affinity), rabbit anti-GAPDH (1:1,000 dilution; Abcam), mouse anti-β-actin (1:1,000 dilution; CST), rabbit anti-Cyclin E1 (1:1,000 dilution; CST), and rabbit anti-FLAG (1:1,000 dilution; SIGMA) at 4°C. Then, the PVDF membrane was washed and incubated with anti-rabbit or anti-mouse IgG for 1 h at room temperature. The immunoreactive bands were detected by chemiluminescence methods and visualized using Luminescent Imaging Workstation, and the relative intensity was measured and analyzed using ImageJ software.

## Immunohistochemical Staining

The clinical tissue samples were collected from prostate surgery and the tumors of null mice were collected and preserved in formalin. The specimens were frozen, embedded in paraffin, and cut into 5 µm sections. The tissue sections were roasted at 65°C for 45 min, next de-waxed in xylene and rehydrated in graded alcohol. Citric acid buffer solution (pH adjusted to 6.0) was used for antigen recovery, under high fire for 5 min and middle-low fire for 10 min in turn. Endogenous peroxidase was blocked in 0.3% hydrogen peroxide and 1.5% horse serum for 10 min. Then the tissue sections were incubated with primary antibody (anti-OTUB1, 1:100 from affinity; anti-Cyclin E1 1:100 from affinity; Ki67 1:100 from Abcam) overnight at 4°C. After using rabbit/mouse universal secondary antibody IgG (1 h), the secondary antibody was detected with the Ultraview DAB detection kit (Zhongshan Co, China). The nuclei were stained with hematoxylin, then dehydrated and transparent, and the slides were sealed with neutral glue. The expression levels of OTUB1, ki-67, and Cyclin E1 were observed under Zeiss microscope (×200).

## Wound Healing Assay

PC3 and C4-2 cells were seeded on 6-well plate and grew to the pavement overnight. After 24 hours of transfection, a channel was drawn on the monolayer cells with 10 µL micropipette tip. Then PC3 and C4-2 cells were washed with PBS twice and cultured in 10% FBS 1640 at 5% CO<sub>2</sub>, 37°C for an additional 24 h. Photographs were taken by an inverted Leica phase contrast microscope at 0 h and 24 h.

## Clone Formation Assay

PC3 and C4-2 cells were digested and  $2.0 \times 10^3$  cells in each group were seeded into 6-well plate. After 24 h, OTUB1 siRNA, Cyclin E1 siRNA, negative control siRNA, OTUB1-overexpression, and otub1 c91s were transfected, respectively. The cells were cultured for 1 week. After washing with phosphate-buffered saline (PBS) buffer twice, 4% paraformaldehyde was used to fixate for 20 min. Then, an appropriate amount of crystal violet solution was added and stained for 30 min. After washing with PBS again and air drying, the software Image J was used for clones counting.

## MTT Assay

After 48 h of transfection,  $2.0 \times 10^3$  cells per well were seeded into 96-well plates and cultured at 37°C for 24 h, 48 h, 72 h, and 96 h. Then 30 µL MTT solution was added into each well at the indicated time, and cells were cultured for another 2 h at 37°C. Subsequently, the MTT solution was removed and 150 µL dimethyl sulfoxide (DMSO) was added into each well to dissolve formazan crystals. The absorbance was measured with a microplate reader at 490 nm.

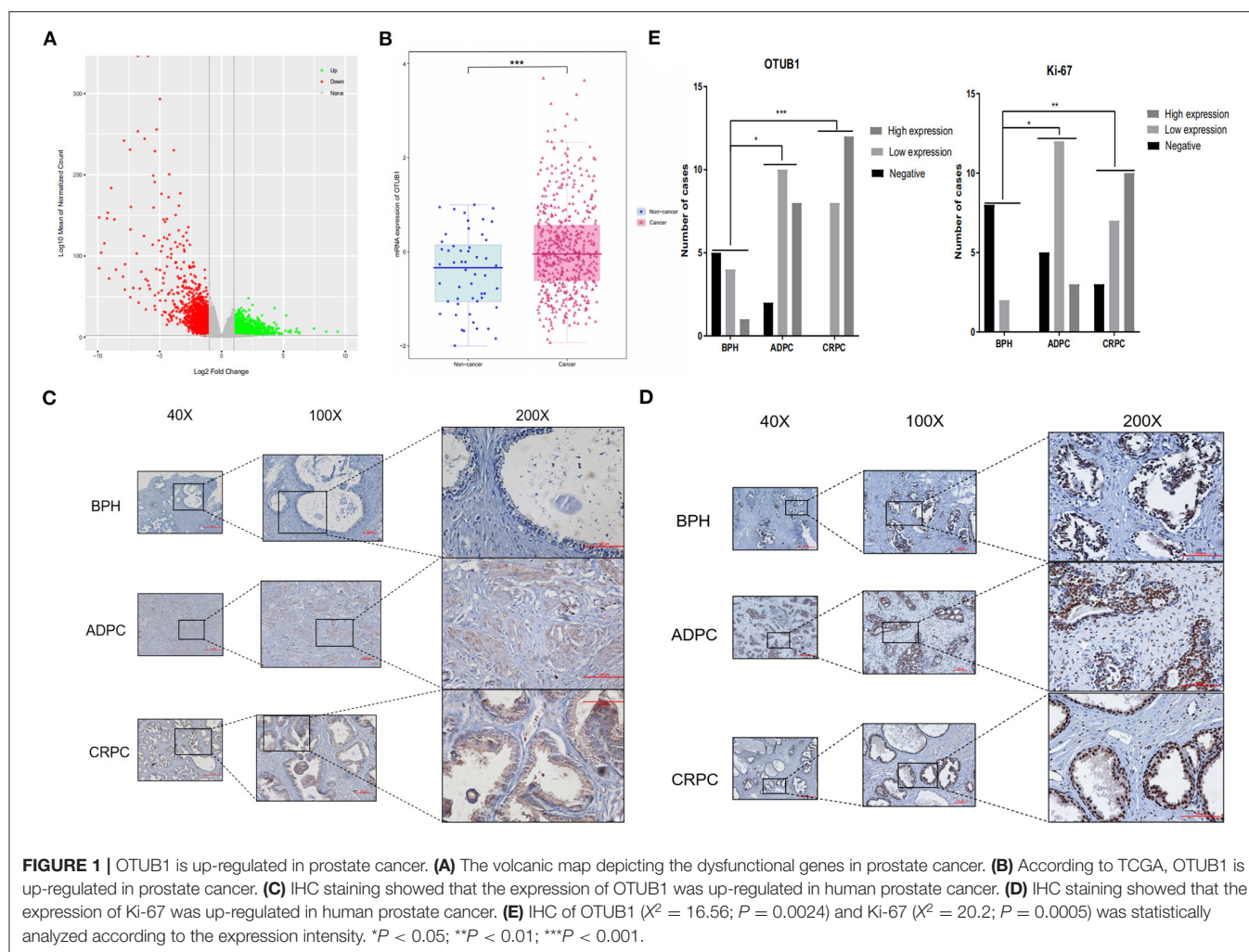
## Transwell Migration Assay

PC3 and C4-2 cells were transfected with OTUB1-siRNA or negative-control siRNA and pcDNA3.1-OTUB1 plasmid respectively, which were suspended in 1,640 containing 10% FBS, and  $2 \times 10^4$  cells were added to the top chamber of 24-well transwell plates (Corning, 8 µm pore size), and 1,640 containing 10% FBS was added to the bottom chamber. After incubating at 37°C for 48 h, the chambers were washed with PBS twice, and these cells which migrated to the bottom chambers were fixed with paraformaldehyde and stained with crystal violet. Then the number of transitional cells in all chambers was calculated in the 5 visual fields.

## Animal Studies

Five-week-old male Balb/c mice (HFK Bio-Technology Co. Ltd, Beijing) were injected subcutaneously with  $2 \times 10^6$  PC3 cells with control, otub1, and otub1-c91s groups suspended in 0.1 mL of Matrigel (BD Biosciences) and 1,640. These cells were implanted subcutaneously into the dorsal flank on both sides of the mice. Once the diameter of tumors reached nearly 2 mm, the volume of tumor was measured daily for 10 days. These mice with overexpression otub1 were divided into two groups: one group was used as control group, and another were treated with RO-3306 4 mg/kg every 2 days via oral feeding. Tumor volume was recorded by digital caliper and the volume was estimated the formula  $0.52 \times L \times W^2$  ( $L$  = the length of tumor and  $W$  = the maximum width). At the 10th day, these mice were killed and tumors were extracted and measured. The tumors were fixated with paraformaldehyde, then immunohistochemistry staining was performed for OTUB1, Ki 67, and Cyclin E1. All procedures involving mice were approved by the University Committee on Use and Care of Animals at the Tianjin Medical University and met all regulatory standards.





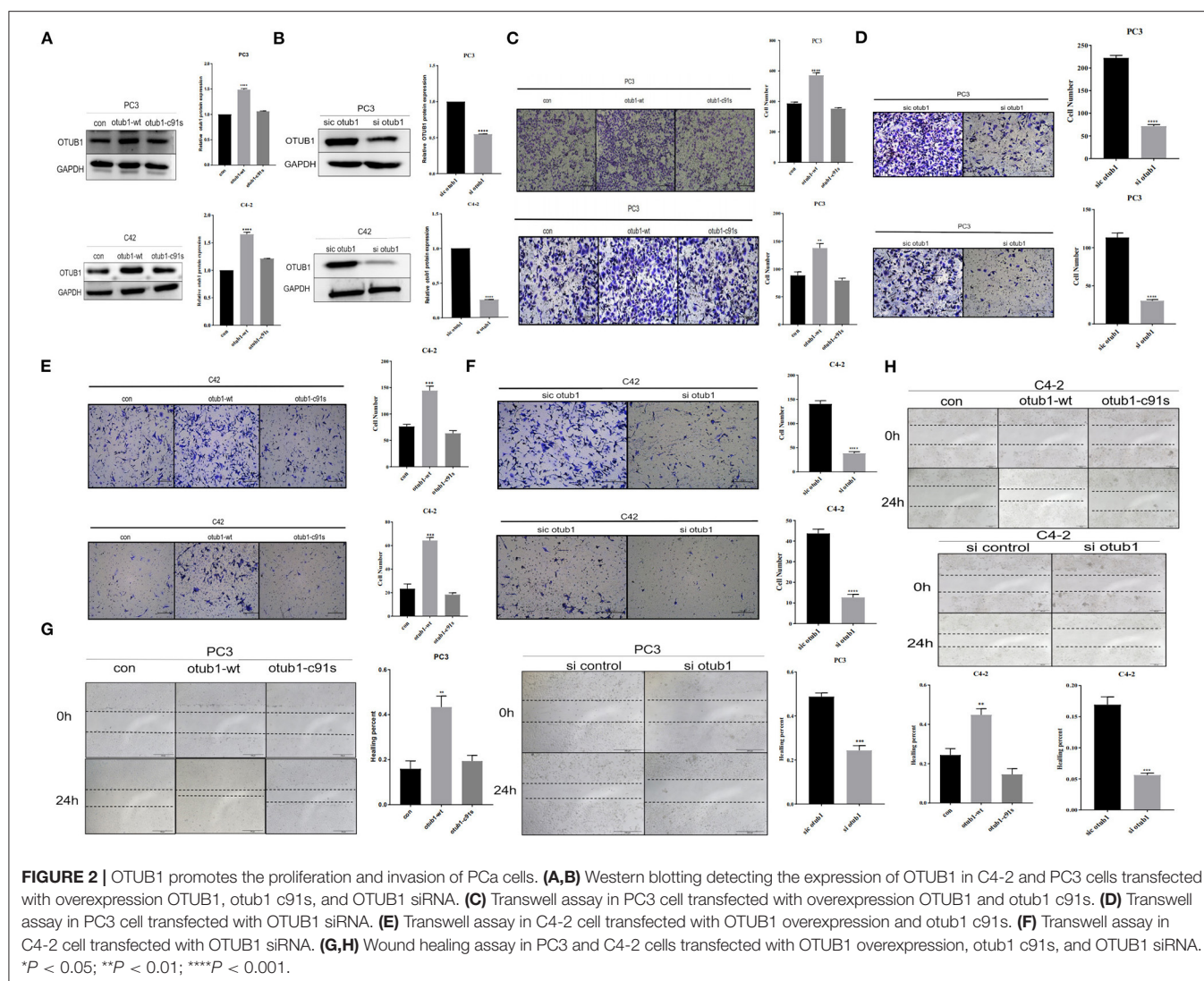
## RESULTS

### OTUB1 is Up-regulated in Prostate Cancer

We filtered all dysregulated genes in prostate cancer profiles from TCGA database, identified 3,480 up-regulated genes and 2,592 down-regulated genes, and the results were presented in the volcano map (Figure 1A). Of the up-regulated genes, we observed that the expression of OTUB1 in PCa was higher than para-carcinoma tissue (Figure 1B). To further identify the deubiquitinating enzymes OTUB1 driving the prostate cancer progression, we conducted subsequent experiments and assays. In order to identify whether clinical data was consistent with the database, we collected clinical prostate cancer tissue and immunohistochemical staining was performed with OTUB1 (Figure 1C) and ki-67 antibody (Figure 1D). A Chi-square test was performed, and the results demonstrated that the expression of OTUB1 in PCa groups was higher than that in BPH group ( $\chi^2 = 16.56$ ;  $P = 0.0024$ ), and the results of ki-67 were consistent with OTUB1 ( $\chi^2 = 20.2$ ;  $P = 0.0005$ ). The detailed statistical results showed that the positive ratios of OTUB1 and Ki67 in ADPC and CRPC groups were higher than BPH group (Figure 1E).

### OTUB1 Promotes Proliferation and Invasion of PCa Cell

We transfected PC3 and C42 cells with OTUB1 overexpression and otub1 c91s, and the expression level of OTUB1 was detected by Western blotting. The results showed that, compared with the control group, the expression level of OTUB1 transfected with otub1-c91s group (cells introduced by the mutated OTUB1 fragment) was not significantly changed, but the expression level of OTUB1 transfected with OTUB1 overexpression was significantly increased (Figure 2A). The gray value of OTUB1 was detected by Image analysis software Image J (Figure 2A). For further explanation, we transfected PC3 and C4-2 cells with OTUB1 siRNA, and the expression level of OTUB1 was decreased distinctly compared with the control group (Figure 2B). Recent studies have shown that OTUB1 is highly expressed in invasive tumor cells and plays an important role in its proliferation and invasion (Zhou et al., 2014, 2019, 2020; Weng et al., 2016; Yuan et al., 2017; Sun et al., 2020). The results showed that the migration and invasion ability of PC3 and C4-2 cells was significantly enhanced in increased OTUB1 group compared

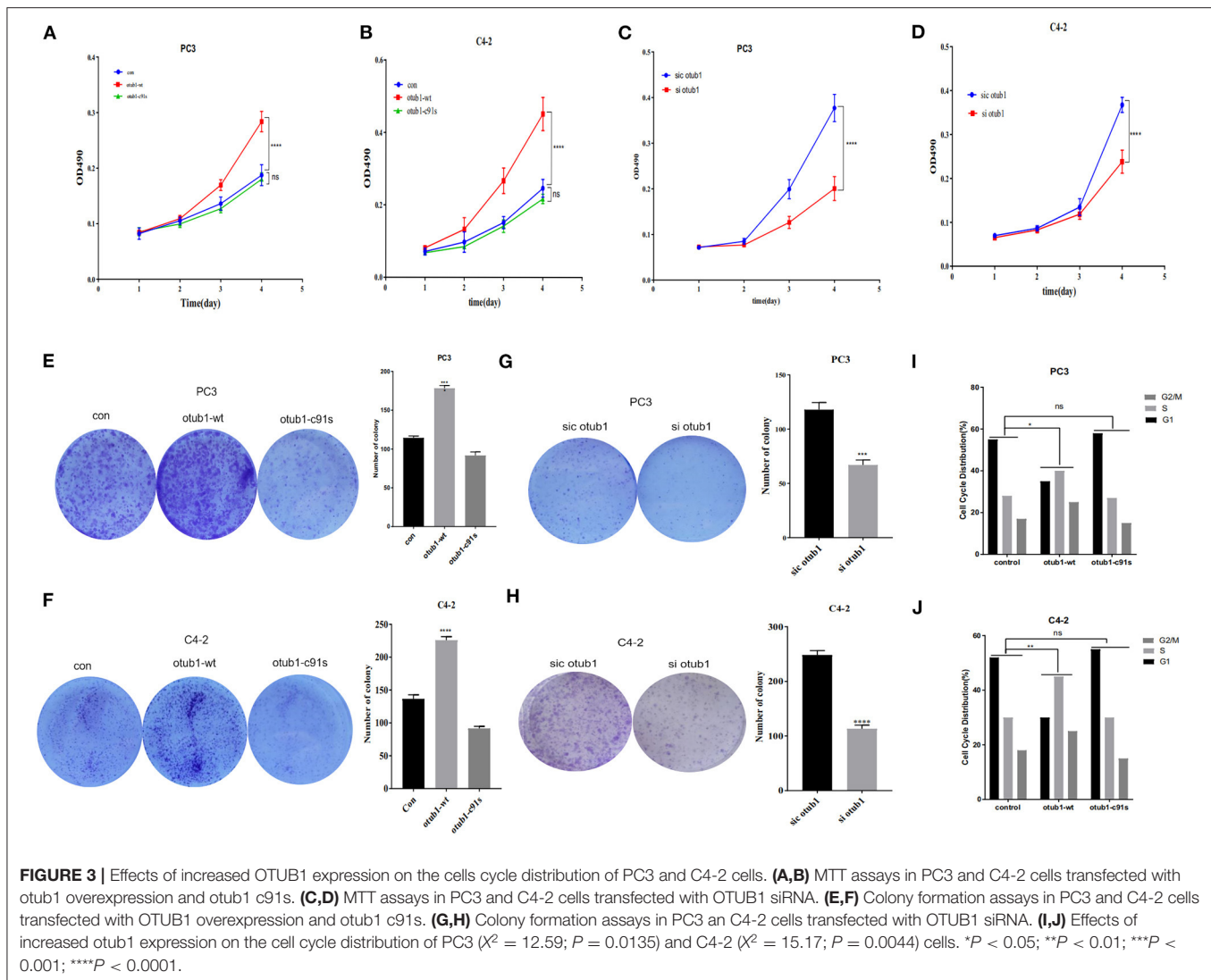


with control group (Figures 2C,E). On the contrary, PC3 and C4-2 cells transfected with OTUB1 siRNA dramatically attenuated the migration and invasion ability (Figures 2D,F).

Cell healing assays is one of the methods to determine the movement characteristics of tumor cells. In order to eliminate the interference of cell proliferation and observe the migration ability of tumor cells, the scratch injury was applied to monolayer cells *in vitro*. The effect of OTUB1 expression level on the migration ability of prostate cancer PC3 and C4-2 cells was observed. The results showed that the migration of OTUB1 overexpression group was significantly improved compared with the control group (Figure 2G), but there was no significant difference between the otub1 c91s group and the control group. The difference was statistically significant ( $P < 0.01$ ). The similar results were also found in PC3 and C4-2 cells transfected with OTUB1 siRNA, the migration ability of PC3 and C4-2 cells was dramatically attenuated (Figure 2H). The results showed that OTUB1 expression significantly influenced cells migration (Figures 2G,H).

## Effects of Increased OTUB1 Expression on PC3 and C4-2 Cells Cycle Distribution

The cell growth curve was drawn, and the proliferation absorbance of the control group, OTUB1 overexpression, and otub1 c91s at 24, 48, 72, and 96 h were detected, respectively. The results showed that the cells with increased OTUB1 expression had significantly higher growth ability than the control group, while the proliferation ability of otub1 c91s group had no significant change compared with the control group ( $P < 0.01$ ; Figures 3A,B). In the same way, we transfected PC3 and C4-2 cells with OTUB1 siRNA and found the opposite results (Figures 3C,D). The results demonstrated that the expression of OTUB1 significantly affected the proliferation of PC3 and C4-2 cells ( $P < 0.01$ ; Figures 3A–D). Clone formation rate is defined as the rate at which a single cell grows and forms small cell groups (clones). The cells were inoculated at a low density ( $2 \times 10^3$  cells/chamber). After 7 days of culture, all cells formed obvious colonies. The colony forming ability of PC3 and C4-2 cells was significantly enhanced in increased OTUB1 group ( $P < 0.01$ ;



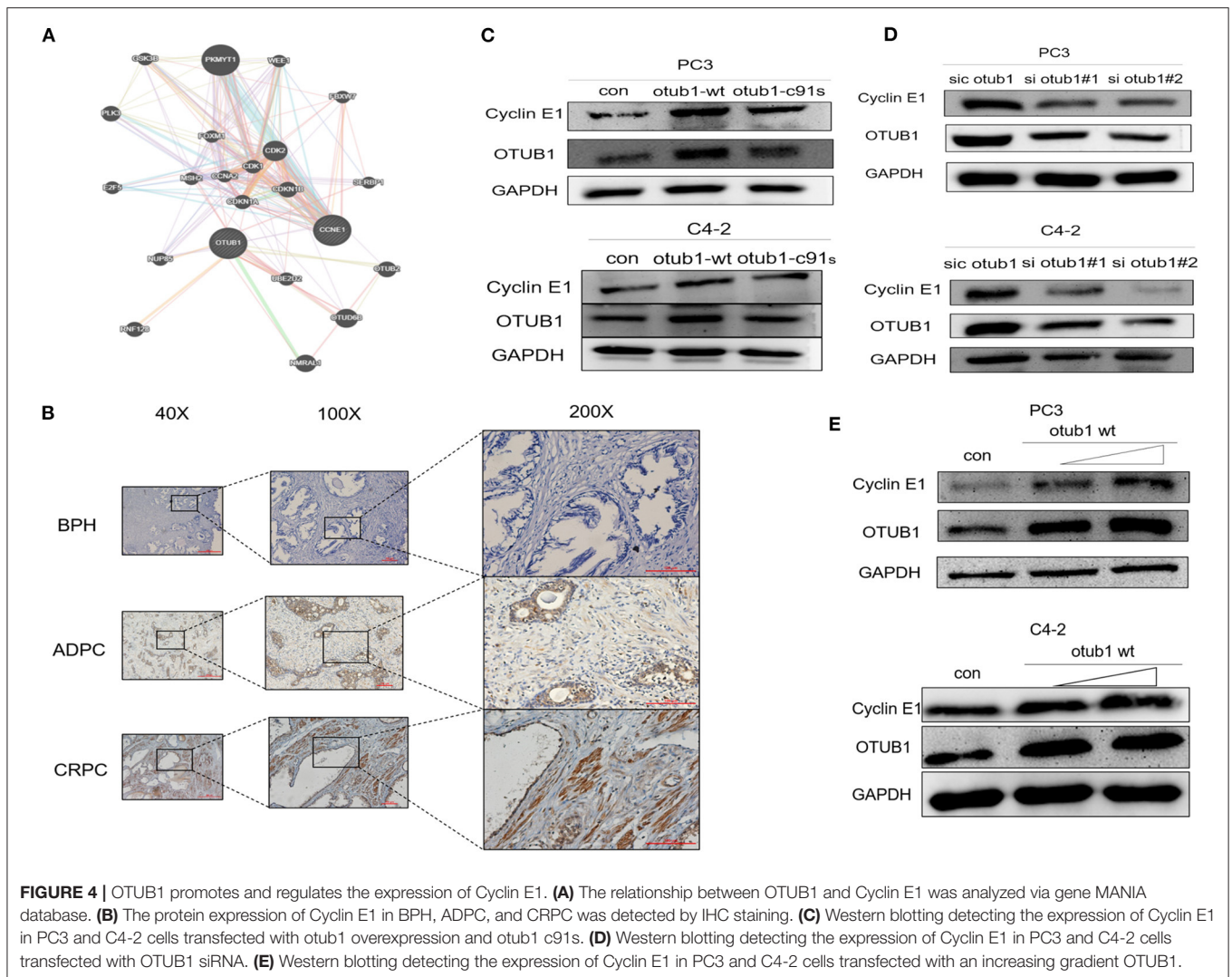
**Figures 3E,F).** Similarly, we transfected PC3 and C4-2 cells with OTUB1 siRNA and the colony forming ability of PC3 and C4-2 cells was reduced significantly ( $P < 0.01$ ; **Figures 3G,H**). Based on the above results, it could be seen that the expression levels of OTUB1 influence the ability of colony formation.

Cell cycle refers to the whole process from the end of the last mitosis to the completion of the next mitosis, including quiescent phase (G0), early DNA synthesis phase (G1), DNA synthesis phase (S), late DNA synthesis phase (G2), and division phase (M). After increasing the expression of OTUB1, the proliferation ability of prostate cancer cells was significantly enhanced ( $P < 0.01$ ; **Figures 3A–D**). Cell cycle test results of PC3 and C4-2 showed that the ratio of G1 phase decreased in increased OTUB1 expression group, while the ratio of G2/M+S phase increased, the Chi-square test results of PC3 ( $\chi^2 = 12.59$ ;  $P = 0.0135$ ) and C4-2 ( $\chi^2 = 15.17$ ;  $P = 0.0044$ ) showed the statistical difference (**Figures 3I,J**). In conclusion, these experiments suggested that OTUB1 might influence the proliferation of PCa cells through altering the distribution of cell cycle (**Figures 3I,J**).

## OTUB1 Rescues Cyclin E1 From Proteasomal Degradation

Next, we investigated how OTUB1 promotes the G1 cell cycle progression, and analyzed a series of OTUB1-related proteins through gene MANIA online database. Cyclin E1, a cell cycle-relative regulative key protein, was found to interact with OTUB1 closely (**Figure 4A**). To explore the relationship between OTUB1 and Cyclin E1, we further observed a consistent result with OTUB1 that the expression level of Cyclin E1 in ADPC and CRPC groups were significantly higher than that in BPH group via IHC assay (**Figure 4B**). To verify whether the function of Cyclin E1 is related to OTUB1, we observed that the expression of Cyclin E1 increased in increased OTUB1 expression group of PC3 and C4-2 cells (**Figure 4C**). In addition, we found a similar experiment result that the protein expression of OTUB1 and Cyclin E1 decreased obviously in PC3 and C4-2 cell transfected with OTUB1 siRNA (**Figure 4D**). The expression level of OTUB1 and Cyclin E1 was found to gradually increase with the gradient overexpression of OTUB1 in PC3 and C4-2 cells (**Figure 4E**).

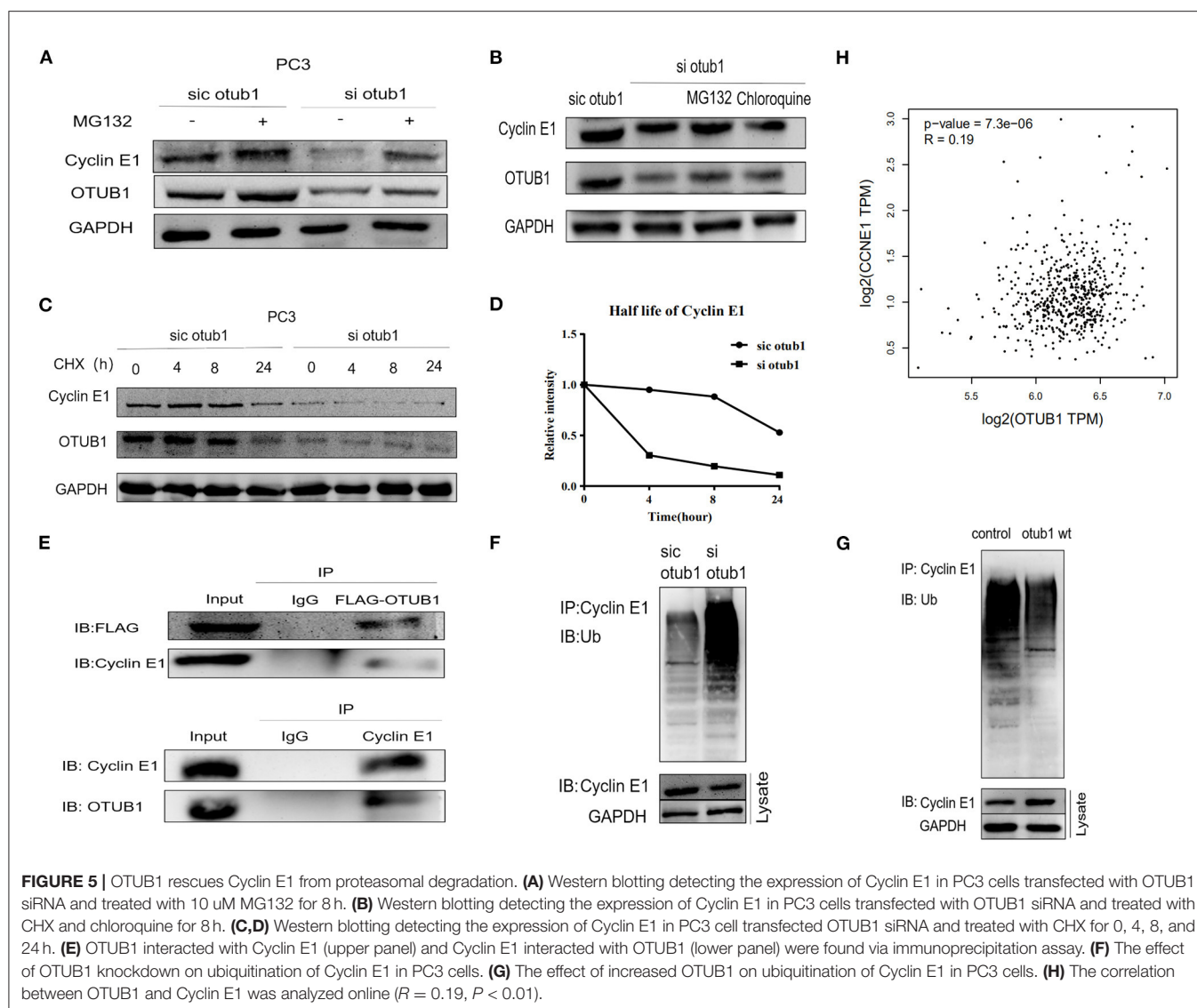




It could be inferred that up-regulated OTUB1 could promote the expression of Cyclin E1 from the above results, and we had sufficient evidence to predict that Cyclin E1 could interact with OTUB1.

Further experiments are needed to verify this conclusion. Thus, we explored how OTUB1 influences the expression of Cyclin E1. PC3 cell transfected with OTUB1 siRNA were treated with DMSO or 10uM MG132 (a protease inhibitor) for 8 h, respectively. The results demonstrated that the expression of Cyclin E1 was decreased significantly in OTUB1 siRNA group compared with the control group, and MG132 could partially preserve the stability, indicating that OTUB1 influenced the expression of Cyclin E1 in a proteasome dependent manner (Figure 5A). Above results implied that Cyclin E1 might be regulated by OTUB1 via a deubiquitinating degradation manner. To identify this hypothesis, we treated PC3 cells transfected with OTUB1 siRNA with 10 uM MG132 and 200 uM chloroquine (a lysosomal enzyme inhibitor) for 8 h. We found that MG132 could partially maintain stability of Cyclin E1 in PC3 cell transfected

with OTUB1 siRNA, while chloroquine could not (Figure 5B). To further explain the above results, PC3 cell transfected with OTUB1 siRNA were treated with 10 mg/ml cycloheximide (CHX), a protein synthesis inhibitor in eukaryotic cells, for 0, 4, 8, and 24 h, respectively. The results showed that CHX promoted the degradation of Cyclin E1 protein, and the decrease rate of Cyclin E1 was increased significantly in PC3 cell transfected with OTUB1 siRNA (Figures 5C,D). The results implied that Cyclin E1 was not a lysosomal enzyme degradation pathway but ubiquitin dependent degradation. The relationship between OTUB1 and Cyclin E1 was determined by immunoprecipitation. The results demonstrated that OTUB1 interacted with Cyclin E1, and Cyclin E1 was also linked with OTUB1 (Figure 5E). Another immunoprecipitation assay presented that knocking down the expression of OTUB1 could strengthen the degree of ubiquitination of Cyclin E1 (Figure 5F), while increased OTUB1 expression could weaken the ubiquitination of Cyclin E1 (Figure 5G). Therefore, these results demonstrated that OTUB1 could promote tumor proliferation and progression in prostate



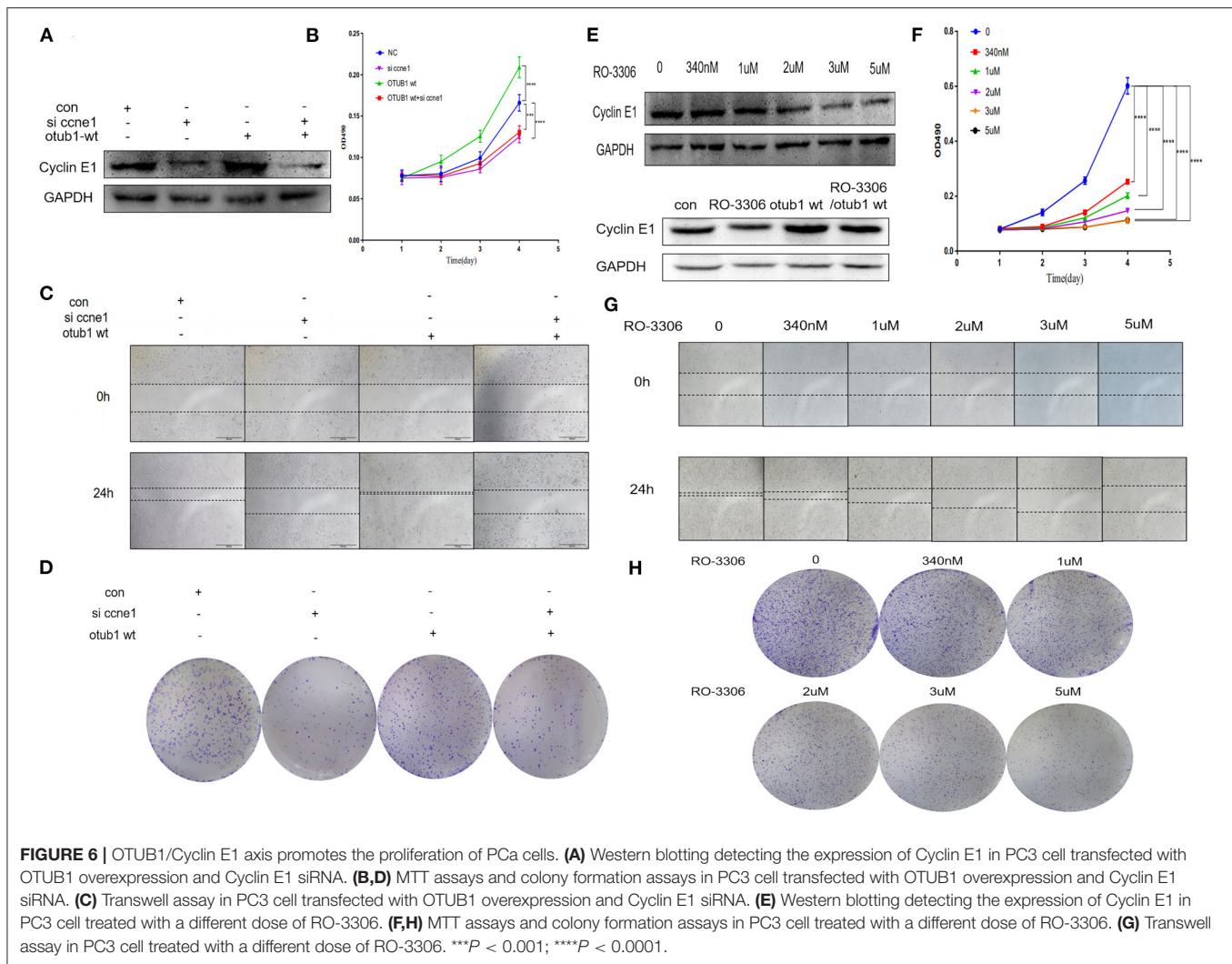
cancer via stabilizing the function and increasing the expression level of Cyclin E1. We analyzed the correlation between OTUB1 and Cyclin E1 via GEPIA online database, and the result presented that OTUB1 was positively correlated with Cyclin E1 ( $R = 0.19$ ;  $P < 0.01$ ; **Figure 5H**).

### OTUB1/Cyclin E1 Axis Promotes Prostate Cancer Cell Proliferation

To further explore the effect of OTUB1/Cyclin E1 axis upon PCa, PC3 cell were co-transfected with Cyclin E1 siRNA and OTUB1 overexpression. The expression of cyclin E1 was detected 48 h after transfection. The results demonstrated that OTUB1 could promote the expression of Cyclin E1, while Cyclin E1 expression was obviously decreased after transfection with Cyclin E1 siRNA. Interestingly, knockdown of Cyclin E1 attenuated the effect of OTUB1 overexpression (increasing the expression of Cyclin E1) (**Figure 6A**). MTT assay was used to detect

cell proliferation, and the results demonstrated that Cyclin E1 knockdown obviously postponed cell proliferation, while the effect of OTUB1 overexpression promoting proliferation was restrained significantly to accompany with Cyclin E1 siRNA group (**Figure 6B**). These results were confirmed by healing assay and clone formation experiments, which were consistent with previous results (**Figures 6C,D**). These results demonstrated that OTUB1/Cyclin E1 axis promotes the proliferation and migration of prostate cancer. Interfering with the contact between OTUB1 and Cyclin E1 might provide a potential therapy for prostate cancer.

To identify the possibility of targeting prostate cancer with OTUB1/Cyclin E1 axis, we treated PC3 cell with RO-3306, a Cyclin E1/CDK2 related inhibitor, in the range dose of 0, 340 nM, 1  $\mu$ M, 2  $\mu$ M, 3  $\mu$ M, and 5  $\mu$ M. After treating with RO-3306 for 24 h, the protein was extracted and Western blotting was performed. We observed the phenomenon of the expression



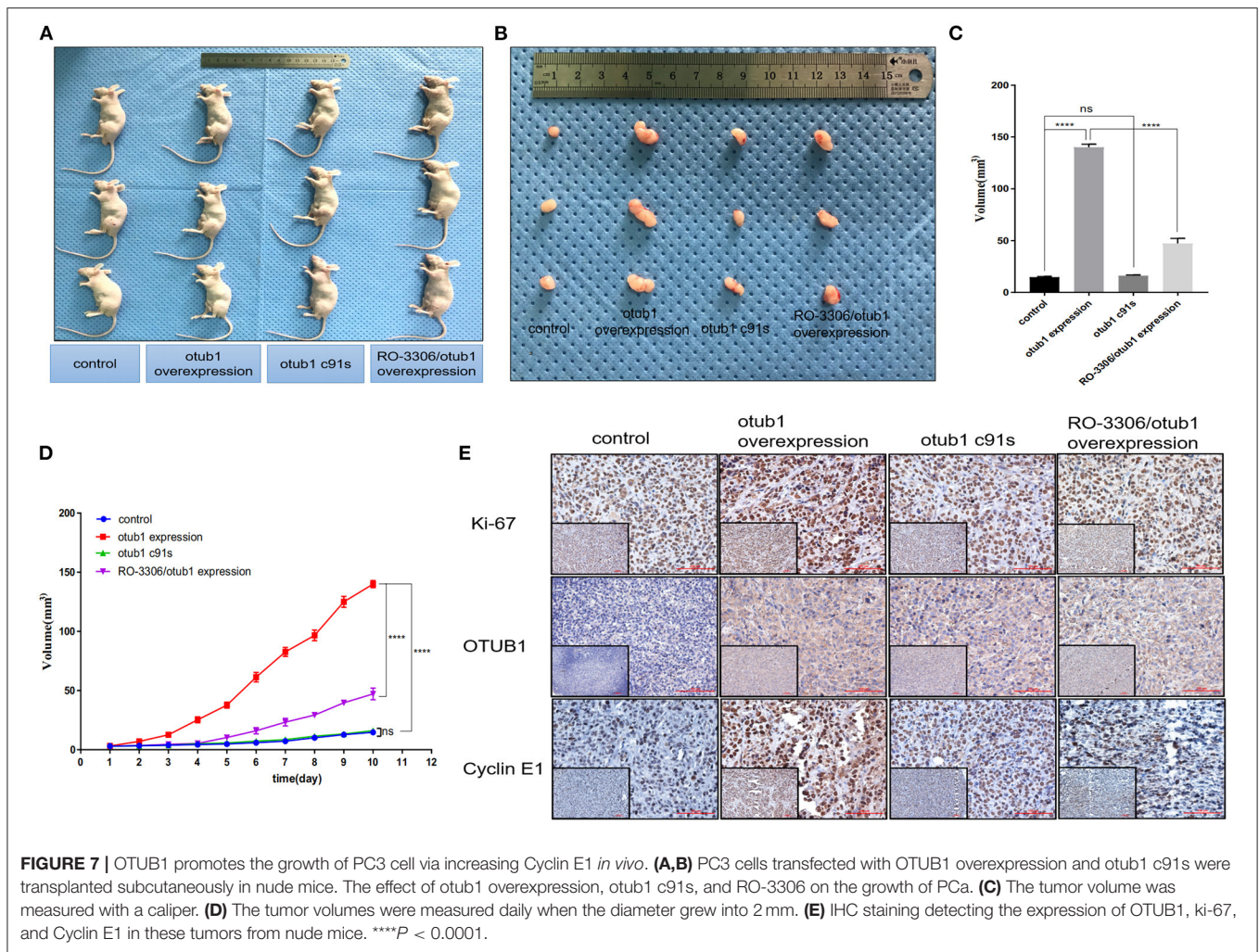
level of Cyclin E1 was degraded in a RO-3306 dose dependent manner. Interestingly, RO-3306 also attenuated the effect of OTUB1 overexpression on promoting Cyclin E1 (**Figure 6E**). The results were consistent with the knock down of Cyclin E1. More experiments were performed to further explore the effect of RO-3306 on cell proliferation and migration. MTT assays and clone formation assays demonstrated that the proliferation and migration ability declined gradually with the increase of RO-3306 concentration (**Figures 6F,H**). And the results of healing assays were coincided with those mentioned earlier results (**Figure 6G**). RO-3306 treatment significantly postponed the migration and proliferation ability of prostate cancer, and the clinical application of RO-3306 in the treatment of PCa might be a potential and effective measure, which could decrease the mortality of PCa patients.

### OTUB1 Promotes the Growth of PC3 Cell via Increasing Cyclin E1 *in vivo*

Male nude mice aged 4–6 weeks were selected as animal models. We planted  $2 \times 10^6$  PC3 cells transfected with overexpressed

OTUB1 and otub1 c91s in mouse groin, respectively. We began to measure the size of the tumors daily with a vernier caliper for 10 days, when the tumor grew to a diameter of 2 mm (**Figure 7D**). After 10 days, the animals were sacrificed with cervical dislocation, and the solid tumor was removed under sterile conditions. The tumor volume of OTUB1 overexpression group was distinctly different from that of the control group, but there was no obvious change in the otub1 c91s group compared with the control group (**Figures 7A–C**). We further found an interesting result that the tumor volume was restrained significantly compared with OTUB1 overexpression group, when these mice were oral administrated with RO-3306 in a dose of 4 mg/kg every day (**Figures 7A–C**). In addition, we found that tumor incidence in OTUB1 overexpressed group was significantly faster than that in the control group, while RO-3306 restrained the tumor incidence in the OTUB1 overexpression group (**Figure 7D**), indicating the critical role of OTUB1/Cyclin E1 axis in tumor formation. Immunohistochemical staining assay showed that the protein expression levels of OTUB1, Ki-67, and Cyclin E1 were higher in the tumors tissue with increased otub1





compared with the control group, and the expression of Cyclin E1 declined after the use of RO-3306, while the expression level of OTUB1 did not decrease (**Figure 7E**). The results further illustrated that OTUB1 regulated the expression and function of Cyclin E1 *in vivo*, and targeting OTUB1/Cyclin E1 axis might provide a potential therapeutic method for these patients with prostate cancer.

## DISCUSSION

In our research, we found that the expression levels of OTUB1 are up-regulated in PCa, OTUB1 could promote the proliferation and progression of PCa via deubiquitinating and stabilizing the expression of Cyclin E1 protein. Many previous researches have shown that OTUB1 is frequently up-regulated in many cancers, such as esophageal squamous cell carcinoma and colon cancer (Liu et al., 2014). Based on these findings of previous studies, OTUB1 promotes the metastasis of esophageal squamous cell carcinoma by modulating snail stability (Zhou et al., 2018), while different expression of OTUB1 affects the

migration and progression of colorectal cancer through the regulation of ERR $\alpha$  or mir-542-3p (Yuan et al., 2017; Zhou et al., 2019). OTUB1 not only regulates cancer metastasis but also chemoresistance. Karunarathna et al. found that OTUB1 inhibited the ubiquitination and degradation of FOXM1 in breast cancer, and mediated epirubicin resistance (Karunarathna et al., 2016). Recently, some researchers have proved that OTUB1 could attenuate interferon response to hepatitis B virus infection (Xie et al., 2020). The effects of OTUB1 in a variety of tumors reminds us that OTUB1 might play an important role during cancer evolution and some physiological activities.

In our research, we first found the expression of OTUB1 was up-regulated in PCa compared with normal prostate tissue from TCGA database. Next, we conducted immunohistochemical staining with PCa tissues and BPH to prove the above conclusion. The results were consistent with the database conclusion (**Figure 1**). To further explore the specific role of OTUB1 in the progression of prostate cancer, we performed a series of experiments to monitor the changes of migration ability by altering the expression of OTUB, and the results demonstrated that increased OTUB1 could significantly promote the migration

and invasion ability of PC3 cell and C4-2 cells. When we knocked down the expression of OTUB1, the ability to influence migration and invasion was obviously decreased compared with untreated PC3 cell and C4-2 cells (**Figure 2**). Previous studies found the effect of OTUB1 on prostate cancer, which showed that there was no significant deviation in PCa proliferation between decreased OTUB1 and the control group (Iglesias-Gato et al., 2015). In this research, we found that increased OTUB1 could promote proliferation of PC3 and C4-2 cells. We also found that G1 phase of cell cycle was shortened with the elevated expression of OTUB1 (**Figure 3**). To investigate the effect of OTUB1 on cell proliferation, we found that increased OTUB1 could increase the expression of Cyclin E1. Further experiments presented that Cyclin E1 interacted with OTUB1. OTUB1 could mediate the deubiquitination of Cyclin E1 and stabilize the expression level and function of Cyclin E1. Compared with PC3 cells transfected with OTUB1 overexpression alone, the proliferation of PC3 cell was decreased when co-transfected with OTUB1 overexpression and Cyclin E1 siRNA (**Figures 4–6**). These results suggested that OTUB1 might promote the proliferation of PCa via mediating Cyclin E1. The experimental results *in vivo* were consistent with those of the above-mentioned cell results *in vitro* (**Figure 7**). So far, we have a lot of evidence to identify the hypothesis that OTUB1 promotes the progression and proliferation of prostate cancer via mediating and stabilizing Cyclin E1. Previous researches had proved that Cyclin E1 belongs to a highly conserved Cyclin family, and its members are characterized by a dramatic periodicity in protein abundance through the cell cycle (Masaki et al., 2003). Cyclins could function as the regulators of CDK kinases (Hu et al., 2014; Asghar et al., 2015). This cyclin forms a complex and functions as a regulatory subunit of CDK2, whose activity is required for G1/S transition of cell cycle (Xu et al., 2019). Many researches have presented that Cyclin E1 could mediate the progression of many tumors, such as hepatocellular carcinoma (Sonntag et al., 2018; Xu et al., 2019), ovarian cancer (Au-Yeung et al., 2017), and breast cancer (Turner et al., 2019). Previous researches have proved that Cyclin E1 has several functional domains, mainly including a central cyclin homology district (interacting with CDK2), a unique N-terminal region, and a C-terminal PEST sequence, which are often detected in protein degraded through the ubiquitin system (Lew et al., 1991; Richardson et al., 1993; Honda et al., 2005; Rath and Senapati, 2014). As an unstable protein, Cyclin E1 is degraded by two distinct pathways involving the ubiquitin-proteasome system mediated by Cul1 or Cul3, which belongs to the cullin-RING family of ubiquitin ligases (Welcker et al., 2003; Davidge et al., 2019). And Cul1 mediated-degradation requires phosphorylation of Cyclin E1 at T77 and T395 to produce ubiquitylation of cyclin E (Minella et al., 2008). Previous studies have shown that Cul3 degrades Cyclin E that was not bound to Cdk2 and regulation of Cyclin E by Cul3 (McEvoy et al., 2007; Davidge et al., 2019). Although our research found that the deubiquitinase OTUB1 promotes the stability of Cyclin E1 and the progression of prostate cancer, the specific mechanism of OTUB1 mediated function of Cyclin E1 remains to be further studied. The interaction among OTUB1, Cul1, and Cul3 might become the internal reason for the stable functions of Cyclin E1 and its

subsequent functions. The next aim of our research focuses on the relationship between OTUB1 and ubiquitin ligases. Not only prostate cancer and the above-mentioned cancers, Kai Zhou et al. found that OTUB1 could promote the progression of renal cell carcinoma via mediating the deubiquitination of FOXM1 and up-regulating the expression of ECT-2 (K. Zhou et al., 2020). Other researchers have proved that SP1 regulates the progression of non-small-cell lung cancer by recruiting OTUB1 (Xie et al., 2019).

Based on the above results, we found that the high expression level of OTUB1 promoted the migration and invasion of PCa cells, while the low expression of OTUB1 decreased the migration and invasion of PCa cells. Previous studies on the biological function of OTUB1 are contradictory. The initial study found that OTUB1 attributed to the stability of P53 protein, and thus inhibiting cell proliferation. Recent studies have indicated that OTUB1 is involved in the invasion and migration of malignant tumors. However, in our study, we discovered that high level of OTUB1 promoted cell proliferation, while low expression of OTUB1 had the opposite effect. And we further found that OTUB1 promoted the progression of PCa via regulating the stability and interacting with Cyclin E1. Cyclin E1 was mainly degraded in a ubiquitination manner, yet OTUB1 inhibited the ubiquitination of Cyclin E1 and stabilized its function to promote the cell proliferation. This mechanism and relationship reminded us that OTUB1/Cyclin E1 pathway might serve as a potential therapeutic target for PCa. When we interfere or interrupt the connection between OTUB1 and Cyclin E1, the proliferation and progression of PCa might be slowed or stopped. The results of RO-3306 treatment are the direct evidence of targeting OTUB1/Cyclin E1 axis for prostate cancer.

This new treatment may become an effective therapy for patients with PCa. The specific mechanism of OTUB1/Cyclin E1 axis needs further experiments to investigate and reinforce. Furthermore, the limitations of this research are also obvious, the role of Cyclin E1 in OTUB1 induced PC is not strong enough and it is only a correlation established from a mechanism. And the design of *in vivo* animal experiments was simple. The specific function of OTUB1/Cyclin E1 axis *in vivo* could not be fully explained by subcutaneous tumor related experiments. Although we have found that otub1 promoted the proliferation and progression of PCa via mediating and stabilizing Cyclin E1, in which one ubiquitination enzyme directly causing to the ubiquitination degradation of Cyclin E1 remains unclear, and the manner of OTUB1 regulating the expression of Cyclin E1 directly or indirectly are still yet not determined. Therefore, this research preliminarily proposed that OTUB1 could promote the progression and proliferation of PCa via regulating the expression of Cyclin E1, thus the specific internal mechanism will become the main work and direction in the next step.

## CONCLUSIONS

Here, our study shows that OTUB1 deubiquitinates and stabilizes Cyclin E1 to promote the progression, migration, and proliferation of prostate cancer. The OTUB1/Cyclin E1 axis may



serve as a potential therapeutic target for patients with prostate cancer. The prognosis of patients with prostate cancer may be improved when the connection between OTUB1 and Cyclin E1 are interrupted or disturbed.

## DATA AVAILABILITY STATEMENT

The datasets presented in this study can be found in online repositories. The names of the repository/repositories and accession number(s) can be found in the article/**Supplementary Material**.

## ETHICS STATEMENT

The animal study was reviewed and approved by Ethics Committee of the Second Hospital of Tianjin Medical University.

## AUTHOR CONTRIBUTIONS

YL: project development, perform experiment, data analysis, and manuscript writing. NW: project development. KW: perform experiment. MW: data analysis. YW: perform experiment. JG:

data collection. BZ: data collection. FM: project development. YW: data analysis. NJ: project development. All authors contributed to the article and approved the submitted version.

## FUNDING

This work was supported by the National Natural Science Foundation of China (81872079 and 81572538), and the Science Foundation of Tianjin (Nos. 11JCZDJC19700, 16JCZDJC34400, 18JCQNJC13100, 20140117, and 16KG118).

## ACKNOWLEDGMENTS

Thanks to all the experimental technicians of Tianjin Institute of Urology for their help. This manuscript has been released as a Pre-Print at bioarxiv.org (Liao et al., 2020).

## SUPPLEMENTARY MATERIAL

The Supplementary Material for this article can be found online at: <https://www.frontiersin.org/articles/10.3389/fcell.2020.617758/full#supplementary-material>

## REFERENCES

- Altwayjry, N., Somani, S., and Dufès, C. (2018). Targeted nonviral gene therapy in prostate cancer. *Int. J. Nanomedicine* 13, 5753–5767. doi: 10.2147/IJN.S139080
- Asghar, U., Witkiewicz, A. K., Turner, N. C., and Knudsen, E. S. (2015). The history and future of targeting cyclin-dependent kinases in cancer therapy. *Nat. Rev. Drug Discov.* 14, 130–146. doi: 10.1038/nrd4504
- Au-Yeung, G., Lang, F., Azar, W. J., Mitchell, C., Jarman, K. E., Lackovic, K., et al. (2017). Selective targeting of cyclin E1-amplified high-grade serous ovarian cancer by cyclin-dependent kinase 2 and AKT inhibition. *Clin. Cancer Res.* 23, 1862–1874. doi: 10.1158/1078-0432.CCR-16-0620
- Bastos, D. A., and Antonarakis, E. S. (2018). CTC-derived AR-V7 detection as a prognostic and predictive biomarker in advanced prostate cancer. *Expert Rev. Mol. Diagn.* 18, 155–163. doi: 10.1080/14737159.2018.1427068
- Bisteau, X., Caldez, M. J., and Kaldis, P. (2014). The complex relationship between liver cancer and the cell cycle: a story of multiple regulations. *Cancers* 6, 79–111. doi: 10.3390/cancers6010079
- Davidge, B., Rebola, K. G. O., Agbor, L. N., Sigmund, C. D., and Singer, J. D. (2019). Cul3 regulates cyclin E1 protein abundance via a degron located within the N-terminal region of cyclin E. *J. Cell Sci.* 132:jcs233049. doi: 10.1242/jcs.233049
- Ehedego, H., Mohs, A., Jansen, B., Hiththetiya, K., Sicinski, P., Liedtke, C., et al. (2018). Loss of Cyclin E1 attenuates hepatitis and hepatocarcinogenesis in a mouse model of chronic liver injury. *Oncogene* 37, 3329–3339. doi: 10.1038/s41388-018-0181-8
- Fang, D., Huang, S., and Su, S. B. (2016). Cyclin E1-CDK 2, a potential anticancer target. *Aging* 8, 571–572. doi: 10.18632/aging.100946
- Gasnier, A., and Parvizi, N. (2017). Updates on the diagnosis and treatment of prostate cancer. *Br. J. Radiol.* 90:20170180. doi: 10.1259/bjr.20170180
- Geng, Y., Yu, Q., Sicinska, E., Das, M., Schneider, J. E., Bhattacharya, S., et al. (2003). Cyclin E ablation in the mouse. *Cell* 114, 431–443. doi: 10.1016/S0092-8674(03)00645-7
- Honda, R., Lowe, E. D., Dubinina, E., Skamnaki, V., Cook, A., Brown, N. R., et al. (2005). The structure of cyclin E1/CDK2: implications for CDK2 activation and CDK2-independent roles. *EMBO J.* 24, 452–463. doi: 10.1038/sj.emboj.7600554
- Hossain, M. K., Nahar, K., Donkor, O., and Apostolopoulos, V. (2018). Immune-based therapies for metastatic prostate cancer: an update. *Immunotherapy* 10, 283–298. doi: 10.2217/imt-2017-0123
- Hu, W., Nevzorova, Y. A., Haas, U., Moro, N., Sicinski, P., Geng, Y., et al. (2014). Concurrent deletion of cyclin E1 and cyclin-dependent kinase 2 in hepatocytes inhibits DNA replication and liver regeneration in mice. *Hepatology* 59, 651–660. doi: 10.1002/hep.26584
- Iglesias-Gato, D., Chuan, Y. C., Jiang, N., Svensson, C., Bao, J., Paul, I., et al. (2015). OTUB1 de-ubiquitinating enzyme promotes prostate cancer cell invasion *in vitro* and tumorigenesis *in vivo*. *Mol. Cancer* 14:8. doi: 10.1186/s12943-014-0280-2
- Kanska, J., Zakhour, M., Taylor-Harding, B., Karlan, B. Y., and Wiedemeyer, W. R. (2016). Cyclin E as a potential therapeutic target in high grade serous ovarian cancer. *Gynecol. Oncol.* 143, 152–158. doi: 10.1016/j.ygyno.2016.07.111
- Karunaratna, U., Kongsema, M., Zona, S., Gong, C., Cabrera, E., Gomes, A. R., et al. (2016). OTUB1 inhibits the ubiquitination and degradation of FOXM1 in breast cancer and epirubicin resistance. *Oncogene* 35, 1433–1444. doi: 10.1038/ncr.2015.208
- Komura, K., Sweeney, C. J., Inamoto, T., Ibuki, N., Azuma, H., and Kantoff, P. W. (2018). Current treatment strategies for advanced prostate cancer. *Int. J. Urol.* 25, 220–231. doi: 10.1111/iju.13512
- Lew, D. J., Dulić, V., and Reed, S. I. (1991). Isolation of three novel human cyclins by rescue of G1 cyclin (Cln) function in yeast. *Cell* 66, 1197–1206. doi: 10.1016/0092-8674(91)90042-W
- Liao, Y., Wu, N., Wang, K., Wang, M., Wang, Y., Gao, J., et al. (2020). OTUB1 promotes progression and proliferation of prostate cancer via deubiquitinating and stabilizing cyclin E1. *bioarxiv*. 8, 1–13. doi: 10.3389/fcell.2020.617758
- Liu, T., Jiang, L., Tavana, O., and Gu, W. (2019). The deubiquitylase OTUB1 mediates ferroptosis via stabilization of SLC7A11. *Cancer Res.* 79, 1913–1924. doi: 10.1158/0008-5472.CAN-18-3037
- Liu, X., Jiang, W. N., Wang, J. G., and Chen, H. (2014). Colon cancer bears overexpression of OTUB1. *Pathol. Res. Pract.* 210, 770–773. doi: 10.1016/j.prp.2014.05.008
- Malumbres, M., and Barbacid, M. (2009). Cell cycle, CDKs and cancer: a changing paradigm. *Nat. Rev. Cancer* 9, 153–166. doi: 10.1038/nrc2602
- Masaki, T., Shiratori, Y., Rengifo, W., Igarashi, K., Yamagata, M., Kurokohchi, K., et al. (2003). Cyclins and cyclin-dependent kinases: comparative study of hepatocellular carcinoma versus cirrhosis. *Hepatology* 37, 534–543. doi: 10.1053/jhep.2003.50112

- McEvoy, J. D., Kossatz, U., Malek, N., and Singer, J. D. (2007). Constitutive turnover of cyclin E by Cul3 maintains quiescence. *Mol. Cell. Biol.* 27, 3651–3666. doi: 10.1128/MCB.00720-06
- Minella, A. C., Loeb, K. R., Knecht, A., Welcker, M., Varnum-Finney, B. J., Bernstein, I. D., et al. (2008). Cyclin E phosphorylation regulates cell proliferation in hematopoietic and epithelial lineages *in vivo*. *Genes Dev.* 22, 1677–1689. doi: 10.1101/gad.1650208
- Murillo-Garzón, V., and Kypta, R. (2017). WNT signalling in prostate cancer. *Nat. Rev. Urol.* 14, 683–696. doi: 10.1038/nrurol.2017.144
- Nakada, S., Tai, I., Panier, S., Al-Hakim, A., Iemura, S., Juang, Y. C., et al. (2010). Non-canonical inhibition of DNA damage-dependent ubiquitination by OTUB1. *Nature* 466, 941–946. doi: 10.1038/nature09297
- Nguyen-Nielsen, M., and Borre, M. (2016). Diagnostic and therapeutic strategies for prostate cancer. *Semin. Nucl. Med.* 46, 484–490. doi: 10.1053/j.semnuclmed.2016.07.002
- Ni, Q., Chen, J., Li, X., Xu, X., Zhang, N., Zhou, A., et al. (2017). Expression of OTUB1 in hepatocellular carcinoma and its effects on HCC cell migration and invasion. *Acta Biochim. Biophys. Sin.* 49, 680–688. doi: 10.1093/abbs/gmx056
- Popovic, D., Vucic, D., and Dikic, I. (2014). Ubiquitination in disease pathogenesis and treatment. *Nat. Med.* 20, 1242–1253. doi: 10.1038/nm.3739
- Rath, S. L., and Senapati, S. (2014). Why are the truncated cyclin Es more effective CDK2 activators than the full-length isoforms? *Biochemistry* 53, 4612–4624. doi: 10.1021/bi5004052
- Richardson, H. E., O'Keefe, L. V., Reed, S. I., and Saint, R. (1993). A Drosophila G1-specific cyclin E homolog exhibits different modes of expression during embryogenesis. *Development* 119, 673–690.
- Saldana, M., VanderVorst, K., Berg, A. L., Lee, H., and Carraway, K. L. (2019). Otubain 1: a non-canonical deubiquitinase with an emerging role in cancer. *Endocr. Relat. Cancer* 26, R1–r14. doi: 10.1530/ERC-18-0264
- Sebesta, E. M., and Anderson, C. B. (2017). The surgical management of prostate cancer. *Semin. Oncol.* 44, 347–357. doi: 10.1053/j.seminoncol.2018.01.003
- Siegel, R. L., Miller, K. D., and Jemal, A. (2019). Cancer statistics, 2019. *CA Cancer J. Clin.* 69, 7–34. doi: 10.3322/caac.21551
- Sivakumar, D., Kumar, V., Naumann, M., and Stein, M. (2020). Activation and selectivity of OTUB-1 and OTUB-2 deubiquitinylases. *J. Biol. Chem.* 295, 6972–6982. doi: 10.1074/jbc.RA120.013073
- Smolle, M. A., Bauernhofer, T., Pummer, K., Calin, G. A., and Pichler, M. (2017). Current insights into long non-coding rnas (LncRNAs) in prostate cancer. *Int. J. Mol. Sci.* 18:473. doi: 10.3390/ijms18020473
- Sonntag, R., Giebler, N., Nevzorova, Y. A., Bangen, J. M., Fahrenkamp, D., Lambertz, D., et al. (2018). Cyclin E1 and cyclin-dependent kinase 2 are critical for initiation, but not for progression of hepatocellular carcinoma. *Proc. Natl. Acad. Sci. U. S. A.* 115, 9282–9287. doi: 10.1073/pnas.1807155115
- Sun, J., Deng, Y., Shi, J., and Yang, W. (2020). MicroRNA-542-3p represses OTUB1 expression to inhibit migration and invasion of esophageal cancer cells. *Mol. Med. Rep.* 21, 35–42. doi: 10.3892/mmr.2019.10836
- Turner, N. C., Liu, Y., Zhu, Z., Loi, S., Colleoni, M., Loibl, S., et al. (2019). Cyclin E1 expression and palbociclib efficacy in previously treated hormone receptor-positive metastatic breast cancer. *J. Clin. Oncol.* 37, 1169–1178. doi: 10.1200/JCO.18.00925
- Wang, Y., Zhou, X., Xu, M., Weng, W., Zhang, Q., Yang, Y., et al. (2016). OTUB1-catalyzed deubiquitination of FOXM1 facilitates tumor progression and predicts a poor prognosis in ovarian cancer. *Oncotarget* 7, 36681–36697. doi: 10.18632/oncotarget.9160
- Wei, R., Thanindratarn, P., Dean, D. C., Hornicek, F. J., Guo, W., and Duan, Z. (2020). Cyclin E1 is a prognostic biomarker and potential therapeutic target in osteosarcoma. *J. Orthop. Res.* 38, 1952–1964. doi: 10.1002/jor.24659
- Welcker, M., Singer, J., Loeb, K. R., Grim, J., Bloecher, A., Gurien-West, M., et al. (2003). Multisite phosphorylation by Cdk2 and GSK3 controls cyclin E degradation. *Mol. Cell* 12, 381–392. doi: 10.1016/S1097-2765(03)00287-9
- Weng, W., Zhang, Q., Xu, M., Wu, Y., Zhang, M., Shen, C., et al. (2016). OTUB1 promotes tumor invasion and predicts a poor prognosis in gastric adenocarcinoma. *Am. J. Transl. Res.* 8, 2234–2244.
- Wiener, R., Zhang, X., Wang, T., and Wolberger, C. (2012). The mechanism of OTUB1-mediated inhibition of ubiquitination. *Nature* 483, 618–622. doi: 10.1038/nature10911
- Xie, J. J., Guo, Q. Y., Jin, J. Y., and Jin, D. (2019). SP1-mediated overexpression of lncRNA LINC01234 as a ceRNA facilitates non-small-cell lung cancer progression via regulating OTUB1. *J. Cell. Physiol.* 234, 22845–22856. doi: 10.1002/jcp.28848
- Xie, M., Yin, Y., Chen, L., Yin, A., Liu, Y., Liu, Y., et al. (2020). Scavenger receptor A impairs interferon response to HBV infection by limiting TRAF3 ubiquitination through recruiting OTUB1. *FEBS J.* 287, 310–324. doi: 10.1111/febs.15035
- Xu, J., Huang, F., Yao, Z., Jia, C., Xiong, Z., Liang, H., et al. (2019). Inhibition of cyclin E1 sensitizes hepatocellular carcinoma cells to regorafenib by mcl-1 suppression. *Cell Commun. Signal.* 17:85. doi: 10.1186/s12964-019-0398-3
- Xu, L., Li, J., Bao, Z., Xu, P., Chang, H., Wu, J., et al. (2017). Silencing of OTUB1 inhibits migration of human glioma cells *in vitro*. *Neuropathology* 37, 217–226. doi: 10.1111/neup.12366
- Yuan, L., Yuan, P., Yuan, H., Wang, Z., Run, Z., Chen, G., et al. (2017). miR-542-3p inhibits colorectal cancer cell proliferation, migration and invasion by targeting OTUB1. *Am. J. Cancer Res.* 7, 159–172.
- Zhou, H., Liu, Y., Zhu, R., Ding, F., Cao, X., Lin, D., et al. (2018). OTUB1 promotes esophageal squamous cell carcinoma metastasis through modulating Snail stability. *Oncogene* 37, 3356–3368. doi: 10.1038/s41388-018-0224-1
- Zhou, K., Mai, H., Zheng, S., Cai, W., Yang, X., Chen, Z., et al. (2020). OTUB1-mediated deubiquitination of FOXM1 up-regulates ECT-2 to promote tumor progression in renal cell carcinoma. *Cell Biosci.* 10:50. doi: 10.1186/s13578-020-00408-0
- Zhou, Y., Jia, Q., Meng, X., Chen, D., and Zhu, B. (2019). ERRα regulates OTUB1 expression to promote colorectal cancer cell migration. *J. Cancer* 10, 5812–5819. doi: 10.7150/jca.30720
- Zhou, Y., Wu, J., Fu, X., Du, W., Zhou, L., Meng, X., et al. (2014). OTUB1 promotes metastasis and serves as a marker of poor prognosis in colorectal cancer. *Mol. Cancer* 13:258. doi: 10.1186/1476-4598-13-258

**Conflict of Interest:** The authors declare that the research was conducted in the absence of any commercial or financial relationships that could be construed as a potential conflict of interest.

Copyright © 2021 Liao, Wu, Wang, Wang, Wang, Gao, Zhong, Ma, Wu and Jiang. This is an open-access article distributed under the terms of the Creative Commons Attribution License (CC BY). The use, distribution or reproduction in other forums is permitted, provided the original author(s) and the copyright owner(s) are credited and that the original publication in this journal is cited, in accordance with accepted academic practice. No use, distribution or reproduction is permitted which does not comply with these terms.



# Cullin3-TNFAIP1 E3 Ligase Controls Inflammatory Response in Hepatocellular Carcinoma Cells via Ubiquitination of RhoB

Yue Liu<sup>1,2,3,4†</sup>, Wenjuan Zhang<sup>2†</sup>, Shiwen Wang<sup>1,2,3,4†</sup>, Lili Cai<sup>2</sup>, Yanyu Jiang<sup>2</sup>, Yongfu Pan<sup>2</sup>, Yupei Liang<sup>2</sup>, Jingrong Xian<sup>1,2,3,4</sup>, Lijun Jia<sup>2</sup>, Lihui Li<sup>2\*</sup>, Hu Zhao<sup>1,3,4\*</sup> and Yanmei Zhang<sup>1,3,4\*</sup>

## OPEN ACCESS

### Edited by:

Lingqiang Zhang,  
Beijing Proteome Research Center,  
National Center for Protein Sciences  
Shanghai, China

### Reviewed by:

Mark Nathaniel Adams,  
Queensland University of Technology,  
Australia  
Chiaki Takahashi,  
Kanazawa University, Japan

### \*Correspondence:

Lihui Li  
dm-li@163.com  
Hu Zhao  
hubertzhao@163.com  
Yanmei Zhang  
15618653286@163.com

<sup>†</sup>These authors have contributed  
equally to this work

### Specialty section:

This article was submitted to  
Cell Growth and Division,  
a section of the journal  
Frontiers in Cell and Developmental  
Biology

**Received:** 14 October 2020

**Accepted:** 04 January 2021

**Published:** 21 January 2021

### Citation:

Liu Y, Zhang W, Wang S, Cai L,  
Jiang Y, Pan Y, Liang Y, Xian J, Jia L,  
Li L, Zhao H and Zhang Y (2021)  
Cullin3-TNFAIP1 E3 Ligase Controls  
Inflammatory Response  
in Hepatocellular Carcinoma Cells via  
Ubiquitination of RhoB.  
Front. Cell Dev. Biol. 9:617134.  
doi: 10.3389/fcell.2021.617134

<sup>1</sup> Department of Laboratory Medicine, Huadong Hospital Affiliated to Fudan University, Shanghai, China, <sup>2</sup> Longhua Hospital, Cancer Institute, Shanghai University of Traditional Chinese Medicine, Shanghai, China, <sup>3</sup> Research Center on Aging and Medicine, Fudan University, Shanghai, China, <sup>4</sup> Shanghai Key Laboratory of Clinical Geriatric Medicine, Shanghai, China

Rho family GTPase RhoB is the critical signaling component controlling the inflammatory response elicited by pro-inflammatory cytokines. However, the underlying mechanisms of RhoB degradation in inflammatory response remain unclear. In this study, for the first time, we identified that TNFAIP1, an adaptor protein of Cullin3 E3 ubiquitin ligases, coordinated with Cullin3 to mediate RhoB degradation through ubiquitin proteasome system. In addition, we demonstrated that downregulation of TNFAIP1 induced the expression of pro-inflammatory cytokines IL-6 and IL-8 in TNF $\alpha$ -stimulated hepatocellular carcinoma cells through the activation of p38/JNK MAPK pathway via blocking RhoB degradation. Our findings revealed a novel mechanism of RhoB degradation and provided a potential strategy for anti-inflammatory intervention of tumors by targeting TNFAIP1-RhoB axis.

**Keywords:** RhoB, CRL3s, TNFAIP1, inflammatory response, MAPK signaling

## INTRODUCTION

Cullin-RING Ligases (CRLs), one major type of E3 ubiquitin ligases, regulate about 20% cellular proteins degradation by ubiquitin-proteasome system (UPS) (Petroski and Deshaies, 2005; Zhao and Sun, 2013). Most of the CRLs consist of Cullin proteins, adaptor proteins, substrate receptor proteins and RING-finger proteins (Cui et al., 2016). Eukaryotic genomes encode eight Cullin proteins (Cullin 1-3, Cullin 4A/4B, Cullin 5, Cullin 7, and Cullin 9) serving as scaffolds of different CRLs (Merlet et al., 2009; Chen and Chen, 2016). The C-terminus of Cullins tightly binds with the Ring finger protein RBX1 or RBX2 which transfers Ub from the Ub-conjugating E2 to the substrates. The N-terminus of Cullins interacts with receptor proteins to recognize specific substrates (Duda et al., 2011). In particular, Cullin3-RING ligases (CRL3s), without receptor proteins, utilize substrates specific Bric-a-Brac/Tramtrack/Broad (BTB) domain proteins to recognize their corresponding substrates and to regulate various biological processes (Kwon et al., 2006; Genschik et al., 2013). Dysregulation of CRL3s leads to tumorigenesis and tumor development (Li et al., 2014; Chen and Chen, 2016; Dubiel et al., 2017). Furthermore, CRL3s play pivotal roles in the innate immune response to infection (Awuh et al., 2015; Dinkova-Kostova et al., 2017). For example, knockdown of the component of Cullin3-Keap1 complex activates NF- $\kappa$ B and

drives the expression of pro-inflammatory cytokines (Awuh et al., 2015). However, the regulatory role of CRL3s in inflammatory response has not been fully elucidated.

RhoB, together with RhoA and RhoC, is a member of the Rho family small GTPases that controls numerous essential biological processes, including actin cytoskeleton dynamics, vesicle trafficking, cell cycle and apoptosis (Wheeler and Ridley, 2004; Karlsson et al., 2009; Kim et al., 2009; Li et al., 2011; Vega and Ridley, 2018). As a short-lived protein, the expression of RhoB is induced by a variety of stimuli including epidermal growth factor, UV irradiation, hypoxia and pro-inflammatory cytokines, such as tumor necrosis factor  $\alpha$  (TNF $\alpha$ ), interferon  $\gamma$  (IFN $\gamma$ ) and interleukin-1 (IL-1) (Fritz and Kaina, 2001; Huang and Prendergast, 2006; Gutierrez et al., 2019). It has been reported that RhoB is the key signaling component in regulating the inflammatory response in endothelial cells and macrophages induced by pro-inflammatory cytokines (Rodriguez et al., 2007; Shi and Wei, 2013; Marcosramiro et al., 2016; Huang et al., 2017). In addition, pro-inflammatory cytokines secreted by tumor cells trigger inflammatory response, which regulate tumor inflammatory microenvironment and promote cancer development and progression (Landskron et al., 2014; Greten and Grivennikov, 2019). However, whether RhoB also regulates the inflammatory response in tumor cells and the underlying mechanisms of RhoB degradation needs to be further explored.

Tumor necrosis factor alpha induced protein 1 (TNFAIP1) is a well-known BTB domain protein that constitutes Cullin3-based ubiquitin ligases, which plays crucial roles in DNA synthesis, apoptosis and cell migration (Chen et al., 2009; Zhu et al., 2014; Liu et al., 2016; Xiao et al., 2020). TNFAIP1 is an immediate-early gene, which is activated by cytokines and chemokines such as TNF $\alpha$  and IL-6 in endothelial cells (Liu et al., 2010; Hu et al., 2012). Recent studies revealed that TNFAIP1 functioned as an inflammatory modulator in Alzheimer's disease by regulating NF- $\kappa$ B signaling pathway (Zhao et al., 2018). Moreover, TNFAIP1 controls actin cytoskeleton structure and cell movement through mediating the degradation of RhoA (Chen et al., 2009). However, whether RhoB degradation is regulated by TNFAIP1 in inflammatory response remains unknown.

In this study, we demonstrated that Cullin3-TNFAIP1 complex targeted RhoB for ubiquitination and subsequent proteasome-dependent degradation in hepatocellular carcinoma (HCC) cells. Moreover, TNFAIP1 downregulation blocked RhoB degradation, thereby inducing the expression of inflammatory genes IL-6 and IL-8 through activating MAPK signaling pathway upon TNF $\alpha$  stimulation. Our studies revealed a previously unknown mechanism that CRL3 E3 ligases regulating inflammatory response through TNFAIP1-mediated RhoB degradation in HCC cells.

## MATERIALS AND METHODS

### Cell Culture

HepG2, Huh7, and HEK293T cells were obtained from the Type Culture Collection of the Chinese Academy of Sciences (Shanghai, China), and cultured at 37°C in 5% CO<sub>2</sub> atmosphere.

DMEM medium supplemented with fetal bovine serum (FBS, 10%) and Penicillin-Streptomycin Solution (1%) from Gibco was used for culturing cells.

### RNA Interference

The cells were transfected with siRNA oligonucleotides using Lipofectamine RNAiMAX Transfection Reagent (Invitrogen, United States) according to the manufacturer's instruction. The sequences of siRNA are as follows: for Cullin3, 5'-TTGACGTGAACTGACATCCACATTC-3' and 5'-TACATATGTGTATACTTTGCGATCC-3'; for TNFAIP1, 5'-TAGAGTAGGACGTTGAGTGTCTCCT-3' and 5'-CACUC AACGUCCUACUCUATT-3'; for RhoB, 5'-GGCAUUCUCU AAAGCUAUG-3'; for KCTD10, 5'-GAAUGAGCGUCUAA AUCGUTT-3'. All of the above siRNAs were obtained from GenePharma (Shanghai, China).

### Plasmids Construction and Transfection

To generate Flag-RhoB, HA-TNFAIP1, Myc-Cullin3 and His-Ub constructs, Human RhoB, TNFAIP1, Cullin3, and Ub were amplified by PCR and cloned into the modified pCMV-Tag2B, pCMV-HA, pCMV-Myc and pCMV-His vector, respectively. All constructs were verified by sequence analysis. Plasmids transfection were carried out using Lipofectamine 2000 (Invitrogen, United States) following the manufacturer's instructions.

### Reagents and Antibodies

Recombinant human TNF $\alpha$  was from Beyotime Biotechnology. MG132 and cycloheximide (CHX) were from sigma. The cell lysates for immunoblotting analysis used antibodies against rabbit Cullin3 (Cell Signaling Technology, United States), mouse  $\beta$ -actin (Cwbiotech, China), mouse RhoB (Santa Cruz, United States), rabbit Ubiquitin (Cell Signaling Technology, United States), mouse TNFAIP1 (Santa Cruz, United States), rabbit KCTD10 (Proteintech, United States), mouse Flag (Abmart, China), rabbit Flag (Huabio, China), rabbit Myc (Huabio, China), rabbit HA (Huabio, China), rabbit p-p38 (Cell Signaling Technology, United States), rabbit p38 (Cell Signaling Technology, United States), rabbit p-JNK (Cell Signaling Technology, United States), and rabbit JNK (Cell Signaling Technology, United States). Densitometric analysis of the band intensities was performed using ImageJ.

### Endogenous Immunoprecipitation Assay

Immunoprecipitation of endogenous RhoB or TNFAIP1 was performed with mouse RhoB antibody and mouse TNFAIP1 antibody (Santa Cruz, United States), respectively. Before lysis, the cells were treated with MG132 (Sigma-Aldrich, United States) for 6 h. Five hundred microliter lysis buffer (Thermo Fisher Scientific, United States) was added into dishes. The cells were collected into tube and spun at 13,000 rpm for 15 min. The supernatant was transferred to new tube and incubated with 1  $\mu$ g RhoB antibody or TNFAIP1 antibody overnight at 4°C. Complexes were pulled down by incubation with protein A/G (Santa Cruz, United States) for another 2 h. The



immunoprecipitate was washed 3 times with lysis buffer and analyzed with SDS-PAGE.

## Exogenous Immunoprecipitation Assay

HEK293T cells were transfected with Flag-RhoB and HA-TNFAIP1. After 24 h, the cells were pretreated with MG132 (Sigma-Aldrich, United States) for 6 h. A 500  $\mu$ L lysis buffer (Thermo Fisher Scientific, United States) was added into dishes. The cells were collected into tube and spun at 13,000 rpm for 15 min. The supernatant was transferred to new tube and incubated with anti-Flag M2 beads (Santa Cruz, United States) overnight at 4°C. The immunoprecipitate was washed 3 times with lysis buffer and analyzed with SDS-PAGE.

## Immunofluorescence

To detect endogenous RhoB and TNFAIP1 colocalization, HepG2 and HEK293T cells were seeded into 3 mm plates with glass slide. After 24 h, the cells were fixed with 4% paraformaldehyde for 20 min. Upon fixation, cells were treated with 0.1% Triton X-100 for 20 min and unspecific staining was blocked by 2% BSA in PBS for 1 h. Cells were incubated with primary antibodies overnight at 4°C. Cells were washed 3 times with PBS and incubated with secondary antibody for 1 h. Secondary antibodies used in this study were goat anti-mouse Alexa Fluor 488 and goat anti-rabbit Alexa Fluor 647 (Invitrogen, United States). Hoechst (Invitrogen, United States) was used to stain nuclei. The plates were analyzed using confocal microscope Leica SP9.

## Ubiquitination Assay

For RhoB ubiquitination analysis, HEK293T cells were transfected with plasmids expressing RhoB, Ub, and TNFAIP1 or Cullin3. The cells were pretreated with MG132 (Sigma-Aldrich, United States) for 6 h. Lyse cells with 100  $\mu$ L cell lysis buffer (Thermo Fisher Scientific, United States) with 1% SDS (Sangon biotech, China) per plate. Cell lysates were boiled for 10 min. Then diluted in 10 volumes of lysis buffer without SDS. Samples were subjected to immunoprecipitation with anti-Flag M2 beads (Sigma-Aldrich, United States) and immunoblotting with anti-ubiquitin antibody. To detect endogenous RhoB ubiquitination, the cells were transfected with siRNA oligonucleotide. After 96 h post-transfection, the cells were treated with MG132 for 6 h and subjected to immunoprecipitation with RhoB antibody and immunoblotting with ubiquitin.

## RNA Extraction and qPCR

Total RNA was isolated using the Trizol reagent (Invitrogen, United States). The reverse transcription reaction was performed on 1  $\mu$ g of total RNA per sample using the PrimerScript reverse transcription reagent kit (TaKaRa, Japan) according to the manufacturer's protocol. After the RT reaction, the quantitative polymerase chain reaction was performed using the Power SYBR Green PCR MasterMix (Applied Biosystems, CA) and specific PCR primers on the ABI 7500 thermocycler (Applied Biosystems) according to the instrument manual. For each sample, the mRNA abundance was normalized to the amount of  $\beta$ -actin. Primers were as follows:

for TNFAIP1, F: 5'-ACCTCCGAGATGACACCATCA-3',  
R: 5'-GGCACTCTGGCACATATTAC-3',  
for RhoB, F: 5'-CTGCTGATCGTGTTCAGTAAGG-3',  
R: 5'-TCAATGTCGGCCACATAGTTC-3',  
for IL-6, F: 5'-ACTCACCTCTTCAGAACGAATTG-3',  
R: 5'-CCATCTTTGGAAGGTTTCAGGTTG-3',  
for IL-8, F: 5'-TTTTGCCAAGGAGTGCTAAAGA-3',  
R: 5'-AACCCTCTGCACCCAGTTTTC-3',  
for  $\beta$ -actin, F: 5'-CATGTACGTTGCTATCCAGGC-3',  
R: 5'-CTCCTTAATGTACGCACGAT-3'.

## Statistical Analysis

The statistical significance of differences between groups was assessed using the GraphPad Prism5 software (GraphPad Software, Inc., San Diego, CA, United States). For comparison of two groups of samples, the two-tailed Student's *t*-test was used.  $P < 0.05$  was considered a statistically significant change (\* $P < 0.05$ , \*\* $P < 0.01$ , \*\*\* $P < 0.001$ , ## $P < 0.01$ , ### $P < 0.001$ , n.s. = not significant).

## RESULTS

### CRL3s Regulates the Degradation of RhoB

To determine whether RhoB served as a substrate of CRL3s, we first detected the protein level of RhoB upon downregulation of Cullin3 in HCC cells. We found that knockdown of Cullin3 using siRNA induced remarkable RhoB accumulation in both Huh7 and HepG2 cells (Figure 1A). Furthermore, we showed that the RhoB expression were suppressed by overexpression of Myc-Cullin3 in a dose-dependent manner (Figure 1B). Next, the RhoB protein stability in Cullin3-silenced cells was measured in the presence of cycloheximide (CHX), which was applied to impede protein synthesis. The results showed that downregulation of Cullin3 dramatically extended the half-life of RhoB (Figures 1C,D). Taken together, our data indicated that Cullin3 targets RhoB for degradation.

### TNFAIP1 Functioned as the Adaptor Protein for CRL3s to Mediate RhoB Degradation

Previous studies demonstrated that TNFAIP1 mediated RhoA degradation and controlled actin cytoskeleton structure in Hela cells (Chen et al., 2009). We determined whether TNFAIP1 also regulated the protein level of RhoB. Two pairs of siRNAs specifically against TNFAIP1 were transfected into Huh7 and HepG2 cells. As shown, ablation of TNFAIP1 induced the accumulation of RhoB in Huh7 and HepG2 cells (Figure 2A), while did not affect the expression of Cullin3 (Supplementary Figure 1). In contrast, overexpression of HA-TNFAIP1 promoted the RhoB degradation in a dose-dependent manner (Figure 2B). To further investigate whether TNFAIP1 promote RhoB degradation, we applied CHX to block protein translation and determined the turnover rate of RhoB. We

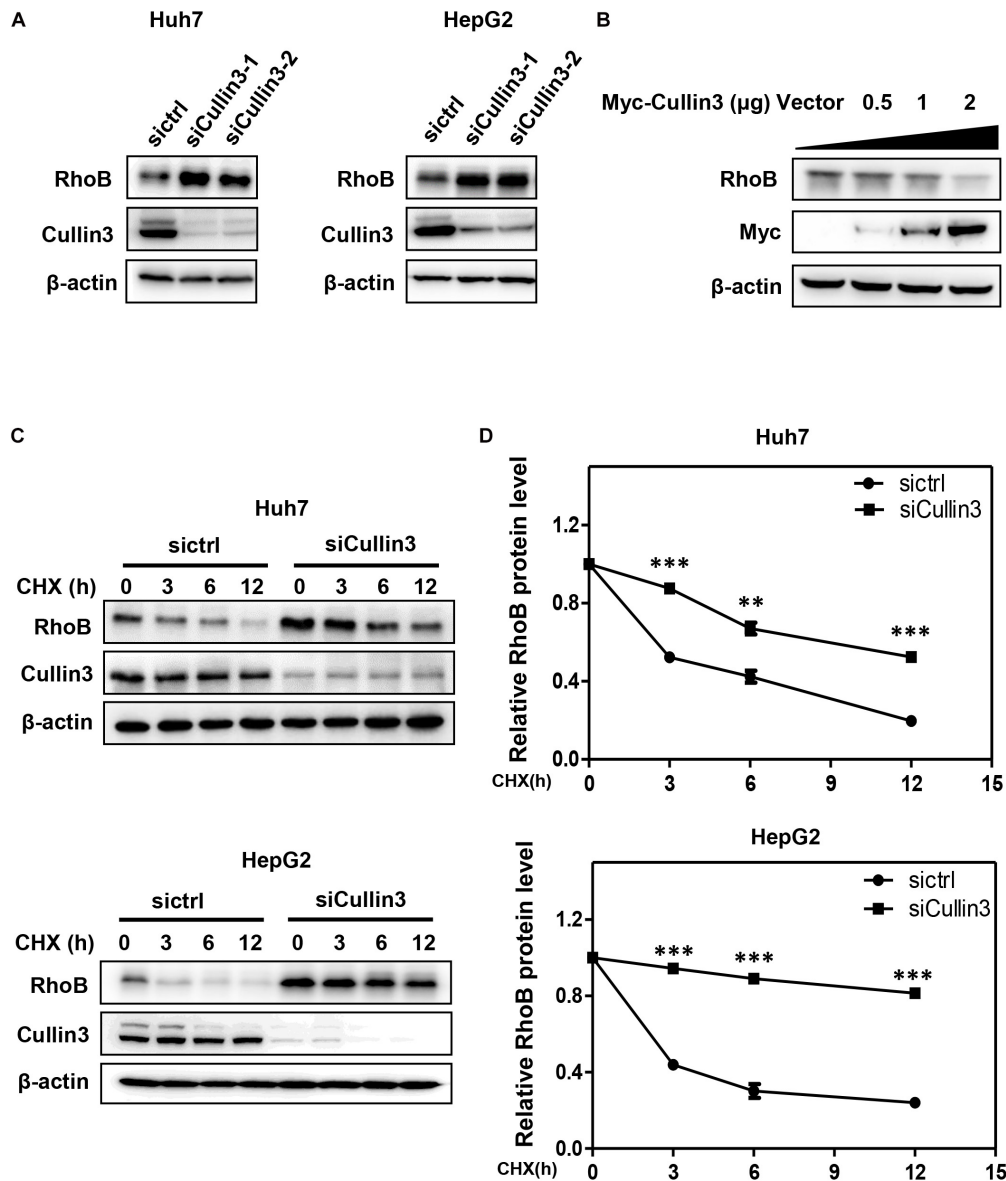


**FIGURE 1 |** Cullin3 regulated protein degradation of RhoB. **(A)** Downregulation of Cullin3 induced remarkable RhoB accumulation in both Huh7 and HepG2 cells. Cells were transfected with ctrl (control), Cullin3-1 or Cullin3-2 siRNA for 96 h, and cell lysates were harvested for western blot analysis. **(B)** Cullin3 overexpression decreased the protein levels of endogenous RhoB. HEK293T cells were transfected with indicated concentration of Myc-Cullin3 plasmid or empty vector, and cell lysates were harvested for western blot analysis. **(C)** Knockdown of Cullin3 extended the half-life of RhoB. Cells were transfected with indicated siRNAs then treated with 50  $\mu$ g/mL cycloheximide (CHX) for the indicated time and harvested for western blot analysis. **(D)** The protein levels were quantified by densitometric analysis and statistical analysis was performed.  $**P < 0.01$  and  $***P < 0.001$  vs. control group.

found that knockdown of TNFAIP1 using siRNA significantly extended the half-life of RhoB in both Huh7 and HepG2 cells (Figures 2C,D). These data suggested that TNFAIP1 regulated RhoB degradation.

### TNFAIP1 Interacted With RhoB

To determine whether TNFAIP1, a well-defined adaptor protein of CRL3 complex, interacted with RhoB, co-immunoprecipitation assay was applied. First, immunoprecipitation assay with anti-RhoB antibody was

performed. As shown in Figure 3A, endogenous RhoB could specifically pull-down TNFAIP1 in HepG2 cells. Furthermore, endogenous TNFAIP1 specifically combined with RhoB (Figure 3B). Consistently, overexpression of HA-TNFAIP1 in transfected HEK293T cells also interacted with Flag-RhoB (Figure 3C). Next, we used immunofluorescence assay to determine whether RhoB co-localize with TNFAIP1 in cells, and found that the endogenous protein RhoB co-localized with TNFAIP1 in the cytoplasm and plasma membrane of both HepG2 and HEK293T cells (Figure 3D). Taken

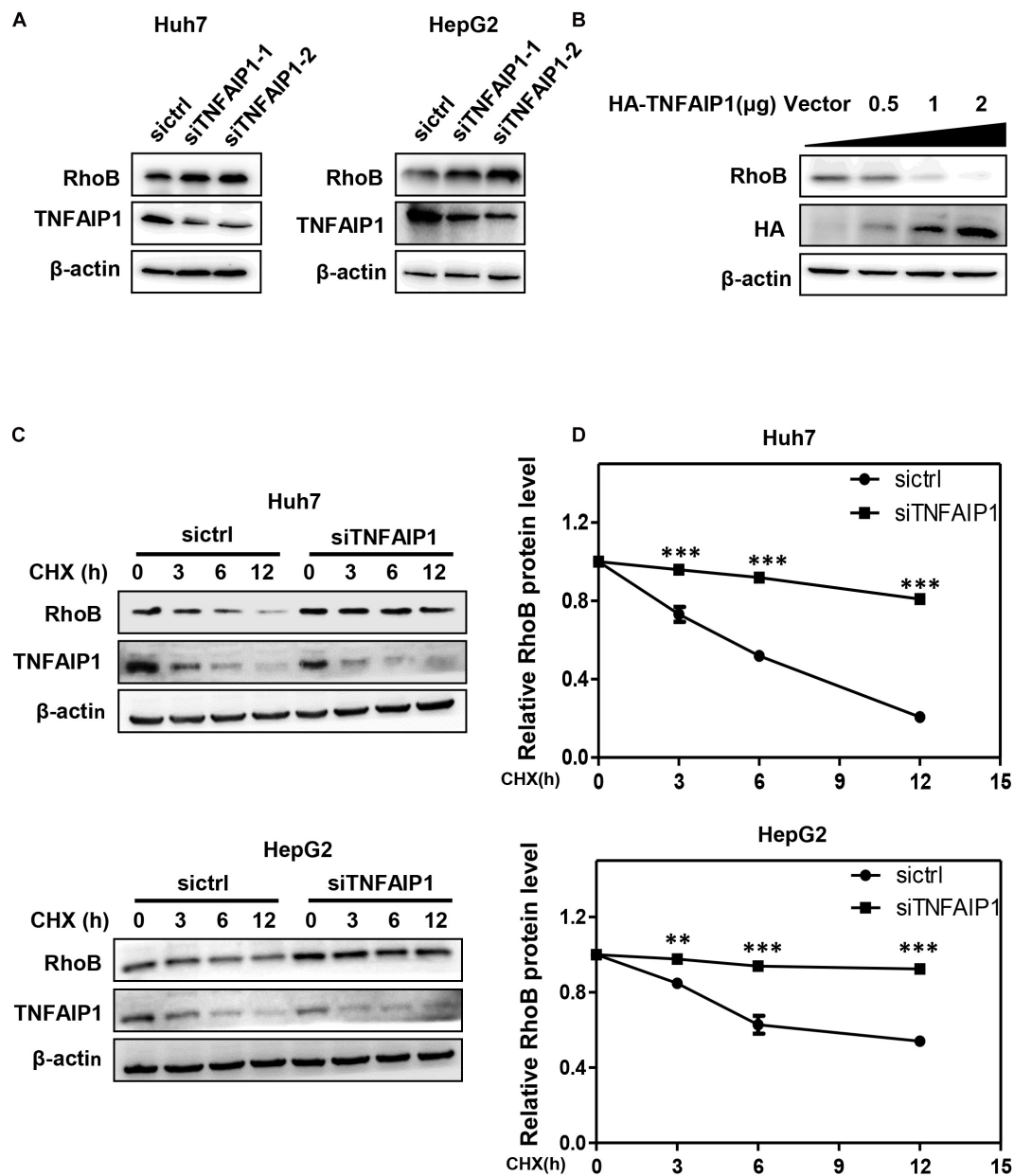


**FIGURE 2 |** The BTB domain protein TNFAIP1 regulated RhoB degradation. **(A)** Knockdown of TNFAIP1 led to RhoB accumulation in both Huh7 and HepG2 cells. Cells were transfected with ctrl (control), TNFAIP1-1 or TNFAIP1-2 siRNA for 96 h, and cell lysates were harvested for western blot analysis. **(B)** Overexpression of TNFAIP1 down-regulated the protein levels of endogenous RhoB. HEK293T cells were transfected with indicated concentration of HA-TNFAIP1 plasmid or empty vector, and cell lysates were harvested for western blot analysis. **(C)** Ablation of TNFAIP1 prolonged the half-life of RhoB. Huh7 and HepG2 cells were transfected with indicated siRNAs for 96 h. After 50 μg/mL cycloheximide (CHX) treatment at the indicated time, cell lysates were harvested for western blot analysis. **(D)** The protein levels were quantified by densitometric analysis and statistical analysis was performed. \*\* $P < 0.01$  and \*\*\* $P < 0.001$  vs. control group.

together, our data demonstrated that TNFAIP1 specifically bound with RhoB.

## The Ubiquitination of RhoB Was Mediated by Cullin3-TNFAIP1 Complex

Next, we determine whether downregulation of Cullin3 and TNFAIP1 affected RhoB ubiquitination. As shown in

**Figures 4A,B**, downregulation of Cullin3 or TNFAIP1 via siRNA silencing significantly reduced the ubiquitination level of RhoB in both Huh7 and HepG2 cells. Furthermore, the ubiquitination level of RhoB was also strongly promoted upon Cullin3 or TNFAIP1 overexpression in HEK293T cells (**Figures 4C,D**). These findings demonstrated that Cullin3-TNFAIP1 complex functioned as an E3 ubiquitin ligase to mediate RhoB degradation.

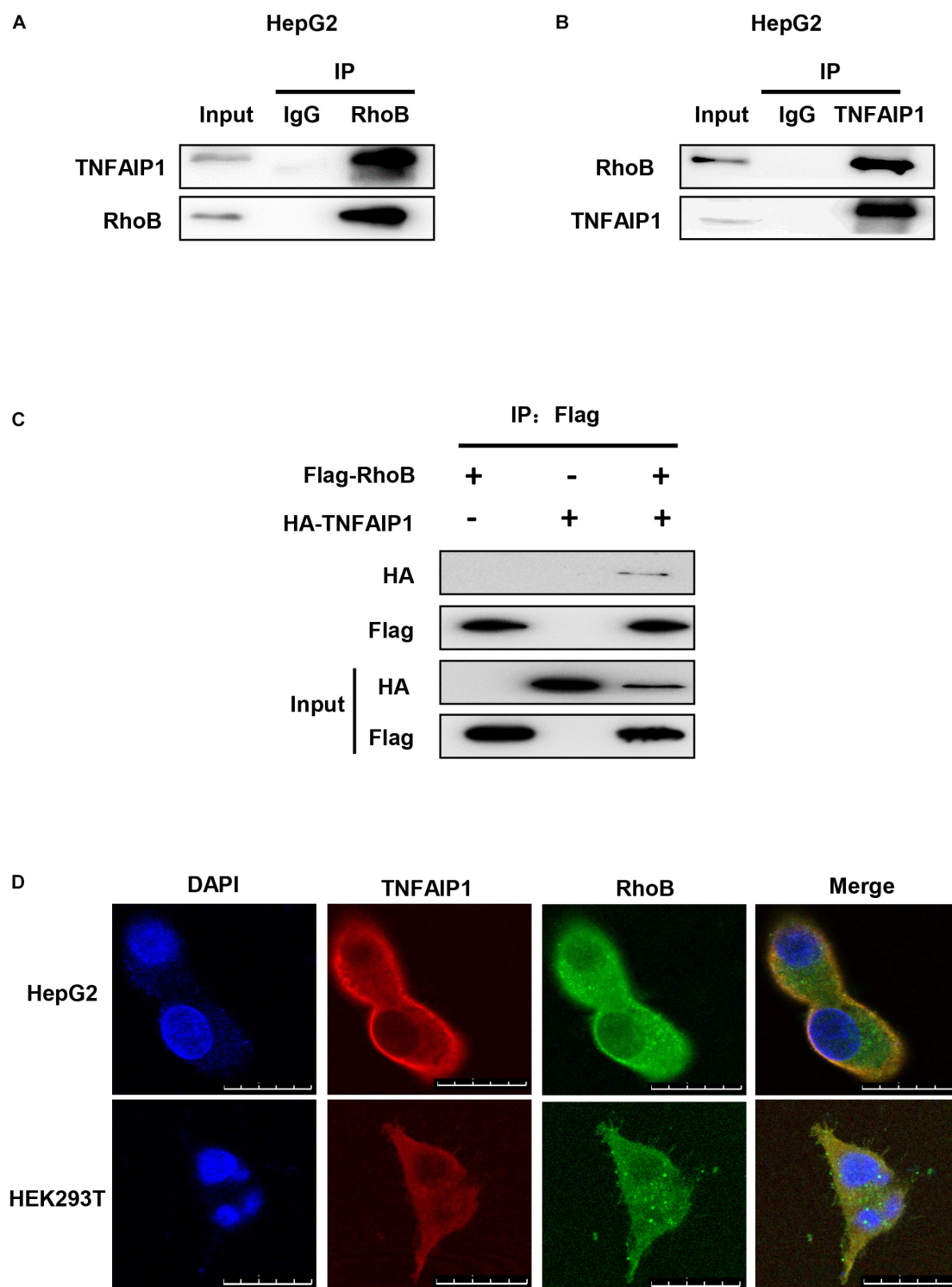


**FIGURE 3 |** TNFAIP1 interacted with RhoB. **(A)** Endogenous RhoB interacted with TNFAIP1. HepG2 cells were treated with MG132 (5  $\mu$ M) for 6 h, then cells lysates were subjected to immunoprecipitation with anti-RhoB antibody. **(B)** Endogenous TNFAIP1 interacted with RhoB. HepG2 cells were treated with MG132 (5  $\mu$ M) for 6 h, then cell lysates were subjected to immunoprecipitation with anti-TNFAIP1 antibody. **(C)** Exogenous RhoB and TNFAIP1 bound to each other. Plasmids expressed Flag-RhoB or HA-TNFAIP1 alone or expressed Flag-RhoB and HA-TNFAIP1 simultaneously were transfected into HEK293T cells. Cell lysates were subjected to immunoprecipitation with anti-Flag M2 beads. **(D)** Endogenous TNFAIP1 and RhoB co-localized in cytoplasm and plasma membrane. HepG2 and HEK293T cells were fixed and stained for TNFAIP1 and RhoB. Bars, 25  $\mu$ m.



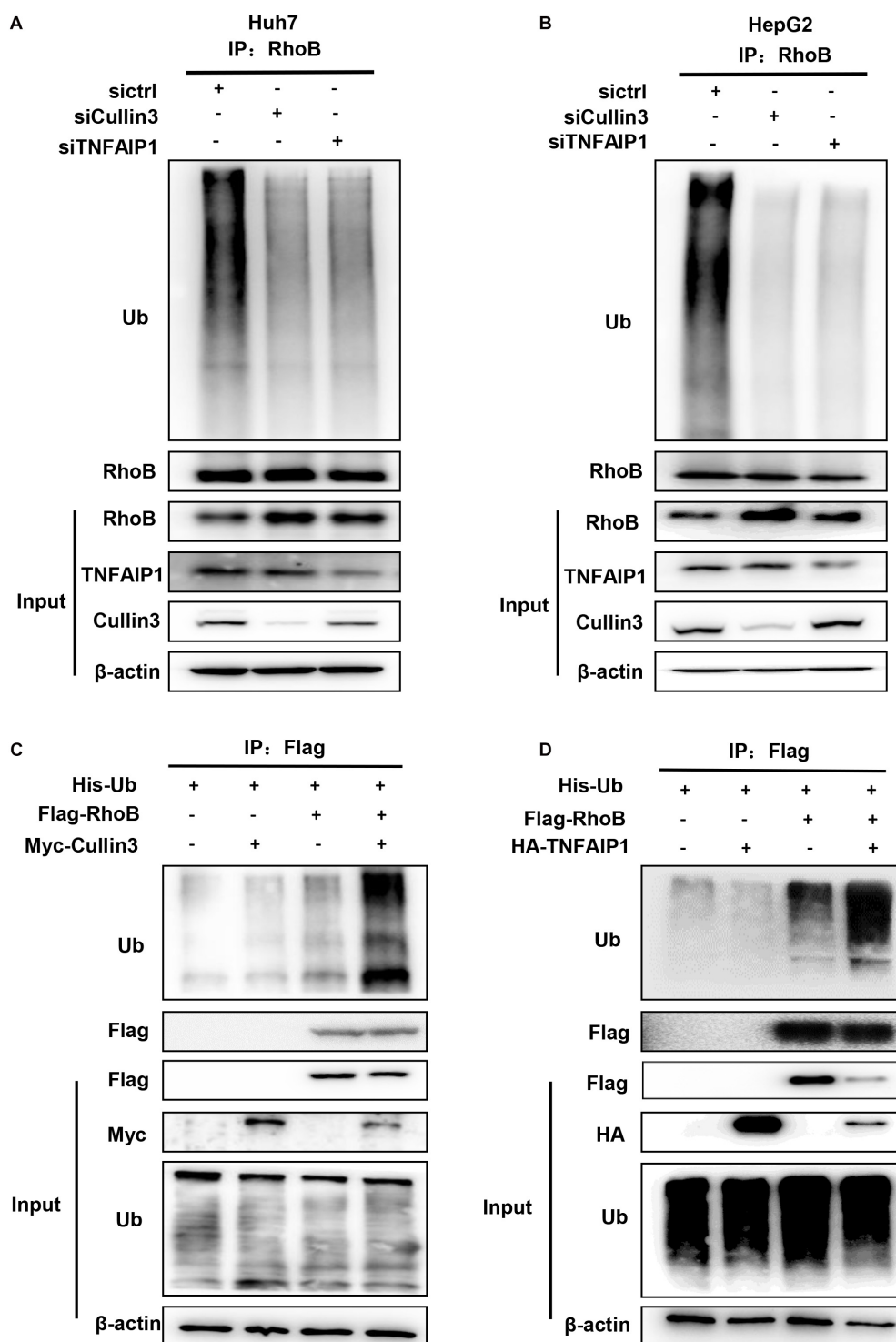


**FIGURE 4 |** Component of CRL3 mediated RhoB ubiquitination. **(A)** Downregulation of Cullin3 and TNFAIP1 inhibited RhoB polyubiquitination in Huh7 cells. Huh7 cells were transfected with ctrl (control), Cullin3 or TNFAIP1 siRNA for 96 h and followed with MG132 (5  $\mu$ M) for 6 h. Cell lysates were subjected to immunoprecipitation with anti-RhoB antibody. **(B)** Cullin3 and TNFAIP1 depletion suppressed ubiquitination of RhoB in HepG2 cells. HepG2 cells were transfected with ctrl (control), Cullin3 or TNFAIP1 siRNA for 96 h and followed with MG132 (5  $\mu$ M) treatment. Cell lysates were harvested and subjected to immunoprecipitation with anti-RhoB antibody. **(C)** Cullin3 promoted RhoB ubiquitination. HEK293T cells were transfected with indicated plasmids combinations of His-tagged Ub (His-Ub), Flag-tagged RhoB (Flag-RhoB), and Myc-tagged Cullin3 (Myc-Cullin3). Cell lysates were subjected to immunoprecipitation assay with anti-Flag beads. **(D)** TNFAIP1 promoted RhoB ubiquitination. HEK293T cells were transfected with indicated plasmids combinations of His-tagged Ub (His-Ub), Flag-tagged RhoB (Flag-RhoB), and HA-tagged TNFAIP1 (HA-TNFAIP1). Cell lysates were subjected to immunoprecipitation assay with anti-Flag beads.

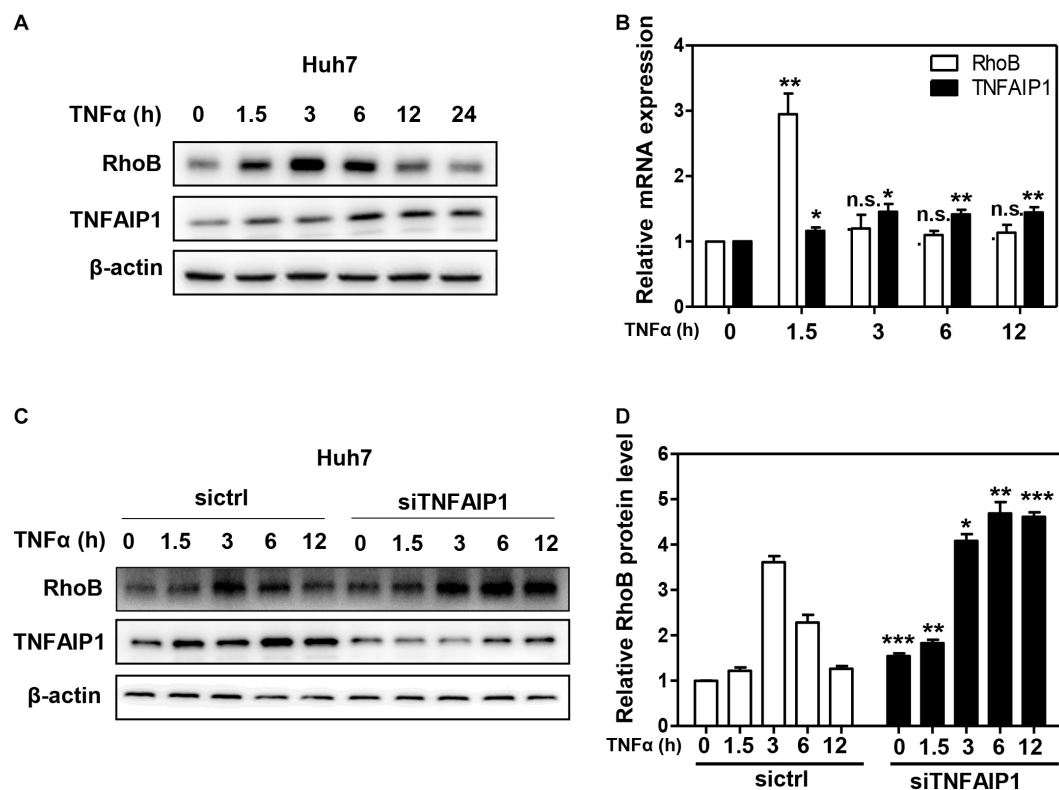


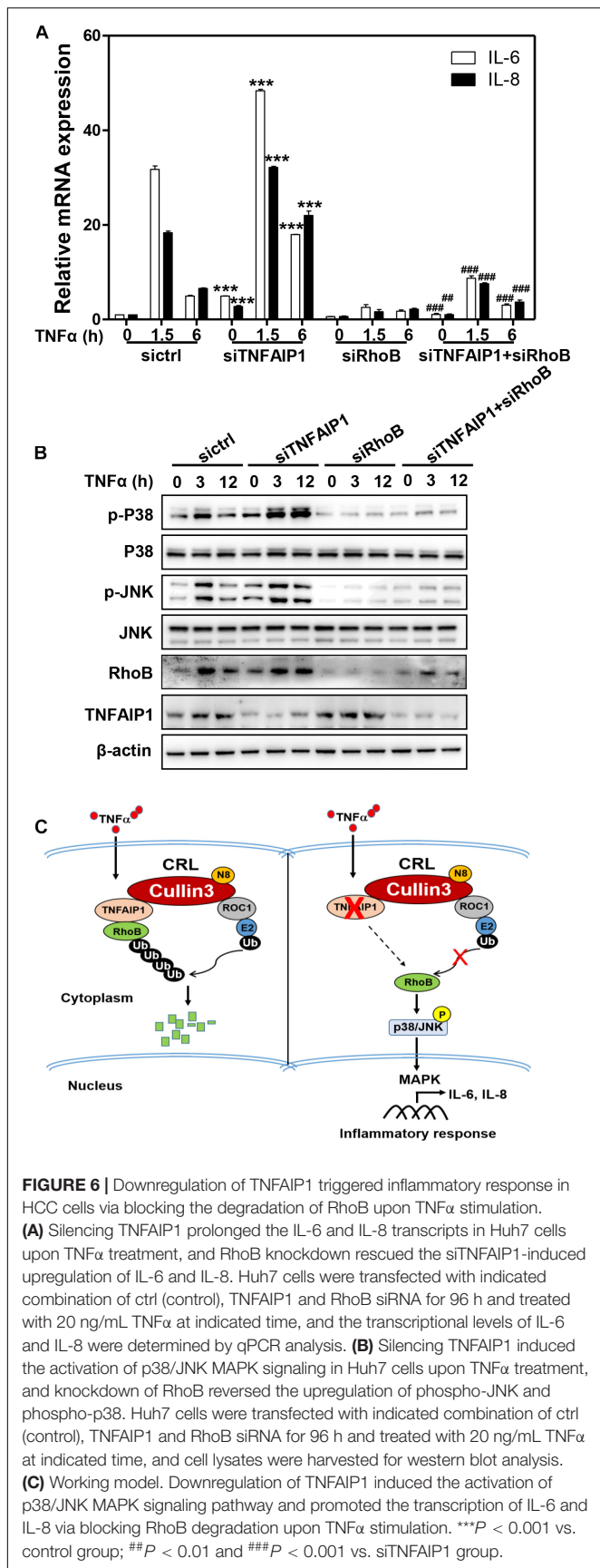
**FIGURE 5 |** The turnover of RhoB upon TNF $\alpha$  stimulation is regulated by TNFAIP1. **(A)** Time course of induction of TNFAIP1 and RhoB protein levels upon TNF $\alpha$  treatment in Huh7 cells. Huh7 cells were treated with 20 ng/mL TNF $\alpha$  at indicated time and determined the protein levels of RhoB and TNFAIP1 by western blot analysis with  $\beta$ -actin as a loading control. **(B)** Time course of induction of TNFAIP1 and RhoB transcripts upon TNF $\alpha$  treatment in Huh7 cells. Huh7 cells were treated with 20 ng/mL TNF $\alpha$  at indicated time and determined the transcriptional levels of RhoB and TNFAIP1 by qPCR analysis. **(C)** Silencing TNFAIP1 extended the half-life of RhoB in Huh7 cells upon TNF $\alpha$  treatment. Huh7 cells were treated with 20 ng/mL TNF $\alpha$  at indicated time and western blot was used to analyze the RhoB protein levels upon TNFAIP1 knockdown via siRNA silencing with  $\beta$ -actin as a loading control. **(D)** The protein levels were quantified by densitometric analysis and statistical analysis was performed. \* $P < 0.05$ , \*\* $P < 0.01$ , and \*\*\* $P < 0.001$  vs. control group; n.s. = not significant.

## Downregulation of TNFAIP1 Enhanced Inflammatory Response via Blocking the Degradation of RhoB Upon TNF $\alpha$ Stimulation

Given that RhoB participated in the inflammatory response upon TNF $\alpha$  stimulation (Kroon et al., 2013; Marcosramiro et al., 2016), we further determined the role of TNFAIP1-mediated RhoB degradation in TNF $\alpha$ -induced inflammatory response. First, we examined the expression of TNFAIP1 and RhoB in TNF $\alpha$ -stimulated Huh7 cells. As shown in **Figure 5A**, the protein levels of RhoB reached highest at 3 h after TNF $\alpha$  stimulation, and then gradually decreased with the increase of TNFAIP1 expression. Consistently, the mRNA levels of RhoB reached its peak at 1.5 h, accompanied by the transcriptional activation of TNFAIP1 upon TNF $\alpha$  stimulation (**Figure 5B**). To determine whether the degradation of RhoB after 3 h with TNF $\alpha$  treatment was elicited by TNFAIP1, we examined the turnover rate of RhoB when silencing TNFAIP1. As shown, knockdown of TNFAIP1 significantly blocked the degradation of RhoB after TNF $\alpha$  treatment for 3 h (**Figures 5C,D**). These results indicated that the

turnover of RhoB after TNF $\alpha$  stimulation is regulated by TNFAIP1 in HCC cells.

Previous studies demonstrated that RhoB plays a pivotal role in the TNF $\alpha$ -induced inflammatory response of endothelial cells and macrophages by activating MAP kinase pathway (Nwariaku et al., 2003; Kroon et al., 2013; Liu et al., 2017). Furthermore, endothelial cells respond to TNF $\alpha$  stimulation by upregulating the expression of pro-inflammatory cytokines, such as IL-6 and IL-8 (Bradley, 2008; Kalliolias and Ivashkiv, 2016). Together with our aforementioned results, we hypothesized that TNF $\alpha$  regulated pro-inflammatory cytokines expression in HCC cells through TNFAIP1-mediated RhoB degradation. As expected, ablation of TNFAIP1 via siRNA silencing markedly upregulated the expression of pro-inflammatory molecules IL-6 and IL-8 in TNF $\alpha$ -stimulated Huh7 cells. Furthermore, the upregulation of IL-6 and IL-8 induced by TNFAIP1 depletion were rescued by simultaneous RhoB knocking down (**Figure 6A**). We further showed that TNFAIP1 knockdown resulted in the increased levels of phospho-JNK and phospho-p38 upon TNF $\alpha$  stimulation. Rescue experiment results demonstrated that additional RhoB depletion reversed the TNFAIP1 knockdown-induced the accumulations of the



phospho-JNK and phospho-p38 (**Figure 6B**). Taken together, our finding demonstrated that inactivation of TNFAIP1 blocked RhoB degradation, thereby enhancing the inflammatory response of HCC cells induced by activation of MAPK signaling pathway (**Figure 6C**).

## DISCUSSION

The small GTPase RhoB is critically required for the inflammatory response elicited by pro-inflammatory cytokines (Biro et al., 2014; Zhang et al., 2017). However, the underlying mechanisms of RhoB degradation in inflammatory response remain exclusive. In this study, for the first time, we demonstrated that TNFAIP1 functioned as the novel adaptor connecting RhoB to Cullin3 to target RhoB for ubiquitination and degradation, and TNF $\alpha$ -induced inflammatory response is regulated by TNFAIP1-mediated RhoB expression in HCC cells. Our findings highlight a crucial role of TNFAIP1-induced RhoB degradation in regulating tumor inflammatory response. It is worth noting that Cullin3-KCTD10 complex has also been reported to ubiquitinate RhoB (Kovacevic et al., 2018; Murakami et al., 2019). Therefore, we speculated that KCTD10 and TNFAIP1 might have redundancy or compensation mechanism for RhoB expression. As shown, we found that downregulation of TNFAIP1 or KCTD10 alone induced RhoB upregulation in both Huh7 and HepG2 cells. In addition, knocking down TNFAIP1 and KCTD10 simultaneously resulted in the more accumulation of RhoB compared with TNFAIP1 and KCTD10 knockdown alone (**Supplementary Figure 2**). Our results suggested that TNFAIP1 and KCTD10 collectively mediated the RhoB expression in HCC cells.

Previous studies found that the pro-inflammatory mediators such as TNF $\alpha$  potentially stimulated RhoB expression (Nübel et al., 2004; Rodriguez et al., 2007; Vega and Ridley, 2018). However, it is not clear how RhoB degradation after TNF $\alpha$  stimulation is regulated. In our study, we demonstrated that TNF $\alpha$  induced the transcriptional activation of TNFAIP1 and RhoB at 1.5 h upon TNF $\alpha$  stimulation in HCC cells. Subsequently, RhoB protein levels reached a peak at 3 h, and then gradually decreased to the baseline level with the increase of TNFAIP1 protein expression. While TNFAIP1 was silenced, the half-life of RhoB was significantly delayed after TNF $\alpha$  stimulation for 3 h. Therefore, our findings revealed a previous unknown mechanism by which TNFAIP1 regulated RhoB stability upon TNF $\alpha$  stimulation.

TNF $\alpha$  triggered pro-inflammatory gene expression through the activation of both NF- $\kappa$ B and MAP kinase pathways (Kyriakis and Avruch, 2001; Zelová and Hošek, 2013; Webster and Vucic, 2020). Therefore, we determined the two main signalling cascades activated by TNF $\alpha$  after TNFAIP1 silencing. Consistent with the previous reports that RhoB regulated TNF $\alpha$ -dependent stress-activated MAPKs in endothelial cells (Nwariaku et al., 2003; Kroon et al., 2013). Our data suggested that activation of p38 MAP kinase and JNK by TNF $\alpha$  was critically dependent on TNFAIP1-induced RhoB degradation in HCC cells. However, downregulation of TNFAIP1 had no effect on NF- $\kappa$ B activation

upon TNF $\alpha$  stimulation (data not shown). Thus, TNFAIP1-mediated RhoB degradation regulated stress-activated MAPKs in HCC cells. In view of TNFAIP1 was highly expressed in many human cancer cells including lung cancer cells and osteosarcoma cells, and modulated tumorigenesis and cancer cell migration (Zhang et al., 2014; Li et al., 2020). Future study will be performed to elucidate the effect of TNFAIP1-mediated RhoB degradation on tumor inflammatory microenvironment and tumorigenesis.

In summary, our study highlighted a pivotal role of Cullin3-TNFAIP1 complex in mediating RhoB ubiquitination and degradation, and uncovered new mechanisms of CRL3 E3 ligase regulating inflammatory response through TNFAIP1-mediated RhoB degradation. TNFAIP1-RhoB axis played a key role in the regulation of tumor inflammatory microenvironment and could be considered as an attractive target for intervention in human cancers.

## DATA AVAILABILITY STATEMENT

The original contributions presented in the study are included in the article/Supplementary Material, further inquiries can be directed to the corresponding author/s.

## AUTHOR CONTRIBUTIONS

YZ, HZ, LJ, SW, and LL conceived and designed the experiments. YueL, SW, WZ, and LL performed the experiments and wrote the manuscript. LJ, SW, and LL revised and finalized the manuscript. LC, YP, and YupL contributed to critical experiment assistances.

## REFERENCES

- Awuh, J. A., Haug, M., Mildnerberger, J., Marstad, A., Do, C. P., Louet, C., et al. (2015). Keap1 regulates inflammatory signaling in *Mycobacterium avium*-infected human macrophages. *Proc. Natl. Acad. Sci. U.S.A.* 112, E4272–E4280. doi: 10.1073/pnas.1423449112
- Biro, M., Munoz, M. A., and Weninger, W. (2014). Targeting Rho-GTPases in immune cell migration and inflammation. *Br. J. Pharmacol.* 171, 5491–5506. doi: 10.1111/bph.12658
- Bradley, J. R. (2008). TNF-mediated inflammatory disease. *J. Pathol.* 214, 149–160. doi: 10.1002/path.2287
- Chen, H. Y., and Chen, R. (2016). Cullin 3 ubiquitin ligases in cancer biology: functions and therapeutic implications. *Front. Oncol.* 6:113. doi: 10.3389/fonc.2016.00113
- Chen, Y., Yang, Z., Meng, M., Zhao, Y., Dong, N., Yan, H., et al. (2009). Cullin mediates degradation of RhoA through evolutionarily conserved BTB adaptors to control actin cytoskeleton structure and cell movement. *Mol. Cell* 35, 841–855. doi: 10.1016/j.molcel.2009.09.004
- Cui, D., Xiong, X., and Zhao, Y. (2016). Cullin-RING ligases in regulation of autophagy. *Cell Div.* 11:8. doi: 10.1186/s13008-016-0022-5
- Dinkova-Kostova, A. T., Kostov, R. V., and Canning, P. (2017). Keap1, the cysteine-based mammalian intracellular sensor for electrophiles and oxidants. *Arch. Biochem. Biophys.* 617, 84–93. doi: 10.1016/j.abb.2016.08.005
- Dubiel, W., Dubiel, D., Wolf, D. A., and Naumann, M. (2017). Cullin 3-based ubiquitin ligases as master regulators of mammalian cell differentiation. *Trends Biochem. Sci.* 43, 95–107. doi: 10.1016/j.tibs.2017.11.010
- Duda, D. M., Scott, D. C., Calabrese, M. F., Zimmerman, E. S., Zheng, N., and Schulman, B. A. (2011). Structural regulation of cullin-RING ubiquitin ligase complexes. *Curr. Opin. Struct. Biol.* 21, 257–264. doi: 10.1016/j.sbi.2011.01.003
- Fritz, G., and Kaina, B. (2001). Transcriptional activation of the small GTPase gene rhoB by genotoxic stress is regulated via a CCAAT element. *Nucleic Acids Res.* 29, 792–798. doi: 10.1093/nar/29.3.792
- Genschik, P., Sumara, I., and Lechner, E. (2013). The emerging family of CULLIN3-RING ubiquitin ligases (CRL3s): cellular functions and disease implications. *EMBO J.* 32, 2307–2320. doi: 10.1038/emboj.2013.173
- Greten, F. R., and Grivnenkov, S. I. (2019). Inflammation and cancer: triggers, mechanisms, and consequences. *Immunity* 51, 27–41. doi: 10.1016/j.immuni.2019.06.025
- Gutierrez, E., Cahatol, I., Bailey, C. A. R., Lafargue, A., Zhang, N., Song, Y., et al. (2019). Regulation of RhoB gene expression during tumorigenesis and aging process and its potential applications in these processes. *Cancers* 11:818. doi: 10.3390/cancers11060818
- Hu, X., Yan, F., Wang, F., Yang, Z., Xiao, L., Li, L., et al. (2012). TNFAIP1 interacts with KCTD10 to promote the degradation of KCTD10 proteins and inhibit the transcriptional activities of NF- $\kappa$ B and AP-1. *Mol. Biol. Rep.* 39, 9911–9919. doi: 10.1007/s11033-012-1858-7
- Huang, G., Su, J., Zhang, M., Jin, Y., Wang, Y., Zhou, P., et al. (2017). RhoB regulates the function of macrophages in the hypoxia-induced inflammatory response. *Cell Mol. Immunol.* 14, 265–275. doi: 10.1038/cmi.2015.78
- Huang, M., and Prendergast, G. C. (2006). RhoB in cancer suppression. *Histol. Histopathol.* 21, 213–218. doi: 10.14670/hh-21.213
- Kalliolias, G. D., and Ivashkiv, L. B. (2016). TNF biology, pathogenic mechanisms and emerging therapeutic strategies. *Nat. Rev. Rheumatol.* 12, 49–62. doi: 10.1038/nrrheum.2015.169

JX and YJ performed statistical analysis of the data. All authors read and approved the final manuscript.

## FUNDING

This research was supported by the National Natural Science Foundation of China (Nos. 81602072, 81902380, and 81625018), National High Technology Research and Development Program of China (No. 2015AA021107-019), Scientific Research Project of Shanghai Science and Technology Commission (No. 18411960600), Shanghai Technological Innovation Action Projects (No. 18411950800), Shanghai Sailing Program (No. 17YF1405000), and Shanghai “Rising Stars of Medical Talent” Youth Development Program, Outstanding Youth Medical Talents, 2018.

## SUPPLEMENTARY MATERIAL

The Supplementary Material for this article can be found online at: <https://www.frontiersin.org/articles/10.3389/fcell.2021.617134/full#supplementary-material>

**Supplementary Figure 1** | Downregulation of TNFAIP1 did not affect the protein level of Cullin3 in Huh7 or HepG2 cells. Cells were transfected with ctrl (control), TNFAIP1-1 or TNFAIP1-2 siRNA for 96 h, and cell lysates were harvested for western blot analysis.

**Supplementary Figure 2** | Knocking down TNFAIP1 and KCTD10 simultaneously resulted in the more accumulation of RhoB compared with TNFAIP1 and KCTD10 knockdown alone. Huh7 and HepG2 cells were transfected with indicated combination of ctrl (control), TNFAIP1 and KCTD10 siRNA for 96 h and cell lysates were harvested for western blot analysis.



- Karlsson, R., Pedersen, E. D. K., Wang, Z., and Brakebusch, C. (2009). Rho GTPase function in tumorigenesis. *Biochim. Biophys. Acta* 1796, 91–98. doi: 10.1016/j.bbcan.2009.03.003
- Kim, D., Chung, K., Choi, S., Jung, Y., Park, S., Han, G., et al. (2009). RhoB induces apoptosis via direct interaction with TNFAIP1 in HeLa cells. *Int. J. Cancer* 125, 2520–2527. doi: 10.1002/ijc.24617
- Kovacevic, I., Sakaue, T., Majolee, J., Pronk, M., Maekawa, M., Geerts, D., et al. (2018). The Cullin-3-Rbx1-KCTD10 complex controls endothelial barrier function via K63 ubiquitination of RhoB. *J. Cell Biol.* 217, 1015–1032. doi: 10.1083/jcb.201606055
- Kroon, J., Tol, S., van Amstel, S., Elias, J. A., and Fernandez-Borja, M. (2013). The small GTPase RhoB regulates TNF $\alpha$  signaling in endothelial cells. *PLoS One* 8:e75031. doi: 10.1371/journal.pone.0075031
- Kwon, J. E., La, M., Oh, K. H., Oh, Y. M., Kim, G. R., Seol, J. H., et al. (2006). BTB domain-containing Speckle-type POZ Protein (SPOP) serves as an adaptor of Daxx for Ubiquitination by Cul3-based ubiquitin ligase. *J. Biol. Chem.* 281, 12664–12672. doi: 10.1074/jbc.M600204200
- Kyriakis, J. M., and Avruch, J. (2001). Mammalian mitogen-activated protein kinase signal transduction pathways activated by stress and inflammation. *Physiol. Rev.* 81, 807–869. doi: 10.1152/physrev.2001.81.2.807
- Landskron, G., De la Fuente, M., Thuwajit, P., Thuwajit, C., and Hermoso, M. A. (2014). Chronic inflammation and cytokines in the tumor microenvironment. *J. Immunol. Res.* 2014:149185. doi: 10.1155/2014/149185
- Li, G., Ci, W., Karmakar, S., Chen, K., Dhar, R., Fan, Z., et al. (2014). SPOP promotes tumorigenesis by acting as a key regulatory hub in kidney cancer. *Cancer Cell* 25, 455–468. doi: 10.1016/j.ccr.2014.02.007
- Li, L., Zhang, W., Liu, Y., Liu, X., Cai, L., Kang, J., et al. (2020). The CRL3(BTBD9) E3 ubiquitin ligase complex targets TNFAIP1 for degradation to suppress cancer cell migration. *Signal. Transduct. Target Ther.* 5:42. doi: 10.1038/s41392-020-0140-z
- Li, Y. D., Liu, Y.-P., Cao, D.-M., Yan, Y.-M., Hou, Y.-N., Zhao, J.-Y., et al. (2011). Induction of small G protein RhoB by non-genotoxic stress inhibits apoptosis and activates NF- $\kappa$ B. *J. Cell Physiol.* 226, 729–738. doi: 10.1002/jcp.22394
- Liu, M., Sun, Z., Zhou, A., Li, H., Yang, L., Zhou, C., et al. (2010). Functional characterization of the promoter region of human TNFAIP1 gene. *Mol. Biol. Rep.* 37, 1699–1705. doi: 10.1007/s11033-009-9588-1
- Liu, N., Yu, Z., Xun, Y., Li, M., Peng, X., Xiao, Y., et al. (2016). TNFAIP1 contributes to the neurotoxicity induced by Abeta25–35 in Neuro2a cells. *BMC Neurosci.* 17:51. doi: 10.1186/s12868-016-0286-3
- Liu, S., Huang, L., Lin, Z., Hu, Y., Chen, R., Wang, L., et al. (2017). RhoB induces the production of proinflammatory cytokines in TLR-triggered macrophages. *Mol. Immunol.* 87, 200–206. doi: 10.1016/j.molimm.2017.04.015
- Marcosramiro, B., García-Weber, D., Barroso, S., Feito, J., Ortega, M. C., Cernuda-Morollón, E., et al. (2016). RhoB controls endothelial barrier recovery by inhibiting Rac1 trafficking to the cell border. *J. Cell Biol.* 213, 385–402. doi: 10.1083/jcb.201504038
- Merlet, J., Burger, J., Gomes, J. E., and Pintard, L. (2009). Regulation of cullin-RING E3 ubiquitin-ligases by neddylation and dimerization. *Cell Mol. Life Sci.* 66, 1924–1938. doi: 10.1007/s00018-009-8712-7
- Murakami, A., Maekawa, M., Kawai, K., Nakayama, J., Araki, N., Semba, K., et al. (2019). Cullin-3/KCTD10 E3 complex is essential for Rac1 activation through RhoB degradation in human epidermal growth factor receptor 2-positive breast cancer cells. *Cancer Sci.* 110, 650–661. doi: 10.1111/cas.13899
- Nübel, T., Dippold, W., Kleinert, H., Kaina, B., and Fritz, G. (2004). Lovastatin inhibits Rho-regulated expression of E-selectin by TNF $\alpha$  and attenuates tumor cell adhesion. *FASEB J.* 18, 140–142. doi: 10.1096/fj.03-0261fj
- Nwariaku, F. E., Rothenbach, P., Liu, Z., Zhu, X., Turnage, R. H., and Terada, L. S. (2003). Rho inhibition decreases TNF-induced endothelial MAPK activation and monolayer permeability. *J. Appl. Physiol.* 95, 1889–1895. doi: 10.1152/japplphysiol.00225.2003
- Petroski, M. D., and Deshaies, R. J. (2005). Function and regulation of cullin-RING ubiquitin ligases. *Nat. Rev. Mol. Cell Biol.* 6, 9–20. doi: 10.1038/nrm1547
- Rodriguez, P. L., Sahay, S., Olabisi, O. O., and Whitehead, I. P. (2007). ROCK I-mediated activation of NF- $\kappa$ B by RhoB. *Cell Signal.* 19, 2361–2369. doi: 10.1016/j.cellsig.2007.07.021
- Shi, J., and Wei, L. (2013). Rho kinases in cardiovascular physiology and pathophysiology: the effect of fasudil. *J. Cardiovasc. Pharmacol.* 62, 341–354. doi: 10.1097/FJC.0b013e3182a3718f
- Vega, F. M., and Ridley, A. J. (2018). The RhoB small GTPase in physiology and disease. *Small GTPases* 9, 384–393. doi: 10.1080/21541248.2016.1253528
- Webster, J. D., and Vucic, D. (2020). The balance of TNF mediated pathways regulates inflammatory cell death signaling in healthy and diseased tissues. *Front. Cell Dev. Biol.* 8:365. doi: 10.3389/fcell.2020.00365
- Wheeler, A. P., and Ridley, A. J. (2004). Why three Rho proteins? RhoA, RhoB, RhoC, and cell motility. *Exp. Cell Res.* 301, 43–49. doi: 10.1016/j.yexcr.2004.08.012
- Xiao, Y., Huang, S., Qiu, F., Ding, X., Sun, Y., and Wei, C. (2020). Tumor necrosis factor  $\alpha$ -induced protein 1 as a novel tumor suppressor through selective downregulation of CSNK2B blocks nuclear factor- $\kappa$ B activation in hepatocellular carcinoma. *EBioMedicine* 51:102603. doi: 10.1016/j.ebiom.2019.102603
- Zelová, H., and Hošek, J. (2013). TNF- $\alpha$  signalling and inflammation: interactions between old acquaintances. *Inflamm. Res.* 62, 641–651. doi: 10.1007/s00011-013-0633-0
- Zhang, C.-L., Wang, C., Yan, W.-J., Gao, R., Li, Y.-H., and Zhou, X.-H. (2014). Knockdown of TNFAIP1 inhibits growth and induces apoptosis in osteosarcoma cells through inhibition of the nuclear factor- $\kappa$ B pathway. *Oncol. Rep.* 32, 1149–1155. doi: 10.3892/or.2014.3291
- Zhang, N., Fu, L., Bu, Y., Yao, Y., and Wang, Y. (2017). Downregulated expression of miR-223 promotes Toll-like receptor-activated inflammatory responses in macrophages by targeting RhoB. *Mol. Immunol.* 91, 42–48. doi: 10.1016/j.molimm.2017.08.026
- Zhao, Y., Li, S., Xia, N., Shi, Y., and Zhao, C. M. (2018). Effects of XIST/miR-137 axis on neuropathic pain by targeting TNFAIP1 in a rat model. *J. Cell Physiol.* 233, 4307–4316. doi: 10.1002/jcp.26254
- Zhao, Y., and Sun, Y. (2013). Cullin-RING Ligases as attractive anti-cancer targets. *Curr. Pharm. Des.* 19, 3215–3225. doi: 10.2174/13816128113199990300
- Zhu, Y., Yao, Z., Wu, Z., Mei, Y., and Wu, M. (2014). Role of tumor necrosis factor alpha-induced protein 1 in paclitaxel resistance. *Oncogene* 33, 3246–3255. doi: 10.1038/onc.2013.299

**Conflict of Interest:** The authors declare that the research was conducted in the absence of any commercial or financial relationships that could be construed as a potential conflict of interest.

Copyright © 2021 Liu, Zhang, Wang, Cai, Jiang, Pan, Liang, Xian, Jia, Li, Zhao and Zhang. This is an open-access article distributed under the terms of the Creative Commons Attribution License (CC BY). The use, distribution or reproduction in other forums is permitted, provided the original author(s) and the copyright owner(s) are credited and that the original publication in this journal is cited, in accordance with accepted academic practice. No use, distribution or reproduction is permitted which does not comply with these terms.



# Low-Dose Decitabine Augments the Activation and Anti-Tumor Immune Response of IFN- $\gamma$ <sup>+</sup> CD4<sup>+</sup> T Cells Through Enhancing I $\kappa$ B $\alpha$ Degradation and NF- $\kappa$ B Activation

Xiang Li<sup>1,2</sup>, Liang Dong<sup>2</sup>, Jiejie Liu<sup>2</sup>, Chunmeng Wang<sup>2</sup>, Yan Zhang<sup>2</sup>, Qian Mei<sup>2</sup>, Weidong Han<sup>2</sup>, Ping Xie<sup>1\*</sup> and Jing Nie<sup>2\*</sup>

## OPEN ACCESS

### Edited by:

Lingqiang Zhang,  
National Center for Protein Sciences  
Shanghai, China

### Reviewed by:

Murugan Kalimutho,  
QIMR Berghofer Medical Research  
Institute, Australia  
Jiyan Zhang,  
Independent Researcher,  
Beijing, China

### \*Correspondence:

Ping Xie  
xiep@ccmu.edu.cn  
Jing Nie  
nnj2002@163.com

### Specialty section:

This article was submitted to  
Cell Growth and Division,  
a section of the journal  
Frontiers in Cell and Developmental  
Biology

**Received:** 30 December 2020

**Accepted:** 23 February 2021

**Published:** 15 March 2021

### Citation:

Li X, Dong L, Liu J, Wang C,  
Zhang Y, Mei Q, Han W, Xie P and  
Nie J (2021) Low-Dose Decitabine  
Augments the Activation  
and Anti-Tumor Immune Response  
of IFN- $\gamma$ <sup>+</sup> CD4<sup>+</sup> T Cells Through  
Enhancing I $\kappa$ B $\alpha$  Degradation  
and NF- $\kappa$ B Activation.  
Front. Cell Dev. Biol. 9:647713.  
doi: 10.3389/fcell.2021.647713

<sup>1</sup> Department of Cell Biology, The Municipal Key Laboratory for Liver Protection and Regulation of Regeneration, Capital Medical University, Beijing, China, <sup>2</sup> Department of Bio-therapeutic, The First Medical Center, Chinese PLA General Hospital, Beijing, China

**Background:** CD4<sup>+</sup> T cells play multiple roles in controlling tumor growth and increasing IFN- $\gamma$ <sup>+</sup> T-helper 1 cell population could promote cell-mediated anti-tumor immune response. We have previously showed that low-dose DNA demethylating agent decitabine therapy promotes CD3<sup>+</sup> T-cell proliferation and cytotoxicity; however, direct regulation of purified CD4<sup>+</sup> T cells and the underlying mechanisms remain unclear.

**Methods:** The effects of low-dose decitabine on sorted CD4<sup>+</sup> T cells were detected both *in vitro* and *in vivo*. The activation, proliferation, intracellular cytokine production and cytotoxic activity of CD4<sup>+</sup> T cells were analyzed by FACS and DELFIA time-resolved fluorescence assays. *In vivo* ubiquitination assay was performed to assess protein degradation. Moreover, phosphor-p65 and I $\kappa$ B $\alpha$  levels were detected in sorted CD4<sup>+</sup> T cells from solid tumor patients with decitabine-based therapy.

**Results:** Low-dose decitabine treatment promoted the proliferation and activation of sorted CD4<sup>+</sup> T cells, with increased frequency of IFN- $\gamma$ <sup>+</sup> Th1 subset and enhanced cytolytic activity *in vitro* and *in vivo*. NF- $\kappa$ B inhibitor, BAY 11-7082, suppressed decitabine-induced CD4<sup>+</sup> T cell proliferation and IFN- $\gamma$  production. In terms of mechanism, low-dose decitabine augmented the expression of E3 ligase  $\beta$ -TrCP, promoted the ubiquitination and degradation of I $\kappa$ B $\alpha$  and resulted in NF- $\kappa$ B activation. Notably, we observed that *in vitro* low-dose decitabine treatment induced NF- $\kappa$ B activation in CD4<sup>+</sup> T cells from patients with a response to decitabine-primed chemotherapy rather than those without a response.

**Conclusion:** These data suggest that low-dose decitabine potentiates CD4<sup>+</sup> T cell anti-tumor immunity through enhancing I $\kappa$ B $\alpha$  degradation and therefore NF- $\kappa$ B activation and IFN- $\gamma$  production.

**Keywords:** decitabine, CD4<sup>+</sup> T cells, immune response, NF- $\kappa$ B activation, I $\kappa$ B $\alpha$  degradation

## INTRODUCTION

Immunotherapy has become a standard approach for the treatment of some types of cancers and has the potential to control tumor development. Most immunotherapy strategies devote to reinvigorate T cell function to evoke effective anti-tumor immune responses (Borst et al., 2018) and most clinical settings focus on the exploiting of cytotoxic CD8<sup>+</sup> T lymphocytes (CD8<sup>+</sup> CTLs) (Rosenberg and Restifo, 2015; Ott et al., 2017). CD4<sup>+</sup> T helper cells are recognized to be required for the formation of CD8<sup>+</sup> CTLs. Currently, numerous studies have demonstrated that CD4<sup>+</sup> T cells actively participate in shaping anti-tumor immunity (Kim and Cantor, 2014; Zander et al., 2019). Based on their functions and cytokine-producing patterns, CD4<sup>+</sup> T helper cells are comprised of different functional subsets, including IFN- $\gamma$ -producing T-helper 1 (Th1), T-helper 2 (Th2), T-helper 17 (Th17) and regulatory T cells (Tregs), which carry out specialized immunoregulatory functions to either enhance or inhibit immune response (Kim and Cantor, 2014). Th1 cells enhance CD8<sup>+</sup> CTLs function and enable CD8<sup>+</sup> CTLs to overcome the obstacles that typically hamper anti-tumor immunity, and Tregs are essential for maintenance of T cell homeostasis and prevention of autoimmunity. In addition, the cytotoxic effector CD4<sup>+</sup> T cells, most closely related to Th1 subset, can directly eliminate tumor cells through the MHC class II-dependent manner, which destroy target cells by secreting granzyme B and perforin (Takeuchi and Saito, 2017). However, the functional diversity of CD4<sup>+</sup> T cells and disorders of CD4<sup>+</sup> T cell subsets weaken the anti-tumor responses (Lee et al., 2012). Thus, boosting Th1 and cytotoxic CD4<sup>+</sup> T cell responses and inhibiting Tregs functions may obtain optimal anti-tumor responses.

Epigenetic modifying agent decitabine (5-Aza-2'-deoxycytidine, DAC) is a unique cytosine analog and an inhibitor of DNA methyltransferases (DNMTs) (Jones and Taylor, 1980). Decitabine has been approved for the treatment of hematological diseases, such as myelodysplastic syndrome (MDS) (Kantarjian et al., 2007) and acute myelogenous leukemia (AML) (Kelly et al., 2010). At the very beginning, decitabine was used as a chemotherapy drug with relatively high doses (Aparicio and Weber, 2002). Unfortunately, extreme cytotoxicity and myelosuppression limited the clinical applications of decitabine (Oki et al., 2007). Recently, preclinical investigations and clinical trials have shown that low doses of decitabine have minimal cytotoxicity and combination therapy could achieve an optimal anti-tumor effect (Mei et al., 2015; Yu et al., 2018). Genome-wide DNA methylation is a stable epigenetic characteristic in tumor cells and closely associates with tumor development and progression (Chatterjee et al., 2018). Moreover, emerging evidences have revealed that DNA hypermethylation impairs the immunogenicity and immune recognition, resulting in tumor immune escape (Maio et al., 2003). Low-dose decitabine suppresses function and induces degradation of DNMTs, considered as an immunotherapeutic drug to control tumor progression (Li et al., 2015; Yu et al., 2018). It is worth noting that most previous studies involved with the mechanism of low-dose decitabine therapy mainly focus on cancer cells and

CD8<sup>+</sup> T cells rather than CD4<sup>+</sup> T cells (Li et al., 2015; Topper et al., 2020). Epigenetic modification plays an important role in the differentiation of CD4<sup>+</sup> T cells (Shih et al., 2014; Tripathi and Lahesmaa, 2014), while the regulation of CD4<sup>+</sup> T cells in anti-tumor activity still needs to be deeply explored.

In our previous clinical trials, we have demonstrated that low-dose decitabine treatment increases CD4/CD8 ratio among peripheral T cells (Nie et al., 2016) and CD4<sup>+</sup> T cells infiltration in tumors. Furthermore, low-dose decitabine results in increased frequency of IFN- $\gamma$ <sup>+</sup> T cells (Li et al., 2017). However, the direct effect of low-dose decitabine on purified CD4<sup>+</sup> T cells and regulation mechanisms remain unclear. In this study, we sorted CD4<sup>+</sup> T cells, treated with low-dose decitabine, and detected the phenotype and cytotoxic activity. Moreover, we investigated the mechanism of low-dose decitabine-mediated increased frequency of IFN- $\gamma$ <sup>+</sup> CD4<sup>+</sup> T cells, and found that this effect was mediated by decitabine-induced protein degradation of I $\kappa$ B $\alpha$ , and this process was dependent on E3 ligase  $\beta$ -TrCP.

## MATERIALS AND METHODS

### Human Peripheral Blood

The peripheral blood was obtained from the cancer patients enrolled in the clinical trials of Chinese PLA general hospital ([www.clinicaltrials.gov](http://www.clinicaltrials.gov): NCT01799083). The collection and storage of peripheral blood were consistent with our previous study (Li et al., 2017) and normal peripheral blood was obtained from healthy donors. All peripheral blood was collected with the informed consent as approved by the ethics committee of the Chinese PLA general hospital, Beijing, China.

### CD4<sup>+</sup> T Cells Sorting, Culture, and Decitabine Treatment

Mouse CD4<sup>+</sup> T cells were purified from splenocytes of C57BL/6J using CD4<sup>+</sup> T Cell Isolation Kit (Miltenyi, Cat#130-104-454) according to the manufacturer's guide. CD4<sup>+</sup> T cells were activated *in vitro* with plate-bound 2  $\mu$ g/ml anti-CD3 (Biolegend, Cat#100340) and 2  $\mu$ g/ml anti-CD28 (Biolegend, Cat#102116) and recombinant IL-2 (cyagen, Cat#MEILP-0201) for 24 h. Human CD4<sup>+</sup> T cells were isolated from peripheral blood mononuclear cells of healthy donors and cancer patients using CD4<sup>+</sup> T cell Isolation (Miltenyi, Cat#130-045-101). The sorted human CD4<sup>+</sup> T cells were activated with plate-bound anti-CD3 antibody (Takara, Cat#T210) and rIL-2 (cyagen, Cat#HEILP-0201) for 24 h. Activated CD4<sup>+</sup> T cells were treated with PBS (CON) or decitabine (10 nM or indicated concentrations, Sigma-Aldrich, Cat#A3656) plus rIL-2 for 3 days. After decitabine treatment, CD4<sup>+</sup> T cells were analyzed by flow cytometry or adoptively transferred into tumor-bearing mice.

### *In vitro* Th1 Differentiation

CD4<sup>+</sup> T cells were sorted from mouse splenocytes and stimulated with plate-bound anti-CD3/CD28 in the presence of IL-12 (10 ng/mL) and anti-IL-4 (10  $\mu$ g/ml) for 24 h. Activated T cells were

treated with PBS or decitabine in the presence of IL-12 and anti-IL-4 for 3 days and flow cytometry was performed to detect the frequency of IFN- $\gamma^+$  cells in CD4 $^+$  T cells.

## Flow Cytometry and Reagents

The following antibodies were purchased from Biolegend: CD3 PerCP (Cat#300326), CD4 APC (Cat#357408), CD4 PerCP (Cat#100432), Ki67 FITC (Cat#652410), Ki67 FITC (Cat#151212), IFN- $\gamma$  PE (Cat#505808), IFN- $\gamma$  BV421 (Cat#505830), IFN- $\gamma$  FITC (Cat#502506), CD69 FITC (Cat#104506), CD28 PE (Cat#102106), CD25 APC (Cat#101910), T-bet PE (Cat#644812), CD45 BV510 (Cat#103138), CD107a PE (Cat#121612), Granzyme B FITC (Cat#515403), Perforin PE (Cat#154406), TNF- $\alpha$  APC (Cat#506308), and isotype-matched antibodies.

Surface marker staining was performed with mAbs for 15 min in PBS using indicated antibodies. For the intracellular cytokine expression detection, CD4 $^+$  T cells were stimulated with Cell Stimulation Cocktail (plus protein transport inhibitors) (eBioscience, Cat#00-4975-03) for 4 h prior to staining. For the *in vitro* co-culture assay, CD4 $^+$  T cells were co-cultured with colon cancer MC38 cells as the indicated ratio for 6 h, and intracellular protein transport inhibitor Brefeldin A (BFA, Beyotime, Cat#S1536) was added for 5 h before collection when assessing the intracellular proteins. To evaluate cell apoptosis, freshly collected CD4 $^+$  T cells were processed into single-cell suspensions and stained with annexin V and 7-AAD according to the manufacturer's instructions (BD, Cat#559763). Cells were detected on DxFLEX (Beckman Coulter) and analyzed with the Kaluza Analysis 2.1 software (Beckman Coulter).

## CFSE Proliferation Assay

Purified CD4 $^+$  T cells were activated with *in vitro* plate-bound anti-CD3/CD28 and recombinant IL-2 for 24 h. CD4 $^+$  T cells were incubated at 37°C for 5 min with 2  $\mu$ M CFSE diluted in PBS, and then an equal volume of cold FBS was used to stop the reaction. Subsequently, cells were washed twice with RPMI 1640 containing 10% FBS. Finally, CFSE-labeled CD4 $^+$  T cells were treated with PBS or decitabine for 3 days, and analyzed by flow cytometry.

## Cytotoxicity Assay

To detect the cytotoxicity of CD4 $^+$  T cells, DELFIA time-resolved fluorescence (TRF) assays were performed (PerkinElmer, Cat#AD0116). The processes of the staining, incubation and measure time-resolved fluorescence were operated according to the manufacturer's instructions. Specific release represents the cytotoxic activity of CD4 $^+$  T cells. MC38 (mouse colon cancer cell line) or HCT116 (human colon cancer cell line) cells were used as targets to study the cytotoxicity of mouse or human CD4 $^+$  T cells, respectively.

## Inhibitors Treatment

CD4 $^+$  T cells were treated with respective five inhibitors, Ruxolitinib (Cat#S1378, 10  $\mu$ M), Rapamycin (Cat#S1039, 100 nM), LY294002 (Cat# S1105, 10  $\mu$ M), BAY 11-7082 (Cat#S2913,

10  $\mu$ M), and ICG-001 (Cat#S2662, 5  $\mu$ M) for 12 h followed by decitabine treatment. All inhibitors were purchased from Selleck.

## Quantitative Real-Time PCR (qRT-PCR)

Total RNA was isolated using TRIzol Reagent (ambion, Cat#15596018). Reverse transcription to cDNA was performed using RevertAid First Strand cDNA Synthesis Kit (Thermo Fisher Scientific, Cat#K1622). Real-time PCR was performed using SYBR Green Realtime PCR Master Mix (TOYOBO, Cat#QPK-201) and Applied Biosystems 7500 (life technologies). The following primers were used: IkB $\alpha$ , F, 5'-TGA AGGACGAGGAGTACGAGC-3', R, 5'-TGCAGGAACGAGTC TCCGT-3',  $\beta$ -TrCP: F, 5'-TCCCAAATGTGTCACTACCAGC-3', R, 5'-AGTGCAGTTATGAAATCCCTCTG-3', GAPDH, F, 5'-AACCTGCCAAGTATGATGA-3', R, 5'-GGAGTTGCTGTT GAAGTC-3'.

## Western Blot and *in vivo* Ubiquitination Assays

T cells were collected and washed with cold PBS and then lysed in lysis buffer to isolated total protein. Nuclear protein extracts were isolated using a nuclear and cytoplasmic extraction kit (Thermo Fisher Scientific, Cat#78835). Protein extracts were quantified using BCA assays and equalized using the extraction reagent. The following antibodies were purchased from Cell Signaling Technology: primary antibodies against phosphor-IKK $\alpha$ / $\beta$  Ser176/Ser177 (2697)/IKK $\beta$  (8943), phosphor-IkB $\alpha$  Ser32 (2859)/IkB $\alpha$  (9242), phosphor-p65 Ser536 (3031)/p65 (6956),  $\beta$ -TrCP (11984),  $\beta$ -actin (3700). Anti-SP1 antibody was purchased from Abcam (ab157123). The relevant secondary antibodies were performed. All the antibodies were purchased from Cell Signaling Technology.

For *in vivo* ubiquitination assay, sorted CD4 $^+$  T cells were treated with MG132 (50  $\mu$ M, Sigma-Aldrich, Cat#M7449) before collection, and cells were lysed in modified RIPA lysis buffer [10 mM Tris-HCl (pH 7.5), 150 mM NaCl, 5 mM EDTA, 1% (v/v) NP-40, 1% sodium deoxycholate, 0.025% SDS, 1  $\times$  protease inhibitors]. The lysates were immunoprecipitated with anti-IkB $\alpha$  antibody and detected by western blot.

## Animal Experiments, Adoptive T Cell Transfer, and Tumor Digestion

Six to eight weeks old Balb/c nude mice were purchased from the SPF Biotechnology Co., Ltd. (Beijing, China). All mice were housed under pathogen-free conditions and all animal experiments were performed under protocols approved by Scientific Investigation Board of Chinese PLA General Hospital, Beijing, China. Mouse colon cancer MC38 cells were cultured with RPMI-1640 medium containing 10% fetal bovine serum and 1% penicillin and streptomycin. MC38 cells ( $1 \times 10^5$ ) were harvested and washed twice with PBS then implanted subcutaneously into the right flank.

The tumor-bearing animals received intravenous injection of PBS or decitabine-treated CD4 $^+$  T cells ( $1 \times 10^6$  per mouse)



when tumor volumes reached a size of around 100 mm<sup>3</sup>. Tumor size was measured every 3 days in two dimensions by caliper. The tumor volume was calculated according to the formula (length  $\times$  width<sup>2</sup>)/2 and mice were sacrificed at the indicated time points or when tumor volume reached >1.5 cm<sup>3</sup> (endpoint). Survival analysis was performed for mice that received decitabine or PBS-treated CD4<sup>+</sup> T cells transfer.

On the indicated days, tumors were excised, manually dissociated and digested with Tumor Dissociation Kit for 1 h (Miltenyi, Cat#130-096-730), followed by mashing through 70  $\mu$ m nylon cell strainer. Cells were harvested and washed twice with PBS then cells were resuspended in PBS for further detection.

## Statistical Analysis

Data are presented as the mean  $\pm$  S.D. of at least three independent experiments. Statistical comparisons between experimental groups were analyzed using the Student *t*-test. Kaplan-Meier survival analysis was performed to estimate the survival curves for tumor-bearing mice that received PBS or decitabine-treated CD4<sup>+</sup> T cells transfer and significant differences were evaluated by a log-rank test. A two-way repeated-measures analysis of variance (ANOVA) was conducted to evaluate the effect of time-group interaction. Statistical analysis was performed using GraphPad Prism software 8.0. A two-tailed *p* < 0.05 was considered statistically significant.

## RESULTS

### Low-Dose Decitabine Promotes the Activation and Proliferation of Sorted CD4<sup>+</sup> T Cells

Previous studies demonstrated that low-dose decitabine (10 nM) has anti-tumor activity in solid tumors *in vivo* (Tsai et al., 2012; Li et al., 2017). To investigate the direct effect of low-dose decitabine on CD4<sup>+</sup> T cell activation, mouse CD4<sup>+</sup> T cells were sorted from splenocytes, activated with immobilized anti-CD3/CD28, and treated with different concentrations of decitabine (0, 1, 10, 100, and 1,000 nM). We observed a significant increase in CD69<sup>+</sup> cells as a percentage of CD4<sup>+</sup> cells following decitabine treatment at a concentration of 10 nM or higher (100 and 1,000 nM), indicating that 10 nM low-dose of decitabine could enhance the activation of purified CD4<sup>+</sup> T cells (Figure 1A). The ratio of CD25<sup>+</sup> cells in CD4<sup>+</sup> T cells was not changed with 10 nM decitabine treatment (Figure 1B). Moreover, we examined the expression of CD28, a co-stimulatory molecule, which played a pivotal role in triggering CD4<sup>+</sup> T cell activation. The results showed that 10 nM of low-dose decitabine markedly increased the percentage of CD28<sup>+</sup>CD4<sup>+</sup> T cells (Figure 1C). We further detected the proliferation capacity of CD4<sup>+</sup> T cells in response to decitabine. The CD4<sup>+</sup> T cells were activated by anti-CD3/CD28, and the CFSE labeled CD4<sup>+</sup> T cells were administrated with PBS or decitabine for 3 days and analyzed by flow cytometry. As shown

in Figure 1D, low-dose decitabine enhanced the proliferation of CD4<sup>+</sup> T cells (Figure 1D). The upregulated expression of Ki67 further confirmed that 10 nM of low-dose decitabine mediated proliferation of activated CD4<sup>+</sup> T cells, and we noticed that the ratio of Ki67<sup>+</sup> cells was reduced with decitabine at a relative higher concentration of 1,000 nM as compared to that with lower dose of 10 nM (Figure 1E). These results suggested that low-dose decitabine treatment promoted the activation and proliferation of CD4<sup>+</sup> T cells.

### Low-Dose Decitabine Increases the Frequency of Th1 Subset and CD4<sup>+</sup> T Cell Cytolysis Activity

CD4<sup>+</sup> T cells include distinct functional subsets based on their function and cytokine secretion patterns, such as Th1, Th2, Th17, and Tregs (Kim and Cantor, 2014). We next explored the effect of low-dose decitabine on CD4<sup>+</sup> T cell subsets. Purified CD4<sup>+</sup> T cells were treated with different concentrations of decitabine for 3 days. The flow cytometry assay showed that the frequency of Th1 subset, which produced IFN- $\gamma$ , was increased following 10 nM of low-dose decitabine treatment (Figure 2A). Notably, low-dose decitabine-induced Th1 cell expansion was not a transient action and required an exposure longer than 2 days, consistently with the slow and memory response of low doses of decitabine *in vivo* (Figure 2B). Moreover, under *in vitro* Th1 polarization conditions, treatment of low-dose decitabine markedly increased the frequency of IFN- $\gamma$ <sup>+</sup> cells in CD4<sup>+</sup> T cells (Figure 2C). As expected, the expression of T-bet was increased after low-dose decitabine treatment (Figure 2D), which was a key transcription factor associated with Th1 differentiation (Pritchard et al., 2019; Xia et al., 2019).

The cytotoxic CD4<sup>+</sup> T cells played important roles in anti-tumor immunity and were reported to be a close relative of Th1 cells. To investigate whether low-dose decitabine affects the cytotoxicity of CD4<sup>+</sup> cells, we performed the DELFIA time-resolved fluorescence (TRF) assays. The results showed that low-dose decitabine-treated CD4<sup>+</sup> T cells exhibited an elevated cytotoxicity against mouse colon carcinoma MC38 cells as compared with control CD4<sup>+</sup> T cells (Figure 2E). Being a marker of cytotoxic T cell degranulation, CD107a, was markedly enhanced on the surface of CD4<sup>+</sup> T cells with low-dose decitabine pretreatment (Figure 2F). Consistently, low-dose decitabine promoted the expression of IFN- $\gamma$ , granzyme B, perforin and TNF- $\alpha$  on CD4<sup>+</sup> T cells when co-cultured with MC38 cells (Figures 2G–J). Furthermore, the proliferating potential of CD4<sup>+</sup> T cells was also increased with decitabine treatment (Figure 2K). Taken together, low-dose decitabine could potentiate the cytotoxic activity of CD4<sup>+</sup> T cells *in vitro*.

### Low-Dose Decitabine-Pretreated CD4<sup>+</sup> T Cells Inhibits Tumor Growth *in vivo*

To further study the anti-tumor capacity of low-dose decitabine-pretreated CD4<sup>+</sup> T cells *in vivo*, we performed a tumor-bearing xenograft model of mouse colon cancer MC38 cells and transferred low-dose decitabine-pretreated

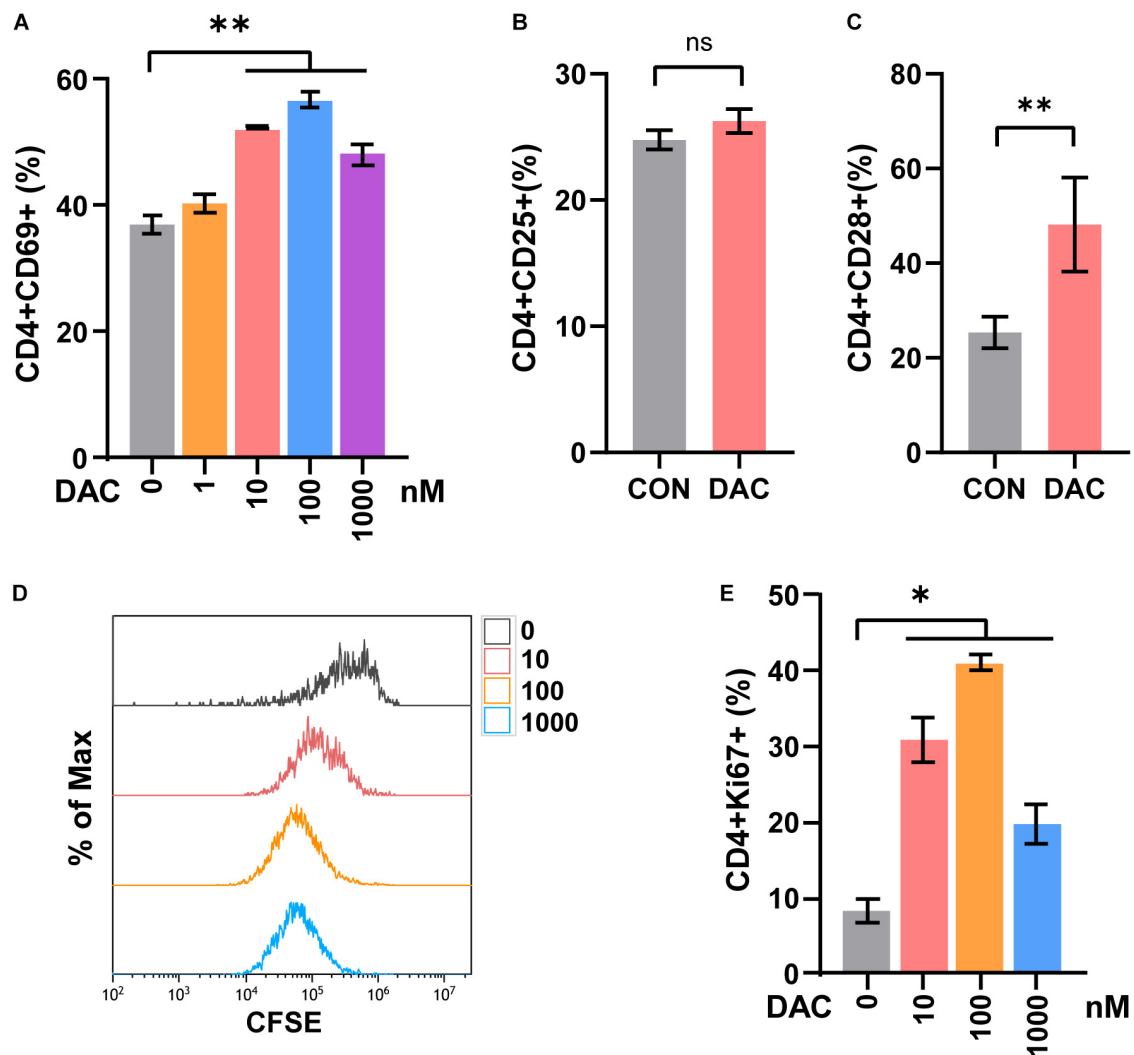


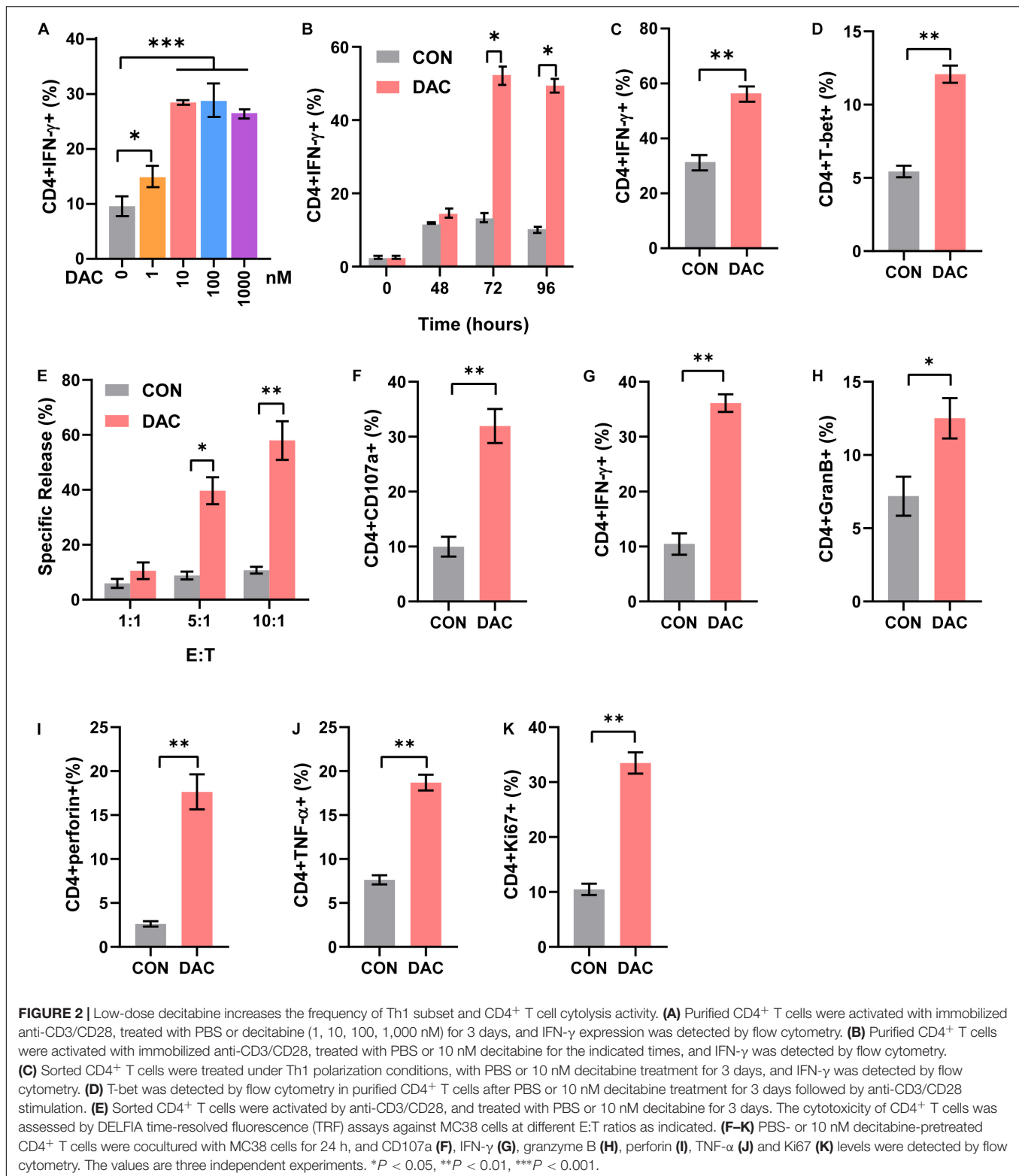
**FIGURE 1 |** Low-dose decitabine promotes the activation and viability of sorted CD4<sup>+</sup> T cells *in vitro*. **(A)** To detect T cell early activation markers, mouse CD4<sup>+</sup> T cells were sorted from splenocytes, activated with immobilized anti-CD3/CD28 for 24 h, and treated with different concentrations of decitabine (DAC, 0, 1, 10, 100, and 1,000 nM) plus IL-2 for 2 days. The surface marker CD69 was detected by flow cytometry. **(B,C)** After anti-CD3/CD28 activation, CD4<sup>+</sup> T cells were treated with PBS (CON) or 10 nM DAC for 3 days, the expressions of CD25 **(B)** and CD28 **(C)** were detected by flow cytometry. **(D)** Sorted CD4<sup>+</sup> T cells were activated with anti-CD3/CD28, the CFSE-labeled (2  $\mu$ M) T cells were then treated with PBS or different concentrations of decitabine for 3 days, and detected by flow cytometry. **(E)** Ki67 was detected by flow cytometry on day three after PBS or decitabine treatment. All results from three independent experiments are shown. \* $P < 0.05$  and \*\* $P < 0.01$ . ns, not significant.

CD4<sup>+</sup> T cells. The results showed that infusion of low-dose decitabine-pretreated CD4<sup>+</sup> T cells significantly inhibited tumor growth and prolonged survival as compared to control CD4<sup>+</sup> T cells (**Figures 3A,B**). Importantly, higher number of infiltrated CD4<sup>+</sup> T cells was observed in tumors treated with decitabine-primed CD4<sup>+</sup> T cells (**Figure 3C**). Moreover, the frequencies of IFN- $\gamma$ <sup>+</sup> and Ki67<sup>+</sup> cells as in tumor infiltrated CD4<sup>+</sup> T cells were dramatically increased in mice transferring low-dose decitabine-pretreated CD4<sup>+</sup> T cells comparing transferring control CD4<sup>+</sup> T cells (**Figure 3D**). In these mice received low-dose decitabine-pretreated CD4<sup>+</sup> T cells, the expression levels of cytotoxic marker granzyme B and TNF- $\alpha$  were also upregulated in tumor infiltrated

CD4<sup>+</sup> T cells (**Figure 3E**). Therefore, low-dose decitabine treated CD4<sup>+</sup> T cells had improved anti-tumor activity *in vivo*.

### Low-Dose Decitabine Promotes CD4<sup>+</sup> T Cell Anti-Tumor Immune Response Dependent on NF- $\kappa$ B Signaling

In order to investigate the mechanism underlying low-dose decitabine-induced CD4<sup>+</sup> T cell proliferation and function, we explored the upstream signaling pathway that controlled the viability of CD4<sup>+</sup> T cells. Inhibitors targeting JAK1/2 (ruxolitinib), mTOR (rapamycin), PI3K (LY294002), NF- $\kappa$ B



(BAY 11-7082) and Wnt/ $\beta$ -catenin (ICG-001) signaling were used. First, low-dose decitabine treatment had minimal effect on CD4<sup>+</sup> T cell apoptosis, and all these inhibitors did not result in increased apoptosis in low-dose decitabine pretreated-CD4<sup>+</sup>

T cells (Figure 4A). Interestingly, we noticed that addition of NF- $\kappa$ B inhibitor markedly suppressed decitabine-induced proliferative capacity and IFN- $\gamma$  secretion in CD4<sup>+</sup> T cells (Figures 4B,C). Results confirmed that NF- $\kappa$ B inhibitor

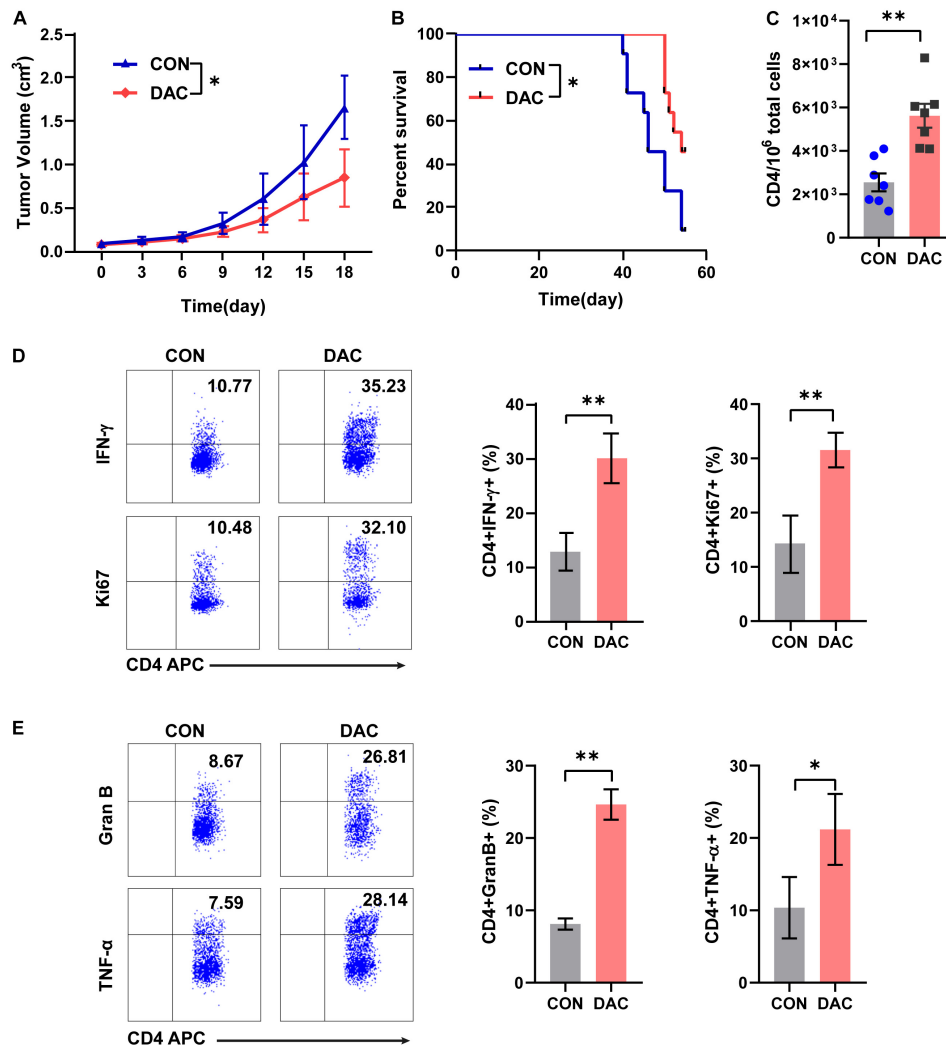


**FIGURE 3 |** Low-dose decitabine-treated CD4<sup>+</sup> T cells inhibit tumor growth *in vivo*. Subcutaneously implantation of MC38 cells received PBS- or 10 nM decitabine-treated CD4<sup>+</sup> T cells when the tumor volume reached 100 mm<sup>3</sup>. **(A)** The tumor volume was measured every 3 days ( $n = 6/\text{group}$ ). **(B)** Survival curves of MC38-bearing mice received PBS- or 10 nM decitabine-treated CD4<sup>+</sup> T cells ( $n = 11/\text{group}$ ). **(C–E)** The MC38-bearing mice were sacrificed on day 18 after CD4<sup>+</sup> T cell transfer, the absolute number of tumor infiltrated CD4<sup>+</sup> T cells were assessed **(C)**; and percentages of IFN- $\gamma$ <sup>+</sup>, Ki67<sup>+</sup> **(D)**, granzyme B<sup>+</sup> and TNF- $\alpha$ <sup>+</sup> **(E)** cells among tumor infiltrated CD4<sup>+</sup> T cells were detected by flow cytometry. All results from three independent experiments are shown. \* $P < 0.05$ . \*\* $P < 0.01$ .

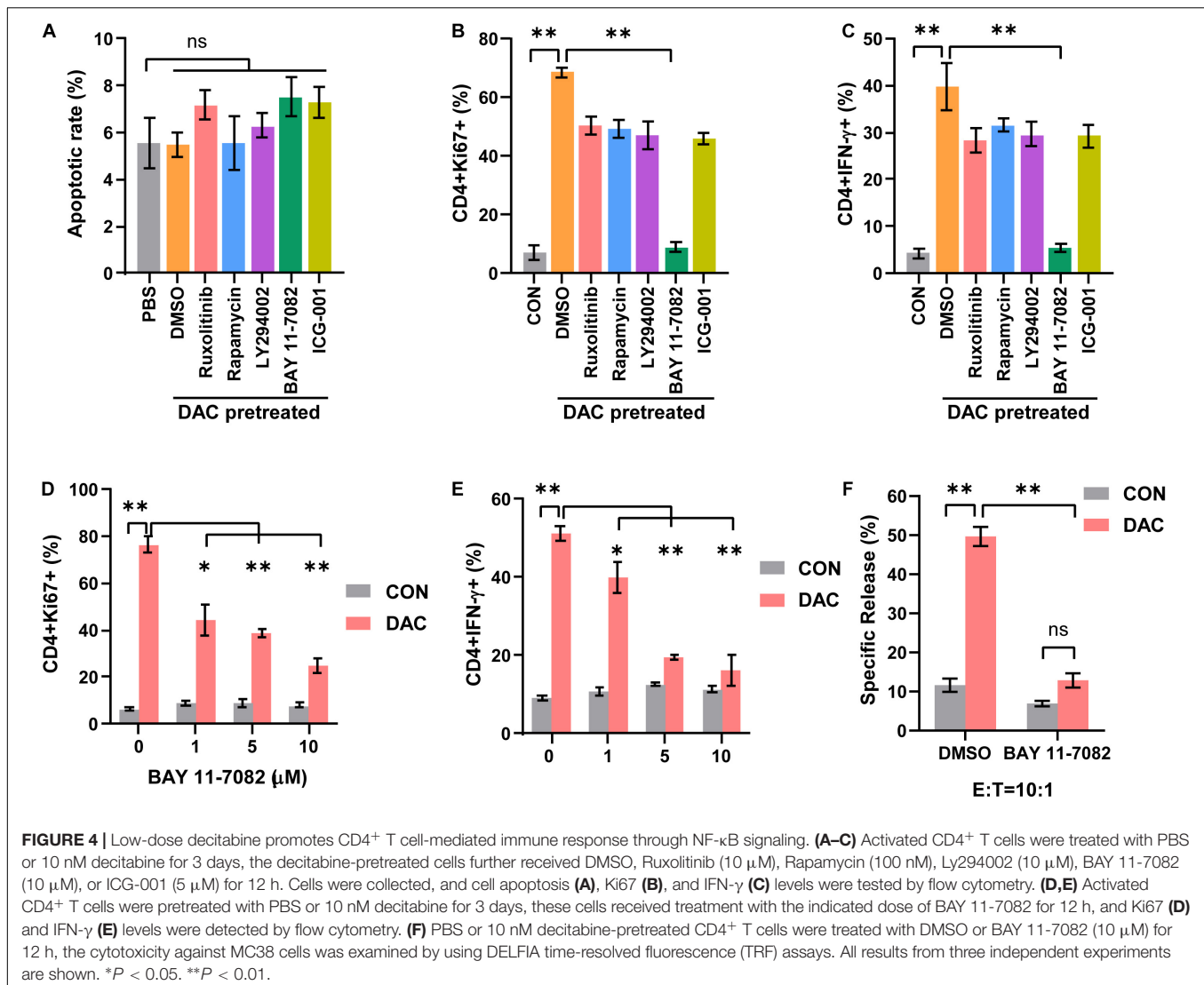
attenuated decitabine-mediated CD4<sup>+</sup> T cell viability and IFN- $\gamma$  expression in a dose-dependent manner (**Figures 4D,E**). Moreover, we observed that NF- $\kappa$ B inhibitor decreased the cytotoxicity of decitabine-treated CD4<sup>+</sup> T cells against colon cancer MC38 cells (**Figure 4F**).

### Low-Dose Decitabine Reinforces NF- $\kappa$ B Activation by Promoting I $\kappa$ B $\alpha$ Ubiquitination and Degradation

NF- $\kappa$ B signaling was crucial and activated in T cells following anti-CD3 stimulation (Gerondakis et al., 2014). In canonical NF- $\kappa$ B signaling pathway, the phosphorylation and ubiquitination of I $\kappa$ B $\alpha$  results in I $\kappa$ B $\alpha$  degradation, which allows NF- $\kappa$ B p50/p65 heterodimer nucleus translocation. NF- $\kappa$ B activation

was characterized by the detection of p65 nuclear staining and phosphorylation of p65 at Ser536 (Gerondakis et al., 2014). We next assessed the influence of low-dose decitabine on NF- $\kappa$ B activation in CD4<sup>+</sup> T cells. As shown in **Figure 5A**, PMA/Ionomycin (P/I) stimulation induced NF- $\kappa$ B activation as the increased phosphorylation of IKK $\alpha$ / $\beta$ , p65 and downregulation of I $\kappa$ B $\alpha$  in sorted CD4<sup>+</sup> T cells. We found that low-dose decitabine-primed CD4<sup>+</sup> T cells might display more robust NF- $\kappa$ B activation upon P/I stimulation as compared to control CD4<sup>+</sup> T cells, since the higher level of phospho-p65 (**Figure 5A**). We next prepared nuclear and cytoplasmic fractions from PBS or decitabine-primed CD4<sup>+</sup> T cells treated with or without PMA/Ionomycin. Low-dose decitabine pretreated CD4<sup>+</sup> T cells revealed dramatic translocation of p65 from the cytosol to the nucleus and diminished I $\kappa$ B $\alpha$  level in response to





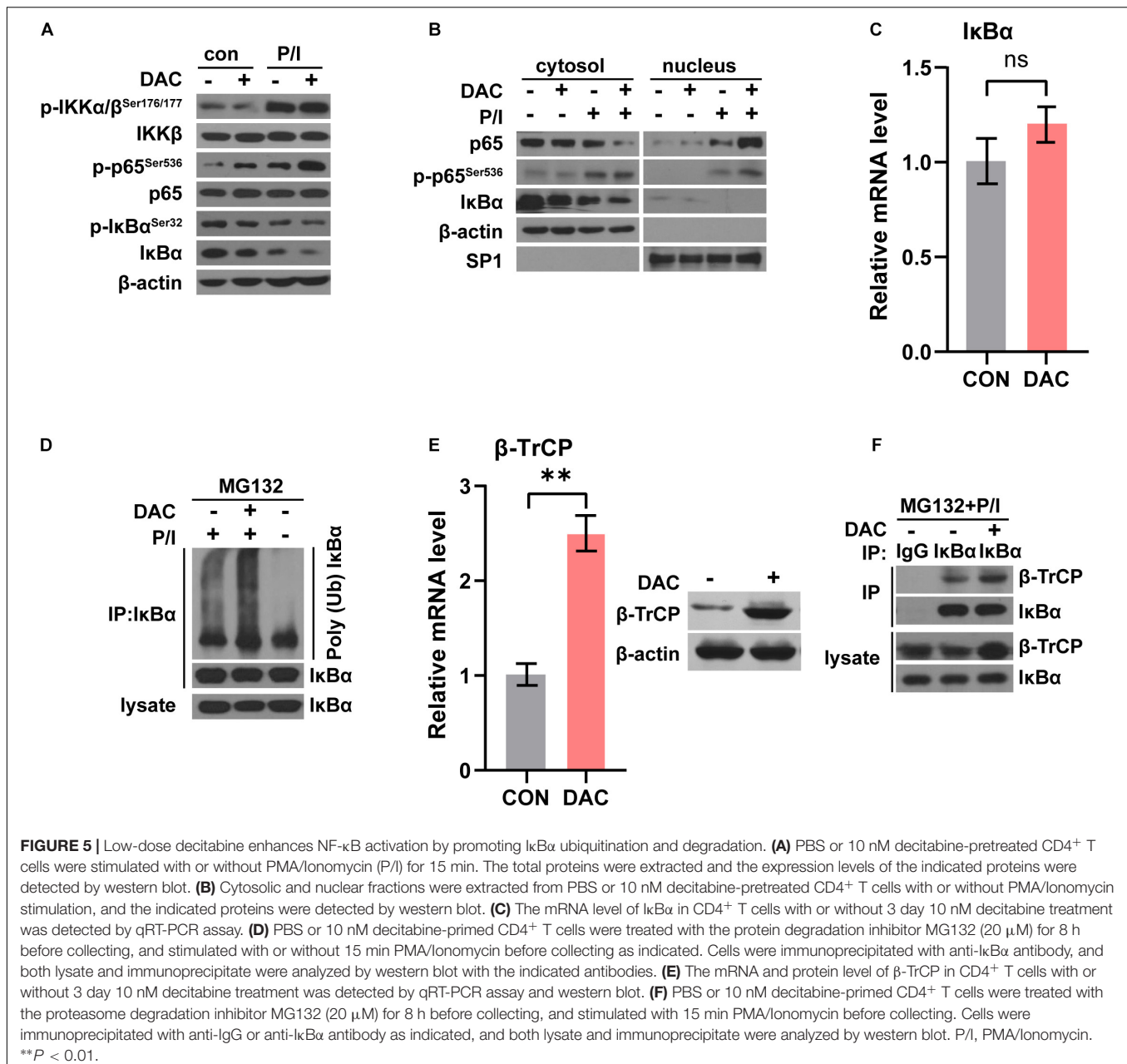
P/I stimulation, further confirming the enhanced activation of NF-κB (Figure 5B). In these cells, we noticed that the level of phosphor-IKKα/β was minimal elevated, and IκBα expression was reduced, suggesting that the increased IκBα degradation might trigger NF-κB activation.

To test this possibility, we first detected IκBα mRNA level and the qRT-PCR assay showed that the mRNA level of IκBα was not changed with low-dose decitabine treatment (Figure 5C). The *in vivo* ubiquitination assay demonstrated that IκBα ubiquitination was significantly enhanced in decitabine-pretreated CD4<sup>+</sup> T cells with P/I stimulation as compared to control CD4<sup>+</sup> T cells (Figure 5D). IκBα is degraded followed by polyubiquitination by the SCF<sup>β-TrCP</sup> complex, among which β-TrCP associates with IκBα for ubiquitination (Winston et al., 1999). It has been reported that low expression of β-TrCP was associated with promoter hypermethylation and decitabine treatment restored mRNA and protein expression of β-TrCP with demethylation at promoter region (Tseng et al., 2008). Similarly, we observed that both the mRNA and protein levels of β-TrCP

were increased after low-dose decitabine treatment in CD4<sup>+</sup> T cells (Figure 5E). Therefore, the protein interaction between β-TrCP and IκBα was boosted in decitabine-primed CD4<sup>+</sup> T cells (Figure 5F). These results suggest that low-dose decitabine potentiates NF-κB activation in CD4<sup>+</sup> T cells by enhancing β-TrCP expression and mediated IκBα degradation.

### Low-Dose Decitabine Therapy Enhances NF-κB Activation in Human CD4<sup>+</sup> T Cells and Associates With Clinical Response in Solid Tumor Patients

To further examine the effect of low-dose decitabine on human CD4<sup>+</sup> T cells, purified CD4<sup>+</sup> T cells were prepared from peripheral blood of healthy donors, activated by using anti-CD3 antibody plus IL2 for 24 h, and treated with or without 10 nM decitabine for 3 days. The frequencies of IFN-γ<sup>+</sup> and Ki67<sup>+</sup> cells were increased after *in vitro* decitabine treatment (Figure 6A). In addition, low-dose decitabine enhanced the



cytotoxicity of CD4<sup>+</sup> T cells against colon cancer HCT116 cells, and increased CD107a expression (**Figure 6B**). To further explore whether decitabine-mediated NF- $\kappa$ B activation in CD4<sup>+</sup> T cells plays an important role with decitabine-based therapy in solid tumor patients, we sorted peripheral CD4<sup>+</sup> T cells from patients before treatment. We observed that in patients (P1 and P2) who had a response to decitabine-based therapy, *in vitro* low-dose decitabine pretreatment promoted I $\kappa$ B $\alpha$  degradation and increased p65 phosphorylation with P/I stimulation in CD4<sup>+</sup> T cells; while in patients (P4 and P5) who did not acquired a response to decitabine-based therapy, *in vitro* decitabine pretreatment displayed no ability to enhance NF- $\kappa$ B activity (**Figure 6C**). Moreover, low-dose decitabine treatment increased IFN- $\gamma$  production and Ki67 level in CD4<sup>+</sup> T cells

from decitabine-based therapy responders P1 and P2 rather than non-responders P4 and P5 (**Figures 6D,E**). These results suggested that low-dose decitabine therapy augmented CD4<sup>+</sup> T cell immune response in solid tumor patients by promoting NF- $\kappa$ B transcription activation and thus inflammatory cytokine IFN- $\gamma$  secretion, which was achieved by the upregulation of I $\kappa$ B $\alpha$  E3 ligase  $\beta$ -TrCP and the enhanced ubiquitination and degradation of I $\kappa$ B $\alpha$  (**Figure 6F**).

## DISCUSSION

DNA methylation represents an important layer of silencing of gene expression and plays important roles in various biological

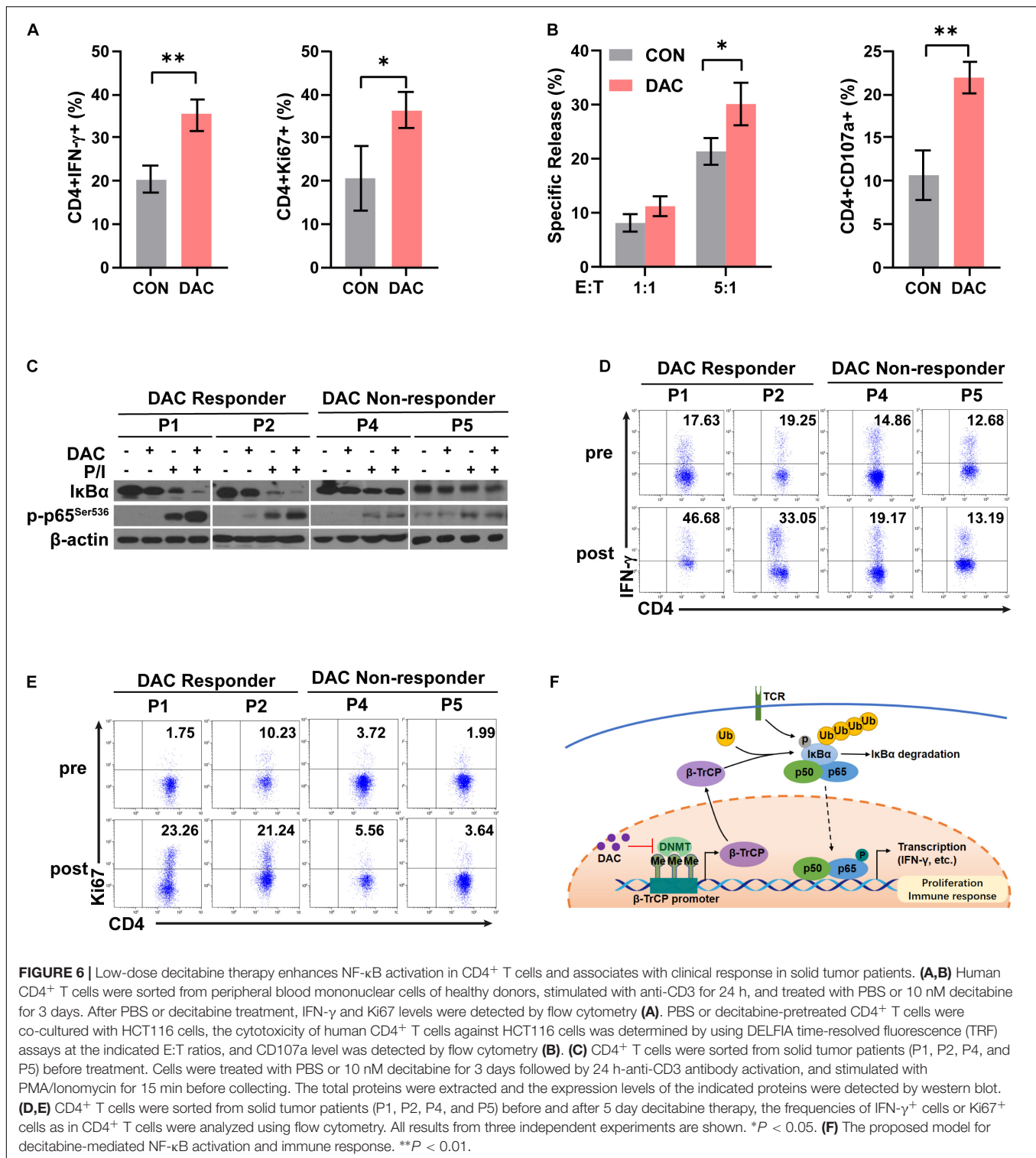


**FIGURE 6 |** Low-dose decitabine therapy enhances NF- $\kappa$ B activation in CD4 $^{+}$  T cells and associates with clinical response in solid tumor patients. **(A,B)** Human CD4 $^{+}$  T cells were sorted from peripheral blood mononuclear cells of healthy donors, stimulated with anti-CD3 for 24 h, and treated with PBS or 10 nM decitabine for 3 days. After PBS or decitabine treatment, IFN- $\gamma$  and Ki67 levels were detected by flow cytometry **(A)**. PBS or decitabine-pretreated CD4 $^{+}$  T cells were co-cultured with HCT116 cells, the cytotoxicity of human CD4 $^{+}$  T cells against HCT116 cells was determined by using DELFIA time-resolved fluorescence (TRF) assays at the indicated E:T ratios, and CD107a level was detected by flow cytometry **(B)**. **(C)** CD4 $^{+}$  T cells were sorted from solid tumor patients (P1, P2, P4, and P5) before treatment. Cells were treated with PBS or 10 nM decitabine for 3 days followed by 24 h-anti-CD3 antibody activation, and stimulated with PMA/Ionomycin for 15 min before collecting. The total proteins were extracted and the expression levels of the indicated proteins were detected by western blot. **(D,E)** CD4 $^{+}$  T cells were sorted from solid tumor patients (P1, P2, P4, and P5) before and after 5 day decitabine therapy, the frequencies of IFN- $\gamma$  $^{+}$  cells or Ki67 $^{+}$  cells as in CD4 $^{+}$  T cells were analyzed using flow cytometry. All results from three independent experiments are shown. \* $P < 0.05$ . **(F)** The proposed model for decitabine-mediated NF- $\kappa$ B activation and immune response. \*\* $P < 0.01$ .

processes. Decitabine, a DNA methyltransferase inhibitor, was effective in treating hematological tumors, such as MDS and AML. It has been widely investigated that genome-wide DNA promoter demethylation occurred in tumor cells after decitabine treatment, resulting in an increased immunogenicity

and immune recognition (Li et al., 2015; Topper et al., 2020). However, the anti-tumor mechanisms of the epigenetic modifying agents were not fully clarified.

Besides cancer cells, the effect of epigenetic modulation on T cells has been concerned in recent years. As the main cytotoxic

effector cell, decitabine-mediated reprogramming of CD8<sup>+</sup> T cells were extensively explored, and emerging evidence has demonstrated that DNA methylation was directly involved in CD8<sup>+</sup> T cell differentiation and function (Chiappinelli et al., 2016; Ghoneim et al., 2017; Henning et al., 2018). Our previous study reported that low-dose decitabine promoted the activation and viability of IFN- $\gamma$ <sup>+</sup> T cells in CD3<sup>+</sup> T cells (Li et al., 2017). Herein, we focused on the regulation of purified CD4<sup>+</sup> T cells by decitabine, and demonstrated that 10 nM of low-dose decitabine enhanced CD4<sup>+</sup> T cell proliferation and activation, especially the IFN- $\gamma$ <sup>+</sup>CD4<sup>+</sup> T cells. The epigenetic modifying agents might play distinct roles with different concentrations and in diverse models. Decitabine induced FOXP3 expression in CD4<sup>+</sup>CD25<sup>-</sup> T cells at a concentration of 1  $\mu$ M or higher, and could convert the non-Tregs into Tregs with suppressor functions (Choi et al., 2010). While 1  $\mu$ M of decitabine treatment impeded the proliferation of CD4<sup>+</sup>CD25<sup>high</sup>FOXP3<sup>+</sup> Tregs and fostered Th1 polarization in Tregs (Landman et al., 2018). In an experimental autoimmune encephalomyelitis mouse model characterized by autoreactive T cells and dysregulated innate immune response, Wang et al. found that long-term higher-dose of decitabine treatment inhibited T cell proliferation due to the increased expression of TET2 and cell cycle inhibitors (Wang et al., 2017). We also identified low-dose decitabine directly increased the cytotoxic activity of CD4<sup>+</sup> T cells against tumor cells *in vitro*, which might be due to the elevated frequency of IFN- $\gamma$ <sup>+</sup>CD4<sup>+</sup> T subset following decitabine treatment. However, since the lack of antigen-specific CD4<sup>+</sup> T cells, we could not determine whether low-dose decitabine promoted the activation and cytotoxic capacity of cytotoxic CD4<sup>+</sup> T cells.

Low-dose decitabine induced upregulation of a series of genes. In addition to direct DNA demethylation-mediated gene activation, the epigenetic agents could also affect the action of protein posttranslational modifications. In the canonical NF- $\kappa$ B signaling pathway, ubiquitination and degradation of I $\kappa$ B $\alpha$  leads to NF- $\kappa$ B translocation to the nucleus and transcription activation of a series of genes in immune response and proliferation (Hayden and Ghosh, 2011). NF- $\kappa$ B pathway regulates T cell differentiation and development through TCR and CD28 activation (Oh and Ghosh, 2013). In this study, we observed that low-dose decitabine treatment augments the expression of E3 ligase  $\beta$ -TrCP, which potentiates the degradation of I $\kappa$ B $\alpha$ , and thus enhancing the activation of NF- $\kappa$ B. The  $\beta$ -TrCP/I $\kappa$ B $\alpha$ /NF- $\kappa$ B pathway provided a new regulation pattern of NF- $\kappa$ B signaling in T cells. Moreover, NF- $\kappa$ B was aberrantly activated in most tumor cells, and we did not detect further NF- $\kappa$ B activation in tumor cells (data not shown), suggesting the distinct regulation of epigenetic agents in different types of cells.

Besides the hematological malignancies, low-dose decitabine therapy had efficacy in some solid tumors. Decitabine pretreatment could increase the sensitivity of cancer cells to chemotherapy or targeted therapy in a part of patients. No or weak association between decitabine response and DNA methylation status of specific genes were reported (Fandy et al., 2009). We previously reported that response

to decitabine-primed chemotherapy might be related to the increased frequency of IFN- $\gamma$ <sup>+</sup> T cells in solid tumor patients (Li et al., 2017). In the current study, we demonstrated that low-dose decitabine-induced activation of IFN- $\gamma$ <sup>+</sup>CD4<sup>+</sup> T cell subset was dependent on the enhancement of NF- $\kappa$ B pathway. Moreover, we found that the NF- $\kappa$ B signaling was activated in response to *in vitro* decitabine treatment in CD4<sup>+</sup> T cells from responsive patients, which was related to an increased frequency of peripheral IFN- $\gamma$ <sup>+</sup>CD4<sup>+</sup> T cells following *in vivo* decitabine therapy in ovarian cancer patients, further confirming the I $\kappa$ B $\alpha$ /NF- $\kappa$ B/IFN- $\gamma$  regulation mechanism by low-dose decitabine in CD4<sup>+</sup> T cells. However, due to limited clinical samples, the levels of  $\beta$ -TrCP in CD4<sup>+</sup> T cells from responder and non-responder patients with decitabine therapy were still unclear. Whether the regulation of NF- $\kappa$ B pathway in CD4<sup>+</sup> T cells played an essential role in producing anti-tumor response to decitabine-primed chemotherapy in solid tumor patients, and exploring the potential role of  $\beta$ -TrCP as a biomarker in decitabine-mediated CD4<sup>+</sup> T-cell activation in patients is worthy of our further investigation.

## CONCLUSION

In conclusion, our study demonstrates that low-dose decitabine induces degradation of I $\kappa$ B $\alpha$  by  $\beta$ -TrCP through a proteasome degradation pathway, to boost NF- $\kappa$ B activation and thus promotes the proliferation of IFN- $\gamma$ <sup>+</sup>CD4<sup>+</sup> T cells and enhances the anti-tumor immune activity of CD4<sup>+</sup> T cells (Figure 6F).

## DATA AVAILABILITY STATEMENT

The original contributions presented in the study are included in the article, further inquiries can be directed to the corresponding authors.

## ETHICS STATEMENT

The studies involving human participants were reviewed and approved by the Ethics Committee of the Chinese PLA general hospital. The patients/participants provided their written informed consent to participate in this study. The animal study was reviewed and approved by the Ethics Committee of the Chinese PLA general hospital.

## AUTHOR CONTRIBUTIONS

XL and LD performed experiments and analyzed data. JL and QM acquired data. CW and YZ analyzed clinical data. PX and WH given material support and reviewed the manuscript. JN designed the project and wrote the manuscript. All authors contributed to the article and approved the submitted version.



## FUNDING

This study was supported by the National Key Research and Development Program of China (2019YFC1316205 to JN), the National Natural Science Foundation of China (Nos. 81872479, 81803071, 31870873, 81903153, and 31971229), Fostering Funds of Chinese PLA General Hospital for National Excellent Young Scholar Science

Fund (2017-YQPY-001), and Beijing excellent talents training project.

## ACKNOWLEDGMENTS

The technical assistance of Jinbo Fan was gratefully acknowledged.

## REFERENCES

- Aparicio, A., and Weber, J. S. (2002). Review of the clinical experience with 5-azacytidine and 5-aza-2'-deoxycytidine in solid tumors. *Curr. Opin. Investig. Drugs* 3, 627–633.
- Borst, J., Ahrends, T., Babala, N., Melief, C. J. M., and Kastenmuller, W. (2018). CD4(+) T cell help in cancer immunology and immunotherapy. *Nat. Rev. Immunol.* 18, 635–647. doi: 10.1038/s41577-018-0044-0
- Chatterjee, A., Rodger, E. J., and Eccles, M. R. (2018). Epigenetic drivers of tumorigenesis and cancer metastasis. *Semin. Cancer Biol.* 51, 149–159. doi: 10.1016/j.semcancer.2017.08.004
- Chiappinelli, K. B., Strissel, P. L., Desrichard, A., Li, H., Henke, C., Akman, B., et al. (2016). Inhibiting DNA methylation causes an interferon response in cancer via dsRNA including endogenous retroviruses. *Cell* 164, 974–986. doi: 10.1016/j.cell.2015.10.020
- Choi, J., Ritchey, J., Prior, J. L., Holt, M., Shannon, W. D., Deych, E., et al. (2010). In vivo administration of hypomethylating agents mitigate graft-versus-host disease without sacrificing graft-versus-leukemia. *Blood* 116, 129–139. doi: 10.1182/blood-2009-12-257253
- Fandy, T. E., Herman, J. G., Kerns, P., Jiemjit, A., Sugar, E. A., Choi, S. H., et al. (2009). Early epigenetic changes and DNA damage do not predict clinical response in an overlapping schedule of 5-azacytidine and entinostat in patients with myeloid malignancies. *Blood* 114, 2764–2773. doi: 10.1182/blood-2009-02-203547
- Gerondakis, S., Fulford, T. S., Messina, N. L., and Grumont, R. J. (2014). NF- $\kappa$ B control of T cell development. *Nat. Immunol.* 15, 15–25. doi: 10.1038/ni.2785
- Ghoneim, H. E., Fan, Y., Moustaki, A., Abdelsamed, H. A., Dash, P., Dogra, P., et al. (2017). De novo epigenetic programs inhibit PD-1 blockade-mediated T cell rejuvenation. *Cell* 170, 142.e19–157.e19. doi: 10.1016/j.cell.2017.06.007
- Hayden, M. S., and Ghosh, S. (2011). NF- $\kappa$ B in immunobiology. *Cell Res.* 21, 223–244. doi: 10.1038/cr.2011.13
- Henning, A. N., Roychoudhuri, R., and Restifo, N. P. (2018). Epigenetic control of CD8(+) T cell differentiation. *Nat. Rev. Immunol.* 18, 340–356. doi: 10.1038/nri.2017.146
- Jones, P. A., and Taylor, S. M. (1980). Cellular differentiation, cytidine analogs and DNA methylation. *Cell* 20, 85–93. doi: 10.1016/0092-8674(80)90237-8
- Kantarjian, H., Oki, Y., Garcia-Manero, G., Huang, X., O'Brien, S., Cortes, J., et al. (2007). Results of a randomized study of 3 schedules of low-dose decitabine in higher-risk myelodysplastic syndrome and chronic myelomonocytic leukemia. *Blood* 109, 52–57. doi: 10.1182/blood-2006-05-021162
- Kelly, T. K., De Carvalho, D. D., and Jones, P. A. (2010). Epigenetic modifications as therapeutic targets. *Nat. Biotechnol.* 28, 1069–1078. doi: 10.1038/nbt.1678
- Kim, H. J., and Cantor, H. (2014). CD4 T-cell subsets and tumor immunity: the helpful and the not-so-helpful. *Cancer Immunol. Res.* 2, 91–98. doi: 10.1158/2326-6066.CIR-13-0216
- Landman, S., Cruisjes, M., Urbano, P. C. M., Huls, G., van Erp, P. E. J., van Rijssen, E., et al. (2018). DNA methyltransferase inhibition promotes Th1 polarization in human CD4(+)CD25(high) FOXP3(+) regulatory T cells but does not affect their suppressive capacity. *J. Immunol. Res.* 2018:4973964. doi: 10.1155/2018/4973964
- Lee, W. C., Wu, T. J., Chou, H. S., Yu, M. C., Hsu, P. Y., Hsu, H. Y., et al. (2012). The impact of CD4+ CD25+ T cells in the tumor microenvironment of hepatocellular carcinoma. *Surgery* 151, 213–222. doi: 10.1016/j.surg.2011.07.029
- Li, X., Mei, Q., Nie, J., Fu, X., and Han, W. (2015). Decitabine: a promising epi-immunotherapeutic agent in solid tumors. *Expert Rev. Clin. Immunol.* 11, 363–375. doi: 10.1586/1744666x.2015.1002397
- Li, X., Zhang, Y., Chen, M., Mei, Q., Liu, Y., Feng, K., et al. (2017). Increased IFN $\gamma$ (+) T cells are responsible for the clinical responses of low-dose DNA-demethylating agent decitabine antitumor therapy. *Clin. Cancer Res.* 23, 6031–6043. doi: 10.1158/1078-0432.Ccr-17-1201
- Maio, M., Coral, S., Fratta, E., Altomonte, M., and Sigalotti, L. (2003). Epigenetic targets for immune intervention in human malignancies. *Oncogene* 22, 6484–6488. doi: 10.1038/sj.onc.1206956
- Mei, Q., Chen, M., Lu, X., Li, X., Duan, F., Wang, M., et al. (2015). An open-label, single-arm, phase I/II study of lower-dose decitabine based therapy in patients with advanced hepatocellular carcinoma. *Oncotarget* 6, 16698–16711. doi: 10.18632/oncotarget.3677
- Nie, J., Zhang, Y., Li, X., Chen, M., Liu, C., and Han, W. (2016). DNA demethylating agent decitabine broadens the peripheral T cell receptor repertoire. *Oncotarget* 7, 37882–37892. doi: 10.18632/oncotarget.9352
- Oh, H., and Ghosh, S. (2013). NF- $\kappa$ B: roles and regulation in different CD4(+) T-cell subsets. *Immunol. Rev.* 252, 41–51. doi: 10.1111/imr.12033
- Oki, Y., Aoki, E., and Issa, J. P. (2007). Decitabine-bedside to bench. *Crit. Rev. Oncol. Hematol.* 61, 140–152. doi: 10.1016/j.critrevonc.2006.07.010
- Ott, P. A., Hu, Z., Keskin, D. B., Shukla, S. A., Sun, J., Bozym, D. J., et al. (2017). An immunogenic personal neoantigen vaccine for patients with melanoma. *Nature* 547, 217–221. doi: 10.1038/nature22991
- Pritchard, G. H., Kedl, R. M., and Hunter, C. A. (2019). The evolving role of T-bet in resistance to infection. *Nat. Rev. Immunol.* 19, 398–410. doi: 10.1038/s41577-019-0145-4
- Rosenberg, S. A., and Restifo, N. P. (2015). Adoptive cell transfer as personalized immunotherapy for human cancer. *Science* 348, 62–68. doi: 10.1126/science.aaa4967
- Shih, H. Y., Sciumè, G., Poholek, A. C., Vahedi, G., Hirahara, K., Villarino, A. V., et al. (2014). Transcriptional and epigenetic networks of helper T and innate lymphoid cells. *Immunol. Rev.* 261, 23–49. doi: 10.1111/imr.12208
- Takeuchi, A., and Saito, T. (2017). CD4 CTL, a cytotoxic subset of CD4(+) T Cells, their differentiation and function. *Front. Immunol.* 8:194. doi: 10.3389/fimmu.2017.00194
- Topper, M. J., Vaz, M., Marrone, K. A., Brahmer, J. R., and Baylin, S. B. (2020). The emerging role of epigenetic therapeutics in immuno-oncology. *Nat. Rev. Clin. Oncol.* 17, 75–90. doi: 10.1038/s41571-019-0266-5
- Tripathi, S. K., and Lahesmaa, R. (2014). Transcriptional and epigenetic regulation of T-helper lineage specification. *Immunol. Rev.* 261, 62–83. doi: 10.1111/imr.12204
- Tsai, H. C., Li, H., Van Neste, L., Cai, Y., Robert, C., Rassool, F. V., et al. (2012). Transient low doses of DNA-demethylating agents exert durable antitumor effects on hematological and epithelial tumor cells. *Cancer Cell* 21, 430–446. doi: 10.1016/j.ccr.2011.12.029
- Tseng, R. C., Lin, R. K., Wen, C. K., Tseng, C., Hsu, H. S., Hsu, W. H., et al. (2008). Epigenetic silencing of AXIN2/betaTrCP and deregulation of p53-mediated control lead to wild-type beta-catenin nuclear accumulation in lung tumorigenesis. *Oncogene* 27, 4488–4496. doi: 10.1038/nc.2008.83
- Wang, X., Wang, J., Yu, Y., Ma, T., Chen, P., Zhou, B., et al. (2017). Decitabine inhibits T cell proliferation via a novel TET2-dependent mechanism and exerts potent protective effect in mouse auto- and allo-immunity models. *Oncotarget* 8, 56802–56815. doi: 10.18632/oncotarget.18063

- Winston, J. T., Strack, P., Beer-Romero, P., Chu, C. Y., Elledge, S. J., and Harper, J. W. (1999). The SCFbeta-TRCP-ubiquitin ligase complex associates specifically with phosphorylated destruction motifs in IkappaBalpha and beta-catenin and stimulates IkappaBalpha ubiquitination in vitro. *Genes Dev.* 13, 270–283. doi: 10.1101/gad.13.3.270
- Xia, A., Zhang, Y., Xu, J., Yin, T., and Lu, X. J. (2019). T cell dysfunction in cancer immunity and immunotherapy. *Front. Immunol.* 10:1719. doi: 10.3389/fimmu.2019.01719
- Yu, J., Qin, B., Moyer, A. M., Nowsheen, S., Liu, T., Qin, S., et al. (2018). DNA methyltransferase expression in triple-negative breast cancer predicts sensitivity to decitabine. *J. Clin. Invest.* 128, 2376–2388. doi: 10.1172/JCI97924
- Zander, R., Schauder, D., Xin, G., Nguyen, C., Wu, X., Zajac, A., et al. (2019). CD4(+) T cell help is required for the formation of a cytolytic CD8(+) T cell subset that protects against chronic infection and cancer. *Immunity* 51, 1028.e4–1024.e4. doi: 10.1016/j.immuni.2019.10.009
- Conflict of Interest:** The authors declare that the research was conducted in the absence of any commercial or financial relationships that could be construed as a potential conflict of interest.

Copyright © 2021 Li, Dong, Liu, Wang, Zhang, Mei, Han, Xie and Nie. This is an open-access article distributed under the terms of the Creative Commons Attribution License (CC BY). The use, distribution or reproduction in other forums is permitted, provided the original author(s) and the copyright owner(s) are credited and that the original publication in this journal is cited, in accordance with accepted academic practice. No use, distribution or reproduction is permitted which does not comply with these terms.



# Advances in Cancer Treatment by Targeting the Neddylation Pathway

Wenbin Gai<sup>1†</sup>, Zhiqiang Peng<sup>2†</sup>, Cui Hua Liu<sup>3\*</sup>, Lingqiang Zhang<sup>1,2,4\*</sup> and Hong Jiang<sup>1\*</sup>

<sup>1</sup> Department of Physiology, Shandong Provincial Key Laboratory of Pathogenesis and Prevention of Neurological Disorders and State Key Disciplines: Physiology, School of Basic Medicine, Medical College, Qingdao University, Qingdao, China, <sup>2</sup> State Key Laboratory of Proteomics, Beijing Proteome Research Center, National Center for Protein Sciences (Beijing), Beijing Institute of Lifeomics, Beijing, China, <sup>3</sup> CAS Key Laboratory of Pathogenic Microbiology and Immunology, Institute of Microbiology, Chinese Academy of Sciences, Beijing, China, <sup>4</sup> Peixian People's Hospital, Xuzhou, China

## OPEN ACCESS

### Edited by:

Tomokazu Tomo Fukuda,  
Iwate University, Japan

### Reviewed by:

Guangyang Yu,  
Center for Cancer Research, National  
Cancer Institute, United States  
Lijun Jia,  
Shanghai University of Traditional  
Chinese Medicine, China

### \*Correspondence:

Cui Hua Liu  
liucuihua@im.ac.cn  
Lingqiang Zhang  
zhanglq@nic.bmi.ac.cn  
Hong Jiang  
hongjiang@qdu.edu.cn

<sup>†</sup>These authors have contributed  
equally to this work

### Specialty section:

This article was submitted to  
Cell Growth and Division,  
a section of the journal  
Frontiers in Cell and Developmental  
Biology

**Received:** 15 January 2021

**Accepted:** 10 March 2021

**Published:** 08 April 2021

### Citation:

Gai W, Peng Z, Liu C, Zhang L  
and Jiang H (2021) Advances  
in Cancer Treatment by Targeting  
the Neddylation Pathway.  
Front. Cell Dev. Biol. 9:653882.  
doi: 10.3389/fcell.2021.653882

Developmental down-regulation protein 8 (NEDD8), expressed by neural progenitors, is a ubiquitin-like protein that conjugates to and regulates the biological function of its substrates. The main target of NEDD8 is cullin-RING E3 ligases. Upregulation of the neddylation pathway is closely associated with the progression of various tumors, and MLN4924, which inhibits NEDD8-activating enzyme (NAE), is a promising new antitumor compound for combination therapy. Here, we summarize the latest progress in anticancer strategies targeting the neddylation pathway and their combined applications, providing a theoretical reference for developing antitumor drugs and combination therapies.

**Keywords:** developmental down-regulation protein 8 (NEDD8), neddylation, MLN4924, treatment, cancer

## INTRODUCTION

As a post-translational modification, protein neddylation refers to a process where substrate proteins are tagged with a ubiquitin-like protein NEDD8 and participate in cellular activity by regulating protein function. NEDD8 encodes an 81-amino acid polypeptide, which is highly homologous to ubiquitins and is connected to its substrates by forming isopeptide chains. For NEDD8, this linkage occurs between Gly-76 at NEDD8's C-terminus and the Lys-48 residue of the substrates (Kamitani et al., 1997). Different from ubiquitin, as a precursor, NEDD8 is initially synthesized with five additional downstream residues of Gly-76 that must be cracked by a C-terminal hydrolase (Rabut and Peter, 2008), mainly ubiquitin carboxyl-terminal esterase L3 (UCH-L3) (Johnston et al., 1997) and NEDD8 specific-protease cysteine (NEDP1) (Gan-Erdene et al., 2003; Mendoza et al., 2003). After that, an adenosine triphosphate (ATP) and an E1 NEDD8-activating enzyme (NAE) first adenylate and activate mature NEDD8, respectively. NAE is a heterodimer comprising NAE1 (also called APPBP1) and UBA3 (also called NAE $\beta$ ) (Bohnsack and Haas, 2003; Walden et al., 2003; Kurz et al., 2008). Next, activated NEDD8 transfers to one of two NEDD8-conjugating E2 enzymes (UBC12/UBE2M or UBE2F) (Kamitani et al., 1997; Huang et al., 2005). Finally, the E3 ligase catalyzes the production of isomers of the C-terminal Gly-76 and lysine residue of the substrate protein via covalent attachment, ultimately transferring NEDD8 to the substrates to complete the neddylation process (Kamitani et al., 1997).

E3 ubiquitin ligases are numerous, but 10 NEDD8 E3 ligases are available. Except for defective cullin neddylation 1 (DCN1) (Kurz et al., 2005, 2008) and DCN1-like proteins (Kurz et al., 2008; Meyer-Schaller et al., 2009), most of these contain the novel gene (RING) domain structure. The 10 NEDD8 E3 ligases are DCN1, RING-box proteins 1 (RBX1) and RBX2 [also known as regulators of cullin 1 (ROC1) and ROC2/SAG, respectively] (Duan et al., 1999; Kamura et al., 1999;

Huang et al., 2009), murine double minute 2 (MDM2) (Xirodimas et al., 2004), casitas B-lineage lymphoma (c-CBL) (Oved et al., 2006; Zuo et al., 2013), SCFFBXO11 (Zuo et al., 2013), ring finger protein 111 (RNF111) (Ma et al., 2013), inhibitors of apoptosis (IAPs) (Broemer et al., 2010), TFB3 (TFIIH/NER complex subunit TFB3) (Rabut et al., 2011), and tripartite motif containing 40 (TRIM40) (Noguchi et al., 2011). The RING-type neddylation ligase acts as a scaffold to bind the E2 ubiquitin complex directly to the substrate, enhancing ubiquitin transfer to the substrate protein (Metzger et al., 2014). Different from RING-type neddylation ligases, HECT-type neddylation ligases act catalytically by constituting a thioester bond with the C-terminal lobe of the HECT domain before the transfer of ubiquitin to its intended substrate (Berndsen and Wolberger, 2014; Zheng and Shabek, 2017). HECT-type neddylation ligases remain less defined than RING-type neddylation ligases, such as Yeast Rsp5, Itch (Li et al., 2016) (E3 ubiquitin-protein ligase Itchy homolog), Smad ubiquitination regulatory factor 1 (Smurf1) (Xie et al., 2014), Smad ubiquitination regulatory factor 2 (Smurf2) (Shu et al., 2016), NEDL1 (NEDD4-like E3 ubiquitin-protein ligase 1) and NEDL2 (NEDD4-like E3 ubiquitin-protein ligase 1) (Qiu et al., 2016) (Table 1). Furthermore, all NEDD8 E3 ligases identified thus far can be used as ubiquitin E3 ligases (Zhao et al., 2014).

NEDD8 regulates the activities of substrates and participates in various signaling pathways, including cell proliferation, autophagy and transformation. Cullins are the most typical target proteins for neddylation. Typical substrates of cullin-RING ligases (CRLs) include proteins related to cell cycle regulation (e.g., Cyclin D/E, p21, p27, and WEE1) (Jia et al., 2011; Luo et al., 2012; Gao et al., 2014; Li et al., 2014; Hua et al., 2015; Paiva et al., 2015; Han et al., 2016; Lan et al., 2016; Xie et al., 2017; Zhang et al., 2016), apoptosis (e.g., BIM, NOXA, BIK, Bcl-xL, Mcl-1, and c-FLIP) (Jia et al., 2011; Dengler et al., 2014; Godbersen et al., 2014; Yao et al., 2014; Knorr et al., 2015; Chen et al., 2016; Czuczman et al., 2016; Leclerc et al., 2016; Tong et al., 2017; Wang et al., 2017) and signal transduction pathways (e.g., HIF1 $\alpha$ , REDD1,  $\beta$ -catenin, and Deptor) (Milhollen et al., 2010; Swords et al., 2010; Zhao et al., 2012; Godbersen et al., 2014). Activation of their substrates contributes to cancer progression and degradation of their substrates (Xirodimas, 2008). In addition to cullins, several other targets of neddylation, involving tumor suppressor p53 (Xirodimas et al., 2004), Hu antigen R (HuR) (Stickle et al., 2004), von Hippel-Lindau protein (pVHL) (Stickle et al., 2004; Embade et al., 2012), epidermal growth factor receptor (EGFR)

(Oved et al., 2006), oncoprotein mouse double minute 2 (Mdm2) (Xirodimas et al., 2004), ribosomal proteins (Xirodimas et al., 2008), AKT, liver kinase B1 (LKB1) (Barbier-Torres et al., 2015), and PTEN (Xie et al., 2020), also effectively affect disease onset and progression. Therefore, targeting neddylation is an effective treatment for treating disease (Figure 1).

The substrate properties dictate the critical effect of neddylation in regulating biological processes and disease management. Recent studies have proposed the relevance of neddylation modifications in cell cycle control, DNA replication regulation, cell cycle progression and cell division. The neddylation pathway is hyperactivated during human cancer evolution (Zhou L. et al., 2019). Blocking the neddylation pathway has become an appealing anti-cancer treatment (Jiang and Jia, 2015). However, inhibiting the neddylation pathway significantly upregulates the expression of the T-cell minus modulator programmed death-ligand 1 (PD-L1), possibly explaining the underlying resistance by evading immune surveillance checkpoints (Zhou S. et al., 2019). In this review, we summarize and analyse the promising potential of the targeted neddylation pathway as a new therapeutic method and effects of MLN4924/pevonedistat/TAK-924 treatment combined with

TABLE 1 | Classification of NEDD8 E3 ligases.

Neddylation E3 ligases

HECT E3s	RING E3s	
Itch	CBLs	SCFFBXO11
NEDL1	DCN1	TFB3
NEDL2	IAPs	TRIM40
Smurf1	MDM2	
Smurf2	RNF111	
Yeast Rsp5	Roc1/2	

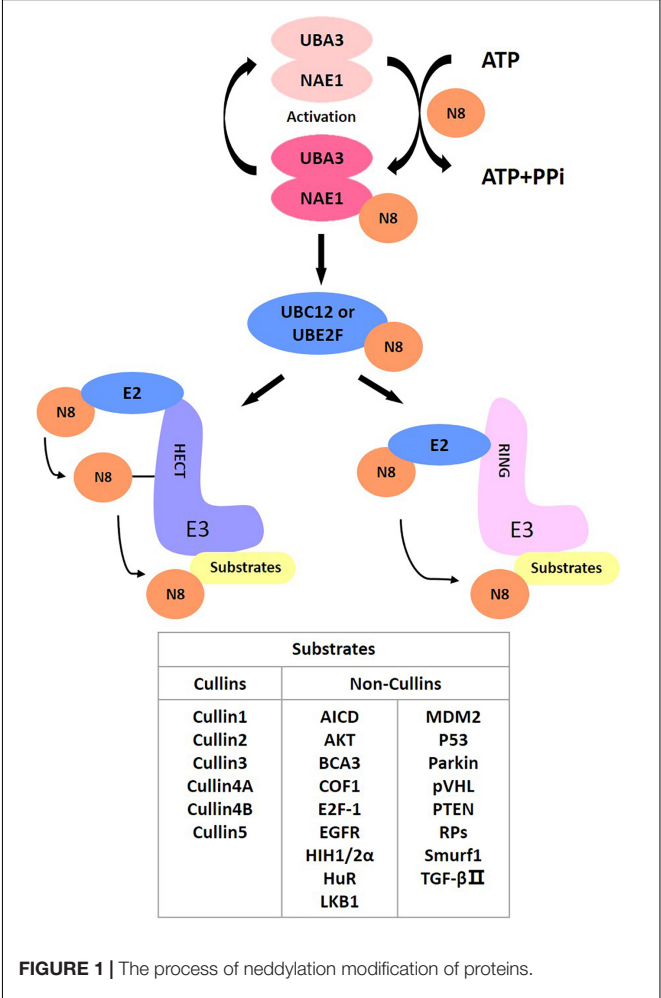


FIGURE 1 | The process of neddylation modification of proteins.



other anticancer therapies, particularly those targeting the antitumor immune axis.

## TARGET PROTEINS OF NEDDYLATION

After activation by neddylation, CRLs are the largest group of multi-unit E3 ubiquitin ligases responsible for ubiquitination, with roughly 20 percent of cellular proteins targeted then degraded by the ubiquitin-proteasome system (UPS) (Petroski and Deshaies, 2005). The connection between NEDD8 and the lysine residues at the C-terminus of cullins activates CRLs (Sakata et al., 2007; Merlet et al., 2009), resulting in a structural alteration in the CRL complex: it adopts an open conformation to increase the entry of ubiquitinated substrates (Zheng et al., 2002; Duda et al., 2008; Saha and Deshaies, 2008). CRL is a multi-unit E3 comprising the following four components: cullin, a substrate recognition receptor, an adaptor protein, and one RING protein. There are eight cullins, including CUL1-3, CUL4A, CUL4B, CUL5, CUL7, and CUL9, which are the optimal substrates of the NEDD8 pathway; they have an evolutionarily conserved cullin homology domain (Petroski and Deshaies, 2005). Every cullin protein is regarded as a molecular framework that promotes the combination of an adaptor protein, an N-terminal substrate receptor protein and a C-terminal RING protein (RBX1 or RBX2) to assemble a CRL (Feldman et al., 1997; Deshaies, 1999; Seol et al., 1999; Petroski and Deshaies, 2005). CRLs regulate many important biological processes, such as cell survival, apoptosis, genomic integrity, tumorigenesis and signal transduction, by facilitating the ubiquitination and degradation of critical zymolytes (Feldman et al., 1997; Nakayama and Nakayama, 2006; Deshaies and Joazeiro, 2009).

Cullin neddylation activates CRLs, but some non-cullin proteins are also protein substrates of neddylation. In 1979, p53 was originally recognized as a factor related to transformation, and researchers have gradually discovered that it is closely associated with the tumor process. *In vivo*, p53 modifications occur mainly in pathways that promote ubiquitination, phosphorylation and acetylation (Brooks and Gu, 2003). Research has indicated that p53 is an essential target for neddylation as well. The stability and function of p53, a tumor suppressor, are tightly regulated by post-translational modifications, including ubiquitylation and neddylation, in which the MDM2 oncoprotein plays a critical role. Mdm2, as an E3 ubiquitin ligase, binds directly to p53, thereby promoting its polyubiquitination and proteasomal degradation (Nakamura et al., 2000). Furthermore, Mdm2 and F-box protein 11 (FBXO11) facilitate the combination of NEDD8 with p53, thus inhibiting p53 activity (Xirodimas et al., 2004; Abida et al., 2007). Several ribosomal proteins have been identified as potential NEDD8 substrates (Xirodimas et al., 2008). L11 was found to be neddylated by Mdm2 and deneddylated by NEDP1. MDM2-mediated L11 neddylation protects L11 from degradation, and both L11 (Lohrum et al., 2003; Zhang et al., 2003) and S14 (Zhou et al., 2013) bind to MDM2 and regulate p53 stability. Furthermore, the expression level of the RNA-binding protein HuR is associated with MDM2. HuR could be protected from degradation by neddylation through Mdm2-dependent

stabilization (Embade et al., 2012). Other non-cullin substrates of neddylation have been reported, including the following: the tumor suppressor pVHL (Stickle et al., 2004); receptor proteins such as EGFR (Oved et al., 2006) and TGF- $\beta$  type II receptor (Zuo et al., 2013); and transcriptional regulators such as HIF1 $\alpha$ /HIF2 $\alpha$  (Ryu et al., 2011), breast cancer-associated protein 3 (BCA3) (Gao et al., 2006), APP intracellular domain (AICD) (Lee et al., 2008), E2F-1 (Loftus et al., 2012), HECT-domain ubiquitin E3 ligase SMURF1 and RBR ubiquitin E3 ligase Parkin (Xie et al., 2014; Enchev et al., 2015). Additionally, new potential neddylation targets exist for LKB1 and Akt (Barbier-Torres et al., 2015).

In addition to the substrates mentioned above, Vogl et al. (2020) recently developed a series of NEDD8-ubiquitin-substrate spectra (sNUSP) that can be used to identify new substrates, such as COF1. The identification of a growing number of substrates suggests that neddylation plays an extensive role in cells with more complex cancer-promoting mechanisms than previously thought, providing a theoretical basis for targeting the neddylation pathway in the treatment of various diseases.

## TARGETING PROTEIN NEDDYLATION AS AN ANTICANCER STRATEGY

NEDD8 was initially identified as a gene whose expression is downregulated during development in the mouse brain (Kumar et al., 1992). However, it was demonstrated subsequently to exist in various mouse tissues and is highly conserved in vertebrate species and somewhat conserved in yeast (Kumar et al., 1993), suggesting that the neddylation pathway is essential during species evolution. Neddylation is a type of posttranslational modification that modulates substrate protein activity. Neddylation modification is catalyzed by an NAE (E1), a NEDD8-conjugating enzyme (E2), and a NEDD8 ligase (E3); these factors link a ubiquitin-like molecule, NEDD8, to the lysine residues of the substrate protein. Accumulating evidence shows that NEDD8 is overexpressed in some human diseases, such as neurodegenerative disorders (Dil Kuazi et al., 2003; Mori et al., 2005) and cancers (Chairatvit and Ngamkitidechakul, 2007; Salon et al., 2007). Thus, targeting protein neddylation has recently been recognized as a popular anticancer method (Watson et al., 2011; Zhou et al., 2018). We summarized previous and recent findings in Table 2.

### NEDD8-Activating Enzyme (NAE)

NEDD8 is activated through an ATP-dependent reaction via NAE and then is transferred to NEDD8-conjugating enzyme E2. MLN4924 is a selective, effective, first-rate inhibitor of NAE (Gong and Yeh, 1999). This micromolecule inhibits the protein neddylation pathway and is currently under multiple clinical investigations of its anticancer effect against solid tumors and leukemia (Soucy et al., 2009; Godbersen et al., 2014; Swords et al., 2018). The MLN4924 antitumor activity is mediated by its ability to induce cell-associated autophagy, apoptosis and senescence (Milhollen et al., 2010; Han et al., 2016). For example, in liver cancer, MLN4924 induces the DNA damage response (DDR) and apoptosis to inhibit hepatoma cell development

**TABLE 2 |** Neddylation modification as an inhibition.

Ligase	Product Name	Mechanism and Principal Action	Target	References
E1	MLN4924	Pevonedistat (MLN4924) inhibits NAE activity more selectively than the closely related ubiquitin-activating enzyme (UAE, also known as UBA1) and SUMO-activating enzyme (SAE; a heterodimer of SAE1 and UBA2 subunits), in purified enzyme and cellular assays. MLN4924 exhibits potent cytotoxic activity against a variety of human tumor-derived cell lines.	NAE1	Soucy et al., 2009
E2	WS-383	WS-383 is a potent, selective and reversible inhibitor of the DCN1-UBC12 interaction. WS-383 inhibits Cul3/1 neddylation and induces the accumulation of p21, p27 and NRF2.	DCN1-UBC12 interaction	Wang et al., 2019
	DI-591	DI-591 binds to purified recombinant human DCN1 and DCN2 protein and disrupts the DCN1-UBC12 interaction in cells. Treatment with DI-591 selectively converts cellular cullin 3 into an un-neddylated inactive form with no or minimum effect on other cullin members.	DCN1-UBC12 interaction	Zhou H. et al., 2017
	NAcM-OPT	NAcM-OPT is an orally bioavailable cullin neddylation 1 (DCN1) inhibitor, which potently inhibits the DCN1-UBE2M interaction.	DCN1	Hammill et al., 2018

*in vitro* and *in vivo* and also induces autophagy, whereas MLN4924 induces autophagy mediated by accumulating the mTOR inhibitory protein Deptor and inducing reactive oxygen species (ROS)-mediated oxidative stress (Peterson et al., 2009; Luo et al., 2012). Identical to its effect in liver cancer, MLN4924 effectively suppresses lymphoma cell growth by inducing cycle arrest of G2 cells and subsequent cell line-dependent apoptosis or senescence. Apoptosis induced by MLN4924 is mediated by the apoptotic signaling pathway, with significantly upregulated pro-apoptotic proteins Bik and Noxa and downregulated anti-apoptotic proteins XIAP, c-IAP1 and c-IAP2, while aging induced by neddylation suppression seemingly depends on the expression of tumor suppressors p21/p27 (Brownell et al., 2010). Mechanistically, when tumor cells are treated with MLN4924, MLN4924 blocks the activities of NAE by binding to its active site to constitute a covalent NEDD8-MLN4924 adduct. Therefore, CRLs are inactivated, leading to the accumulation of tumor-suppressive substrates of CRLs and apoptosis or senescence induction to inhibit cancer cell progression (Karin et al., 2002; Wang et al., 2015).

Consistent with NAE inhibition, MLN4924 treatment of cultured tumor cells results in the inhibition of CRL neddylation and a reciprocal rise in the levels of foregone CRL substrates such as p-Ik $\beta$  (Soucy et al., 2009). The accumulation of p-Ik $\beta$  in the cytoplasm inhibits the nuclear translocation of NF- $\kappa$ B transcription factors and suppresses the NF- $\kappa$ B pathway, affecting tumorigenesis and development through transcriptionally controlling genes related to cell growth, angiogenesis, apoptosis, metastasis and cell migration (Karin et al., 2002). For example, in activated B-cell-like diffuse large B-cell lymphoma (ABC-DLBCL), MLN4924 causes G1-phase cell cycle arrest and apoptosis induction by blocking the classic NF- $\kappa$ B pathway. Thus, MLN4924 treatment leads to G1 phase arrest, P-Ik $\beta$  accumulation and decreased inhibition of NF- $\kappa$ B target genes, significantly affecting MLN4924-mediated antitumor effects (Milhollen et al., 2010).

Autophagy plays a critical role in maintaining cellular homeostasis and is closely associated with the development of many human diseases (Wang and Zhang, 2019). MLN4924 significantly inhibits CRL neddylation modifications and effectively induces autophagy in both dose- and time-dependently in multiple human cancer cell lines (Zhao et al., 2012). MLN4924 inhibits the activity of CRLs, induces

the accumulation of its substrate Ik $\beta$ , blocks the activation of NF- $\kappa$ B and expression of catalase, and promotes the expression of ATF3, thereby inducing autophagy in oesophageal cancer cells (Liang et al., 2020). mTOR is a well-established negative regulator of autophagy (Kim and Guan, 2015). By inactivating CRLs/SCF E3s, MLN4924 can inhibit mTORC1 activity by causing DEPTOR accumulation directly and DEPTOR and HIF1 $\alpha$  accumulation via the HIF1-REDD1-TSC1 axis (HIF1 $\alpha$ ) (Zhao et al., 2012). MLN4924 also triggers autophagy in colon cancer cells by suppressing the PI3K/AKT/mTOR pathway (Lv et al., 2018). Autophagy may be a novel anti-cancer mechanism for MLN4924 in cancer treatment, providing conceptual evidence for the strategic combination of MLN4924 with autophagy inhibitors to maximize tumor cell killing through enhanced apoptosis.

MLN4924 leads to DNA re-replication, which triggers checkpoint activation, apoptosis, and senescence in cancer cells (Soucy et al., 2009). The replication of genetic material is a critical process of the cell cycle. Re-replication is a known signal that induces DNA damage and causes DNA damage signaling in cells (Zhu et al., 2004; Archambault et al., 2005). Cdt1 is the initiation factor for the induction of DNA re-replication in cells treated with MLN4924 (Lin et al., 2010). Similarly, the DNA damage signaling factors P21 and P53 are important substrates of the NEDD8-mediated neddylation pathway. P21 is crucial in the S-phase of the cell cycle, DNA replication and the cellular senescence pathway (Pérez-Yépez et al., 2018). MLN4924-induced senescence in human colorectal cancer cells relies on recruiting p53 and its downstream adaptor P21 (Lin et al., 2010). For other human tumor-derived cell lines, including HCT116 (colon), Calu-6 (lung), SKOV-3 (ovarian), H460 (lung), DLD-1 (colon), MCF-7 (mammary gland), CWR22 (prostate) and OCI-LY19 (lymphoma), MLN4924 treatment also inhibits proliferation and migration.

Currently, phase I trials for MLN4924 are ongoing in cancers, such as metastatic melanoma (Bhatia et al., 2016), advanced solid tumors (Bhatia et al., 2016), acute myeloid leukemia (Swords et al., 2015), myelodysplastic syndromes (Shah et al., 2016), lymphoma and multiple myeloma (Shah et al., 2016), and these studies have revealed that critical therapeutic effects can be obtained by antagonizing NEDD8-mediated protein degradation (**Supplementary Table 1**).

Although excellent activity of MLN4924 was observed in early trials, drug resistance was also found in large number of

patients. Early preclinical studies have shown that treatment-emergent NAE $\beta$  mutations promotes resistance to MLN4924. Additionally, in human leukemic cells, UBA3 mutations increase the enzyme's affinity for ATP while decreasing its affinity for NEDD8 (Milhollen et al., 2012; Xu et al., 2014); these mutations effectively contribute to decreased MLN4924 potency *in vitro*. In TCGA, PanCancer Atlas, the frequency of mutations in UBA3 is about 20%, that may suggest that mutations in UBA3 are not the main cause of MLN4924 resistance. Mutations of key molecules are often associated with drug resistance, and in addition to mutations of NAE $\beta$  and UBA3, the upregulation of ABCG2 transcription in resistant cells drives clinical resistance (Kathawala et al., 2020; Wei et al., 2020). Thus, MLN4924 is widely used as an anti-cancer drug in clinical practice but still has some limitations.

### NEDD8-Conjugating Enzyme

Activated NEDD8 can be transferred to the subunits of the substrate by the NEDD8-conjugating enzyme E2, which includes two members: UBE2F and UBE2M/Ubc12. RBX proteins can be divided into RBX1 and RBX2 in humans (Nakamura et al., 2000; Brooks and Gu, 2003; Nakayama and Nakayama, 2006; Abida et al., 2007). UBE2F pairs with RBX2 to modulate cullin 5 neddylation dependent on E2 RING, while UBE2M functions through RRB1 to mediate the neddylation of cullin 1, 2, 3, 4a, 4b, and 7 (Zhou W. et al., 2017). The E2-RBX-cullin interaction combination determines the *in vivo* selectivity of neddylation (Huang et al., 2009). The cellular levels of different RBX partners determine the cellular levels of distinct cullins. The two NEDD8 E2s exert different effects in cullin neddylation *in vivo* (Huang et al., 2009).

Inhibition of E2s, which inhibit one subset of NEDD8 substrates compared with all neddylation substrates, may provide better cytotoxic selectivity than inhibition of E1s, which inactivates the entire neddylation pathway. In lung cancer, targeting UBC12 causes accumulation of the CRL substrates p21, p27, and Wee1, inactivating CRL ubiquitin ligase and arresting the cell cycle in the G2 phase (Li et al., 2019). Therefore, targeting E2s to inhibit neddylation modification blocks the protein neddylation pathway and deactivates CRLs, triggering the aggregation of tumor-suppressive CRL substrates, stopping the cell cycle and impeding tumor growth and metastasis.

### NEDD8 E3 Ligases

E3 ubiquitin ligases based on Cullin are activated by NEDD8 binding to Cullins. Therefore, targeting E2s to inhibit neddylation modification blocks the protein neddylation pathway and deactivates CRLs, triggering the aggregation of tumor-suppressive CRL substrates, stopping the cell cycle and impeding tumor growth and metastasis (Kurz et al., 2008). Human cells express 5 DCN1-like (DCNL) proteins, termed DCNL1–DCNL5 (also named DCUN1D1–5), each encompassing a C-terminal potentiating neddylation domain and an N-terminal ubiquitin-binding (UBA) domain, which we termed the PONY domain, with distinct amino-terminal extensions (Kurz et al., 2005; Kurz et al., 2008; Meyer-Schaller et al., 2009). For example, in various human tumors, activation

of squamous cell carcinoma-associated oncogene (SCCRO) triggers its function as an oncogene, and the UBA domain in SCCRO (also called DCUN1D1) works as a feedback regulator of biochemical and oncogenic activity (Huang et al., 2015). Conversely, DCNL3 levels are downregulated in the liver, bladder, and renal tumors (Ma et al., 2008) compared with those in normal controls, indicating that DCNL regulation is critical for human cancer development. Considering the conserved binding characteristics of the UBA domain, targeting these vital proteins could possess therapeutic implications for human cancer treatment.

## TARGETING PROTEIN NEDDYLATION-BASED COMBINATION THERAPIES

### NAE Inhibitor MLN4924 Combined With Chemotherapy Drugs

The effectiveness of radiotherapy for cancer is limited by some of the toxic side effects of dose increases, although existing radiotherapy remains the preferred problem for local cancer control (Lyons et al., 2011; Venur and Leone, 2016). Chemotherapy can improve the efficiency of ionizing radiation by inhibiting DNA repair and overcoming apoptotic resistance (Bandugula and N, 2013). Among anticancer drugs, 2-deoxy-D-glucose (2-DG) is the most effective inhibitor of glycolysis, glucose metabolism and ATP production (Dwarakanath, 2009). 2-DG increases the efficacy of chemotherapy drugs (such as doxorubicin [DOX] and paclitaxel) in human osteosarcoma and non-small cell lung cancer *in vivo* (Kern and Norton, 1987). 2-DG + DOX and buthionine sulfoximine (BSO) dramatically promotes cytotoxicity by regulating oxidative stress and interfering with thioethanol metabolism in breast cancer cells (Tagg et al., 2008). MLN4924 can sensitize drug-resistant pancreatic, lung and breast cancer cells to ionizing radiation, although it has little effect on normal lung fibroblasts, indicating that MLN4924 is a new radiation sensitizer (Wei et al., 2012; Yang et al., 2012; Sun and Li, 2013). Therefore, 2-DG plus MLN4924 could be an anti-proliferative and radiation-sensitizing strategy for various human cancers, providing insights on breast cancer treatment (Oladghaffari et al., 2017).

### NAE Inhibitor MLN4924 Combined With Targeted Drugs

Endocrine therapy is the standard treatment for oestrogen receptor (ER)-positive breast cancer and can significantly reduce the risk of disease recurrence and mortality (Anbalagan and Rowan, 2015). However, nearly one-third of patients still experience disease recurrence and metastasis mediated by endocrine resistance at the beginning of treatment or during treatment (deConinck et al., 1995; Anbalagan and Rowan, 2015). Fulvestrant has been approved as a selective oestrogen receptor downregulator (SERD) to cure locally advanced or metastatic breast carcinoma and significantly extends the progression-free survival of patients (Johnston and Cheung, 2010). The



neddylation modification pathway is activated in breast carcinoma and is associated with ER- $\alpha$  expression. In anti-breast cancer treatment, the neddylation pathway can downregulate ER- $\alpha$  expression and inhibit ER inactivation, which can have a synergistic anticancer effect with fulvestrant (Jia et al., 2019).

Inhibitors of apoptosis proteins (IAPs) are anti-apoptotic regulators that prevent apoptosis and are often overexpressed in many human tumors, in which they promote apoptosis evasion and cell survival (Gyrd-Hansen and Meier, 2010). IAP antagonists, also regarded as second mitochondria-derived activator of caspase (SMAC) mimetics, have been recognized as new apoptosis-inducing agents for treatment, either alone or in combination with other antitumor drugs (Dineen et al., 2010; Sumi et al., 2013). MLN4924 activates stress-response signaling and works synergistically with IAP antagonists and DNA damage-inducing chemotherapies. The oral IAP antagonist T-3256336 synergistically promotes the anti-proliferative results of the NAE inhibitor MLN4924 in cancer cells (Sumi et al., 2016). The combination of IAP antagonists with MLN4924 inhibits tumor proliferation, demonstrating the promise of a novel cancer combination treatment.

## NAE Inhibitor MLN4924 Combined With Drugs Targeting the Antitumor Immune Axis

Because the FDA approved the anti-PD-1 (programmed death-1) antibodies nivolumab and pembrolizumab, as well as the anti-PD-L1 antibodies atezolimumab, durvalumab and avelumab, the signaling pathway involving PD-1 and its ligand PD-L1 has become a research hotspot in the field of tumor immunology and oncology (Dong et al., 2002). However, not all tumors are sensitive to these compounds. Inhibitors of neddylation are potential cancer treatment and may promote cancer-related immunosuppression. Increasing evidence has demonstrated that some traditional and targeted cancer therapies modulate antitumor immunity (Galluzzi et al., 2015; Patel and Minn, 2018), suggesting that cytotoxic anticancer drugs combined with immune checkpoint blockade therapy may be an effective combination. Thus, the combination of MLN4924 and anti-PD-L1 therapy might significantly increase the therapeutic efficacy *in vivo* compared with that with either agent alone.

## CONCLUSION

MLN4924/pevonedistat/TAK-924, as a micromolecule inhibitor, inhibits NEDD8-activating enzyme (NAE), which impedes the ubiquitination modification cascade, inactivating CRLs. MLN4924 is the critical element of the dynamic protein homeostasis pathway. Many clinical studies have shown the impressive antitumor activity of MLN4924, but single-drug treatment has some limitations. Clinical trials have demonstrated that MLN4924 alone or combined with chemotherapy has a good treatment effect. MLN4924 is currently under phase II/III clinical trials for antitumor treatment and shows good safety and tolerability, indicating its good development

prospects. We summarize the previous and recent findings in **Supplementary Table 1**.

Recent studies have shown that MLN4924 has good anti-ubiquitination activity and several activities independent of its ubiquitination effects. MLN4924 induces EGFR dimerization, thus triggering AKT1 activation. However, AKT1 and EGFR inhibitors can eliminate MLN4924's inhibition of cilia formation (Mao et al., 2019). These results suggest that MLN4924 may have new applications in human cancer therapy that exhibit cilia-dependent increase or drug resistance (Zhou et al., 2016). MLN4924 can also promote glycolysis, and MLN4924 significantly increases the activity of pyruvate kinase (PK), which could improve the survival rate of breast carcinoma cells. Therefore, PKM2 activation, which promotes glycolysis and cell survival, is an adverse outcome of MLN4924 for cancer treatment and careful monitoring is required when using this drug (Zhou Q. et al., 2019). The dosage of MLN4924 is also worthy of our attention. Studies on various signal inhibitors have shown that the tumor sphere stimulation of MLN4924 is primarily regulated by the RAS/MAPK pathway. In mouse skin, MLN4924 accelerates EGF-induced injury recovery. Therefore, a low dose of MLN4924 controls the proliferation and differentiation of stem cells and has different anticancer properties than the high dose. Additionally, MLN4924 has promising application in stem cell treatment and tissue regeneration. In addition to the dosage of MLN4924 that requires caution, the drug resistance of MLN4924 also deserves our attention. In TCGA, PanCancer Atlas, the frequency of mutations in UBA3 in all tumors is approximately 20%, which may suggest that there are other reasons for MLN4924 resistance and that no key gene mutations but the upregulation of ABCG2 transcripts were found in relapsed/refractory patients with MLN4924. Therefore, we can use this hint to look for other causes of drug resistance in MLN4924, and that bring new understanding to the resistance of MLN4924 to better overcome it. To overcome resistance to MLN4924, refining the drug combination may be a more routine and convenient clinical tool, in contrast to the development of a new generation of NAE inhibitors. In parallel, mutant molecules or ABCG2 can be used as clinical biomarkers to predict therapeutic resistance to MLN4924.

Immunotherapy has become a hot topic in cancer precision medicine and has gradually developed into the fourth tumor treatment mode after surgery, chemotherapy and radiotherapy. However, it is not universally effective, and even the most popular PD-1/PDL-1 therapy only leads to a good response in approximately 20% of patients. The body's immune system has the function of immune surveillance. When malignant cells appear in the body, the immune system recognizes and specifically clears these "non-self" cells. However, tumor cells can still grow in the body, suggesting that they can either evade attack by the host immune system or somehow modulate the body's effective antitumor immune response. The inhibition of cell activation caused by tumor cell modification is an important mechanism of tumor immune escape. According to recent research progress, targeted therapy is expected to inhibit tumor immune escape, improve the therapeutic effect of tumor treatment and improve the prognosis of patients.



## AUTHOR CONTRIBUTIONS

LZ, HJ, and CL contributed to the conception of the review. WG wrote the manuscript. ZP helped perform the analysis with constructive discussions. All the authors contributed to the article and approved the submitted version.

## FUNDING

This work was supported by the National Natural Science Foundation of China (31771110), Shandong Province

Natural Science Foundation (ZR2019ZD31), Taishan Scholars Construction Project, and Innovative Research Team of High-Level Local Universities in Shanghai.

## SUPPLEMENTARY MATERIAL

The Supplementary Material for this article can be found online at: <https://www.frontiersin.org/articles/10.3389/fcell.2021.653882/full#supplementary-material>

**Supplementary Table 1** | Combined application and clinical staging of MLN4924.

## REFERENCES

- Abida, W. M., Nikolaev, A., Zhao, W., Zhang, W., and Gu, W. (2007). FBXO11 promotes the Neddylation of p53 and inhibits its transcriptional activity. *J. Biol. Chem.* 282, 1797–1804. doi: 10.1074/jbc.M609001200
- Anbalagan, M., and Rowan, B. G. (2015). Estrogen receptor alpha phosphorylation and its functional impact in human breast cancer. *Mol. Cell. Endocrinol.* 418(Pt 3), 264–272. doi: 10.1016/j.mce.2015.01.016
- Archambault, V., Ikui, A. E., Drapkin, B. J., and Cross, F. R. (2005). Disruption of mechanisms that prevent rereplication triggers a DNA damage response. *Mol. Cell. Biol.* 25, 6707–6721. doi: 10.1128/mcb.25.15.6707-6721.2005
- Bandugula, V. R., and N, R. P. (2013). 2-Deoxy-D-glucose and ferulic acid modulates radiation response signaling in non-small cell lung cancer cells. *Tumour Biol.* 34, 251–259. doi: 10.1007/s13277-012-0545-6
- Barbier-Torres, L., Delgado, T. C., García-Rodríguez, J. L., Zubiete-Franco, I., Fernández-Ramos, D., Buqué, X., et al. (2015). Stabilization of LKB1 and Akt by neddylation regulates energy metabolism in liver cancer. *Oncotarget* 6, 2509–2523. doi: 10.18632/oncotarget.3191
- Berndsen, C. E., and Wolberger, C. (2014). New insights into ubiquitin E3 ligase mechanism. *Nat. Struct. Mol. Biol.* 21, 301–307. doi: 10.1038/nsmb.2780
- Bhatia, S., Pavlick, A. C., Boasberg, P., Thompson, J. A., Mulligan, G., Pickard, M. D., et al. (2016). A phase I study of the investigational NEDD8-activating enzyme inhibitor pevonedistat (TAK-924/MLN4924) in patients with metastatic melanoma. *Invest. New Drugs* 34, 439–449. doi: 10.1007/s10637-016-0348-5
- Bohnsack, R. N., and Haas, A. L. (2003). Conservation in the mechanism of Nedd8 activation by the human AppBp1-Uba3 heterodimer. *J. Biol. Chem.* 278, 26823–26830. doi: 10.1074/jbc.M303177200
- Broemer, M., Tenev, T., Rigbolt, K. T., Hempel, S., Blagoev, B., Silke, J., et al. (2010). Systematic in vivo RNAi analysis identifies IAPs as NEDD8-E3 ligases. *Mol. Cell* 40, 810–822. doi: 10.1016/j.molcel.2010.11.011
- Brooks, C. L., and Gu, W. (2003). Ubiquitination, phosphorylation and acetylation: the molecular basis for p53 regulation. *Curr. Opin. Cell Biol.* 15, 164–171. doi: 10.1016/s0955-0674(03)00003-6
- Brownell, J. E., Sintchak, M. D., Gavin, J. M., Liao, H., Bruzzese, F. J., Bump, N. J., et al. (2010). Substrate-assisted inhibition of ubiquitin-like protein-activating enzymes: the NEDD8 E1 inhibitor MLN4924 forms a NEDD8-AMP mimetic in situ. *Mol. Cell* 37, 102–111. doi: 10.1016/j.molcel.2009.12.024
- Chairatvit, K., and Ngamkitdechakul, C. (2007). Control of cell proliferation via elevated NEDD8 conjugation in oral squamous cell carcinoma. *Mol. Cell. Biochem.* 306, 163–169. doi: 10.1007/s11010-007-9566-7
- Chen, P., Hu, T., Liang, Y., Li, P., Chen, X., Zhang, J., et al. (2016). Neddylation inhibition activates the extrinsic apoptosis pathway through ATF4-CHOP-DR5 axis in human esophageal cancer cells. *Clin. Cancer Res.* 22, 4145–4157. doi: 10.1158/1078-0432.Ccr-15-2254
- Czuczman, N. M., Barth, M. J., Gu, J., Neppalli, V., Mavis, C., Frys, S. E., et al. (2016). Pevonedistat, a NEDD8-activating enzyme inhibitor, is active in mantle cell lymphoma and enhances rituximab activity in vivo. *Blood* 127, 1128–1137. doi: 10.1182/blood-2015-04-640920
- deConinck, E. C., McPherson, L. A., and Weigel, R. J. (1995). Transcriptional regulation of estrogen receptor in breast carcinomas. *Mol. Cell. Biol.* 15, 2191–2196. doi: 10.1128/mcb.15.4.2191
- Dengler, M. A., Weilbacher, A., Gutekunst, M., Staiger, A. M., Vöhringer, M. C., Horn, H., et al. (2014). Discrepant NOXA (PMAIP1) transcript and NOXA protein levels: a potential Achilles' heel in mantle cell lymphoma. *Cell Death Dis.* 5:e1013. doi: 10.1038/cddis.2013.552
- Deshaies, R. J. (1999). SCF and cullin/ring H2-based ubiquitin ligases. *Annu. Rev. Cell Dev. Biol.* 15, 435–467. doi: 10.1146/annurev.cellbio.15.1.435
- Deshaies, R. J., and Joazeiro, C. A. (2009). RING domain E3 ubiquitin ligases. *Annu. Rev. Biochem.* 78, 399–434. doi: 10.1146/annurev.biochem.78.101807.093809
- Dil Kuazi, A., Kito, K., Abe, Y., Shin, R. W., Kamitani, T., and Ueda, N. (2003). NEDD8 protein is involved in ubiquitinated inclusion bodies. *J. Pathol.* 199, 259–266. doi: 10.1002/path.1283
- Dineen, S. P., Roland, C. L., Greer, R., Carbon, J. G., Toombs, J. E., Gupta, P., et al. (2010). Smac mimetic increases chemotherapy response and improves survival in mice with pancreatic cancer. *Cancer Res.* 70, 2852–2861. doi: 10.1158/0008-5472.Can-09-3892
- Dong, H., Strome, S. E., Salomao, D. R., Tamura, H., Hirano, F., Flies, D. B., et al. (2002). Tumor-associated B7-H1 promotes T-cell apoptosis: a potential mechanism of immune evasion. *Nat. Med.* 8, 793–800. doi: 10.1038/nm730
- Duan, H., Wang, Y., Aviram, M., Swaroop, M., Loo, J. A., Bian, J., et al. (1999). SAG, a novel zinc RING finger protein that protects cells from apoptosis induced by redox agents. *Mol. Cell. Biol.* 19, 3145–3155. doi: 10.1128/mcb.19.4.3145
- Duda, D. M., Borg, L. A., Scott, D. C., Hunt, H. W., Hammel, M., and Schulman, B. A. (2008). Structural insights into NEDD8 activation of cullin-RING ligases: conformational control of conjugation. *Cell* 134, 995–1006. doi: 10.1016/j.cell.2008.07.022
- Dwarakanath, B. S. (2009). Cytotoxicity, radiosensitization, and chemosensitization of tumor cells by 2-deoxy-D-glucose in vitro. *J. Cancer Res. Ther.* 5(Suppl. 1), S27–S31. doi: 10.4103/0973-1482.55137
- Embade, N., Fernández-Ramos, D., Varela-Rey, M., Beraza, N., Sini, M., Gutiérrez de Juan, V., et al. (2012). Murine double minute 2 regulates Hu antigen R stability in human liver and colon cancer through NEDDylation. *Hepatology* 55, 1237–1248. doi: 10.1002/hep.24795
- Enchev, R. I., Schulman, B. A., and Peter, M. (2015). Protein neddylation: beyond cullin-RING ligases. *Nat. Rev. Mol. Cell Biol.* 16, 30–44. doi: 10.1038/nrm3919
- Feldman, R. M., Correll, C. C., Kaplan, K. B., and Deshaies, R. J. (1997). A complex of Cdc4p, Skp1p, and Cdc53p/cullin catalyzes ubiquitination of the phosphorylated CDK inhibitor Sic1p. *Cell* 91, 221–230. doi: 10.1016/s0092-8674(00)80404-3
- Galluzzi, L., Buqué, A., Kepp, O., Zitvogel, L., and Kroemer, G. (2015). Immunological effects of conventional chemotherapy and targeted anticancer agents. *Cancer Cell* 28, 690–714. doi: 10.1016/j.ccell.2015.10.012
- Gan-Erdene, T., Nagamalleswari, K., Yin, L., Wu, K., Pan, Z. Q., and Wilkinson, K. D. (2003). Identification and characterization of DEN1, a deneddylase of the ULP family. *J. Biol. Chem.* 278, 28892–28900. doi: 10.1074/jbc.M302890200
- Gao, F., Cheng, J., Shi, T., and Yeh, E. T. (2006). Neddylation of a breast cancer-associated protein recruits a class III histone deacetylase that represses NFκappaB-dependent transcription. *Nat. Cell Biol.* 8, 1171–1177. doi: 10.1038/ncb1483
- Gao, Q., Yu, G. Y., Shi, J. Y., Li, L. H., Zhang, W. J., Wang, Z. C., et al. (2014). Neddylation pathway is up-regulated in human intrahepatic

- cholangiocarcinoma and serves as a potential therapeutic target. *Oncotarget* 5, 7820–7832. doi: 10.18632/oncotarget.2309
- Godbersen, J. C., Humphries, L. A., Danilova, O. V., Kebbekus, P. E., Brown, J. R., Eastman, A., et al. (2014). The Nedd8-activating enzyme inhibitor MLN4924 thwarts microenvironment-driven NF- $\kappa$ B activation and induces apoptosis in chronic lymphocytic leukemia B cells. *Clin. Cancer Res.* 20, 1576–1589. doi: 10.1158/1078-0432.Ccr-13-0987
- Gong, L., and Yeh, E. T. (1999). Identification of the activating and conjugating enzymes of the NEDD8 conjugation pathway. *J. Biol. Chem.* 274, 12036–12042. doi: 10.1074/jbc.274.17.12036
- Gyrd-Hansen, M., and Meier, P. (2010). IAPs: from caspase inhibitors to modulators of NF-kappaB, inflammation and cancer. *Nat. Rev. Cancer* 10, 561–574. doi: 10.1038/nrc2889
- Hammill, J. T., Bhasin, D., Scott, D. C., Min, J., Chen, Y., Lu, Y., et al. (2018). Discovery of an orally bioavailable inhibitor of defective in cullin neddylation 1 (DCN1)-mediated cullin neddylation. *J. Med. Chem.* 61, 2694–2706. doi: 10.1021/acs.jmedchem.7b01282
- Han, K., Wang, Q., Cao, H., Qiu, G., Cao, J., Li, X., et al. (2016). The NEDD8-activating enzyme inhibitor MLN4924 induces G2 arrest and apoptosis in T-cell acute lymphoblastic leukemia. *Oncotarget* 7, 23812–23824. doi: 10.18632/oncotarget.8068
- Hua, W., Li, C., Yang, Z., Li, L., Jiang, Y., Yu, G., et al. (2015). Suppression of glioblastoma by targeting the overactivated protein neddylation pathway. *Neuro Oncol.* 17, 1333–1343. doi: 10.1093/neuonc/nov066
- Huang, D. T., Ayrault, O., Hunt, H. W., Taherbhoy, A. M., Duda, D. M., Scott, D. C., et al. (2009). E2-RING expansion of the NEDD8 cascade confers specificity to cullin modification. *Mol. Cell* 33, 483–495. doi: 10.1016/j.molcel.2009.01.011
- Huang, D. T., Paydar, A., Zhuang, M., Waddell, M. B., Holton, J. M., and Schulman, B. A. (2005). Structural basis for recruitment of Ubc12 by an E2 binding domain in NEDD8's E1. *Mol. Cell* 17, 341–350. doi: 10.1016/j.molcel.2004.12.020
- Huang, G., Towe, C. W., Choi, L., Yonekawa, Y., Bommeljé, C. C., Bains, S., et al. (2015). The ubiquitin-associated (UBA) domain of SCCRO/DCUN1D1 protein serves as a feedback regulator of biochemical and oncogenic activity. *J. Biol. Chem.* 290, 296–309. doi: 10.1074/jbc.M114.560169
- Jia, L., Li, H., and Sun, Y. (2011). Induction of p21-dependent senescence by an NAE inhibitor, MLN4924, as a mechanism of growth suppression. *Neoplasia* 13, 561–569. doi: 10.1593/neo.11420
- Jia, X., Li, C., Li, L., Liu, X., Zhou, L., Zhang, W., et al. (2019). Neddylation inactivation facilitates FOXO3a nuclear export to suppress estrogen receptor transcription and improve fulvestrant sensitivity. *Clin. Cancer Res.* 25, 3658–3672. doi: 10.1158/1078-0432.Ccr-18-2434
- Jiang, Y., and Jia, L. (2015). Neddylation pathway as a novel anti-cancer target: mechanistic investigation and therapeutic implication. *Anticancer Agents Med. Chem.* 15, 1127–1133. doi: 10.2174/1871520615666150305111257
- Johnston, S. C., Larsen, C. N., Cook, W. J., Wilkinson, K. D., and Hill, C. P. (1997). Crystal structure of a deubiquitinating enzyme (human UCH-L3) at 1.8 Å resolution. *EMBO J.* 16, 3787–3796. doi: 10.1093/emboj/16.13.3787
- Johnston, S. J., and Cheung, K. L. (2010). Fulvestrant – a novel endocrine therapy for breast cancer. *Curr. Med. Chem.* 17, 902–914. doi: 10.2174/092986710790820633
- Kamitani, T., Kito, K., Nguyen, H. P., and Yeh, E. T. (1997). Characterization of NEDD8, a developmentally down-regulated ubiquitin-like protein. *J. Biol. Chem.* 272, 28557–28562. doi: 10.1074/jbc.272.45.28557
- Kamura, T., Conrad, M. N., Yan, Q., Conaway, R. C., and Conaway, J. W. (1999). The Rbx1 subunit of SCF and VHL E3 ubiquitin ligase activates Rub1 modification of cullins Cdc53 and Cul2. *Genes Dev.* 13, 2928–2933. doi: 10.1101/gad.13.22.2928
- Karin, M., Cao, Y., Greten, F. R., and Li, Z. W. (2002). NF-kappaB in cancer: from innocent bystander to major culprit. *Nat. Rev. Cancer* 2, 301–310. doi: 10.1038/nrc780
- Kathawala, R. J., Espitia, C. M., Jones, T. M., Islam, S., Gupta, P., Zhang, Y. K., et al. (2020). ABCG2 overexpression contributes to pevonedistat resistance. *Cancers* 12:429. doi: 10.3390/cancers12020429
- Kern, K. A., and Norton, J. A. (1987). Inhibition of established rat fibrosarcoma growth by the glucose antagonist 2-deoxy-D-glucose. *Surgery* 102, 380–385.
- Kim, Y. C., and Guan, K. L. (2015). mTOR: a pharmacologic target for autophagy regulation. *J. Clin. Invest.* 125, 25–32. doi: 10.1172/jci73939
- Knorr, K. L., Schneider, P. A., Meng, X. W., Dai, H., Smith, B. D., Hess, A. D., et al. (2015). MLN4924 induces Noxa upregulation in acute myelogenous leukemia and synergizes with Bcl-2 inhibitors. *Cell Death Differ.* 22, 2133–2142. doi: 10.1038/cdd.2015.74
- Kumar, S., Tomooka, Y., and Noda, M. (1992). Identification of a set of genes with developmentally down-regulated expression in the mouse brain. *Biochem. Biophys. Res. Commun.* 185, 1155–1161. doi: 10.1016/0006-291x(92)91747-e
- Kumar, S., Yoshida, Y., and Noda, M. (1993). Cloning of a cDNA which encodes a novel ubiquitin-like protein. *Biochem. Biophys. Res. Commun.* 195, 393–399. doi: 10.1006/bbrc.1993.2056
- Kurz, T., Chou, Y. C., Willems, A. R., Meyer-Schaller, N., Hecht, M. L., Tyers, M., et al. (2008). Dcn1 functions as a scaffold-type E3 ligase for cullin neddylation. *Mol. Cell* 29, 23–35. doi: 10.1016/j.molcel.2007.12.012
- Kurz, T., Ozl , N., Rudolf, F., O'Rourke, S. M., Luke, B., Hofmann, K., et al. (2005). The conserved protein DCN-1/Dcn1p is required for cullin neddylation in *C. elegans* and *S. cerevisiae*. *Nature* 435, 1257–1261. doi: 10.1038/nature03662
- Lan, H., Tang, Z., Jin, H., and Sun, Y. (2016). Neddylation inhibitor MLN4924 suppresses growth and migration of human gastric cancer cells. *Sci. Rep.* 6:24218. doi: 10.1038/srep24218
- Leclerc, G. M., Zheng, S., Leclerc, G. J., DeSalvo, J., Swords, R. T., and Barredo, J. C. (2016). The NEDD8-activating enzyme inhibitor pevonedistat activates the eIF2 $\alpha$  and mTOR pathways inducing UPR-mediated cell death in acute lymphoblastic leukemia. *Leuk. Res.* 50, 1–10. doi: 10.1016/j.leukres.2016.09.007
- Lee, M. R., Lee, D., Shin, S. K., Kim, Y. H., and Choi, C. Y. (2008). Inhibition of APP intracellular domain (AICD) transcriptional activity via covalent conjugation with Nedd8. *Biochem. Biophys. Res. Commun.* 366, 976–981. doi: 10.1016/j.bbrc.2007.12.066
- Li, H., Zhu, H., Liu, Y., He, F., Xie, P., and Zhang, L. (2016). Itch promotes the neddylation of JunB and regulates JunB-dependent transcription. *Cell. Signal.* 28, 1186–1195. doi: 10.1016/j.cellsig.2016.05.016
- Li, L., Kang, J., Zhang, W., Cai, L., Wang, S., Liang, Y., et al. (2019). Validation of NEDD8-conjugating enzyme UBC12 as a new therapeutic target in lung cancer. *EBioMedicine* 45, 81–91. doi: 10.1016/j.ebiom.2019.06.005
- Li, L., Wang, M., Yu, G., Chen, P., Li, H., Wei, D., et al. (2014). Overactivated neddylation pathway as a therapeutic target in lung cancer. *J. Natl. Cancer Inst.* 106:dju083. doi: 10.1093/jnci/dju083
- Liang, Y., Jiang, Y., Jin, X., Chen, P., Heng, Y., Cai, L., et al. (2020). Neddylation inhibition activates the protective autophagy through NF- $\kappa$ B-catalase-ATF3 Axis in human esophageal cancer cells. *Cell Commun. Signal.* 18:72. doi: 10.1186/s12964-020-00576-z
- Lin, J. J., Milhollen, M. A., Smith, P. G., Narayanan, U., and Dutta, A. (2010). NEDD8-targeting drug MLN4924 elicits DNA rereplication by stabilizing Cdt1 in S phase, triggering checkpoint activation, apoptosis, and senescence in cancer cells. *Cancer Res.* 70, 10310–10320. doi: 10.1158/0008-5472.Can-10-2062
- Loftus, S. J., Liu, G., Carr, S. M., Munro, S., and La Thangue, N. B. (2012). NEDDylation regulates E2F-1-dependent transcription. *EMBO Rep.* 13, 811–818. doi: 10.1038/embo.2012.113
- Lohrum, M. A., Ludwig, R. L., Kubbutat, M. H., Hanlon, M., and Vousden, K. H. (2003). Regulation of HDM2 activity by the ribosomal protein L11. *Cancer Cell* 3, 577–587. doi: 10.1016/s1535-6108(03)00134-x
- Luo, Z., Yu, G., Lee, H. W., Li, L., Wang, L., Yang, D., et al. (2012). The Nedd8-activating enzyme inhibitor MLN4924 induces autophagy and apoptosis to suppress liver cancer cell growth. *Cancer Res.* 72, 3360–3371. doi: 10.1158/0008-5472.Can-12-0388
- Ly, Y., Li, B., Han, K., Xiao, Y., Yu, X., Ma, Y., et al. (2018). The Nedd8-activating enzyme inhibitor MLN4924 suppresses colon cancer cell growth via triggering autophagy. *Korean J. Physiol. Pharmacol.* 22, 617–625. doi: 10.4196/kjpp.2018.22.6.617
- Lyons, J. A., Woods, C., Galanopoulos, N., and Silverman, P. (2011). Emerging radiation techniques for early-stage breast cancer after breast-conserving surgery. *Future Oncol.* 7, 915–925. doi: 10.2217/fon.11.61
- Ma, T., Chen, Y., Zhang, F., Yang, C. Y., Wang, S., and Yu, X. (2013). RNF111-dependent neddylation activates DNA damage-induced ubiquitination. *Mol. Cell* 49, 897–907. doi: 10.1016/j.molcel.2013.01.006
- Ma, T., Shi, T., Huang, J., Wu, L., Hu, F., He, P., et al. (2008). DCUN1D3, a novel UVC-responsive gene that is involved in cell cycle progression and cell growth. *Cancer Sci.* 99, 2128–2135. doi: 10.1111/j.1349-7006.2008.00929.x

- Mao, H., Tang, Z., Li, H., Sun, B., Tan, M., Fan, S., et al. (2019). Neddylation inhibitor MLN4924 suppresses cilia formation by modulating AKT1. *Protein Cell* 10, 726–744. doi: 10.1007/s13238-019-0614-3
- Mendoza, H. M., Shen, L. N., Botting, C., Lewis, A., Chen, J., Ink, B., et al. (2003). NEDP1, a highly conserved cysteine protease that deNEDDylates cullins. *J. Biol. Chem.* 278, 25637–25643. doi: 10.1074/jbc.M212948200
- Merlet, J., Burger, J., Gomes, J. E., and Pintard, L. (2009). Regulation of cullin-RING E3 ubiquitin-ligases by neddylation and dimerization. *Cell. Mol. Life Sci.* 66, 1924–1938. doi: 10.1007/s00018-009-8712-7
- Metzger, M. B., Pruneda, J. N., Klevit, R. E., and Weissman, A. M. (2014). RING-type E3 ligases: master manipulators of E2 ubiquitin-conjugating enzymes and ubiquitination. *Biochim. Biophys. Acta* 1843, 47–60. doi: 10.1016/j.bbamcr.2013.05.026
- Meyer-Schaller, N., Chou, Y. C., Sumara, I., Martin, D. D., Kurz, T., Katheder, N., et al. (2009). The human Dcn1-like protein DCN13 promotes Cul3 neddylation at membranes. *Proc. Natl. Acad. Sci. U.S.A.* 106, 12365–12370. doi: 10.1073/pnas.0812528106
- Milhollen, M. A., Thomas, M. P., Narayanan, U., Traore, T., Riceberg, J., Amidon, B. S., et al. (2012). Treatment-emergent mutations in NAE $\beta$  confer resistance to the NEDD8-activating enzyme inhibitor MLN4924. *Cancer Cell* 21, 388–401. doi: 10.1016/j.ccr.2012.02.009
- Milhollen, M. A., Traore, T., Adams-Duffy, J., Thomas, M. P., Berger, A. J., Dang, L., et al. (2010). MLN4924, a NEDD8-activating enzyme inhibitor, is active in diffuse large B-cell lymphoma models: rationale for treatment of NF- $\kappa$ B-dependent lymphoma. *Blood* 116, 1515–1523. doi: 10.1182/blood-2010-03-272567
- Mori, F., Nishie, M., Piao, Y. S., Kito, K., Kamitani, T., Takahashi, H., et al. (2005). Accumulation of NEDD8 in neuronal and glial inclusions of neurodegenerative disorders. *Neuropathol. Appl. Neurobiol.* 31, 53–61. doi: 10.1111/j.1365-2990.2004.00603.x
- Nakamura, S., Roth, J. A., and Mukhopadhyay, T. (2000). Multiple lysine mutations in the C-terminal domain of p53 interfere with MDM2-dependent protein degradation and ubiquitination. *Mol. Cell. Biol.* 20, 9391–9398. doi: 10.1128/mcb.20.24.9391-9398.2000
- Nakayama, K. I., and Nakayama, K. (2006). Ubiquitin ligases: cell-cycle control and cancer. *Nat. Rev. Cancer* 6, 369–381. doi: 10.1038/nrc1881
- Noguchi, K., Okumura, F., Takahashi, N., Kataoka, A., Kamiyama, T., Todo, S., et al. (2011). TRIM40 promotes neddylation of IKK $\gamma$  and is downregulated in gastrointestinal cancers. *Carcinogenesis* 32, 995–1004. doi: 10.1093/carcin/bgr068
- Oladghaffari, M., Shabestani Monfared, A., Farajollahi, A., Baradaran, B., Mohammadi, M., Shانهbandi, D., et al. (2017). MLN4924 and 2DG combined treatment enhances the efficiency of radiotherapy in breast cancer cells. *Int. J. Radiat. Biol.* 93, 590–599. doi: 10.1080/09553002.2017.1294272
- Oved, S., Mosesson, Y., Zwang, Y., Santonic, E., Shtiegman, K., Marmor, M. D., et al. (2006). Conjugation to Nedd8 instigates ubiquitylation and down-regulation of activated receptor tyrosine kinases. *J. Biol. Chem.* 281, 21640–21651. doi: 10.1074/jbc.M513034200
- Paiva, C., Godbersen, J. C., Berger, A., Brown, J. R., and Danilov, A. V. (2015). Targeting neddylation induces DNA damage and checkpoint activation and sensitizes chronic lymphocytic leukemia B cells to alkylating agents. *Cell Death Dis.* 6:e1807. doi: 10.1038/cddis.2015.161
- Patel, S. A., and Minn, A. J. (2018). Combination cancer therapy with immune checkpoint blockade: mechanisms and strategies. *Immunity* 48, 417–433. doi: 10.1016/j.immuni.2018.03.007
- Pérez-Yépez, E. A., Saldívar-Cerón, H. I., Villamar-Cruz, O., Pérez-Plasencia, C., and Arias-Romero, L. E. (2018). p21 Activated kinase 1: nuclear activity and its role during DNA damage repair. *DNA Repair (Amst)* 65, 42–46. doi: 10.1016/j.dnarep.2018.03.004
- Peterson, T. R., Laplante, M., Thoreen, C. C., Sancak, Y., Kang, S. A., Kuehl, W. M., et al. (2009). DEPTOR is an mTOR inhibitor frequently overexpressed in multiple myeloma cells and required for their survival. *Cell* 137, 873–886. doi: 10.1016/j.cell.2009.03.046
- Petroski, M. D., and Deshaies, R. J. (2005). Function and regulation of cullin-RING ubiquitin ligases. *Nat. Rev. Mol. Cell Biol.* 6, 9–20. doi: 10.1038/nrm1547
- Qiu, X., Wei, R., Li, Y., Zhu, Q., Xiong, C., Chen, Y., et al. (2016). NEDL2 regulates enteric nervous system and kidney development in its Nedd8 ligase activity-dependent manner. *Oncotarget* 7, 31440–31453. doi: 10.18632/oncotarget.8951
- Rabut, G., and Peter, M. (2008). Function and regulation of protein neddylation. ‘Protein modifications: beyond the usual suspects’ review series. *EMBO Rep.* 9, 969–976. doi: 10.1038/embor.2008.183
- Rabut, G., Le Dez, G., Verma, R., Makhnevych, T., Knebel, A., Kurz, T., et al. (2011). The TFIIB subunit Tfb3 regulates cullin neddylation. *Mol. Cell* 43, 488–495. doi: 10.1016/j.molcel.2011.05.032
- Ryu, J. H., Li, S. H., Park, H. S., Park, J. W., Lee, B., and Chun, Y. S. (2011). Hypoxia-inducible factor  $\alpha$  subunit stabilization by NEDD8 conjugation is reactive oxygen species-dependent. *J. Biol. Chem.* 286, 6963–6970. doi: 10.1074/jbc.M110.188706
- Saha, A., and Deshaies, R. J. (2008). Multimodal activation of the ubiquitin ligase SCF by Nedd8 conjugation. *Mol. Cell* 32, 21–31. doi: 10.1016/j.molcel.2008.08.021
- Sakata, E., Yamaguchi, Y., Miyauchi, Y., Iwai, K., Chiba, T., Saeki, Y., et al. (2007). Direct interactions between NEDD8 and ubiquitin E2 conjugating enzymes upregulate cullin-based E3 ligase activity. *Nat. Struct. Mol. Biol.* 14, 167–168. doi: 10.1038/nsmb1191
- Salon, C., Brambilla, E., Brambilla, C., Lantuejoul, S., Gazzeri, S., and Eymin, B. (2007). Altered pattern of Cul-1 protein expression and neddylation in human lung tumours: relationships with CAND1 and cyclin E protein levels. *J. Pathol.* 213, 303–310. doi: 10.1002/path.2223
- Seol, J. H., Feldman, R. M., Zachariae, W., Shevchenko, A., Correll, C. C., Lyapina, S., et al. (1999). Cdc53/cullin and the essential Hrt1 RING-H2 subunit of SCF define a ubiquitin ligase module that activates the E2 enzyme Cdc34. *Genes Dev.* 13, 1614–1626. doi: 10.1101/gad.13.12.1614
- Shah, J. J., Jakubowiak, A. J., O’Connor, O. A., Orlowski, R. Z., Harvey, R. D., Smith, M. R., et al. (2016). Phase I study of the novel investigational NEDD8-activating enzyme inhibitor pevonedistat (MLN4924) in patients with relapsed/refractory multiple myeloma or lymphoma. *Clin. Cancer Res.* 22, 34–43. doi: 10.1158/1078-0432.Ccr-15-1237
- Shu, J., Liu, C., Wei, R., Xie, P., He, S., and Zhang, L. (2016). Nedd8 targets ubiquitin ligase Smurf2 for neddylation and promote its degradation. *Biochem. Biophys. Res. Commun.* 474, 51–56. doi: 10.1016/j.bbrc.2016.04.058
- Soucy, T. A., Smith, P. G., Milhollen, M. A., Berger, A. J., Gavin, J. M., Adhikari, S., et al. (2009). An inhibitor of NEDD8-activating enzyme as a new approach to treat cancer. *Nature* 458, 732–736. doi: 10.1038/nature07884
- Stickle, N. H., Chung, J., Klco, J. M., Hill, R. P., Kaelin, W. G. Jr., and Ohh, M. (2004). pVHL modification by NEDD8 is required for fibronectin matrix assembly and suppression of tumor development. *Mol. Cell. Biol.* 24, 3251–3261. doi: 10.1128/mcb.24.8.3251-3261.2004
- Sumi, H., Inazuka, M., Morimoto, M., Hibino, R., Hashimoto, K., Ishikawa, T., et al. (2016). An inhibitor of apoptosis protein antagonist T-3256336 potentiates the antitumor efficacy of the Nedd8-activating enzyme inhibitor pevonedistat (TAK-924/MLN4924). *Biochem. Biophys. Res. Commun.* 480, 380–386. doi: 10.1016/j.bbrc.2016.10.058
- Sumi, H., Yabuki, M., Iwai, K., Morimoto, M., Hibino, R., Inazuka, M., et al. (2013). Antitumor activity and pharmacodynamic biomarkers of a novel and orally available small-molecule antagonist of inhibitor of apoptosis proteins. *Mol. Cancer Ther.* 12, 230–240. doi: 10.1158/1535-7163.Mct-12-0699
- Sun, Y., and Li, H. (2013). Functional characterization of SAG/RBX2/ROC2/RNF7, an antioxidant protein and an E3 ubiquitin ligase. *Protein Cell* 4, 103–116. doi: 10.1007/s13238-012-2105-7
- Swords, R. T., Coutre, S., Maris, M. B., Zeidner, J. F., Foran, J. M., Cruz, J., et al. (2018). Pevonedistat, a first-in-class NEDD8-activating enzyme inhibitor, combined with azacitidine in patients with AML. *Blood* 131, 1415–1424. doi: 10.1182/blood-2017-09-805895
- Swords, R. T., Erba, H. P., DeAngelo, D. J., Bixby, D. L., Altman, J. K., Maris, M., et al. (2015). Pevonedistat (MLN4924), a first-in-class NEDD8-activating enzyme inhibitor, in patients with acute myeloid leukaemia and myelodysplastic syndromes: a phase 1 study. *Br. J. Haematol.* 169, 534–543. doi: 10.1111/bjh.13323
- Swords, R. T., Kelly, K. R., Smith, P. G., Garnsey, J. J., Mahalingam, D., Medina, E., et al. (2010). Inhibition of NEDD8-activating enzyme: a novel approach for the treatment of acute myeloid leukemia. *Blood* 115, 3796–3800. doi: 10.1182/blood-2009-11-254862
- Tagg, S. L., Foster, P. A., Leese, M. P., Potter, B. V., Reed, M. J., Purohit, A., et al. (2008). 2-Methoxyoestradiol-3,17-O,O-bis-sulphamate and 2-deoxy-D-glucose



- in combination: a potential treatment for breast and prostate cancer. *Br. J. Cancer* 99, 1842–1848. doi: 10.1038/sj.bjc.6604752
- Tong, S., Si, Y., Yu, H., Zhang, L., Xie, P., and Jiang, W. (2017). MLN4924 (Pevonedistat), a protein neddylation inhibitor, suppresses proliferation and migration of human clear cell renal cell carcinoma. *Sci. Rep.* 7:5599. doi: 10.1038/s41598-017-06098-y
- Venur, V. A., and Leone, J. P. (2016). Targeted therapies for brain metastases from breast cancer. *Int. J. Mol. Sci.* 17:1543. doi: 10.3390/ijms17091543
- Vogl, A. M., Phu, L., Becerra, R., Giusti, S. A., Verschuere, E., Hinkle, T. B., et al. (2020). Global site-specific neddylation profiling reveals that NEDDylated cofilin regulates actin dynamics. *Nat. Struct. Mol. Biol.* 27, 210–220. doi: 10.1038/s41594-019-0370-3
- Walden, H., Podgorski, M. S., Huang, D. T., Miller, D. W., Howard, R. J., Minor, D. L. Jr., et al. (2003). The structure of the APPBP1-UBA3-NEDD8-ATP complex reveals the basis for selective ubiquitin-like protein activation by an E1. *Mol. Cell* 12, 1427–1437. doi: 10.1016/s1097-2765(03)00452-0
- Wang, J., Wang, S., Zhang, W., Wang, X., Liu, X., Liu, L., et al. (2017). Targeting neddylation pathway with MLN4924 (Pevonedistat) induces NOXA-dependent apoptosis in renal cell carcinoma. *Biochem. Biophys. Res. Commun.* 490, 1183–1188. doi: 10.1016/j.bbrc.2017.06.179
- Wang, S., Zhao, L., Shi, X. J., Ding, L., Yang, L., Wang, Z. Z., et al. (2019). Development of highly potent, selective, and cellular active Triazolo[1,5-a]pyrimidine-based inhibitors targeting the DCN1-UBC12 protein-protein interaction. *J. Med. Chem.* 62, 2772–2797. doi: 10.1021/acs.jmedchem.9b00113
- Wang, Y., and Zhang, H. (2019). Regulation of autophagy by mTOR signaling pathway. *Adv. Exp. Med. Biol.* 1206, 67–83. doi: 10.1007/978-981-15-0602-4\_3
- Wang, Y., Luo, Z., Pan, Y., Wang, W., Zhou, X., Jeong, L. S., et al. (2015). Targeting protein neddylation with an NEDD8-activating enzyme inhibitor MLN4924 induced apoptosis or senescence in human lymphoma cells. *Cancer Biol. Ther.* 16, 420–429. doi: 10.1080/15384047.2014.1003003
- Watson, I. R., Irwin, M. S., and Ohh, M. (2011). NEDD8 pathways in cancer, Sine Quibus Non. *Cancer Cell* 19, 168–176. doi: 10.1016/j.ccr.2011.01.002
- Wei, D., Li, H., Yu, J., Sebolt, J. T., Zhao, L., Lawrence, T. S., et al. (2012). Radiosensitization of human pancreatic cancer cells by MLN4924, an investigational NEDD8-activating enzyme inhibitor. *Cancer Res.* 72, 282–293. doi: 10.1158/0008-5472.Can-11-2866
- Wei, L. Y., Wu, Z. X., Yang, Y., Zhao, M., Ma, X. Y., Li, J. S., et al. (2020). Overexpression of ABCG2 confers resistance to pevonedistat, an NAE inhibitor. *Exp. Cell Res.* 388:111858. doi: 10.1016/j.yexcr.2020.111858
- Xie, P., Peng, Z., Chen, Y., Li, H., Du, M., Tan, Y., et al. (2020). Neddylation of PTEN regulates its nuclear import and promotes tumor development. *Cell Res.* 31, 291–311. doi: 10.1038/s41422-020-00443-z
- Xie, P., Yang, J. P., Cao, Y., Peng, L. X., Zheng, L. S., Sun, R., et al. (2017). Promoting tumorigenesis in nasopharyngeal carcinoma, NEDD8 serves as a potential theranostic target. *Cell Death Dis.* 8:e2834. doi: 10.1038/cddis.2017.195
- Xie, P., Zhang, M., He, S., Lu, K., Chen, Y., Xing, G., et al. (2014). The covalent modifier Nedd8 is critical for the activation of Smurf1 ubiquitin ligase in tumorigenesis. *Nat. Commun.* 5:3733. doi: 10.1038/ncomms4733
- Xirodimas, D. P. (2008). Novel substrates and functions for the ubiquitin-like molecule NEDD8. *Biochem. Soc. Trans.* 36, 802–806. doi: 10.1042/bst0360802
- Xirodimas, D. P., Saville, M. K., Bourdon, J. C., Hay, R. T., and Lane, D. P. (2004). Mdm2-mediated NEDD8 conjugation of p53 inhibits its transcriptional activity. *Cell* 118, 83–97. doi: 10.1016/j.cell.2004.06.016
- Xirodimas, D. P., Sundqvist, A., Nakamura, A., Shen, L., Botting, C., and Hay, R. T. (2008). Ribosomal proteins are targets for the NEDD8 pathway. *EMBO Rep.* 9, 280–286. doi: 10.1038/embor.2008.10
- Xu, G. W., Toth, J. I., da Silva, S. R., Paiva, S. L., Lukkarila, J. L., Hurren, R., et al. (2014). Mutations in UBA3 confer resistance to the NEDD8-activating enzyme inhibitor MLN4924 in human leukemic cells. *PLoS One* 9:e93530. doi: 10.1371/journal.pone.0093530
- Yang, D., Tan, M., Wang, G., and Sun, Y. (2012). The p21-dependent radiosensitization of human breast cancer cells by MLN4924, an investigational inhibitor of NEDD8 activating enzyme. *PLoS One* 7:e34079. doi: 10.1371/journal.pone.0034079
- Yao, W. T., Wu, J. F., Yu, G. Y., Wang, R., Wang, K., Li, L. H., et al. (2014). Suppression of tumor angiogenesis by targeting the protein neddylation pathway. *Cell Death Dis.* 5:e1059. doi: 10.1038/cddis.2014.21
- Zhang, Y., Shi, C. C., Zhang, H. P., Li, G. Q., and Li, S. S. (2016). MLN4924 suppresses neddylation and induces cell cycle arrest, senescence, and apoptosis in human osteosarcoma. *Oncotarget* 7, 45263–45274. doi: 10.18632/oncotarget.9481
- Zhang, Y., Wolf, G. W., Bhat, K., Jin, A., Allio, T., Burkhart, W. A., et al. (2003). Ribosomal protein L11 negatively regulates oncoprotein MDM2 and mediates a p53-dependent ribosomal-stress checkpoint pathway. *Mol. Cell. Biol.* 23, 8902–8912. doi: 10.1128/mcb.23.23.8902-8912.2003
- Zhao, Y., Morgan, M. A., and Sun, Y. (2014). Targeting neddylation pathways to inactivate cullin-RING ligases for anticancer therapy. *Antioxid. Redox Signal.* 21, 2383–2400. doi: 10.1089/ars.2013.5795
- Zhao, Y., Xiong, X., Jia, L., and Sun, Y. (2012). Targeting cullin-RING ligases by MLN4924 induces autophagy via modulating the HIF1-REDD1-TSC1-mTORC1-DEPTOR axis. *Cell Death Dis.* 3:e386. doi: 10.1038/cddis.2012.125
- Zheng, N., and Shabek, N. (2017). Ubiquitin ligases: structure, function, and regulation. *Annu. Rev. Biochem.* 86, 129–157. doi: 10.1146/annurev-biochem-060815-014922
- Zheng, N., Schulman, B. A., Song, L., Miller, J. J., Jeffrey, P. D., Wang, P., et al. (2002). Structure of the Cul1-Rbx1-Skp1-F boxSkp2 SCF ubiquitin ligase complex. *Nature* 416, 703–709. doi: 10.1038/416703a
- Zhou, H., Lu, J., Liu, L., Bernard, D., Yang, C. Y., Fernandez-Salas, E., et al. (2017). A potent small-molecule inhibitor of the DCN1-UBC12 interaction that selectively blocks cullin 3 neddylation. *Nat. Commun.* 8:1150. doi: 10.1038/s41467-017-01243-7
- Zhou, L., Jiang, Y., Luo, Q., Li, L., and Jia, L. (2019). Neddylation: a novel modulator of the tumor microenvironment. *Mol. Cancer* 18:77. doi: 10.1186/s12943-019-0979-1
- Zhou, L., Zhang, W., Sun, Y., and Jia, L. (2018). Protein neddylation and its alterations in human cancers for targeted therapy. *Cell. Signal.* 44, 92–102. doi: 10.1016/j.cellsig.2018.01.009
- Zhou, Q., Li, H., Li, Y., Tan, M., Fan, S., Cao, C., et al. (2019). Inhibiting neddylation modification alters mitochondrial morphology and reprograms energy metabolism in cancer cells. *JCI Insight* 4:e121582. doi: 10.1172/jci.insight.121582
- Zhou, S., Zhao, X., Yang, Z., Yang, R., Chen, C., Zhao, K., et al. (2019). Neddylation inhibition upregulates PD-L1 expression and enhances the efficacy of immune checkpoint blockade in glioblastoma. *Int. J. Cancer* 145, 763–774. doi: 10.1002/ijc.32379
- Zhou, W., Xu, J., Li, H., Xu, M., Chen, Z. J., Wei, W., et al. (2017). Neddylation E2 UBE2F promotes the survival of lung cancer cells by activating CRL5 to degrade NOXA via the K11 linkage. *Clin. Cancer Res.* 23, 1104–1116. doi: 10.1158/1078-0432.Ccr-16-1585
- Zhou, X., Hao, Q., Liao, J., Zhang, Q., and Lu, H. (2013). Ribosomal protein S14 unties the MDM2-p53 loop upon ribosomal stress. *Oncogene* 32, 388–396. doi: 10.1038/onc.2012.63
- Zhou, X., Tan, M., Nyati, M. K., Zhao, Y., Wang, G., and Sun, Y. (2016). Blockage of neddylation modification stimulates tumor sphere formation in vitro and stem cell differentiation and wound healing in vivo. *Proc. Natl. Acad. Sci. U.S.A.* 113, E2935–E2944. doi: 10.1073/pnas.1522367113
- Zhu, W., Chen, Y., and Dutta, A. (2004). Rereplication by depletion of geminin is seen regardless of p53 status and activates a G2/M checkpoint. *Mol. Cell. Biol.* 24, 7140–7150. doi: 10.1128/mcb.24.16.7140-7150.2004
- Zuo, W., Huang, F., Chiang, Y. J., Li, M., Du, J., Ding, Y., et al. (2013). c-Cbl-mediated neddylation antagonizes ubiquitination and degradation of the TGF- $\beta$  type II receptor. *Mol. Cell* 49, 499–510. doi: 10.1016/j.molcel.2012.12.002

**Conflict of Interest:** The authors declare that the research was conducted in the absence of any commercial or financial relationships that could be construed as a potential conflict of interest.

Copyright © 2021 Gai, Peng, Liu, Zhang and Jiang. This is an open-access article distributed under the terms of the Creative Commons Attribution License (CC BY). The use, distribution or reproduction in other forums is permitted, provided the original author(s) and the copyright owner(s) are credited and that the original publication in this journal is cited, in accordance with accepted academic practice. No use, distribution or reproduction is permitted which does not comply with these terms.





# Targeting RFWD2 as an Effective Strategy to Inhibit Cellular Proliferation and Overcome Drug Resistance to Proteasome Inhibitor in Multiple Myeloma

Mengjie Guo<sup>1,2†</sup>, Pinggang Ding<sup>1†</sup>, Zhen Zhu<sup>3†</sup>, Lu Fan<sup>1</sup>, Yanyan Zhou<sup>1</sup>, Shu Yang<sup>1</sup>, Ye Yang<sup>1\*</sup> and Chunyan Gu<sup>1,2\*</sup>

## OPEN ACCESS

### Edited by:

Daming Gao,

Shanghai Institute of Biochemistry  
and Cell Biology, Chinese Academy  
of Sciences (CAS), China

### Reviewed by:

Lei Qiang,

China Pharmaceutical University,  
China

Hongbo Wang,

Yantai University, China

### \*Correspondence:

Ye Yang

yangye876@sina.com

Chunyan Gu

guchunyan@njucm.edu.cn

<sup>†</sup>These authors have contributed  
equally to this work

### Specialty section:

This article was submitted to

Cell Growth and Division,

a section of the journal

Frontiers in Cell and Developmental  
Biology

**Received:** 04 March 2021

**Accepted:** 30 March 2021

**Published:** 21 April 2021

### Citation:

Guo M, Ding P, Zhu Z, Fan L,  
Zhou Y, Yang S, Yang Y and Gu C  
(2021) Targeting RFWD2 as an  
Effective Strategy to Inhibit Cellular  
Proliferation and Overcome Drug  
Resistance to Proteasome Inhibitor  
in Multiple Myeloma.  
*Front. Cell Dev. Biol.* 9:675939.  
doi: 10.3389/fcell.2021.675939

<sup>1</sup> School of Medicine & Holistic Integrative Medicine, Nanjing University of Chinese Medicine, Nanjing, China, <sup>2</sup> Large Data Center, Nanjing Hospital of Chinese Medicine affiliated to Nanjing University of Chinese Medicine, Nanjing, China, <sup>3</sup> College of Health and Rehabilitation & College of Acupuncture and Massage, Nanjing University of Chinese Medicine, Nanjing, China

The potential to overcome resistance to proteasome inhibitors is greatly related with ubiquitin-proteasome system during multiple myeloma (MM) treatment process. The constitutive photomorphogenic 1 (RFWD2), referred to an E3 ubiquitin ligase, has been identified as an oncogene in multiple cancers, yet important questions on the role of RFWD2 in MM biology and treatment remain unclear. Here we demonstrated that MM patients with elevated RFWD2 expression achieved adverse outcome and drug resistance by analyzing gene expression profiling. Moreover, we proved that RFWD2 participated in the process of cell cycle, cell growth and death in MM by mass spectrometry analysis. *In vitro* study indicated that inducible knockdown of RFWD2 hindered cellular growth and triggered apoptosis in MM cells. Mechanism study revealed that RFWD2 controlled MM cellular proliferation via regulating the degradation of P27 rather than P53. Further exploration unveiled that RFWD2 mediated P27 ubiquitination via interacting with RCHY1, which served as an E3 ubiquitin ligase of P27. Finally, *in vivo* study illustrated that blocking RFWD2 in BTZ-resistant MM cells overcame the drug resistance in a myeloma xenograft mouse model. Taken together, these findings provide compelling evidence for prompting that targeting RFWD2 may be an effective strategy to inhibit cellular proliferation and overcome drug resistance to proteasome inhibitor in MM.

**Keywords:** multiple myeloma, RFWD2, proliferation, drug resistance, P27, ubiquitination, RCHY1

## INTRODUCTION

The uncontrolled expansion of plasma cells has been pinpointed as the major feature of multiple myeloma (MM), which synthesize and excrete a substantial amount of paraproteins (Gandolfi et al., 2017). In order to avoid the accumulation of the proteins involved in tumor pathogenesis, the MM cells are largely reliant on proteasome complexes, especially on the 26S proteasome, which is responsible for degrading intracellular proteins through ubiquitination pathway

(Gandolfi et al., 2017). Therefore, MM cells are more sensitive to proteasome inhibition. Proteasome inhibitors (PIs) have emerged as an effective therapy for the treatment of MM patients in the past two decades (Richardson et al., 2018), which trigger endoplasmic reticulum stress to induce MM cell apoptosis. The three classic PIs like bortezomib (BTZ), carfilzomib (CFZ) and ixazomib (IXZ), as well as the novel PIs under clinical investigation including marizomib and oprozomib, have been used in combination with other regimens, which have formed one of the backbones of treatment paradigm throughout the whole course of MM (Song et al., 2019). However, current therapy might result in unideal effects and the acquisition of drug resistance. Consequently, the prospect of overcoming drug resistance has made the ubiquitin (Ub) plus proteasome system (UPS) as a potential therapeutic target in MM.

An attractively therapeutic strategy for treating MM is focusing on non-proteasomal components within the UPS, such as the E3 ubiquitin ligases, determining the substrate selectivity for ubiquitination and degradation (Snoek et al., 2013). Current evidence demonstrates that overexpression or mutation of E3 ubiquitin ligases could drive tumor development (Huang et al., 2020). In our previous research, we identified an E3 ubiquitin ligase, known as the gene constitutive photomorphogenic 1 (RFWD2, also called COP1) (Gu et al., 2020). Multiple literature have reported that RFWD2 is engaged in tumorigenesis via meditating several biological processes like transcription, DNA repair, cell cycle arrest and apoptosis (Migliorini et al., 2011; Zou et al., 2017; Abbastabar et al., 2018). Since both tumor suppressor (like p53) and oncogene (like JUN) are among putative targets of RFWD2, the potential role of RFWD2 in a wide variety of cancers remains controversial (Song et al., 2020). Few reports showed a tumor suppressor role of RFWD2 in prostate cancer and gastric cancer (Vitari et al., 2011; Sawada et al., 2013). Conversely, RFWD2 was regarded as a tumor promoter in human hepatocellular carcinoma, breast cancer, ovarian adenocarcinoma and acute myeloid leukemia (Dornan et al., 2004a; Lee et al., 2010; Yoshida et al., 2013). One study by our group has demonstrated that inducible upregulation of RFWD2 is closely associated with myeloma cellular proliferation and contributes to PIs resistance (Gu et al., 2020). To complement the studies on RFWD2 overexpression with the inverse experiment, the action mode of depletion of endogenous RFWD2 in MM needs to be further explored.

The cyclin/CDK2 inhibitor P27 has been recognized as a vitally negative regulator of cell cycle, which disrupts the G1-to-S phase cell cycle transition (Yoon et al., 2019), functioning as a tumor suppressor. Aberrant activities of P27 cause abnormal alterations in cell cycle regulation and alleviate P27-suppressed target genes, which contribute to uncontrolled cell proliferation, thereby inducing tumors (Li et al., 2018). It has been well documented that the expression of P27 is mainly dominated by its rate of proteasome degradation, making E3 ubiquitin ligases as the key regulators involved in targeting P27 (Egozi et al., 2007; Rodriguez et al., 2020). RFWD2 serves as a negative regulator of P27 (Ko et al., 2019), leading to CSN6-mediated P27 degradation in HCT116 and HEK-293T cells (Choi et al., 2015a). Consistently, our previous work initially illustrated the

interaction between RFWD2 and P27 (Gu et al., 2020). To intensively delineate the precise mechanisms associated with RFWD2-induced drug resistance in MM via targeting P27, we continued to investigate which E3 ubiquitin ligases involving P27 degradation interacted with RFWD2.

Heartened by the current studies on the biological aggressiveness of RFWD2 in various cancers, we herein continued with the previous findings in the impact of RFWD2 on MM progression and drug resistance, further proved that targeting RFWD2 could work as a potential treatment approach for MM.

## MATERIALS AND METHODS

### Database Analysis

Message levels of RFWD2 in MM were determined using the gene expression profiling (GEP) cohorts, which were mined from the GEO database as previously described (Zhou et al., 2013). The outcome data were based on Total therapy 2 (TT2, GSE2658), TT3 (GSE2658), and the evaluation of proteasome inhibition for extending remission (APEX, GSE9782). The Dutch-Belgian Cooperative Trial Group for Hematology Oncology Group-65 (HOVON65) trials was collected from GSE19784.

### Antibodies and Reagents

Antibodies were purchased from Abcam (Cambridge, Cambs, United Kingdom) (RFWD2, catalog number ab56400; KPC2, catalog number ab177519) or ProteinTech Group (Chicago, IL, United States) (P27, catalog number 25614-1-AP). Other antibodies were purchased from Cell Signaling Technology (Danvers, MA, United States). Rabbit IgG (a7016), mouse IgG (a7028) and doxycycline (DOX) were obtained from Beyotime Institute of Biotechnology (Shanghai, China). Bortezomib (BTZ) and other chemical reagents were obtained from Shanghai Aladdin Bio-Chem Technology (Shanghai, China).

### Cell Lines and Culture

Human MM cell lines, ARP1, H929, RPMI 8226, ANBL6, OCI-MY5, JIN3, XG1, U266 and MM1S were maintained in RPMI-1640 (Biological Industries, Kibbutz Beit Haemek, Israel), supplemented with 10% fetal bovine serum (Biological Industries, Kibbutz Beit Haemek, Israel), 100 U/mL penicillin and 100 µg/mL streptomycin (Sigma, St. Louis, MO). 293T cells were cultured in DMEM (Hyclone, Los Angeles, CA, United States). The BTZ-resistant MM cell lines, 8226/BTZ were produced by increasing BTZ concentration gradient in our institute. All cells were propagated *in vitro* under the condition of 37°C in a humidified atmosphere containing 5% CO<sub>2</sub>.

### Plasmids and Transfection

The plasmids including the human RFWD2 cDNA or shRNA cassettes were obtained from Genaray Biotech (Shanghai, China). The RFWD2 cDNA was cloned into the lentiviral vector, CD513B-1. Under the control of a DOX-inducible gene promoter, RFWD2-targeted shRNA was cloned into the vector of pTRIPZ. Lenti-viruses containing cDNA or shRNA were

created by co-transfection of the CD513B-1-RFWD2 vector or RFWD2 shRNA vector with packaging vectors (PLP1, PLP2, and PLP-VSVG) into 293T cells (attained 70-80% confluency) using Lipofectamine2000 Transfection Reagent. The virus supernatant was collected after 48 h and stored at  $-80^{\circ}\text{C}$ , which were used for subsequent experiments. MM cells were transfected with the lentivirus and selected by puromycin treatment. Transduction efficiency was validated by Quantitative Real time-PCR assays (qPCR) or western blotting (WB).

## Myeloma Xenografts in NOD-SCID Mice

8226 WT, 8226/BTZ, 8226 RFWD2 KD and 8226/BTZ RFWD2 KD cells ( $5 \times 10^6$ ) were injected subcutaneously into the left and right abdominal flanks of 6-8 weeks old NOD-SCID mice, respectively. On day 3 after injection, DOX (2 mg/mL) was employed on mice through drinking to induce the reduction of RFWD2. On day 7 mice were treated with intraperitoneal (IP) administrations of BTZ (1 mg/kg) twice weekly.

Tumor diameter was measured 2-3 times weekly by using calipers. Mice were sacrificed by IP injection of chloral hydrate and then tumor tissues were collected, weighed, photographed and stored frozen in case the tumor diameter reached 20 mm. All experimental procedures were performed in accordance with government-published recommendations for the Care and Use of laboratory animals and approved by the guidelines of Institutional Ethics Review Boards of Nanjing University of Chinese Medicine (Ethics Registration no. 201905A003) (Zhou et al., 2013).

## Cell Proliferation and Viability Assay

Cell viability was evaluated using Thiazolyl Blue Tetrazolium Bromide (MTT) assay, which was performed according to the manufacturer's instructions (Beijing Solarbio Science & Technology) (Yuan et al., 2018). Cells were cultured in 96-well plates at a density of  $1 \times 10^4$  cells/well with repeats for 3 wells in each group. Absorbance was read at 570 nm using microplate reader (Thermo Fisher Scientific).

## Flow Cytometric Analysis of Cell Apoptosis

APC 5-Bromo-2'-Deoxyuridine (BrdU) Flow Kit (BD Pharmingen) was used to measure the stage of apoptosis and cell cycle by a FlowSight flow cytometer. Briefly, cells were resuspended with 195  $\mu\text{L}$  staining buffer, and then added 5  $\mu\text{L}$  (0.125  $\mu\text{g}$ ) of APC-BrdU antibody per well, and incubated at  $4^{\circ}\text{C}$  for 30 min in the dark. 488 nm excitation wavelength and 520 nm emission wavelength were termed as the working condition of FlowSight flow cytometer.

## WB and Co-immunoprecipitation (Co-IP)

Protein levels were determined by WB analysis under the procedure as previous described (Yang et al., 2018). Co-IP was performed according to the instructions of the Pierce Direct Magnetic IP/Co-IP kit as mentioned (Gu et al., 2016). As the RFWD2 cDNA used in the current study carrying the FLAG tag, FLAG antibody was used instead of RFWD2 antibody for IP. And

the IgG antibody sharing the same host with the IP antibody was chosen as a negative control.

## In vitro Ubiquitylation Assay

MM cells were incubated with 20  $\mu\text{M}$  MG132 (a proteasome inhibitor) for 12 h before collection, and lysed in IP lysis buffer. Afterward, the cell lysate was subjected to immunoprecipitation with an ubiquitin antibody, and immunoprecipitation was subsequently separated by SDS-PAGE and immunoblotted with a P27 antibody to detect the ubiquitination level of P27 (Wang et al., 2019).

## Mass Spectrometry (MS) Analysis

SDS-PAGE was used to separate proteins in ARP1 WT & OE cells, and gel bands at the expected size were excised and digested with sequencing-grade trypsin (Promega, United States). The MS was performed by Lianchuan Biotech (Hangzhou, China), which was conducted by using LC-MS technology (Q-Exactive, Thermo). The first process was to quantify the protein and then open the three-dimensional structure of the protein by reductive alkylation. After enzymolysis, the peptides were extracted, and MS was used to obtain the mass spectra of these peptides. Finally, the peptides were identified by the related software.

## Statistical Analysis

All data were expressed as means  $\pm$  SD. The statistical analysis was carried out using GraphPad Prism 6.01 or SPSS 22.0 version. Two-tailed Student's *t*-test (2 groups) and one-way analysis of variance ( $\geq 3$  groups) were employed to determine the significant differences among experimental groups. The survival data were plotted using Kaplan-Meier curve and sketched by log-rank test. Hazard ratios were estimated using Cox's proportional hazard model. Array CGH data analysis building on the Agilent 180,000-feature human CGH microarray was performed as described previously (Zhou et al., 2013). Significance was set at  $P < 0.05$ .  $P < 0.05$  was labeled as\*,  $P < 0.01$  as\*\*.

## RESULTS

### Increased RFWD2 Expression Is Correlated With Poor Survival and Relapse in MM

To assess the role of RFWD2 in MM, we analyzed the array-based comparative genomic hybridization (aCGH) data gained from 67 MM patients and found that RFWD2 locus was amplified in MM patient samples to a major extent (Figure 1A left). To determine the clinical significance of RFWD2 in MM, the prognosis of patients was best captured by analyzing GEP cohorts collected from the GEO database. As expected, Kaplan-Meier survival curves showed that MM patients with amplification of RFWD2 were significantly associated with poor overall survival (OS) in 3 independent MM cohorts (TT3, APEX and HOVON65) [Figures 1A,B (A-right)], which were in sync with the results of TT2 (a

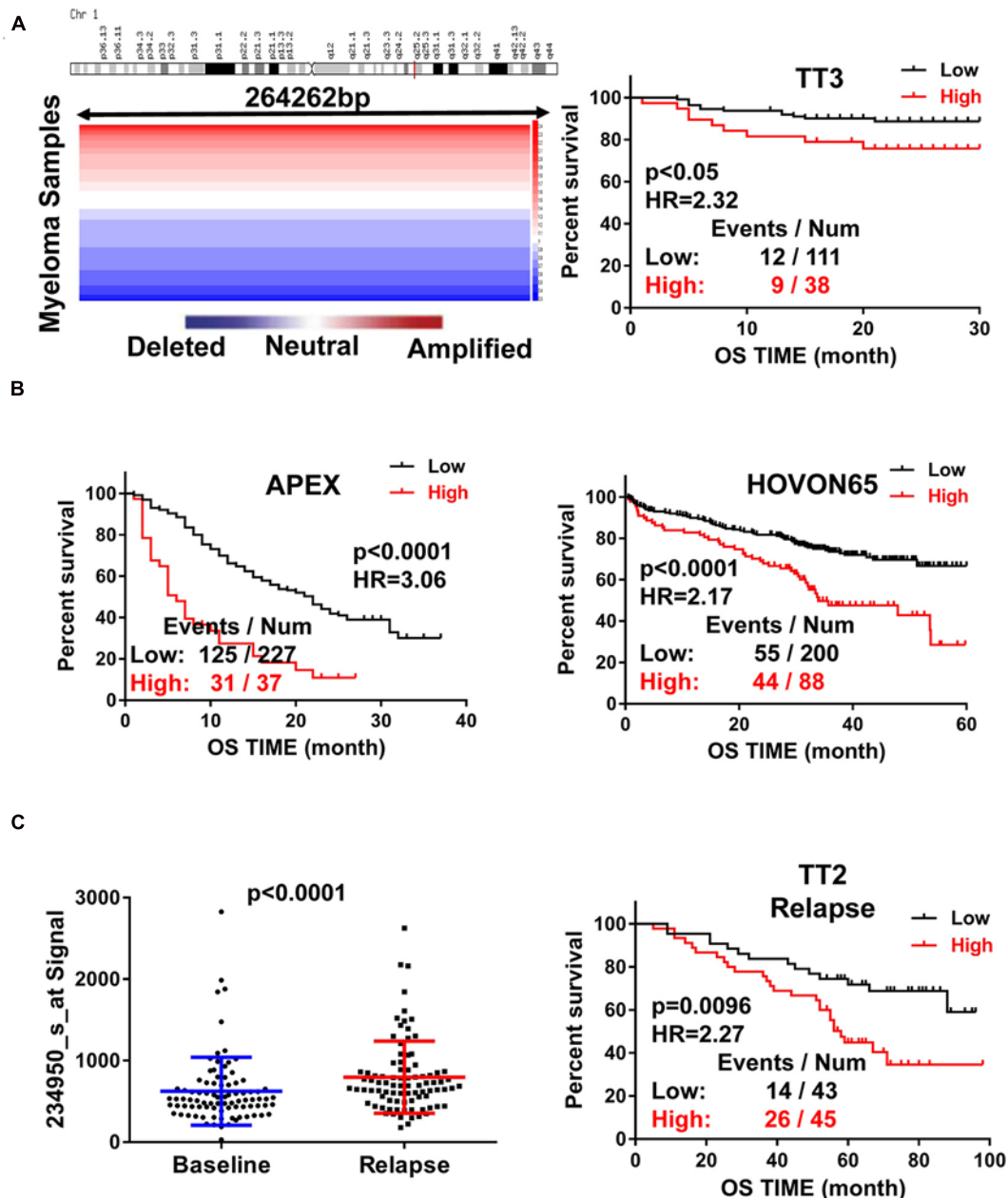


**FIGURE 1 |** Increased RFWD2 expression is correlated with poor survival and relapse in MM. **(A)** Left: Array-based comparative genomic hybridization analysis illustrated RFWD2 copy number variation in 67 primary MM samples; Right: MM patients with high RFWD2 level were positively associated with poor overall survival (OS) in TT3 cohort. **(B)** MM patients with elevated RFWD2 level exhibited positive correlation with poor overall survival (OS) in APEX and HOVON65 cohorts. **(C)** Left: RFWD2 expression in relapsed MM patients was significantly elevated compared with the corresponding newly diagnosed samples. Right: upregulation of RFWD2 was correlated with decreased OS in relapsed TT2 patients. The data were expressed as mean  $\pm$  SD.

well-annotated, mature data set) and GMMG-HD4 cohort (Gu et al., 2020). Moreover, we found that elevated RFWD2 expression was impressively germane to clinical parameters, such as  $\beta$ 2-microglobulin, hemoglobin concentration, and high-risk genetic parameters, such as chromosomal abnormalities (by G-banding) and g70high37 ( $P < 0.05$ ; Table 1). It indicated that abnormal elevation of RFWD2 in MM leads to poor prognosis. Then we compared RFWD2 expression among 88

paired baseline/relapse samples. As illustrated in Figure 1C left, the RFWD2 expression in the relapse samples exhibited a dramatic upward trend compared with the corresponding newly diagnosed samples ( $P < 0.0001$ ). Furthermore, overexpression of RFWD2 prognosticated inferior OS in the relapsed MM patients ( $P = 0.0096$ ; Figure 1C right). These findings consolidate that RFWD2 acts as a valuable prognostic biomarker even in relapsed MM.



**TABLE 1 |** The Correlation of RFWD2 Expression and Clinical Characteristics in TT2.

Characteristics	High RFWD2 Low RFWD2		p Value
	(%, n = 186)	(%, n = 165)	
Age at least 65 years	25.3	18.2	0.122
Female sex	42.5	44.2	0.747
White race	90.3	86.7	0.315
IgA isotype	28.4	23.0	0.271
CRP at least 4.0 mg/L	6.52	5.45	0.822
$\beta$ 2-Microglobulin at least 4.0 mg/L	42.5	25.4	0.001
Creatinine at least 2.0 mg/dL	14.0	8.64	0.129
Hemoglobin less than 10 g/dL	31.1	18.8	0.009
Albumin less than 3.5 g/dL	37.1	35.7	0.825
Chromosomal abnormalities (by G-banding)	40.3	29.7	0.044
MRI focal bone lesions, at least three	59.8	57.2	0.659
LDH at least 190 IU/L	37.5	30.3	0.175
Hyperdiploid	18.3	18.8	1.000
Hypodiploid	21.5	8.48	0.001
Amplification of 1q21	54.5	43.6	0.058
g70high	39.2	12.7	0.000
MRI1	74.9	77.3	0.612
7grp	60.5	23.6	0.000
Strata(train)	51.6	49.1	0.669

## MS Analysis Reveals the Potential Signaling Pathway for RFWD2 Function in MM

To address the potential role of RFWD2 in myeloma biology, we adopted two independent MM cell lines ARP1 and H929 as *in vitro* experimental models for MM. ARP1 and H929 cells were transfected with CRISPR lentiviral activation particles to functionally overexpress (OE) RFWD2. WB analysis confirmed the increment of RFWD2 expression in RFWD2 OE cells relative to wild-type cells (WT) serving as controls (**Figure 2A**). Furthermore, MS was conducted to assess activation of RFWD2-related signaling pathways. Representative gene ontology (GO) Biological Process terms and Kyoto Encyclopedia of Genes and Genomes (KEGG) pathways chosen from the most enriched charts were presented in **Figure 2B**, suggesting the top 20 most significantly enriched pathways. Above data indicated that the activation of two pathways related to RFWD2 in MM progression were mitotic cell cycle and cell growth and death, which would be basic guidance for further research on RFWD2.

## The Decrease of RFWD2 Hinders Cellular Proliferation in MM Cells

In our previous paper, it has been illustrated that enforced expression of RFWD2 executed positive function in regulating MM cellular proliferation (Gu et al., 2020). Here, we continued to investigate the mechanism in depth. Flow cytometry analysis showed that the proportions of cells in the S phase were increased in RFWD2 OE cells relative to the controls (**Figure 3A**). Lentiviral shRNA transfection technology was conducted to knockdown the endogenous expression of RFWD2 in ARP1 and H929 cells.

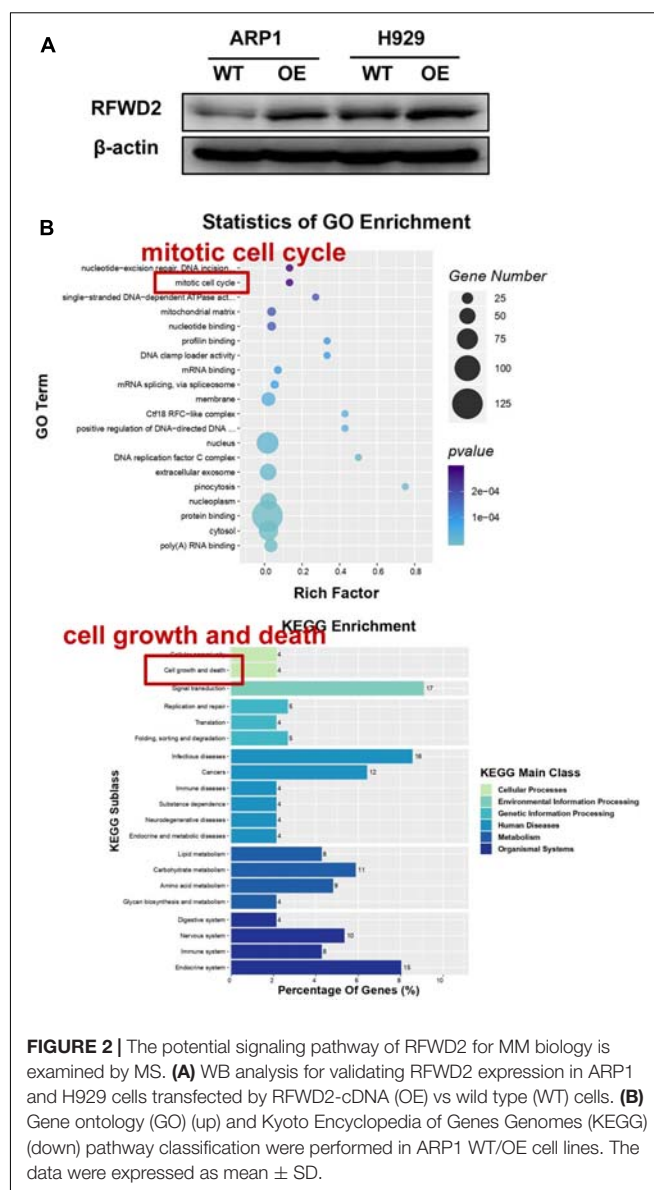


**FIGURE 2 |** The potential signaling pathway of RFWD2 for MM biology is examined by MS. **(A)** WB analysis for validating RFWD2 expression in ARP1 and H929 cells transfected by RFWD2-cDNA (OE) vs wild type (WT) cells. **(B)** Gene ontology (GO) (up) and Kyoto Encyclopedia of Genes Genomes (KEGG) (down) pathway classification were performed in ARP1 WT/OE cell lines. The data were expressed as mean  $\pm$  SD.

Then, qPCR and WB were recruited to validate the efficiency of shRNA, which demonstrated the significant decrease of RFWD2 at mRNA and protein levels in RFWD2-shRNA transfected MM cells (KD) compared to the WT cells (**Figure 3B** up and down). A prominent decrease of cell growth rate in ARP1 and H929 cells was provoked by silencing RFWD2 ( $P < 0.05$ ) in a time-dependent manner (**Figure 3B**, middle), further confirming that RFWD2 facilitated MM cell proliferation. PARP and Caspase-3 have been authenticated as two key proapoptotic molecules in a broad spectrum of cancers. WB examination indicated that the expression of PARP and cleaved Caspase-3 expression was increased in RFWD2-shRNA cells compared to that in WT cells (**Figure 3B** down). Taken together, we further confirm that RFWD2 activation is critical for promoting MM cellular proliferation via controlling cell cycle and apoptosis *in vitro*.

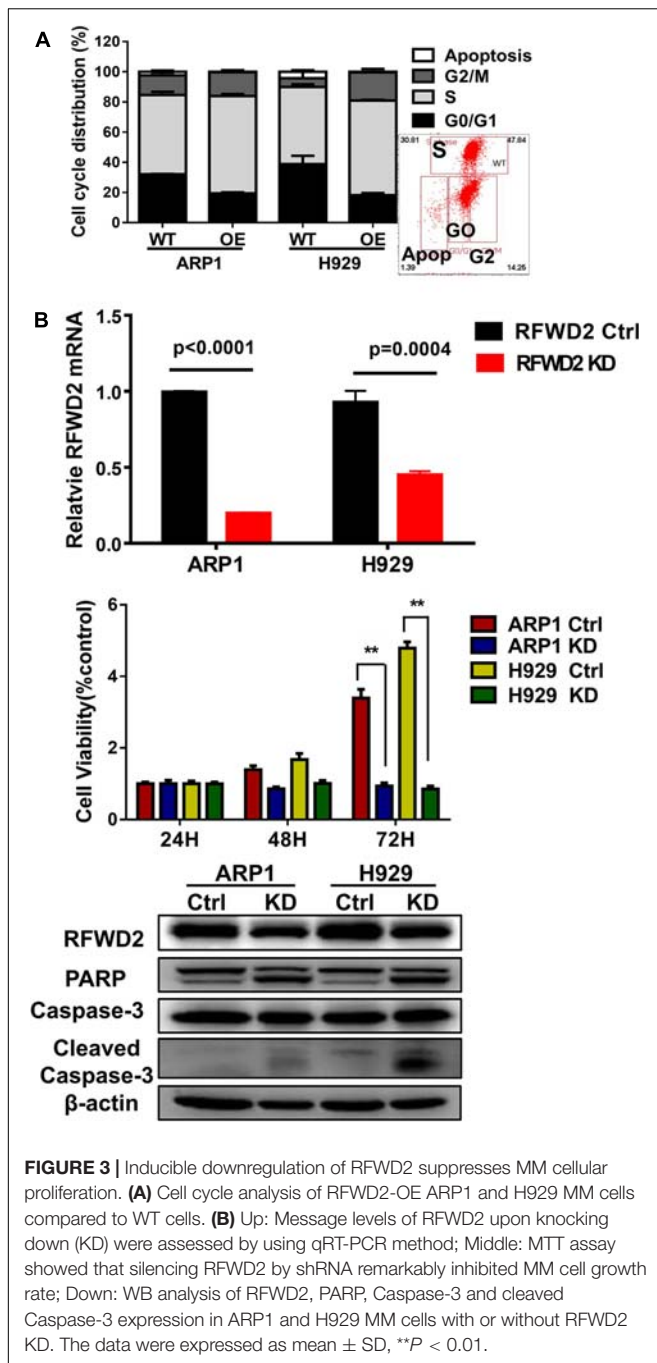


**FIGURE 3 |** Inducible downregulation of RFWD2 suppresses MM cellular proliferation. **(A)** Cell cycle analysis of RFWD2-OE ARP1 and H929 MM cells compared to WT cells. **(B)** Up: Message levels of RFWD2 upon knocking down (KD) were assessed by using qRT-PCR method; Middle: MTT assay showed that silencing RFWD2 by shRNA remarkably inhibited MM cell growth rate; Down: WB analysis of RFWD2, PARP, Caspase-3 and cleaved Caspase-3 expression in ARP1 and H929 MM cells with or without RFWD2 KD. The data were expressed as mean  $\pm$  SD,  $^{**}P < 0.01$ .

## RFWD2 Mediates P27 Degradation to Influence MM Cell Growth

Since RFWD2 is modulating both P27 and P53 (Dornan et al., 2004a; Ko et al., 2019), the two vital factors mediating cellular proliferation, we aim to identify which one is the major downstream factor of RFWD2. As **Figure 4A** shown, relatively higher level of P27 was ubiquitously observed in 8 MM cell lines with wild-type, negative or mutated expression of P53 (Xiong et al., 2008) by WB, while P53 expression was comparatively lower than P27 in 7 of 8 cells no matter mutated or not.

More importantly, Co-IP assay demonstrated that the interaction between RFWD2 and P27 was more pronounced than with P53 (**Figure 4B**). Under overexpression of RFWD2, the interaction between P53 and RFWD2 did not increase and remained at a low level, supporting that P27 was the major target of RFWD2 in MM. The function of P27 is triggering cell cycle arrest by repressing cyclin-dependent kinase (CDK) activity (Sharma and Pledger, 2016; Fang et al., 2017), and P27 level is dominantly monitored by polyubiquitination, while RFWD2 acts as an E3 ubiquitin ligase. As proved by WB analysis, the protein level of P27 was up-regulated by blocking RFWD2 (**Figure 4C** up). After cells were treated with MG132, a reversible proteasome inhibitor, substantial increment of ubiquitylated P27 was shown by *in vitro* ubiquitylation assay. Additionally, the amount of ubiquitylated P27 in RFWD2 KD cells was well below that of the WT cells (**Figure 4C** down), implicating that RFWD2 participated in the ubiquitination modification and degradation of P27 through the proteasome pathway. On the basis of these observations, we propose that targeting RFWD2 impedes MM cellular proliferation via regulating the degradation of P27.

## RFWD2 Collaborates With RCHY1 E3 Ubiquitin Ligase to Mediate P27 Ubiquitination in MM

Kip ubiquitination-promoting complex (KPC) complex, RING-finger and CHY-zinc-finger domain-containing protein 1 (RCHY1, also known as Pirh2) and CRL4DDB2-Artemis E3 ligases are identified as E3 ubiquitin ligases of P27 (Zhao et al., 2013; Masumoto and Kitagawa, 2016; Dobashi et al., 2017; Li et al., 2019). To find the detailed factor by which RFWD2 mediated P27 degradation, we examined the correlation between RFWD2 and the three E3 ubiquitin ligases. WB analysis showed only RCHY1 expression was increased in RFWD2 OE cells (**Figure 5A** left), and the expression of RCHY1 was reduced in RFWD2 KD cells (**Figure 5A** right). Then, the physical interaction between RFWD2 and RCHY1 was verified by Co-IP assay. With using FLAG antibody for IP and RCHY1 antibody for IB, RCHY1 band could be detected and vice versa (**Figure 5B**). Strikingly, intervention of RCHY1 by siRNA resulted in decreased ubiquitination of P27 in RFWD2 OE cell lines (**Figure 5C**) that validated RFWD2 mediating P27 expression through interacting with RCHY1 E3 ubiquitin ligase. In addition, **Figure 5D** presented that patients in TT2 or APEX cohorts with a high/high co-expression of RFWD2-RCHY1 experienced poor survival outcomes relative to patients with low/low co-expression or medium expression. The findings indicate a potentially synergistic effect of RFWD2 and RCHY1 on MM patient prognosis.

## Reduction of RFWD2 Reverses BTZ Resistance in MM Xenograft Model

Our previous research has shed light on the vital role of RFWD2 in MM PIs resistance; we further verified whether RFWD2 inhibition could overcome drug resistance *in vivo* (Gu et al., 2020). To this end, RFWD2 shRNA was transfected to 8226 WT and 8226 BTZ-resistant (DR) cells. DOX was applied to induce

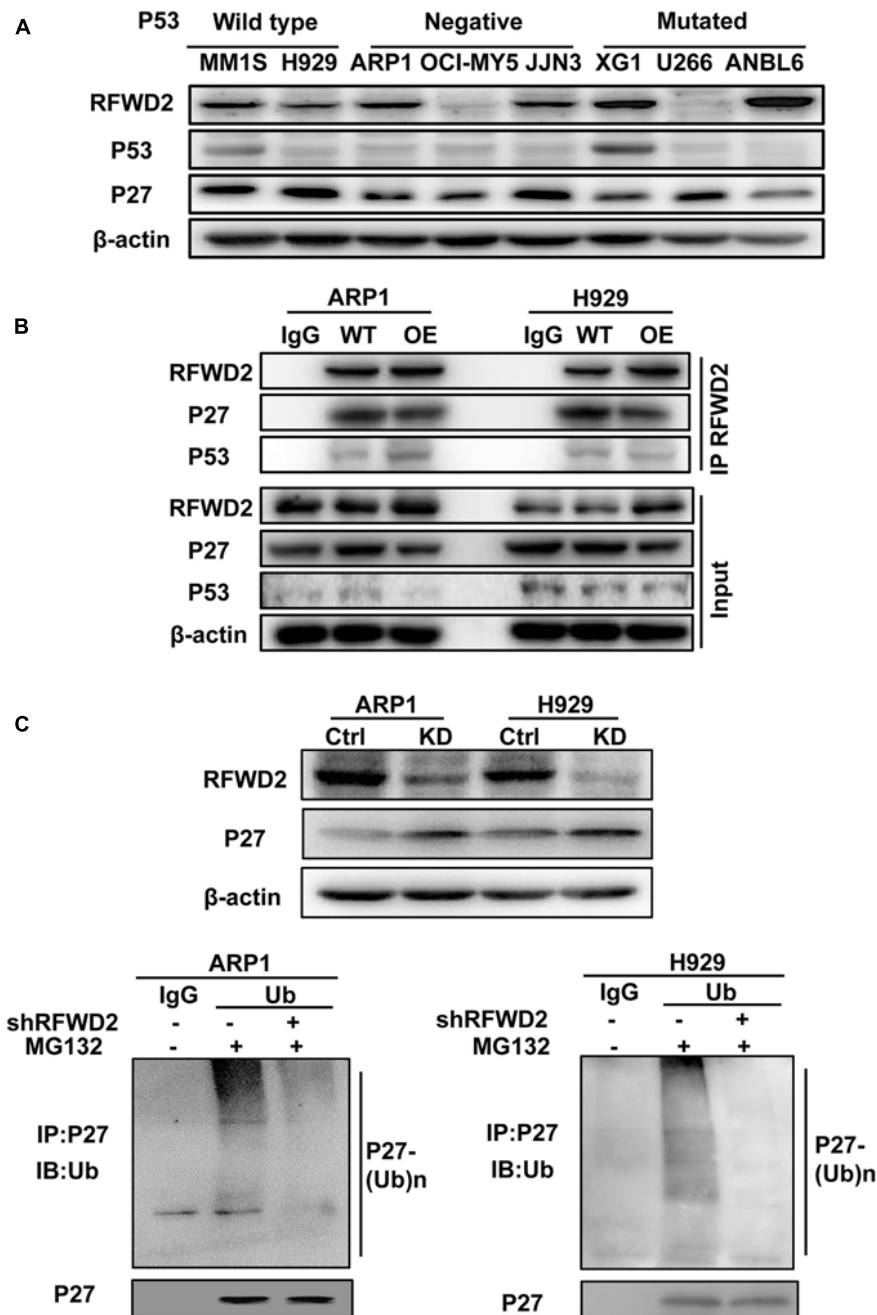


**FIGURE 4 |** RFWD2 mediates P27 degradation to influence MM cell growth. **(A)** WB results showed the expression of RFWD2, P27 and P53 in 8 MM cell lines with wild-type, negative or mutated expression of P53. **(B)** Co-IP assay for the interaction between RFWD2 and P27, as well as P53 in RFWD2 WT/OE ARP1 and H929 cells. **(C)** Up: Detection of RFWD2 and P27 protein levels in WT/RFWD2-shRNA transfected MM cells; Down: Depletion of RFWD2 expression in MM cells resulting in reduction of ubiquitylated P27 expression.

shRNA expression. The 8226 WT and 8226 DR cells with genetic ablation of RFWD2 were injected into NOD-SCID mice with or without DOX stimulation. Elevated amounts of RFWD2 protein were observed in the DR group compared with the untreated WT group, while RFWD2 expression was downregulated in both WT and DR groups by shRNA (Figure 6A). RFWD2 KD tumors in both WT and DR groups harvested at study endpoint were

extremely smaller than the tumors with normal expression of RFWD2 (Figure 6B). The similar trend was also exhibited in tumor weight (Figure 6C left) and volume (Figure 6C right), suggesting that RFWD2 inhibition could decrease the tolerance to BTZ *in vivo*. Combined with the data *in vitro*, we conclude that targeting RFWD2 offers a suitable therapeutic approach for halting MM progression and overcoming drug resistance.

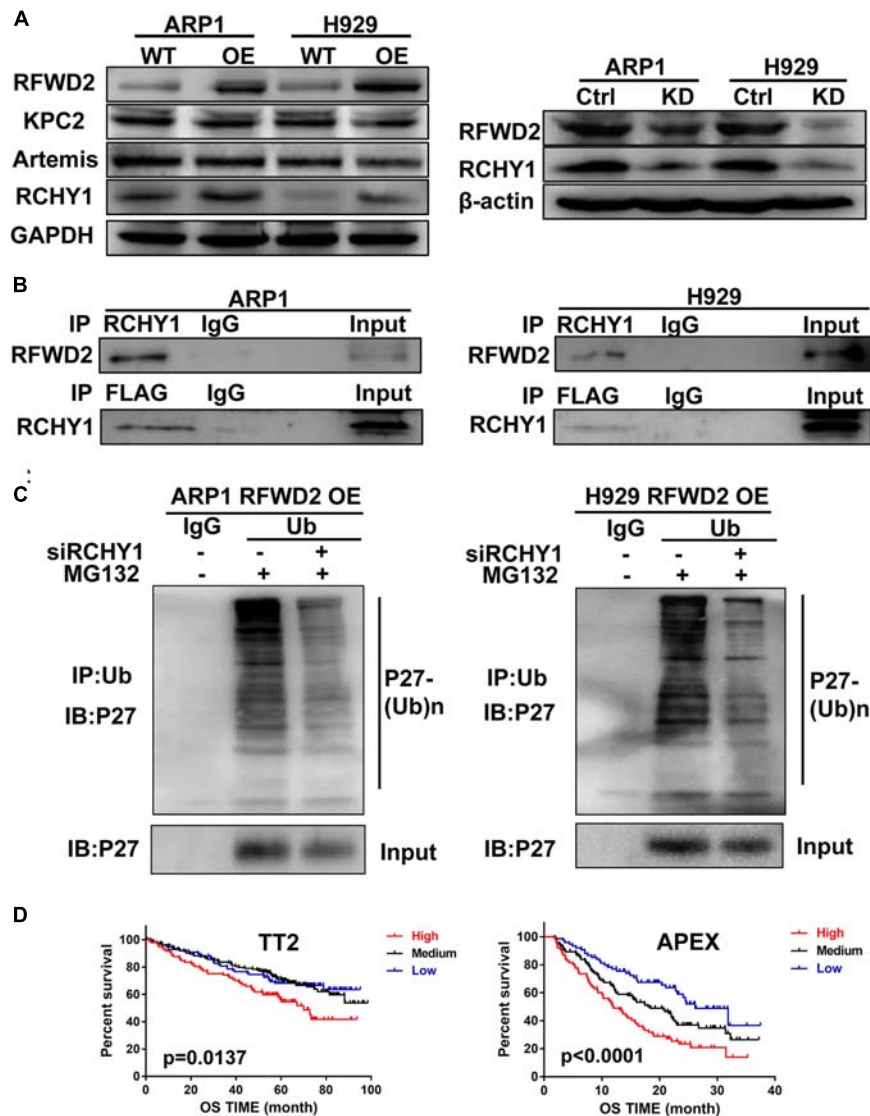


**FIGURE 5 |** RFWD2 regulates P27 ubiquitination through interacting with RCHY1 E3 ubiquitin ligase in MM. **(A)** Left: Protein levels of E3 ubiquitin ligases (KPC2, Artemis and RCHY1) of P27 were measured by WB in RFWD2 WT/OE ARP1 and H929 cell lines; Right: Protein levels of RCHY1 E3 ubiquitin ligase were detected in ARP1 and H929 cells with or without RFWD2 KD. **(B)** The physical interaction between RFWD2 and RCHY1 was identified by Co-IP experiment. **(C)** The ubiquitination level of P27 was detected in RFWD2 OE cells upon transfection of RCHY1 siRNA or not. **(D)** Kaplan-Meier analysis for MM patients with different levels of RFWD2 and RCHY1 expression. The patient survival classified by high/low RFWD2 expression and high/low RCHY1 expression were described. The cases were designated as high expressers while both RFWD2 and RCHY1 message were above (indicated in red) the medium level, or stratified as low expressers while both RFWD2 and RCHY1 message were below (blue) the medium level in the TT2 and APEX dataset. All remaining cases (RFWD2<sup>High</sup>/RCHY1<sup>Low</sup> or RFWD2<sup>Low</sup>/RCHY1<sup>High</sup>) were stratified as medium expressers (black).

## DISCUSSION

The ubiquitin-proteasome system (UPS) plays a key role in regulating the levels and activities of a multitude of proteins as well as modulation of cell cycle, gene expression, cell survival, cell proliferation and apoptosis in MM (Crawford et al., 2020). MM cells typically produce a substantial amount of paraprotein and deeply rely on the UPS to maintain cellular homeostasis (Franqui-Machin et al., 2018). Ubiquitination is a process in which ubiquitin molecules bind to the

target protein under the action of E1 ubiquitin activating enzyme, E2 ubiquitin conjugating enzyme and E3 ubiquitin ligase to modify the ubiquitination of the target protein (Mulder et al., 2016). Preclinical studies have highlighted a rich source of E3 ubiquitin ligases rendering resistance to PIs in MM cells and developed anti-E3s based cancer therapeutics for MM treatment (Zhang et al., 2016; Chen et al., 2018; Barrio et al., 2020; Huang et al., 2020). In the current study, we introduced an E3 ubiquitin ligase RFWD2 located at the long arm of chromosomal position 1q25,



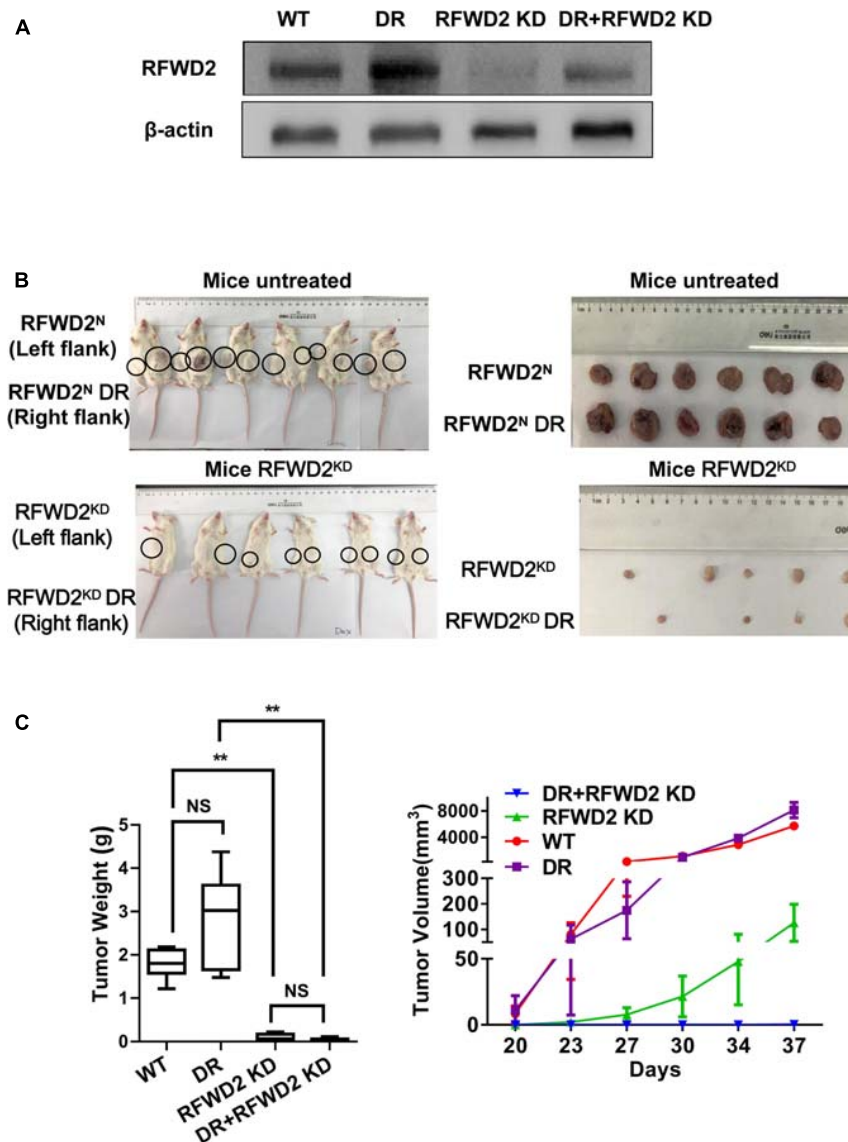


**FIGURE 6 |** Reduction of RFWD2 reverses BTZ resistance in MM xenograft model. **(A)** WB assay was conducted to evaluate RFWD2 protein levels in 8226 WT, 8226 RFWD2 KD, 8226/BTZ and 8226/BTZ RFWD2 KD xenografts. **(B)** Photographic images of xenograft-bearing mice (left) and tumor growth (right) from each group were captured. **(C)** Left: Mean tumor weight in the four experimental groups at day 28 post implantation of the specified MM cells; Right: Time course of tumor growth in myeloma xenografts received 8226 WT, 8226 RFWD2 KD, 8226/BTZ and 8226/BTZ RFWD2 KD cells in each flank. The data were expressed as mean  $\pm$  SD,  $**P < 0.01$ , NS, no significance.

which is of particular interest in MM (Shaughnessy, 2005; De Boussac et al., 2020). The data of gene expression profiling from 3 independent MM cohorts (TT3, HOVON65 and APEX) were analyzed, which indicated that high RFWD2-expression patients were intimately associated with adverse prognosis, disease relapse and myeloma cell proliferation, as consistent with our previous results in TT2 and GMMG-HD4 cohort (Gu et al., 2020). All these provide ample experimental evidence for RFWD2 acting as an attractively molecular predictor in advanced myeloma.

Since RFWD2 governs a series of biological activities, we further develop a deeper knowledge surrounding RFWD2 and

MM using lentivirus knockdown and overexpressing approaches. MS analysis showed that the impact of RFWD2 on cell cycle, cell growth and death were involved in MM process. Inducible downregulation of RFWD2 elicited an apparent decrease in growth rates of ARP1 and H929 cells via regulating cell cycle and apoptosis, which made a complementary to our previous report on overexpression of RFWD2 (Gu et al., 2020). The function of RFWD2 differs in diverse tumors largely depending on degradation of its specific downstream substrates, such as c-Jun (Migliorini et al., 2011), FOXO1 (Kato et al., 2008), P53 (Dornan et al., 2004b) and ETS transcription factors (Vitari et al., 2011). Several research have highlighted the significance of

P53 and P27 for cell cycle and apoptosis involved in RFWD2-driven carcinogenesis (Choi et al., 2015a; Ka et al., 2018). Guided by the data of WB and Co-IP assessment on P53 and P27, we found the higher expression of P27 and the stronger linkage of RFWD2 and P27, which suggested that P27 was the major target of RFWD2 in MM. Next, we unraveled that depletion of RFWD2 impaired ubiquitination and degradation of P27 to induce cell cycle arrest, thereby blunt MM cell growth.

To query the mechanism underlying RFWD2-induced tumorigenesis via mediating P27, we further evaluated the moderator involved in the interaction between RFWD2 and P27. Mounting evidence has pointed out that P27 is predominately regulated by KPC2 at G1 phase, leading to translocation-coupled cytoplasmic ubiquitination (Kamura et al., 2004; Masumoto and Kitagawa, 2016). In addition, P27 is found to be degraded through CRL4DDB2-Artemis E3 ligases (Zhao et al., 2013). Recently, RCHY1 has been proved to act as a novel E3 ubiquitin ligase for P27 via directly binding and ubiquitylating P27 from late G1 to S phase (Shimada et al., 2009; Masumoto and Kitagawa, 2016). Both RCHY1 and RFWD2 are RING type E3 ubiquitin ligases. RFWD2 serves as one of the RCHY1-binding partners, and functional interplay between them can inhibit P53 activity synergistically in non-small cell lung cancer (Wang et al., 2011). We first explored these specific E3 ubiquitin ligases in MM and found that the positive relationship was observed only between RCHY1 and RFWD2. Co-IP assay was employed to further validate the physical interaction of RCHY1 and RFWD2. In addition, silencing RCHY1 by siRNA abolished the ubiquitination of P27 in RFWD2 OE cell lines. However, the study performed in human 293T, HeLa and MDA-MB231 cells demonstrated that the E3 ubiquitin ligases of P27 like RCHY1 did not participate in RFWD2-mediated P27 degradation (Choi et al., 2015b). The reason of the two distinctive conclusions may be attributed to diverse genetic backgrounds, molecular manipulators and signal pathways presented in different types of cancer. Notably, we found that the increased co-expression of RFWD2 and RCHY1 yielded a severe detrimental impact on the prognosis of MM patients. Collectively, we infer that RFWD2 mediates P27 ubiquitination to facilitate MM progression by interacting with the RCHY1 E3 ubiquitin ligase, which contributes to a potentially novel mechanism regarding RFWD2-driven carcinogenesis.

It has been well recognized that P27 is one of the major targets of PIs like BTZ (Iskandarani et al., 2016; Fotouhi et al., 2019), while RFWD2 is the key regulator of P27. We have proved that targeting RFWD2 potentially overcomes BTZ resistance *in vitro*. To put forward our findings into *in vivo* study, we adopted paired 8226 WT and BTZ-resistant cells with RFWD2 KD in MM xenograft model. Both 8226 WT or 8226/BTZ RFWD2 KD tumor

expansion were outstandingly lagged behind their corresponding partner control, indicating that targeting RFWD2 could repress tumor expansion and overcome BTZ resistance both *in vitro* and *in vivo*.

In summary, we provide more preclinical evidence to strengthen the notion that targeting RFWD2 can inhibit MM cellular proliferation and drug resistance to proteasome inhibitor via regulating P27. In addition, our findings provide important insights into the mechanism by which RFWD2 and RCHY1 collaborate to negatively regulate P27 stability, indicating that blocking the RFWD2-RCHY1 signaling axis is a feasible strategy with reduced P27 to potentiate PIs therapy for combating MM. The development of advanced techniques on screening chemical inhibition of RFWD2 for MM therapy is entered into new research frontier.

## DATA AVAILABILITY STATEMENT

The original contributions presented in the study are publicly available. This data can be found here: the ProteomeXchange Consortium: PXD024507.

## ETHICS STATEMENT

The animal study was reviewed and approved by Institutional Ethics Review Boards of Nanjing University of Chinese Medicine.

## AUTHOR CONTRIBUTIONS

CG and MG conceived the manuscript and provided critical input. MG drafted the manuscript. PD, SY, MG, LE, and YZ performed the experiments. ZZ provided technical counseling on experiments. CG and YY reviewed the data and edited the manuscript. All authors read and approved the final manuscript.

## FUNDING

This work was supported by National Natural Science Foundation of China 82003832 (to MG); National Natural Science Foundation of China 81970196 (to CG), 82073885 (to YY); Natural Science Foundation of Jiangsu Province BK20200097 (to CG); and a Project Funded by the Priority Academic Program Development of Jiangsu Higher Education Institutions (Integration of Chinese and Western Medicine).

## REFERENCES

- Abbastabar, M., Kheyrollah, M., Azizian, K., Bagherlou, N., Tehrani, S. S., Maniati, M., et al. (2018). Multiple functions of p27 in cell cycle, apoptosis, epigenetic modification and transcriptional regulation for the control of cell growth: a double-edged sword protein. *DNA Repair (Amst)* 69, 63–72. doi: 10.1016/j.dnarep.2018.07.008
- Barrio, S., Munawar, U., Zhu, Y. X., Giesen, N., Shi, C. X., Via, M. D., et al. (2020). IKZF1/3 and CRL4(CRBN) E3 ubiquitin ligase mutations and resistance to immunomodulatory drugs in multiple myeloma. *Haematologica* 105, e237–e241. doi: 10.3324/haematol.2019.217943
- Chen, Y., Zhao, J., Li, D., Hao, J., He, P., Wang, H., et al. (2018). TRIM56 suppresses multiple myeloma progression by activating TLR3/TRIF signaling. *Yonsei Med. J.* 59, 43–50. doi: 10.3349/ymj.2018.59.1.43

- Choi, H. H., Guma, S., Fang, L., Phan, L., Ivan, C., Baggerly, K., et al. (2015a). Regulating the stability and localization of CDK inhibitor p27(Kip1) via CSN6-COP1 axis. *Cell Cycle* 14, 2265–2273. doi: 10.1080/15384101.2015.1046655
- Choi, H. H., Phan, L., Chou, P. C., Su, C. H., Yeung, S. C., Chen, J. S., et al. (2015b). COP1 enhances ubiquitin-mediated degradation of p27Kip1 to promote cancer cell growth. *Oncotarget* 6, 19721–19734. doi: 10.18632/oncotarget.3821
- Crawford, L. J., Campbell, D. C., Morgan, J. J., Lawson, M. A., Down, J. M., Chauhan, D., et al. (2020). The E3 ligase HUWE1 inhibition as a therapeutic strategy to target MYC in multiple myeloma. *Oncogene* 39, 5001–5014. doi: 10.1038/s41388-020-1345-x
- De Boussac, H., Bruyer, A., Jourdan, M., Maes, A., Robert, N., Gourzones, C., et al. (2020). Kinome expression profiling to target new therapeutic avenues in multiple myeloma. *Haematologica* 105, 784–795. doi: 10.3324/haematol.2018.208306
- Dobashi, Y., Tsubochi, H., Minegishi, K., Kitagawa, M., Otani, S., and Ooi, A. (2017). Regulation of p27 by ubiquitin ligases and its pathological significance in human lung carcinomas. *Hum. Pathol.* 66, 67–78. doi: 10.1016/j.humpath.2017.05.022
- Dornan, D., Bheddah, S., Newton, K., Ince, W., Frantz, G. D., Dowd, P., et al. (2004a). COP1, the negative regulator of p53, is overexpressed in breast and ovarian adenocarcinomas. *Cancer Res.* 64, 7226–7230. doi: 10.1158/0008-5472.CAN-04-2601
- Dornan, D., Wertz, I., Shimizu, H., Arnott, D., Frantz, G. D., Dowd, P., et al. (2004b). The ubiquitin ligase COP1 is a critical negative regulator of p53. *Nature* 429, 86–92. doi: 10.1038/nature02514
- Egozi, D., Shapira, M., Paor, G., Ben-Izhak, O., Skorecki, K., and Hershko, D. D. (2007). Regulation of the cell cycle inhibitor p27 and its ubiquitin ligase Skp2 in differentiation of human embryonic stem cells. *FASEB J.* 21, 2807–2817. doi: 10.1096/fj.06-7758com
- Fang, J. S., Coon, B. G., Gillis, N., Chen, Z., Qiu, J., Chittenden, T. W., et al. (2017). Shear-induced Notch-Cx37-p27 axis arrests endothelial cell cycle to enable arterial specification. *Nat. Commun.* 8:2149. doi: 10.1038/s41467-017-01742-7
- Fotouhi, O., Kjellin, H., Juhlin, C. C., Pan, Y., Vesterlund, M., Ghaderi, M., et al. (2019). Proteomics identifies neddylation as a potential therapy target in small intestinal neuroendocrine tumors. *Oncogene* 38, 6881–6897. doi: 10.1038/s41388-019-0938-8
- Franqui-Machin, R., Hao, M., Bai, H., Gu, Z., Zhan, X., Habelhah, H., et al. (2018). Destabilizing NEK2 overcomes resistance to proteasome inhibition in multiple myeloma. *J. Clin. Invest.* 128, 2877–2893. doi: 10.1172/JCI98765
- Gandolfi, S., Laubach, J. P., Hideshima, T., Chauhan, D., Anderson, K. C., and Richardson, P. G. (2017). The proteasome and proteasome inhibitors in multiple myeloma. *Cancer Metastasis Rev.* 36, 561–584. doi: 10.1007/s10555-017-9707-8
- Gu, C., Lu, T., Wang, W., Shao, M., Wei, R., Guo, M., et al. (2020). RFWD2 induces cellular proliferation and selective proteasome inhibitor resistance by mediating P27 ubiquitination in multiple myeloma. *Leukemia* doi: 10.1038/s41375-020-01033-z [Epub ahead of print].
- Gu, C., Yang, Y., Sompallae, R., Xu, H., Tompkins, V. S., Holman, C., et al. (2016). FOXM1 is a therapeutic target for high-risk multiple myeloma. *Leukemia* 30, 873–882. doi: 10.1038/leu.2015.334
- Huang, X., Gu, H., Zhang, E., Chen, Q., Cao, W., Yan, H., et al. (2020). The NEDD4-1 E3 ubiquitin ligase: a potential molecular target for bortezomib sensitivity in multiple myeloma. *Int. J. Cancer* 146, 1963–1978. doi: 10.1002/ijc.32615
- Iskandarani, A., Bhat, A. A., Siveen, K. S., Prabhu, K. S., Kuttikrishnan, S., Khan, M. A., et al. (2016). Bortezomib-mediated downregulation of S-phase kinase protein-2 (SKP2) causes apoptotic cell death in chronic myelogenous leukemia cells. *J. Transl. Med.* 14:69. doi: 10.1186/s12967-016-0823-y
- Ka, W. H., Cho, S. K., Chun, B. N., Byun, S. Y., and Ahn, J. C. (2018). The ubiquitin ligase COP1 regulates cell cycle and apoptosis by affecting p53 function in human breast cancer cell lines. *Breast Cancer* 25, 529–538. doi: 10.1007/s12282-018-0849-5
- Kamura, T., Hara, T., Matsumoto, M., Ishida, N., Okumura, F., Hatakeyama, S., et al. (2004). Cytoplasmic ubiquitin ligase KPC regulates proteolysis of p27(Kip1) at G1 phase. *Nat. Cell Biol.* 6, 1229–1235. doi: 10.1038/ncb1194
- Kato, S., Ding, J., Pisch, E., Jhala, U. S., and Du, K. (2008). COP1 functions as a FoxO1 ubiquitin E3 ligase to regulate FoxO1-mediated gene expression. *J. Biol. Chem.* 283, 35464–35473. doi: 10.1074/jbc.M801011200
- Ko, E. J., Oh, Y. L., Kim, H. Y., Eo, W. K., Kim, H., Kim, K. H., et al. (2019). Correlation of constitutive photomorphogenic 1 (COP1) and p27 tumor suppressor protein expression in ovarian cancer. *Genes Genomics* 41, 879–884. doi: 10.1007/s13258-019-00818-6
- Lee, Y. H., Andersen, J. B., Song, H. T., Judge, A. D., Seo, D., Ishikawa, T., et al. (2010). Definition of ubiquitination modulator COP1 as a novel therapeutic target in human hepatocellular carcinoma. *Cancer Res.* 70, 8264–8269. doi: 10.1158/0008-5472.CAN-10-0749
- Li, L., Kang, J., Zhang, W., Cai, L., Wang, S., Liang, Y., et al. (2019). Validation of NEDD8-conjugating enzyme UBC12 as a new therapeutic target in lung cancer. *EBioMedicine* 45, 81–91. doi: 10.1016/j.ebiom.2019.06.005
- Li, N., Zeng, J., Sun, F., Tong, X., Meng, G., Wu, C., et al. (2018). p27 inhibits CDK6/CCND1 complex formation resulting in cell cycle arrest and inhibition of cell proliferation. *Cell Cycle* 17, 2335–2348. doi: 10.1080/15384101.2018.1526598
- Masumoto, K., and Kitagawa, M. (2016). E3 ubiquitin ligases as molecular targets in human oral cancers. *Curr. Cancer Drug Targets* 16, 130–135. doi: 10.2174/1568009616666151112122336
- Migliorini, D., Bogaerts, S., Defever, D., Vyas, R., Denecker, G., Radaelli, E., et al. (2011). Cop1 constitutively regulates c-Jun protein stability and functions as a tumor suppressor in mice. *J. Clin. Invest.* 121, 1329–1343. doi: 10.1172/JCI45784
- Mulder, M. P. C., Witting, K., Berlin, I., Pruneda, J. N., Wu, K. P., and Chang, J. G. (2016). A cascading activity-based probe sequentially targets E1-E2-E3 ubiquitin enzymes. *Nat. Chem. Biol.* 12, 523–530. doi: 10.1038/nchembio.2084
- Richardson, P. G., Zweegman, S., O'donnell, E. K., Laubach, J. P., Raj, N., Voorhees, P., et al. (2018). Ixazomib for the treatment of multiple myeloma. *Expert Opin. Pharmacother.* 19, 1949–1968. doi: 10.1080/14656566.2018.1528229
- Rodriguez, S., Abundis, C., Boccalatte, F., Mehrotra, P., Chiang, M. Y., Yui, M. A., et al. (2020). Therapeutic targeting of the E3 ubiquitin ligase SKP2 in T-ALL. *Leukemia* 34, 1241–1252. doi: 10.1038/s41375-019-0653-z
- Sawada, G., Ueo, H., Matsumura, T., Uchi, R., Ishibashi, M., Mima, K., et al. (2013). Loss of COP1 expression determines poor prognosis in patients with gastric cancer. *Oncol. Rep.* 30, 1971–1975. doi: 10.3892/or.2013.2664
- Sharma, S. S., and Pledger, W. J. (2016). The non-canonical functions of p27(Kip1) in normal and tumor biology. *Cell Cycle* 15, 1189–1201. doi: 10.1080/15384101.2016.1157238
- Shaughnessy, J. (2005). Amplification and overexpression of CKS1B at chromosome band 1q21 is associated with reduced levels of p27Kip1 and an aggressive clinical course in multiple myeloma. *Hematology* 10(Suppl. 1), 117–126. doi: 10.1080/10245330512331390140
- Shimada, M., Kitagawa, K., Dobashi, Y., Isobe, T., Hattori, T., Uchida, C., et al. (2009). High expression of Pirh2, an E3 ligase for p27, is associated with low expression of p27 and poor prognosis in head and neck cancers. *Cancer Sci.* 100, 866–872. doi: 10.1111/j.1349-7006.2009.01122.x
- Snoek, B. C., De Wilt, L. H., Jansen, G., and Peters, G. J. (2013). Role of E3 ubiquitin ligases in lung cancer. *World J. Clin. Oncol.* 4, 58–69. doi: 10.5306/wjco.v4.i3.58
- Song, Y., Liu, Y., Pan, S., Xie, S., Wang, Z. W., and Zhu, X. (2020). Role of the COP1 protein in cancer development and therapy. *Semin. Cancer Biol.* 67(Pt 2), 43–52. doi: 10.1016/j.semcancer.2020.02.001
- Song, Y., Park, P. M. C., Wu, L., Ray, A., Picaud, S., Li, D., et al. (2019). Development and preclinical validation of a novel covalent ubiquitin receptor Rpn13 degrader in multiple myeloma. *Leukemia* 33, 2685–2694. doi: 10.1038/s41375-019-0467-z
- Vitari, A. C., Leong, K. G., Newton, K., Yee, C., O'rourke, K., Liu, J., et al. (2011). COP1 is a tumour suppressor that causes degradation of ETS transcription factors. *Nature* 474, 403–406. doi: 10.1038/nature10005
- Wang, L., He, G., Zhang, P., Wang, X., Jiang, M., and Yu, L. (2011). Interplay between MDM2, MDMX, Pirh2 and COP1: the negative regulators of p53. *Mol. Biol. Rep.* 38, 229–236. doi: 10.1007/s11033-010-0099-x
- Wang, W., Wei, R., Liu, S., Qiao, L., Hou, J., Gu, C., et al. (2019). BTK induces CAM-DR through regulation of CXCR4 degradation in multiple myeloma. *Am. J. Transl. Res.* 11, 4139–4150.
- Xiong, W., Wu, X., Starnes, S., Johnson, S. K., Haessler, J., Wang, S., et al. (2008). An analysis of the clinical and biologic significance of TP53 loss and the identification of potential novel transcriptional targets of TP53 in multiple myeloma. *Blood* 112, 4235–4246. doi: 10.1182/blood-2007-10-119123

- Yang, Z., Guan, Y., Li, J., Li, L., and Li, Z. (2018). Chrysin attenuates carrageenan-induced pleurisy and lung injury via activation of SIRT1/NRF2 pathway in rats. *Eur. J. Pharmacol.* 836, 83–88. doi: 10.1016/j.ejphar.2018.08.015
- Yoon, H., Kim, M., Jang, K., Shin, M., Besser, A., Xiao, X., et al. (2019). p27 transcriptionally coregulates cJun to drive programs of tumor progression. *Proc. Natl. Acad. Sci. U.S.A.* 116, 7005–7014. doi: 10.1073/pnas.1817415116
- Yoshida, A., Kato, J. Y., Nakamae, I., and Yoneda-Kato, N. (2013). COP1 targets C/EBPalpha for degradation and induces acute myeloid leukemia via Trib1. *Blood* 122, 1750–1760. doi: 10.1182/blood-2012-12-476101
- Yuan, Z. Z., Suo, Y. R., Hao, X. Y., Wang, S. L., Li, G., and Wang, H. L. (2018). Triterpenic acids from *potentilla parvifolia* and their protective effects against okadaic acid induced neurotoxicity in differentiated sh-sy5y cells. *Biol. Pharm. Bull.* 41, 885–890. doi: 10.1248/bpb.b17-01010
- Zhang, Z., Tong, J., Tang, X., Juan, J., Cao, B., Hurren, R., et al. (2016). The ubiquitin ligase HERC4 mediates c-Maf ubiquitination and delays the growth of multiple myeloma xenografts in nude mice. *Blood* 127, 1676–1686. doi: 10.1182/blood-2015-07-658203
- Zhao, H., Bauzon, F., Fu, H., Lu, Z., Cui, J., Nakayama, K., et al. (2013). Skp2 deletion unmasks a p27 safeguard that blocks tumorigenesis in the absence of pRb and p53 tumor suppressors. *Cancer Cell* 24, 645–659. doi: 10.1016/j.ccr.2013.09.021
- Zhou, W., Yang, Y., Xia, J., Wang, H., Salama, M. E., Xiong, W., et al. (2013). NEK2 induces drug resistance mainly through activation of efflux drug pumps and is associated with poor prognosis in myeloma and other cancers. *Cancer Cell* 23, 48–62. doi: 10.1016/j.ccr.2012.12.001
- Zou, S., Zhu, Y., Wang, B., Qian, F., Zhang, X., Wang, L., et al. (2017). The ubiquitin ligase COP1 promotes glioma cell proliferation by preferentially downregulating tumor suppressor p53. *Mol. Neurobiol.* 54, 5008–5016. doi: 10.1007/s12035-016-0033-x

**Conflict of Interest:** The authors declare that the research was conducted in the absence of any commercial or financial relationships that could be construed as a potential conflict of interest.

Copyright © 2021 Guo, Ding, Zhu, Fan, Zhou, Yang, Yang and Gu. This is an open-access article distributed under the terms of the Creative Commons Attribution License (CC BY). The use, distribution or reproduction in other forums is permitted, provided the original author(s) and the copyright owner(s) are credited and that the original publication in this journal is cited, in accordance with accepted academic practice. No use, distribution or reproduction is permitted which does not comply with these terms.





# The Absence of PTEN in Breast Cancer Is a Driver of MLN4924 Resistance

Meng-ge Du<sup>1†</sup>, Zhi-qiang Peng<sup>2,3†</sup>, Wen-bin Gai<sup>2,4†</sup>, Fan Liu<sup>1</sup>, Wei Liu<sup>1</sup>, Yu-jiao Chen<sup>1</sup>, Hong-chang Li<sup>2</sup>, Xin Zhang<sup>2</sup>, Cui Hua Liu<sup>5</sup>, Ling-qiang Zhang<sup>2,3</sup>, Hong Jiang<sup>4\*</sup> and Ping Xie<sup>1\*</sup>

<sup>1</sup> The Municipal Key Laboratory for Liver Protection and Regulation of Regeneration, Department of Cell Biology, Capital Medical University, Beijing, China, <sup>2</sup> State Key Laboratory of Proteomics Beijing Proteome Research Center, National Center for Protein Sciences (Beijing), Beijing Institute of Lifeomics, Beijing, China, <sup>3</sup> School of Medicine, Tsinghua University, Beijing, China, <sup>4</sup> Shandong Provincial Key Laboratory of Pathogenesis and Prevention of Neurological Disorders and State Key Disciplines: Physiology, Department of Physiology, School of Basic Medicine, Medical College, Qingdao University, Qingdao, China, <sup>5</sup> CAS Key Laboratory of Pathogenic Microbiology and Immunology, Institute of Microbiology (Chinese Academy of Sciences), Savaid Medical School, University of Chinese Academy of Sciences, Beijing, China

## OPEN ACCESS

### Edited by:

Gordon Chan,  
University of Alberta, Canada

### Reviewed by:

Yongchao Zhao,  
Zhejiang University, China  
Alo Ray,  
The Ohio State University,  
United States

### \*Correspondence:

Hong Jiang  
hongjiang@qdu.edu.cn  
Ping Xie  
xiep@ccmu.edu.cn

<sup>†</sup> These authors have contributed  
equally to this work

### Specialty section:

This article was submitted to  
Cell Growth and Division,  
a section of the journal  
Frontiers in Cell and Developmental  
Biology

**Received:** 13 February 2021

**Accepted:** 19 March 2021

**Published:** 30 April 2021

### Citation:

Du M-g, Peng Z-q, Gai W-b, Liu F,  
Liu W, Chen Y-j, Li H-c, Zhang X,  
Liu CH, Zhang L-q, Jiang H and Xie P  
(2021) The Absence of PTEN  
in Breast Cancer Is a Driver  
of MLN4924 Resistance.  
Front. Cell Dev. Biol. 9:667435.  
doi: 10.3389/fcell.2021.667435

**Background:** Numerous studies have indicated that the neddylation pathway is closely associated with tumor development. MLN4924 (Pevonedistat), an inhibitor of the NEDD8-activating E1 enzyme, is considered a promising chemotherapeutic agent. Recently, we demonstrated that neddylation of the tumor suppressor PTEN occurs under high glucose conditions and promotes breast cancer development. It has been shown, however, that PTEN protein levels are reduced by 30–40% in breast cancer. Whether this PTEN deficiency affects the anti-tumor function of MLN4924 is unknown.

**Methods:** In the present study, cell counting kit-8 and colony formation assays were used to detect cell proliferation, and a transwell system was used to quantify cell migration. A tumor growth assay was performed in BALB/c nude mice. The subcellular location of PTEN was detected by fluorescence microscopy. The CpG island of the UBA3 gene was predicted by the Database of CpG Islands and UCSC database. Western blotting and qRT-PCR were used to measure the expression of indicated proteins. The Human Protein Atlas database, the Cancer Genome Atlas and Gene Expression Omnibus datasets were used to validate the expression levels of UBA3 in breast cancer.

**Results:** Our data show that the anti-tumor efficacy of MLN4924 in breast cancer cells was markedly reduced with the deletion of PTEN. PI3K/Akt signaling pathway activity correlated positively with UBA3 expression. Pathway activity correlated negatively with NEDP1 expression in PTEN-positive breast cancer patients, but not in PTEN-negative patients. We also demonstrate that high glucose conditions upregulate UBA3 mRNA by inhibiting UBA3 promoter methylation, and this upregulation results in the overactivation of PTEN neddylation in breast cancer cells.

**Conclusion:** These data suggest a mechanism by which high glucose activates neddylation. PTEN is critical, if not indispensable, for MLN4924 suppression of tumor growth; PTEN status thus may help to identify MLN4924-responsive breast cancer patients.

**Keywords:** MLN4924, UBA3, neddylation, PTEN, breast cancer

## INTRODUCTION

Breast cancer has overtaken lung cancer as the world's most common cancer. Effective therapy of breast cancer requires precise treatments that are tailored to genomic status. Therefore, it is important to identify new diagnostic methods, drug targets and prognostic tools from the results of studies of the pathogenesis and molecular mechanisms underlying breast cancer (Waks and Winer, 2019; Hanks et al., 2020).

Phosphatase and tension homolog on chromosome 10 (PTEN) is one of the most frequently mutated genes in human cancers and inherited syndromes (Song et al., 2012). Absence of PTEN results in the activation of the phosphatidylinositol 3-kinase (PI3K)/Akt oncogenic pathway, which controls cell growth and survival (Di Cristofano et al., 1998; Stambolic et al., 1998). Recently, we reported that PTEN is a novel target for modification with NEDD8. High concentrations of glucose trigger PTEN neddylation, resulting in PTEN nuclear import. In breast cancer patients, neddylated PTEN correlates with tumor stages and with a poor prognosis (Xie et al., 2021). NEDD8 is a ubiquitin-like protein (UBL) that is covalently conjugated to substrates in a manner similar to the ubiquitin system. The neddylation system includes an activating enzyme (E1, which consists of a heterodimer of UBA3 and NAE1/APP-BP1), two conjugating enzymes (E2s, which are known as UBE2M/Ubc12 and UBE2F), and various E3 ligases (Enchev et al., 2015). Neddylation is reversible through the deneddylases NEDP1 and JAB1/CSN5 (Cope et al., 2002; Mendoza et al., 2003).

An inhibitor of the NEDD8-activating enzyme E1, MLN4924 (Pevonedistat), has shown promise as an anti-cancer agent. Previous studies indicated that MLN4924 inhibits breast cancer cell growth and migration (Chen et al., 2018, 2020; Naik et al., 2020), and it displays potent preclinical activity for patients with acute myelocytic leukemia, acute lymphocytic leukemia, glioblastomas, Wilms tumors, rhabdomyosarcomas, and neuroblastomas (Soucy et al., 2009; Wang et al., 2011; Nawrocki et al., 2012). Accordingly, MLN4924 has been evaluated in a series of phase 1, 2, and 3 clinical trials, both alone and in combination with other chemo- and radiotherapies (Soucy et al., 2009; Abidi and Xirodimas, 2015). MLN4924 serves as a chemo- or radiosensitizer in pancreatic (Wei et al., 2012), colorectal (Wan et al., 2016), prostate (Wang et al., 2016), and ovarian (Nawrocki et al., 2013) cancer cells, and it has been found to be more effective in combination with other chemo- or radiotherapies, including azacytidine (Swords et al., 2018) and 2-deoxy-D-glucose (2-DG) (Oladghaffari et al., 2017). Unfortunately, loss or reduction of PTEN protein is common in numerous tumors, including breast cancer (Perren et al., 1999; Costa et al., 2020), and PTEN is thought to be a necessary factor for MLN4924 sensitivity.

Here, we specifically studied the role of PTEN presence in the biological activities of MLN4924. Our data showed that MLN4924 suppressed Akt signaling in a PTEN-dependent manner. Loss of PTEN particularly weakened the anti-tumor ability of MLN4924 in breast cancer. Furthermore, we found that high glucose inhibits UBA3 promoter methylation and increases UBA3 mRNA levels, and these outcomes correlate with the overactivation of PTEN neddylation in breast cancer cells. The PI3K/Akt signaling pathway is positively correlated with the expression of UBA3, but the correlation is not significant in PTEN-null breast cancer patients. Therefore, our data suggest that those patients with cancer that harbor complete *PTEN*-loss may be resistant to MLN4924. In addition, we suggest that low levels of UBA3 promoter methylation in breast cancer patients could suggest promising tumor therapeutic targets.

## MATERIALS AND METHODS

### Cell Culture and Transfections

MCF-7, BT-549, MDA-MB-231, SKBR3, and T-47D were obtained from the American Type Culture Collection (ATCC). MCF-7 cells were cultured in DMEM (GIBCO-Invitrogen) supplemented with 10% fetal bovine serum (FBS). BT-549 and T-47D cells were cultured in RPMI-1640 (GIBCO-Invitrogen) supplemented with 10% FBS. MDA-MB-231 cells were cultured in Leibovitz's L-15 Medium supplemented with 10% FBS. SKBR3 cells were cultured in Dulbecco's modified Eagle's medium and GlutaMAX-1 (Gibco Life Technologies) containing 10% FBS. Cells were transfected with various plasmids using TurboFect (Thermo Fisher Scientific, R0531), Lipofectamine 3000 (Invitrogen, L3000001) reagent according to the manufacturer's protocol.

### Antibodies and Regents

Antibodies used in this work: Anti-Akt (CST, #9272, 1:1,000), anti-pThr308-Akt (CST, #9275, 1:1,000), anti-pSer473-Akt (CST, #4060, D9E, 1:1,000), anti-p70 S6K (CST, #9202, 1:1,000), anti-pThr389-p70 S6K (CST, no. 9209, 1:1,000), anti-pSer235/236-S6 (CST, #4858, 1:1,000), anti-S6 (CST, #2317, 1:1,000), anti-4E-BP1 (CST, #9452, 1:1,000), anti-pSer65-4E-BP1 (CST, #9451, 1:1,000), anti-PTEN (CST, #9559, 1:1,000), anti-pSer2448-mTOR (CST, #5536, 1:500), anti-mTOR (CST, #2972, 1:500), anti-UBE1a (CST, #4890, 1:1,000) and anti-pAMPK (CST, #2535, 1:1,000) were purchased from Cell Signaling Technology. Anti-GAPDH (Santa Cruz, sc-293335, 1:1,000), Anti-UBA3 (Santa Cruz, sc-377212, 1:200), anti-NAE1 (Santa Cruz, sc-390002, 1:200) and anti-NEDP1 (Santa Cruz, sc-271498, 1:100) were from

Santa Cruz Biotechnologies. Anti-UBE2D3 (Abcam, ab176568, 1:1,000), anti-Cullin1 (Abcam, ab75817, 1:1,000) and anti-SAE1 (Abcam, ab185552, 1:1,000) were purchased from Abcam. Anti-Nedd8-K402-PTEN antibody was from PTM Biolabs, Inc. The NAE inhibitor MLN4924 (HY-70062), 2-Deoxy-D-glucose (a glucose analog and a competitive inhibitor of glucose metabolism) (2-DG, HY-13966), 5-Azacytidine (Azacitidine; 5-AzaC; Ladakmycin) (HY-10586) were purchased from MCE.

## RNA-Seq and Data Analysis

Total RNA was isolated using Trizol (Sigma, Saint Louis, MO) and cDNAs were synthesized by reverse transcription kit (Bio-Rad, Hercules, CA). The cDNA library products were sequenced on an Illumina HiSeq 2000 (Illumina, San Diego, CA). Results from reads that could be uniquely mapped to a gene were used to calculate the expression level. FASTQC was used to check the quality of reads of all samples<sup>1</sup>. Raw data preprocessing was performed as previously described (Liu et al., 2019). The expression of each gene was normalized by the reads per kilobase per million mapped reads among different samples.

## Fluorescence Microscopy

For detection of subcellular localization by immunofluorescence, after fixation with 4% paraformaldehyde and permeabilization in 0.2% Triton X-100 (PBS), cells were incubated with the indicated antibodies for 8 h at 4°C, followed by incubation with TRITC-conjugated or FITC-conjugated secondary antibody for 1 h at 37°C. The nuclei were stained with DAPI. The images were visualized with a Zeiss LSM 510 Meta inverted confocal microscope.

## Real-Time Quantitative PCR Analyses

Total RNA was isolated using Trizol (Sigma, Saint Louis, MO) and cDNAs were synthesized by reverse transcription kit (Bio-Rad, Hercules, CA). Quantitative PCR reactions were performed using SYBR Green master mixture on HT7500 system (Applied Biosystems).

## Generation of Knock-Out Cells

The knock-out cell lines were generated using the Crispr-Cas9 method. Crispr guide sequences targeting *UBA3* was designed by software at <http://crispr.mit.edu> and cloned into Lenti-Crispr pXPR\_001. The sgUBA3 sequences were: 5'-CACCGTGAAGGGTCCAGATCGCTCG-3'. The MCF-7 cells were co-transfected with the Lenti-Crispr vector and packaging plasmids pVSVg and psPAX2. Puromycin-resistant single cells were plated in a 96-well dish to screen for positive monoclonal cells.

## Prediction of CpG Island and Methylation-Specific PCR

The CpG island of *UBA3* gene was predicted by Database of CpG Islands<sup>2</sup> and UCSC database<sup>3</sup>. Genomic DNA was extracted

for methylation analysis from cells in culture by using Genomic DNA Miniprep Kit (sigma). One microgram of genomic DNA was modified with sodium bisulfite using the DNA Bisulfite Conversion Kit (TIANGEN) according to the specifications of the manufacturer. Methylation-specific PCR (MSP) was run in a total volume of 20 µl. MSP reactions were subjected to initial incubation at 95°C for 5 min, followed by 35 cycles of 94°C for 20 s, and annealing at the 60°C for 30 s and 72°C for 20 s. Final extension was done by incubation at 72°C for 5 min. MSP products were separated on 2% agarose gels and visualized after ethidium bromide staining. The following primers were used:

Unmethylated Forward 5'-TTAAAGTTTATGGGAGTTT AGTTGT-3'

Unmethylated Reverse 5'-CAAAATATATAAAAAATCCA AATCACTCA-3'

Methylated Forward 5'-TTAAAGTTTATGGGAGTTTA GTCGT-3'

Methylated Reverse 5'-ATATATAAAAAATCCAAATCGC TCG-3'

## The Human Protein Atlas Database

The Human Protein Atlas database<sup>4</sup> was used to validate the protein expression level of *UBA3* in breast cancer.

## The Cancer Genome Atlas (TCGA) Data

The mRNA data (RNA Seq v2), DNA methylation and clinical information for patients in TCGA-BRCA dataset were downloaded from <https://www.synapse.org> and cBioPortal database<sup>5</sup>, respectively and used for differential mRNA expression, correlation and gene set enrichment analysis.

## GEO Datasets Collection and Differential Expression Analysis

Microarray data were obtained from three datasets. The three series were accessed at the National Centers for Biotechnology Information (NCBI), Gene Expression Omnibus (GEO) database<sup>6</sup> which served as a public repository for gene expression datasets, and the accession numbers were GSE66695 and GSE14088. Differentially expressed genes were obtained using GEO2R<sup>7</sup>. GEO2R is an interactive web tool that compares two groups of samples under the same experimental conditions and can analyze almost any GEO series.

## RNA Interference

Sequence information of the shRNAs are as follows:

shPTEN: 5'-TGCAGATAATGACAAGGAA-3';

shNC: 5'-TTCTCCGAACGTGTCACGT-3'.

## Colony Formation Assay

Cells were seeded into 6-well plates with 600 cells per well. After 12 days, cells were fixed with 4% paraformaldehyde for 15min

<sup>1</sup><http://www.bioinformatics.babraham.ac.uk/projects/fastqc>

<sup>2</sup><http://dbcat.cgm.ntu.edu.tw/>

<sup>3</sup><http://genome.ucsc.edu/index.html>

<sup>4</sup><https://www.proteinatlas.org/>

<sup>5</sup>[www.cbioportal.org](http://www.cbioportal.org)

<sup>6</sup><http://www.ncbi.nlm.nih.gov/geo/>

<sup>7</sup><http://www.ncbi.nlm.nih.gov/geo/geo2r/>

and stained with 0.5% crystal violet solution. The experiment was conducted in three independent triplicates.

## Cell Migration Assay

The assay was performed in an invasion chamber consisting of a 24-well tissue culture plate with 12 cell culture inserts (Becton–Dickinson). Briefly, cells ( $2 \times 10^4$  per well) were seeded in the upper chambers in serum free cell culture medium (in triplicate), and medium containing 10% FBS was added to the bottom wells. Cells were allowed to migrate for 24–48 h in a humidified chamber at 37°C with 5% CO<sub>2</sub>. Then filter was removed and fixed with 4% formaldehyde for 20 min. Cells located in the lower filter were stained with 0.1% crystal violet for 15 min and photographed.

## Cell Proliferation Assay

Cell proliferation was assayed using the Cell Counting Kit-8 (CCK8) assay (Promega) according to the manufacturer's protocol. The transfected cells were planted in 96-well plates (2,000 cells/well). Cell proliferation was detected every 24 h according to the manufacturer's protocol. Briefly, 100 µl of 10% CCK8 solution was added to each well and incubated for 1 h at 37°C. The solution was then measured spectrophotometrically at 450 nm.

## Tumor Growth Assay

The experimental procedures in mice have been approved by the Animal Care and Use Committee of Academy of Military and Medical Sciences. BALB/c nude mice (6-weeks old,  $18.0 \pm 2.0$  g) were obtained from Shanghai Laboratory Animal Center (SLAC, China). Cells ( $5 \times 10^6$  per mouse) were inoculated subcutaneously into the right flank of the mice. Tumor size was measured every 2 days and converted to TV according to the following formula: TV (mm<sup>3</sup>) =  $(a \times b^2)/2$ , where a and b are the largest and smallest diameters, respectively. All animals were killed 4 weeks after injection, and the transplanted tumors were removed, weighed and fixed for further study.

## KEGG Pathway Enrichment Analysis

The online analysis tool DAVID (the Database for Annotation, Visualization and Integrated Discovery, Version 6.7) was used to determine the Kyoto Encyclopedia of Genes and Genomes (KEGG) ( $P < 0.05$ ), in which we focused on the KEGG feature.

## Gene Set Enrichment Analysis

The association between phenotypes, pathways and UBA3/NEDP1 expression was analyzed using Gene Set Enrichment Analysis (GSEA v2.2)<sup>8</sup>. GSEA calculates a gene set Enrichment Score (ES) that estimates whether genes from pre-defined gene set [obtained from the Molecular Signatures Database (MSigDB)]<sup>9</sup> are enriched among the highest- (or lowest-) ranked genes or distributed randomly. Default settings were used. Thresholds for significance were determined by permutation analysis (1,000 permutations). False Discovery Rate

(FDR) was calculated. A gene set is considered significantly enriched when the FDR score is  $< 0.05$ .

## Statistical Analysis

Data were analyzed with GraphPad Prism 5 and SPSS 19.0 software. The statistical significance of differences between various groups was calculated with the Mann-Whitney or two-tailed, Student's *t*-test and error bars represent standard deviation of the mean (SD). Data are shown as mean  $\pm$  SD and  $P < 0.05$  were considered to be statistically significant.

## RESULTS

### MLN4924 Suppresses the Akt Signaling Pathway

On the basis of high-throughput RNA-Seq, 1908 genes whose expression was changed in MCF-7 cells treated with MLN4924 were identified (Figure 1A and Supplementary Table 1). Notably, upon MLN4924 treatment, Kyoto Encyclopedia of Genes and Genomes (KEGG) pathway analysis indicated that the PI3K/Akt signaling pathway was one of the most significantly impacted pathways (Figure 1B). Furthermore, a heatmap analysis revealed that genes downstream of PI3K/Akt signaling, such as the cell cycle control protein cyclin D1 (Cnd1), were robustly decreased upon MLN4924 treatment, while FOXO1, FOXO2, p21, Bax, Bim, p27<sup>kip1</sup>, p15<sup>INK4b</sup> were increased (Figure 1C). Notably, a previous expression analysis showed that the PI3K/Akt pathway target gene Cnd1 was decreased in NIH3T3 cells after knockdown of *Ubc12*, which encodes for a NEDD8-conjugating enzyme. Bim, a Bcl-2 family member, and p27<sup>kip1</sup>, one of the cyclin-CDK inhibitors, were both upregulated when *Ubc12* was depleted (Figure 1D). These data indicate that MLN4924 inhibits the activity of the PI3K/Akt signaling pathway.

Next, we examined the potential correlation between PTEN expression levels and the effect of neddylation on the PI3K/Akt signaling pathway in breast cancer patients. Among breast cancer patients harboring high PTEN expression, the PI3K/Akt signaling pathway activation gene-set was markedly enriched in the genes encoding for the NEDD8-activating enzyme UBA3, whose expression was increased, and the deneddylase NEDP1, whose expression was decreased (Figures 1E,F). In contrast, among patients with low PTEN expression, there was no correlation between the PI3K/Akt signaling pathway activation gene set and UBA3 (Figure 1G) or NEDP1 (Figure 1H).

### PTEN Is Indispensable for MLN4924 Suppressing PI3K/Akt Signaling Pathway

Consistent with our previous study (Xie et al., 2021), in MCF-7 cells, we observed a dose-dependent reduction in phosphorylation of Akt, S6K, 4EBP1, and mTOR within 12 h of exposure to MLN4924, while total protein levels of Akt, S6K, 4EBP1, and mTOR were unchanged (Figure 2A, left). PTEN neddylation on K402 was also decreased by MLN4924 treatment in a dose-dependent manner. However, in the PTEN-deficient

<sup>8</sup><http://www.broad.mit.edu/gsea/>

<sup>9</sup><http://software.broadinstitute.org>



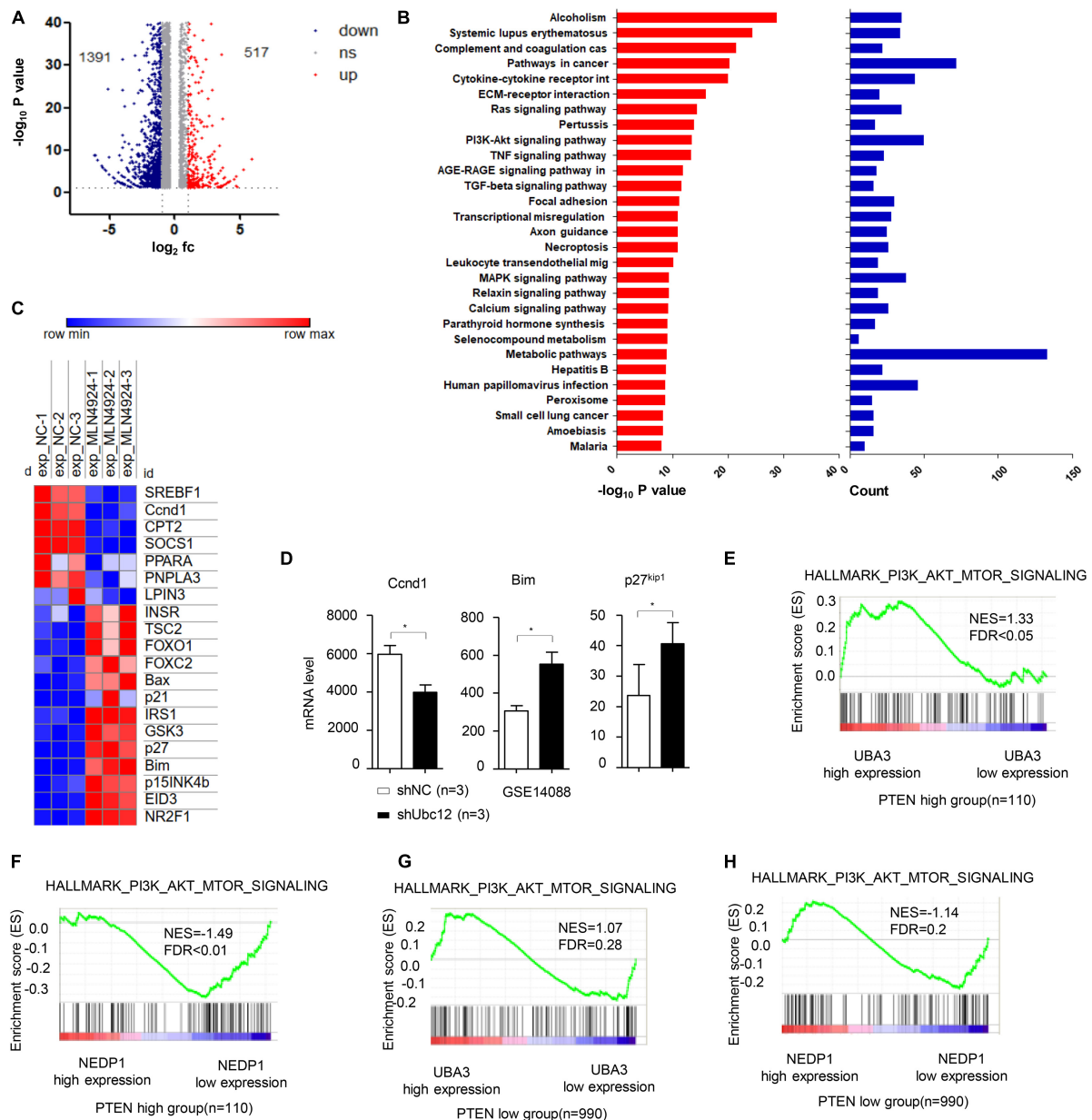
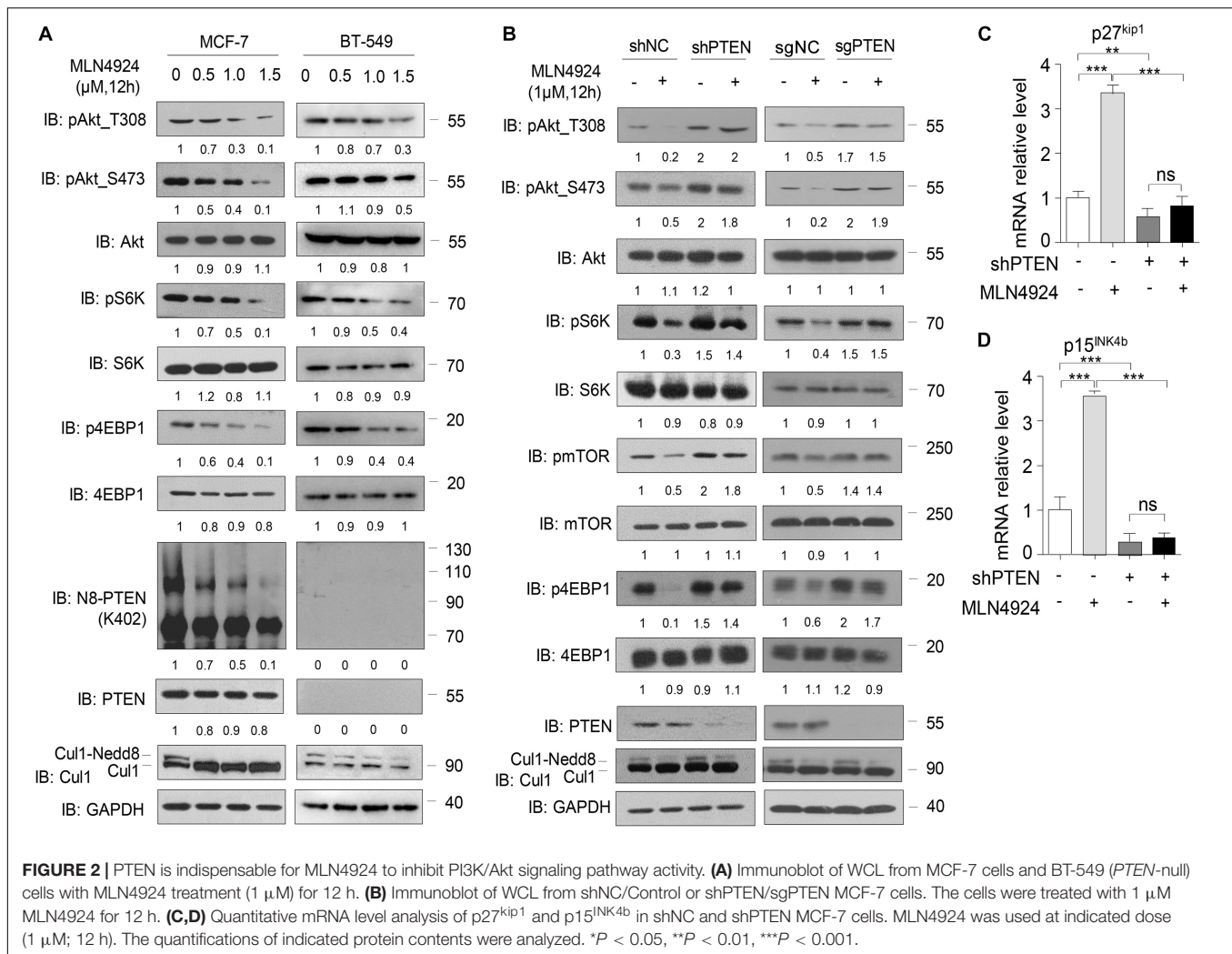


**FIGURE 1 |** MLN4924 inhibits the PI3K/Akt signaling pathway. **(A)** Differentially expressed genes in MCF-7 cells between DMSO and MLN4924 (5  $\mu$ M; 24 h) treatment groups are plotted as a volcano plot. **(B)** Bar charts depict the top ranked pathway analyzed from the KEGG pathway database. Blue (upper) and red (bottom) bars represent counts and significance ( $-\log_{10}$  P-value), respectively. **(C)** Heat map of the downstream target genes of Akt signaling pathway between the DMSO and MLN4924 treatment group. **(D)** The mRNA level of Ccnd1, Bim and p27 were analyzed in Ubc12 knockdown NIH 3T3 cells. The GEO2R online tool was used to analyze differentially expressed genes on GSE14088 microarray. \* $P < 0.05$ , \*\* $P < 0.01$ , \*\*\* $P < 0.001$ . **(E,F)** Enrichment plots of gene expression signatures for PI3K/Akt signaling according to UBA3 mRNA levels by gene set enrichment analysis (GSEA) of TCGA BRCA dataset in PTEN high expression group (NES = 1.33, FDR < 0.05) and PTEN low (with almost undetectable PTEN level) expression group (NES = 1.07, FDR = 0.28), respectively. Samples were divided into high and low UBA3 expression groups. False discovery rate (FDR) gives the estimated probability that a gene set with a given normalized ES (NES) represents a false-positive finding; FDR < 0.05 is a widely accepted cutoff for the identification of biologically significant gene sets. **(G,H)** Enrichment plots of gene expression signatures for PI3K/Akt signaling according to NEDP1 mRNA levels by gene set enrichment analysis (GSEA) of TCGA BRCA dataset in PTEN high expression group (NES = -1.49, FDR < 0.01) and PTEN low (with almost undetectable PTEN level) expression group (NES = -1.14, FDR = 0.2), respectively.

breast cancer cell line BT-549, loss of PTEN negated the inhibitory effects of MLN4924 on PI3K/Akt signaling activity. In BT-549 cells, PTEN neddylation was undetectable under all conditions, and phosphorylation of Akt, S6K, 4EBP1, and

mTOR was not decreased upon treatment with MLN4924 (Figure 2A, right).

Considering the facts that PTEN is a key upstream regulator of PI3K/Akt signaling, and that PTEN is covalently modified with



Nedd8, we intended to further investigate whether MLN4924 regulates PI3K/Akt signaling via PTEN. To that end, we used a lentiviral strategy to establish an MCF-7 cell line with a stable knockdown of endogenous *PTEN* and the Lenti-crispr-cas9 method to create an MCF-7 line with a *PTEN* knockout. As shown in **Figure 2B**, silencing *PTEN* negated the inhibitory effects of MLN4924 on PI3K/Akt signaling activity. MLN4924 lost the ability to decrease the phosphorylation levels of Akt, S6K, 4EBP1, and mTOR in these lines. In addition, treatment of wild type cells with MLN4924 upregulated the Akt downstream genes p27<sup>kip1</sup> and p15<sup>INK4b</sup>, and that effect was weakened when *PTEN* was depleted (**Figures 2C,D**). Hence, we conclude that *PTEN* is essential for inhibition of the activity of the PI3K/Akt signaling pathway by MLN4924.

## Involvement of PTEN in MLN4924-Mediated Inhibition of Breast Cancer Cell Growth and Migration

Next, we evaluated the ability of MLN4924 to reduce cell viability in different breast cancer cell lines. As shown in

**Figure 3A**, MLN4924 showed a marked and dose-dependent reduction of cell viability in MDA-MB-231, MDA-MB-468, and MCF-7 cells. However, in BT-549 cells, which is a *PTEN* deficient cell line, MLN4924 did not indicate marked inhibition effect on cell proliferation. Moreover, MLN4924 clearly reduced clone formation in MDA-MB-231, MDA-MB-468, and MCF-7 cells (**Figures 3B–D**), except for in BT-549 cells (**Figure 3E**). Moreover, MLN4924 inhibited breast cancer cell migration, including MCF-7 cells and MDA-MB-231 cells (**Figures 3F,G**). In BT-549 cells, loss of *PTEN* correlated with an abrogation of the inhibitory effects of MLN4924 on tumor cell invasion (**Figure 3H**). Then, we generated stably transduced MCF-7 breast cancer cells by performing lentiviral transduction with Lenti-shNC (negative control), Lenti-shPTEN. It is worth noting that deletion of *PTEN* from MCF-7 cells abrogated the inhibitory effects of MLN4924 on cell proliferation (**Figures 4A,B**), and tumor invasion (**Figure 4C**). Moreover, we determined that loss of *PTEN* inhibited reduction of anchorage growth and tumor formation by MLN4924 in xenografts (**Figures 4D–G**). Collectively, we conclude that *PTEN* is indispensable for the tumor growth suppression activity of MLN4924.

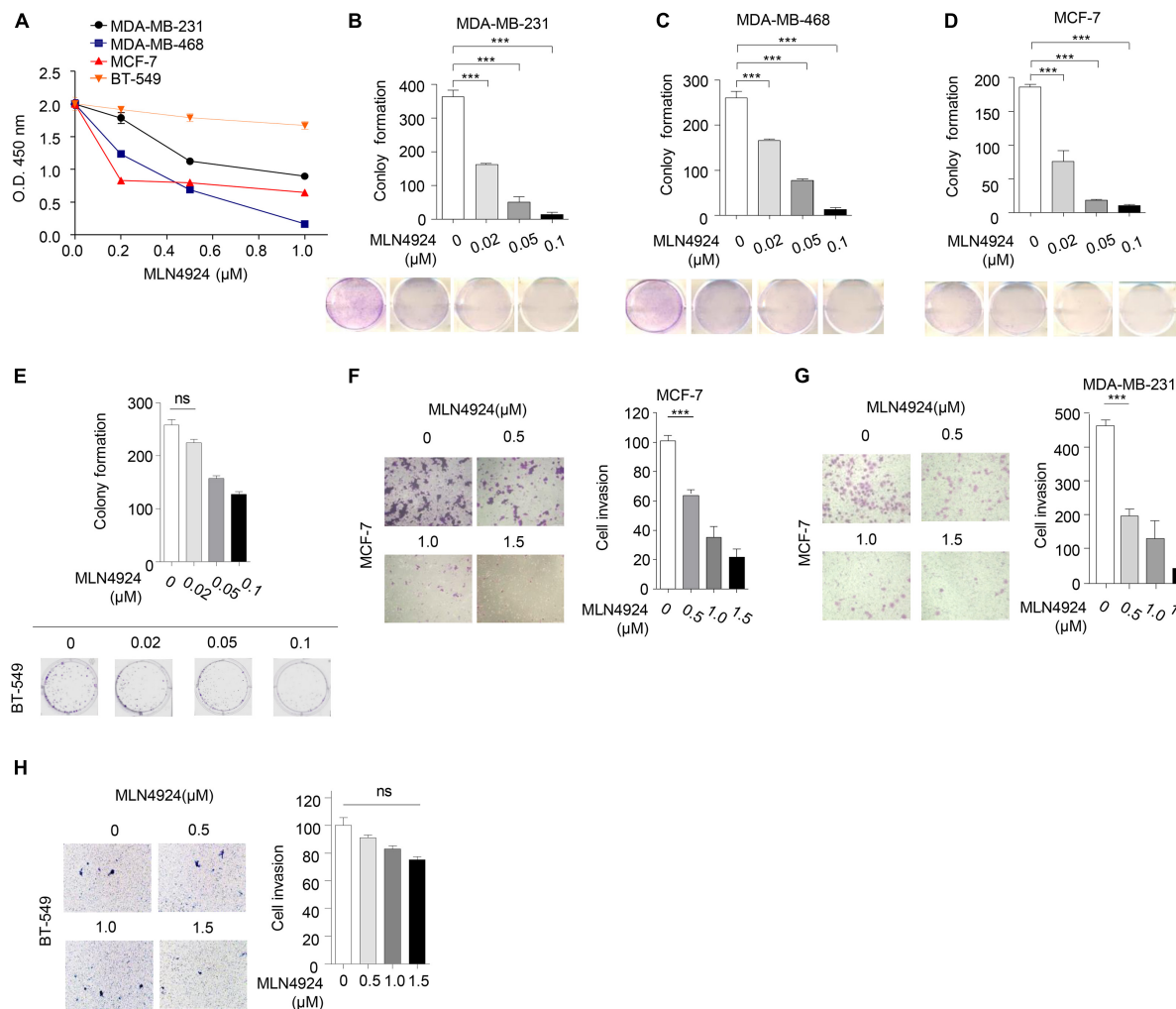


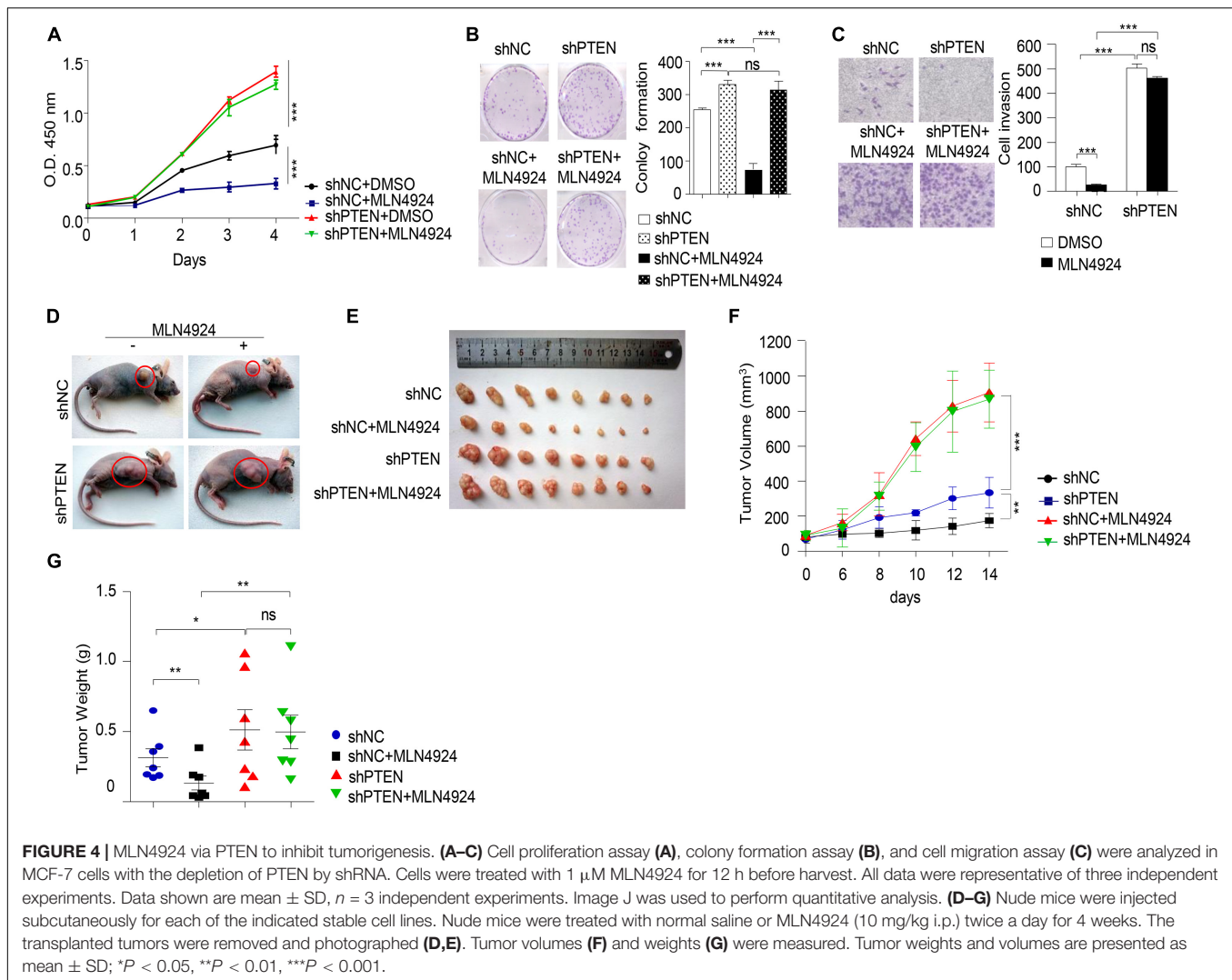
**FIGURE 3 |** Anti-tumor effect of MLN4924 is dependent on PTEN. **(A)** Cells were treated with serial dilutions of MLN4924 for 72 h and cell viability was determined using CCK8 assays. Representative inhibitory curves from three independent experiments are shown for each cell line. **(B–E)** Cells were seeded into 6-well plates petri-dishes at 500 cells per dish in triplicate and treated with MLN4924 for 12 days, followed by 0.01% (w/v) crystal violet staining and colony counting. Representative images of three independent experiments are shown for colony formation. Image J was used to perform quantitative analysis. **(F–H)** Cells were treated with indicated concentrations of MLN4924 for 12 h before being subjected to trans-well migration analysis. Shown are representative images. Image J was used to perform quantitative analysis. Shown are representative images. Image J was used to perform quantitative analysis. Data are shown as the mean  $\pm$  SD. *P*-values were calculated by one-way ANOVA test **(B–H)** and two-way ANOVA test **(A)**. \**P* < 0.05, \*\**P* < 0.01, \*\*\**P* < 0.001.

## 2-DG Decreases PTEN Neddylolation via Downregulating the mRNA Level of UBA3

Co-treatment with the glycolysis inhibitor 2-DG and MLN4924 greatly improves the efficacy of radiotherapy in breast cancer cells (Oladghaffari et al., 2017), suggesting an interplay between glucose metabolism and MLN4924-sensitive neddylolation pathways. Importantly, breast cancer cells, like many other cancers, also exhibit an increased rate of glucose uptake (Martinez-Outschoorn et al., 2017). Our previous study showed that high concentrations of glucose trigger PTEN neddylolation and that neddylolated PTEN subsequently undergoes nuclear import (Xie et al., 2021). PTEN neddylolation is known to promote the progression of breast cancer, thus providing another mechanistic link between glucose uptake and progression, but

the mechanism by which glucose triggers PTEN neddylolation remains unknown.

In the present study, consistent with previous results, PTEN nuclear import increased in a time-dependent manner in the presence of high glucose concentrations (25 mM), but MLN4924 inhibited the accumulation of neddylolated PTEN in the nucleus (**Figure 5A**). An inhibitor of SUMOylation, 2-D08 had no effect on glucose induced PTEN nuclear import (**Figure 5A**). Meanwhile, neddylolated PTEN and the phosphorylation of Akt increased with the addition of glucose in the cell culture, but MLN4924 treatment abolished these effects (**Figure 5B**). Interestingly, we noticed that high glucose concentrations upregulated the protein level of UBA3 and this affect was unaffected by MLN4924 (**Figure 5B**). Then, our results showed



that high glucose concentrations increased the mRNA level of UBA3, but not of the SUMO-activating enzyme SAE1 (Figure 5C). The glycolysis inhibitor, 2-DG, inhibited the expression of UBA3 and Ubc12, but not NAE1, Nedd8, SAE1, UBE1a or UBE2D3 (Figure 5D). The mono-neddylation of Cul1 was also declined under the treatment of 2-DG (Figure 5D). Importantly, we noticed that 2-DG treatment reduced the mRNA level of UBA3, not SAE1 (Figure 5E). Moreover, treatment with 2-DG did not affect the subcellular localization of UBA3, but the expression of UBA3 was reduced (Figure 5F). To investigate whether glucose regulates subcellular location of PTEN by increasing UBA3, we generated *UBA3* knock-out MCF-7 cells using the Crispr-Cas9 method. The result showed that PTEN was markedly retained in the cytoplasm in *UBA3*-deleted cells (Figure 5G). As shown in Figure 5H, 2-DG promotes PTEN nucleus export in a time dependent manner, and treatment with MLN4924 or the deletion of *UBA3* strengthened the accumulation of PTEN in the cytoplasm. Interestingly, the interaction of UBA3 and NAE1 was strengthened under the high glucose concentration (Figure 5I). We noticed that the

formation of UBA3-NAE1 heterodimer was not strengthened under the treatment of CHX, an inhibitor of protein synthesis (Figure 5I). It seems like high glucose concentration triggered the mRNA expression of UBA3, and more UBA3 proteins were produced. Therefore, the enhanced interaction between UBA3-NAE1 is due to increased UBA3 expression rather than changes in protein conformation or activity. Hence, we suggest that glucose triggers PTEN neddylation and nuclear import by upregulating the expression of UBA3 and strengthened the interaction between UBA3-NAE1. However, we could not to rule out the possible change of Ubc12 to promote PTEN neddylation. The precise mechanism of how glucose enhances the expression of Ubc12 also needs further investigation.

## High Concentration of Glucose Inhibits UBA3 Promoter Methylation

Next, we sought to determine the underlying mechanism by which glucose regulates the UBA3 mRNA level. Sequence analyses using the Database of CpG Islands (see text footnote 2)



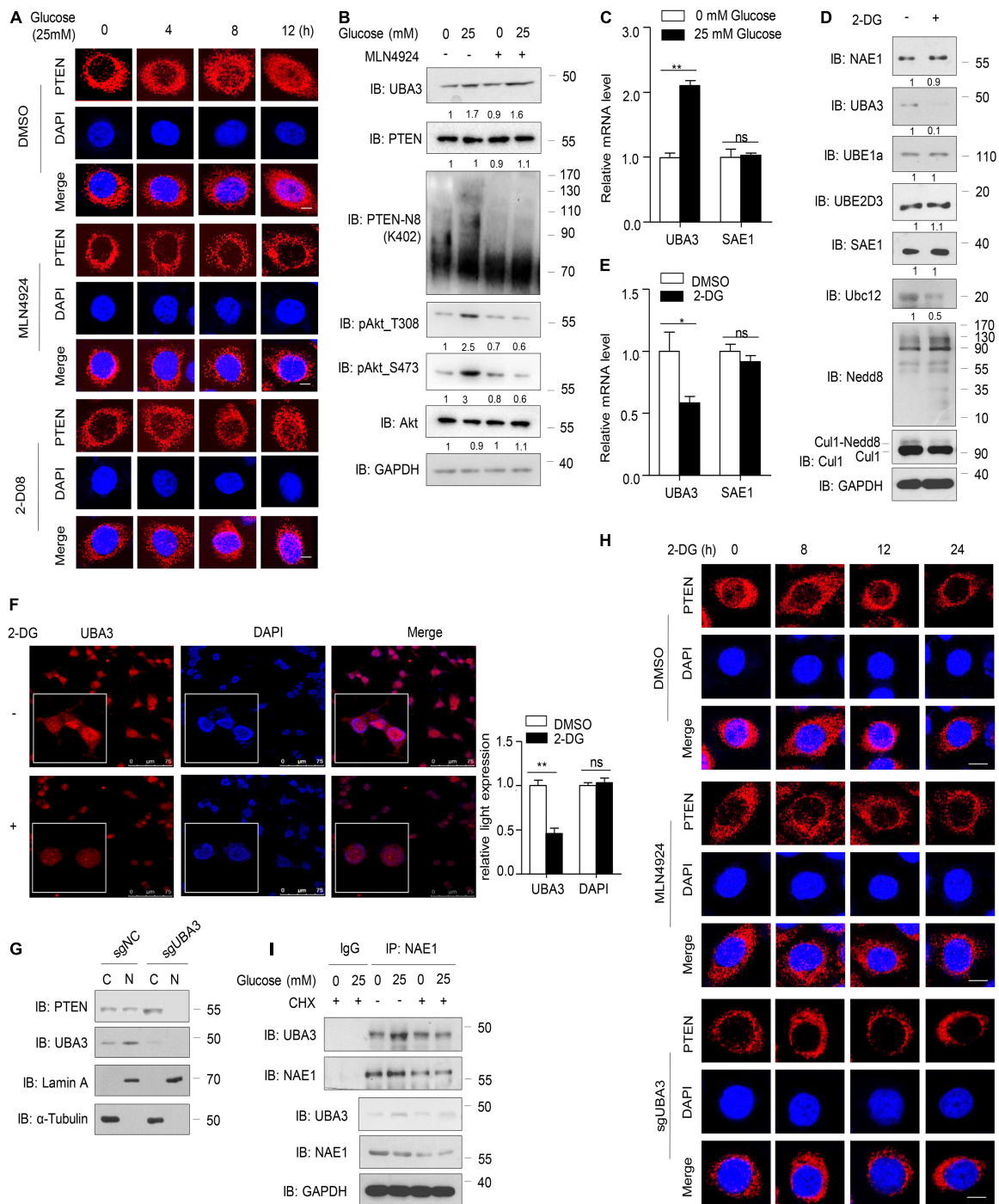


**FIGURE 5 |** High concentration of glucose increases UBA3 expression. **(A)** Immunofluorescence of endogenous PTEN in MCF-7 cells. Cells were deprived for glucose for 12 h followed by glucose stimulation (25 mM) for different time. Cells were treated with DMSO, MLN4924 (1  $\mu$ M; 12 h) or 2-D08 (5 mM; 24 h) before harvested, respectively. Scale bar, 25  $\mu$ m. **(B)** Immunoblot of WCL from MCF-7 cells cultured in cell medium containing different glucose concentrations. The cells were treated with DMSO or 1  $\mu$ M MLN4924 for 12 h. The quantifications of indicated protein contents were analyzed. **(C)** UBA3 and SAE1 mRNA levels were analyzed by qPCR in MCF-7 cells cultured in different glucose concentrations. \* $P$  < 0.05, \*\* $P$  < 0.01, \*\*\* $P$  < 0.001. **(D)** Immunoblot analysis of WCL from MCF-7 cells. MCF-7 cells were treated without or with 2-DG (5 mM, 24 h) before harvested. The quantifications of indicated protein contents were analyzed. **(E)** UBA3 and SAE1 mRNA levels were analyzed by qPCR in MCF-7 cells with or without 2-DG (5 mM; 72 h) treatment. Data are shown as the mean  $\pm$  SD. \* $P$  < 0.05, \*\* $P$  < 0.01, \*\*\* $P$  < 0.001. **(F)** Immunofluorescence of UBA3 in MCF-7 cells with or without 2-DG (5 mM, 24 h) treatment. Scale bar, 75  $\mu$ m. The quantifications of indicated protein expression were analyzed. \* $P$  < 0.05, \*\* $P$  < 0.01, \*\*\* $P$  < 0.001. **(G)** Cell fractionation assay of PTEN in UBA3 knockout MCF-7 stable cells. **(H)** Immunofluorescent assay of PTEN in MCF-7 or UBA3 knockout MCF-7 cells. Cells were deprived for glucose for 12 h followed by glucose stimulation (25 mM) for different time. MCF-7 cells were treated without or with 1  $\mu$ M of MLN4924 for 12 h. Scale bar, 25  $\mu$ m. **(I)** Co-IP of interaction between UBA3 and NAE1 in MCF-7 cells. Anti-UBA3 immunoprecipitants were analyzed by western blotting with anti-NAE1 antibodies. Cells were deprived of glucose and followed by glucose stimulation (25 mM). Cells were treated with 100 ng/ml of CHX for 6 h.

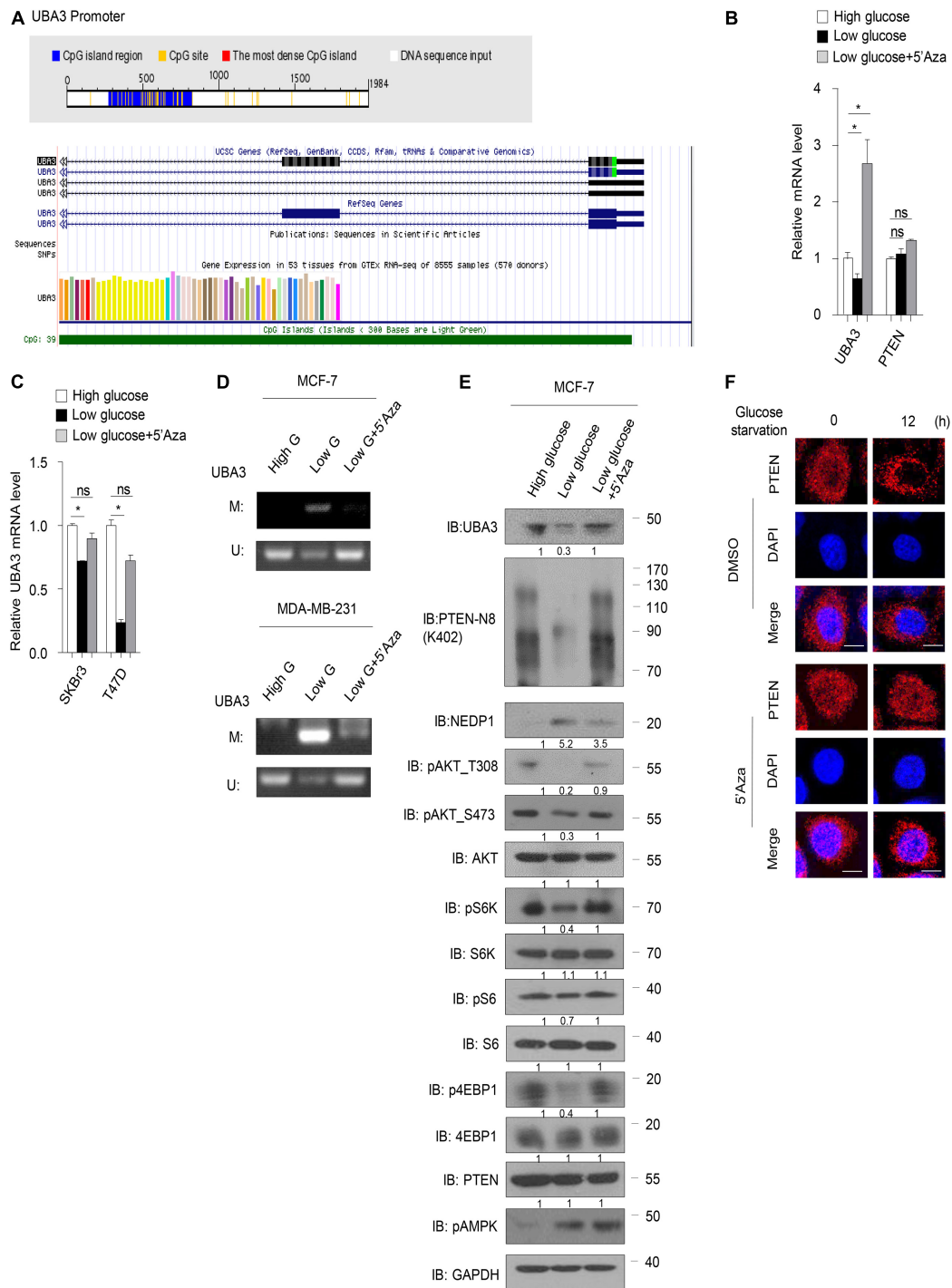
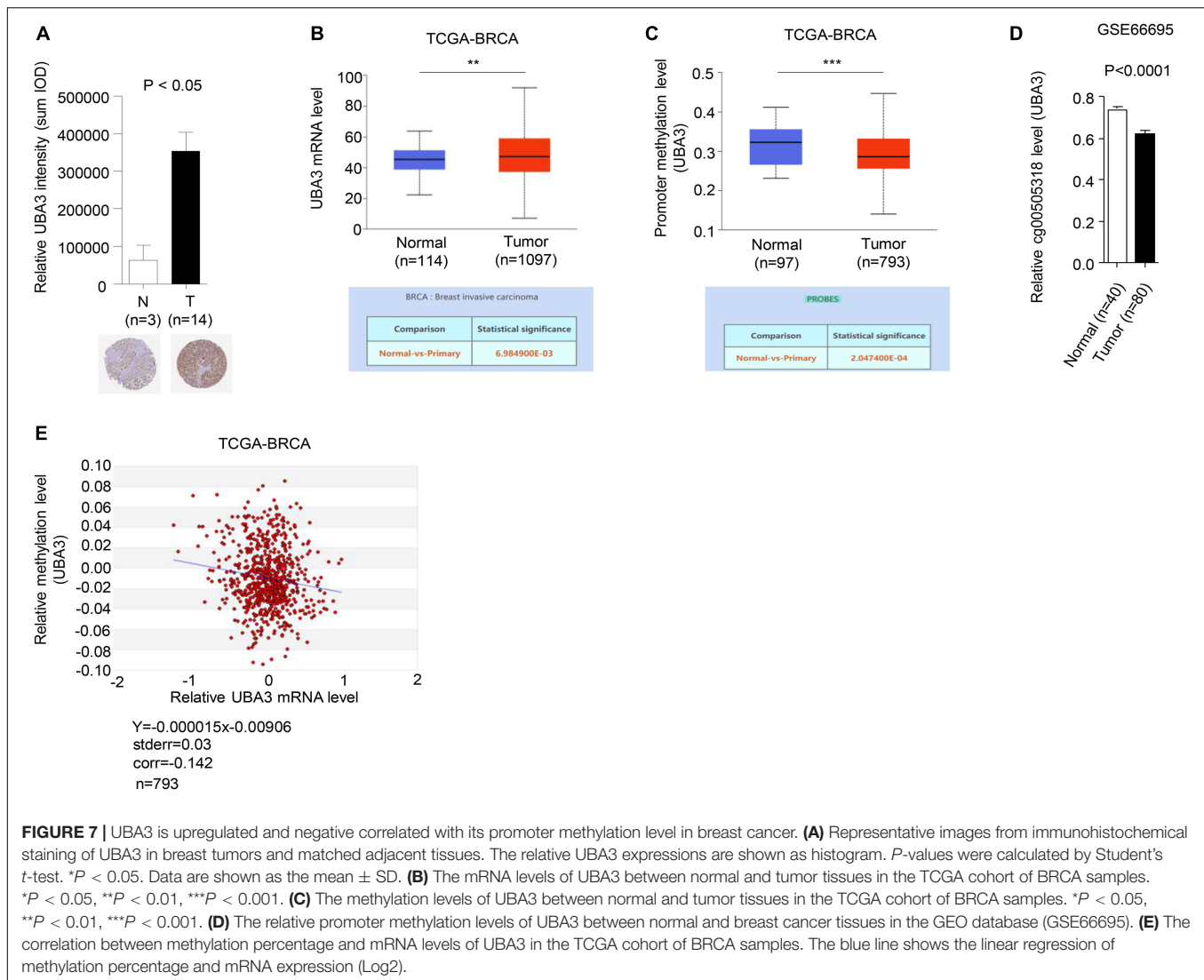


**FIGURE 6 |** High concentration of glucose inhibits UBA3 promoter methylation. **(A)** The CpG Island within the UBA3 gene promoter region (upstream 2000bp of the UBA3). Blue line depicts the CpG island region and the yellow vertical bars represent a CpG site. White line depicts the DNA sequence (Top). The green line indicates the CpG Island of UBA3 in UCSC database (Bottom). **(B)** UBA3, NEDP1, PTEN expression was analyzed by qPCR in MCF-7 cells (high glucose, 25  $\mu$ M; low glucose, 5  $\mu$ M), without or with 5-Aza-2'-deoxycytidine (5'Aza) treatment. Cells were treated with 5 mM 5'Aza for 72 h, and the medium was replaced with freshly added 5'Aza for every 24 h. Data are shown as the mean  $\pm$  SD. \* $P$  < 0.05, \*\* $P$  < 0.01, \*\*\* $P$  < 0.001. **(C)** UBA3 mRNA level was analyzed by qPCR in breast cancer cell lines. Data are shown as the mean  $\pm$  SD. \* $P$  < 0.05, \*\* $P$  < 0.01, \*\*\* $P$  < 0.001. **(D)** The methylation status of the UBA3 promoter in breast cancer cell lines medium containing different glucose concentrations, without or with 5'Aza treatment. The CpG islands of UBA3 were analyzed by methylation-specific PCR (MSP). U, unmethylated; M, methylated. **(E)** Immunoblot analysis of WCL from MCF-7 cells cultured in cell medium containing different glucose concentrations, without or with 5'Aza treatment. The quantifications of indicated protein contents were analyzed. **(F)** Immunofluorescence of PTEN in MCF-7 cells. Cells were deprived for glucose for different time. Cells were treated without or with 1  $\mu$ M 5'Aza for 12 h. Scale bar, 25  $\mu$ m.



and the University of California, Santa Cruz Genome Browser database (see text footnote 3) revealed that a CpG island is located within the UBA3 promoter region (Figure 6A). Low glucose reduced the mRNA level of UBA3 in breast cancer cells (Figure 6B). However, treatment with 5-azacytidine (5'Aza), a DNA methylation inhibitor, reversed that effect. As a comparison, PTEN was not affected by lowering the glucose concentration or by the 5'Aza treatment. Similar results were found in other breast cancer cells (Figure 6C). Then we performed a methylation-specific PCR assay to clarify whether glucose regulates the UBA3 promoter methylation in breast cancer cells. The data indicated that UBA3 promoter methylation was increased under low glucose concentrations and that 5'Aza treatment reversed this trend (Figure 6D). Moreover, lowering glucose concentrations correlated with lower UBA3 protein levels, PTEN neddylation levels and the Akt/mTOR signaling pathway activity (Figure 6E). Glucose starvation-induced PTEN nuclear export was abolished by 5'Aza treatment (Figure 6F). Taken together, our data suggest that

high glucose concentrations might increase UBA3 mRNA and promote PTEN neddylation via inhibition of methylation of the UBA3 promoter.

### UBA3 Expression Is Negative Correlated With Hypomethylation of Upstream CpG-Island in Breast Cancer

To further investigate the relevance of the connections between promoter methylation and transcriptional activity of UBA3 in breast cancer, the expression and promoter methylation levels of UBA3 were analyzed in the Human Protein Atlas, the database of the Cancer Genome Atlas Program of the National Cancer Institute (CGAP), and the Gene Expression Omnibus (GEO) database. The expression of UBA3 was found to be upregulated in tumor tissues relative to adjacent normal tissues (Figures 7A,B). Conversely, promoter methylation of UBA3 is downregulated in breast cancer (Figures 7C,D). A correlation assay between methylation and mRNA level of UBA3 was also performed

utilizing the MethHC database. A linear regression demonstrated that UBA3 mRNA levels are negatively correlated with promoter methylation levels (**Figure 7E**). These data demonstrate that promoter hypomethylation results in UBA3 overexpression in breast cancer.

## DISCUSSION

Neddylation is necessary for development, and overactivation of neddylation often leads to tumorigenesis (Huang et al., 2009; Zhou et al., 2018, 2019). MLN4924 is an effective small molecule inhibitor of NEDD8-activating enzyme E1, and this molecule has been evaluated in a series of phase 1, 2, and 3 clinical trials for oncotherapy (Soucy et al., 2009; Zhou and Jia, 2020). Recently, PTEN, a well-known tumor suppressor, was identified as a novel target for modification with NEDD8, and PTEN neddylation has been associated with tumor development in all types of breast cancers (Xie et al., 2021). PTEN loss of function is one of the most common events observed in multiple cancers (Hollander et al., 2011), and we previously reported that neddylation is a key regulatory mechanism that leads to loss of the tumor-suppressive function of PTEN and activation of Akt signaling pathways. Meanwhile, PTEN expression is often associated with anti-tumor drug resistance (Wein and Loi, 2017). Thus, we hypothesized that PTEN status might affect the anti-tumor effectiveness of MLN4924.

In this study, we found that MLN4924 strongly inhibits the PI3K/Akt signaling pathway in breast cancer. The neddylation pathway is positively correlated with Akt signaling pathway activity in patients with high PTEN expression but not in low expression patients according to the Cancer Genome Atlas Breast Invasive Carcinoma dataset. Moreover, PTEN loss abolished the anti-tumor and Akt signaling inhibitory effects of MLN4924. These data imply that PTEN neddylation may be the crucial therapeutic target of MLN4924 in breast cancer. Taken together, PTEN loss may act as a driver of MLN4924 resistance in breast cancer, and this study may thus provide a more focused treatment strategy.

Neddylation affects numerous important biological processes, such as cell cycle progression (Jia et al., 2011; Luo et al., 2012; Mackintosh et al., 2013; Yao et al., 2014; Chen et al., 2016). Cullins have been reported as major substrates for neddylation, but a growing number of non-Cullin targets of Nedd8 have also been identified, including p53, Smurf1 and PTEN (Xirodimas et al., 2004; Xie et al., 2014, 2021). Although the promotion of tumor growth by neddylation has been established, mechanisms by which neddylation promotes tumorigenesis are still poorly understood. More importantly, the physiological conditions leading to neddylation pathway activation remain unclear.

Recently, we reported that high glucose triggers UBA3 upregulation and downstream PTEN neddylation in breast cancer (Xie et al., 2021). In the present report, we found that high glucose increased UBA3 mRNA levels by inhibiting UBA3 promoter methylation in breast cancer cells. High glucose concentration triggered the expression of UBA3 and enhanced the formation of heterodimer with NAE1. Once the cells were

treated with CHX, the interaction between UBA3-NAE1 could not increase even under the high glucose concentration, which indicated that the strengthened UBA3-NAE1 heterodimer was due to increased UBA3 expression rather than changes in protein conformation or activity. Moreover, the mRNA level of UBA3 is negatively correlated with UBA3 promoter methylation level in breast cancer patients. A previous study showed that high glucose triggers cytoplasmic translocation of a key DNA methylase, DNMT3A, and reduces the level of DNA promoter methylation (Zhang et al., 2016). DNMT3A is essential for genome regulation and development and has been associated with tumorigenesis, and structural studies have indicated an enzymatic preference of DNMT3A for CpG sites of target genes (Zhang et al., 2018). Therefore, we conjecture that glucose may upregulate via promoter hypomethylation UBA3 induced by cytoplasmic translocation of DNMT3A; this proposed mechanism calls for additional study.

## CONCLUSION

In conclusion, these results in this work support a mechanism in which high concentrations of glucose activate a neddylation pathway via downregulation of UBA3 promoter methylation, and this mechanism may be closely correlate with the overactivation of the neddylation pathway in cancers. In addition, to our knowledge, this is the first report on physiological conditions leading to neddylation activation. We also demonstrate that targeting the neddylation pathway is an attractive therapeutic approach for breast cancer patients with PTEN expression. Our findings provide insight into the clinical significance of MLN4924 precision therapies in breast cancer, and PTEN neddylation may be a useful marker to guide MLN4924 therapy for breast cancer in the future.

## DATA AVAILABILITY STATEMENT

The original contributions presented in the study are publicly available. This data can be found here: <https://www.ncbi.nlm.nih.gov/sra/PRJNA723112>; accession number: PRJNA723112.

## ETHICS STATEMENT

The animal study was reviewed and approved by the Institutional Animal Care and Use Committee (IACUC) at the Beijing Institute of Lifeomics.

## AUTHOR CONTRIBUTIONS

PX, MD, ZP, WG, FL, WL, YC, HL, XZ, and CL performed the experiments. PX and HJ designed the experiments and analyzed the data. PX, ZP, WG, and MD co-wrote the manuscript. PX, LZ, and HJ conceived the idea and supervised the study. All authors contributed to the article and approved the submitted version.



## FUNDING

This work was jointly supported by the Chinese National Natural Science Foundation Project (Grant No. 31971229), Open Project Program of the State Key Laboratory of Proteomics (Grant No. SKLP-O201901), Beijing excellent talents training project, Chinese National Natural Science Foundation Project (Grant No. 31771110), Shandong Province Natural Science Foundation (Grant No. ZR2019ZD31), and Taishan Scholars Construction

## REFERENCES

- Abidi, N., and Xirodimas, D. P. (2015). Regulation of cancer-related pathways by protein NEDDylation and strategies for the use of NEDD8 inhibitors in the clinic. *Endocr. Relat. Cancer* 22, T55–T70. doi: 10.1530/ERC-14-0315
- Chen, P., Hu, T., Liang, Y., Li, P., Chen, X., Zhang, J., et al. (2016). Neddylation inhibition activates the extrinsic apoptosis pathway through ATF4-CHOP-DR5 axis in human esophageal Cancer cells. *Clin. Cancer Res.* 22, 4145–4157. doi: 10.1158/1078-0432.CCR-15-2254
- Chen, X., Cui, D., Bi, Y., Shu, J., Xiong, X., and Zhao, Y. (2018). AKT inhibitor MK-2206 sensitizes breast cancer cells to MLN4924, a first-in-class NEDD8-activating enzyme (NAE) inhibitor. *Cell. Cycle* 17, 2069–2079. doi: 10.1080/15384101.2018.1515550
- Chen, Y., Du, M., Yusuying, S., Liu, W., Tan, Y., and Xie, P. (2020). Nedd8-activating enzyme inhibitor MLN4924 (Pevonedistat), inhibits miR-1303 to suppress human breast cancer cell proliferation via targeting p27(Kip1). *Exp. Cell. Res.* 392:112038. doi: 10.1016/j.yexcr.2020.112038
- Cope, G. A., Suh, G. S., Aravind, L., Schwarz, S. E., Zipursky, S. L., Koonin, E. V., et al. (2002). Role of predicted metalloprotease motif of Jab1/Csn5 in cleavage of Nedd8 from Cul1. *Science* 298, 608–611. doi: 10.1126/science.1075901
- Costa, C., Wang, Y., Ly, A., Hosono, Y., Murchie, E., Walmsley, C. S., et al. (2020). PTEN loss mediates clinical cross-resistance to CDK4/6 and PI3K $\alpha$  inhibitors in Breast Cancer. *Cancer. Discov.* 10, 72–85. doi: 10.1158/2159-8290.CD-18-0830
- Di Cristofano, A., Pesce, B., Cordon-Cardo, C., and Pandolfi, P. P. (1998). Pten is essential for embryonic development and tumour suppression. *Nat. Genet.* 19, 348–355. doi: 10.1038/1235
- Enchev, R. I., Schulman, B. A., and Peter, M. (2015). Protein neddylation: beyond cullin-RING ligases. *Nat. Rev. Mol. Cell. Biol.* 16, 30–44. doi: 10.1038/nrm3919
- Hanker, A. B., Sudhan, D. R., and Arteaga, C. L. (2020). Overcoming endocrine resistance in Breast Cancer. *Cancer Cell* 37, 496–513. doi: 10.1016/j.ccell.2020.03.009
- Hollander, M. C., Blumenthal, G. M., and Dennis, P. A. (2011). PTEN loss in the continuum of common cancers, rare syndromes and mouse models. *Nat. Rev. Cancer* 11, 289–301. doi: 10.1038/nrc3037
- Huang, D. T., Ayrault, O., Hunt, H. W., Taherbhoy, A. M., Duda, D. M., Scott, D. C., et al. (2009). E2-RING expansion of the NEDD8 cascade confers specificity to cullin modification. *Mol. Cell* 33, 483–495. doi: 10.1016/j.molcel.2009.01.011
- Jia, L., Li, H., and Sun, Y. (2011). Induction of p21-dependent senescence by an NAE inhibitor, MLN4924, as a mechanism of growth suppression. *Neoplasia* 13, 561–569. doi: 10.1593/neo.11420
- Liu, L., Xie, P., Li, W., Wu, Y., and An, W. (2019). Augmenter of liver regeneration protects against ethanol-induced acute liver injury by promoting autophagy. *Am. J. Pathol.* 189, 552–567. doi: 10.1016/j.ajpath.2018.11.006
- Luo, Z., Yu, G., Lee, H. W., Li, L., Wang, L., Yang, D., et al. (2012). The Nedd8-activating enzyme inhibitor MLN4924 induces autophagy and apoptosis to suppress live-r cancer cell growth. *Cancer Res.* 72, 3360–3371. doi: 10.1158/0008-5472.CAN-12-0388
- Mackintosh, C., García-Domínguez, D. J., Ordóñez, J. L., Ginel-Picardo, A., Smith, P. G., Sacristán, M. P., et al. (2013). WEE1 accumulation and deregulation of S-phase proteins mediate MLN4924 potent inhibitory effect on ewing sarcoma cells. *Oncogene* 32, 1441–1451. doi: 10.1038/onc.2012.153
- Martinez-Outschoorn, U. E., Peiris-Pagés, M., Pestell, R. G., Sotgia, F., and Lisanti, M. P. (2017). Cancer metabolism: a therapeutic perspective. *Nat. Rev. Clin. Oncol.* 14, 11–31. doi: 10.1038/nrclinonc.2016.60
- Mendoza, H. M., Shen, L. N., Botting, C., Lewis, A., Chen, J., Ink, B., et al. (2003). NEDP1, a highly conserved cysteine protease that deNEDDylates Cullins. *J. Biol. Chem.* 278, 25637–25643. doi: 10.1074/jbc.M212948200
- Naik, S. K., Lam, E. W., Parija, M., Prakash, S., Jiramongkol, Y., Adhya, A. K., et al. (2020). NEDDylation negatively regulates ERR $\beta$  expression to promote breast cancer tumorigenesis and progression. *Cell. Death. Dis.* 11:703. doi: 10.1038/s41419-020-02838-7
- Nawrocki, S. T., Griffin, P., Kelly, K. R., and Carew, J. S. (2012). MLN4924: a novel first-in-class inhibitor of NEDD8-activating enzyme for cancer therapy. *Expert. Opin. Investig. Drugs* 21, 1563–1573. doi: 10.1517/13543784.2012.707192
- Nawrocki, S. T., Kelly, K. R., Smith, P. G., Espitia, C. M., Possemato, A., Beausoleil, S. A., et al. (2013). Disrupting protein NEDDylation with MLN4924 is a novel strategy to target cisplatin resistance in ovarian cancer. *Clin. Cancer Res.* 19, 3577–3590. doi: 10.1158/1078-0432.CCR-12-3212
- Oladghaffari, M., Shabestani, M. A., Farajollahi, A., Baradaran, B., Mohammadi, M., Shانهbandi, D., et al. (2017). MLN4924 and 2DG combined treatment enhances the efficiency of radiotherapy in breast cancer cells. *Int. J. Radiat. Biol.* 93, 590–599. doi: 10.1080/09553002.2017.1294272
- Perren, A., Weng, L. P., Boag, A. H., Ziebold, U., Thakore, K., Dahia, P. L., et al. (1999). Immunohistochemical evidence of loss of PTEN expression in primary ductal adenocarcinomas of the breast. *Am. J. Pathol.* 155, 1253–1260. doi: 10.1016/S0002-9440(10)65227-3
- Song, M. S., Salmena, L., and Pandolfi, P. P. (2012). The functions and regulation of the PTEN tumour suppressor. *Nat. Rev. Mol. Cell. Biol.* 13, 283–296. doi: 10.1038/nrm3330
- Soucy, T. A., Smith, P. G., Milhollen, M. A., Berger, A. J., Gavin, J. M., Adhikari, S., et al. (2009). An inhibitor of NEDD8-activating enzyme as a new approach to treat cancer. *Nature* 458, 732–736. doi: 10.1038/nature07884
- Stambolic, V., Suzuki, A., de la Pompa, J. L., Brothers, G. M., Mirtsos, C., Sasaki, T., et al. (1998). Negative regulation of PKB/Akt-dependent cell survival by the tumor suppressor PTEN. *Cell* 95, 29–39. doi: 10.1016/s0092-8674(00)81780-8
- Swords, R. T., Coutre, S., Maris, M. B., Zeidner, J. F., Foran, J. M., Cruz, J., et al. (2018). Pevonedistat, a first-in-class NEDD8-activating enzyme inhibitor, combined with azacitidine in patients with AML. *Blood* 131, 1415–1424. doi: 10.1182/blood-2017-09-805895
- Waks, A. G., and Winer, E. P. (2019). Breast Cancer treatment: a review. *JAMA* 321, 288–300. doi: 10.1001/jama.2018.19323
- Wan, J., Zhu, J., Li, G., and Zhang, Z. (2016). Radiosensitization of human colorectal cancer cells by MLN4924: an inhibitor of NEDD8-Activating enzyme. *Technol. Cancer Res. Treat.* 15, 527–534. doi: 10.1177/1533034615588197
- Wang, M., Medeiros, B. C., Erba, H. P., DeAngelo, D. J., Giles, F. J., Swords, R. T., et al. (2011). Targeting protein neddylation: a novel therapeutic strategy for the treatment of cancer. *Expert. Opin. Ther. Targets* 15, 253–264. doi: 10.1517/14728222.2011.550877
- Wang, X., Zhang, W., Yan, Z., Liang, Y., Li, L., Yu, X., et al. (2016). Radiosensitization by the investigational NEDD8-activating enzyme inhibitor MLN4924 (pevonedistat) in hormone-resistant prostate cancer cells. *Oncotarget* 7, 38380–38391. doi: 10.18632/oncotarget.9526
- Wei, D., Li, H., Yu, J., Sebolt, J. T., Zhao, L., Lawrence, T. S., et al. (2012). Radiosensitization of human pancreatic cancer cells by MLN4924, an investigational NEDD8-activating enzyme inhibitor. *Cancer Res.* 72, 282–293. doi: 10.1158/0008-5472.CAN-11-2866
- Wein, L., and Loi, S. (2017). Mechanisms of resistance of chemotherapy in early-stage triple negative breast cancer (TNBC). *Breast* 34(Suppl. 1), S27–S30. doi: 10.1016/j.breast.2017.06.023

Project and Innovative Research Team of High-Level Local Universities in Shanghai.

## SUPPLEMENTARY MATERIAL

The Supplementary Material for this article can be found online at: <https://www.frontiersin.org/articles/10.3389/fcell.2021.667435/full#supplementary-material>

- Xie, P., Peng, Z., Chen, Y., Li, H., Du, M., Tan, Y., et al. (2021). Neddylation of PTEN regulates its nuclear import and promotes tumor development. *Cell. Res.* 31, 291–311. doi: 10.1038/s41422-020-00443-z
- Xie, P., Zhang, M. H., He, S., Lu, K. F., Chen, Y. H., Xing, G. C., et al. (2014). The covalent modifier Nedd8 is critical for the activation of Smurf1 ubiquitin ligase in tumorigenesis. *Nat. Commun.* 5:3733. doi: 10.1038/ncomms4733
- Xirodimas, D. P., Saville, M. K., Bourdon, J. C., Hay, R. T., and Lane, D. P. (2004). Mdm2-mediated NEDD8 conjugation of p53 inhibits its transcriptional activity. *Cell* 118, 83–97. doi: 10.1016/j.cell.2004.06.016
- Yao, W. T., Wu, J. F., Yu, G. Y., Wang, R., Wang, K., Li, L. H., et al. (2014). Suppression of tumor angiogenesis by targeting the protein neddylation pathway. *Cell. Death. Dis.* 5:e1059. doi: 10.1038/cddis.2014.21
- Zhang, H., Li, A., Zhang, W., Huang, Z., Wang, J., and Yi, B. (2016). High glucose-induced cytoplasmic translocation of Dnmt3a contributes to CTGF hypo-methylation in mesangial cells. *Biosci. Rep.* 36:e00362. doi: 10.1042/BSR20160141
- Zhang, Z. M., Lu, R., Wang, P., Yu, Y., Chen, D., Gao, L., et al. (2018). Structural basis for DNMT3A-mediated de novo DNA methylation. *Nature* 554, 387–391. doi: 10.1038/nature25477
- Zhou, L., and Jia, L. (2020). Targeting protein neddylation for cancer therapy. *Adv. Exp. Med. Biol.* 1217, 297–315. doi: 10.1007/978-981-15-1025-0\_18
- Zhou, L., Jiang, Y., Luo, Q., Li, L., and Jia, L. (2019). Neddylation: a novel modulator of the tumor microenvironment. *Mol. Cancer* 18, 77. doi: 10.1186/s12943-019-0979-1
- Zhou, L., Zhang, W., Sun, Y., and Jia, L. (2018). Protein neddylation and its alterations in human cancers for targeted therapy. *Cell. Signal.* 44, 92–102. doi: 10.1016/j.cellsig.2018.01.009

**Conflict of Interest:** The authors declare that the research was conducted in the absence of any commercial or financial relationships that could be construed as a potential conflict of interest.

Copyright © 2021 Du, Peng, Gai, Liu, Liu, Chen, Li, Zhang, Liu, Zhang, Jiang and Xie. This is an open-access article distributed under the terms of the Creative Commons Attribution License (CC BY). The use, distribution or reproduction in other forums is permitted, provided the original author(s) and the copyright owner(s) are credited and that the original publication in this journal is cited, in accordance with accepted academic practice. No use, distribution or reproduction is permitted which does not comply with these terms.



# Ubiquitin Modification Patterns of Clear Cell Renal Cell Carcinoma and the Ubiquitin Score to Aid Immunotherapy and Targeted Therapy

## OPEN ACCESS

### Edited by:

Daming Gao,

Shanghai Institute of Biochemistry  
and Cell Biology, Chinese Academy  
of Sciences (CAS), China

### Reviewed by:

Hu Zhou,

Shanghai Institute of Materia Medica,  
Chinese Academy of Sciences, China

Yongbin Chen,

Key Laboratory of Animal Models  
and Human Disease Mechanisms,  
Kunming Institute of Zoology (CAS),  
China

Huadong Pei,

The George Washington University,  
United States

### \*Correspondence:

Jia Hu

Jiahutjm@163.com

Shaogang Wang

sgwangtjm@163.com

### Specialty section:

This article was submitted to  
Cell Growth and Division,  
a section of the journal  
*Frontiers in Cell and Developmental  
Biology*

**Received:** 27 January 2021

**Accepted:** 08 April 2021

**Published:** 13 May 2021

### Citation:

Zhou P, Lu Y, Xun Y, Xu J, Liu C,  
Xia Q, Lu J, Wang S and Hu J (2021)  
Ubiquitin Modification Patterns  
of Clear Cell Renal Cell Carcinoma  
and the Ubiquitin Score to Aid  
Immunotherapy and Targeted  
Therapy.  
*Front. Cell Dev. Biol.* 9:659294.  
doi: 10.3389/fcell.2021.659294

**Peng Zhou, Yuchao Lu, Yang Xun, Jinzhou Xu, Chenqian Liu, Qidong Xia, Junlin Lu, Shaogang Wang\* and Jia Hu\***

Department of Urology, Tongji Hospital, Tongji Medical College, Huazhong University of Science and Technology, Wuhan, China

Ubiquitin modification is the most common protein post-translational modification (PTM) process in organisms, and 1332 ubiquitin regulators have been identified in humans. Ubiquitin regulators, especially E3 ligases and deubiquitinases, are widely involved in immune processes. This study aims to explore the ubiquitin modification features of clear cell renal cell carcinoma (ccRCC) and to elucidate the role of such ubiquitin modifications in shaping anti-tumor immunity and individual benefits from immune checkpoint blockade (ICB). A comprehensive analysis was performed in the TCGA cohort ( $n = 530$ ) and GEO cohort ( $n = 682$ ). RNA sequencing data of 758 differentially expressed regulators, which was validated by the proteomics data, was used for k-means unsupervised consensus clustering and three ubiquitin patterns of ccRCC were identified. Then, we focused on the ubiquitin modification and tumor progression signatures, immune infiltration characteristics, and prognostic value. The three patterns with different ubiquitin modification signatures correspond to “immune desert phenotype,” “immune resistance phenotype,” and “immune-inflammatory phenotype,” respectively. To facilitate clinical application, we constructed a ubiquitin score to evaluate individual patients’ ubiquitination outcome, and it was demonstrated to be an independent risk factor for overall survival (OS) in multivariate Cox analysis. It was found that the high score group was correlated to higher immune cells infiltrating level and PD-1/PD-L1/CTLA-4 expression. More importantly, we found that the high score group was predicted to be sensitive to anti-PD-1 treatment, while the low-score group showed lower predicted IC50 values in treatment with Pazopanib and Axitinib. In summary, this study elucidated the potential link between ubiquitin modification and immune infiltration landscape of ccRCC for the first time and provided a new assessment protocol for the precise selection of treatment strategies for patients with advanced ccRCC.

**Keywords:** ubiquitin code, unsupervised consensus clustering, clear-cell renal-cell carcinoma, immune signature, immune checkpoint blockade, targeted therapy

## INTRODUCTION

Ubiquitin is a 76-amino acid small molecule protein that is highly conserved in sequence. The most common ubiquitination modification is sequentially catalyzed by ubiquitin-activating enzymes (E1s), ubiquitin-conjugating enzymes (E2s), and ubiquitin protein-ligases (E3s) (Kerscher et al., 2006). Ubiquitin itself can continue to bind ubiquitin molecules at multiple residues (i.e., K6, K11, K27, K29, K33, K48, K63, and Met1), thus forming complex structured ubiquitin chains on the substrates, known as the “ubiquitin code.” Besides, the ubiquitin-binding domain-containing protein (UBD) (Husnjak and Dikic, 2012), proteins containing ubiquitin-like domains (ULDs) (Upadhyay and Hegde, 2003), and deubiquitinases (DUBs) (Nijman et al., 2005; Reyes-Turcu et al., 2009) act as “deciphers” of the “ubiquitin code” and negative regulators of this process. Accelerating evidence has shown that the dysregulation of the ubiquitin system plays a critical role in a variety of diseases, such as DNA repair damage, cellular autophagy, neurodegenerative pathologies, autoimmune diseases, and malignancies (Schwertman et al., 2016; Seeler and Dejean, 2017; Grumati and Dikic, 2018; Rape, 2018).

The expression of immune checkpoint molecules and the maturation of immune cells were regulated by the ubiquitin system. Meng et al. (2018) identified Lys48-linked polyubiquitination as the first post-translational modification (PTM) process of PD-1 and FBX038 as the mediator of the process. Lim et al. (2016) identified CSN5 as a DUB that inhibits the PD-L1 degradation. Blocking CSN5 with curcumin attenuated this inhibition and sensitized the cells to anti-CTLA4 treatment. Another study on triple-negative breast cancer (TNBC) identified  $\beta$ -TrCP as an E3 ligase participating in the poly-ubiquitination modification of PD-L1 (Li et al., 2016). Zhang et al. (2018) demonstrated that CDK4/6 degrades PD-L1 via Cullin3-SPOP E3 ligase in prostate cancer and the nonsense mutations of SPOP resulted in elevated PD-L1 expression level. Similar ubiquitin modification regulation was also found in the PTM process of LAG-3, CTLA4, and CD80/CD86 (Yao and Xu, 2020). Moreover, ubiquitin modifications also profoundly affected the maturation of immune cells and shaped the tumor microenvironment (TME) (Zhu et al., 2020). Alix et al. (2020) found that WWP2 blocked DC cell-induced T cell activation by targeting and degrading MHC-II expression in DC cells. A recent study showed that the deubiquitination enzyme TRABID can also affect DC cell-induced Th1 and Th17 cell differentiation

by targeting the epigenetic regulation of IL-12/IL-23 (Jin et al., 2016). These studies indicated that ubiquitin modifications profoundly affected the fates of immune cells and the formation of an anti- or pro-tumorigenic microenvironment.

Renal cancer is a malignancy with a moderate mutation burden, but it dramatically responds to immune checkpoint blockade (ICB) therapy (Braun et al., 2020). Results from several clinical trials have shown that anti-PD-1/CTLA-4 combination therapy has a superior clinical effect over VEGFR-targeted therapy, marking a new era of immunotherapy for renal cell carcinoma (Grimm et al., 2020). Although there were abundant infiltrating T cells in clear cell renal cell carcinoma (ccRCC), the anti-tumor response was suppressed by Tregs and myeloid cells, resulting in inadequate durable benefit from ICB (Díaz-Montero et al., 2020). Indicated by the available evidence that ubiquitin system involving in the regulation of immune checkpoints (Hsu et al., 2018), an in-depth investigation of the ubiquitin patterns in ccRCC would further clarify the mechanism of immune resistance and help to identify reliable biomarkers of ICB responsiveness. The large number of ubiquitin regulators makes it difficult to depict the macroscopic immune landscape shaped by ubiquitination modifications of individual tumors using traditional research methods. Moreover, tumorigenesis is an interaction of multiple regulators in a highly coordinated manner, thus a more comprehensive and efficient analysis is needed to characterize the ubiquitin modifications in ccRCC. Based on this, we explored the ubiquitin patterns of ccRCC and comprehensively evaluated the underlying role in shaping immune maturation by analyzing the genomic information from a total of 1212 ccRCC samples. Herein, we identified three ubiquitin patterns in ccRCC, which correspond to three distinct immune phenotypes. Besides, we proposed a new ubiquitin score to evaluate samples' ubiquitination modification outcomes and initially demonstrated its potentiality in predicting immunotherapy and targeted therapy responsiveness in this study.

## MATERIALS AND METHODS

### ccRCC Datasets Collecting and Pre-processing

The datasets for this study were collected from the TCGA, GEO, and the Clinical Proteomic Tumor Analysis Consortium (CPTAC) databases. As discovery cohort, we downloaded the RNA sequencing data (read counts and FPKM values) and phenotype information of the TCGA-KIRC dataset<sup>1</sup>. Somatic mutation data of the TCGA dataset ( $N = 451$ ) was downloaded from the cBioPortal website<sup>2</sup>. FPKM values were converted to TPM values for subsequent analysis, as it is identical to the microarray values (Wagner et al., 2012). To reduce noise, ubiquitin regulators with median absolute deviation values  $\leq 0.5$  were excluded. The testing cohort is composed of 5 Affymetrix GPL570 platform-based microarray datasets:

**Abbreviations:** PTM, post-translational modification; ccRCC, clear cell renal cell carcinoma; ICB, immune checkpoint blockade; OS, overall survival; E1s, ubiquitin-activating enzymes; E2s, ubiquitin-conjugating enzymes; E3s, ubiquitin protein-ligases; UBD, ubiquitin-binding domain-containing protein; ULDs, ubiquitin-like domains; TNBC, triple-negative breast cancer; DC, dendritic cell; PCA, principal components analysis; DFS, disease-free survival; CC, cellular components; ME, molecular functions; TME, tumor microenvironment; WES, whole exon sequencing; SUMOs, Small ubiquitin-like modifiers; ORR, overall response rate; TMB, tumor mutational load; APAP, antigen processing and presenting; NLR, NOD-like receptor signaling pathway; TLR, toll-like receptor signaling pathway; TCR, T-cell receptor signaling pathway; CPTAC, Clinical Proteomic Tumor Analysis Consortium; GSEA, Gene Set Variation Analysis; ssGSEA, single sample gene set enrichment analysis.

<sup>1</sup><https://portal.gdc.cancer.gov/repository>

<sup>2</sup>[http://www.cbioportal.org/study/summary?id=kirc\\_tcg](http://www.cbioportal.org/study/summary?id=kirc_tcg)



GSE73731 ( $N = 265$ ), GSE53757 ( $N = 144$ ), GSE46699 ( $N = 130$ ), GSE66272 ( $N = 54$ ), and GSE36895 ( $N = 76$ ). GPL10558 platform-based microarray datasets GSE65615 ( $N = 138$ ) and GSE40435 ( $N = 202$ ) were compiled as the external validating cohorts. We downloaded the original “CEL” files from the GEO database<sup>3</sup>, adjusted the background and quantile normalized the data sets using “RMA” algorithm of the “affy” package, and then removed the batch effect using the “ComBat” algorithm of the “sva” package to merge these datasets into one for validation (Johnson et al., 2007). For GSE29609 ( $N = 39$ ), the expression matrix (normalized log10 values) and clinical information were directly downloaded and used to validate the prognostic value. Log ratio transformed proteomics data and the biospecimen features of ccRCC were download from the CPTAC website<sup>4</sup> to validate the protein level of the ubiquitin regulators (Clark et al., 2019).

## Different Expressed Ubiquitin Regulators Analysis and Survival Analysis

Twenty-seven E1s, 109 E2s, 1153 E3s, 164 DUBs, 396 UBDs, and 183 ULDs were collected from the iUUCD 2.0 database (Gao et al., 2013), and there were 1332 regulators after duplication removal. DEG of ubiquitin regulators was performed in the discovery and testing datasets using “DESeq2” and “Limma” methods, respectively. DEGs of the discovery cohort were filtered at adjusted  $p$ -value  $< 0.01$ , and results of the testing cohort were screened at adjusted  $p$ -value  $< 0.05$ . Finally, 758 overlapped regulators were identified as the hub regulators in ccRCC. Significantly mutated regulators ( $q < 0.05$ ) were inferred using the MutSigCV algorithm as described before (Lawrence et al., 2013). Prognostic values were assessed using univariate and multivariate-cox regression, and the survival differences were visualized using Kaplan-Meier curves.

## Identification of Ubiquitin Pattern and Molecular Characterization

Unsupervised consensus clustering of the 758 ubiquitin regulators was performed using the k-means algorithm, the cluster algorithm was set as “km,” and the similarity of samples was determined by “Euclidean” distance. This step was repeated 1000 times in the “ConsensusClusterPlus” package to ensure the stability of the classification (Wilkerson and Hayes, 2010). The 127 ubiquitin and proteasome-related biological processes were collected from the “c2.cp.kegg.v7.2.symbols” gene set (MSigDB database)<sup>5</sup>. “Gene Set Variation Analysis (GSVA)” method and “Limma” difference analysis were used for subsequent molecular characterization (Hanzelmann, 2013ga). Meanwhile, the “ClusterProfiler” package was used to annotate the function of each subgroup.

## Estimating the Immune Cell Infiltrating

Single sample gene set enrichment analysis (ssGSEA) is a method developed to estimate the relative abundance of immune cells

based on the expression profile of a single sample. We obtained the gene set signatures of 28 immune cells (18 adaptive and 10 innate immune cell types) from the study of Charoentong et al. (2017), and the estimated score was calculated to represent the abundance of each cell type. CIBERSORT is an algorithm that deconvolves the expression matrix of bulk sequencing data based on the principle of linear support vector regression, and the sum of the percentages of each immune cell in the estimation result is 100% (Yoshihara et al., 2013; Newman et al., 2015). We used the “cibersort” package to analyze the discovery dataset, and samples with  $p < 0.05$  in the results were included for comparison.

## Dimensional Reduction and Ubiquitin Score Generation

Here, we proposed to quantitatively assess the ubiquitin modification degree of ccRCC samples using the “ubiquitin score.” The ubiquitin score was derived as follows: Firstly, the Pearson correlation coefficients of 758 ubiquitin regulators with the identified ubiquitin patterns were calculated. Then the positively and negatively correlated genes were downscaled using the Boruta algorithm, respectively. Thus we obtained the signature genes A and signature genes B. Finally, the principal components analysis (PCA) was used to calculate the first principal components of signature genes A and B in each sample (Zhang X. et al., 2020). The ubiquitin scores of each sample were extracted as:

$$\text{Ubiquitin score} = \Sigma \text{PC1}_A - \Sigma \text{PC1}_B$$

## Predicting the Benefits of Ubiquitin Score for Immunotherapy and Targeted Therapy

The Tumor Immune Dysfunction and Exclusion (TIDE) is developed by Jiang et al. (2018) to predict the responsiveness to immunotherapy based on simulating tumor immune evasion mechanism. Due to the lack of open-access data of ccRCC cohorts accepting immunotherapy, we used the TIDE algorithm to preliminarily explore the responsiveness of the discovery cohort to ICB. Besides, we also used subclass mapping (Submap) to compare the similarity of gene expression profiles with 47 melanoma patients receiving anti-CTLA-4/PD-1 treatment to validate the results of TIDE prediction (Roh et al., 2017; Lu et al., 2019). Considering that VEGFR-targeted therapy remains the first-line treatment option for metastatic ccRCC (cc-mRCC), we explored the sensitivity of each subgroup to Sorafenib, Sunitinib, Pazopanib, and Axitinib. The tumor cell line genomic data and the corresponding IC50 of drug treatment from GDSC database<sup>6</sup> were used as training dataset to estimate the IC50 values of tumor samples by ridge regression using the “pRRophetic” package, and the accuracy of the prediction results was assessed by 10-fold cross-validation (Geeleher et al., 2014).

## Statistical Analysis

All calculation and statistical analyses were performed in RStudio 3.6.3. Student's  $t$ -test and Wilcoxon test were used for two-group

<sup>3</sup><http://www.ncbi.nlm.nih.gov/geo/>

<sup>4</sup><https://cptac-data-portal.georgetown.edu/study-summary/S044>

<sup>5</sup><https://www.gsea-msigdb.org/gsea/msigdb/collections.jsp#C5>

<sup>6</sup><https://www.cancerrxgene.org/>

comparison of normally or skewed distribution data, respectively. For multiple groups, Kruskal–Wallis test and one-way ANOVA were used for parametric or non-parametric comparisons. Component differences in subgroups were compared by Fisher's exact test. All statistical tests were two-sided, and  $p < 0.05$  was considered statistically significant.

## RESULTS

### Identification of the Differentially Expressed Ubiquitin Regulators and the Ubiquitin Patterns

The analysis flowchart of this study was shown in **Figure 1A**. There were 947 differentially expressed ubiquitin regulators in the discovery dataset, and 1032 regulators differentially expressed in the testing cohort. 758 overlapped regulators shared by the two datasets were shown in **Supplementary Figure 1A** and detailed in **Supplementary Table 1**. To clarify that these regulators were similarly differentially expressed at the protein level, we checked the CPTAC dataset. In total, 562 regulators were involved in the proteomic data, 459 of which were statistically significant ( $p < 0.05$ ), with a compliance rate of 81.68% (**Supplementary Table 2**). Subsequently, we explored the prognostic value of the 758 regulators for overall survival (OS) and disease-free survival (DFS) using univariate cox method (**Supplementary Table 3**).

To explore the ubiquitin patterns of ccRCC, unsupervised consensus clustering of the 758 regulators was performed. After comprehensive consideration of CDF curves and Delta area, we chose  $k = 3$  as the number of subgroups (**Figures 1B,C** and **Supplementary Figures 1B–F**). In the discovery cohort, 123 patients were classified into Pattern A, 246 patients were classified into Pattern B, and 161 patients were classified into Pattern C. To verify the robustness of this classification, we used the t-SNE method for dimensional reduction and observed the discrimination of subgroups. As shown in **Figure 1D**, there was only individual cross-over, indicating good discrimination among subgroups. We also performed unsupervised consensus clustering in the testing cohort (**Supplementary Figures 1G–N**), and the results also showed three patterns of ubiquitin regulator expression in ccRCC samples. Regulators that were significantly higher expressed in each pattern ( $\log_{2}FC > 0$ , adjusted  $p$ -value  $< 0.05$ ) were identified as hub regulators of each pattern (**Supplementary Figure 3A** and **Supplementary Table 4**). In detail, there were 82 hub regulators for pattern A, 166 hub regulators for pattern B, and 264 hub regulators for pattern C. Besides, we found that these hub regulators were mainly composed of E3 ligases and UBD (**Supplementary Table 5**).

Then we compared the prognosis of the subgroups. The results showed that pattern B had a significant survival advantage with a median DFS time (123.7 months), while pattern A had the shortest median DFS time of 84.5 months (**Figure 1F**, log-rank test,  $p = 0.075$ ). In pattern C we observed the shortest median OS of 65.7 months (log-rank test,  $p = 0.0045$ ), while pattern A and B did not reach 50% median OS (**Figure 1E**). These results showed that the ubiquitin regulators in ccRCC exhibited

three types of expression patterns, with each pattern possessing a different prognosis.

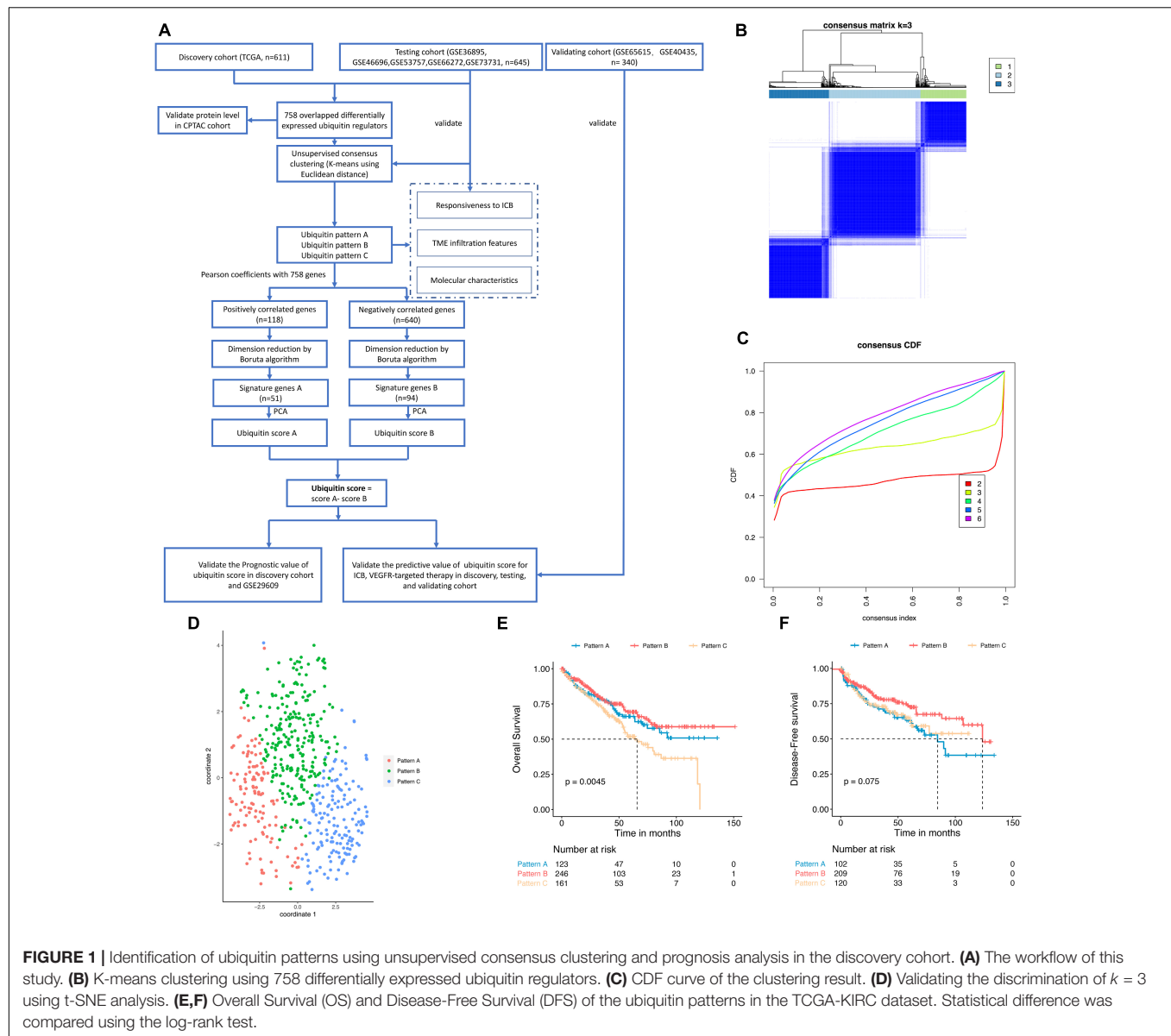
### Molecular Characteristics of the Distinct Ubiquitin Patterns

Considering that the classification is based on ubiquitin regulators, here we characterized the “ubiquitination code” signatures of each pattern. We calculated the enrichment scores of 127 ubiquitin and proteasome system-related biological processes using the GSVA algorithm, and ubiquitination relevant signatures of each pattern were defined as processes with higher enrichment scores in the limma analysis ( $\log_{2}FC > 0.15$ , adjusted  $p$ -value  $< 0.05$ ). The results showed the leading role of Culling-4b Ring E3 and proteasome complex  $\beta$  components and negative regulation of the ubiquitination process in pattern A. Pattern B is characterized by a deubiquitination process mediated by the K29 amino acid site. However, we did not find the ubiquitin-relevant signatures of pattern C under the criterion (**Figure 2A**).

Corresponding to the biological effects of distinct ubiquitin patterns, we further evaluated 14 renal cell cancer progression-relevant signatures. Patients in pattern A had higher DNA repair, p53, hypoxia, and EMT signaling pathway enrichment scores (**Figures 2B,C**), and activation of HIF-1 and Notch signaling were observed in GSEA analysis (**Supplementary Figure 2A** and **Supplementary Table 6**), suggesting greater tumor proliferation activity in pattern A, which explained the reason of shorter median DFS in pattern A (**Figure 1F**). Interestingly, key biological processes promoting kidney cancer progression such as angiogenesis, WNT, PI3K/Akt/mTOR signaling were more enriched in pattern B. On the other side, immune response-related signals such as pan-TNF and pan-IFN signaling were enriched in pattern B. GSVA analysis showed that pattern B exhibited both stromal activation and active immune response activity, suggesting a complex immune homeostatic mechanism in pattern B. We found that immune activation-related signals, such as antigen processing and presenting (APAP), NOD-like receptor (NLR), toll-like receptor (TLR), T-cell receptor (TCR), TNF were activated in pattern B (**Supplementary Figures 2B,C**). The GO enrichment results further characterized the leading role of neutrophil-mediated innate immunity in pattern B. At the same time, stroma-associated cellular components (CC) and molecular functions (MF) were also enriched in pattern B, which verified our speculation (**Figure 3D**).

### Tumor Microenvironment (TME) Infiltration Characteristics of the Distinct Expression Patterns

The imbalance of immune-related signatures among subtypes prompted further exploration of the immune infiltration profile. We firstly compared the tumor purity of the subtypes. By the ESTIMATE algorithm, we found a higher tumor purity of pattern A over pattern B and C, while no difference was found between pattern B and C. The immune scores of pattern B and pattern C were both higher than pattern A, indicating that the two groups had similar immune activation characteristics. In contrast, the stromal scores of pattern B were higher than



pattern A and C, agreeing with the significant stromal activation of pattern B (Figure 3A). We then compare the proportion of immune cells among the three patterns (Supplementary Figure 2F). The results showed no statistical differences in the composition of immune cell types, suggesting that ubiquitin modification did not alter the overall TME infiltrating pattern (Fisher's exact test,  $p = 0.924$ ). Subsequently, we estimated the abundance of 18 adaptive immune cells and 10 innate immune cells in the samples using ssGSEA (Figures 3B,C). In general, pattern A showed a low abundance of almost all immune cell types in contrast to patterns B and C, and we termed it as "immune desert pattern." Pattern B had more B cells, Treg, Th1, Th2, memory CD4+/CD8+ T cells, memory DC cells, and more neutrophils, NK cells, and other innate immune cells along with stromal activation, thus, corresponded to the "immune resistance phenotype." Meanwhile, pattern C possessed

more abundant Th17, activated CD4+/CD8+ T cells, DC cells, CD56+ NK cells, MDSC, and macrophages, corresponding to "immune-inflammatory phenotype." However, patients in pattern C survived worst, which was inconsistent with the immune features of this subgroup (Figure 1E). One possible reason is that the anti-tumor response in pattern C was blocked by the simultaneous high expressed immune checkpoints. As we speculated, PD-1, CTLA4, GZMA, GZMB, IFNG, LAG3, TBX2, and TNF were higher expressed in pattern C (Figure 3E). The pair-wise comparison results revealed that these genes were significantly higher in group C compared with group A, while no significant difference existed when compared with group B except for TBX2 (Supplementary Table 7).

VHL mutation has been demonstrated to play an important role in ccRCC, but it is not clear whether it affects the immune landscape. MutSig results showed that the overall mutation rate

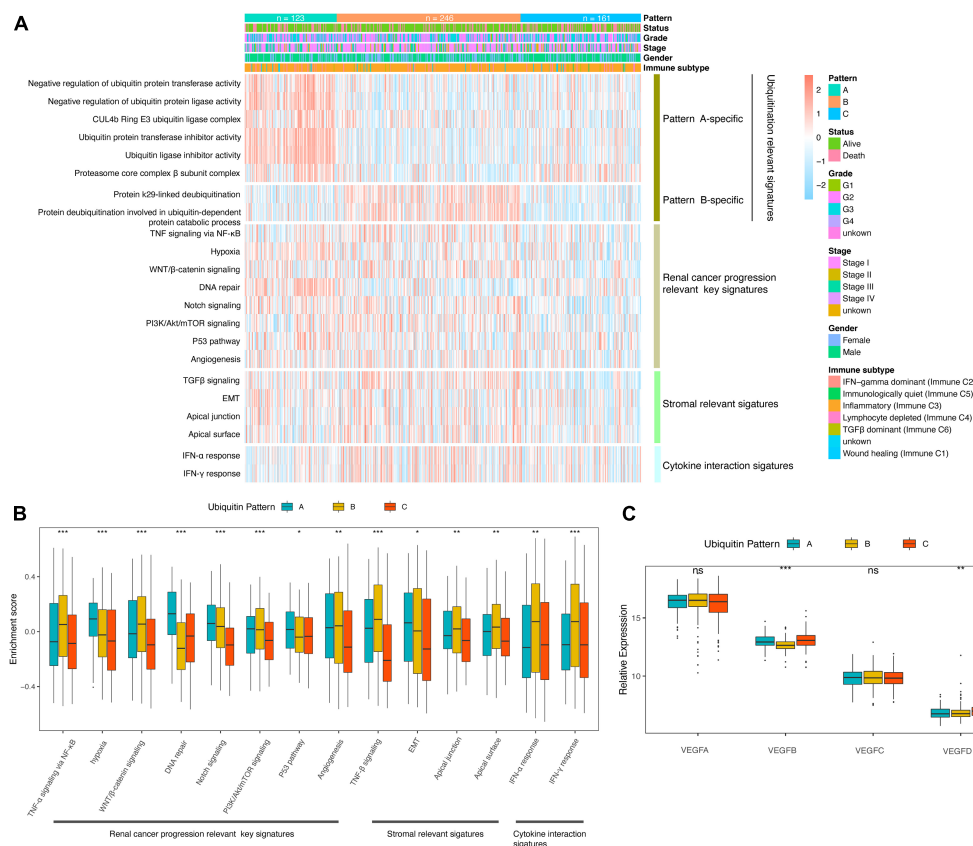


**FIGURE 2 |** Molecular characteristics of the ubiquitin pattern. **(A)** Heatmap of the ubiquitin-relevant signature of the subclasses. **(B)** Boxplot of the GSVA enrichment score of ccRCC progression-relevant signatures. **(C)** Relative expression of VEGF family distinguished by ubiquitin patterns. The median values of the enrichment scores were compared using the Kruskal-Wallis test. Statistical significance levels were indicated with asterisks above the boxplot (ns, no statistical difference, \*  $p < 0.05$ , \*\*  $p < 0.01$ , \*\*\*  $p < 0.001$ ).

of VHL was 50% in all samples, much higher than the other significantly mutated regulators (**Supplementary Figure 3B**). Therefore, we focused on exploring the potential role of VHL in the patterns we identified. There was no significant differences in VHL mutation rates among the three patterns (**Supplementary Figure 3D**, Fischer's exact test,  $p = 0.448$ ), but VHL expression levels were significantly lower in pattern A than in pattern B and C (**Supplementary Figure 2C**, Wilcoxon test,  $p = 1.1e-10$ ,  $9.6e-08$ , respectively). Furthermore, we found no significant difference in immune cell abundance between the mut/wild subtypes except for CD56bright NK cells. For PD-1, PD-L1, CTLA4, no statistical difference was found between the mut/wild VHL subtypes (**Supplementary Figure 3H**), which is in consistent with the findings of Hong et al. (2019).

## Correlation of the Ubiquitin Patterns With the Immunotherapy Benefits

The abundance of infiltrating immune cells and expression of immune checkpoint molecules in pattern C suggest the need to further explore the responsiveness of pattern C to ICB therapy. Based on the TIDE algorithm, we found significantly higher predicted response rates of pattern C (50.93%) in contrast to

pattern A and B (38.21, 35.77%, respectively) (**Figure 4A** and **Supplementary Table 10**, Fisher exact test,  $p = 0.008$ ). The testing cohort resulted similarly with a 54.46% predicted response rate of pattern A (**Figure 4C** and **Supplementary Table 11**, Fisher exact test,  $p < 0.0001$ ). The expression profiles of each pattern were subsequently applied to Submap analysis. However, no definite similarity to ICB responders was found. None of the subgroups in the discovery cohort exhibited similarity to ICB responders, whereas pattern A in the testing cohort showed strong similarity to ICB responders (**Figures 4B,D**). This indicated the limitation and instability of population-based classification in predicting ICB treatment benefit.

## Ubiquitin Scores of Individual ccRCC Sample and the Prognostic Value

Previous studies demonstrated the close relationship between ubiquitin modification and anti-tumor immune activity. However, this patient population-based classification cannot accurately describe the ubiquitination outcome of the individual patients, which greatly limited its clinical application. Therefore, we continued to construct a ubiquitin score to quantify the ubiquitination outcome of single tumor sample. As the methods



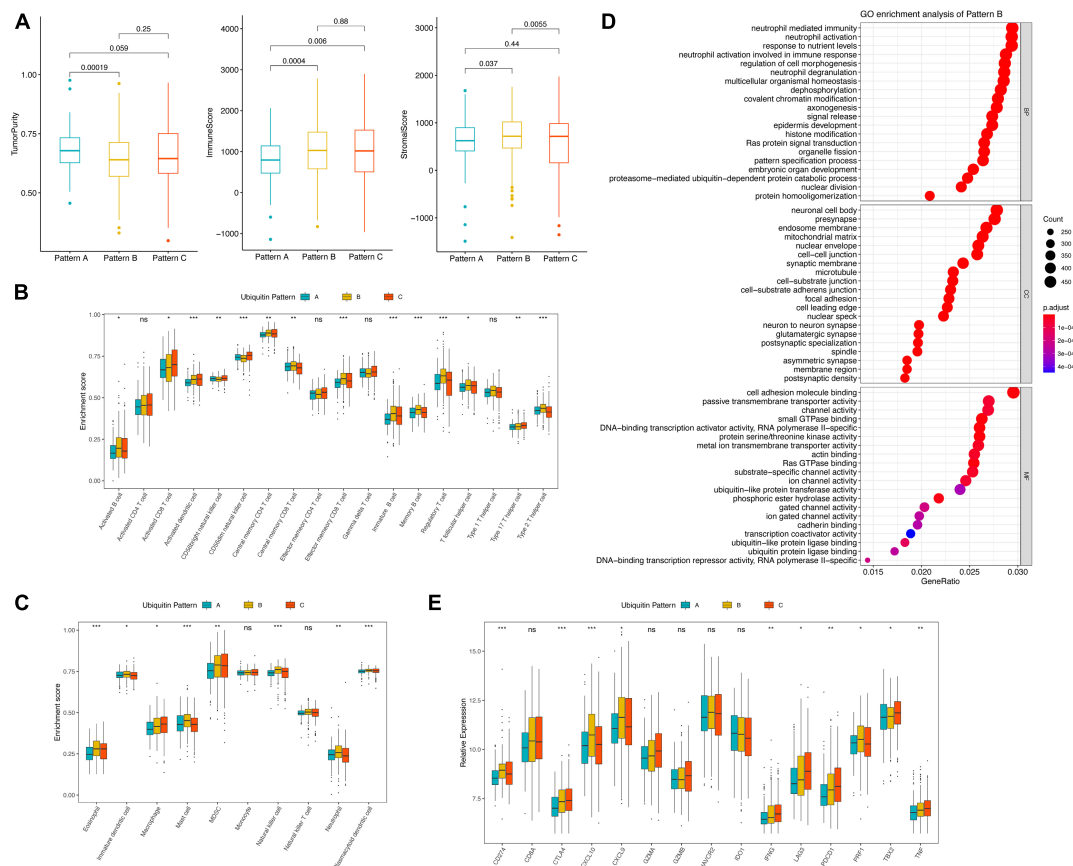


**FIGURE 3 |** TME features of distinct ubiquitin patterns. **(A)** Tumor purity, immune score, and the stromal score of the subclasses generated by the “ESTIMATE” algorithm. The comparison was performed by Student’s *t*-test. **(B,C)** Estimated abundance of 18 adaptive and 10 innate immune cells using ssGSEA. Inter-subgroup comparison was performed by one-way ANOVA. **(D)** GO enrichment results of pattern B. The Top 20 of biological process (BP), cellular component (CC), and molecular function (MF) were displayed. **(E)** Association of ubiquitin patterns with immune checkpoint molecules. Kruskal–Wallis test, ns, no statistical difference, \*  $p < 0.05$ , \*\*  $p < 0.01$ , \*\*\*  $p < 0.001$ .

described, we downsampled the 758 regulators and obtained 51 and 94 genes that were positively and negatively associated with the ubiquitin patterns, which were termed as signature genes A and B, respectively (Supplementary Table 8). Supplementary Figure 4A displayed the expression landscape of 758 genes in each pattern. GO enrichment analysis showed that signature genes A were enriched in Cullin3-Ring ligase, which was involved in protein poly-ubiquitination and phosphorylation modifications (Supplementary Figure 4B), while signature genes B were predominated in Cullin-4 Ring E3 ligases, which was participating in proteasome-dependent protein degradation and deubiquitination process (Supplementary Figure 4C). The ubiquitin score was obtained by applying PCA performance to each signature gene (Supplementary Table 9). We compared the ubiquitin scores of the three patterns and found significant differences among the subgroups (Supplementary Figure 4D), with mode C having the highest ubiquitin score (median value of 5.079), mode A having the lowest score (median value of  $-3.931$ ), and group B having an intermediate score (median value of  $-2.079$ ). discovery cohort patients were classified into two groups using the best separation method, with 309

samples sorted into the high score group and 221 samples into the low score group. Prognosis analysis showed that the high score group had a significantly shorter median OS time (Figure 5E,  $p < 0.0001$ ). To validate, the higher score group in the GSE29609 cohort also showed a significantly shorter median OS (Figure 5G,  $p = 0.031$ ). Inclusion of the ubiquitin score along with the clinicopathological factors in multivariate analysis revealed that the ubiquitin score was an independent risk factor for OS (Figure 5F, HR = 1.47,  $p < 0.001$ ). These results demonstrated the prognostic value of the ubiquitination score.

As shown in the heatmap (Figure 5A), IL6/JAK/STAT3, IFN $\gamma$ , and K-ras signaling were upregulated in high score groups, while TGF $\beta$  signaling was downregulated ( $\log_{2}FC > 0.1$ , adjusted  $p$ -value  $< 0.05$ ). The majority of key signatures for renal cancer progression were enriched in the low score group, including EMT, WNT, mTORC1, Angiogenesis, Myc, and Hedgehog signaling. The high score group exhibited an advantage of activated CD4 $^{+}$ /CD8 $^{+}$  T, MDSC, macrophages, and various types of DC cell infiltration (Figure 5B). Recent studies have shown that ubiquitinases (including E3 ubiquitinases

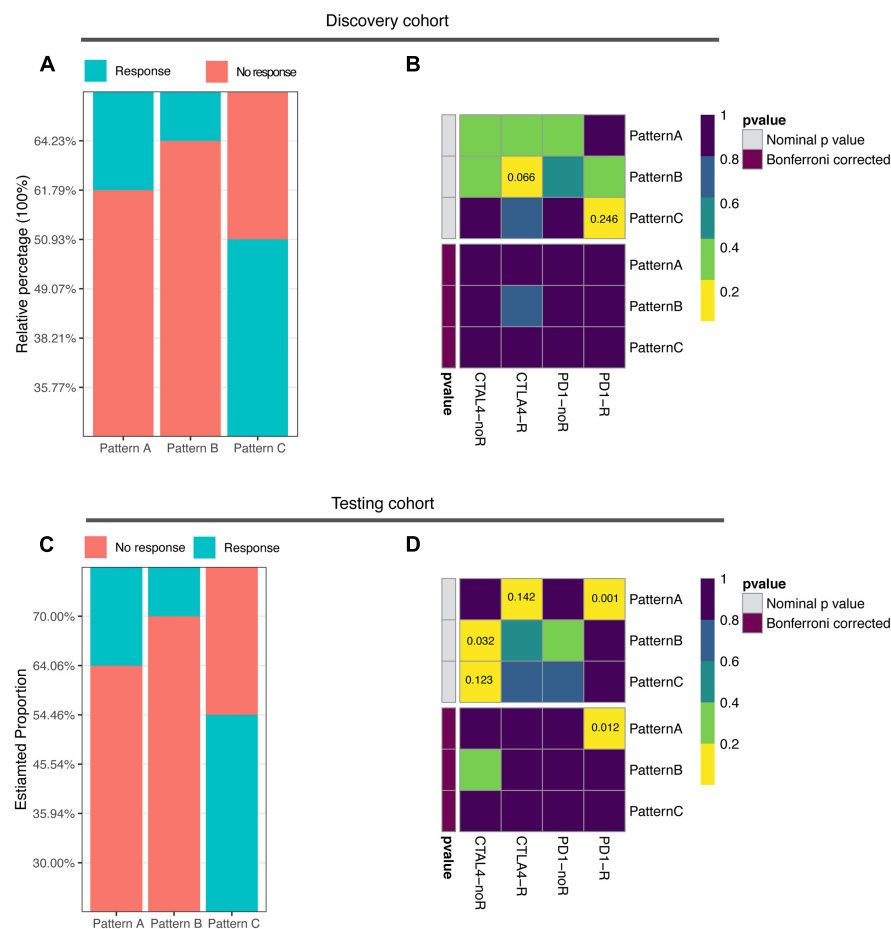


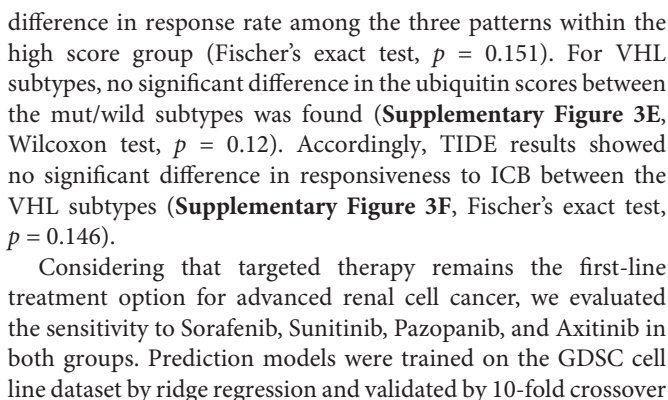
**FIGURE 4 |** Correlation of ubiquitin patterns with immunotherapy benefit. **(A,C)** The predicted response rate in TIDE analysis of discovery and testing cohorts. Fisher's exact test,  $p = 0.008$ ,  $p < 0.0001$ , respectively. **(B,D)** The similarity of gene expression profiles between ubiquitin patterns and melanoma patients treated with ICB ( $n = 47$ ). CTLA4-noR, patients no respond to anti-CTLA4 treatment, CTLA4-R, patients respond to anti-CTLA4 treatment, PD1-noR, patients no respond to anti-PD1 treatment, PD1-R, patients respond to anti-PD1 treatment.

and DUB) are key regulators of DC function (Jin et al., 2016). Activation of DC cells depends on the high expression of MHC molecules, co-stimulatory molecules, and adhesion factors (Qian and Cao, 2018). And we noted that high ubiquitin scores were accompanied by an overall elevation of MHC, adhesion molecules, and co-stimulatory molecules (Figure 5C). Subsequent comparison of immune activation-related pathways (including APAP, NFKB, NLR, TLR, and TCR) revealed a significant enhancement of APAP and TCR signaling in the high group (Figure 5D). These results demonstrated that ubiquitin modifications in ccRCC ultimately promote DC maturation and antigen presentation process.

## Correlation of the Ubiquitin Score With ICB Treatment Responsiveness and Targeted Therapy Sensitivity

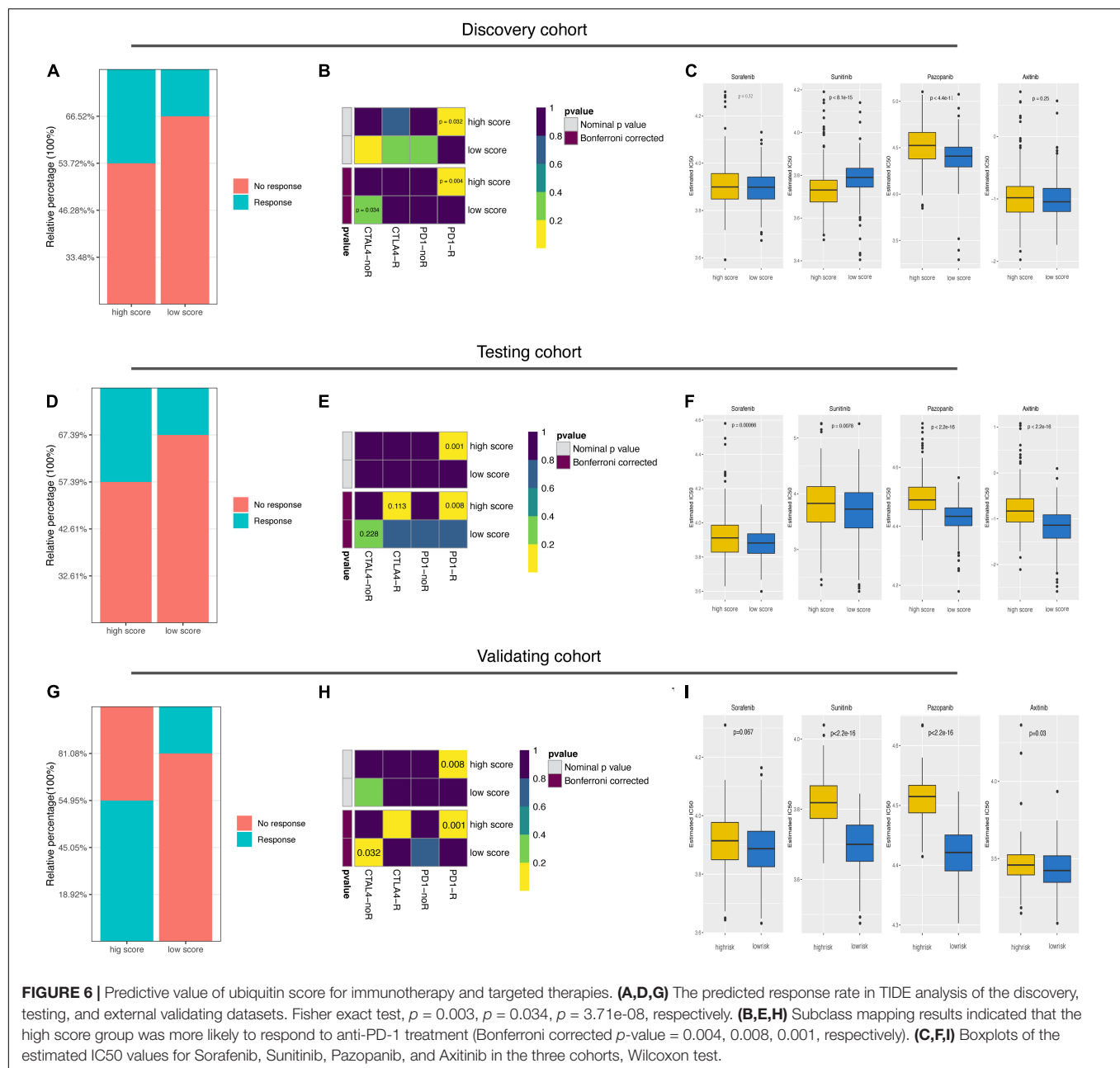
Finally, we explored the predictive value of the ubiquitin score to immunotherapy and targeted therapy. The TIDE results showed a higher predicted response rate in the high score group (46.28%

vs. 33.48%, Figure 6A,  $p = 0.0032$ ). In addition, we were delighted to see the consistent results with TIDE analysis that the high score group was more likely to respond to anti-PD-1 treatment (Figure 6B,  $p = 0.032$ , 0.004, respectively). To validate, we generated the ubiquitin score for patients in the testing cohort. In the testing cohort, Pattern C had the highest ubiquitin score, while pattern A had the lowest ubiquitin score, with significant statistical differences in the pair-wise comparison (Supplementary Figure 4E). After dividing all patients into high/low score groups based on median ubiquitin score, the response rate was 42.61% in the high score group, while 32.61% in the low score group (Figure 6D, Fisher's exact test,  $p = 0.034$ ). The Submap analysis yielded positive results with high similarity in expression profiles between the high score group and the anti-PD-1 responders (Figure 6E,  $p = 0.001$ , 0.008, respectively). Because of the differential distribution of pattern A and B in high and low score groups, we performed subgroup analysis. For pattern A and B, there was no significant difference in responsive rates to ICB between the high and low subgroups (Fischer's exact test,  $p = 1$ ,  $p = 0.083$ , respectively). And there was no significant



to make the prediction results stable. IC50 values were estimated for each sample and the differences were compared. In the discovery cohort, we found that the high score group was more likely to be sensitive to Sunitinib ( $p < 8.1\text{e-}15$ ), while the low score group more sensitive to Pazopanib and Axitinib (**Figure 6C**,  $p < 4.4\text{e-}11$ ,  $p = 0.25$ , respectively). In the testing cohort, the low score group showed a lower predicted IC50 value in treating with the four candidate drugs (**Figure 6F**). Since mTOR signaling, VEGFR family, PDGFR family, and KIT expressed higher in the low score group (**Supplementary Figure 3G**), the above prediction results were reasonable.

Lastly, these findings were all validated in an external independent cohort. The results of the TIDE and Submap



analysis again demonstrated that the high ubiquitin score group may respond to ICB treatment, while the low score group is more sensitive to Sunitinib, Pazopanib, and Axitinib (Figures 6G–I and Supplementary Table 12). All in all, these results firmly proposed that ubiquitin scores to be used to predict patient benefits from ICB and targeted therapy.

## DISCUSSION

The role of ubiquitin regulators in ccRCC has been of interest to researchers since the E3 ubiquitin ligase pVHL deficiency was identified as an essential feature of ccRCC

(Gossage et al., 2015). Recently, Guo et al. (2012) identified 12 novel high-frequency mutated genes that were enriched in the ubiquitin-mediated protein hydrolysis pathway by whole exon sequencing (WES) assay, and these genes were closely associated with overexpression of HIF factors. In addition, ubiquitin factors involved in key signaling of renal cell cancer, such as p53, PI3K/Akt, and Angiogenesis, are being increasingly identified (Ma et al., 2015; Guo et al., 2019; Hao et al., 2019; Yu et al., 2019; Zhang E. et al., 2020). However, there was a small number of studies investigating the role of ubiquitin regulators on the immune system of ccRCC. To our knowledge, this is the first time to comprehensively assess the ubiquitin modification pattern of renal cell carcinoma and to characterize their biological



outcomes, especially the ubiquitin regulator-mediated immune features using bioinformatics method. The newly published proteomics data provide important supporting evidence for our study (Clark et al., 2019). Due to the limitations of detection technology and rapid protein degradation, proteomic data usually have a large disparity with the transcriptomic data. In the CPTAC ccRCC dataset, only 9964 proteins were detected in total, which is half amount of the coding genes. However, 562 of the 758 ubiquitin regulators used in our study were detected, with a detection rate of 74.14% and a compliance rate of 81.68%. Based on this, we suggest that it is meaningful to use RNA seq data for subsequent analysis.

In contrast to the conventional perception of immunology, highly infiltrative macrophages, Treg, and CD8+ T cells in ccRCC tend to be associated with worse oncologic outcomes (OS and PFS) (Bruni et al., 2020). The study by Braun et al. (2020) further showed that although about 73% of advanced ccRCC was infiltrated by CD8+ T cells, this high infiltration status was not associated with anti-PD-1 treatment benefit. It was demonstrated that the presence of pro-angiogenic, pro-inflammatory TME in ccRCC induced upregulation of multiple immune checkpoint expression on CD8+ toxic T cells, which present an “immune depleted phenotype” (Nakano et al., 2001; Giraldo et al., 2015; Granier et al., 2017). On the contrary, CD8+ T cells were more active in patients with a lower level of vascular factors, and these patients had a better oncology outcome (Giraldo et al., 2015). This suggests that renal cell carcinoma progression-relevant signatures were negatively associated with immune activation signatures. In our study, both the ubiquitin pattern C and the high score group had an immune infiltration advantage but worse OS and PFS, which is in line with the previously described phenomenon. In the comparison of the VEGF superfamily, pattern C was found to have a significantly higher expression of VEGFB and VEGFD (Figure 2C). Thus, high level of vascular factors and immune checkpoints blocked its anti-tumor immune response, ultimately lead to the worst prognosis of pattern C. Interestingly, however, these patients with the worst prognosis were most likely to benefit from ICB. The TIDE results showed a predicted response rate of 50.93% in pattern C, which was higher than 35.77% in pattern B and 38.21% in pattern A. Among the three patterns, pattern A lacked infiltrating immune cells, immune cells of pattern B were trapped in the stroma and cannot actually reach the tumor cells, and only the immune cells in pattern C infiltrated into the tumor nest, therefore anti-tumor immunity was restored the best when drugs unlocked the immune checkpoint.

In advantage of the “Boruta” algorithm and PCA analysis, we generated the ubiquitin score of single patients and demonstrated its prognostic value. Analysis of the signature genes revealed the prominent role of Culling-Ring ubiquitin ligase (E3), ubiquitin-protein transferase (E2), and ubiquitin-like protein protease (ULD) in the ubiquitin system of ccRCC (Supplementary Figures 3B,C). Besides, we found that signature gene A was enriched to protein phosphorylation modification process in ccRCC, and the oxidative phosphorylation pathway was down-regulated in the high ubiquitin score group, suggesting that the phosphorylation process may be involved in the ubiquitin modification process of ccRCC (Supplementary Figures 3B

and Figure 5A). Small ubiquitin-like modifiers (SUMOs), including SUMO1/SUMO2/SUMO3/SUMO4/WDR48, are intranuclear PTM regulators well-studied in recent years. The results of a recent proteomics study showed that the intranuclear modification sites of SUMOs are mainly determined by pre-existing phosphorylation events, and these co-modification processes are regulated by cell cycle protein-dependent kinases (Hendriks et al., 2017). In the difference analysis of the GSVA enrichment scores, we found that signals related to immune shaping and cytokine responses, such as IL6/JAK/STAT3 and IFN- $\gamma$  signaling, were more enriched in the high score group while signaling related to proliferation and epithelial-mesenchymal transition were downregulated. Notably, TGF $\beta$  signaling was negatively correlated to ubiquitination signaling (Figure 5A), and Fukasawa et al. (2010) showed that the ubiquitination degradation process of TGF $\beta$ -RII mediated by Smurf2 was significantly enhanced in renal cell cancer, which might be the reason for the TGF $\beta$  signaling attenuation in ccRCC.

In the latest edition of EAU guidelines, the anti-PD-1/CTLA4 combination treatment is recommended as the first-line treatment option for high-risk cc-mRCC patients (Ljungberg et al., 2020). In Phase 3 clinical trial of CheckMate-214 (NCT02231749), anti-PD-1 antibody Nivolumab combined with anti-CTLA-4 antibody Ipilimumab resulted in an overall response rate (ORR) of 41.6% (OS in 18 months was 75%) in the treatment of advanced renal cancer (Motzer et al., 2018). Despite these advances, reliable biomarkers of ICB therapeutic efficacy remain for further discussion. The instability of a single biomarker to predict benefit from immunotherapy strategies is now recognized. In our study, almost all patients in pattern C and part of patients from pattern B and A with high ubiquitin scores were categorized into high score group, which had both an anti-tumor immune infiltration advantage and high expression of immune checkpoints (Figures 5B–D and Supplementary Figure 3F). Therefore, it is reasonable that the high score group has a higher response rate to ICB treatment. The predicted response rates of 46.28, 42.61, and 36.96% in the three cohorts were close to the result of CheckMate-214, which strengthened our confidence in the predictive value of ubiquitin score. Meanwhile, we observed consistent trends of PD-1/PD-L1/CTLA-4 expression in the high score group, so we suggest it more appropriate to be used to assess the patients' benefit from the anti-CTLA-4/PD-1 combination therapeutic strategy. In regard to this, further validation of the veracity should be performed in a ccRCC dataset receiving immunotherapy. The latest guidelines raise the recommendation grade (1b) of Pembrolizumab and Axitinib for the first-line treatment option for low- and intermediate-risk cc-mRCC patients, while Sunitinib (1b) and Cabozantinib (2a) were recommended as an alternative for patients who cannot tolerate or receive ICB treatment, and Pazopanib (1b) only recommended for intermediate-risk patients (Ljungberg et al., 2020). In particular, the combination of Pembrolizumab and Axitinib, approved for m-ccRCC treatment in 2019, may bring an exciting shift to the therapeutic field (Rini et al., 2019). For Sunitinib, the discovery cohort showed an opposite result with testing and validation cohorts. Analysis of the target molecules revealed that the predicted IC50 values in

the TCGA dataset contradicted the expression level of VEGFR and PDGFR (**Supplementary Figure 3G**). Considering the fact that tumor proliferation and mTOR signaling were more active in the low score group, it was more reasonable than the high score group to be more sensitive to Sunitinib. Limited by the types of candidate drugs currently available in the algorithm, we could not estimate the IC50 values of Pembrolizumab and Cabozantinib in this study. In a recent study including 91 patients with cc-mRCC (treated with Nivolumab or Sunitinib), neither transcriptome nor exome sequencing data showed a correlation between VHL and clinical benefit, and our predicted results were consistent with that fact (Dizman et al., 2020).

## CONCLUSION

In conclusion, we identified three ubiquitin patterns in ccRCC with different oncological outcomes, which had distinctly different immune characteristics and prognostic outcomes. In clinical application, the “ubiquitin score” could be used to predict patients’ responsiveness to immunotherapy (high score group) and sensitivity to Pazopanib and Axitinib (low score group). Our study illustrated the key role of ubiquitin regulators in the TME of ccRCC and immunotherapy outcome, and provided a new reference for the management strategies of advanced ccRCC.

## DATA AVAILABILITY STATEMENT

The datasets presented in this study can be found in online repositories. The names of the repository/repositories and accession number(s) can be found below: <https://www.ncbi.nlm.nih.gov/geo/>, GSE53757; <https://www.ncbi.nlm.nih.gov/geo/>, GSE46699; <https://www.ncbi.nlm.nih.gov/geo/>, GSE66272; <https://www.ncbi.nlm.nih.gov/geo/>, GSE36895; <https://www.ncbi.nlm.nih.gov/geo/>, GSE73731; <https://portal.gdc.cancer.gov/repository>, TCGA-KIRC; <https://www.ncbi.nlm.nih.gov/geo/>, GSE65615; and <https://www.ncbi.nlm.nih.gov/geo/>, GSE40435.

## AUTHOR CONTRIBUTIONS

SW and JH proposed and designed the framework of this study. JX, QX, and CL completed the collation and pre-processing of the raw data required for subsequent analysis. PZ performed a detailed analysis of the data, drafted this manuscript. YX, JL, and YL reviewed and critically revised the manuscript. The manuscript was confirmed by all authors before submitted for peer review.

## REFERENCES

Alix, E., Godlee, C., Cerny, O., Blundell, S., Tocci, R., Matthews, S., et al. (2020). The Tumour Suppressor TMEM127 Is a Nedd4-Family E3 Ligase Adaptor Required by *Salmonella* SteD to Ubiquitinate and Degrade MHC Class II Molecules. *Cell Host Microbe* 28, 54–57. doi: 10.1016/j.chom.2020.04.024

## FUNDING

This presented study was supported by the National Natural Science Foundation of China (Grant Number: 81772729) and the Chen Xiao-ping Foundation for The Development of Science and Technology of Hubei Province (No.202094).

## ACKNOWLEDGMENTS

We would like to thank Dr. Xiaofan Lu (State Key Laboratory of Natural Medicines, Research Center of Biostatistics and Computational Pharmacy, China Pharmaceutical University) for his help with the analytical methods of this study.

## SUPPLEMENTARY MATERIAL

The Supplementary Material for this article can be found online at: <https://www.frontiersin.org/articles/10.3389/fcell.2021.659294/full#supplementary-material>

**Supplementary Figure 1** | Unsupervised consensus clustering in GEO-KIRC datasets. **(A)** The 758 overlapped differentially expressed ubiquitin regulators in the Venn diagram. **(B–F)** Consensus clustering results when  $k = 2, 4, 5, 6$  in the discovery cohort and delta area plot. **(G–M)** Consensus clustering result when  $k = 2, 3, 4, 5, 6$  in the testing cohort. **(N)** t-SNE result of the testing cohorts.

**Supplementary Figure 2** | GSEA of ubiquitin patterns. **(A–E)** The enrichment results by GSEA for patterns A, B, and C. **(F)** Comparison of immune infiltration difference among subgroups by CIBERSORT deconvolution, Fisher exact test,  $p = 0.924$ .

**Supplementary Figure 3** | Correlation of VHL mut/wild subtypes with ubiquitin patterns and immunotherapy responsiveness. **(A)** Heatmap of the distinct patterns’ hub regulators. 82 regulators for pattern A, 166 regulators for pattern B, and 264 regulators for pattern C. **(B)** Significantly mutated ubiquitin regulators in ccRCC inferred by MutSigCV method. The oncoplot showed that VHL was the most frequently mutated ubiquitin regulators with a 50% mutation rate. **(C)** VHL expression and **(D)** mutation status of the three patterns. There was no significant difference in the proportion of VHL mutant phenotype among the three patterns,  $p = 0.448$ , Fischer’s exact test. **(E)** No difference of ubiquitin score between the VHL mut/wild subtypes, Wilcoxon test,  $p = 0.12$ . **(F)** No difference of immunotherapy response rate between the VHL mut/wild subtypes was found by TIDE method,  $p = 0.146$ , Fischer’s exact test. **(G)** Immune cell abundance between the VHL mut/wild subtypes, Wilcoxon test. **(H)** PD-L1(CD274), CTLA4, PD-1(PDCD1) expression level between the VHL mut/wild subtype, Wilcoxon test.

**Supplementary Figure 4** | Generation of the ubiquitin score. **(A)** heatmap of the positive and negatively correlated regulators in three ubiquitin patterns. **(B,C)** GO enrichment of signature gene A and B. **(D,E)** ubiquitin scores of distinct ubiquitin pattern in the discovery **(D)** and testing **(E)** cohorts, pair-wise comparison using Wilcoxon test. **(F,G)** Drug targets of immunotherapy **(F)** and VEGFR-targeted therapy **(G)** expression level, Wilcoxon test.

Braun, D. A., Hou, Y., Bakouny, Z., Ficial, M., Sant’ Angelo, M., Forman, J., et al. (2020). Interplay of somatic alterations and immune infiltration modulates response to PD-1 blockade in advanced clear cell renal cell carcinoma. *Nat. Med.* 26, 909–918. doi: 10.1038/s41591-020-0839-y

Bruni, D., Angell, H. K., and Galon, J. (2020). The immune contexture and Immunoscore in cancer prognosis and therapeutic efficacy. *Nat. Rev. Cancer* 20, 662–680. doi: 10.1038/s41568-020-0285-7

- Charoentong, P., Finotello, F., Angelova, M., Mayer, C., Efremova, M., Rieder, D., et al. (2017). Pan-cancer Immunogenomic Analyses Reveal Genotype-Immunophenotype Relationships and Predictors of Response to Checkpoint Blockade. *Cell Rep.* 18, 248–262. doi: 10.1016/j.celrep.2016.12.019
- Clark, D. J., Dhanasekaran, S. M., Petralia, F., Pan, J., Song, X., Hu, Y., et al. (2019). Integrated Proteogenomic Characterization of Clear Cell Renal Cell Carcinoma. *Cell* 179, 964–983.e31.
- Díaz-Montero, C. M., Rini, B. I., and Finke, J. H. (2020). The immunology of renal cell carcinoma. *Nat. Rev. Nephrol.* 16, 721–735.
- Dizman, N., Lyou, Y., Salgia, N., Bergerot, P. G., Hsu, J., Enriquez, D., et al. (2020). Correlates of clinical benefit from immunotherapy and targeted therapy in metastatic renal cell carcinoma: comprehensive genomic and transcriptomic analysis. *J. Immunother. Cancer* 8:e000953. doi: 10.1136/jitc-2020-000953
- Fukasawa, H., Yamamoto, T., Fujigaki, Y., Misaki, T., Ohashi, N., Takayama, T., et al. (2010). Reduction of transforming growth factor-beta type II receptor is caused by the enhanced ubiquitin-dependent degradation in human renal cell carcinoma. *Int. J. Cancer* 127, 1517–1525. doi: 10.1002/ijc.25164
- Gao, T., Liu, Z., Wang, Y., Cheng, H., Yang, Q., Guo, A., et al. (2013). UUCD: a family-based database of ubiquitin and ubiquitin-like conjugation. *Nucleic Acids Res.* 41, D445–D451.
- Geeleher, P., Cox, N. J., and Huang, R. S. (2014). Clinical drug response can be predicted using baseline gene expression levels and in vitro drug sensitivity in cell lines. *Genome Biol.* 15:R47.
- Giraldo, N. A., Becht, E., Pagès, F., Skliris, G., Verkarre, V., Vano, Y., et al. (2015). Orchestration and Prognostic Significance of Immune Checkpoints in the Microenvironment of Primary and Metastatic Renal Cell Cancer. *Clin. Cancer Res.* 21, 3031–3040. doi: 10.1158/1078-0432.ccr-14-2926
- Gossage, L., Eisen, T., and Maher, E. R. (2015). VHL, the story of a tumour suppressor gene. *Nat. Rev. Cancer* 15, 55–64. doi: 10.1038/nrc3844
- Granier, C., Dariane, C., Combe, P., Verkarre, V., Urien, S., Badoual, C., et al. (2017). Tim-3 Expression on Tumor-Infiltrating PD-1+CD8+ T Cells Correlates with Poor Clinical Outcome in Renal Cell Carcinoma. *Cancer Res.* 77, 1075–1082. doi: 10.1158/0008-5472.can-16-0274
- Grimm, M.-O., Leucht, K., Grünwald, V., and Foller, S. (2020). New First Line Treatment Options of Clear Cell Renal Cell Cancer Patients with PD-1 or PD-L1 Immune-Checkpoint Inhibitor-Based Combination Therapies. *J. Clin. Med.* 9:565. doi: 10.3390/jcm9020565
- Grumati, P., and Dikic, I. (2018). Ubiquitin signaling and autophagy. *J. Biol. Chem.* 293, 5404–5413. doi: 10.1074/jbc.tml117.000117
- Guo, F., Liu, J., Han, X., Zhang, X., Lin, T., Wang, Y., et al. (2019). FBXO22 Suppresses Metastasis in Human Renal Cell Carcinoma via Inhibiting MMP-9-Mediated Migration and Invasion and VEGF-Mediated Angiogenesis. *Int. J. Biol. Sci.* 15, 647–656. doi: 10.7150/ijbs.31293
- Guo, G., Gui, Y., Gao, S., Tang, A., Hu, X., Huang, Y., et al. (2012). Frequent mutations of genes encoding ubiquitin-mediated proteolysis pathway components in clear cell renal cell carcinoma. *Nat. Genet.* 44, 17–19.
- Hao, P., Kang, B., Li, Y., Hao, W., and Ma, F. (2019). UBE2T promotes proliferation and regulates PI3K/Akt signaling in renal cell carcinoma. *Mol. Med. Rep.* 20, 1212–1220.
- Hendriks, I. A., Lyon, D., Young, C., Jensen, L. J., Vertegaal, A. C. O., and Nielsen, M. L. (2017). Site-specific mapping of the human SUMO proteome reveals co-modification with phosphorylation. *Nat. Struct. Mol. Biol.* 24, 325–336. doi: 10.1038/nsmb.3366
- Hong, B., Cai, L., Wang, J., Liu, S., Zhou, J., Ma, K., et al. (2019). Differential Expression of PD-L1 Between Sporadic and VHL-Associated Hereditary Clear-Cell Renal Cell Carcinoma and Its Correlation With Clinicopathological Features. *Clin. Genitourin. Cancer* 17, 97–104.e1.
- Hsu, J.-M., Li, C.-W., Lai, Y.-J., and Hung, M.-C. (2018). Posttranslational Modifications of PD-L1 and Their Applications in Cancer Therapy. *Cancer Res.* 78, 6349–6353. doi: 10.1158/0008-5472.can-18-1892
- Husnjak, K., and Dikic, I. (2012). Ubiquitin-Binding Proteins: decoders of Ubiquitin-Mediated Cellular Functions. *Annu. Rev. Biochem.* 81, 291–322. doi: 10.1146/annurev-biochem-051810-094654
- Jiang, P., Gu, S., Pan, D., Fu, J., Sahu, A., Hu, X., et al. (2018). Signatures of T cell dysfunction and exclusion predict cancer immunotherapy response. *Nat. Med.* 24, 1550–1558. doi: 10.1038/s41591-018-0136-1
- Jin, J., Xie, X., Xiao, Y., Hu, H., Zou, Q., Cheng, X., et al. (2016). Epigenetic regulation of the expression of IL12 and IL23 and autoimmune inflammation by the deubiquitinase TRABID. *Nat. Immunol.* 17, 259–268. doi: 10.1038/ni.3347
- Johnson, W. E., Li, C., and Rabinovic, A. (2007). Adjusting batch effects in microarray expression data using empirical Bayes methods. *Biostatistics* 8, 118–127. doi: 10.1093/biostatistics/kxj037
- Kerscher, O., Felberbaum, R., and Hochstrasser, M. (2006). Modification of proteins by ubiquitin and ubiquitin-like proteins. *Annu. Rev. Cell Dev. Biol.* 22, 159–180. doi: 10.1146/annurev.cellbio.22.010605.093503
- Lawrence, M. S., Stojanov, P., Polak, P., Kryukov, G. V., Cibulskis, K., Sivachenko, A., et al. (2013). Mutational heterogeneity in cancer and the search for new cancer-associated genes. *Nature* 499, 214–218.
- Li, C.-W., Lim, S.-O., Xia, W., Lee, H.-H., Chan, L.-C., Kuo, C.-W., et al. (2016). Glycosylation and stabilization of programmed death ligand-1 suppresses T-cell activity. *Nat. Commun.* 7:12632.
- Lim, S.-O., Li, C.-W., Xia, W., Cha, J.-H., Chan, L.-C., Wu, Y., et al. (2016). Deubiquitination and Stabilization of PD-L1 by CSN5. *Cancer Cell* 30, 925–939. doi: 10.1016/j.ccell.2016.10.010
- Ljungberg, B., Albiges, L., Bensalah, K., Bex, A., Giles, R. H., Hora, M., et al. (2020). *EAU Guidelines on Renal Cell Carcinoma 2020*. In: *European Association of Urology Guidelines 2020 Edition*. Arnhem: European Association of Urology Guidelines Office.
- Lu, X., Jiang, L., Zhang, L., Zhu, Y., Hu, W., Wang, J., et al. (2019). Immune Signature-Based Subtypes of Cervical Squamous Cell Carcinoma Tightly Associated with Human Papillomavirus Type 16 Expression, Molecular Features, and Clinical Outcome. *Neoplasia* 21, 591–601. doi: 10.1016/j.neo.2019.04.003
- Ma, J., Peng, J., Mo, R., Ma, S., Wang, J., Zang, L., et al. (2015). Ubiquitin E3 ligase UHRF1 regulates p53 ubiquitination and p53-dependent cell apoptosis in clear cell Renal Cell Carcinoma. *Biochem. Biophys. Res. Commun.* 464, 147–153. doi: 10.1016/j.bbrc.2015.06.104
- Meng, X., Liu, X., Guo, X., Jiang, S., Chen, T., Hu, Z., et al. (2018). FBXO38 mediates PD-1 ubiquitination and regulates anti-tumour immunity of T cells. *Nature* 564, 130–135. doi: 10.1038/s41586-018-0756-0
- Motzer, R. J., Tannir, N. M., McDermott, D. F., Arén Frontera, O., Melichar, B., Choueiri, T. K., et al. (2018). Nivolumab plus Ipilimumab versus Sunitinib in Advanced Renal-Cell Carcinoma. *N. Engl. J. Med.* 378, 1277–1290.
- Nakano, O., Sato, M., Naito, Y., Suzuki, K., Orikasa, S., Aizawa, M., et al. (2001). Proliferative activity of intratumoral CD8(+) T-lymphocytes as a prognostic factor in human renal cell carcinoma: clinicopathologic demonstration of antitumor immunity. *Cancer Res.* 61, 5132–5136.
- Newman, A. M., Liu, C. L., Green, M. R., Gentles, A. J., Feng, W., Xu, Y., et al. (2015). Robust enumeration of cell subsets from tissue expression profiles. *Nat. Methods* 12, 453–457. doi: 10.1038/nmeth.3337
- Nijman, S., Luna-Vargas, M., Velds, A., Brummelkamp, T. R., Dirac, A., Sixma, T. K., et al. (2005). A genomic and functional inventory of deubiquitinating enzymes. *Cell* 123, 773–786. doi: 10.1016/j.cell.2005.11.007
- Qian, C., and Cao, X. (2018). Dendritic cells in the regulation of immunity and inflammation. *Semin Immunol.* 35, 3–11. doi: 10.1016/j.smim.2017.12.002
- Rape, M. (2018). Ubiquitylation at the crossroads of development and disease. *Nat. Rev. Mol. Cell Biol.* 19, 59–70. doi: 10.1038/nrm.2017.83
- Reyes-Turcu, F. E., Ventii, K. H., and Wilkinson, K. D. (2009). Regulation and Cellular Roles of Ubiquitin-Specific Deubiquitinating Enzymes. *Annu. Rev. Biochem.* 78, 363–397. doi: 10.1146/annurev.biochem.78.082307.091526
- Rini, B. I., Battle, D., Figlin, R. A., George, D. J., Hammers, H., Hutson, T., et al. (2019). The society for immunotherapy of cancer consensus statement on immunotherapy for the treatment of advanced renal cell carcinoma (RCC). *J. Immunother. Cancer* 7:354.
- Roh, W., Chen, P.-L., Reuben, A., Spencer, C. N., Prieto, P. A., Miller, J. P., et al. (2017). Integrated molecular analysis of tumor biopsies on sequential CTLA-4 and PD-1 blockade reveals markers of response and resistance. *Sci. Transl. Med.* 9:eaa3560. doi: 10.1126/scitranslmed.aah3560
- Schwertman, P., Bekker-Jensen, S., and Mailand, N. (2016). Regulation of DNA double-strand break repair by ubiquitin and ubiquitin-like modifiers. *Nat. Rev. Mol. Cell Biol.* 17, 379–394. doi: 10.1038/nrm.2016.58
- Seeler, J.-S., and Dejean, A. (2017). SUMO and the robustness of cancer. *Nat. Rev. Cancer* 17, 184–197. doi: 10.1038/nrc.2016.143

- Upadhyay, S. C., and Hegde, A. N. (2003). A potential proteasome-interacting motif within the ubiquitin-like domain of parkin and other proteins. *Trends Biochem. Sci.* 28, 280–283. doi: 10.1016/s0968-0004(03)00092-6
- Wagner, G. P., Kin, K., and Lynch, V. J. (2012). Measurement of mRNA abundance using RNA-seq data: RPKM measure is inconsistent among samples. *Theory Biosci.* 131, 281–285. doi: 10.1007/s12064-012-0162-3
- Wilkerson, M. D., and Hayes, D. N. (2010). ConsensusClusterPlus: a class discovery tool with confidence assessments and item tracking. *Bioinformatics* 26, 1572–1573. doi: 10.1093/bioinformatics/btq170
- Yao, H., and Xu, J. (2020). Regulation of Cancer Immune Checkpoint: mono- and Poly-Ubiquitination: tags for Fate. *Adv. Exp. Med. Biol.* 1248, 295–324. doi: 10.1007/978-981-15-3266-5\_13
- Yoshihara, K., Shahmoradgoli, M., Martínez, E., Vegesna, R., Kim, H., Torres-García, W., et al. (2013). Inferring tumour purity and stromal and immune cell admixture from expression data. *Nat. Commun.* 4:2612.
- Yu, S., Dai, J., Ma, M., Xu, T., Kong, Y., Cui, C., et al. (2019). RBCK1 promotes p53 degradation via ubiquitination in renal cell carcinoma. *Cell Death Dis.* 10:254.
- Zhang, E., Dong, X., Chen, S., Shao, J., Zhang, P., Wang, Y., et al. (2020). Ubiquitin ligase KLHL2 promotes the degradation and ubiquitination of ARHGEF7 protein to suppress renal cell carcinoma progression. *Am. J. Cancer Res.* 10, 3345–3357.
- Zhang, J., Bu, X., Wang, H., Zhu, Y., Geng, Y., Nihira, N. T., et al. (2018). Cyclin D-CDK4 kinase destabilizes PD-L1 via cullin 3-SPOP to control cancer immune surveillance. *Nature* 553, 91–95. doi: 10.1038/nature25015
- Zhang, X., Shi, M., Chen, T., and Zhang, B. (2020). Characterization of the Immune Cell Infiltration Landscape in Head and Neck Squamous Cell Carcinoma to Aid Immunotherapy. *Mol. Ther. Nucleic Acids* 22, 298–309. doi: 10.1016/j.omtn.2020.08.030
- Zhu, B., Zhu, L., Xia, L., Xiong, Y., Yin, Q., and Rui, K. (2020). Roles of Ubiquitination and Deubiquitination in Regulating Dendritic Cell Maturation and Function. *Front. Immunol.* 11:586613. doi: 10.3389/fimmu.2020.586613

**Conflict of Interest:** The authors declare that the research was conducted in the absence of any commercial or financial relationships that could be construed as a potential conflict of interest.

Copyright © 2021 Zhou, Lu, Xun, Xu, Liu, Xia, Lu, Wang and Hu. This is an open-access article distributed under the terms of the Creative Commons Attribution License (CC BY). The use, distribution or reproduction in other forums is permitted, provided the original author(s) and the copyright owner(s) are credited and that the original publication in this journal is cited, in accordance with accepted academic practice. No use, distribution or reproduction is permitted which does not comply with these terms.





# Intricate Regulatory Mechanisms of the Anaphase-Promoting Complex/Cyclosome and Its Role in Chromatin Regulation

Tatyana Bodrug<sup>1†</sup>, Kaeli A. Welsh<sup>2†</sup>, Megan Hinkle<sup>2</sup>, Michael J. Emanuele<sup>2</sup> and Nicholas G. Brown<sup>2\*</sup>

<sup>1</sup> Department of Biochemistry and Biophysics, Lineberger Comprehensive Cancer Center, University of North Carolina at Chapel Hill, Chapel Hill, NC, United States, <sup>2</sup> Department of Pharmacology, Lineberger Comprehensive Cancer Center, University of North Carolina School of Medicine, Chapel Hill, NC, United States

## OPEN ACCESS

### Edited by:

Lixin Wan,  
Moffitt Cancer Center, United States

### Reviewed by:

Matthew K. Summers,  
The Ohio State University,  
United States  
Steve Cappell,  
National Cancer Institute (NCI),  
United States

### \*Correspondence:

Nicholas G. Brown  
nbrown1@med.unc.edu

<sup>†</sup> These authors have contributed  
equally to this work

### Specialty section:

This article was submitted to  
Cell Growth and Division,  
a section of the journal  
Frontiers in Cell and Developmental  
Biology

**Received:** 29 March 2021

**Accepted:** 26 April 2021

**Published:** 24 May 2021

### Citation:

Bodrug T, Welsh KA, Hinkle M,  
Emanuele MJ and Brown NG (2021)  
Intricate Regulatory Mechanisms of  
the Anaphase-Promoting  
Complex/Cyclosome and Its Role  
in Chromatin Regulation.  
*Front. Cell Dev. Biol.* 9:687515.  
doi: 10.3389/fcell.2021.687515

The ubiquitin (Ub)-proteasome system is vital to nearly every biological process in eukaryotes. Specifically, the conjugation of Ub to target proteins by Ub ligases, such as the Anaphase-Promoting Complex/Cyclosome (APC/C), is paramount for cell cycle transitions as it leads to the irreversible destruction of cell cycle regulators by the proteasome. Through this activity, the RING Ub ligase APC/C governs mitosis, G1, and numerous aspects of neurobiology. Pioneering cryo-EM, biochemical reconstitution, and cell-based studies have illuminated many aspects of the conformational dynamics of this large, multi-subunit complex and the sophisticated regulation of APC/C function. More recent studies have revealed new mechanisms that selectively dictate APC/C activity and explore additional pathways that are controlled by APC/C-mediated ubiquitination, including an intimate relationship with chromatin regulation. These tasks go beyond the traditional cell cycle role historically ascribed to the APC/C. Here, we review these novel findings, examine the mechanistic implications of APC/C regulation, and discuss the role of the APC/C in previously unappreciated signaling pathways.

**Keywords:** ubiquitin, cell cycle, chromatin, structural biology, ubiquitin ligase (E3), cryo-EM, Anaphase-Promoting Complex/Cyclosome

## INTRODUCTION

The post-translational modification of cellular proteins with ubiquitin (Ub) is a predominant form of eukaryotic regulation (Rape, 2018). Since the initial discoveries of Ub-dependent processes, there was an intimate link between the role of Ub in the cell cycle and the regulation of chromatin (Goldknopf et al., 1975; Matsui et al., 1979; West and Bonner, 1980; Irniger et al., 1995; King et al., 1995, 1996; Sudakin et al., 1995; Yamano et al., 1996; Robzyk et al., 2000). In the 1990s, the cell cycle and Ub fields were significantly advanced by the discovery of Ub-dependent protein turnover of cycling proteins (Yamano et al., 1996). Specifically, cullin-RING Ub ligases, SCFs (SKP1-CUL1-F-box protein) and the Anaphase-Promoting Complex/Cyclosome (APC/C) drive the cell cycle by tagging key regulators with polyubiquitin chains, resulting in their destruction by the proteasome (King et al., 1996; Peters, 1998). Changes in chromatin architecture have also been tightly linked to the cell cycle (Kouzarides, 2007; Bannister and Kouzarides, 2011; Struhl and Segal, 2013).

Chromatin modifications, such as acetylation, methylation, and ubiquitination, are important contributing factors in mediating changes of key cell cycle regulators at the transcriptional level (Whitfield et al., 2002; Kouzarides, 2007; Bar-Joseph et al., 2008; Bannister and Kouzarides, 2011; Grant et al., 2013; Pena-Diaz et al., 2013; Breiling and Lyko, 2015). Recent developments have shown a link between transcriptional processes involving chromatin modification and protein turnover, including a role for E3 ligases such as the APC/C.

The 1.2 MDa APC/C is a molecular machine required for the cell cycle in all eukaryotes (Alfieri et al., 2017; Watson et al., 2019a). Polyubiquitination by the APC/C is responsible for the degradation of several substrates, e.g., Securin and Cyclin B, and is selectively regulated by a variety of factors (Irniger et al., 1995; King et al., 1995, 1996; Lahav-Baratz et al., 1995; Sudakin et al., 1995; Tugendreich et al., 1995; Aristarkhov et al., 1996; Yamano et al., 1996; Yu et al., 1996). This regulation is at the heart of the G1/S transition, mitotic checkpoint, and genome stability; consequently, APC/C dysregulation is common in cancer (Lukas et al., 1999; Garcia-Higuera et al., 2008; Kim and Yu, 2011; Cappell et al., 2016; Choudhury et al., 2017; Sansregret et al., 2017; Wan et al., 2017). The APC/C is a multisubunit Ub ligase with several moving parts, numerous substrates, and is involved in a number of non-mitotic processes (Konishi et al., 2004; Eguren et al., 2011; Kim and Yu, 2011; Primorac and Musacchio, 2013; Davey and Morgan, 2016; Huang and Bonni, 2016; Alfieri et al., 2017; Bakos et al., 2018; Watson et al., 2019a). However, new mechanisms of substrate recruitment and their subsequent ubiquitination have continued to be identified along with novel substrates. Here, we will review several recent studies of APC/C-dependent ubiquitination and examine how the APC/C is at the nexus of both the cell cycle and chromatin biology.

## THE UBIQUITIN SYSTEM

An intricate set of enzymes serve as writers (E1-E2-E3 cascade), erasers (deubiquitinases), and readers (proteins that recognize Ub) of the Ub system (Figure 1A). E3 Ub ligases collaborate with E2s to decorate substrates with Ub, creating the Ub code (Komander and Rape, 2012; Yau and Rape, 2016; Haakonsen and Rape, 2019). E3s can be separated into three classes- RING (really interesting new gene), HECT (homologous to E6AP C-terminus), and RBR (RING-between-RING) (Metzger et al., 2014; Streich and Lima, 2014). Each E3 class uses a unique mechanism to transfer Ub from the E2 to the substrate. HECTs and RBRs accept the Ub from the E2, forming a covalent E3~Ub conjugate (~ denotes the covalent intermediate), and then transfer the Ub to the substrate (Buetow and Huang, 2016; Dove and Klevit, 2017). RINGs co-recruit the substrate and the E2, and facilitate the transfer of Ub from the E2 directly to the substrate (Buetow and Huang, 2016). Deubiquitinases (DUBs) fine-tune the Ub code by editing or removing the Ub chains (Mevisen and Komander, 2017). The edited Ub code is ultimately read by effector proteins that alter the polyubiquitinated target's half-life, cellular localization, and enzymatic activity, depending on the Ub signal (Komander and Rape, 2012; Yau and Rape, 2016;

Haakonsen and Rape, 2019). These diverse proteins can vary widely in both their enzymatic mechanisms and Ub-linkage specificities. It is the successful integration of E2s (~40), E3 ligases (~600), DUBs (~100), and countless readers that result in a plethora of signaling outcomes that flow from the ubiquitin system.

During various cellular processes, a vast array of Ub chains can be formed because of the numerous amino groups on the protein target and on the Ub (M1, K6, K11, K27, K29, K33, K48, and K63) previously linked to the target (Figure 1A; reviewed in Komander and Rape, 2012; Yau and Rape, 2016; Clague et al., 2019; Griewahn et al., 2019; Haakonsen and Rape, 2019; Mattern et al., 2019). These polyubiquitin chains can either be homotypic, composed of a single chain type (e.g., K48), or heterotypic, containing mixed or branched linkages. Mixed chains are comprised of at least two different chain types (e.g., K11 and K48), but each Ub monomer is only modified at a single lysine site. In branched chains, a Ub monomer is modified at two or more lysine sites (e.g., K11/K48). These complex chains and topologies can be regarded as a code, because the linkage type dictates the fate of the substrate and cellular outcome. Different substrates are polyubiquitinated with different Ub linkage types. Some of the Ub tags are used for substrate degradation by the proteasome, whereas others are non-degradative. Often, the biological function and enzymes involved in forming heterotypic branched chains are unknown, even though 10–20% of polymerized Ub are modified at two or more lysines (Swatek et al., 2019).

## APC/C FUNDAMENTALS

The APC/C itself forms multiple types of Ub linkages, e.g., K11, K48, K63, and K11/K48 branched chains, and can monoubiquitinate its substrate target using a complex mechanism involving the E2s UBE2C and UBE2S (Aristarkhov et al., 1996; Yu et al., 1996; Kirkpatrick et al., 2006; Garnett et al., 2009; Williamson et al., 2009; Wu et al., 2010; Dimova et al., 2012; Meyer and Rape, 2014; Brown et al., 2016; Yau et al., 2017). Deciphering the structural organization and basic mechanisms of the APC/C and its E2s was made possible through two decades of work involving x-ray crystallography, native mass spectrometry, NMR, and cryo-Electron microscopy and relied on characterization of both human and yeast APC/C. Through advances in these techniques and our reconstitution capabilities of the complex assemblies that make up the APC/C, a detailed view of APC/C structure and function has emerged, with numerous aspects of the APC/C ubiquitination mechanisms uncovered through the combination of careful mutagenesis studies and artificially cross-linked intermediates.

The APC/C consists of 19 subunits, four of which are homodimers, that can be divided into two subcomplexes (Figure 1B). The "Platform" (APC1, 2, 4, 5, 8, 11, and 15) contains the catalytic core (APC2 and APC11) and the "Arc Lamp" (APC3, 6, 7, 10, 12, 13, and 16) provides a scaffolding element and a binding site for the substrate receptor/coactivator. Within the Arc Lamp, the subunits APC7, APC3, and APC6 are each dimers

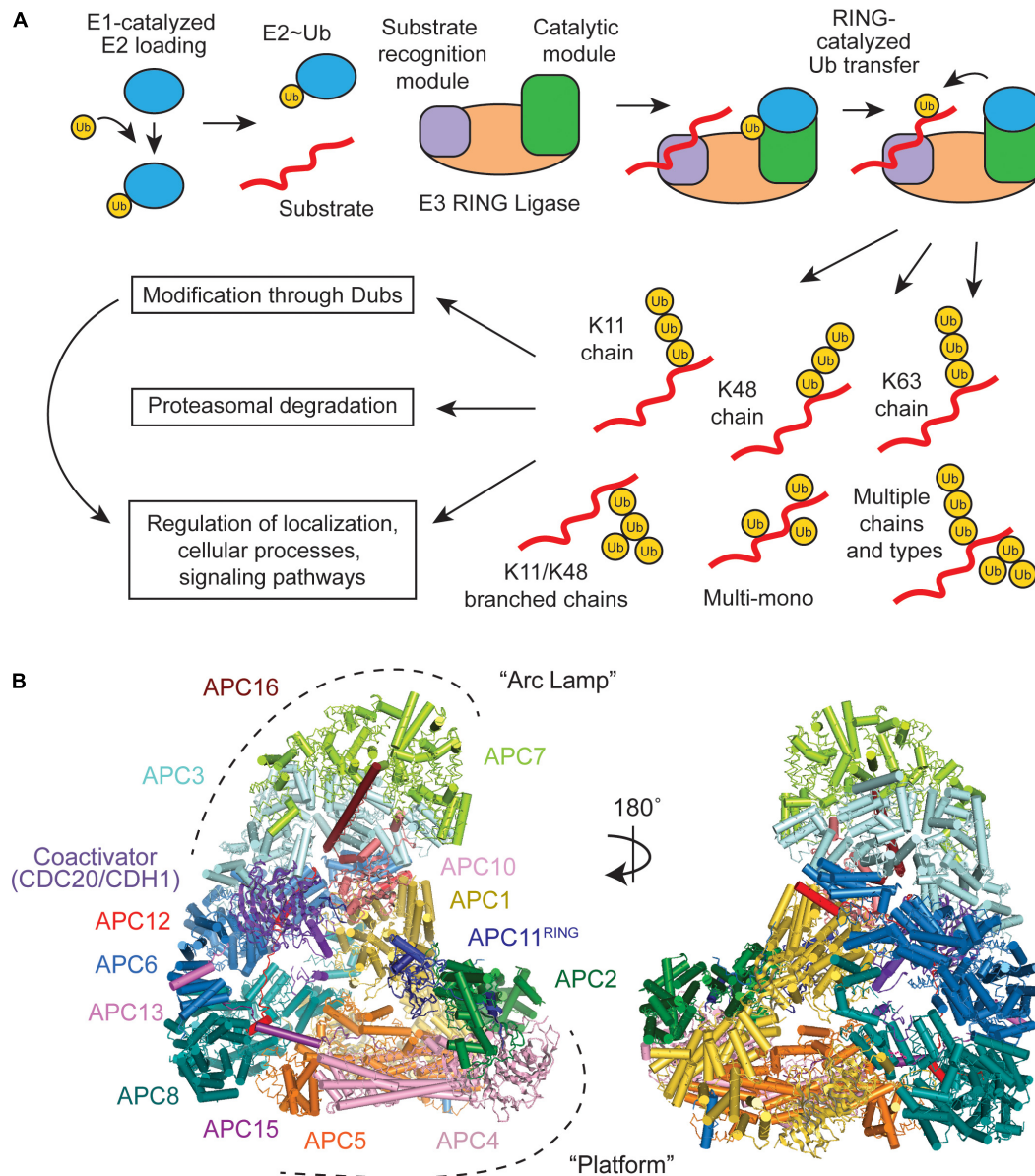


**FIGURE 1 |** Overview of a RING E3 Ub ligase mechanism and structural overview of the Anaphase-Promoting Complex/Cyclosome (APC/C). **(A)** Substrate ubiquitination occurs through an E1-E2-E3 cascade, with RING E3s containing both a receptor for recognizing substrates and catalytic domains that facilitate Ub transfer. Multiple E2 binding events result in an array of Ub chain types that have specific downstream effects. **(B)** The APC/C consists of 19 polypeptides, which can be broken down into two large subdomains, the "Arc Lamp" and the "Platform" (PDB ID code 5G04) (Zhang et al., 2016).

made up of TPR domain repeats (King et al., 1995; da Fonseca et al., 2011; Uzunova et al., 2012; Frye et al., 2013; Chang et al., 2014). Together, these subcomplexes work to facilitate and fine tune the APC/C's highly dynamic ubiquitination activities.

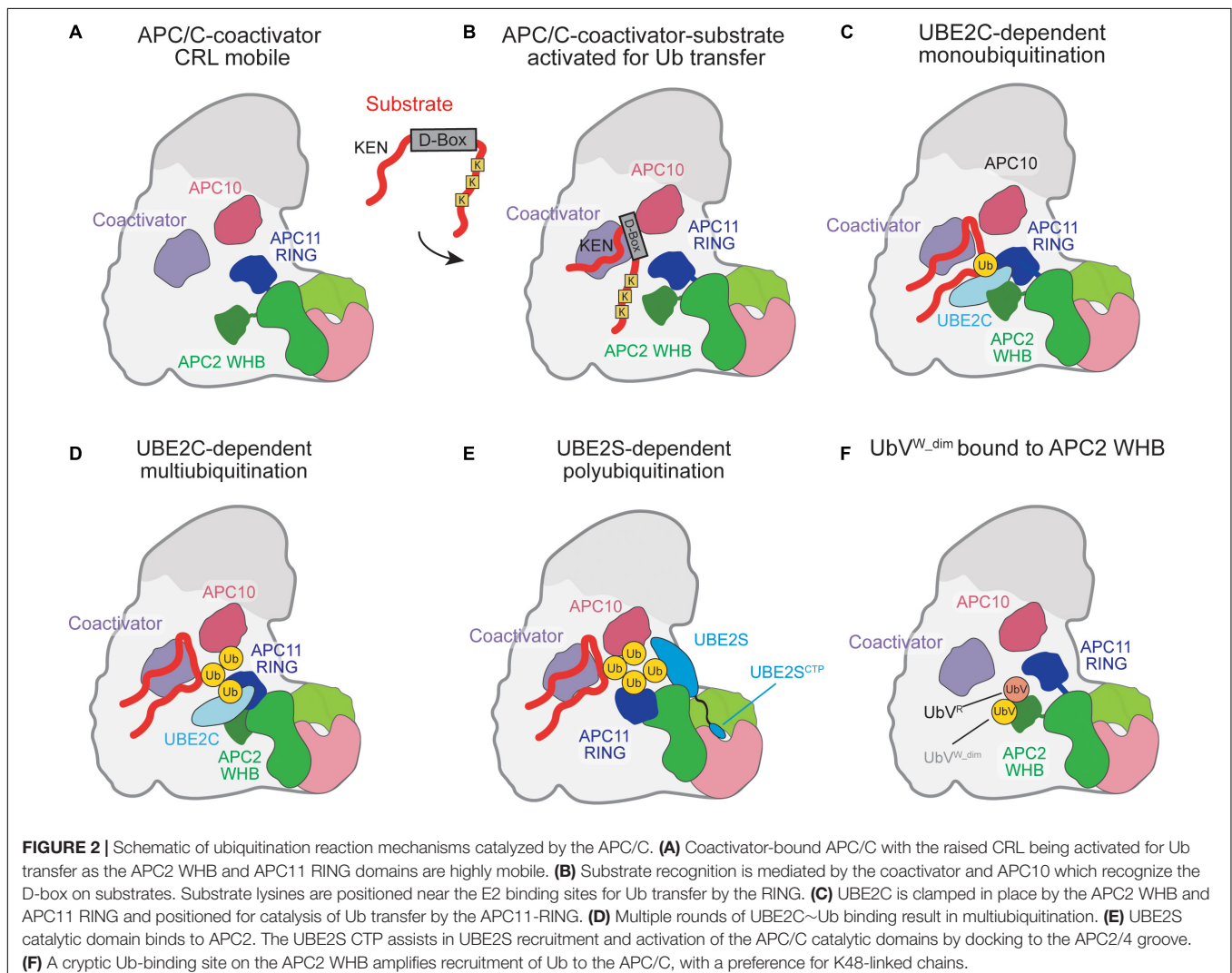
The recruitment of substrates to the APC/C and the positioning of its catalytic domains for ubiquitin transfer occur simultaneously through the binding one of two APC/C-specific coactivators, CDC20 or CDH1 (Visintin et al., 1997; Kraft et al., 2005; Buschhorn et al., 2011; da Fonseca et al., 2011; Chang et al., 2015). Binding of either coactivator to the APC/C occurs through sequences on their flexible N- or C-terminal domains,

with C-terminal Ile-Arg motifs (IR tail) that bind on APC3, and an N-terminal C-box motif recognized by APC8 (Kimata et al., 2008; Matyskiela and Morgan, 2009; Chang et al., 2014; Yamaguchi et al., 2015). Also important for substrate recognition is APC10, which also contains an IR tail that binds to the second APC3 dimer and was found to be important for both substrate recognition and processivity (Buschhorn et al., 2011; da Fonseca et al., 2011; Chang et al., 2014). The coactivators thus provide binding sites for recruited substrates by recognizing ABBA and KEN box motifs on substrates (reviewed in Davey and Morgan, 2016) or working in conjunction with APC10



to bind D-box sequences (**Figures 2A,B**; Buschhorn et al., 2011; da Fonseca et al., 2011; Chang et al., 2014). The binding of coactivators is cell-cycle dependent and mediated through phosphorylation (Lahav-Baratz et al., 1995; Visintin et al., 1997; Lukas et al., 1999; Kramer et al., 2000). CDH1 is inactivated through phosphorylation prior to metaphase onset, while Cyclin-dependent kinase (CDK) activity is high, and CDC20 is active during mitosis (Lukas et al., 1999; Kramer et al., 2000; Kernan et al., 2018). CDC20 recruitment to the APC/C is only allowed upon phosphorylation of APC1, which allows for APC3 to be phosphorylated and for the binding of the CDC20 IR tail (Kramer et al., 2000; Fujimitsu et al., 2016; Qiao et al., 2016; Zhang et al., 2016). CDH1, in turn, ensures CDC20 is inactivated in late mitosis-G1 through APC/C-dependent ubiquitination and through autoubiquitination (Visintin et al., 1997; Uzunova et al., 2012). In addition to the recognition, recruitment, and positioning of substrates near the active site, coactivator binding mobilizes the cullin-RING ligase (CRL) core for E2 recruitment and binding (**Figures 2A,B**; Yu et al., 1998; Tang et al., 2001; Chang et al., 2014, 2015; Li et al., 2016).

For substrate ubiquitination to occur, the APC/C utilizes a dual E2 mechanism where UBE2C initially primes the substrate with Ub and UBE2S extends K11-linked Ub chains (Sudakin et al., 1995; Aristarkhov et al., 1996; Yu et al., 1996; Garnett et al., 2009; Williamson et al., 2009; Wu et al., 2010; Wickliffe et al., 2011). In the complete absence of these well-established E2s, UBE2D/UBCH5 can also be used as the E2 (Wild et al., 2016). Detailed biochemical and structural studies have been performed to capture the multiple steps of ubiquitination by APC/C and its E2s. Upon CRL mobilization by the coactivators, UBE2C is grasped by the winged-helix B (WHB) and RING domains of APC2 and APC11, respectively, and positioned to transfer the Ub onto a substrate lysine (**Figure 2C**; Chang et al., 2014, 2015; Van Voorhis and Morgan, 2014; Brown et al., 2015; Li et al., 2016). In addition to substrate lysine modification, UBE2C can build short chains on substrate-linked Ub, catalyzing K11, K48, and K63 Ub chains (**Figure 2D**; Kirkpatrick et al., 2006; Dimova et al., 2012; Brown et al., 2015, 2016). Next, the Ub-conjugating domain (UBC) domain of UBE2S is activated for Ub transfer by a separate site on APC2, termed [UBE2S-interacting





(Si) helices] (Brown et al., 2014, 2016; Kelly et al., 2014). Instead of binding and activating UBE2S, as in UBE2C, the APC11 RING domain accommodates the substrate-linked acceptor Ub to receive the Ub from UBE2S~Ub (**Figure 2E**; Brown et al., 2014, 2016; Yamaguchi et al., 2016). To facilitate binding to the APC/C, UBE2S contains a C-terminal extension off its UBC that contains a positively charged peptide and binds in the groove formed between APC2 and APC4 (Williamson et al., 2009; Wickliffe et al., 2011; Chang et al., 2015; Brown et al., 2016; Yamaguchi et al., 2016).

Recent work has shown that the binding of the UBE2S C-terminal peptide (CTP) to the APC2/4 groove facilitates activation of the APC/C catalytic domain in a similar manner to coactivator binding to enhance the catalytic efficiency of UBE2C-dependent ubiquitination (Martinez-Chacin et al., 2020). Therefore, UBE2S facilitates a positive allosteric feedback mechanism to maximize substrate turnover by the APC/C. However, multiple questions remain about how the different APC/C subunits are repositioned for different modes of ubiquitination, how UBE2S is activated by the Si helices of APC2, and how branched Ub chains are formed.

While the substrate is still bound to the APC/C for Ub modification, the substrate-linked Ub has been shown to enhance processivity and substrate turnover rates (Lu et al., 2015; Brown et al., 2016). Ub binding to the APC11 RING domain, which positions the substrate-linked acceptor Ub for Ub-chain elongation by UBE2S, increases the binding affinity of the substrate and increases the processivity of the UBE2C-dependent reaction (Brown et al., 2016). A second, cryptic Ub-binding site was uncovered on the APC2 WHB using a tight-binding Ub variant (**Figure 2F**; Watson et al., 2019b). Interestingly, this binding site on the APC2 WHB is also utilized to position UBE2C and bind to a component of the inhibitory mitotic checkpoint complex (MCC). Therefore, this Ub-WHB interaction likely has multiple roles in regulating APC/C function during the cell cycle.

## THE APC/C AND ITS INHIBITORS

Canonical APC/C activity occurs in M and G1 phases, yet the APC/C is present throughout the cell cycle. The early mitotic inhibitor (EMI1) and the MCC both restrain APC/C function during the G1/S transition and the metaphase-anaphase transition, respectively (Hoyt et al., 1991; Li and Murray, 1991; Reimann et al., 2001b; Fang, 2002; Davenport et al., 2006; Miller et al., 2006; Burton and Solomon, 2007; Cappell et al., 2016). Both inhibitors attach to the APC/C at specific sites to selectively modulate substrate binding and Ub transfer by the E2s, and are regulated by ubiquitination-dependent degradation, releasing the APC/C from their inhibition.

### The Interphase APC/C Inhibitor EMI1

APC/C activity during interphase is regulated through several factors, including CDK-dependent phosphorylation, coactivator regulation, E2 degradation, and transcription of APC/C subunits (Kernan et al., 2018; Kataria and Yamano, 2019). One regulatory factor of note is EMI1, a protein that inhibits APC/C

activity during G1/S phase transition to allow sufficient cyclin accumulation for mitotic entry (Reimann et al., 2001a,b). Since its discovery in *Xenopus* embryos, the significance of EMI1 has been elevated through numerous cell-cycle and cancer biology studies, including a live cell imaging study where EMI1 was identified as a key “point of no return” step for cell cycle reentry by inactivating the APC/C at the G1/S boundary (Di Fiore and Pines, 2008; Shimizu et al., 2013; Barr et al., 2016; Cappell et al., 2016; Guan et al., 2016; Vaidyanathan et al., 2016; Marzio et al., 2019; Moustafa et al., 2021). Therefore, several biochemical and structural studies have uncovered how EMI1 tightly binds and shuts down APC/C activity.

Multiple domains of EMI1 cooperate together to block multiple steps of the ubiquitination mechanisms (**Figure 3A**). Reimann et al. initially characterized the mode of inhibition by EMI1 by mapping its domains to their effects on APC/C activity (Reimann et al., 2001b). Although EMI1 is an F-box containing protein that is 50 kDa in size, only its C-terminus (16 kDa) contains the domains that are expected to function in APC/C inhibition (Reimann et al., 2001b; Frye et al., 2013; Wang and Kirschner, 2013). Within its C-terminus, EMI1 contains a D-box motif, linker, zinc binding region (ZBR), and a C-terminal peptide (Reimann et al., 2001b; Miller et al., 2006; Frye et al., 2013; Wang and Kirschner, 2013; Chang et al., 2015). The early studies of EMI1-mediated APC/C inhibition focused primarily on the D-box and ZBR (Reimann et al., 2001b; Miller et al., 2006). For example, EMI1 becomes a D-box-dependent APC/C<sup>CDH1</sup> substrate upon ZBR inactivation, suggesting it functions as an APC/C<sup>CDH1</sup> pseudo-substrate inhibitor (Miller et al., 2006). However, the intricate and specific mechanism was not fully appreciated yet, as UBE2S had not been identified as the chain-elongating E2.

Subsequent ubiquitination and structural studies expanded on this complex mechanism of E3 ligase inhibition by providing specific inhibitory roles for the individual domains. First, low-resolution EM structures demonstrated that the EMI1 D-box binds to CDH1 and APC10, while the ZBR and rest of the C-terminus was bound to the APC/C catalytic core and platform (Frye et al., 2013; Wang and Kirschner, 2013). Second, while the D-box of EMI1 does inhibit APC/C-dependent ubiquitination by itself, it is comparatively weak, suggesting that additional domains are needed to effectively inhibit the APC/C (Frye et al., 2013). Third, a linker between the D-box and ZBR was identified (Frye et al., 2013). Together with the ZBR, the linker contributes to EMI1-dependent inhibition of UBE2C-mediated monoubiquitination (Frye et al., 2013; Wang and Kirschner, 2013). Lastly, the EMI1 C-terminal tail was found to have a similar sequence to the UBE2S C-terminus and is sufficient to inhibit UBE2S-mediated Ub-chain elongation (Frye et al., 2013; Wang and Kirschner, 2013). Removal of this sequence significantly impairs the inhibition constant of EMI1. Taken together with additional NMR and other biophysical studies that suggest that the EMI1 C-terminal domain is largely disordered, except for the ZBR, these EMI1 domains synergize for strong APC/C<sup>CDH1</sup> inhibition (Frye et al., 2013; Wang and Kirschner, 2013).

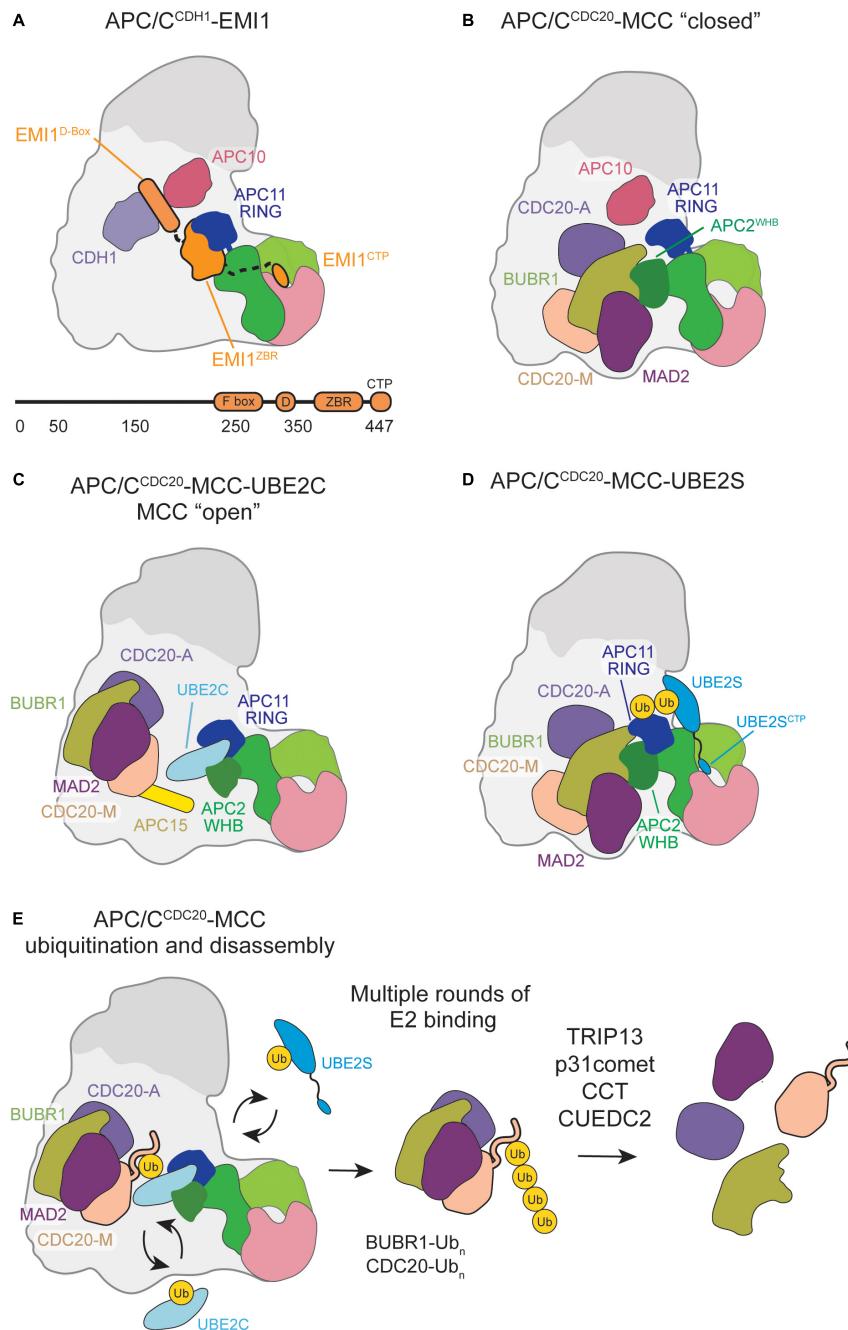


**FIGURE 3 |** Schematic of APC/C inhibition by EMI1 or MCC binding. **(A)** EMI1 binds in a multimodal fashion, the D-box binds at the CDH1-APC10 D-box receptor site, binds and immobilizes the APC11 RING, and contains a CTP similar to the UBE2S CTP that binds in the APC2/4 groove. **(B)** MCC bound to the APC/C in a “closed” conformation engages the APC2 WHB and CDC20<sup>A</sup>. **(C)** MCC transitions to an “open” conformation, allowing UBE2C to bind, and some substrates, such as Cyclin-A and NEK2A, to bypass MCC inhibition and be ubiquitinated by the APC/C. **(D)** MCC in the “closed” conformation permits UBE2S to bind, allowing for Ub chain elongation to occur. **(E)** Multiple rounds of E2 binding result in the polyubiquitination of several MCC subunits. CCT/TRIP13 and TRIP13-p31<sup>comet</sup> assist in the release CDC20 and MAD2, respectively, from MCC.

To fully understand the EMI1 inhibition mechanism, a high-resolution structure of the APC/C<sup>CDH1</sup>-EMI1 ternary complex was solved at 3.6 Å by cryo-EM (Chang et al., 2015). Through this structure, the multimodal APC/C<sup>CDH1</sup>-EMI1 interaction network was described in detail, and largely validated previous

biochemical studies. As expected, the EMI1 D-box engages D-box receptors CDH1 and APC10 (**Figure 3A**). The EMI1 linker regions are packed against the ZBR β-sheet and bind the APC2-APC11 catalytic domain, effectively blocking UBE2C binding to APC11 and the RING domain. On the APC/C Platform, the EMI1

C-terminal peptide binds APC2 adjacent to the APC4 WD40 region, blocking UBE2S binding.

Despite this structural and mechanistic understanding, several biological implications have yet to be described. For example, EMI1 has been shown to be a substrate of SCF<sup>TRCP</sup> and the APC/C itself (Margottin-Goguet et al., 2003; Eldridge et al., 2006; Cappell et al., 2018). Further mechanistic studies are needed to describe how ubiquitination events occur and how these different domains are potentially regulated to selectively permit different APC/C ubiquitination mechanisms and/or strip this tight binding inhibitor off the APC/C.

## The Mitotic Checkpoint Complex

The spindle assembly checkpoint (SAC) prevents the cell from transitioning to anaphase prior to complete chromosome bi-orientation by regulating APC/C activity (Hoyt et al., 1991; Li and Murray, 1991; Fang, 2002; Davenport et al., 2006; Burton and Solomon, 2007). Chromosome kinetochores that remain unattached to the spindle apparatus signal the assembly of the MCC—a 250 kDa complex comprised of BUBR1, CDC20, BUB3, and MAD2 that binds and inhibits APC/C (APC/C<sup>MCC</sup>) (Hoyt et al., 1991; Li and Murray, 1991; Fang, 2002; Davenport et al., 2006; Burton and Solomon, 2007). The signaling networks and underlying mechanisms behind MCC assembly during SAC activation are reviewed in Musacchio (2015). Additionally, recent studies have uncovered novel, multiplex interactions that facilitate MAD2 binding to CDC20—the initial, rate-limiting step of MCC assembly—through *in vivo* and *in vitro* work (Lara-Gonzalez et al., 2021; Piano et al., 2021).

A number of pioneering structural studies worked to understand the basic structure of MCC and its inhibition of APC/C. In *Schizosaccharomyces pombe* MCC, MAD2, and MAD3 (BUBR1 in human MCC) were shown to cooperatively bind and inhibit CDC20 through multiplex interactions (Chao et al., 2012). CDC20 and MAD2 primarily interact through the MAD2 safety belt latching onto the CDC20 MAD2-interacting motif while MAD3 coordinates the overall structure of the complex (Fang et al., 1998; Luo et al., 2000, 2004; Sironi et al., 2002; Yu, 2006; Yang et al., 2007; Luo and Yu, 2008; Kim et al., 2014; Rosenberg and Corbett, 2015; Singh et al., 2017). Once assembled, MCC is capable of inhibiting APC/C activity through a “closed” conformation that was first observed through low-resolution single-particle EM of APC/C isolated from SAC-arrested cells (Herzog et al., 2009). In the “closed” conformation, MCC blocks the APC/C central cavity, preventing substrate and UBE2C recruitment. However, this structural model lacked the resolution necessary to map APC/C<sup>CDC20</sup>-MCC interaction networks. Questions remained concerning the mechanisms behind MCC-mediated APC/C inhibition and MCC departure from the APC/C during checkpoint silencing.

For years, it was unknown how MCC leaves in a manner that maintains APC/C-CDC20 association to allow rapid modulation of APC/C<sup>CDC20</sup> activity in response to unattached kinetochores. Biological studies proposed that an MCC subcomplex comprised of BUBR1, BUB3, and CDC20 (BBC) was the main checkpoint effector. The BBC would negate the need to disrupt the complex CDC20-MAD2 interactions required for MAD2 departure and

CDC20's continued association to APC/C. In response, it was suggested that APC/C<sup>MCC</sup> contains two CDC20 molecules, both bound by BUBR1 at either of its two KEN boxes (Primorac and Musacchio, 2013). Biochemical studies confirmed this hypothesis, which showed that recombinant MCC can bind a second CDC20 associated with the APC/C (Izawa and Pines, 2015). MCC contains a CDC20 molecule (CDC20<sup>M</sup>) that binds the BUBR1 KEN1-box. Through the BUBR1 KEN2-box, the MCC may associate with a CDC20 molecule bound to APC/C (CDC20<sup>A</sup>) as a coactivator. This APC/C<sup>MCC</sup> binding configuration would be further confirmed and characterized by high-resolution structural studies mapping APC/C<sup>MCC</sup> interaction and identifying novel conformational states that allow checkpoint silencing.

Through recombinant cryo-EM structures of APC/C<sup>MCC</sup>, MCC was shown to capture key interfaces and domains critical for APC/C activity in the “closed” conformation (Figure 3B; Alfieri et al., 2016; Yamaguchi et al., 2016). CDC20<sup>M</sup> and CDC20<sup>A</sup> interact through their WD40 domains. BUBR1 stabilizes this dual-CDC20 interaction by contacting both CDC20 subunits with its KEN1 box, KEN2 box, D-box, and tetratricopeptide repeat (TPR) domains. Such interactions disrupt the CDC20<sup>A</sup> degron binding sites necessary for APC/C substrate recognition. In contrast, MAD2 solely interacts with MCC subunits BUBR1 and CDC20<sup>M</sup>, which potentially stabilizes their respective interactions with CDC20<sup>A</sup>. Additionally, MCC sterically blocks UBE2C binding within the APC/C central cavity predominantly through BUBR1, whose TPR domain directly interacts with the APC2<sup>WHB</sup>. Overall, key APC/C<sup>MCC</sup> interactions in the “closed” conformation prevent substrate recognition and UBE2C ubiquitination activity to accomplish checkpoint-mediated anaphase inhibition.

Both high-resolution structural studies identified a previously undiscovered APC/C<sup>MCC</sup> “open” conformation in which CDC20<sup>A</sup> remains in contact with BUBR1 and CDC20<sup>M</sup> to prevent substrate recognition (Figure 3C; Alfieri et al., 2016; Yamaguchi et al., 2016). However, the BUBR1<sup>TPR</sup>-APC2<sup>WHB</sup> interface is disrupted and MCC is rotated away from the APC11 RING domain to allow UBE2C binding within the central cavity. During this conformational change, the APC15 N-terminal helix becomes ordered and makes key interactions with APC4 and APC5 to stabilize the “open” conformation (Uzunova et al., 2012; Alfieri et al., 2016; Yamaguchi et al., 2016). UBE2C binding to the “open” APC/C<sup>MCC</sup> results in UBE2C active site positioning toward CDC20<sup>M</sup>, potentially facilitating ubiquitination necessary for MCC departure.

While UBE2C is impacted by the APC/C<sup>MCC</sup> “closed”/“open” transition, UBE2S is not. Previous biochemical work showed that UBE2S escapes this SAC regulatory feature, which was hypothesized to be due to non-canonical UBE2S binding at an APC11 RING exosite (Brown et al., 2014, 2016; Kelly et al., 2014). APC/C<sup>MCC</sup> structures crosslinked with a UBE2S-Ub variant (UBv) conjugate confirmed UBE2S placement adjacent to the APC2 and APC11 subunits away from the central cavity and MCC inhibition (Figure 3D; Yamaguchi et al., 2016).

Several proteins have been implicated in SAC silencing through facilitating MCC disassembly. The AAA-ATPase



TRIP13, its binding partner p31<sup>comet</sup>, and the chaperonin CCT/TRIC facilitate disassembly of free MCC in a multistep process (Eytan et al., 2014; Wang et al., 2014; Miniowitz-Shemtov et al., 2015; Kaisari et al., 2017; Alfieri et al., 2018). P31<sup>comet</sup> binds and recruits MCC to TRIP13 through the MAD2 subunit (Miniowitz-Shemtov et al., 2015; Alfieri et al., 2018). This recruitment allows TRIP13 to trigger a conformational change in MAD2, catalyzed through TRIP13 ATPase activity, and promote MAD2 dissociation from CDC20 (Miniowitz-Shemtov et al., 2015; Alfieri et al., 2018). CCT/TRIC works to further disassemble MCC subcomplexes lacking MAD2, thereby completing the disassembly pathways of free MCC (Kaisari et al., 2017). Whether these SAC silencing effectors also promote MCC departure from APC/C remains to be seen, though one silencing effector has been linked to APC/C-MCC disassembly. A biological study found that the CUE-domain protein CUEDC2 promotes the departure of MAD2 from APC/C<sup>MCC</sup> through direct interactions with CDC20 (Gao et al., 2011). However, this functionality was discovered prior to our understanding that two CDC20 molecules exist in APC/C<sup>MCC</sup>, and there have yet to be biochemical or structural studies conducted to elucidate CUEDC2-mediated APC/C-MCC disassembly mechanisms. Therefore, much remains to be uncovered regarding the roles and mechanisms of SAC silencing effectors on APC/C<sup>MCC</sup> regulation.

Though structurally resolved, the “closed” and “open” APC/C<sup>MCC</sup> conformational dynamics during checkpoint silencing raise questions surrounding MCC departure. The “open” conformation is necessary for UBE2C-mediated ubiquitination to trigger MCC release and relieve APC/C inhibition, yet this conformation comprises only a small subset of the APC/C<sup>MCC</sup> population in structural studies. Further work is required to determine the dynamics of this conformational change and how it may be influenced by effector proteins during checkpoint silencing to promote rapid APC/C activation. Additionally, the order in which MCC subunits dissociate from the APC/C and how various SAC effector proteins influence this process remains elusive (Figure 3E).

## RECENT STUDIES REVEAL HOW CERTAIN SUBSTRATES ESCAPE MITOTIC CHECKPOINT INHIBITION

While the SAC is capable of preventing most APC/C<sup>CDC20</sup>-mediated substrate degradation, there are APC/C substrates capable of bypassing this inhibitory mechanism. The privileged ubiquitination of Cyclin A and NEK2A during an active checkpoint presented a multitude of questions regarding what molecular and regulatory factors determine the timing of substrate ubiquitination (den Elzen and Pines, 2001; Hames et al., 2001; Hayes et al., 2006; Di Fiore and Pines, 2010; Wieser and Pines, 2015). Recent high-resolution structures of these two substrates bound to APC/C<sup>MCC</sup> identified unique binding modes that proposed mechanisms by which Cyclin A and NEK2A are able to escape SAC regulation.

## Cyclin A

Cyclin A promotes microtubule detachment from kinetochores during prometaphase, allowing error correction during chromosome bi-orientation and faithful sister chromatid segregation (Kabeche and Compton, 2013). However, persistent cyclin A activity prevents complete bi-orientation, requiring cyclin A stability to be regulated for mitotic progression (den Elzen and Pines, 2001; Kabeche and Compton, 2013). Interestingly, Cyclin A degradation begins in prometaphase after Cyclin B-CDK2 activation in a proteasome- and APC/C-dependent manner, though the SAC is active (den Elzen and Pines, 2001).

Biochemical studies sought to understand how Cyclin A ubiquitination is allowed during an active checkpoint. Cyclin A binding to the APC/C was found to depend on several key interactions. First, Cyclin A associates with Cks, which binds phosphorylated sites on APC/C (Di Fiore and Pines, 2010). Once bound, the Cyclin A N-terminus binds the CDC20 WD40 domain regardless of MCC, and therefore, regardless of checkpoint activation (Di Fiore and Pines, 2010). However, the molecular mechanisms behind this competition and the role of Cks remained unknown in the absence of a structural view of APC/C<sup>MCC</sup> bound to a CDK-Cyclin A-Cks complex.

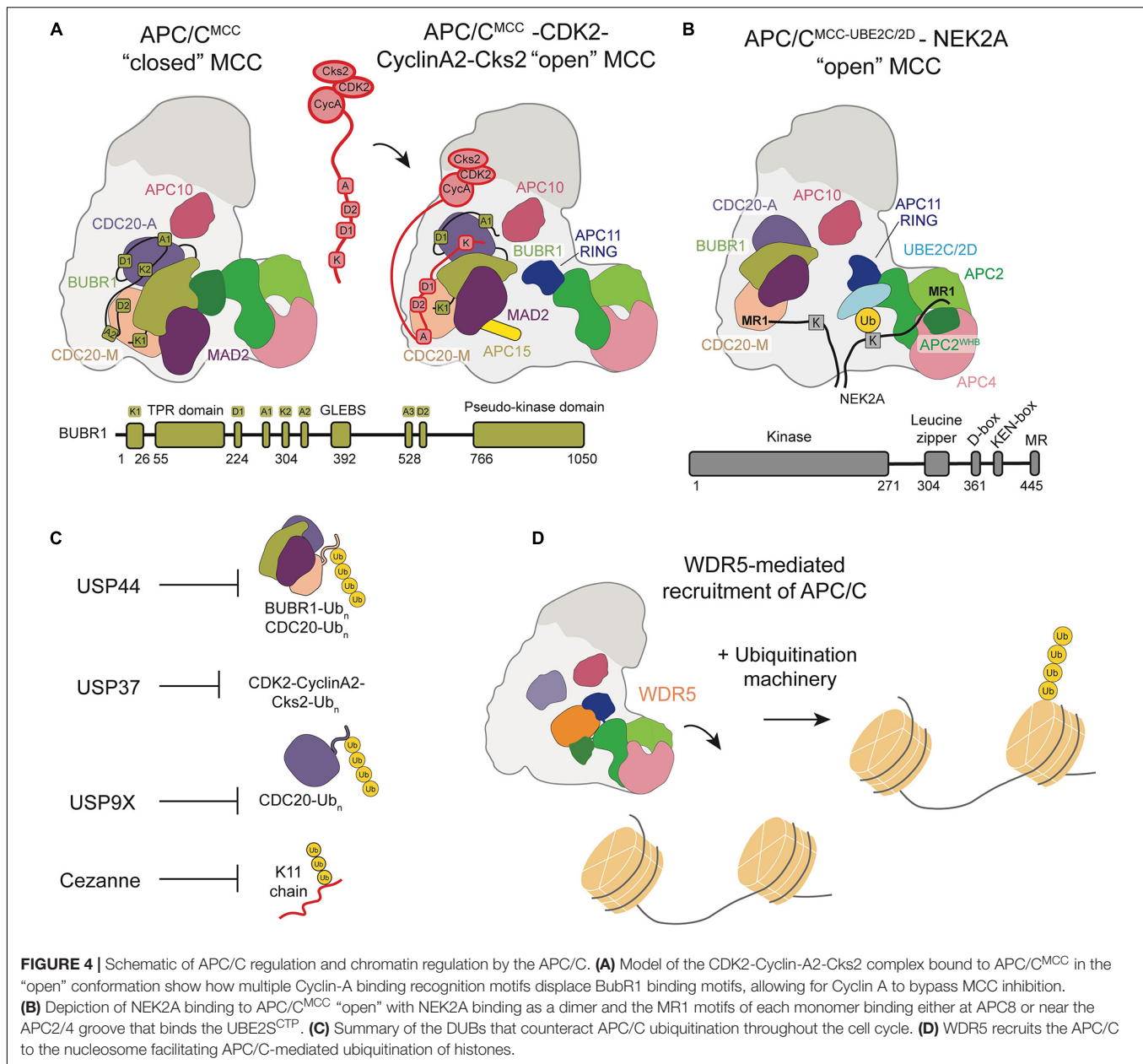
Recently, a high-resolution structure of Cyclin A bound to APC/C<sup>CDC20</sup>, Cks, and CDK2 identified a non-canonical, highly conserved D-box (D2-box) on Cyclin A (Zhang et al., 2019). The canonical D1-box and non-canonical D2-box display differential binding with CDC20 and APC10, resulting in unique, cooperative interactions between the Cyclin A KEN box and ABBA motif and APC/C<sup>CDC20</sup>. Through its distinct binding mode, the Cyclin A D2-box directs more efficient Cyclin A ubiquitination than the canonical D1-box. A subsequent structure of APC/C<sup>MCC</sup> bound to Cyclin A-CDK2-Cks2 proposed a mechanism by which Cyclin A circumvents MCC inhibition of the APC/C through multiple, disruptive interactions (Figure 4A). The Cyclin A D2-box and ABBA motif compete for CDC20<sup>M</sup> binding with BUBR1<sup>ABBA</sup>. The Cyclin A KEN-box also competes with BUBR1<sup>KEN</sup> for interactions with CDC20<sup>A</sup>, allowing Cyclin A to displace BUBR1 from APC/C<sup>CDC20</sup>. This cooperative interaction network is further stabilized by CDK and Cks, which bind both Cyclin A and phosphorylated APC/C sites.

Overall, the privileged ubiquitination of Cyclin A suggests the importance of substrate motifs and their avidity to the E3 ligase relative to regulatory factors in determining the timing and efficiency of substrate ubiquitination. Interestingly, Cyclin A was found to promote the APC/C<sup>MCC</sup> “open” conformation, potentially to allow Cyclin A ubiquitination and degradation (Zhang et al., 2019).

## NEK2A

The kinetochore-associated NIMA-related kinase 2A (NEK2A) is able to evade APC/C inhibition by an active SAC to undergo ubiquitination and proteasomal degradation. Hames et al. first observed NEK2A degradation in early mitosis in an APC/C- and proteasome-dependent manner (Hames et al., 2001). Similar





to canonical APC/C substrates, NEK2A contains a D-box and a KEN-box, as well as a suggested Cyclin A-like D-box motif at its extreme C-terminus. Domain-mapping biochemical studies proposed molecular mechanisms by which NEK2A ubiquitination and destruction may escape SAC-mediated inhibition of APC/C.

Though the KEN box and ABBA motif were found to contribute to NEK2A ubiquitination, two structural features proved to be essential for NEK2A interactions with APC/C. Biochemical studies largely focused on the NEK2A C-terminal motif, which contains a Met-Arg (MR) dipeptide that allows NEK2A to bind apo-APC/C, potentially through TPR domains on APC6 and APC8 (Hayes et al., 2006). This binding mode is in contrast to Cyclin A, which primarily interacts with CDC20.

Additionally, NEK2A contains a leucine zipper region that allows dimerization and contributes to APC/C-recognition, though the mechanism of this contribution was unclear. Though NEK2A may bind apo-APC/C, its degradation is delayed until the arrival of CDC20 and is insensitive to the presence of MCC (Boekhout and Wolthuis, 2015). These observations lacked a structural view to propose a mechanism by which NEK2A is able to escape SAC regulation.

A recent study sought to determine how NEK2A binds APC/C<sup>MCC</sup> for ubiquitination during an active checkpoint by generating a high-resolution structure of NEK2A-APC/C<sup>MCC</sup> (Alfieri et al., 2020). Through refinement of previously determined 3D models, Alfieri et al. discovered that the CDC20<sup>M</sup> IR tail dissociates from its APC8 binding site in the

“open” APC/C<sup>MCC</sup> conformation (Alfieri et al., 2016; Alfieri et al., 2020). This structural change would allow NEK2A to bind APC8 with its MR tail, in agreement with previous studies suggesting the importance of TPR-containing APC/C subunits (**Figure 4B**). As a dimer, NEK2A contains two MR tails. The binding site of the second MR tail was identified in a pocket formed by APC2<sup>WHB</sup>, APC2, and APC4<sup>WD40</sup>, potentially ordering the WHB domain to force an active APC/C configuration for NEK2A ubiquitination. Based on these observations, Alfieri et al. hypothesize that NEK2A promotes the “open” APC/C<sup>MCC</sup> conformation by displacing the CDC20<sup>M</sup> IR tail from APC8 and disrupting BUBR1-WHB binding. NEK2A is able to position the WHB domain 60 Å from its position in the “closed” conformation, prioritizing NEK2A ubiquitination rather than MCC-mediated inhibition.

Overall, current structural studies have uncovered the molecular mechanisms by which Cyclin A and NEK2A are able to evade MCC regulation and undergo APC/C-mediated ubiquitination. However, additional questions remain regarding interactions between these privileged substrates and E2 enzymes. It has been shown that NEK2A is more efficiently ubiquitinated by UBE2D than UBE2C, while the opposite is true for Cyclin A (Zhang et al., 2019; Alfieri et al., 2020). Further structural studies are needed to fully characterize substrate-E2 combinations. Together with current models of substrate-APC/C binding modes, such information will help uncover how the timing of substrate ubiquitination by the APC/C is controlled, with potential implications across E3 ligases.

## DUBS THAT ANTAGONIZE APC/C FUNCTION

The complexity of substrate ubiquitination and APC/C inhibition mechanisms are further compounded by the antagonism of deubiquitinase enzymes (DUBs). DUBs cleave Ub chains from substrates and can therefore prevent degradation. Four DUBs were identified to specifically antagonize APC/C-mediated ubiquitination and degradation of substrates: USP44, USP37, USP9X, Cezanne/OTUD7B (**Figure 4C**). These DUBs work in opposition to the APC/C to regulate cell cycle progression.

Drugs that disrupt the mitotic spindle, including taxol, nocodazole and vincristine, disrupt kinetochore-microtubule attachments and maintain active spindle checkpoint signaling, thus restraining APC/C activation. In a search for DUBs that might regulate cell division, Stegmeier et al. (2007) used RNAi to screen for genes whose loss caused a bypass of mitotic arrest in the presence of taxol. This analysis identified the ubiquitin specific protease, USP44. They showed that USP44 antagonizes the ubiquitination of the MCC (**Figure 4C**). Importantly, MCC ubiquitination leads to spindle checkpoint silencing. Thus, in the absence of USP44, MCC ubiquitination is increased and the ability of the complex to restrain cell division is lost. This study represented the first identification of a DUB linked to APC/C function.

Despite the ability of EMI1 to potently inhibit interphase APC/C, it was later noted that not all APC/C<sup>CDH1</sup> is associated

with EMI1 during G2 phase. This raised the question as to how APC/C substrates remain stable prior to mitosis. Huang et al. hypothesized that an additional mechanism of APC/C<sup>CDH1</sup> inactivation functions to prevent degradation of APC/C<sup>CDH1</sup> substrates after G1 phase (Miller et al., 2006; Bassermann et al., 2008; Huang et al., 2011). Specifically, the presence of a DUB could prevent degradation of APC/C substrates while maintaining a pool of APC/C available to be activated. They identified interactions between USP37 and CDH1, as well as APC/C subunits, implicating USP37 in the regulation of the G1/S transition and characterized the cell cycle regulation of USP37 (**Figure 4C**). Based on this study, Huang et al. describe a model where USP37 is transcribed in late G1 and the resulting protein antagonizes APC/C-mediated ubiquitination of Cyclin A, resulting in accumulation of Cyclin A which then promotes progression to S phase (Huang et al., 2011). Cyclin A accumulation activates CDK2, which also phosphorylates USP37 to positively reinforce its catalytic activity. As cells progress to mitosis, Cyclin A is inactivated and APC/C is activated, at which point USP37 switches from an antagonist of APC/C ubiquitination and is itself ubiquitinated by the APC/C and degraded. This prevents USP37 from antagonizing APC/C substrate degradation. This study demonstrates the role of a DUB in regulating the G1/S transition by opposing APC/C activity through its interaction with Cyclin A. USP37 has also been linked to the regulation of other cell cycle proteins, including Cdt1 and WAPL (Yeh et al., 2015; Hernandez-Perez et al., 2016). Interestingly, USP37 is also a substrate of SCF-type ubiquitin ligases, and this too is cell cycle regulated (Burrows et al., 2012).

The role of the APC/C in promoting progression from metaphase to anaphase during mitosis was also found to be antagonized by the DUB USP9X. Skowyra et al. (2018) showed that USP9X strengthens the SAC by antagonizing APC/C ubiquitination of CDC20, which represents a critical point of regulation to prevent chromosomal instability. During mitosis, the SAC prevents progression to anaphase until all chromosomes are properly attached to microtubules. Until this occurs, the MCC is continuously assembled, of which CDC20 is a component (Lischetti and Nilsson, 2015; Musacchio, 2015). APC/C-mediated CDC20 autoubiquitination results in MCC turnover (Uzunova et al., 2012; Izawa and Pines, 2015; Alfieri et al., 2016; Yamaguchi et al., 2016). The synthesis of new MCC compensates for MCC turnover until all chromosomes are prepared for anaphase. This regulation is very sensitive, although the molecular mechanism for the sensitivity remained unknown until Skowyra et al. investigated the possibility that a DUB opposing APC/C activity could contribute to this phenomenon (Skowyra et al., 2018). They demonstrated that USP9X depletion causes premature mitotic progression in the presence of the microtubule poison nocodazole and that it antagonizes APC/C-mediated ubiquitination of CDC20 (**Figure 4C**). Additionally, they showed that USP9X depletion increases the degradation of CDC20 and leads to bypass of SAC arrest, resulting in chromosomal instability. Thus, USP9X plays an important role in regulating appropriate chromosome segregation and genome stability during mitosis by antagonizing ubiquitination by the APC/C.

An additional DUB opposing ubiquitination by the APC/C was identified by our labs (Bonacci et al., 2018). In a search for K11 linkage specific DUBs, it was confirmed that Cezanne/OTUD7B specifically cleaves K11-linked ubiquitin chains. Notably, Cezanne is itself a strongly cell cycle regulated (Figure 4C; Bremm et al., 2010; Mevissen et al., 2016). Our work demonstrated that Cezanne levels peak during mitosis, in concert with APC/C activity, and that Cezanne specifically interacts with, deubiquitinates, and opposes the degradation of APC/C substrates, including Aurora A and Cyclin B (Bonacci et al., 2018). The functional consequence of Cezanne activity was shown by experiments in which Cezanne depletion resulted in mitotic progression errors and micronuclei formation. This study, along with those previously discussed, indicate key roles for DUBs that specifically oppose APC/C-mediated ubiquitination in regulating proper cell cycle progression. Future studies may identify additional roles and substrates of cell cycle-regulated DUBs. Determining how these DUBs, and perhaps others, coordinate with each other to regulate the kinetics of substrate degradation represents an important area of future investigation.

## APC/C REGULATES CHROMATIN

Chromatin experiences many dynamic changes during the cell cycle, most notably genome replication during S phase and chromosome condensation and segregation during mitosis. Additionally, subsets of genes are transcribed in a cell cycle-dependent manner (Whitfield et al., 2002; Bar-Joseph et al., 2008; Grant et al., 2013; Pena-Diaz et al., 2013). The promoters and enhancers of these genes must be available for binding by transcriptional machinery which requires changes in chromatin structure at these loci during the cell cycle. While aspects of chromatin organization are coordinated with cell cycle progression, the APC/C was only recently identified to play a role in this regulation. The following studies demonstrated direct interactions between the APC/C and nucleosomes, as well as with DNA itself. These observations show new biological functions of APC/C and raise additional questions about the interactions between chromatin and the APC/C.

The fundamental unit of chromatin structure is the nucleosome, consisting of a core octameric subunit of histone proteins around which the DNA double-helix is wound (Luger et al., 1997). Nucleosomes play a role in compacting DNA, but also serve as a key point of signal integration, as many proteins interact with various components of the nucleosome structure to affect local genome accessibility, among other functions (Kouzarides, 2007; Struhl and Segal, 2013). As part of a study to identify the nucleosome interaction network and establish principles for nucleosome-binding proteins, Skrajna et al. (2020) observed multiple protein components of the APC/C bound to the nucleosome by mass spectrometry. Direct binding of the APC/C to the nucleosome was also established, suggesting the possibility that the APC/C may play a fundamental role in nucleosome ubiquitination.

Oh et al. (2020) published a study at a similar time demonstrating a functional role for the APC/C at nucleosomes by showing the ubiquitination of histones by the APC/C in human embryonic stem cells. They identified the APC/C as a potential integrator of cell division and the pluripotency transcriptional program. This transcriptional program is essential to maintaining stem cell identity, but transcription is generally downregulated during mitosis, bringing into question the mechanism by which cells are able to transcribe pluripotency factors immediately following cell division to maintain stem cell identity (Prescott and Bender, 1962; Young, 2011). Oh et al. (2020) demonstrated that the chromatin-associated factor WDR5 recruits the APC/C to the promoters of pluripotency genes marked by stem cell specific transcription factors during mitosis. K11/K48 branched ubiquitin chains, a hallmark of APC/C function, on histones were identified at these promoter regions and shown to be targeted for degradation by the proteasome. Based on this study, they proposed a mechanism in which WDR5 binds promoters of pluripotency genes during interphase and remains bound as cells enter mitosis, at which point the APC/C is recruited to transcription start sites and ubiquitinates histones (Figure 4D). An EM structure of WDR5 bound to the APC/C revealed that WDR5 is bound to the catalytic core APC2-APC11. This structure suggests that WDR5 would have to leave the APC/C for APC/C and its E2s to ubiquitinate the nucleosome, or another unexpected catalytic architecture must be formed. After ubiquitination, the histones are degraded by the proteasome to maintain an open chromatin structure at gene promoters, allowing the transcription of pluripotency genes immediately after the completion of mitosis. This study characterizes a functional role of APC/C interaction with nucleosomes, implicating the APC/C as a regulator of chromatin organization and pluripotency.

An additional study by Mizrak and Morgan (2019) implicated binding of the APC/C to polyanions, including nucleic acid polymers which are components of nucleosomes, as a mechanism to regulate the dissociation of CDC20 and CDH1 from the APC/C. Using lysates from *Saccharomyces cerevisiae* to perform *in vitro* experiments, they show that single-stranded DNA and RNA of about 75 base pairs, as well as polyphosphate species, promote the dissociation of CDC20 and CDH1 from the APC/C. However, the polyanions lose their ability to promote coactivator dissociation when the APC/C is bound to a substrate with high affinity for the complex. Their proposed mechanism described the interaction between the APC/C and polyanions as a way to promote ubiquitination of high-affinity substrates, while reducing the ubiquitination of low-affinity substrates by causing the dissociation of the coactivator from the APC/C. From this conclusion, they hypothesized that polyanion binding could interact with the APC/C at sites adjacent to the coactivators. However, additional studies are required to validate this hypothesis. Confirmation of this model would indicate a new functional interaction between the APC/C and nucleic acids, suggesting that coactivator dissociation could be another point of regulation of APC/C activity and affect how the DNA-wrapped nucleosome is ubiquitinated.



The APC/C was further implicated in the regulation of chromatin biology with the identification of novel APC/C substrates (Franks et al., 2020). Franks et al. (2020) used an *in silico* approach to identify novel APC/C<sup>CDH1</sup> substrates based on two criteria shared by many known APC/C<sup>CDH1</sup> substrates. The first was the presence of a KEN-box degron. The second criterion was that the gene encoding for the protein is transcribed in a cell cycle-dependent manner, as identified in cell cycle transcriptome studies, based on RNA-sequencing and microarrays. These criteria identified 145 proteins, including many previously identified APC/C<sup>CDH1</sup> substrates. The resulting candidate substrates were enriched for GO processes related to chromatin biology. Several candidates were shown to oscillate during the cell cycle, to be degraded when the APC/C is activated, and to co-immunoprecipitate with CDH1, including histone modification writers UHRF1 and TTF2, and the chromatin assembly factor CHAF1B. The ubiquitination of these proteins was previously reported in independent studies (Kim et al., 2011; Elia et al., 2015). We further characterized the mechanism and functional consequence of degradation of UHRF1, a chromatin regulator involved in histone ubiquitylation and maintenance of DNA methylation (Bostick et al., 2007). We demonstrated that disruption of UHRF1 degradation by the APC/C at mitotic exit results in altered DNA methylation patterns across the genome and accelerated progression through G1 phase. This study describes several novel APC/C substrates involved in the regulation of chromatin biology and shows that proper degradation of UHRF1 is important for chromatin biology and for cell cycle progression.

These recent studies indicate that the APC/C regulates aspects of chromatin biology in addition to its role in promoting mitotic progression. Cyclin-dependent kinases (CDKs) were also recently implicated in regulation of chromatin biology with the identification of novel CDK substrates responsible for regulating the epigenetic landscape (Chi et al., 2020; Michowski et al., 2020). Thus, it is likely that chromatin biology is broadly regulated by multiple components of the cell cycle machinery. Future work may identify additional enzyme-substrate relationships connecting these two areas of biology and may elucidate the functional consequences of these interactions.

## DISCUSSION

Understanding how cells orchestrate a delicate balance between protein accumulation and degradation remains a significant challenge. Various rules have been suggested previously. For example, processive substrates, substrates that are highly ubiquitinated in a single binding event, are degraded faster when compared to distributive substrates, i.e., substrates that require multiple binding events to build a proteasome degradation signal (Rape et al., 2006; Buschhorn et al., 2011; Meyer and Rape, 2011; Williamson et al., 2011; Lu et al., 2015). However, the molecular description of this rule and others remains largely uncharacterized. Key questions remain: What makes an APC/C substrate processive—cooperativity between the degrons, lysine accessibility, catalytic rate of ubiquitination, or a combination?

How do multiple ubiquitination mechanisms synergize for accurate cell cycle timing? Given the diversity of APC/C substrates, additional mechanisms are likely to be uncovered. For example, we likely do not know if a certain set of substrates is critically dependent on UBE2S or how the ubiquitination mechanism is altered for the autoubiquitination of CDH1 and its E2s. In addition to post-translational modifications, e.g., phosphorylation and sumoylation, on the APC/C, substrates can also be phosphorylated to alter their degradation rate, but the mechanistic basis for this regulation is unknown (Min et al., 2013; Lu et al., 2014; Davey and Morgan, 2016; Eifler et al., 2018; Lee et al., 2018). To further complicate this process, DUBs fine tune the ubiquitin code by editing or completely removing Ub chains, extending the lifetime of a protein. The ~100 DUBs can vary dramatically in their mechanism, Ub linkage specificities, cellular localization, post-translational modifications, and regulation (Mevisen and Komander, 2017). However, how specific DUBs are cell-cycle regulated or specifically antagonize APC/C function remains unclear.

The timing of cell cycle events is directly coupled to changes in the transcription of several hundred genes by chromatin regulation (Bannister and Kouzarides, 2011; Struhl and Segal, 2013; Ma et al., 2015). Moreover, the chromatin landscape is broadly altered during cellular quiescence, a reversible state of growth arrest and terminal differentiation (Buttitta et al., 2010; Everitt et al., 2013; Ma et al., 2015, 2019). However, the mechanisms underlying these dynamics are largely unknown. The recent data discussed above, and other previous studies, suggest that the APC/C is a significant regulator of cell cycle transcription and chromatin changes. First, the APC/C regulates cell cycle transcription factors, namely FOXM1 and E2F1 (Laoukili et al., 2008; Park et al., 2008; Peart et al., 2010; Ping et al., 2012). Second, the APC/C controls the levels of cell cycle transcriptional repressors, most notably, the atypical repressors E2F7 and E2F8 (Cohen et al., 2013; Boekhout et al., 2016). Third, the APC/C ubiquitinates chromatin modifying enzymes, including UHRF1 (Franks et al., 2020). Lastly, the APC/C directly ubiquitinates histones (Oh et al., 2020). Together, this places the APC/C at the center of proliferative control via the coordination of chromatin dynamics and gene expression.

These observations support the notion that activation of the APC/C acts as a molecular reset switch for proliferative transcriptional programs. APC/C activation can be thought of as the final weight, that when added to a scale, brings the cell back to a point where several proliferative signals are near zero. This reset happens through the inactivation of mitotic CDKs, as well as inactivation of transcriptional and chromatin programs (Guardavaccaro and Pagano, 2006; Skaar and Pagano, 2008; Buttitta et al., 2010; Ma et al., 2015, 2019). Interestingly, we normally consider these changes as being governed by the retinoblastoma (RB) family of transcriptional repressors (Guardavaccaro and Pagano, 2006). However, expression of the APC/C substrate UHRF1 in G1 phase, using a degradation-resistant allele, increases the expression of E2F targets, including cyclin E and E2F1 (Franks et al., 2020). These observations suggest that the regulation of chromatin proteins by APC/C-mediated destruction is indirectly linked to the expression of cell



cycle transcriptional programs. Furthermore, previous studies showed that a non-degradable FOXM1 protein is sufficient to promote S-phase entry (Laoukili et al., 2008; Park et al., 2008). Together, these observations suggest that the destruction of many substrates by the APC/C is necessary to restrain the cell cycle. These findings are consistent with the significantly shortened G1-phase observed in CDH1-KO cells and the ability of CDH1 to suppress tumorigenesis in mice (Garcia-Higuera et al., 2008; Sigl et al., 2009).

There is significant cross talk between RB and APC/C pathways in restraining G1/S (Guardavaccaro and Pagano, 2006; Kernan et al., 2018; Emanuele et al., 2020). This relationship is particularly evident in the regulation of SKP2, which is both an E2F target gene and an APC/C substrate (Carrano et al., 1999; Tsvetkov et al., 1999; Bornstein et al., 2003; Bashir et al., 2004; Assoian and Yung, 2008; Yuan et al., 2014). In this example, the accumulation of SKP2 leads to the destruction of cyclin-dependent kinase inhibitors (CKIs), resulting in the activation of cyclin E/CDK2 complexes that drive S-phase entry through the phosphorylation of RB. The additional findings discussed above suggest that there are many more ways that the APC/C is regulating the transcriptional dynamics of the cell cycle, and we speculate that these pathways are deeply intertwined. Furthermore, the regulatory systems surrounding the APC/C, which involve kinases and DUBs, are likely to tune substrate ubiquitination, thereby shaping the chromatin environment and transcriptional programs. These relationships are likely to be highly relevant to cell cycle progression, and to quiescent or differentiated cells where the APC/C is also active.

The newfound relationship between the APC/C and chromatin may also play a significant role in tissue specific functions as genetic disorders are beginning to be found from the disruption of the APC/C function (Eguren et al., 2011; Huang and Bonni, 2016). For example, a mutation was found in CDH1 that causes neurological defects, e.g., microencephaly

and epilepsy (Rodriguez et al., 2019). In another study, decreased *ANAPC1* transcript and corresponding APC1 protein levels results in Rothmund-Thomson syndrome that effects multiple organ systems (Ajeawung et al., 2019). Deeper genomic studies will likely demonstrate other functions and diseases genetically linked to the APC/C and its role in regulating chromatin. Mechanistically, it remains unclear why the APC/C specifically acts on chromatin regulators in G1, how the APC/C ubiquitinates the nucleosome, or how APC/C activity is regulated by negatively charged polyanions, such as nucleic acids. Additional studies will hopefully shed light on this relatively new and exciting era of APC/C-dependent biology and mechanisms.

## AUTHOR CONTRIBUTIONS

TB, KW, MH, ME, and NB wrote and edited the manuscript. All authors contributed to the article and approved the submitted version.

## FUNDING

This work was supported by NIH T32GM008570 and NSF DGE-1650116 (TB), NIH T32GM135095 (KW and MH), UNC University Cancer Research Fund (UCRF), NIH R01GM120309, and the American Cancer Society RSG-18-220-01-TBG (ME), and NIH R35GM128855 and UCRF (NB).

## ACKNOWLEDGMENTS

We would like to apologize to all of the individuals whose recent work on APC/C regulation was not discussed due to the focus of this review.

## REFERENCES

- Ajeawung, N. F., Nguyen, T. T. M., Lu, L., Kucharski, T. J., Rousseau, J., Molidpere, S., et al. (2019). Mutations in *ANAPC1*, encoding a scaffold subunit of the anaphase-promoting complex, cause rothmund-thomson syndrome type 1. *Am. J. Hum. Genet.* 105, 625–630. doi: 10.1016/j.ajhg.2019.06.011
- Alfieri, C., Chang, L., and Barford, D. (2018). Mechanism for remodelling of the cell cycle checkpoint protein MAD2 by the ATPase TRIP13. *Nature* 559, 274–278. doi: 10.1038/s41586-018-0281-1
- Alfieri, C., Chang, L., Zhang, Z., Yang, J., Maslen, S., Skehel, M., et al. (2016). Molecular basis of APC/C regulation by the spindle assembly checkpoint. *Nature* 536, 431–436. doi: 10.1038/nature19083
- Alfieri, C., Tischer, T., and Barford, D. (2020). A unique binding mode of Nek2A to the APC/C allows its ubiquitination during prometaphase. *EMBO Rep.* 21:e49831. doi: 10.15252/embr.201949831
- Alfieri, C., Zhang, S., and Barford, D. (2017). Visualizing the complex functions and mechanisms of the anaphase promoting complex/cyclosome (APC/C). *Open Biol.* 7:170204. doi: 10.1098/rsob.170204
- Aristarkhov, A., Eytan, E., Moghe, A., Admon, A., Herskho, A., and Ruderman, J. V. (1996). E2-C, a cyclin-selective ubiquitin carrier protein required for the destruction of mitotic cyclins. *Proc. Natl. Acad. Sci. U.S.A.* 93, 4294–4299. doi: 10.1073/pnas.93.9.4294
- Assoian, R. K., and Yung, Y. (2008). A reciprocal relationship between Rb and Skp2: implications for restriction point control, signal transduction to the cell cycle and cancer. *Cell Cycle* 7, 24–27. doi: 10.4161/cc.7.1.5232
- Bakos, G., Yu, L., Gak, I. A., Roumeliotis, T. I., Liakopoulos, D., Choudhary, J. S., et al. (2018). An E2-ubiquitin thioester-driven approach to identify substrates modified with ubiquitin and ubiquitin-like molecules. *Nat. Commun.* 9:4776. doi: 10.1038/s41467-018-07251-5
- Bannister, A. J., and Kouzarides, T. (2011). Regulation of chromatin by histone modifications. *Cell Res.* 21, 381–395. doi: 10.1038/cr.2011.22
- Bar-Joseph, Z., Siegfried, Z., Brandeis, M., Brors, B., Lu, Y., Eils, R., et al. (2008). Genome-wide transcriptional analysis of the human cell cycle identifies genes differentially regulated in normal and cancer cells. *Proc. Natl. Acad. Sci. U.S.A.* 105, 955–960. doi: 10.1073/pnas.0704723105
- Barr, A. R., Heldt, F. S., Zhang, T., Bakal, C., and Novak, B. (2016). a dynamical framework for the all-or-none G1/S transition. *Cell Syst.* 2, 27–37. doi: 10.1016/j.cels.2016.01.001
- Bashir, T., Dorrello, N. V., Amador, V., Guardavaccaro, D., and Pagano, M. (2004). Control of the SCF(Skp2-Cks1) ubiquitin ligase by the APC/C(Cdh1) ubiquitin ligase. *Nature* 428, 190–193. doi: 10.1038/nature02330
- Bassermann, F., Frescas, D., Guardavaccaro, D., Busino, L., Peschiaroli, A., and Pagano, M. (2008). The Cdc14B-Cdh1-Plk1 axis controls the G2 DNA-damage-response checkpoint. *Cell* 134, 256–267. doi: 10.1016/j.cell.2008.05.043

- Boekhout, M., and Wolthuis, R. (2015). Nek2A destruction marks APC/C activation at the prophase-to-prometaphase transition by spindle-checkpoint-restricted Cdc20. *J. Cell Sci.* 128, 1639–1653. doi: 10.1242/jcs.163279
- Boekhout, M., Yuan, R., Wondergem, A. P., Segeren, H. A., van Liere, E. A., Awol, N., et al. (2016). Feedback regulation between atypical E2Fs and APC/Cdh1 coordinates cell cycle progression. *EMBO Rep.* 17, 414–427. doi: 10.15252/embr.201540984
- Bonacci, T., Suzuki, A., Grant, G. D., Stanley, N., Cook, J. G., Brown, N. G., et al. (2018). Cezanne/OTUD7B is a cell cycle-regulated deubiquitinase that antagonizes the degradation of APC/C substrates. *EMBO J.* 37:e98701. doi: 10.15252/embr.201798701
- Bornstein, G., Bloom, J., Sitry-Shevah, D., Nakayama, K., Pagano, M., and Hershko, A. (2003). Role of the SCF<sup>Skp2</sup> ubiquitin ligase in the degradation of p21<sup>Cip1</sup> in S phase. *J. Biol. Chem.* 278, 25752–25757. doi: 10.1074/jbc.M301774200
- Bostick, M., Kim, J. K., Esteve, P. O., Clark, A., Pradhan, S., and Jacobsen, S. E. (2007). UHRF1 plays a role in maintaining DNA methylation in mammalian cells. *Science* 317, 1760–1764. doi: 10.1126/science.1147939
- Breiling, A., and Lyko, F. (2015). Epigenetic regulatory functions of DNA modifications: 5-methylcytosine and beyond. *Epigenet. Chromatin* 8:24. doi: 10.1186/s13072-015-0016-6
- Bremm, A., Freund, S. M., and Komander, D. (2010). Lys11-linked ubiquitin chains adopt compact conformations and are preferentially hydrolyzed by the deubiquitinase Cezanne. *Nat. Struct. Mol. Biol.* 17, 939–947. doi: 10.1038/nsmb.1873
- Brown, N. G., VanderLinden, R., Watson, E. R., Qiao, R., Grace, C. R., Yamaguchi, M., et al. (2015). RING E3 mechanism for ubiquitin ligation to a disordered substrate visualized for human anaphase-promoting complex. *Proc. Natl. Acad. Sci. U.S.A.* 112, 5272–5279. doi: 10.1073/pnas.1504161112
- Brown, N. G., VanderLinden, R., Watson, E. R., Weissmann, F., Ordureau, A., Wu, K. P., et al. (2016). Dual RING E3 architectures regulate Multiubiquitination and Ubiquitin chain elongation by APC/C. *Cell* 165, 1440–1453. doi: 10.1016/j.cell.2016.05.037
- Brown, N. G., Watson, E. R., Weissmann, F., Jarvis, M. A., VanderLinden, R., Grace, C. R. R., et al. (2014). Mechanism of polyubiquitination by human anaphase-promoting complex: RING repurposing for ubiquitin chain assembly. *Mol. Cell* 56, 246–260. doi: 10.1016/j.molcel.2014.09.009
- Buetow, L., and Huang, D. T. (2016). Structural insights into the catalysis and regulation of E3 ubiquitin ligases. *Nat. Rev. Mol. Cell Biol.* 17, 626–642. doi: 10.1038/nrm.2016.91
- Burrows, A. C., Prokop, J., and Summers, M. K. (2012). Skp1-Cul1-F-box ubiquitin ligase (SCF<sup>(betaTrCP)</sup>)-mediated destruction of the ubiquitin-specific protease USP37 during G2-phase promotes mitotic entry. *J. Biol. Chem.* 287, 39021–39029. doi: 10.1074/jbc.M112.390328
- Burton, J. L., and Solomon, M. J. (2007). Mad3p, a pseudosubstrate inhibitor of APC<sup>Cdc20</sup> in the spindle assembly checkpoint. *Genes Dev.* 21, 655–667. doi: 10.1101/gad.1511107
- Buschhorn, B. A., Petzold, G., Galova, M., Dube, P., Kraft, C., Herzog, F., et al. (2011). Substrate binding on the APC/C occurs between the coactivator Cdh1 and the processivity factor Doc1. *Nat. Struct. Mol. Biol.* 18, 6–13. doi: 10.1038/nsmb.1979
- Buttitta, L. A., Katzaroff, A. J., and Edgar, B. A. (2010). A robust cell cycle control mechanism limits E2F-induced proliferation of terminally differentiated cells in vivo. *J. Cell Biol.* 189, 981–996. doi: 10.1083/jcb.200910006
- Cappell, S. D., Chung, M., Jaimovich, A., Spencer, S. L., and Meyer, T. (2016). Irreversible APC(Cdh1) inactivation underlies the point of no return for cell-cycle entry. *Cell* 166, 167–180. doi: 10.1016/j.cell.2016.05.077
- Cappell, S. D., Mark, K. G., Garbett, D., Pack, L. R., Rape, M., and Meyer, T. (2018). EMI1 switches from being a substrate to an inhibitor of APC/C(CDH1) to start the cell cycle. *Nature* 558, 313–317. doi: 10.1038/s41586-018-0199-7
- Carrano, A. C., Eytan, E., Hershko, A., and Pagano, M. (1999). SKP2 is required for ubiquitin-mediated degradation of the CDK inhibitor p27. *Nat. Cell Biol.* 1, 193–199. doi: 10.1038/12013
- Chang, L., Zhang, Z., Yang, J., McLaughlin, S. H., and Barford, D. (2015). Atomic structure of the APC/C and its mechanism of protein ubiquitination. *Nature* 522, 450–454. doi: 10.1038/nature14471
- Chang, L. F., Zhang, Z., Yang, J., McLaughlin, S. H., and Barford, D. (2014). Molecular architecture and mechanism of the anaphase-promoting complex. *Nature* 513, 388–393. doi: 10.1038/nature13543
- Chao, W. C., Kulkarni, K., Zhang, Z., Kong, E. H., and Barford, D. (2012). Structure of the mitotic checkpoint complex. *Nature* 484, 208–213. doi: 10.1038/nature10896
- Chi, Y., Carter, J. H., Swanger, J., Mazin, A. V., Moritz, R. L., and Clurman, B. E. (2020). A novel landscape of nuclear human CDK2 substrates revealed by in situ phosphorylation. *Sci. Adv.* 6:eaz9899. doi: 10.1126/sciadv.aaz9899
- Choudhury, R., Bonacci, T., Wang, X., Truong, A., Arceci, A., Zhang, Y., et al. (2017). The E3 ubiquitin ligase SCF(Cyclin F) transmits AKT signaling to the cell-cycle machinery. *Cell Rep.* 20, 3212–3222. doi: 10.1016/j.celrep.2017.08.099
- Clague, M. J., Urbe, S., and Komander, D. (2019). Breaking the chains: deubiquitylating enzyme specificity begets function. *Nat. Rev. Mol. Cell Biol.* 20, 338–352. doi: 10.1038/s41580-019-0099-1
- Cohen, M., Vecsler, M., Liberzon, A., Noach, M., Zlotorynski, E., and Tzur, A. (2013). Unbiased transcriptome signature of in vivo cell proliferation reveals pro- and antiproliferative gene networks. *Cell Cycle* 12, 2992–3000. doi: 10.4161/cc.26030
- da Fonseca, P. C., Kong, E. H., Zhang, Z., Schreiber, A., Williams, M. A., Morris, E. P., et al. (2011). Structures of APC/C(Cdh1) with substrates identify Cdh1 and Apc10 as the D-box co-receptor. *Nature* 470, 274–278. doi: 10.1038/nature09625
- Davenport, J., Harris, L. D., and Goorha, R. (2006). Spindle checkpoint function requires Mad2-dependent Cdc20 binding to the Mad3 homology domain of BubR1. *Exp. Cell Res.* 312, 1831–1842. doi: 10.1016/j.yexcr.2006.02.018
- Davey, N. E., and Morgan, D. O. (2016). Building a regulatory network with short linear sequence motifs: lessons from the degrons of the anaphase-promoting complex. *Mol. Cell* 64, 12–23. doi: 10.1016/j.molcel.2016.09.006
- den Elzen, N., and Pines, J. (2001). Cyclin A is destroyed in prometaphase and can delay chromosome alignment and anaphase. *J. Cell Biol.* 153, 121–136. doi: 10.1083/jcb.153.1.121
- Di Fiore, B., and Pines, J. (2008). Defining the role of Emi1 in the DNA replication-segregation cycle. *Chromosoma* 117, 333–338. doi: 10.1007/s00412-008-0152-x
- Di Fiore, B., and Pines, J. (2010). How cyclin A destruction escapes the spindle assembly checkpoint. *J. Cell Biol.* 190, 501–509. doi: 10.1083/jcb.201001083
- Dimova, N. V., Hathaway, N. A., Lee, B. H., Kirkpatrick, D. S., Berkowitz, M. L., Gygi, S. P., et al. (2012). APC/C-mediated multiple monoubiquitylation provides an alternative degradation signal for cyclin B1. *Nat. Cell Biol.* 14, 168–176. doi: 10.1038/ncb2425
- Dove, K. K., and Klevit, R. E. (2017). RING-between-RING E3 ligases: emerging themes amid the variations. *J. Mol. Biol.* 429, 3363–3375. doi: 10.1016/j.jmb.2017.08.008
- Eguren, M., Manchado, E., and Malumbres, M. (2011). Non-mitotic functions of the anaphase-promoting complex. *Semin. Cell Dev. Biol.* 22, 572–578. doi: 10.1016/j.semcdb.2011.03.010
- Eifler, K., Cuijpers, S. A. G., Willemstein, E., Raaijmakers, J. A., El Atmioui, D., Ovaa, H., et al. (2018). SUMO targets the APC/C to regulate transition from metaphase to anaphase. *Nat. Commun.* 9:1119. doi: 10.1038/s41467-018-03486-4
- Eldridge, A. G., Loktev, A. V., Hansen, D. V., Verschuren, E. W., Reimann, J. D., and Jackson, P. K. (2006). The evi5 oncogene regulates cyclin accumulation by stabilizing the anaphase-promoting complex inhibitor emi1. *Cell* 124, 367–380. doi: 10.1016/j.cell.2005.10.038
- Elia, A. E., Boardman, A. P., Wang, D. C., Huttlin, E. L., Everley, R. A., Dephoure, N., et al. (2015). Quantitative proteomic atlas of ubiquitination and acetylation in the DNA damage response. *Mol. Cell* 59, 867–881. doi: 10.1016/j.molcel.2015.05.006
- Emanuel, M. J., Enrico, T. P., Mouery, R. D., Wasserman, D., Nachum, S., and Tzur, A. (2020). Complex cartography: regulation of E2F transcription factors by Cyclin F and ubiquitin. *Trends Cell Biol.* 30, 640–652. doi: 10.1016/j.tcb.2020.05.002
- Everetts, A. G., Manning, A. L., Wang, X., Dyson, N. J., Garcia, B. A., and Collier, H. A. (2013). H4K20 methylation regulates quiescence and chromatin compaction. *Mol. Biol. Cell* 24, 3025–3037. doi: 10.1091/mbc.E12-07-0529
- Eytan, E., Wang, K., Miniowitz-Shemtov, S., Sitry-Shevah, D., Kaisari, S., Yen, T. J., et al. (2014). Disassembly of mitotic checkpoint complexes by the joint action of the AAA-ATPase TRIP13 and p31(comet). *Proc. Natl. Acad. Sci. U.S.A.* 111, 12019–12024. doi: 10.1073/pnas.1412901111

- Fang, G. (2002). Checkpoint protein BubR1 acts synergistically with Mad2 to inhibit anaphase-promoting complex. *Mol. Biol. Cell* 13, 755–766. doi: 10.1091/mbc.01-09-0437
- Fang, G., Yu, H., and Kirschner, M. W. (1998). The checkpoint protein MAD2 and the mitotic regulator CDC20 form a ternary complex with the anaphase-promoting complex to control anaphase initiation. *Genes Dev.* 12, 1871–1883. doi: 10.1101/gad.12.12.1871
- Franks, J. L., Martinez-Chacin, R. C., Wang, X., Tiedemann, R. L., Bonacci, T., Choudhury, R., et al. (2020). In silico APC/C substrate discovery reveals cell cycle-dependent degradation of UHRF1 and other chromatin regulators. *PLoS Biol.* 18:e3000975. doi: 10.1371/journal.pbio.3000975
- Frye, J. J., Brown, N. G., Petzold, G., Watson, E. R., Grace, C. R., Nourse, A., et al. (2013). Electron microscopy structure of human APC/C(CDH1)-EMI1 reveals multimodal mechanism of E3 ligase shutdown. *Nat. Struct. Mol. Biol.* 20, 827–835. doi: 10.1038/nsmb.2593
- Fujimitsu, K., Grimaldi, M., and Yamano, H. (2016). Cyclin-dependent kinase 1-dependent activation of APC/C ubiquitin ligase. *Science* 352, 1121–1124. doi: 10.1126/science.aad3925
- Gao, Y. F., Li, T., Chang, Y., Wang, Y. B., Zhang, W. N., Li, W. H., et al. (2011). Cdk1-phosphorylated CUEDC2 promotes spindle checkpoint inactivation and chromosomal instability. *Nat. Cell Biol.* 13, 924–933. doi: 10.1038/ncb2287
- García-Higuera, I., Manchado, E., Dubus, P., Canamero, M., Mendez, J., Moreno, S., et al. (2008). Genomic stability and tumour suppression by the APC/C cofactor Cdh1. *Nat. Cell Biol.* 10, 802–811. doi: 10.1038/ncb1742
- Garnett, M. J., Mansfeld, J., Godwin, C., Matsusaka, T., Wu, J., Russell, P., et al. (2009). UBE2S elongates ubiquitin chains on APC/C substrates to promote mitotic exit. *Nat. Cell Biol.* 11, 1363–1369. doi: 10.1038/ncb1983
- Goldknopf, I. L., Taylor, C. W., Baum, R. M., Yeoman, L. C., Olson, M. O., Prestayko, A. W., et al. (1975). Isolation and characterization of protein A24, a "histone-like" non-histone chromosomal protein. *J. Biol. Chem.* 250, 7182–7187.
- Grant, G. D., Brooks, L. III, Zhang, X., Mahoney, J. M., Martyanov, V., Wood, T. A., et al. (2013). Identification of cell cycle-regulated genes periodically expressed in U2OS cells and their regulation by FOXM1 and E2F transcription factors. *Mol. Biol. Cell* 24, 3634–3650. doi: 10.1091/mbc.E13-05-0264
- Griewahn, L., Koser, A., and Maurer, U. (2019). Keeping cell death in check: ubiquitylation-dependent control of TNFR1 and TLR signaling. *Front. Cell. Dev. Biol.* 7:117. doi: 10.3389/fcell.2019.00117
- Guan, C., Zhang, J., Zhang, J., Shi, H., and Ni, R. (2016). Enhanced expression of early mitotic inhibitor-1 predicts a poor prognosis in esophageal squamous cell carcinoma patients. *Oncol. Lett.* 12, 114–120. doi: 10.3892/ol.2016.4611
- Guardavaccaro, D., and Pagano, M. (2006). Stabilizers and destabilizers controlling cell cycle oscillators. *Mol. Cell* 22, 1–4. doi: 10.1016/j.molcel.2006.03.017
- Haakonsen, D. L., and Rape, M. (2019). Branching out: improved signaling by heterotypic ubiquitin chains. *Trends Cell Biol.* 29, 704–716. doi: 10.1016/j.tcb.2019.06.003
- Hames, R. S., Wattam, S. L., Yamano, H., Bacchieri, R., and Fry, A. M. (2001). APC/C-mediated destruction of the centrosomal kinase Nek2A occurs in early mitosis and depends upon a cyclin A-type D-box. *EMBO J.* 20, 7117–7127. doi: 10.1093/emboj/20.24.7117
- Hayes, M. J., Kimata, Y., Wattam, S. L., Lindon, C., Mao, G., Yamano, H., et al. (2006). Early mitotic degradation of Nek2A depends on Cdc20-independent interaction with the APC/C. *Nat. Cell Biol.* 8, 607–614. doi: 10.1038/ncb1410
- Hernandez-Perez, S., Cabrera, E., Amoedo, H., Rodriguez-Acebes, S., Koundrioukoff, S., Debatise, M., et al. (2016). USP37 deubiquitinates Cdt1 and contributes to regulate DNA replication. *Mol. Oncol.* 10, 1196–1206. doi: 10.1016/j.molonc.2016.05.008
- Herzog, F., Primorac, I., Dube, P., Lenart, P., Sander, B., Mechtler, K., et al. (2009). Structure of the anaphase-promoting complex/cyclosome interacting with a mitotic checkpoint complex. *Science* 323, 1477–1481. doi: 10.1126/science.1163300
- Hoyt, M. A., Totis, L., and Roberts, B. T. (1991). *S. cerevisiae* genes required for cell cycle arrest in response to loss of microtubule function. *Cell* 66, 507–517. doi: 10.1016/0092-8674(81)90014-3
- Huang, J., and Bonni, A. (2016). A decade of the anaphase-promoting complex in the nervous system. *Genes Dev.* 30, 622–638. doi: 10.1101/gad.274324.115
- Huang, X., Summers, M. K., Pham, V., Lill, J. R., Liu, J., Lee, G., et al. (2011). Deubiquitinase USP37 is activated by CDK2 to antagonize APC(CDH1) and promote S phase entry. *Mol. Cell* 42, 511–523. doi: 10.1016/j.molcel.2011.03.027
- Irniger, S., Piatti, S., Michaelis, C., and Nasmyth, K. (1995). Genes involved in sister chromatid separation are needed for B-type cyclin proteolysis in budding yeast. *Cell* 81, 269–278. doi: 10.1016/0092-8674(95)90337-2
- Izawa, D., and Pines, J. (2015). The mitotic checkpoint complex binds a second CDC20 to inhibit active APC/C. *Nature* 517, 631–634. doi: 10.1038/nature13911
- Kabeche, L., and Compton, D. A. (2013). Cyclin A regulates kinetochore microtubules to promote faithful chromosome segregation. *Nature* 502, 110–113. doi: 10.1038/nature12507
- Kaisari, S., Sitry-Shevah, D., Miniowitz-Shemtov, S., Teichner, A., and Hershko, A. (2017). Role of CCT chaperonin in the disassembly of mitotic checkpoint complexes. *Proc. Natl. Acad. Sci. U.S.A.* 114, 956–961. doi: 10.1073/pnas.1620451114
- Kataria, M., and Yamano, H. (2019). Interplay between phosphatases and the anaphase-promoting complex/cyclosome in mitosis. *Cells* 8, 814. doi: 10.3390/cells8080814
- Kelly, A., Wickliffe, K. E., Song, L., Fedrigo, I., and Rape, M. (2014). Ubiquitin chain elongation requires E3-dependent tracking of the emerging conjugate. *Mol. Cell* 56, 232–245. doi: 10.1016/j.molcel.2014.09.010
- Kernan, J., Bonacci, T., and Emanuele, M. J. (2018). Who guards the guardian? Mechanisms that restrain APC/C during the cell cycle. *Biochim. Biophys. Acta Mol. Cell Res.* 1865, 1924–1933. doi: 10.1016/j.bbamcr.2018.09.011
- Kim, S., and Yu, H. (2011). Mutual regulation between the spindle checkpoint and APC/C. *Semin. Cell Dev. Biol.* 22, 551–558. doi: 10.1016/j.semcdb.2011.03.008
- Kim, W., Bennett, E. J., Huttlin, E. L., Guo, A., Li, J., Possemato, A., et al. (2011). Systematic and quantitative assessment of the ubiquitin-modified proteome. *Mol. Cell* 44, 325–340. doi: 10.1016/j.molcel.2011.08.025
- Kim, Y., Rosenberg, S. C., Kugel, C. L., Kostow, N., Rog, O., Davydov, V., et al. (2014). The chromosome axis controls meiotic events through a hierarchical assembly of HORMA domain proteins. *Dev. Cell* 31, 487–502. doi: 10.1016/j.devcel.2014.09.013
- Kimata, Y., Baxter, J. E., Fry, A. M., and Yamano, H. (2008). A role for the Fizzy/Cdc20 family of proteins in activation of the APC/C distinct from substrate recruitment. *Mol. Cell* 32, 576–583. doi: 10.1016/j.molcel.2008.09.023
- King, R. W., Deshaies, R. J., Peters, J. M., and Kirschner, M. W. (1996). How proteolysis drives the cell cycle. *Science* 274, 1652–1659. doi: 10.1126/science.274.5293.1652
- King, R. W., Peters, J. M., Tugendreich, S., Rolfe, M., Hieter, P., and Kirschner, M. W. (1995). A 20S complex containing CDC27 and CDC16 catalyzes the mitosis-specific conjugation of ubiquitin to cyclin B. *Cell* 81, 279–288. doi: 10.1016/0092-8674(95)90338-0
- Kirkpatrick, D. S., Hathaway, N. A., Hanna, J., Elsasser, S., Rush, J., Finley, D., et al. (2006). Quantitative analysis of in vitro ubiquitinated cyclin B1 reveals complex chain topology. *Nat. Cell Biol.* 8, 700–710. doi: 10.1038/ncb1436
- Komander, D., and Rape, M. (2012). The ubiquitin code. *Annu. Rev. Biochem.* 81, 203–229. doi: 10.1146/annurev-biochem-060310-170328
- Konishi, Y., Stegmüller, J., Matsuda, T., Bonni, S., and Bonni, A. (2004). Cdh1-APC controls axonal growth and patterning in the mammalian brain. *Science* 303, 1026–1030. doi: 10.1126/science.1093712
- Kouzarides, T. (2007). Chromatin modifications and their function. *Cell* 128, 693–705. doi: 10.1016/j.cell.2007.02.005
- Kraft, C., Vodermaier, H. C., Maurer-Stroh, S., Eisenhaber, F., and Peters, J. M. (2005). The WD40 propeller domain of Cdh1 functions as a destruction box receptor for APC/C substrates. *Mol. Cell* 18, 543–553. doi: 10.1016/j.molcel.2005.04.023
- Kramer, E. R., Scheuringer, N., Podtelejnikov, A. V., Mann, M., and Peters, J. M. (2000). Mitotic regulation of the APC activator proteins CDC20 and CDH1. *Mol. Biol. Cell* 11, 1555–1569. doi: 10.1091/mbc.11.5.1555
- Lahav-Baratz, S., Sudakin, V., Ruderman, J. V., and Hershko, A. (1995). Reversible phosphorylation controls the activity of cyclosome-associated cyclin-ubiquitin ligase. *Proc. Natl. Acad. Sci. U.S.A.* 92, 9303–9307. doi: 10.1073/pnas.92.20.9303
- Laoukili, J., Alvarez-Fernandez, M., Stahl, M., and Medema, R. H. (2008). FoxM1 is degraded at mitotic exit in a Cdh1-dependent manner. *Cell Cycle* 7, 2720–2726. doi: 10.4161/cc.7.17.6580



- Lara-Gonzalez, P., Kim, T., Oegema, K., Corbett, K., and Desai, A. (2021). A tripartite mechanism catalyzes Mad2-Cdc20 assembly at unattached kinetochores. *Science* 371, 64–67. doi: 10.1126/science.abc1424
- Lee, C. C., Li, B., Yu, H., and Matunis, M. J. (2018). Sumoylation promotes optimal APC/C activation and timely anaphase. *eLife* 7:e29539. doi: 10.7554/eLife.29539
- Li, Q., Chang, L., Aibara, S., Yang, J., Zhang, Z., and Barford, D. (2016). WD40 domain of Apc1 is critical for the coactivator-induced allosteric transition that stimulates APC/C catalytic activity. *Proc. Natl. Acad. Sci. U.S.A.* 113, 10547–10552. doi: 10.1073/pnas.1607147113
- Li, R., and Murray, A. W. (1991). Feedback control of mitosis in budding yeast. *Cell* 66, 519–531. doi: 10.1016/0092-8674(81)90015-5
- Lischetti, T., and Nilsson, J. (2015). Regulation of mitotic progression by the spindle assembly checkpoint. *Mol. Cell Oncol.* 2:e970484. doi: 10.4161/23723548.2014.970484
- Lu, D., Hsiao, J. Y., Davey, N. E., Van Voorhis, V. A., Foster, S. A., Tang, C., et al. (2014). Multiple mechanisms determine the order of APC/C substrate degradation in mitosis. *J. Cell Biol.* 207, 23–39. doi: 10.1083/jcb.201402041
- Lu, Y., Wang, W., and Kirschner, M. W. (2015). Specificity of the anaphase-promoting complex: a single-molecule study. *Science* 348:1248737. doi: 10.1126/science.1248737
- Luger, K., Mader, A. W., Richmond, R. K., Sargent, D. F., and Richmond, T. J. (1997). Crystal structure of the nucleosome core particle at 2.8 Å resolution. *Nature* 389, 251–260. doi: 10.1038/38444
- Lukas, C., Sorensen, C. S., Kramer, E., Santoni-Rugiu, E., Lindene, C., Peters, J. M., et al. (1999). Accumulation of cyclin B1 requires E2F and cyclin-A-dependent rearrangement of the anaphase-promoting complex. *Nature* 401, 815–818. doi: 10.1038/44611
- Luo, X., Fang, G., Coldiron, M., Lin, Y., Yu, H., Kirschner, M. W., et al. (2000). Structure of the Mad2 spindle assembly checkpoint protein and its interaction with Cdc20. *Nat. Struct. Biol.* 7, 224–229. doi: 10.1038/73338
- Luo, X., Tang, Z., Xia, G., Wassmann, K., Matsumoto, T., Rizo, J., et al. (2004). The Mad2 spindle checkpoint protein has two distinct natively folded states. *Nat. Struct. Mol. Biol.* 11, 338–345. doi: 10.1038/nsmb748
- Luo, X., and Yu, H. (2008). Protein metamorphosis: the two-state behavior of Mad2. *Structure* 16, 1616–1625. doi: 10.1016/j.str.2008.10.002
- Ma, Y., Kanakousaki, K., and Buttitta, L. (2015). How the cell cycle impacts chromatin architecture and influences cell fate. *Front. Genet.* 6:19. doi: 10.3389/fgene.2015.00019
- Ma, Y., McKay, D. J., and Buttitta, L. (2019). Changes in chromatin accessibility ensure robust cell cycle exit in terminally differentiated cells. *PLoS Biol.* 17:e3000378. doi: 10.1371/journal.pbio.3000378
- Margottin-Goguet, F., Hsu, J. Y., Loktev, A., Hsieh, H. M., Reimann, J. D., and Jackson, P. K. (2003). Prophase destruction of Emi1 by the SCF(betaTrCP/Slimb) ubiquitin ligase activates the anaphase promoting complex to allow progression beyond prometaphase. *Dev. Cell* 4, 813–826. doi: 10.1016/s1534-5807(03)00153-9
- Martinez-Chacin, R. C., Bodrug, T., Bolhuis, D. L., Kedziora, K. M., Bonacci, T., Ordureau, A., et al. (2020). Ubiquitin chain-elongating enzyme UBE2S activates the RING E3 ligase APC/C for substrate priming. *Nat. Struct. Mol. Biol.* 27, 550–560. doi: 10.1038/s41594-020-0424-6
- Marzio, A., Puccini, J., Kwon, Y., Maverakis, N. K., Arbini, A., Sung, P., et al. (2019). The F-box domain-dependent activity of EMI1 regulates PARPi sensitivity in triple-negative breast cancers. *Mol. Cell* 73, 224–237.e226. doi: 10.1016/j.molcel.2018.11.003
- Matsui, S. I., Seon, B. K., and Sandberg, A. A. (1979). Disappearance of a structural chromatin protein A24 in mitosis: implications for molecular basis of chromatin condensation. *Proc. Natl. Acad. Sci. U.S.A.* 76, 6386–6390. doi: 10.1073/pnas.76.12.6386
- Mattern, M., Sutherland, J., Kadimisetty, K., Barrio, R., and Rodriguez, M. S. (2019). Using ubiquitin binders to decipher the ubiquitin code. *Trends Biochem. Sci.* 44, 599–615. doi: 10.1016/j.tibs.2019.01.011
- Matyskiel, M. E., and Morgan, D. O. (2009). Analysis of activator-binding sites on the APC/C supports a cooperative substrate-binding mechanism. *Mol. Cell* 34, 68–80. doi: 10.1016/j.molcel.2009.02.027
- Metzger, M. B., Pruneda, J. N., Klevit, R. E., and Weissman, A. M. (2014). RING-type E3 ligases: master manipulators of E2 ubiquitin-conjugating enzymes and ubiquitination. *Biochim. Biophys. Acta* 1843, 47–60. doi: 10.1016/j.bbamcr.2013.05.026
- Mevissen, T. E. T., and Komander, D. (2017). Mechanisms of deubiquitinase specificity and regulation. *Annu. Rev. Biochem.* 86, 159–192. doi: 10.1146/annurev-biochem-061516-044916
- Mevissen, T. E. T., Kulathu, Y., Mulder, M. P. C., Geurink, P. P., Maslen, S. L., Gersch, M., et al. (2016). Molecular basis of Lys11-polyubiquitin specificity in the deubiquitinase Cezanne. *Nature* 538, 402–405. doi: 10.1038/nature19836
- Meyer, H. J., and Rape, M. (2011). Processive ubiquitin chain formation by the anaphase-promoting complex. *Semin. Cell. Dev. Biol.* 22, 544–550. doi: 10.1016/j.semcdb.2011.03.009
- Meyer, H. J., and Rape, M. (2014). Enhanced protein degradation by branched ubiquitin chains. *Cell* 157, 910–921. doi: 10.1016/j.cell.2014.03.037
- Michowski, W., Chick, J. M., Chu, C., Kolodziejczyk, A., Wang, Y., Suski, J. M., et al. (2020). Cdk1 controls global epigenetic landscape in embryonic stem cells. *Mol. Cell* 78, 459–476.e413. doi: 10.1016/j.molcel.2020.03.010
- Miller, J. J., Summers, M. K., Hansen, D. V., Nachury, M. V., Lehman, N. L., Loktev, A., et al. (2006). Emi1 stably binds and inhibits the anaphase-promoting complex/cyclosome as a pseudosubstrate inhibitor. *Genes Dev.* 20, 2410–2420. doi: 10.1101/gad.1454006
- Min, M., Mayor, U., and Lindon, C. (2013). Ubiquitination site preferences in anaphase promoting complex/cyclosome (APC/C) substrates. *Open Biol.* 3:130097. doi: 10.1098/rsob.130097
- Miniowitz-Shemtov, S., Eytan, E., Kaisari, S., Sitry-Shevah, D., and Hershko, A. (2015). Mode of interaction of TRIP13 AAA-ATPase with the Mad2-binding protein p31comet and with mitotic checkpoint complexes. *Proc. Natl. Acad. Sci. U.S.A.* 112, 11536–11540. doi: 10.1073/pnas.1515358112
- Mizrak, A., and Morgan, D. O. (2019). Polyanions provide selective control of APC/C interactions with the activator subunit. *Nat. Commun.* 10:5807. doi: 10.1038/s41467-019-13864-1
- Moustafa, D., Elwahed, M. R. A., Elsaid, H. H., and Parvin, J. D. (2021). Modulation of Early Mitotic Inhibitor 1 (EMI1) depletion on the sensitivity of PARP inhibitors in BRCA1 mutated triple-negative breast cancer cells. *PLoS One* 16:e0235025. doi: 10.1371/journal.pone.0235025
- Musacchio, A. (2015). The molecular biology of spindle assembly checkpoint signaling dynamics. *Curr. Biol.* 25, R1002–R1018. doi: 10.1016/j.cub.2015.08.051
- Oh, E., Mark, K. G., Mocciano, A., Watson, E. R., Prabhu, J. R., Cha, D. D., et al. (2020). Gene expression and cell identity controlled by anaphase-promoting complex. *Nature* 579, 136–140. doi: 10.1038/s41586-020-2034-1
- Park, H. J., Costa, R. H., Lau, L. F., Tyner, A. L., and Raychaudhuri, P. (2008). Anaphase-promoting complex/cyclosome-CDH1-mediated proteolysis of the forkhead box M1 transcription factor is critical for regulated entry into S phase. *Mol. Cell Biol.* 28, 5162–5171. doi: 10.1128/MCB.00387-08
- Pearl, M. J., Poyurovsky, M. V., Kass, E. M., Urist, M., Verschuren, E. W., Summers, M. K., et al. (2010). APC/C(Cdc20) targets E2F1 for degradation in prometaphase. *Cell Cycle* 9, 3956–3964. doi: 10.4161/cc.9.19.13162
- Pena-Diaz, J., Hegre, S. A., Anderssen, E., Aas, P. A., Mjelle, R., Gilfillan, G. D., et al. (2013). Transcription profiling during the cell cycle shows that a subset of Polycomb-targeted genes is upregulated during DNA replication. *Nucleic Acids Res.* 41, 2846–2856. doi: 10.1093/nar/gks1336
- Peters, J. M. (1998). SCF and APC: the Yin and Yang of cell cycle regulated proteolysis. *Curr. Opin. Cell Biol.* 10, 759–768. doi: 10.1016/s0955-0674(98)80119-1
- Piano, V., Alex, A., Stege, P., Maffini, S., Stoppiello, G. A., Huis In 't Veld, P. J., et al. (2021). CDC20 assists its catalytic incorporation in the mitotic checkpoint complex. *Science* 371, 67–71. doi: 10.1126/science.abc1152
- Ping, Z., Lim, R., Bashir, T., Pagano, M., and Guardavaccaro, D. (2012). APC/C (Cdh1) controls the proteasome-mediated degradation of E2F3 during cell cycle exit. *Cell Cycle* 11, 1999–2005. doi: 10.4161/cc.20402
- Prescott, D. M., and Bender, M. A. (1962). Synthesis of RNA and protein during mitosis in mammalian tissue culture cells. *Exp. Cell Res.* 26, 260–268. doi: 10.1016/0014-4827(62)90176-3
- Primorac, I., and Musacchio, A. (2013). Panta rhei: the APC/C at steady state. *J. Cell Biol.* 201, 177–189. doi: 10.1083/jcb.201301130
- Qiao, R., Weissmann, F., Yamaguchi, M., Brown, N. G., VanderLinden, R., Imre, R., et al. (2016). Mechanism of APC/CCDC20 activation by mitotic phosphorylation. *Proc. Natl. Acad. Sci. U.S.A.* 113, E2570–E2578. doi: 10.1073/pnas.1604929113



- Rape, M. (2018). Ubiquitylation at the crossroads of development and disease. *Nat. Rev. Mol. Cell Biol.* 19, 59–70. doi: 10.1038/nrm.2017.83
- Rape, M., Reddy, S. K., and Kirschner, M. W. (2006). The processivity of multiubiquitination by the APC determines the order of substrate degradation. *Cell* 124, 89–103. doi: 10.1016/j.cell.2005.10.032
- Reimann, J. D., Freed, E., Hsu, J. Y., Kramer, E. R., Peters, J. M., and Jackson, P. K. (2001a). Emi1 is a mitotic regulator that interacts with Cdc20 and inhibits the anaphase promoting complex. *Cell* 105, 645–655. doi: 10.1016/s0092-8674(01)00361-0
- Reimann, J. D., Gardner, B. E., Margottin-Goguet, F., and Jackson, P. K. (2001b). Emi1 regulates the anaphase-promoting complex by a different mechanism than Mad2 proteins. *Genes Dev.* 15, 3278–3285. doi: 10.1101/gad.945701
- Robzyk, K., Recht, J., and Osley, M. A. (2000). Rad6-dependent ubiquitination of histone H2B in yeast. *Science* 287, 501–504. doi: 10.1126/science.287.5452.501
- Rodriguez, C., Sanchez-Moran, I., Alvarez, S., Tirado, P., Fernandez-Mayoralas, D. M., Calleja-Perez, B., et al. (2019). A novel human Cdh1 mutation impairs anaphase promoting complex/cyclosome activity resulting in microcephaly, psychomotor retardation, and epilepsy. *J. Neurochem.* 151, 103–115. doi: 10.1111/jnc.14828
- Rosenberg, S. C., and Corbett, K. D. (2015). The multifaceted roles of the HORMA domain in cellular signaling. *J. Cell. Biol.* 211, 745–755. doi: 10.1083/jcb.201509076
- Sansregret, L., Patterson, J. O., Dewhurst, S., Lopez-Garcia, C., Koch, A., McGranahan, N., et al. (2017). APC/C dysfunction limits excessive cancer chromosomal instability. *Cancer Discov.* 7, 218–233. doi: 10.1158/2159-8290.CD-16-0645
- Shimizu, N., Nakajima, N. I., Tsunematsu, T., Ogawa, I., Kawai, H., Hirayama, R., et al. (2013). Selective enhancing effect of early mitotic inhibitor 1 (Emi1) depletion on the sensitivity of doxorubicin or X-ray treatment in human cancer cells. *J. Biol. Chem.* 288, 17238–17252. doi: 10.1074/jbc.M112.446351
- Sigl, R., Wandke, C., Rauch, V., Kirk, J., Hunt, T., and Geley, S. (2009). Loss of the mammalian APC/C activator FZR1 shortens G1 and lengthens S phase but has little effect on exit from mitosis. *J. Cell Sci.* 122(Pt 22), 4208–4217. doi: 10.1242/jcs.054197
- Singh, G. K., Karade, S. S., Ranjan, R., Ahamad, N., and Ahmed, S. (2017). C-terminal region of Mad2 plays an important role during mitotic spindle checkpoint in fission yeast *Schizosaccharomyces pombe*. *Mol. Biol. Rep.* 44, 89–96. doi: 10.1007/s11033-016-4083-y
- Sironi, L., Mapelli, M., Knapp, S., De Antoni, A., Jeang, K. T., and Musacchio, A. (2002). Crystal structure of the tetrameric Mad1-Mad2 core complex: implications of a 'safety belt' binding mechanism for the spindle checkpoint. *EMBO J.* 21, 2496–2506. doi: 10.1093/emboj/21.10.2496
- Skaar, J. R., and Pagano, M. (2008). Cdh1: a master G0/G1 regulator. *Nat. Cell Biol.* 10, 755–757. doi: 10.1038/ncb0708-755
- Skowrya, A., Allan, L. A., Saurin, A. T., and Clarke, P. R. (2018). USP9X limits mitotic checkpoint complex turnover to strengthen the spindle assembly checkpoint and guard against chromosomal instability. *Cell Rep.* 23, 852–865. doi: 10.1016/j.celrep.2018.03.100
- Skraina, A., Goldfarb, D., Kedziora, K. M., Cousins, E. M., Grant, G. D., Spangler, C. J., et al. (2020). Comprehensive nucleosome interactome screen establishes fundamental principles of nucleosome binding. *Nucleic Acids Res.* 48, 9415–9432. doi: 10.1093/nar/gkaa544
- Stegmeier, F., Rape, M., Draviam, V. M., Nalepa, G., Sowa, M. E., Ang, X. L., et al. (2007). Anaphase initiation is regulated by antagonistic ubiquitination and deubiquitination activities. *Nature* 446, 876–881. doi: 10.1038/nature05694
- Streich, F. C. Jr., and Lima, C. D. (2014). Structural and functional insights to ubiquitin-like protein conjugation. *Annu. Rev. Biophys.* 43, 357–379. doi: 10.1146/annurev-biophys-051013-022958
- Struhl, K., and Segal, E. (2013). Determinants of nucleosome positioning. *Nat. Struct. Mol. Biol.* 20, 267–273. doi: 10.1038/nsmb.2506
- Sudakin, V., Ganoth, D., Dahan, A., Heller, H., Hershko, J., Luca, F. C., et al. (1995). The cyclosome, a large complex containing cyclin-selective ubiquitin ligase activity, targets cyclins for destruction at the end of mitosis. *Mol. Biol. Cell* 6, 185–197. doi: 10.1091/mbc.6.2.185
- Swatek, K. N., Usher, J. L., Kueck, A. F., Gladkova, C., Mevissen, T. E. T., Pruneda, J. N., et al. (2019). Insights into ubiquitin chain architecture using Ub-clipping. *Nature* 572, 533–537. doi: 10.1038/s41586-019-1482-y
- Tang, Z., Li, B., Bharadwaj, R., Zhu, H., Ozkan, E., Hakala, K., et al. (2001). APC2 Cullin protein and APC11 RING protein comprise the minimal ubiquitin ligase module of the anaphase-promoting complex. *Mol. Biol. Cell* 12, 3839–3851. doi: 10.1091/mbc.12.12.3839
- Tsvetkov, L. M., Yeh, K. H., Lee, S. J., Sun, H., and Zhang, H. (1999). p27(Kip1) ubiquitination and degradation is regulated by the SCF(Skp2) complex through phosphorylated Thr187 in p27. *Curr. Biol.* 9, 661–664. doi: 10.1016/s0960-9822(99)80290-5
- Tugendreich, S., Tomkiel, J., Earnshaw, W., and Hieter, P. (1995). CDC27Hs colocalizes with CDC16Hs to the centrosome and mitotic spindle and is essential for the metaphase to anaphase transition. *Cell* 81, 261–268. doi: 10.1016/0092-8674(95)90336-4
- Uzunova, K., Dye, B. T., Schutz, H., Ladurner, R., Petzold, G., Toyoda, Y., et al. (2012). APC15 mediates CDC20 autoubiquitination by APC/C(MCC) and disassembly of the mitotic checkpoint complex. *Nat. Struct. Mol. Biol.* 19, 1116–1123. doi: 10.1038/nsmb.2412
- Vaidyanathan, S., Cato, K., Tang, L., Pavey, S., Haass, N. K., Gabrielli, B. G., et al. (2016). In vivo overexpression of Emi1 promotes chromosome instability and tumorigenesis. *Oncogene* 35, 5446–5455. doi: 10.1038/onc.2016.94
- Van Voorhis, V. A., and Morgan, D. O. (2014). Activation of the APC/C ubiquitin ligase by enhanced E2 efficiency. *Curr. Biol.* 24, 1556–1562. doi: 10.1016/j.cub.2014.05.052
- Visintin, R., Prinz, S., and Amon, A. (1997). CDC20 and CDH1: a family of substrate-specific activators of APC-dependent proteolysis. *Science* 278, 460–463. doi: 10.1126/science.278.5337.460
- Wan, L., Chen, M., Cao, J., Dai, X., Yin, Q., Zhang, J., et al. (2017). The APC/C E3 ligase complex activator FZR1 restricts BRAF oncogenic function. *Cancer Discov.* 7, 424–441. doi: 10.1158/2159-8290.CD-16-0647
- Wang, K., Sturt-Gillespie, B., Hittle, J. C., Macdonald, D., Chan, G. K., Yen, T. J., et al. (2014). Thyroid hormone receptor interacting protein 13 (TRIP13) AAA-ATPase is a novel mitotic checkpoint-silencing protein. *J. Biol. Chem.* 289, 23928–23937. doi: 10.1074/jbc.M114.585315
- Wang, W., and Kirschner, M. W. (2013). Emi1 preferentially inhibits ubiquitin chain elongation by the anaphase-promoting complex. *Nat. Cell Biol.* 15, 797–806. doi: 10.1038/ncb2755
- Watson, E. R., Brown, N. G., Peters, J. M., Stark, H., and Schulman, B. A. (2019a). Posing the APC/C E3 ubiquitin ligase to orchestrate cell division. *Trends Cell Biol.* 29, 117–134. doi: 10.1016/j.tcb.2018.09.007
- Watson, E. R., Grace, C. R. R., Zhang, W., Miller, D. J., Davidson, I. F., Prabu, J. R., et al. (2019b). Protein engineering of a ubiquitin-variant inhibitor of APC/C identifies a cryptic K48 ubiquitin chain binding site. *Proc. Natl. Acad. Sci. U.S.A.* 116, 17280–17289. doi: 10.1073/pnas.1902889116
- West, M. H., and Bonner, W. M. (1980). Histone 2B can be modified by the attachment of ubiquitin. *Nucleic Acids Res.* 8, 4671–4680. doi: 10.1093/nar/8.20.4671
- Whitfield, M. L., Sherlock, G., Saldanha, A. J., Murray, J. I., Ball, C. A., Alexander, K. E., et al. (2002). Identification of genes periodically expressed in the human cell cycle and their expression in tumors. *Mol. Biol. Cell* 13, 1977–2000. doi: 10.1091/mbc.02-02-0030
- Wickliffe, K. E., Lorenz, S., Wemmer, D. E., Kuriyan, J., and Rape, M. (2011). The mechanism of linkage-specific ubiquitin chain elongation by a single-subunit E2. *Cell* 144, 769–781. doi: 10.1016/j.cell.2011.01.035
- Wieser, S., and Pines, J. (2015). The biochemistry of mitosis. *Cold Spring Harb. Perspect. Biol.* 7:a015776. doi: 10.1101/cshperspect.a015776
- Wild, T., Larsen, M. S., Narita, T., Schou, J., Nilsson, J., and Choudhary, C. (2016). The spindle assembly checkpoint is not essential for viability of human cells with genetically lowered APC/C activity. *Cell Rep.* 14, 1829–1840. doi: 10.1016/j.celrep.2016.01.060
- Williamson, A., Banerjee, S., Zhu, X., Philipp, I., Iavarone, A. T., and Rape, M. (2011). Regulation of ubiquitin chain initiation to control the timing of substrate degradation. *Mol. Cell* 42, 744–757. doi: 10.1016/j.molcel.2011.04.022
- Williamson, A., Wickliffe, K. E., Mellone, B. G., Song, L., Karpen, G. H., and Rape, M. (2009). Identification of a physiological E2 module for the human anaphase-promoting complex. *Proc. Natl. Acad. Sci. U.S.A.* 106, 18213–18218. doi: 10.1073/pnas.0907887106

- Wu, T., Merbl, Y., Huo, Y., Gallop, J. L., Tzur, A., and Kirschner, M. W. (2010). UBE2S drives elongation of K11-linked ubiquitin chains by the anaphase-promoting complex. *Proc. Natl. Acad. Sci. U.S.A.* 107, 1355–1360. doi: 10.1073/pnas.0912802107
- Yamaguchi, M., VanderLinden, R., Weissmann, F., Qiao, R., Dube, P., Brown, N. G., et al. (2016). Cryo-EM of mitotic checkpoint complex-bound APC/C reveals reciprocal and conformational regulation of ubiquitin ligation. *Mol. Cell* 63, 593–607. doi: 10.1016/j.molcel.2016.07.003
- Yamaguchi, M., Yu, S., Qiao, R., Weissmann, F., Miller, D. J., VanderLinden, R., et al. (2015). Structure of an APC3-APC16 complex: insights into assembly of the anaphase-promoting complex/cyclosome. *J. Mol. Biol.* 427, 1748–1764. doi: 10.1016/j.jmb.2014.11.020
- Yamano, H., Gannon, J., and Hunt, T. (1996). The role of proteolysis in cell cycle progression in *Schizosaccharomyces pombe*. *EMBO J.* 15, 5268–5279.
- Yang, M., Li, B., Tomchick, D. R., Machius, M., Rizo, J., Yu, H., et al. (2007). p31comet blocks Mad2 activation through structural mimicry. *Cell* 131, 744–755. doi: 10.1016/j.cell.2007.08.048
- Yau, R., and Rape, M. (2016). The increasing complexity of the ubiquitin code. *Nat. Cell. Biol.* 18, 579–586. doi: 10.1038/ncb3358
- Yau, R. G., Doerner, K., Castellanos, E. R., Haakonsen, D. L., Werner, A., Wang, N., et al. (2017). Assembly and function of heterotypic ubiquitin chains in cell-cycle and protein quality control. *Cell* 171, 918–933.e920. doi: 10.1016/j.cell.2017.09.040
- Yeh, C., Coyaude, E., Bashkurov, M., van der Lelij, P., Cheung, S. W., Peters, J. M., et al. (2015). The deubiquitinase USP37 regulates chromosome cohesion and mitotic progression. *Curr. Biol.* 25, 2290–2299. doi: 10.1016/j.cub.2015.07.025
- Young, R. A. (2011). Control of the embryonic stem cell state. *Cell* 144, 940–954. doi: 10.1016/j.cell.2011.01.032
- Yu, H. (2006). Structural activation of Mad2 in the mitotic spindle checkpoint: the two-state Mad2 model versus the Mad2 template model. *J. Cell. Biol.* 173, 153–157. doi: 10.1083/jcb.200601172
- Yu, H., King, R. W., Peters, J. M., and Kirschner, M. W. (1996). Identification of a novel ubiquitin-conjugating enzyme involved in mitotic cyclin degradation. *Curr. Biol.* 6, 455–466. doi: 10.1016/s0960-9822(02)00513-4
- Yu, H., Peters, J. M., King, R. W., Page, A. M., Hieter, P., and Kirschner, M. W. (1998). Identification of a cullin homology region in a subunit of the anaphase-promoting complex. *Science* 279, 1219–1222. doi: 10.1126/science.279.5354.1219
- Yuan, X., Srividhya, J., De Luca, T., Lee, J. H., and Pomerening, J. R. (2014). Uncovering the role of APC-Cdh1 in generating the dynamics of S-phase onset. *Mol. Biol. Cell* 25, 441–456. doi: 10.1091/mbc.E13-08-0480
- Zhang, S., Chang, L., Alfieri, C., Zhang, Z., Yang, J., Maslen, S., et al. (2016). Molecular mechanism of APC/C activation by mitotic phosphorylation. *Nature* 533, 260–264. doi: 10.1038/nature17973
- Zhang, S., Tischer, T., and Barford, D. (2019). Cyclin A2 degradation during the spindle assembly checkpoint requires multiple binding modes to the APC/C. *Nat. Commun.* 10:3863. doi: 10.1038/s41467-019-11833-2

**Conflict of Interest:** The authors declare that the research was conducted in the absence of any commercial or financial relationships that could be construed as a potential conflict of interest.

The reviewer MS declared a past collaboration with one of the authors ME to the handling editor.

Copyright © 2021 Bodrug, Welsh, Hinkle, Emanuele and Brown. This is an open-access article distributed under the terms of the Creative Commons Attribution License (CC BY). The use, distribution or reproduction in other forums is permitted, provided the original author(s) and the copyright owner(s) are credited and that the original publication in this journal is cited, in accordance with accepted academic practice. No use, distribution or reproduction is permitted which does not comply with these terms.



# CUL5–ASB6 Complex Promotes p62/SQSTM1 Ubiquitination and Degradation to Regulate Cell Proliferation and Autophagy

Liyan Gong<sup>1,2</sup>, Kaihua Wang<sup>3,4</sup>, Mengcheng Wang<sup>3,4</sup>, Ronggui Hu<sup>4,5</sup>, Huaguang Li<sup>1</sup>, Daming Gao<sup>3,4\*</sup> and Moubin Lin<sup>1,2\*</sup>

<sup>1</sup> Center for Clinical Research and Translational Medicine, Yangpu Hospital, Tongji University School of Medicine, Shanghai, China, <sup>2</sup> Department of General Surgery, Yangpu Hospital, Tongji University School of Medicine, Shanghai, China, <sup>3</sup> State Key Laboratory of Cell Biology, Shanghai Institute of Biochemistry and Cell Biology, Center for Excellence in Molecular Cell Science, Chinese Academy of Sciences, Shanghai, China, <sup>4</sup> University of Chinese Academy of Sciences, Beijing, China, <sup>5</sup> State Key Laboratory of Molecular Biology, Shanghai Institute of Biochemistry and Cell Biology, Center for Excellence in Molecular Cell Science, Chinese Academy of Sciences, Shanghai, China

## OPEN ACCESS

### Edited by:

Biao Kong,  
Fudan University, China

### Reviewed by:

Ceshi Chen,  
Kunming Institute of Zoology, China  
Vibhuti Joshi,  
National Institutes of Health (NIH),  
United States

### \*Correspondence:

Daming Gao  
dgao@sibcb.ac.cn  
Moubin Lin  
lmbin@hotmail.com

### Specialty section:

This article was submitted to  
Cell Growth and Division,  
a section of the journal  
Frontiers in Cell and Developmental  
Biology

**Received:** 24 March 2021

**Accepted:** 06 May 2021

**Published:** 07 June 2021

### Citation:

Gong L, Wang K, Wang M, Hu R,  
Li H, Gao D and Lin M (2021)  
CUL5–ASB6 Complex Promotes  
p62/SQSTM1 Ubiquitination  
and Degradation to Regulate Cell  
Proliferation and Autophagy.  
Front. Cell Dev. Biol. 9:684885.  
doi: 10.3389/fcell.2021.684885

p62/SQSTM1 (sequestosome-1) is a key protein involved in multiple cellular bioprocesses including autophagy, nutrient sensing, cell growth, cell death, and survival. Therefore, it is implicated in human diseases such as obesity and cancer. Here, we show that the CUL5–ASB6 complex is a ubiquitin E3 ligase complex mediating p62 ubiquitination and degradation. Depletion of CUL5 or ASB6 induced p62 accumulation, and overexpression of ASB6 promoted ubiquitination and degradation of p62. Functionally, ASB6 overexpression can inhibit the proliferation of MEF and hepatocellular carcinoma cells by reducing p62 protein level, and impair the occurrence of autophagy. Overall, our study identified a new molecular mechanism regulating p62 stability, which may provide additional insights for understanding the delicate control of p62 and cell proliferation–autophagy control in physiological and pathological settings.

**Keywords:** p62, ubiquitination, CUL5, ASB6, proliferation, autophagy

## INTRODUCTION

p62, encoded by *SQSTM1* gene, is the first discovered autophagic adaptor protein, which participates in many cellular processes, such as cell growth and proliferation, autophagy, malignant transformation, apoptosis, and inflammation (Layfield and Hocking, 2004; McManus and Roux, 2012; Moscat and Diaz-Meco, 2012). During the autophagy process, PB1 domain of p62 promotes the packaging of ubiquitinated substrates through oligomerization (Kraft et al., 2016), and LIR domain of p62 mediates its interaction with LC3, thus transporting the packaged substrates and participating in the formation of autophagosome (Park et al., 2014). It is reported that several kinases including CK2/TBK1 and ULK1 phosphorylate p62 at Ser403 and Ser407 within the UBA region of p62, promoting p62 ubiquitination and the subsequent autophagy degradation (Matsumoto et al., 2011; Pilli et al., 2012; Ro et al., 2014; Lim et al., 2015). In addition to autophagy regulation, p62 interacts with receptor interacting protein (RIP) and connects with aPKCs to activate tumor necrosis factor  $\alpha$  (TNF $\alpha$ )-induced NF- $\kappa$ B signaling pathway (Sanz et al., 1999). On the other hand, p62 recruits TRAF6, the inflammation signaling molecule and E3 ubiquitin ligase,

and promotes TRAF6-dependent ubiquitination and activation of mTORC1 under amino acid-rich conditions (Jadhav et al., 2008; Linares et al., 2013). Moreover, the interaction between p62 and Keap1 can destroy Keap1-mediated ubiquitination of Nrf2, leading to Nrf2 activation (Jain et al., 2010). Reciprocally, Nrf2 can enhance the expression of p62 at the transcription level by directly binding to the promoter region of *p62/SQSTM1* gene, forming a positive feedback loop (Liu et al., 2007). Therefore, p62 acts as a multifunctional signaling hub involved in nutrition sensing (*via* mTORC1), inflammation and apoptosis (*via* NF- $\kappa$ B), and antioxidant response and selective autophagy pathways (*via* Keap1-Nrf2). Since alterations of all these important pathways are associated with human diseases such as cancer, no surprise p62 has been shown playing a role in tumorigenesis. More and more evidences indicate abnormal expression of p62 in various cancers, including liver (Inami et al., 2011), lung (Inoue et al., 2012), breast (Rolland et al., 2007), kidney (Li et al., 2013), colorectal (Ren et al., 2014), ovarian (Yan et al., 2019), and prostate cancers (Kitamura et al., 2006). For example, p62 accumulation can destabilize the genome and promote tumor development; p62 can mediate tumor-induced fat reprogramming in adipocytes and has a potential impact on obesity-promoted cancer (Komatsu, 2011; Huang et al., 2018). Importantly, increased p62 expression in cancer cells is regarded a consequence of defective autophagy, which promotes tumorigenesis (Mathew et al., 2009). Recent results from liver cancer mouse models suggest that high p62 expression exerts its oncogenic activity *via* Nrf2, mTORC1, and c-Myc activation, and hepatocyte-specific deletion of p62 impairs hepatocellular carcinoma (HCC) formation (Umemura et al., 2016). Consistently, elevated p62 levels are often observed in HCC and liver diseases with increased risk of malignant transformation (Aigelsreiter et al., 2017; Sanchez-Martin et al., 2019). Therefore, the de-regulated p62 may be a potential therapeutic target for HCC.

Ubiquitination is a major post-translational modification regulating protein properties including stability, interaction spectrum, localization, and so on. Protein ubiquitination is typically catalyzed by ubiquitin-activating enzymes (E1s), ubiquitin-conjugating enzymes (E2s), and ubiquitin ligase enzymes (E3s) (Hershko and Ciechanover, 1998; Schulman and Harper, 2009; Wenzel et al., 2011). E3 ubiquitin ligases are the most heterogeneous class of enzymes in the ubiquitination pathway, since they control the substrate specificity (Morreale and Walden, 2016). Several E3 ubiquitin ligases have been identified to modulate the expression or functions of p62. Keap1-Cullin3 ubiquitylates p62 at K420, leading to diminished p62 sequestration and degradation activity during autophagy (Lee et al., 2017). TRIM21 and NEDD4 were reported to mediate ubiquitylation of p62 at K7, leading to suppressed protein sequestration and induced inclusion body autophagy (Pan et al., 2016; Lin et al., 2017). The E3 ligase RNF26 ubiquitylates p62 within the UBA domain to facilitate TOLLIP interaction and vesicular cargo sorting (Jongsma et al., 2016), while RNF166 ubiquitylates p62 to modulate the role of p62 in xenophagic targeting of bacteria (Heath et al., 2016). In addition to the E3 ligases that modulate p62 activity, two E3 ligases have been

reported to regulate p62 stability *via* proteasomal degradation. The E3 ubiquitin ligase Parkin directly interacts with and ubiquitinates p62 to promote proteasomal degradation of p62, and dysregulation of Parkin/p62 axis could account for the selective vulnerability during pathogenesis of PD (Song et al., 2016). Another recent study has shown that X-linked inhibitor of apoptosis protein (XIAP) functioned as a ubiquitination E3 ligase toward p62 and suppressed p62 expression through ubiquitin-proteasomal degradation and therefore promoted breast cancer progression (Huang et al., 2019). Therefore, p62 is ubiquitinated in various physiological settings. In the current study, we found that a functional Cullin-Ring E3 ligase (CRL) complex composed of Cullin5 (CUL5), Elongin B (EloB), Elongin C (EloC), and substrate recognition adaptor ASB6 interacts with p62 and mediates its ubiquitination-dependent degradation. Our experimental evidences indicate that ASB6 overexpression inhibits the proliferation of HCC cells and impairs autophagy by reducing the p62 protein levels. Therefore, our study has not only characterized a new functional CRL5-ASB6 E3 complex, but also identified p62 as the first degradation substrate of it, which may provide new insight for cell proliferation and autophagy regulation.

## MATERIALS AND METHODS

### Reagents, Antibodies, and Plasmid Constructs

DMSO and cycloheximide (CHX) were purchased from Sigma. MG132 and MLN4924 were purchased from Selleck Chemicals. Bafilomycin A1 (Baf A1) was purchased from Sigma. DMEM (Dulbecco's Modified Eagle Medium), DMEM/F-12 (Dulbecco's Modified Eagle Medium/Nutrient Mixture F-12), FBS (Fetal Bovine Serum), Penicillin-Streptomycin, and puromycin were purchased from Invitrogen (Thermo Fisher Scientific). Transfection reagent polyethylenimine was purchased from Sigma. Lipofectamine 3000 was purchased from Thermo Fisher Scientific, and siRNA transfection reagent X-tremeGENE was purchased from Roche.

The following antibodies were used for Western blot: p62/SQSTM1 (catalog A11250) was from Abclonal; ASB6 (catalog 21449-1-AP), HA (catalog 51064-2-AP), Myc (catalog 16286-1-AP), and GFP (catalog 66002-1) were from Proteintech; Tubulin (catalog SC23948), CUL5 (catalog SC-373822), and HA (catalog SC-7392) were from Santa Cruz Biotechnology; FLAG (catalog F3165), FLAG (F7425), Vinculin (catalog V4505), and His (catalog H1029) were from Sigma; p27/kip1 (catalog 610241) was from BD.

Human p62 (including p62 and p62S), CUL5, ASB6, EloB, or EloC were PCR amplified and inserted into the pcDNA3.1, pCMV-FLAG, or pLEX-MCS-FLAG vectors. shRNA vectors were generated by inserting synthesized oligos into pLKO.1 vector. The shRNA target sequences for CUL5 were 5'-GCCATCAAGATGATACGGCTT-3', 5'-GCTAGAATGTTTCAGGACATA-3', and 5'-GAGGAACATA TCATTAGTGC-3'. The shRNA target sequences for EloB were 5'-CCAACTCTTGGATGATGGCAA-3' and 5'-CGAACT



GAAGCGCATCGTCGA-3'. The shRNA target sequences for EloC were 5'-CGAAACCAATGAGGTCAATTT-3' and 5'-CGTACAAGGTTTCGCTACACTA-3'. The shRNA target sequences for ASB6 were 5'-GCAGATCCACAATACTGA GAA-3', 5'-CCCGAAACTTCGATATCCAC-3', 5'-AGGAG AGCCGAATCCTTGTTTC-3', and 5'-CACAGTGTTCACCT GCATCAT-3'. The shRNA target sequence for p62 was 5'-CCTCTGGGCATTGAAGTTGAT-3'.

## Cell Culture and Transfection

HeLa, HEK293T, and HepG2 cells were cultured in DMEM at 37°C/5% CO<sub>2</sub>, while SNU739, SNU182, and Huh1 cells were cultured in DMEM/F-12 at 37°C/5% CO<sub>2</sub>. All culture media were added with 10% FBS and 1% penicillin/streptomycin before use. Transfection experiments were performed when the cells were about 60–80% confluent. According to different cell types, we choose different transfection reagents and methods. HEK293T and HeLa cells were transfected with polyethylenimine and Lipofectamine 3000 reagents, respectively. siRNAs were transfected into cells with X-tremeGENE siRNA Transfection Reagent at 50 nM final concentration according to the manufacturer's protocol. The siRNA sequences targeting ASB6 were as follows: 5'-CAGAUCCACAAUACUGAGA-3' and 5'-CGAAAACUUCGAUAUCCA-3'.

## Western Blotting and Immunoprecipitation (IP)

Cells were harvested in EBC lysis buffer (50 mM Tris-HCl, pH 8.0, 120 mM NaCl, and 0.5% Nonidet P-40) supplemented with protease inhibitors (Selleck Chemicals) and phosphatase inhibitors (Selleck Chemicals) to generate cell lysates. Protein concentration of cell lysates was measured using Bio-Rad protein assay kit in a spectrophotometer (Thermo Scientific). Equal amounts of protein were resolved by electrophoresis on SDS-PAGE gels and transferred onto a PVDF membrane. After incubation in blocking buffer [50 mM Tris-buffered saline (pH 7.4) containing 5% non-fat dry milk and 0.1% Tween-20], the membranes were probed with the primary antibodies, followed by incubation with HRP-conjugated rabbit or mouse secondary antibodies. For immunoprecipitation, cell lysates were incubated with anti-FLAG M2 agarose beads or anti-HA agarose beads for 3 h. Beads were then washed five times with NETN buffer (20 mM Tris-HCl, pH 8.0, 100 mM NaCl, 1 mM EDTA, and 0.5% NP-40). After washing, the precipitated samples were resolved on SDS-PAGE and immunoblotted with appropriate antibodies.

## Lentiviral Production and Infection

Lentiviral packaging and infection were done as previously described (Du et al., 2015). Briefly, HEK293T cells were co-transfected with pLKO.1 or pLEX constructs and the packaging plasmids psPAX2 and pMD2.G. All media were removed after 5 h and replaced with fresh DMEM plus 10% FBS. Virus containing medium were collected and filtered with a 0.45-μm membrane (Merck Millipore) 48 h after replacement with fresh media. Polybrene (10 μg/ml) was added into the virus-containing medium to infect the corresponding cells, and

infected cells were selected in puromycin for 48 h before harvest or following experiments.

## Cell Proliferation Assay

For cell proliferation assays, 500 cells were seeded in 96-well plates (Nest), and the viability of the cells was measured at various time points. Ten microliters of CCK8 (Meilunbio) reagent was added to each well, and the cells were incubated at 37°C for 2 h. Next, absorbance was measured in single-wavelength mode (450-nm) using a BioTek Eon Multi-Mode Microplate Readers.

## Colony Formation Assay

For cell colony formation assays, 500 cells were seeded in each well of six-well plates, and cultured for 10 days until visible colonies formed. Colonies were then washed with PBS, fixed, and stained with 0.1% crystal violet for 20 min. After staining, the plates were washed with distilled water and air-dried. Visible colonies were counted.

## Immunofluorescence Analysis

Cells were grown on glass coverslips for treatment as indicated and then fixed with 4% paraformaldehyde in PBS for 15 min at room temperature and permeabilized with 0.5% Triton X-100 in PBS for 5 min. Samples were rinsed three times with PBS (5 min each time). Coverslips were then blocked for 60 min with 5% BSA. After washing three times with PBS (10 min each time), nuclei were counterstained with 4,6-diamidino-2-phenylindole (DAPI) for 10 min. Coverslips were rinsed twice (3 min for each wash) with PBS and mounted onto slides using ProLong Gold Antifade reagent (Invitrogen). All images were obtained with the Leica TCS SP8 fluorescence microscope.

## Statistical Analysis

Each experiment was repeated at least three times, and results were presented as mean ± standard error of the mean. The statistical significance of differences was assessed by the Student's unpaired *t*-test (\*0.01 < *P* < 0.05, \*\*0.001 < *P* < 0.01, and \*\*\**P* < 0.001). Statistical analysis was performed using GraphPad Prism.

# RESULTS

## p62 Is Modulated by CRL5 E3 Ligase Complex

We initially found that proteasome inhibitor MG132, the NEDD8-activating enzyme inhibitor MLN4924 (often used to suppress CRL E3 ligase activity) (Soucy et al., 2009), and the autophagy inhibitor bafilomycin A1 (Baf A1) caused an obvious elevation of endogenous p62 protein levels in HepG2, SNU739, and Huh1 cells (**Figure 1A**), indicating that p62 is an unstable protein that is likely governed by CRL E3 ligase complexes. Moreover, knockdown of CUL5 could upregulate endogenous p62 protein level and co-transfection of shRNAs against EloB/EloC in HeLa cells can dramatically upregulate the expression of ectopically expressed HA-p62 (**Figures 1B,C**).

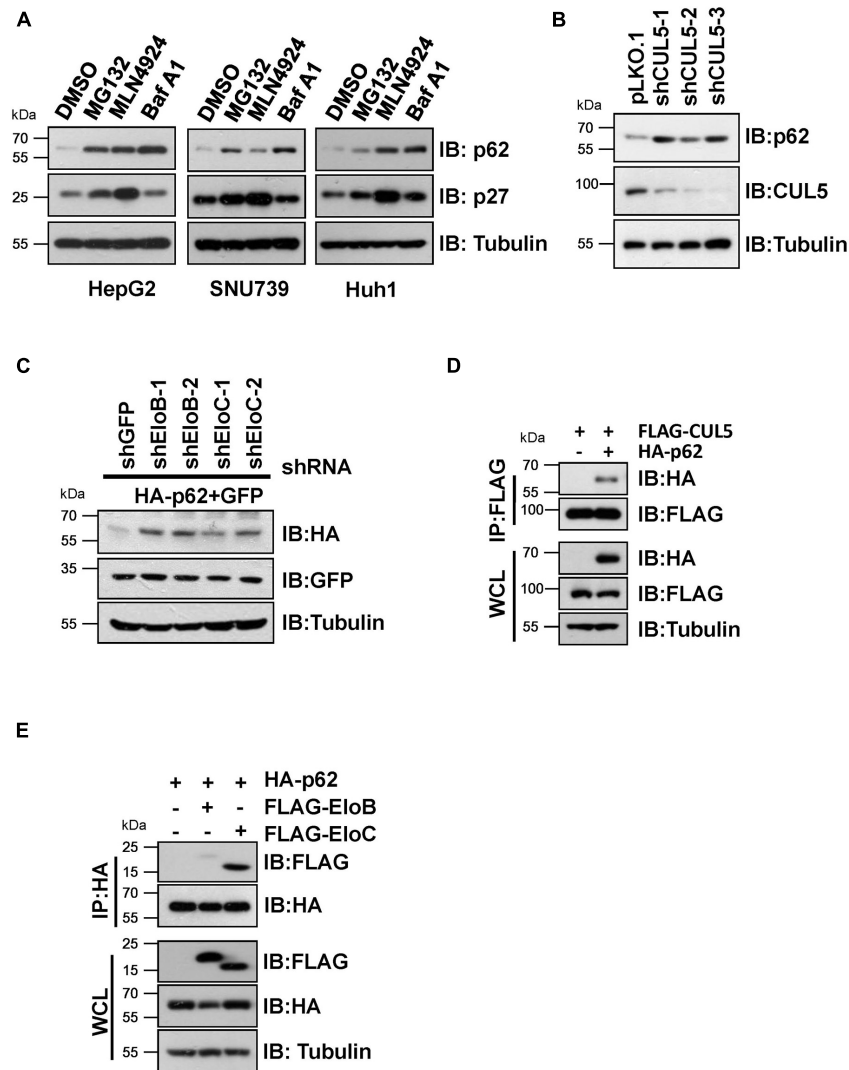


**FIGURE 1 |** CUL5 interacts with p62 and regulates its expression. **(A)** HepG2, SNU739, and Huh1 cells were treated with 10  $\mu$ M MG132, 1  $\mu$ M MLN4924, or 200 nM Baf A1 for 10 h, and the whole-cell lysates (WCL) were generated for immunoblotting (IB) analysis. p27 served as a positive control responding to CRL E3 blocking, and Tubulin served as a loading control. **(B)** Huh1 cells infected with indicated shRNAs were subjected to IB analysis. Tubulin served as a loading control. **(C)** IB analyses of WCL from HeLa cells transfected with plasmids encoding HA-p62, shRNAs targeting EloB/C, and GFP (as an internal transfection control). Tubulin served as a loading control. **(D,E)** HEK293T cells transfected with the indicated plasmids were treated with 10  $\mu$ M MG132 for 10 h before Co-IP and IB analysis.

Then, we further confirmed the interaction between p62 and the CUL5–EloB/EloC complex by transfection/co-immunoprecipitation (IP) experiments (Figures 1D,E). Notably, the interaction between p62 and EloC was stronger than the p62–EloB interaction. These results indicated that p62 is a potential CRL5 ubiquitination substrate, since the substrate recognition subunit of CRL5 directly interacts with the linker protein EloC *via* the SOCS-box region and indirectly interacts with EloB *via* N-terminus of CUL5 protein.

## ASB6 Is the SOCS-Box Protein That Interacts With p62

In order to identify the substrate recognition subunit that specifically mediates CRL5-dependent p62 regulation, we

performed shRNA-based screening and three SOCS-box proteins were identified, including SOCS3, SOCS6, and ASB6. By co-immunoprecipitation (Co-IP) experiment, a strong interaction was observed between p62 and ASB6, but not SOCS3 or SOCS6 (Figure 2A). Meanwhile, HA-ASB6 interacts with both FLAG-EloB and EloC, and the binding affinity of HA-ASB6 to EloC is significantly stronger than to EloB (Figure 2B), a pattern very similar to the interaction of p62 with EloB/EloC (Figure 1E). According to the domain composition of ASB6 (Figure 2C), we generated internal deletion FLAG-ASB6 constructs and co-transfected them with HA-CUL5 or HA-p62 in HEK293T cells to examine the interaction between ASB6 with CUL5 and p62. The Co-IP results suggested that removing SOCS box or Cul5-box domain abolished the ASB6–CUL5 interaction, but did not

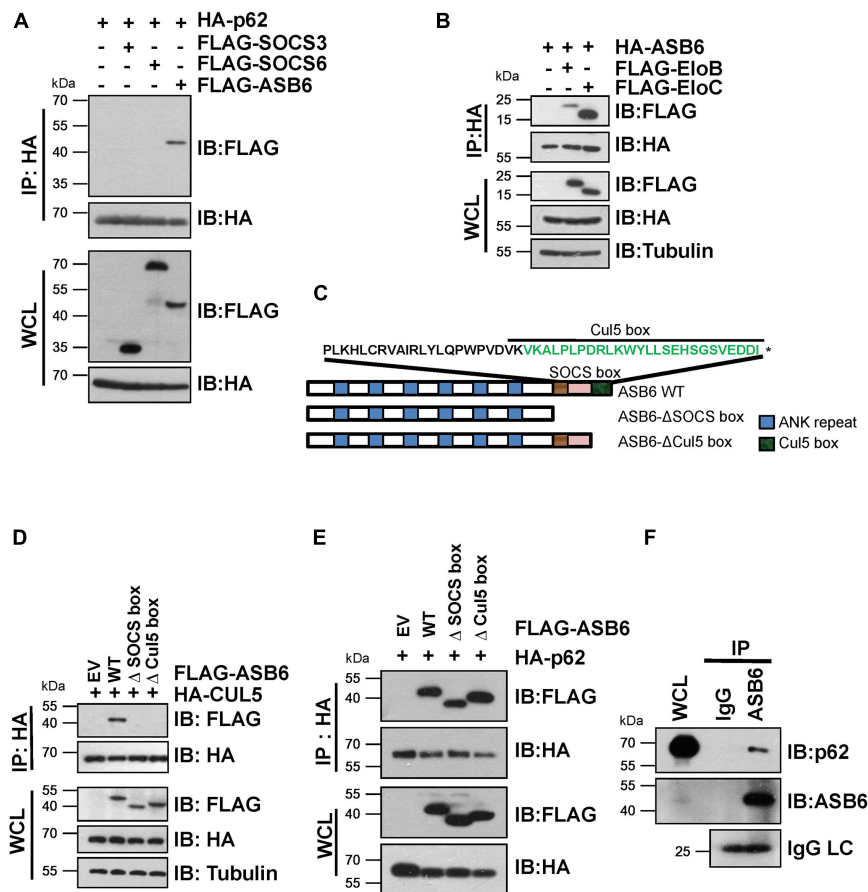


**FIGURE 2 |** ASB6 interacts with p62 and it is part of CRL5 E3 ligase complex. **(A,B)** HEK293T cells transfected with the indicated plasmids were treated with 10  $\mu$ M MG132 for 10 h before harvest for Co-IP and IB analysis. **(C)** Schematic illustration of human ASB6 protein domain composition. **(D,E)** HEK293T cells were co-transfected with ASB6 wild type and mutants ( $\Delta$ -SOCS box,  $\Delta$ -Cul5-box) and HA-CUL5 **(D)** or HA-p62 **(E)** constructs. Cells were treated with 10  $\mu$ M MG132 for 10 h before harvest for Co-IP and IB analysis. **(F)** Huh1 cells were treated with 10  $\mu$ M MG132 for 10 h before harvest to make whole-cell lysates. ASB6 antibody was used to perform endogenous Co-IP experiments with Rabbit IgG as negative control.

impair the interaction between ASB6 and p62 (**Figures 2D,E**). In order to test whether ASB6 is indeed an endogenous interacting protein of p62, we next performed Co-IP experiment with lysate generated from human liver cancer cell line Huh1, in which the tumor-promoting effect of p62 has been validated. As indicated, indeed ASB6 binds to p62 at endogenous level (**Figure 2F**). These results suggest that ASB6 may be the key SOCS box protein in the CRL5 E3 complex that binds and regulates p62.

## ASB6 Promotes Ubiquitination and Degradation of p62

Next, a series of experiments were carried out to determine whether ASB6 is a key p62 regulator. Transient co-transfection of multiple shRNA against ASB6 caused dramatic upregulation of ectopically expressed HA-p62 in 293T cells (**Figure 3A**). Consistently, stable depletion of ASB6 also significantly increased endogenous p62 protein in HeLa cells (**Figure 3B**), with ASB6 knockdown efficiency confirmed by RT-PCR. On the other hand, co-expression of FLAG-ASB6 caused degradation of ectopically

expressed HA-p62 in 293T cells, which could be blocked by proteasome inhibitor MG132 in a dose-dependent manner (**Figure 3C**). Moreover, deletion of either SOCS-box or the smaller Cul5-box impaired the capacity of ASB6 to degrade p62 (**Figure 3D**), which may due to the damaged potential to form functional CRL E3 complex with CUL5 (**Figure 2D**). We also transfected various amounts of FLAG-ASB6 constructs in 293T cells and examined the expression changes of endogenous p62. As shown in **Figure 3G**, the decrease of endogenous p62 is inversely correlated with the amount of overexpressed ASB6. We further performed CHX chase experiment to determine if the observed reduced p62 expression is caused by p62 protein stability change. As indicated in **Figures 3E,F**, p62 is a very stable protein without overexpression of ASB6, and its half-life was significantly shortened in the presence of ASB6. So these results suggested that ASB6 negatively regulates p62 protein stability. We subsequently confirmed that overexpression of CUL5 and ASB6 could promote ubiquitination of endogenous p62 (**Figure 3H**). Therefore, our data suggest that the CUL5-ASB6 complex is a functional E3 ligase promotes ubiquitination and degradation of p62.

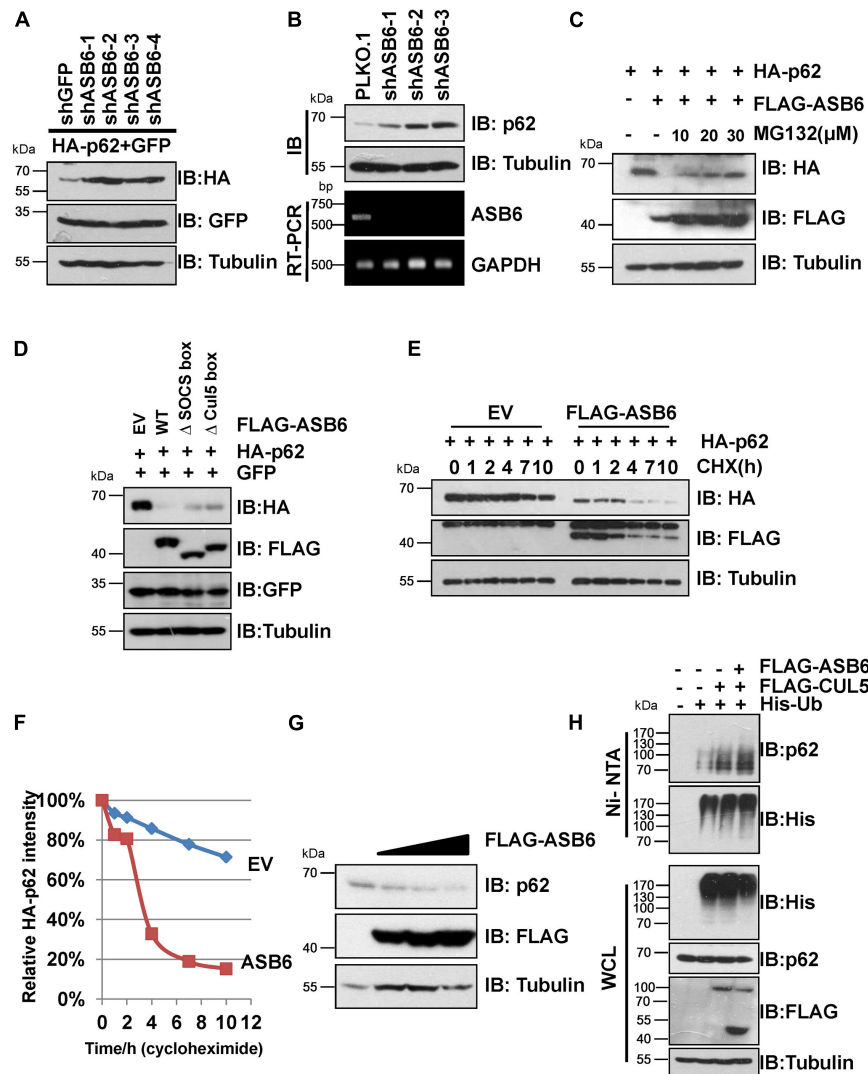


**FIGURE 3 |** CUL5-ASB6 complex promotes ubiquitination and degradation of p62. **(A)** IB analyses of WCL from HEK293T cells co-transfected with plasmids encoding HA-p62, ASB6 shRNAs, and GFP (as an internal transfection control). Tubulin served as a loading control. **(B)** HeLa cells infected with indicated shRNAs were harvested for IB analysis. Tubulin served as a loading control. The knockdown efficiency of ASB6 was examined by RT-PCR. *GAPDH* gene was detected as the internal control. **(C)** HEK293T cells were co-transfected with plasmids encoding HA-p62 and FLAG-ASB6 and were treated with different concentrations of MG132 (10, 20, and 30  $\mu$ M) for 10 h before harvest for IB assay. Tubulin served as a loading control. **(D)** IB analyses of HEK293T cells transfected with plasmids encoding HA-p62 and ASB6 mutants. Tubulin served as a loading control. **(E,F)** HEK293T cells were transfected with plasmids encoding HA-p62 and EV or FLAG-ASB6. Forty-eight hours after transfection, cells were treated with 50  $\mu$ g/ml CHX and harvested at the indicated time for IB analysis. Tubulin served as loading control. Relative HA-p62 protein levels were quantified and normalized to Tubulin with ImageJ software. **(G)** IB analysis of HEK293T cells transfected with a plasmid encoding FLAG-ASB6. Tubulin served as a loading control. **(H)** HEK293T cells transfected with the indicated plasmids were treated with 10  $\mu$ M MG132 for 10 h before harvest for Ni-NTA beads pull down and IB analysis.

It has been reported that p62 has two protein isoforms that are generated by three mRNA variants due to alternative splicing (Wang et al., 2014). Different from the commonly detected 440 amino acid isoform, the shorter p62 isoform (p62S) lacks the N-terminal PB1 domain and contains 356 aa in length (Figure 4A). Therefore, we examined whether p62S is also subject to CUL5-ASB6 mediated regulation. As indicated, p62S also interacted with CUL5 and ASB6, in a manner very similar to the longer p62 isoform (Figures 4B,C). Co-transfection of CUL5 shRNAs can also dramatically upregulate HA-p62S expression

(Figure 4D), while overexpression of CUL5 reduced HA-p62S protein level (Figure 4E). These results suggested that the CUL5-ASB6 E3 ligase regulates not only the classic p62 protein but also the shorter p62 isoform.

### ASB6-Mediated p62 Degradation Is Independent of Autophagy

p62 is the most famous autophagy receptor protein and itself also gets degraded in the autophagosomes together



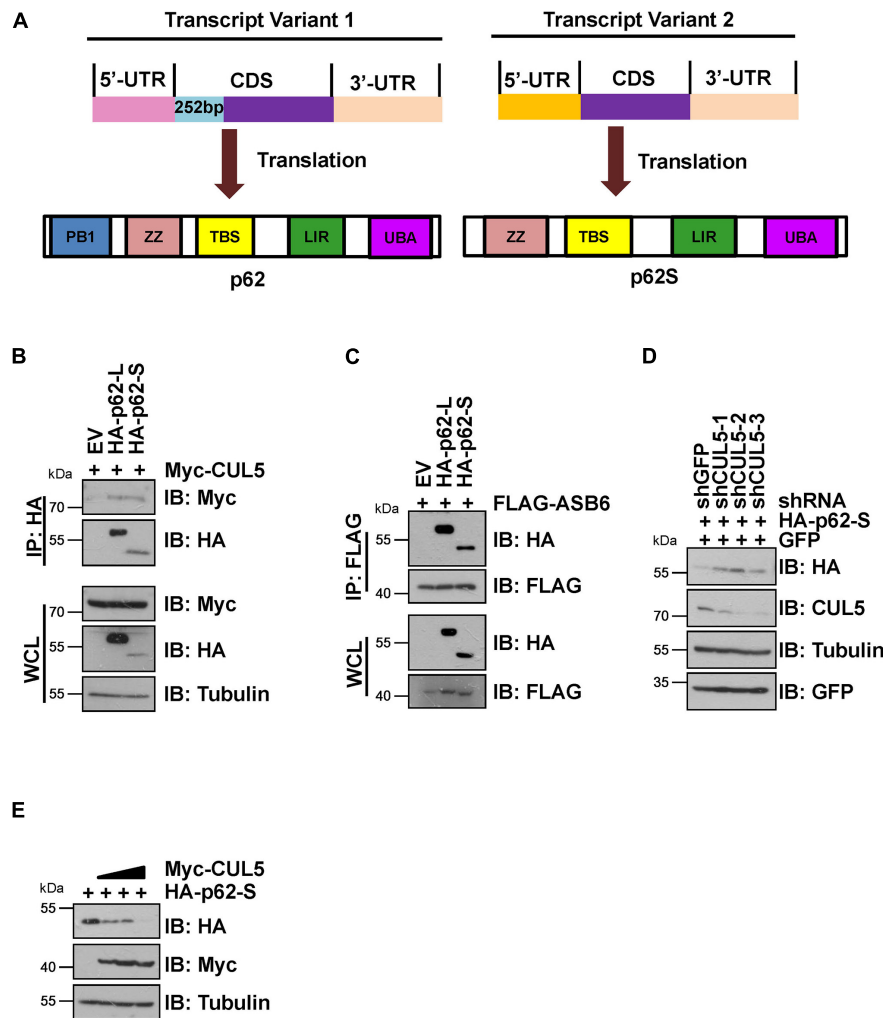


**FIGURE 4 |** CUL5-ASB6 complex interacts with and regulates short p62 isoform. **(A)** Schematic representation of the domain composition of p62 and p62S. **(B,C)** HEK293T cells transfected with the indicated plasmids were treated with 10  $\mu$ M MG132 for 10 h before harvest for IP and IB analysis. **(D)** HEK293T cells were co-transfected with plasmids encoding HA-p62S, shRNAs targeting CUL5, and GFP (as an internal transfection control), and were harvested for IB analysis 48 h later. Tubulin served as a loading control. **(E)** IB analysis of HEK293T cells transfected with HA-p62S plasmid and increasing amount of Myc-CUL5 construct. Tubulin served as a loading control.

with the cargo protein. So, decrease of p62 protein is regarded as an indicator of autophagy process. To dissect whether CUL5-ASB6-mediated p62 degradation depends on autophagy process, we performed multiple experiments with ATG7 knockout (ATG7<sup>-/-</sup>) MEF cells, in which autophagy pathway is defective due to loss of ATG7, a ubiquitin E1-like activating enzyme essential for the assembly and function of ubiquitin-like conjugation systems during autophagy (Nakatogawa et al., 2009). We found that overexpression of ASB6 could downregulate p62 protein levels in ATG7<sup>-/-</sup> MEF cells and shorten p62 half-life in the CHX chase experiment (**Figures 5A,B**). Meanwhile, ASB6 overexpression also inhibited the colony formation and cell proliferation of ATG7<sup>-/-</sup> MEF cells (**Figures 5C,D**). These results suggest that the regulation of p62 by the CUL5-ASB6 complex does not depend on the occurrence of autophagy process. Therefore, the

CUL5-ASB6 complex may regulate cell proliferation *via* p62 independent of autophagy.

## ASB6 Modulates Hepatocellular Carcinoma Cell Proliferation and Autophagy *via* p62

Since p62 has been reported to play an important role in the occurrence and development of liver cancer, we next investigated whether ASB6 has a function in liver cancer cells by regulating p62. We first depleted ASB6 in HCC cell lines SNU739 and SNU182 with siRNAs and shRNAs that target ASB6 (**Figures 6A,B**) and observed significant upregulation of p62 protein. Importantly, depletion of ASB6 with shRNA greatly increased the colony formation of SNU739 cells (**Figure 6C**). Moreover, further depletion of p62 completely reversed the

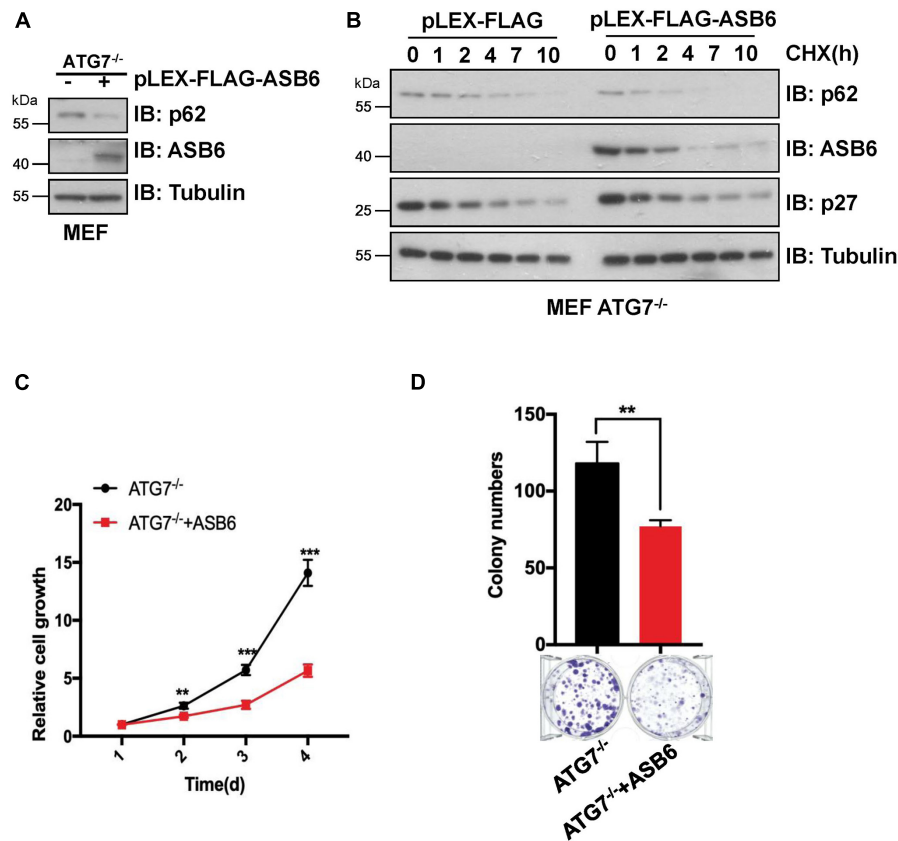


**FIGURE 5 |** The degradation of p62 by ASB6 is independent of autophagy. **(A)** IB analysis of p62 levels in ATG7<sup>-/-</sup> MEF cells stably expressing ectopic ASB6. Tubulin was used as a loading control. **(B)** ATG7<sup>-/-</sup> MEF cells stably expressing ectopic ASB6 were treated with 50  $\mu$ g/ml CHX and harvested at indicated time for IB analysis. Tubulin served as loading control. **(C)** ATG7<sup>-/-</sup> MEF cells stably expressing ectopic ASB6 were counted and seeded into 96-well plates (500 cells per well) to perform CCK8 experiment at the indicated time. Data were shown as mean  $\pm$  SEM ( $n = 3$ ). Statistical analyses were performed using Student's *t*-test. \*\* $P < 0.01$ , \*\*\* $P < 0.001$ . **(D)** ATG7<sup>-/-</sup> MEF cells stably overexpressing ASB6 were counted and seeded into six-well plates (500 cells per well). The number of colonies were measured and analyzed after 10 days. Data represent the mean  $\pm$  SEM. \*\* $P < 0.01$ , by Student's *t*-test.

promoted colony formation caused by ASB6 knockdown in Huh1 cells (Figures 6D,E). Therefore, the increased cell proliferation by ASB6 knockdown is largely due to p62 upregulation.

As p62 is a well-characterized factor in autophagy, we further investigated whether ASB6-mediated p62 degradation would affect the autophagy process. When treated with glucose starvation condition, more advanced autophagy occurred in ASB6-depleted SNU739 cells as evidenced by the much increased shorter LC3-II isoform compared to pLKO.1 vector-treated control cells, and further overexpression of ASB6 could indeed inhibit the LC3-II protein level (Figure 6F). This result indicated that ASB6 may be an inhibitory factor for autophagy. To further prove this point, we constructed a Huh1 cell line stable expressing the autophagy fluorescent reporter protein mCherry-GFP-LC3, and then ectopically expressed FLAG tagged ASB6 wild type and  $\Delta$ SOCS-box ASB6 truncate in it. The expression of endogenous p62 was examined and autophagy was induced by removing glucose from culture medium in these resulting cells. As indicated, expression of ASB6 wild type but not  $\Delta$ SOCS-box ASB6 truncate reduced p62 expression (Figure 6H). More

importantly, the number of mature autophagosomes (marked by red-only puncta, since GFP protein is denatured in acidic condition) significantly reduced in wild-type ASB6 expressed cells (Figure 6G). Consistently, expression of ASB6 wild type, but not  $\Delta$ SOCS-box ASB6 truncate, also strongly reduced the colony formation of the resulted Huh1 cells (Figure 6I). Therefore, these data suggested that ASB6 has an inhibitory role in autophagy and cell proliferation possibly *via* governing p62 abundance in HCC cells.

## DISCUSSION

In the current study, we identified a new functional ubiquitin E3 ligase complex, CUL5-ASB6 complex, as a major regulator governing p62/SQSTM1 abundance (Figure 7). As the largest E3 ligase family, Cullin-Ring E3 ligase complexes are composed of hundreds of members differing in various Cullin proteins, and more importantly, the substrate recognition proteins (Nguyen et al., 2017). Initially designated as VACM-1, CUL5 is a relatively

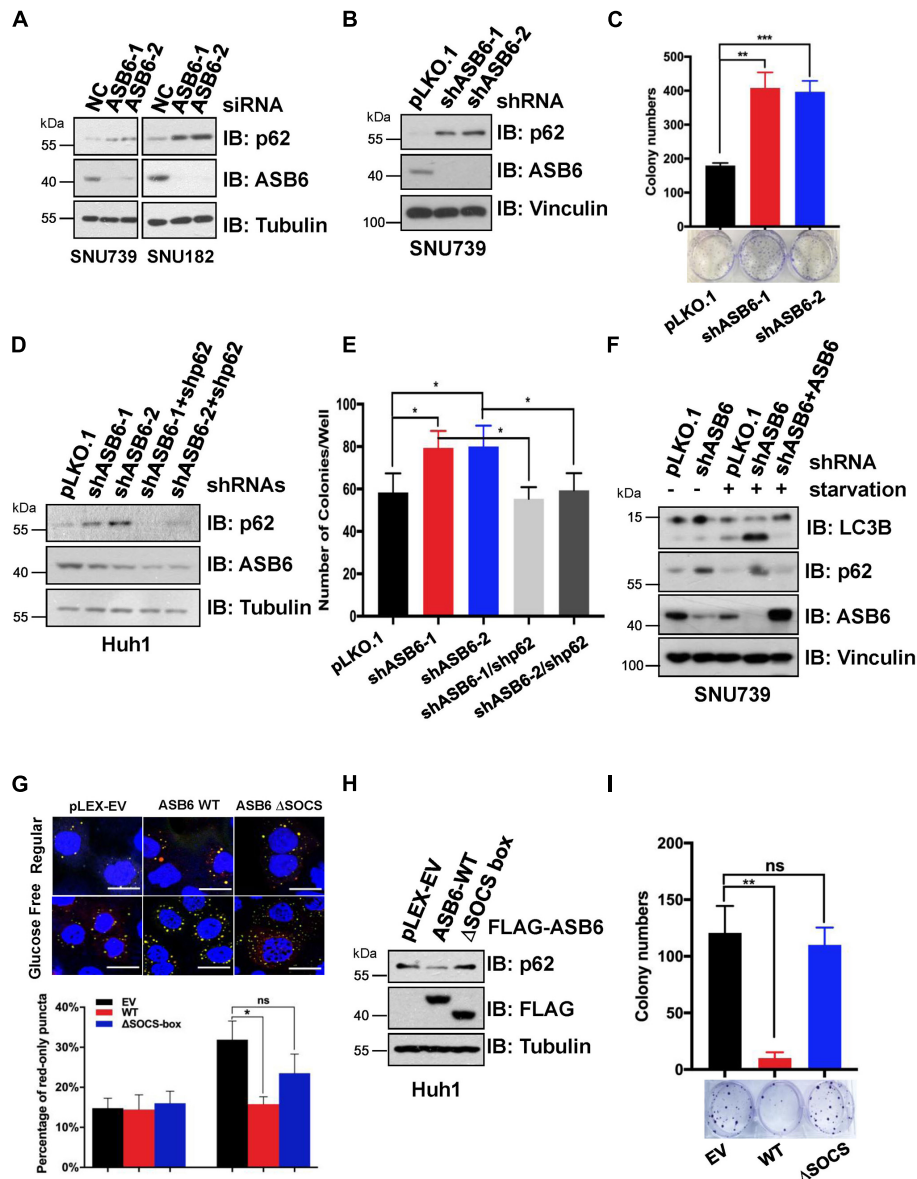
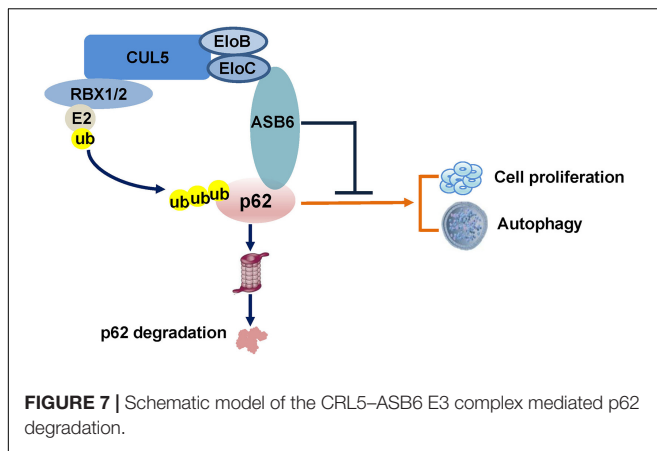


**FIGURE 6 |** ASB6 functions in HCC cells by regulating p62. **(A)** IB analysis of HCC cell lines SNU739 and SNU182 that were transfected with ASB6 siRNAs. Tubulin was used as loading control. **(B)** SNU739 cells infected with indicated shRNAs were harvested for IB analysis. Vinculin served as a loading control. **(C)** The cells from **(B)** were counted and seeded into six-well plates (500 cells per well) to perform colony formation assay. The number of colonies were counted and analyzed. Data represent the mean  $\pm$  SEM.  $^{**}P < 0.01$ ,  $^{***}P < 0.001$ , by Student's *t*-test. **(D)** Huh1 cells were treated with lentiviral shRNAs against ASB6 and p62. The resulting cells were harvested and analyzed by IB with indicated antibodies. Tubulin served as loading control. **(E)** The cells from **(D)** were counted and transferred to six-well plates (500 cells per well) to perform colony formation assay. The number of colonies was measured and analyzed after 10 days. Data represent the mean  $\pm$  SEM.  $^{*}P < 0.05$ , by Student's *t*-test. **(F)** IB analysis of SNU739 cells pre-treated with ASB6 stably knockdown and ASB6 re-expression (a mutant resistant to shRNA treatment). Resulting cells were treated with glucose deprivation for 16 h to induce autophagy. Vinculin was used as loading control. **(G)** Huh1 cells stably expressing mCherry-GFP-LC3 were treated with viral vectors encoding ectopic FLAG-ASB6 WT or  $\Delta$ SOCS-box mutant. Glucose deprivation was performed for 16 h to induce autophagy. GFP and mCherry puncta were measured and analyzed under confocal microscope, and the average percentage of cells containing red-only puncta, which represents the matured autophagosome, was determined and blotted. Scale bars, 20  $\mu$ m. Data represent the mean  $\pm$  SEM. ns, non-significant;  $^{*}P < 0.05$ , by Student's *t*-test. **(H)** IB analysis of Huh1 cells generated in **(G)**. Tubulin was used as loading control. **(I)** The cells from **(G)** were counted and transferred to six-well plates (500 cells per well) to perform colony formation assay. The number of colonies was measured and analyzed after 10 days. Data represent the mean  $\pm$  SEM. ns, non-significant;  $^{**}P < 0.01$ , by Student's *t*-test.

late identified member for the Cullin family (Burnatowska-Hledin et al., 1995). The following studies revealed that CUL5 forms a series of CRL5 E3 ligase complex together with RING

protein RBX1/2, adaptor proteins Elob/C, and, most importantly, the substrate recognition subunit SOCS-box proteins. With more and more studies published, various roles of CRL5 E3 ligase



in viral infection, signaling transduction, and carcinogenesis have been revealed (Zhao and Sun, 2013). Although CUL5 protein is found downregulated in multiple cancers, the exact function of each CUL5 E3 ligase complex in oncogenesis is very diverse since CUL5 E3 ligases could promote the degradation of both oncoproteins and tumor suppressors. For example, we have found that the CUL5-SOCS3 complex degrades ITGB1 to inhibit small cell lung cancer cell migration and metastasis, and the CUL5-SOCS6 complex governs Sin1 level and limits mTORC2 function (Cui et al., 2019; Zhao et al., 2019). Moreover, other groups found that the CUL5-ASB13 complex degrades SNAI2 and the CUL5-SPSB3 complex degrades SNAIL to inhibit cancer metastasis (Liu et al., 2018; Fan et al., 2020). These evidences suggested that certain CUL5 E3 complexes could exert tumor suppressor function in cancer cells. On the other hand, CUL5-WSB1 has been shown to promote tumor metastasis and promote cell cycle *via* degrading tumor suppressors VHL, RhoGDI2, ATM, etc. (Cao et al., 2015; Kim et al., 2015, 2017). Therefore, the role of CUL5 E3 complexes in cancer regulation is very complicated and possibly context dependent. Interestingly, CUL5 has also been implicated in regulating autophagy by promoting the turnover of mTORC1 inhibitor DEPTOR, a process that could be blocked by AMBRA1 (Antonioli et al., 2014). Notably, the reported CUL5-DEPTOR-mTORC1 regulation of autophagy is rather indirect and related to the onset stage of autophagy, since it mainly goes *via* phosphorylation and inhibition of ULK1 (Antonioli et al., 2014). Therefore, our study established a new regulatory role of CUL5 in autophagy *via* governing p62.

ASB6 contains six ankyrin repeats at its N-terminal and a SOCS-box at its C-terminal, which enable it to be integrated as part of the CUL5 E3 complex *via* E2B/C. ASB6 was first identified *via* yeast two hybrid as an interaction protein of APS (also known as SH2B2), an adaptor protein that is involved in the activation of multiple tyrosine kinases (Wilcox et al., 2004). The interaction between APS and ASB6 was further validated by immunoprecipitation and immunofluorescence methods, and ASB6 was shown to possibly recruit E2B/C and other binding partners to the plasma membrane to cause the degradation of APS and ASB6 itself upon activation of insulin receptor. Later, ASB6 was found upregulated in oral

squamous cell carcinoma, which is a possible consequence of exposure to Areca nut extracts and is co-related with poor survival (Hung et al., 2009). Another recent following study from the same group suggested that accumulation of ASB6 may impede ER stress and cause gain of stemness and metastasis feature of oral squamous cell carcinoma, although the underlying molecular mechanism remains elusive (Hung et al., 2019). Therefore, the detailed molecular function of ASB6, especially in pathological conditions, is largely unknown. In the current study, we characterized ASB6 as a substrate recognition subunit of CUL5 E3 ligase that governs p62 abundance. Notably, depletion of ASB6 promotes colony formation of HCC cell line Huh1, which could be reversed by further knockdown of p62, indicating that the function of ASB6 in inhibiting HCC cell proliferation is largely through p62. Consistent with the necessary role of p62 in promoting autophagy, overexpression of ASB6 (but not the  $\Delta$ SOCS-box ASB6 truncate) degrades endogenous p62 and suppresses proceeding of autophagy and colony formation in Huh1 cells. So, it is possible that the function of ASB6 in control cell proliferation-autophagy homeostasis is dependent on p62 status. Nevertheless, a more mechanistic study is required to fully address the biological meaning of the CUL5-ASB6-p62 regulation in physiological and pathological conditions.

Taken together, we have identified the CUL5-ASB6 complex as a functional ubiquitin E3 ligase that promotes the ubiquitination and degradation of p62, through which it regulates cell proliferation and autophagy. Our finding may shed new light on understanding the complex regulation of p62 function and cell proliferation-autophagy homeostasis.

## DATA AVAILABILITY STATEMENT

The raw data supporting the conclusions of this article will be made available by the authors, without undue reservation.

## AUTHOR CONTRIBUTIONS

LG conducted the experiments with help from KW, MW, and HL. DG and ML supervised the project with intellectual input from RH. DG, LG, and ML wrote the manuscript with input from the other authors. All authors contributed to the article and approved the submitted version.

## FUNDING

This work was supported by grants from the Ministry of Science and Technology of China (Nos. 2020YFA0803203 and 2019YFA0802102), grants from the National Science Foundation of China (Nos. 81925029, 91853130, 81790253, and 81874201), the Strategic Priority Research Program of the Chinese Academy of Sciences (XDB19020203), grants from the Natural Science Foundation of Shanghai of China (No. 20ZR1452300), and Shanghai Municipal Health Commission Foundation (No. 201840359).



## REFERENCES

- Aigelsreiter, A., Neumann, J., Pichler, M., Halasz, J., Zatloukal, K., Berghold, A., et al. (2017). Hepatocellular carcinomas with intracellular hyaline bodies have a poor prognosis. *Liver Int.* 37, 600–610. doi: 10.1111/liv.13325
- Antonoli, M., Albiero, F., Nazio, F., Vescovo, T., Perdomo, A. B., Corazzari, M., et al. (2014). AMBRA1 interplay with cullin E3 ubiquitin ligases regulates autophagy dynamics. *Dev. Cell* 31, 734–746. doi: 10.1016/j.devcel.2014.11.013
- Burnatowska-Hledin, M. A., Spielman, W. S., Smith, W. L., Shi, P., Meyer, J. M., and Dewitt, D. L. (1995). Expression cloning of an AVP-activated, calcium-mobilizing receptor from rabbit kidney medulla. *Am. J. Physiol.* 268, F1198–F1210.
- Cao, J., Wang, Y., Dong, R., Lin, G., Zhang, N., Wang, J., et al. (2015). Hypoxia-induced WSB1 promotes the metastatic potential of osteosarcoma cells. *Cancer Res.* 75, 4839–4851. doi: 10.1158/0008-5472.can-15-0711
- Cui, B., Gong, L., Chen, M., Zhang, Y., Yuan, H., Qin, J., et al. (2019). CUL5-SOCS6 complex regulates mTORC2 function by targeting sin1 for degradation. *Cell Discov.* 5:52.
- Du, P., Wang, L., Sliz, P., and Gregory, R. I. (2015). A biogenesis step upstream of microprocessor controls mir-17 approximately 92 expression. *Cell* 162, 885–899. doi: 10.1016/j.cell.2015.07.008
- Fan, H., Wang, X., Li, W., Shen, M., Wei, Y., Zheng, H., et al. (2020). ASB13 inhibits breast cancer metastasis through promoting SNAIL2 degradation and relieving its transcriptional repression of YAP. *Genes Dev.* 34, 1359–1372. doi: 10.1101/gad.339796.120
- Heath, R. J., Goel, G., Baxt, L. A., Rush, J. S., Mohanan, V., Paulus, G. L. C., et al. (2016). RNF166 determines recruitment of adaptor proteins during antibacterial autophagy. *Cell Rep.* 17, 2183–2194. doi: 10.1016/j.celrep.2016.11.005
- Hershko, A., and Ciechanover, A. (1998). The ubiquitin system. *Annu. Rev. Biochem.* 67, 425–479.
- Huang, J., Diaz-Meco, M. T., and Moscat, J. (2018). The macroenvironmental control of cancer metabolism by p62. *Cell Cycle* 17, 2110–2121. doi: 10.1080/15384101.2018.1520566
- Huang, X., Wang, X. N., Yuan, X. D., Wu, W. Y., Lobie, P. E., and Wu, Z. (2019). XIAP facilitates breast and colon carcinoma growth via promotion of p62 depletion through ubiquitination-dependent proteasomal degradation. *Oncogene* 38, 1448–1460. doi: 10.1038/s41388-018-0513-8
- Hung, K. F., Lai, K. C., Liu, T. Y., Liu, C. J., Lee, T. C., and Lo, J. F. (2009). Asb6 upregulation by *Areca* nut extracts is associated with betel quid-induced oral carcinogenesis. *Oral Oncol* 45, 543–548. doi: 10.1016/j.oraloncology.2008.10.004
- Hung, K. F., Liao, P. C., Chen, C. K., Chiu, Y. T., Cheng, D. H., Kawasumi, M., et al. (2019). ASB6 promotes the stemness properties and sustains metastatic potential of oral squamous cell carcinoma cells by attenuating ER stress. *Int. J. Biol. Sci.* 15, 1080–1090. doi: 10.7150/ijbs.31484
- Inami, Y., Waguri, S., Sakamoto, A., Kouno, T., Nakada, K., Hino, O., et al. (2011). Persistent activation of Nrf2 through p62 in hepatocellular carcinoma cells. *J. Cell Biol.* 193, 275–284. doi: 10.1083/jcb.201102031
- Inoue, D., Suzuki, T., Mitsuishi, Y., Miki, Y., Suzuki, S., Sugawara, S., et al. (2012). Accumulation of p62/SQSTM1 is associated with poor prognosis in patients with lung adenocarcinoma. *Cancer Sci.* 103, 760–766. doi: 10.1111/j.1349-7006.2012.02216.x
- Jadhav, T., Geetha, T., Jiang, J., and Wooten, M. W. (2008). Identification of a consensus site for TRAF6/p62 polyubiquitination. *Biochem. Biophys. Res. Commun.* 371, 521–524. doi: 10.1016/j.bbrc.2008.04.138
- Jain, A., Lamark, T., Sjøttem, E., Larsen, K. B., Awuh, J. A., Overvatn, A., et al. (2010). p62/SQSTM1 is a target gene for transcription factor NRF2 and creates a positive feedback loop by inducing antioxidant response element-driven gene transcription. *J. Biol. Chem.* 285, 22576–22591. doi: 10.1074/jbc.m110.118976
- Jongsma, M. L., Berlin, I., Wijdeven, R. H., Janssen, L., Janssen, G. M., Garstka, M. A., et al. (2016). An ER-associated pathway defines endosomal architecture for controlled cargo transport. *Cell* 166, 152–166.
- Kim, J. J., Lee, S. B., Jang, J., Yi, S. Y., Kim, S. H., Han, S. A., et al. (2015). WSB1 promotes tumor metastasis by inducing pVHL degradation. *Genes Dev.* 29, 2244–2257. doi: 10.1101/gad.268128.115
- Kim, J. J., Lee, S. B., Yi, S. Y., Han, S. A., Kim, S. H., Lee, J. M., et al. (2017). WSB1 overcomes oncogene-induced senescence by targeting ATM for degradation. *Cell Res.* 27, 274–293. doi: 10.1038/cr.2016.148
- Kitamura, H., Torigoe, T., Asanuma, H., Hisasue, S. I., Suzuki, K., Tsukamoto, T., et al. (2006). Cytosolic overexpression of p62 sequestosome 1 in neoplastic prostate tissue. *Histopathology* 48, 157–161. doi: 10.1111/j.1365-2559.2005.02313.x
- Komatsu, M. (2011). Potential role of p62 in tumor development. *Autophagy* 7, 1088–1090. doi: 10.4161/auto.7.9.16474
- Kraft, L. J., Dowler, J., Manral, P., and Kenworthy, A. K. (2016). Size, organization, and dynamics of soluble SQSTM1 and LC3-SQSTM1 complexes in living cells. *Autophagy* 12, 1660–1674. doi: 10.1080/15548627.2016.1199299
- Layfield, R., and Hocking, L. J. (2004). SQSTM1 and Paget's disease of bone. *Calcif. Tissue Int.* 75, 347–357. doi: 10.1007/s00223-004-0041-0
- Lee, Y., Chou, T. F., Pittman, S. K., Keith, A. L., Razani, B., and Weihl, C. C. (2017). Keap1/Cullin3 modulates p62/SQSTM1 activity via UBA domain ubiquitination. *Cell Rep.* 20:1994. doi: 10.1016/j.celrep.2017.08.019
- Li, L. J., Shen, C., Nakamura, E., Ando, K., Signoretti, S., Beroukhi, R., et al. (2013). SQSTM1 is a pathogenic target of 5q copy number gains in kidney cancer. *Cancer Cell* 24, 738–750. doi: 10.1016/j.ccr.2013.10.025
- Lim, J., Lachenmayer, M. L., Wu, S., Liu, W., Kundu, M., Wang, R., et al. (2015). Proteotoxic stress induces phosphorylation of p62/SQSTM1 by ULK1 to regulate selective autophagic clearance of protein aggregates. *PLoS Genet.* 11:e1004987. doi: 10.1371/journal.pgen.1004987
- Lin, Q., Dai, Q., Meng, H., Sun, A., Wei, J., Peng, K., et al. (2017). The HECT E3 ubiquitin ligase NEDD4 interacts with and ubiquitylates SQSTM1 for inclusion body autophagy. *J. Cell. Sci.* 130, 3839–3850.
- Linares, J. F., Duran, A., Yajima, T., Pasparakis, M., Moscat, J., and Diaz-Meco, M. T. (2013). K63 polyubiquitination and activation of mTOR by the p62-TRAF6 complex in nutrient-activated cells. *Mol. Cell* 51, 283–296. doi: 10.1016/j.molcel.2013.06.020
- Liu, Y., Kern, J. T., Walker, J. R., Johnson, J. A., Schultz, P. G., and Luesch, H. (2007). A genomic screen for activators of the antioxidant response element. *Proc. Natl. Acad. Sci. U.S.A.* 104, 5205–5210. doi: 10.1073/pnas.0700898104
- Liu, Y., Zhou, H., Zhu, R., Ding, F., Li, Y., Cao, X., et al. (2018). SPSB3 targets SNAIL for degradation in GSK-3beta phosphorylation-dependent manner and regulates metastasis. *Oncogene* 37, 768–776. doi: 10.1038/ncr.2017.370
- Mathew, R., Karp, C. M., Beaudoin, B., Vuong, N., Chen, G., Chen, H. Y., et al. (2009). Autophagy suppresses tumorigenesis through elimination of p62. *Cell* 137, 1062–1075. doi: 10.1016/j.cell.2009.03.048
- Matsumoto, G., Wada, K., Okuno, M., Kurosawa, M., and Nukina, N. (2011). Serine 403 phosphorylation of p62/SQSTM1 regulates selective autophagic clearance of ubiquitinated proteins. *Mol. Cell* 44, 279–289. doi: 10.1016/j.molcel.2011.07.039
- McManus, S., and Roux, S. (2012). The adaptor protein p62/SQSTM1 in osteoclast signaling pathways. *J. Mol. Signal.* 7:1. doi: 10.1186/1750-2187-7-1
- Morreale, F. E., and Walden, H. (2016). Types of ubiquitin ligases. *Cell* 165:248.e1.
- Moscat, J., and Diaz-Meco, M. T. (2012). p62: a versatile multitasker takes on cancer. *Trends Biochem. Sci.* 37, 230–236. doi: 10.1016/j.tibs.2012.02.008
- Nakatogawa, H., Suzuki, K., Kamada, Y., and Ohsumi, Y. (2009). Dynamics and diversity in autophagy mechanisms: lessons from yeast. *Nat. Rev. Mol. Cell Biol.* 10, 458–467. doi: 10.1038/nrm2708
- Nguyen, H. C., Wang, W., and Xiong, Y. (2017). Cullin-RING E3 ubiquitin ligases: bridges to destruction. *Subcell. Biochem.* 83, 323–347. doi: 10.1007/978-3-319-46503-6\_12
- Pan, J. A., Sun, Y., Jiang, Y. P., Bott, A. J., Jaber, N., Dou, Z., et al. (2016). TRIM21 ubiquitylates SQSTM1/p62 and suppresses protein sequestration to regulate redox homeostasis. *Mol. Cell* 62, 149–151. doi: 10.1016/j.molcel.2016.03.015
- Park, S., Choi, S. G., Yoo, S. M., Son, J. H., and Jung, Y. K. (2014). Choline dehydrogenase interacts with SQSTM1/p62 to recruit LC3 and stimulate mitophagy. *Autophagy* 10, 1906–1920. doi: 10.4161/auto.32177
- Pilli, M., Arko-Mensah, J., Ponpuak, M., Roberts, E., Master, S., Mandell, M. A., et al. (2012). TBK-1 promotes autophagy-mediated antimicrobial defense by controlling autophagosome maturation. *Immunity* 37, 223–234. doi: 10.1016/j.immuni.2012.04.015

- Ren, F., Shu, G., Liu, G., Liu, D., Zhou, J., Yuan, L., et al. (2014). Knockdown of p62/sequestosome 1 attenuates autophagy and inhibits colorectal cancer cell growth. *Mol. Cell. Biochem.* 385, 95–102. doi: 10.1007/s11010-013-1818-0
- Ro, S. H., Semple, I. A., Park, H., Park, H., Park, H. W., Kim, M., et al. (2014). Sestrin2 promotes Unc-51-like kinase 1 mediated phosphorylation of p62/sequestosome-1. *FEBS J.* 281, 3816–3827. doi: 10.1111/febs.12905
- Rolland, P., Majid, Z., Durrant, L., Ellis, I. O., Layfield, R., and Spendlove, I. (2007). The ubiquitin-binding protein p62 is expressed in breast cancers showing features of aggressive disease. *Endocr. Relat. Cancer* 14, 73–80. doi: 10.1677/erc.1.01312
- Sanchez-Martin, P., Saito, T., and Komatsu, M. (2019). p62/SQSTM1: 'Jack of all trades' in health and cancer. *FEBS J.* 286, 8–23. doi: 10.1111/febs.14712
- Sanz, L., Sanchez, P., Lallena, M. J., Diaz-Meco, M. T., and Moscat, J. (1999). The interaction of p62 with RIP links the atypical PKCs to NF-kappaB activation. *EMBO J.* 18, 3044–3053. doi: 10.1093/emboj/18.11.3044
- Schulman, B. A., and Harper, J. W. (2009). Ubiquitin-like protein activation by E1 enzymes: the apex for downstream signalling pathways. *Nat. Rev. Mol. Cell Biol.* 10, 319–331. doi: 10.1038/nrm2673
- Song, P., Li, S., Wu, H., Gao, R., Rao, G., Wang, D., et al. (2016). Parkin promotes proteasomal degradation of p62: implication of selective vulnerability of neuronal cells in the pathogenesis of Parkinson's disease. *Protein Cell* 7, 114–129. doi: 10.1007/s13238-015-0230-9
- Soucy, T. A., Smith, P. G., Milhollen, M. A., Berger, A. J., Gavin, J. M., Adhikari, S., et al. (2009). An inhibitor of NEDD8-activating enzyme as a new approach to treat cancer. *Nature* 458, 732–736.
- Umemura, A., He, F., Taniguchi, K., Nakagawa, H., Yamachika, S., Font-Burgada, J., et al. (2016). p62, upregulated during preneoplasia, induces hepatocellular carcinogenesis by maintaining survival of stressed hcc-initiating cells. *Cancer Cell* 29, 935–948. doi: 10.1016/j.ccell.2016.04.006
- Wang, L., Cano, M., and Handa, J. T. (2014). p62 provides dual cytoprotection against oxidative stress in the retinal pigment epithelium. *Biochim. Biophys. Acta.* 1843, 1248–1258. doi: 10.1016/j.bbamcr.2014.03.016
- Wenzel, D. M., Stoll, K. E., and Klevit, R. E. (2011). E2s: structurally economical and functionally replete. *Biochem. J.* 433, 31–42. doi: 10.1042/bj20100985
- Wilcox, A., Katsanakis, K. D., Bheda, F., and Pillay, T. S. (2004). Asb6, an adipocyte-specific ankyrin and SOCS box protein, interacts with APS to enable recruitment of elongins B and C to the insulin receptor signaling complex. *J. Biol. Chem.* 279, 38881–38888. doi: 10.1074/jbc.m406101200
- Yan, X. Y., Zhong, X. R., Yu, S. H., Zhang, L. C., Liu, Y. N., Zhang, Y., et al. (2019). p62 aggregates mediated caspase 8 activation is responsible for progression of ovarian cancer. *J. Cell. Mol. Med.* 23, 4030–4042. doi: 10.1111/jcmm.14288
- Zhao, G., Gong, L., Su, D., Jin, Y., Guo, C., Yue, M., et al. (2019). Cullin5 deficiency promotes small-cell lung cancer metastasis by stabilizing integrin beta1. *J. Clin. Invest.* 129, 972–987. doi: 10.1172/jci122779
- Zhao, Y., and Sun, Y. (2013). Cullin-RING Ligases as attractive anti-cancer targets. *Curr. Pharm. Des.* 19, 3215–3225. doi: 10.2174/13816128113199990300

**Conflict of Interest:** The authors declare that the research was conducted in the absence of any commercial or financial relationships that could be construed as a potential conflict of interest.

Copyright © 2021 Gong, Wang, Wang, Hu, Li, Gao and Lin. This is an open-access article distributed under the terms of the Creative Commons Attribution License (CC BY). The use, distribution or reproduction in other forums is permitted, provided the original author(s) and the copyright owner(s) are credited and that the original publication in this journal is cited, in accordance with accepted academic practice. No use, distribution or reproduction is permitted which does not comply with these terms.



# Neddylation Regulates Macrophages and Implications for Cancer Therapy

Yanyu Jiang<sup>1</sup>, Lihui Li<sup>1</sup>, Yan Li<sup>2</sup>, Guangwei Liu<sup>2</sup>, Robert M. Hoffman<sup>3,4</sup> and Lijun Jia<sup>1\*</sup>

<sup>1</sup> Longhua Hospital, Cancer Institute, Shanghai University of Traditional Chinese Medicine, Shanghai, China, <sup>2</sup> College of Life Sciences, Beijing Normal University, Beijing, China, <sup>3</sup> Department of Surgery, University of California, San Diego, San Diego, CA, United States, <sup>4</sup> AntiCancer Inc., San Diego, CA, United States

Tumor-associated macrophages (TAMs) promote cancer progression via stimulating angiogenesis, invasion/metastasis, and suppressing anti-cancer immunity. Targeting TAMs is a potential promising cancer therapeutic strategy. Neddylation adds the ubiquitin-like protein NEDD8 to substrates, and thereby regulates diverse biological processes in multiple cell types, including macrophages. By controlling cellular responses, the neddylation pathway regulates the function, migration, survival, and polarization of macrophages. In the present review we summarized how the neddylation pathway modulates Macrophages and its implications for cancer therapy.

**Keywords:** macrophage, neddylation, cytokine, migration, polarization

## INTRODUCTION

The tumor microenvironment (TME) comprises multiple cell types, including tumor cells, endothelial cells, fibroblasts and immune cells, interacting with each other continuously (Junttila and de Sauvage, 2013). TME is the critical mediator to inhibit or promote tumor progression and metastasis (Junttila and de Sauvage, 2013). Macrophages are the most abundant immune-cell population in TME (Qian et al., 2011; Izumi et al., 2013; Vakilian et al., 2017). Macrophages can produce various cytokines, such as interleukin-6 (IL-6), tumor necrosis factor- $\alpha$  (TNF- $\alpha$ ), interferon gamma (IFN- $\gamma$ ), which are inflammatory factors (Mantovani, 2010; Cassetta and Pollard, 2018). In turn, chronic inflammation promotes macrophages infiltration to initiate tumor growth via inducing gene mutations and resistance to apoptosis (Coussens and Werb, 2002; Shacter and Weitzman, 2002; Nagarsheth et al., 2017). In established tumors, macrophages stimulate tumor growth, migration, angiogenesis, and metastasis via the following mechanisms: (1) Macrophages create and maintain the tumor vascular network by producing and releasing pro-angiogenic cytokines, such as vascular endothelial growth factor- $\alpha$  (VEGF- $\alpha$ ) and angiogenic CXC chemokines (CXCL8 and CXCL12), transforming growth factor- $\beta$  (TGF- $\beta$ ) and TNF- $\alpha$  (Noy and Pollard, 2014; Cassetta and Pollard, 2018). (2) Macrophages produce pro-invasive extracellular matrix-degrading proteases, such as matrix metalloproteinase 9 (MMP9), to promote cancer cell intravasation and metastasis (Pollard, 2004; Noy and Pollard, 2014; Jinushi and Komohara, 2015; Cassetta and Pollard, 2018). (3) Macrophages serve as an important immunosuppressive regulator to avoid cancer-cell eradication via suppressing T-cell development, activation or function (Cassetta and Pollard, 2018; DeNardo and Ruffell, 2019). Elevated macrophage infiltration in tumors is associated with higher tumor grade and worse overall survival in diverse forms of cancers, such as breast cancer, lung cancer, and lymphoma (Steidl et al., 2010; Zhao et al., 2017; Zhang et al., 2018). An increase of macrophages in tumors suppresses tumor response to first-line therapy, such as

## OPEN ACCESS

### Edited by:

Lingqiang Zhang,  
National Center for Protein Sciences  
Shanghai, China

### Reviewed by:

Xiaofeng Zheng,  
Peking University, China  
Ping Xie,  
Capital Medical University, China

### \*Correspondence:

Lijun Jia  
ljia@shutcm.edu.cn

### Specialty section:

This article was submitted to  
Cell Growth and Division,  
a section of the journal  
Frontiers in Cell and Developmental  
Biology

**Received:** 16 March 2021

**Accepted:** 05 May 2021

**Published:** 07 June 2021

### Citation:

Jiang Y, Li L, Li Y, Liu G,  
Hoffman RM and Jia L (2021)  
Neddylation Regulates Macrophages  
and Implications for Cancer Therapy.  
Front. Cell Dev. Biol. 9:681186.  
doi: 10.3389/fcell.2021.681186

irradiation, chemotherapy, immunotherapy (Ruffell and Coussens, 2015; Petty and Yang, 2017; DeNardo and Ruffell, 2019). A decrease of macrophages in the TME correlates with decreased tumor growth/metastasis and increased survival (Mantovani et al., 2017). Thus, macrophages are a promising target for cancer therapy.

Currently, macrophages are targets in some cancer therapy, including: (1) Depletion macrophages via targeting colony-stimulating factor 1 (CSF1) and colony-stimulating factor 1 receptor (CSF1R) pathway, such as with the small molecule PLX3397 (Butowski et al., 2016; Yan et al., 2017). (2) Promoting macrophage death or inhibiting macrophage proliferation in TME with bisphosphonates (Stresing et al., 2007). (3) Inhibition macrophage infiltration in the TME by targeting the C-C motif chemokine ligand 2 (CCL2) and C-C motif chemokine receptor 2 (CCR2) axis with Carlumab (Loberg et al., 2007). (4) Reprogramming macrophages via anti-CD47 or CD40 antibodies to activate the antitumor activity (Cassetta and Pollard, 2018). These macrophage-targeted therapeutic approaches have shown promise in preclinical models and are being investigated in Phase I/II clinical trials as monotherapy or in combination with chemotherapy or radiation (Cassetta and Pollard, 2018).

Recently, neddylation also has emerged as a critical mechanism in regulating macrophages. Neddylation, a type of post-translational modification, is a biochemical process of adding an ubiquitin-like protein NEDD8 (neuronal precursor cell-expressed developmentally down-regulated protein 8) to substrates via a three-step enzymatic cascades (Kamitani et al., 1997; Xirodimas, 2008; Enchev et al., 2015). Similar to ubiquitination, NEDD8 is first activated by an E1 enzyme (NEDD8 activating enzyme, NAE), transferred to an E2 enzyme (Ubc12/UBE2M and UBE2F), and then conjugated to substrates via a specific E3 enzyme (such as RBX1, RBX2) (Gong and Yeh, 1999; Walden et al., 2003; Huang et al., 2005; Zhao et al., 2014; Enchev et al., 2015; Zhou et al., 2018; **Figure 1**). Neddylation modification regulates diverse biological processes via affecting the stability, conformation, localization and function of its substrate proteins (Zhao et al., 2014; Enchev et al., 2015). The best-characterized physiological substrates of neddylation pathway are the cullin subunits of Cullin-RING ligases (CRLs) (Zhao and Sun, 2013). As the largest family of E3 ubiquitin ligases, CRLs promote the ubiquitination and degradation of approximately 20% of cellular proteins via the ubiquitin-proteasome system (Petroski and Deshaies, 2005; Nakayama and Nakayama, 2006; Deshaies and Joazeiro, 2009; Soucy et al., 2009). Neddylation modification to the C-terminal lysine residue of cullin changes the conformation of CRLs and activates CRLs enzymatic function for protein ubiquitination and degradation (Jia and Sun, 2011; Chen et al., 2016).

Recent studies from our and other groups demonstrate that protein neddylation (NEDD8 and NEDD8-conjugated proteins) and the key components of the neddylation pathway (NAE, UBE2F, UBE2M, RBX1, RBX2) are overactivated in multiple human cancers (Li et al., 2014; Hua et al., 2015; Xie et al., 2017; Zhou et al., 2017; Yu et al., 2018; Tian et al., 2019; Jiang et al., 2020; Wang et al., 2020). The overactivated neddylation pathway activates CRLs to degrade many tumor-suppressor proteins, such

as p21 and p27, leading to tumorigenesis and tumor progression, and resulting in a worse overall patient survival (Li et al., 2014, 2019; Zhou et al., 2018; Jiang et al., 2020).

In 2009, a specific small molecular inhibitor of NAE, called MLN4924 (also known as pevonedistat), was identified via high throughput screening (Soucy et al., 2009). MLN4924 forms a covalent NEDD8-MLN4924 adduct at the active site of NAE to inhibit the first step of the neddylation enzymatic process (Brownell et al., 2010; Enchev et al., 2015). By doing so, MLN4924 inhibits the entire neddylation pathway and blocks the activation of CRLs, thus inducing the accumulation of various tumor-suppressive CRL substrates which trigger cell-cycle arrest, DNA damage, apoptosis or senescence (Zhou et al., 2018; Liang et al., 2020; Zhou and Jia, 2020). Phase II/III clinical trials of MLN4924 have been conducted for the treatment of several solid tumors and hematologic malignancies (Swords et al., 2015, 2018; Bhatia et al., 2016; Sarantopoulos et al., 2016; Shah et al., 2016).

The neddylation pathway also modulates macrophages and their response to different stimulation (Li et al., 2013; Zhou et al., 2019a,b), thus highlighting the connection between neddylation, macrophages, and cancer.

## NEDDYLATION REGULATES THE RELEASE OF INFLAMMATORY CYTOKINES IN MACROPHAGES

Inflammatory cytokines secreted by macrophages are small, secreted proteins that regulate immune-cell development, recruitment and trafficking and are potential targets for cancer therapy (Robinson et al., 2002; Tsuyada et al., 2012; Nagarsheth et al., 2017; Liu et al., 2020). Inactivation the neddylation pathway suppresses proinflammatory cytokine production by macrophages (Chang et al., 2012; Li et al., 2013; Asare et al., 2017). For example, inactivation of neddylation with MLN4924 in macrophages inhibits LPS-induced inflammatory cytokine production, such as IL-6, TNF- $\alpha$ , and IL-1 $\beta$  (Chang et al., 2012; Li et al., 2013; Asare et al., 2017). RBX2-overexpressing macrophages upregulate pro-tumorigenic cytokines (IL-6, TNF- $\alpha$ , and IL-1 $\beta$ ), and downregulate anti-tumorigenic cytokine (IL-12) and anti-inflammatory cytokine (IL-10) (Chang and Ding, 2014). In addition, proteasome inhibitors (e.g., MG-132) repress LPS-induced up-regulation of certain proinflammatory cytokines, such as IL-6, TNF- $\alpha$ , and IL-1 $\beta$  (Ortiz-Lazareno et al., 2008). Furthermore, our group found that neddylation regulates macrophage production of several cytokines (**Figure 2A**). PCR array analysis on MLN4924-treated RAW264.2 demonstrated that the levels of 51 inflammation-related factors were altered (42 down-regulated and 9 up-regulated) compared to lipopolysaccharide (LPS) treated RAW264.2 (**Figure 2A**). Among these factors, the classical inflammatory factors, including IL-6, IL-18, TNF- $\alpha$ , IFN- $\gamma$ , IL-1 $\alpha$ , IL-1 $\beta$ , and CRP (C-reactive protein) were significantly decreased (**Figure 2A**).

Apart from cytokines, our group found that chemokine (C-C motif) ligand families (CCL-1,2,3,4,5,7,8,12,17,19,20,22), chemokine (C-X-C motif) ligand families (CXCL1,5,10,11) and the related receptors (CCR1, CCR3, CCR7, and CXCR4)



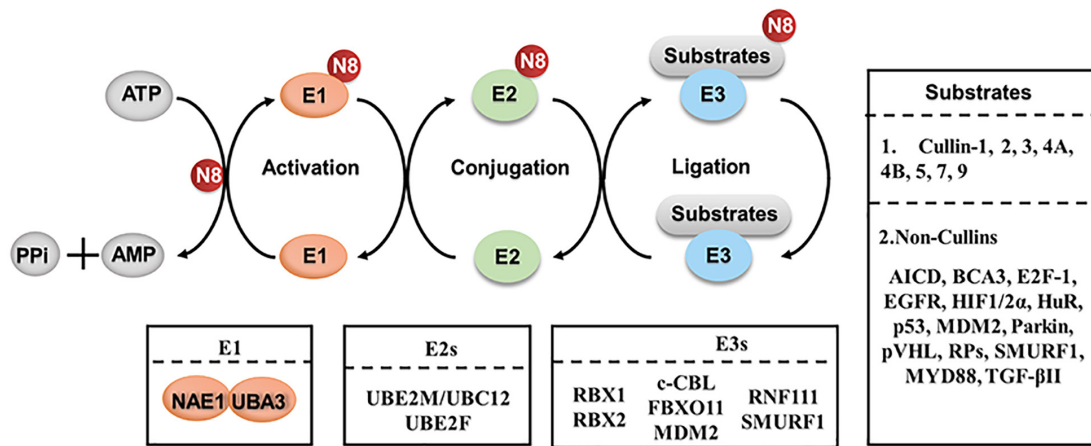


**FIGURE 1 |** The process of protein neddylation. Neddylation is a biochemical process of adding an ubiquitin-like protein, NEDD8, to substrates via a three-step enzymatic cascade involving NEDD8-activating enzyme E1, NEDD8-conjugating enzyme E2 and substrate specific NEDD8-E3 ligases. N8, NEDD8.

were significantly decreased upon MLN4924 treatment in lipopolysaccharide (LPS)-treated RAW264.2 (**Figure 2B**). Among these chemokines, high expression of CCL2, CCL3, CCL7, CCL20, CXCL1, and CXCL10, is correlated with poorer overall survival of cancer patients than patients with low expression ( $p < 0.05$ ) (Gyorffy et al., 2013, 2014; Menyhart et al., 2018; Nagy et al., 2018; **Figure 2C**). CCL2 promotes the infiltration of monocytes, thus promoting cancer-cell vascularization, extravasation and metastasis (Fridlender et al., 2011; Qian et al., 2011; Tsuyada et al., 2012; Wolf et al., 2012; Bonapace et al., 2014; Li et al., 2017). CCL3 promotes tumor extravasation (Robinson et al., 2002; Farmaki et al., 2017). CXCL1 is overexpressed in tumors and recruits the infiltration of monocytes to promote tumor progression, chemoresistance, and metastasis (Acharyya et al., 2012; Miyake et al., 2016; Wang et al., 2016, 2017, 2018; Hsu et al., 2018; Yang et al., 2019). Overactivated neddylation may contribute to tumor progression via promoting the macrophages-mediated inflammation response, but more detailed characterizations and effects are still warranted.

## NEDDYLATION REGULATES INFLAMMATION-RELATED SIGNAL PATHWAYS IN MACROPHAGES

Transcription factors are intracellular molecules that modulate the activity of specific genes. When macrophages are stimulated, transcription factors activate related genes to eliminate pathogens or other dangerous elements. Nuclear factor kappa-B (NF- $\kappa$ B), one of the basic inflammatory-related factors, functions as a precursor to increase the concentration of proinflammatory factors and thus coordinates the inflammatory response (DiDonato et al., 2012). In normal conditions, NF- $\kappa$ B is sequestered in the cytoplasm by interacting with its inhibitory protein I $\kappa$ B $\alpha$  (Bhoj and Chen, 2009). When stimulated by various signals, neddylation modification to the C-terminal lysine residue

of cullin changes the conformation of CRLs and activates CRLs enzymatic function for I $\kappa$ B $\alpha$  ubiquitination and degradation (Bhoj and Chen, 2009; Chang et al., 2012; Jin et al., 2018). The degradation of I $\kappa$ B $\alpha$  by the ubiquitin proteasome system allows NF- $\kappa$ B entering into nucleus where it binds to DNA promoter regions, thus turning on transcription of a wide spectrum of genes and the release of inflammatory factors (Bhoj and Chen, 2009). This process is triggered by I $\kappa$ B $\alpha$  kinases (IKK $\alpha$  or  $\beta$ ), which phosphorylate I $\kappa$ B $\alpha$  at S32 and S36 (Fuchs et al., 1999; Tan et al., 1999), thus, highlighting the underlying cooperative relationship between phosphorylation and neddylation whereas. Inactivation of neddylation inhibits the activity of CRLs and induces the accumulation of its substrate I $\kappa$ B $\alpha$ , which sequesters NF- $\kappa$ B in the cytoplasm to block NF- $\kappa$ B transcriptional activity (Chang et al., 2012; Jin et al., 2018; **Figure 3A**). Moreover, Cullin 5 neddylation following LPS stimulation triggers the interaction with tumor necrosis factor receptor-associated factor 6 (TRAF6), an essential adaptor to promote the activation of NF- $\kappa$ B, thus inducing K63-linked TRAF6 polyubiquitination and leading to NF- $\kappa$ B activation, and eventually facilitating the generation of proinflammatory cytokines (Zhu et al., 2016, 2017).

Apart from the modulation of transcription factors, the neddylation pathway regulates the maturation and secretion processes of inflammatory factors in macrophages. For example, the association of pro-caspase-1 with NLR family pyrin domain containing 3 (NLRP3)/apoptosis-associated speck-like (ASC) protein via caspase recruitment domain (CARD) promotes the autocatalytic activity of pro-caspase-1 to self-cleavage into caspase-1, and thus leads to the maturation of 31 KD pro-interleukin-1 $\beta$  into 17KD IL-1 $\beta$  (Bryant and Fitzgerald, 2009; Dowling and O'Neill, 2012). In this process, neddylation modification to the CARD domain is required for the self-cleavage of pro-caspase-1 to generate its catalytically active subunits (Segovia et al., 2015). NEDD8 silencing or MLN4924 inhibition of neddylation modification of the caspase-1 CARD domain diminishes caspase-1 maturation and inhibits IL-1 $\beta$  maturation and secretion (Segovia et al., 2015; **Figure 3B**). These

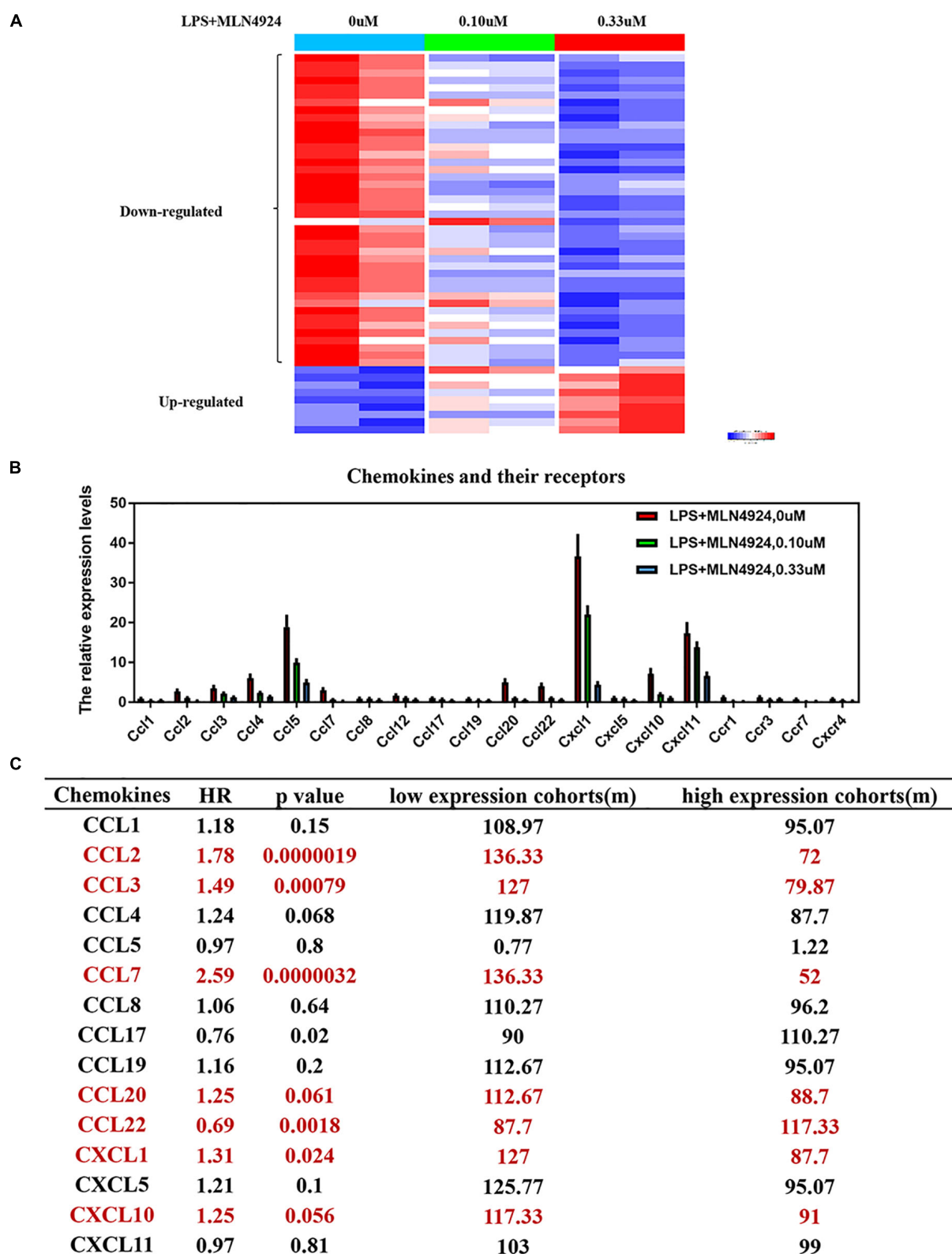


**FIGURE 2 |** Neddylolation regulates the release of inflammatory cytokines in macrophages. **(A)** The results of PCR array analysis on lipopolysaccharide (LPS)-treated RAW264.2 upon MLN4924 treatment, **(B)** MLN4924 treatment decreases the level of chemokines and the related receptors in lipopolysaccharide (LPS)-treated RAW264.2. **(C)** The survival analysis of these chemokines in lung adenocarcinoma using KM plotter website.

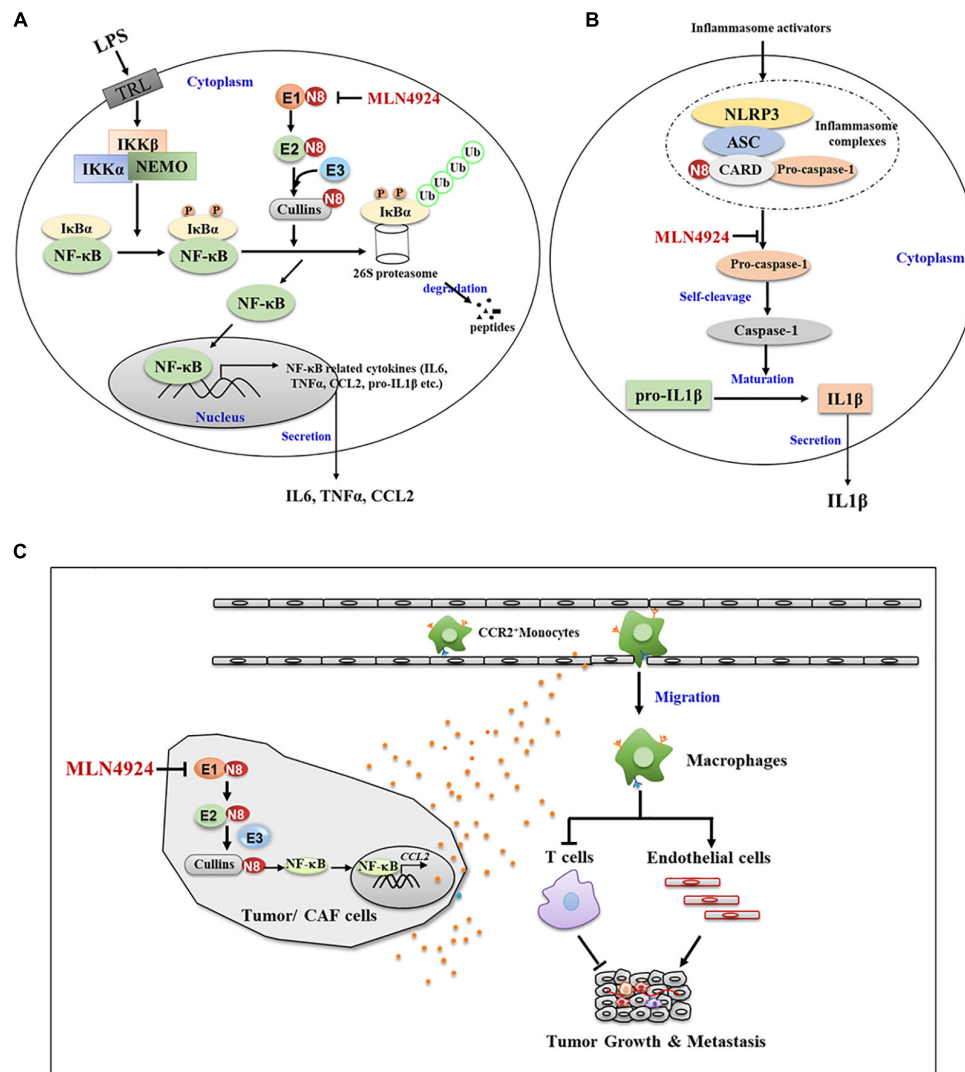


**FIGURE 3 |** Neddylation regulates the function and migration of macrophages. **(A)** Neddylation inactivation by MLN4924 inhibits the activity of CRLs and induces the accumulation of its substrate IκBα, which sequesters NF-κB in the cytoplasm to block NF-κB transcriptional activity. **(B)** MLN4924 inhibits neddylation modification of caspase-1 CARD domain, and thus diminishes caspase-1 maturation and reduces IL-1β maturation and secretion. **(C)** Inactivation neddylation in tumor or CAF cells inhibited CCL2 expression and macrophage infiltration, thus mediating its lung metastasis-inhibitory efficacy.

findings demonstrate how neddylation pathway modulates the macrophage inflammation response, which provides a molecular basis for targeting neddylation pathway in macrophages to ameliorate the inflammation microenvironment in tumors.

## NEDDYLATION REGULATES THE MIGRATION OF MACROPHAGES

The monocyte-derived macrophages are mainly recruited into tumors by chemokines, which can be released from cancer cells or stromal cells (Qian et al., 2011; Izumi et al., 2013; Vakilian et al., 2017). Among these chemokines, CCL2 recruits monocytes into tumors (Qian et al., 2011; Izumi et al., 2013; Vakilian et al., 2017). High CCL2 expression positively correlates with increased

infiltration of tumor associated macrophages and predicts worse prognosis in multiple human and murine cancers (Fridlender et al., 2011; Qian et al., 2011; Tsuyada et al., 2012; Wolf et al., 2012; Bonapace et al., 2014; Li et al., 2017).

A recent study from our group showed that the elevated neddylation pathway in cancer cells led to the accumulation of NF-κB-regulated activation of chemokines CCL2 with promotion of macrophage infiltration (Zhou et al., 2019a). Inactivation neddylation in cancer cells, either pharmacologically (MLN4924) or genetically (NEDD8 knock out via Crisp Cas9), inhibited CCL2 expression and macrophage tumor infiltration, thus inhibiting lung metastasis (Zhou et al., 2019a; **Figure 3C**). MLN4924 also suppressed cancer-associated fibroblasts (CAF)-derived and macrophage-derived CCL2 (Zhou et al., 2019b; **Figure 3C**). Therefore, neddylation activation promotes the

migration of macrophages via regulating tumor/CAF-derived CCL2, indicating synergistic inhibition of neddylation in CCL2-producing cells to target the CCL2-macrophage axis. MLN4924 can thus reduce macrophage accumulation in tumors, which could be an effective cancer therapy.

Functionally, tumor infiltrated macrophages induce an immunosuppressive and tumorigenic phenotype by neutralizing the function of cytotoxic CD8<sup>+</sup> T cells (Cassetta and Pollard, 2018). Neddylation inactivation decreases macrophage tumor infiltration and promotes CD8<sup>+</sup> T cell tumor infiltration (Zhou et al., 2019a). Based on these findings, we postulate that targeting the neddylation pathway to inhibit macrophage recruitment in tumors would be tested in clinical trials.

## NEDDYLATION REGULATES THE PROLIFERATION AND SURVIVAL OF MACROPHAGES

Similar to cancer cells, the neddylation pathway is required for the proliferation and survival of macrophages. Neddylation inactivation inhibits macrophage viability with the following

mechanisms, including: (1) Neddylation inactivation by MLN4924 blocks cullin neddylation and suppresses CRL activity, thus leading to the accumulation of cell-cycle inhibitors (e.g., p21, p27, and Wee1) and inducing G<sub>2</sub>-M- phase cell-cycle arrest in macrophages. (2) MLN4924 activates DNA re-replication stress and DNA damage by inducing the accumulation DNA replication licensing protein of CDT1 and ORC1 in macrophages. (3) MLN4924 triggers the increase of tumor-suppressive CRL substrate NF- $\kappa$ B inhibitor I $\kappa$ B $\alpha$ , and resulting in apoptosis of macrophages (Li et al., 2013; Zhou et al., 2019b; **Figure 4A**). (4) RBX2 depletion in macrophages induces the accumulation of proapoptotic Bax and SARM, and inhibits the expression of anti-apoptotic protein Bcl-2, thereby activating cytosolic cytochrome c, caspase-9 and caspase -3, and leading to macrophage's death (Chang and Ding, 2014).

How dose neddylation modification influence survival and the inflammatory response of macrophages? Firstly, partial inhibition of neddylation by MLN4924 inhibits inflammatory response of macrophages at an early stage when cell viability is not significantly blocked. However, continuous inactivation of neddylation by MLN4924 impairs macrophage viability, indicating that the balance of macrophage survival or death

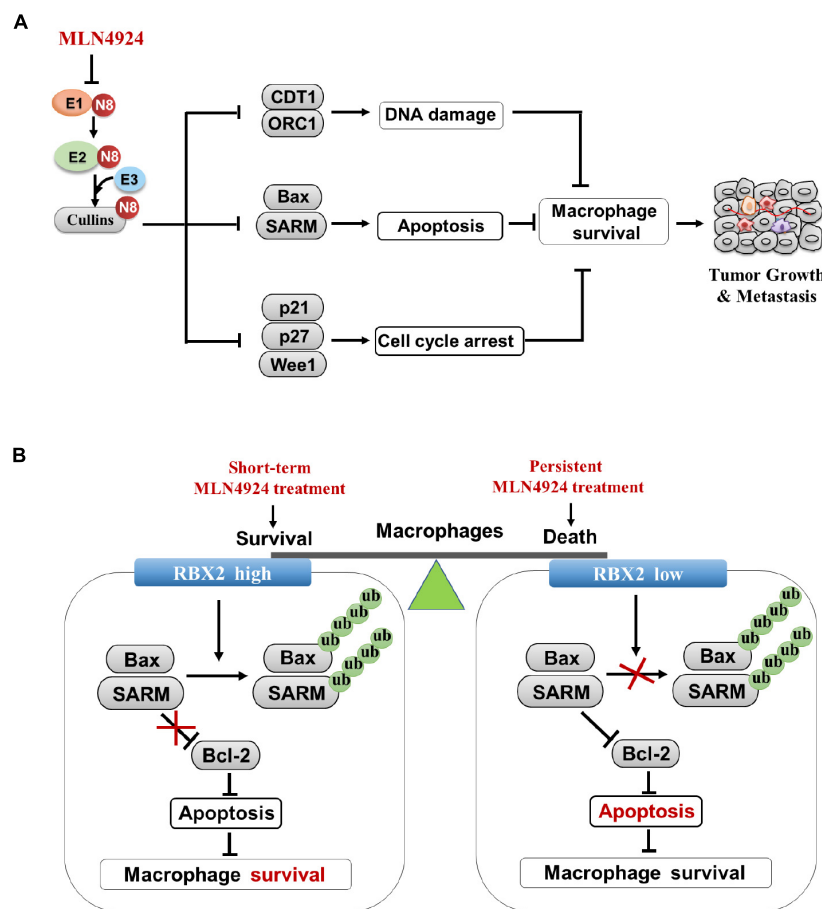


**FIGURE 4 |** Inhibition of neddylation pathway impairs proliferation and survival of macrophages. **(A)** Multiple anti-growth mechanisms in macrophages upon MLN4924 treatment. **(B)** Neddylation modification equilibrates the survival/inflammatory response and death of macrophages.

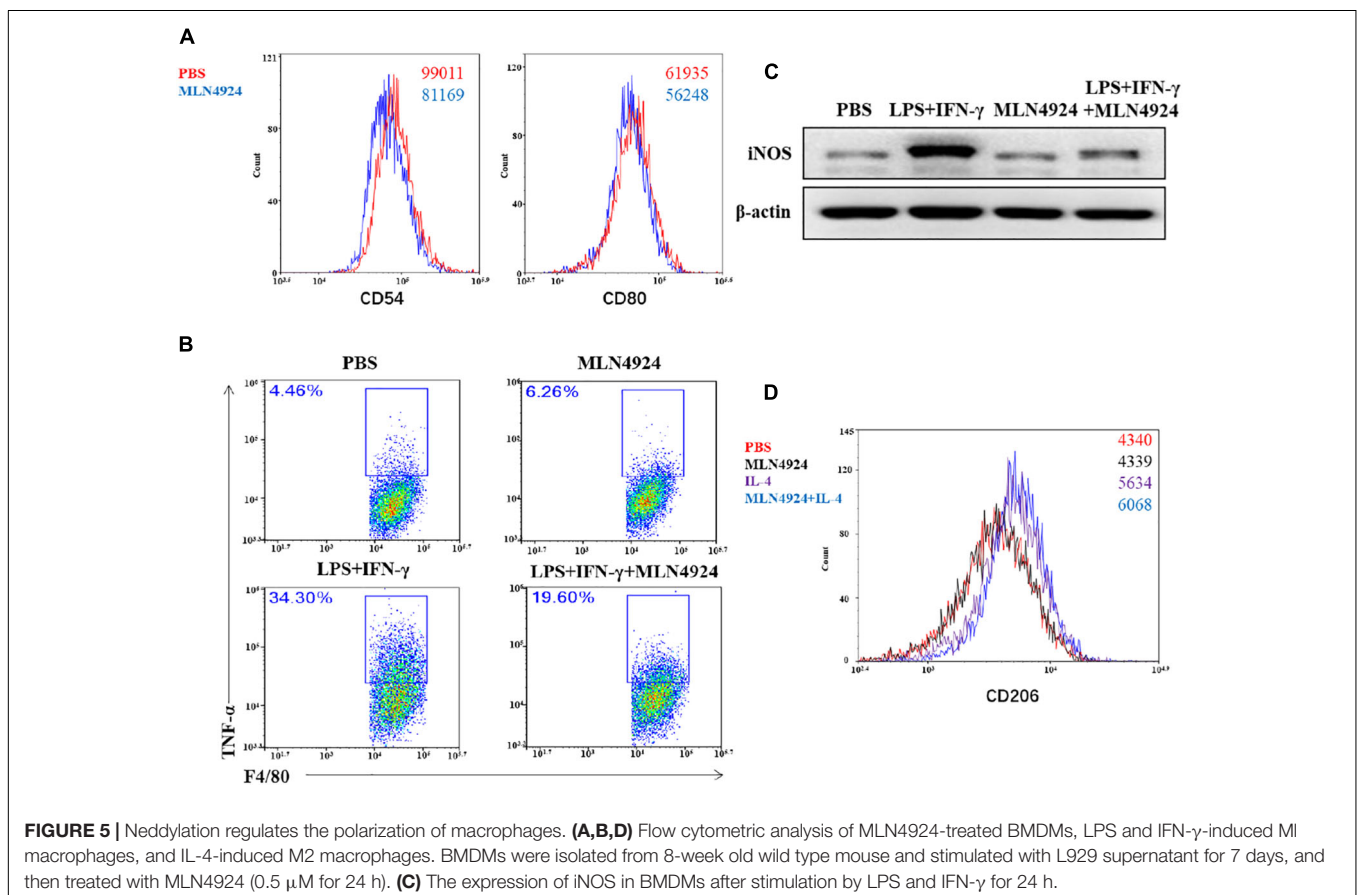


depends on the treatment degree of neddylation inactivation by MLN4924 treatment (Li et al., 2013; **Figure 4B**). Secondly, RBX2-overexpressing macrophages maintain viability via degradation of the pro-apoptotic proteins (BAX and SARM), which facilitate the pathogen-associated molecular patterns (PAMPs)-stimulated inflammatory response. RBX2 knockdown induces the accumulation of BAX and SARM to trigger intrinsic apoptosis (Chang and Ding, 2014; **Figure 4B**), suggesting the RBX2-dependent ubiquitin-proteasome system serves as a checkpoint between the survival and death of macrophages. These results suggest strategies for targeting neddylation to inhibit tumor infiltration macrophages as potential cancer therapy.

## NEDDYLATION REGULATES THE POLARIZATION OF MACROPHAGES

Macrophages can be divided into classically activated macrophages (M1 phenotype) and alternatively activated macrophages (M2 phenotype) (Gordon and Taylor, 2005; Murray, 2017; Chistiakov et al., 2018). M1 produces inducible nitric oxide synthase (iNOS) and pro-inflammatory cytokines upon LPS and/or IFN- $\gamma$  stimulation, which have anti-cancer effects. M2 is triggered by IL-4 or IL-13, to produce arginase 1 (Arg1) and anti-inflammatory cytokines, eventually promoting tumorigenesis (Martinez et al., 2006; Liu et al., 2014).

Asare et al. (2017) reported that MLN4924 drove macrophages to the anti-inflammatory M2 state with increase of M2 makers, arginase-1 and IL-13, and decrease M1 markers, TNF- $\alpha$ , IL-6, and IL-12 in bone marrow-derived macrophages (BMDMs) which were isolated from Apoe<sup>-/-</sup> knockout mice. Our team also found that MLN4924 inhibited macrophages to the M1 phenotype in wild type mouse bone-marrow derived macrophages (**Figure 5**). Flow cytometric analysis demonstrated that the expression level of costimulatory molecules, CD80 and CD54, was decreased in MLN4924-treated BMDMs, indicating that MLN4924 suppressed the polarization of BMDMs into M1 macrophages (**Figure 5A**). To further confirm this hypothesis, we treated BMDMs with MLN4924 to determine the phenotype switching between M1 and M2 macrophages. As shown, the proportion of LPS and IFN- $\gamma$ -induced M1 macrophages (F4/80+/TNF- $\alpha$ +) was significantly reduced upon MLN4924 treatment (**Figure 5B**). Also, after 24 h stimulation, LPS and IFN- $\gamma$  induced the expression of iNOS in BMDMs, which was restored by MLN4924 treatment (**Figure 5C**). IL-4 stimulation resulted in the M2 phenotype (CD11b+/F4/80-/CD206+), while MLN4924 up-regulated the number of M2 macrophages following IL-4 treatment (**Figure 5D**), indicating that inactivation of the neddylation pathway by MLN4924 polarized macrophages toward a M2 phenotype *in vitro*. In a metastatic lung cancer model, NEDD8 knockout significantly reduced the population of both M1 (CD11b+/F4/80+/CD206-) and M2



(CD11b+/F4/80+/CD206+) macrophages, suggesting that neddylation pathway probably mainly regulates the chemotaxis of macrophages but not the polarization in the metastatic lung cancer model (Zhou et al., 2019a).

In summary, these results imply that neddylation regulates the polarization of macrophages in a cell-type and microenvironment-type dependent manner. Additional investigation is needed to further decipher the detailed mechanisms. Nevertheless, in either case, a high number of macrophages in tumor is associated with poor overall survival. Therefore, limiting the numbers of macrophages via inactivating neddylation in tumor is a promising therapeutic strategy.

## CONCLUSION AND REMARKS

Macrophages are a major component of TME. Neddylation inactivation to suppress the accumulation of macrophages in tumor is a novel and promising cancer therapeutic strategy (Zhou et al., 2019a,b). However, some questions still await further investigation.

Firstly, further studies are needed to fully identify macrophage phenotypes and define the determining factors for macrophage's polarization upon MLN4924 treatment in various tumor models. Secondly, the TME comprises different types of infiltrated immune cells, fibroblasts, endothelial cells as well as cancer cells. The role of the neddylation genes (such as NEDD8, UBA3, NAE1, UBE2M, UBE2F, RBX1, and RBX2) in specific cell subsets of the TME needs to be further clarified. Thirdly, we need to learn how neddylation modulates the proliferation and differentiation of hematopoietic stem cells and myeloid progenitor cells, and how neddylation modulates the production of monocytes in multiple tumor models. Fourthly, the efficacy of MLN4924 in

combination with cancer immunotherapy (such as nivolumab, avelumab, ipilimumab) needed to be tested. Finally, identification of the biomarkers indicating the viability of macrophages upon neddylation inhibition could maximize the therapeutic efficacy of MLN4924, and optimize the dose, routine, and schedule.

Once we assure these questions, the regulatory mechanisms of macrophages will be clearly clarified, which would extend our understanding of how neddylation pathway modulates macrophages in fundamental cancer biology, and provide a sound rationale and molecular basis for neddylation-based targeting macrophages therapies for clinical cancer treatment.

## AUTHOR CONTRIBUTIONS

YJ, LL, and YL collected the related manuscript and drafted the manuscript. GL and RMH provided the technical or material support. LJ, YJ, and RMH revised and finalized the manuscript. All authors read and approved the final manuscript.

## FUNDING

This work was supported by the National Natural Science Foundation of China (Grant Nos. 81625018, 81820108022, 82003297), the Innovation Program of Shanghai Municipal Education Commission (2019-01-07-00-10-E00056), the Program of Shanghai Academic/Technology Research Leader (18XD1403800), the National Thirteenth Five-Year Science and Technology Major Special Project for New Drug and Development (2017ZX09304001), and the ChenGuang project supported by the Shanghai Municipal Education Commission and Shanghai Education Development Foundation (19CG49).

## REFERENCES

- Acharyya, S., Oskarsson, T., Vanharanta, S., Malladi, S., Kim, J., Morris, P. G., et al. (2012). A CXCL1 paracrine network links cancer chemoresistance and metastasis. *Cell* 150, 165–178. doi: 10.1016/j.cell.2012.04.042
- Asare, Y., Ommer, M., Azombo, F. A., Alampour-Rajabi, S., Sternkopf, M., Sanati, M., et al. (2017). Inhibition of atherogenesis by the COP9 signalosome subunit 5 in vivo. *Proc. Natl. Acad. Sci. U.S.A.* 114, E2766–E2775.
- Bhatia, S., Pavlick, A. C., Boasberg, P., Thompson, J. A., Mulligan, G., Pickard, M. D., et al. (2016). A phase I study of the investigational NEDD8-activating enzyme inhibitor pevonedistat (TAK-924/MLN4924) in patients with metastatic melanoma. *Invest. New Drugs* 34, 439–449. doi: 10.1007/s10637-016-0348-5
- Bhoj, V. G., and Chen, Z. J. (2009). Ubiquitylation in innate and adaptive immunity. *Nature* 458, 430–437. doi: 10.1038/nature07959
- Bonapace, L., Coissieux, M. M., Wyckoff, J., Mertz, K. D., Varga, Z., Junt, T., et al. (2014). Cessation of CCL2 inhibition accelerates breast cancer metastasis by promoting angiogenesis. *Nature* 515, 130–133. doi: 10.1038/nature13862
- Brownell, J. E., Sintchak, M. D., Gavin, J. M., Liao, H., Bruzzese, F. J., Bump, N. J., et al. (2010). Substrate-assisted inhibition of ubiquitin-like protein-activating enzymes: the NEDD8 E1 inhibitor MLN4924 forms a NEDD8-AMP mimetic in situ. *Mol. Cell* 37, 102–111. doi: 10.1016/j.molcel.2009.12.024
- Bryant, C., and Fitzgerald, K. A. (2009). Molecular mechanisms involved in inflammasome activation. *Trends Cell Biol.* 19, 455–464. doi: 10.1016/j.tcb.2009.06.002
- Butowski, N., Colman, H., De Groot, J. F., Omuro, A. M., Nayak, L., Wen, P. Y., et al. (2016). Orally administered colony stimulating factor 1 receptor inhibitor PLX3397 in recurrent glioblastoma: an Ivy Foundation early phase clinical trials consortium phase II study. *Neuro Oncol.* 18, 557–564. doi: 10.1093/neuonc/nov245
- Cassetta, L., and Pollard, J. W. (2018). Targeting macrophages: therapeutic approaches in cancer. *Nat. Rev. Drug Discov.* 17, 887–904. doi: 10.1038/nrd.2018.169
- Chang, F. M., Reyna, S. M., Granados, J. C., Wei, S. J., Innis-Whitehouse, W., Maffi, S. K., et al. (2012). Inhibition of neddylation represses lipopolysaccharide-induced proinflammatory cytokine production in macrophage cells. *J. Biol. Chem.* 287, 35756–35767. doi: 10.1074/jbc.m112.397703
- Chang, S. C., and Ding, J. L. (2014). Ubiquitination by SAG regulates macrophage survival/death and immune response during infection. *Cell Death Differ.* 21, 1388–1398. doi: 10.1038/cdd.2014.54
- Chen, P., Hu, T., Liang, Y., Li, P., Chen, X., Zhang, J., et al. (2016). Neddylation inhibition activates the extrinsic apoptosis pathway through ATF4-CHOP-DR5 axis in human esophageal cancer cells. *Clin. Cancer Res.* 22, 4145–4157. doi: 10.1158/1078-0432.ccr-15-2254
- Chistiakov, D. A., Myasoedova, V. A., Revin, V. V., Orekhov, A. N., and Bobryshev, Y. V. (2018). The impact of interferon-regulatory factors to macrophage differentiation and polarization into M1 and M2. *Immunobiology* 223, 101–111. doi: 10.1016/j.imbio.2017.10.005
- Coussens, L. M., and Werb, Z. (2002). Inflammation and cancer. *Nature* 420, 860–867.
- DeNardo, D. G., and Ruffell, B. (2019). Macrophages as regulators of tumour immunity and immunotherapy. *Nat. Rev. Immunol.* 19, 369–382. doi: 10.1038/s41577-019-0127-6

- Deshaies, R. J., and Joazeiro, C. A. (2009). RING domain E3 ubiquitin ligases. *Annu. Rev. Biochem.* 78, 399–434.
- DiDonato, J. A., Mercurio, F., and Karin, M. (2012). NF- $\kappa$ B and the link between inflammation and cancer. *Immunol. Rev.* 246, 379–400. doi: 10.1111/j.1600-065x.2012.01099.x
- Dowling, J. K., and O'Neill, L. A. (2012). Biochemical regulation of the inflammasome. *Crit. Rev. Biochem. Mol. Biol.* 47, 424–443. doi: 10.3109/10409238.2012.694844
- Enchev, R. I., Schulman, B. A., and Peter, M. (2015). Protein neddylation: beyond cullin-RING ligases. *Nat. Rev. Mol. Cell Biol.* 16, 30–44. doi: 10.1038/nrm3919
- Farmaki, E., Kaza, V., Papavassiliou, A. G., Chatzistamou, I., and Kiaris, H. (2017). Induction of the MCP chemokine cluster cascade in the periphery by cancer cell-derived Ccl3. *Cancer Lett.* 389, 49–58. doi: 10.1016/j.canlet.2016.12.028
- Fridlender, Z. G., Kapoor, V., Buchlis, G., Cheng, G., Sun, J., Wang, L. C., et al. (2011). Monocyte chemoattractant protein-1 blockade inhibits lung cancer tumor growth by altering macrophage phenotype and activating CD8+ cells. *Am. J. Respir. Cell Mol. Biol.* 44, 230–237. doi: 10.1165/rcmb.2010-0080oc
- Fuchs, S. Y., Chen, A., Xiong, Y., Pan, Z. Q., and Ronai, Z. (1999). HOS, a human homolog of Slimb, forms an SCF complex with Skp1 and Cullin1 and targets the phosphorylation-dependent degradation of I $\kappa$ B and  $\beta$ -catenin. *Oncogene* 18, 2039–2046. doi: 10.1038/sj.onc.1202760
- Gong, L., and Yeh, E. T. (1999). Identification of the activating and conjugating enzymes of the NEDD8 conjugation pathway. *J. Biol. Chem.* 274, 12036–12042. doi: 10.1074/jbc.274.17.12036
- Gordon, S., and Taylor, P. R. (2005). Monocyte and macrophage heterogeneity. *Nat. Rev. Immunol.* 5, 953–964. doi: 10.1038/nri1733
- Gyorffy, B., Bottai, G., Lehmann-Che, J., Keri, G., Orfi, L., Iwamoto, T., et al. (2014). TP53 mutation-correlated genes predict the risk of tumor relapse and identify MP51 as a potential therapeutic kinase in TP53-mutated breast cancers. *Mol. Oncol.* 8, 508–519. doi: 10.1016/j.molonc.2013.12.018
- Gyorffy, B., Surowiak, P., Budczies, J., and Lanczky, A. (2013). Online survival analysis software to assess the prognostic value of biomarkers using transcriptomic data in non-small-cell lung cancer. *PLoS One* 8:e82241. doi: 10.1371/journal.pone.0082241
- Hsu, Y. L., Chen, Y. J., Chang, W. A., Jian, S. F., Fan, H. L., Wang, J. Y., et al. (2018). Interaction between tumor-associated dendritic cells and colon cancer cells contributes to tumor progression via CXCL1. *Int. J. Mol. Sci.* 19:2427. doi: 10.3390/ijms19082427
- Hua, W., Li, C., Yang, Z., Li, L., Jiang, Y., Yu, G., et al. (2015). Suppression of glioblastoma by targeting the overactivated protein neddylation pathway. *Neuro Oncol.* 17, 1333–1343. doi: 10.1093/neuonc/nov066
- Huang, D. T., Paydar, A., Zhuang, M., Waddell, M. B., Holton, J. M., and Schulman, B. A. (2005). Structural basis for recruitment of Ubc12 by an E2 binding domain in NEDD8's E1. *Mol. Cell* 17, 341–350. doi: 10.1016/j.molcel.2004.12.020
- Izumi, K., Fang, L. Y., Mizokami, A., Namiki, M., Li, L., Lin, W. J., et al. (2013). Targeting the androgen receptor with siRNA promotes prostate cancer metastasis through enhanced macrophage recruitment via CCL2/CCR2-induced STAT3 activation. *EMBO Mol. Med.* 5, 1383–1401. doi: 10.1002/emmm.201202367
- Jia, L., and Sun, Y. (2011). SCF E3 ubiquitin ligases as anticancer targets. *Curr. Cancer Drug Targets* 11, 347–356. doi: 10.2174/156800911794519734
- Jiang, Y., Cheng, W., Li, L., Zhou, L., Liang, Y., Zhang, W., et al. (2020). Effective targeting of the ubiquitin-like modifier NEDD8 for lung adenocarcinoma treatment. *Cell Biol. Toxicol.* 36, 349–364. doi: 10.1007/s10565-019-09503-6
- Jin, J., Jing, Z., Ye, Z., Guo, L., Hua, L., Wang, Q., et al. (2018). MLN4924 suppresses lipopolysaccharide-induced proinflammatory cytokine production in neutrophils in a dose-dependent manner. *Oncol. Lett.* 15, 8039–8045.
- Jinushi, M., and Komohara, Y. (2015). Tumor-associated macrophages as an emerging target against tumors: creating a new path from bench to bedside. *Biochim. Biophys. Acta* 1855, 123–130. doi: 10.1016/j.bbcan.2015.01.002
- Junttila, M. R., and de Sauvage, F. J. (2013). Influence of tumour micro-environment heterogeneity on therapeutic response. *Nature* 501, 346–354. doi: 10.1038/nature12626
- Kamitani, T., Kito, K., Nguyen, H. P., and Yeh, E. T. (1997). Characterization of NEDD8, a developmentally down-regulated ubiquitin-like protein. *J. Biol. Chem.* 272, 28557–28562. doi: 10.1074/jbc.272.45.28557
- Li, L., Kang, J., Zhang, W., Cai, L., Wang, S., Liang, Y., et al. (2019). Validation of NEDD8-conjugating enzyme UBC12 as a new therapeutic target in lung cancer. *EBioMedicine* 45, 81–91. doi: 10.1016/j.ebiom.2019.06.005
- Li, L., Liu, B., Dong, T., Lee, H. W., Yu, J., Zheng, Y., et al. (2013). Neddylation pathway regulates the proliferation and survival of macrophages. *Biochem. Biophys. Res. Commun.* 432, 494–498. doi: 10.1016/j.bbrc.2013.02.028
- Li, L., Wang, M., Yu, G., Chen, P., Li, H., Wei, D., et al. (2014). Overactivated neddylation pathway as a therapeutic target in lung cancer. *J. Natl. Cancer Inst.* 106:dju083.
- Li, X., Yao, W., Yuan, Y., Chen, P., Li, B., Li, J., et al. (2017). Targeting of tumour-infiltrating macrophages via CCL2/CCR2 signalling as a therapeutic strategy against hepatocellular carcinoma. *Gut* 66, 157–167. doi: 10.1136/gutjnl-2015-310514
- Liang, Y., Jiang, Y., Jin, X., Chen, P., Heng, Y., Cai, L., et al. (2020). Neddylation inhibition activates the protective autophagy through NF- $\kappa$ B-catalase-ATF3 axis in human esophageal cancer cells. *Cell Commun. Signal.* 18:72.
- Liu, G., Bi, Y., Shen, B., Yang, H., Zhang, Y., Wang, X., et al. (2014). SIRT1 limits the function and fate of myeloid-derived suppressor cells in tumors by orchestrating HIF-1 $\alpha$ -dependent glycolysis. *Cancer Res.* 74, 727–737. doi: 10.1158/0008-5472.can-13-2584
- Liu, H., Yang, Z., Lu, W., Chen, Z., Chen, L., Han, S., et al. (2020). Chemokines and chemokine receptors: a new strategy for breast cancer therapy. *Cancer Med.* 9, 3786–3799. doi: 10.1002/cam4.3014
- Loberg, R. D., Ying, C., Craig, M., Day, L. L., Sargent, E., Neeley, C., et al. (2007). Targeting CCL2 with systemic delivery of neutralizing antibodies induces prostate cancer tumor regression in vivo. *Cancer Res.* 67, 9417–9424. doi: 10.1158/0008-5472.can-07-1286
- Mantovani, A. (2010). Molecular pathways linking inflammation and cancer. *Curr. Mol. Med.* 10, 369–373. doi: 10.2174/156652410791316968
- Mantovani, A., Marchesi, F., Malesci, A., Laghi, L., and Allavena, P. (2017). Tumour-associated macrophages as treatment targets in oncology. *Nat. Rev. Clin. Oncol.* 14, 399–416. doi: 10.1038/nrclinonc.2016.217
- Martinez, F. O., Gordon, S., Locati, M., and Mantovani, A. (2006). Transcriptional profiling of the human monocyte-to-macrophage differentiation and polarization: new molecules and patterns of gene expression. *J. Immunol.* 177, 7303–7311. doi: 10.4049/jimmunol.177.10.7303
- Menyhart, O., Nagy, A., and Gyorffy, B. (2018). Determining consistent prognostic biomarkers of overall survival and vascular invasion in hepatocellular carcinoma. *R. Soc. Open Sci.* 5:181006. doi: 10.1098/rsos.181006
- Miyake, M., Hori, S., Morizawa, Y., Tatsumi, Y., Nakai, Y., Anai, S., et al. (2016). CXCL1-mediated interaction of cancer cells with tumor-associated macrophages and cancer-associated fibroblasts promotes tumor progression in human bladder cancer. *Neoplasia* 18, 636–646. doi: 10.1016/j.neo.2016.08.002
- Murray, P. J. (2017). Macrophage polarization. *Annu. Rev. Physiol.* 79, 541–566.
- Nagarsheth, N., Wicha, M. S., and Zou, W. (2017). Chemokines in the cancer microenvironment and their relevance in cancer immunotherapy. *Nat. Rev. Immunol.* 17, 559–572. doi: 10.1038/nri.2017.49
- Nagy, A., Lanczky, A., Menyhart, O., and Gyorffy, B. (2018). Validation of miRNA prognostic power in hepatocellular carcinoma using expression data of independent datasets. *Sci. Rep.* 8:9227.
- Nakayama, K. I., and Nakayama, K. (2006). Ubiquitin ligases: cell-cycle control and cancer. *Nat. Rev. Cancer* 6, 369–381. doi: 10.1038/nrc1881
- Noy, R., and Pollard, J. W. (2014). Tumor-associated macrophages: from mechanisms to therapy. *Immunity* 41, 49–61. doi: 10.1016/j.immuni.2014.06.010
- Ortiz-Lazareno, P. C., Hernandez-Flores, G., Dominguez-Rodriguez, J. R., Lerma-Diaz, J. M., Jave-Suarez, L. F., Aguilar-Lemarroy, A., et al. (2008). MG132 proteasome inhibitor modulates proinflammatory cytokines production and expression of their receptors in U937 cells: involvement of nuclear factor- $\kappa$ B and activator protein-1. *Immunology* 124, 534–541. doi: 10.1111/j.1365-2567.2008.02806.x
- Petroski, M. D., and Deshaies, R. J. (2005). Function and regulation of cullin-RING ubiquitin ligases. *Nat. Rev. Mol. Cell Biol.* 6, 9–20. doi: 10.1038/nrm1547
- Petty, A. J., and Yang, Y. (2017). Tumor-associated macrophages: implications in cancer immunotherapy. *Immunotherapy* 9, 289–302. doi: 10.2217/imt-2016-0135
- Pollard, J. W. (2004). Tumour-educated macrophages promote tumour progression and metastasis. *Nat. Rev. Cancer* 4, 71–78. doi: 10.1038/nrc1256
- Qian, B. Z., Li, J., Zhang, H., Kitamura, T., Zhang, J., Campion, L. R., et al. (2011). CCL2 recruits inflammatory monocytes to facilitate breast-tumour metastasis. *Nature* 475, 222–225. doi: 10.1038/nature10138



- Robinson, S. C., Scott, K. A., and Balkwill, F. R. (2002). Chemokine stimulation of monocyte matrix metalloproteinase-9 requires endogenous TNF- $\alpha$ . *Eur. J. Immunol.* 32, 404–412. doi: 10.1002/1521-4141(200202)32:2<404::aid-immu404>3.0.co;2-x
- Ruffell, B., and Coussens, L. M. (2015). Macrophages and therapeutic resistance in cancer. *Cancer Cell* 27, 462–472. doi: 10.1016/j.ccr.2015.02.015
- Sarantopoulos, J., Shapiro, G. I., Cohen, R. B., Clark, J. W., Kauh, J. S., Weiss, G. J., et al. (2016). Phase I study of the investigational NEDD8-activating enzyme inhibitor pevonedistat (TAK-924/MLN4924) in patients with advanced solid tumors. *Clin. Cancer Res.* 22, 847–857. doi: 10.1158/1078-0432.ccr-15-1338
- Segovia, J. A., Tsai, S. Y., Chang, T. H., Shil, N. K., Weintraub, S. T., Short, J. D., et al. (2015). Nedd8 regulates inflammasome-dependent caspase-1 activation. *Mol. Cell Biol.* 35, 582–597. doi: 10.1128/mcb.00775-14
- Shacter, E., and Weitzman, S. A. (2002). Chronic inflammation and cancer. *Oncology (Williston Park)* 16, 217–226, 229; discussion 230–232.
- Shah, J. J., Jakubowiak, A. J., O'Connor, O. A., Orlowski, R. Z., Harvey, R. D., Smith, M. R., et al. (2016). Phase I study of the novel investigational NEDD8-activating enzyme inhibitor pevonedistat (MLN4924) in patients with relapsed/refractory multiple myeloma or lymphoma. *Clin. Cancer Res.* 22, 34–43. doi: 10.1158/1078-0432.ccr-15-1237
- Soucy, T. A., Smith, P. G., Milhollen, M. A., Berger, A. J., Gavin, J. M., Adhikari, S., et al. (2009). An inhibitor of NEDD8-activating enzyme as a new approach to treat cancer. *Nature* 458, 732–736.
- Steidl, C., Lee, T., Shah, S. P., Farinha, P., Han, G., and Nayar, T. (2010). Tumor-associated macrophages and survival in classic Hodgkin's lymphoma. *N. Engl. J. Med.* 362, 875–885.
- Strasing, V., Daubine, F., Benzaid, I., Monkkonen, H., and Clezardin, P. (2007). Bisphosphonates in cancer therapy. *Cancer Lett.* 257, 16–35. doi: 10.1016/j.canlet.2007.07.007
- Swords, R. T., Coutre, S., Maris, M. B., Zeidner, J. F., Foran, J. M., Cruz, J., et al. (2018). Pevonedistat, a first-in-class NEDD8-activating enzyme inhibitor, combined with azacitidine in patients with AML. *Blood* 131, 1415–1424. doi: 10.1182/blood-2017-09-805895
- Swords, R. T., Erba, H. P., DeAngelo, D. J., Bixby, D. L., Altman, J. K., Maris, M., et al. (2015). Pevonedistat (MLN4924), a first-in-Class NEDD8-activating enzyme inhibitor, in patients with acute myeloid leukaemia and myelodysplastic syndromes: a phase 1 study. *Br. J. Haematol.* 169, 534–543. doi: 10.1111/bjh.13323
- Tan, P., Fuchs, S. Y., Chen, A., Wu, K., Gomez, C., Ronai, Z., et al. (1999). Recruitment of a ROC1-CUL1 ubiquitin ligase by Skp1 and HOS to catalyze the ubiquitination of I kappa B alpha. *Mol. Cell* 3, 527–533. doi: 10.1016/s1097-2765(00)80481-5
- Tian, D. W., Wu, Z. L., Jiang, L. M., Gao, J., Wu, C. L., and Hu, H. L. (2019). Neural precursor cell expressed, developmentally downregulated 8 promotes tumor progression and predicts poor prognosis of patients with bladder cancer. *Cancer Sci.* 110, 458–467. doi: 10.1111/cas.13865
- Tsuyada, A., Chow, A., Wu, J., Somlo, G., Chu, P., Loera, S., et al. (2012). CCL2 mediates cross-talk between cancer cells and stromal fibroblasts that regulates breast cancer stem cells. *Cancer Res.* 72, 2768–2779. doi: 10.1158/0008-5472.can-11-3567
- Vakilian, A., Khorramdelazad, H., Heidari, P., Sheikh Rezaei, Z., and Hassanshahi, G. (2017). CCL2/CCR2 signaling pathway in glioblastoma multiforme. *Neurochem. Int.* 103, 1–7. doi: 10.1016/j.neuint.2016.12.013
- Walden, H., Podgorski, M. S., Huang, D. T., Miller, D. W., Howard, R. J., Minor, D. L. Jr., et al. (2003). The structure of the APPBP1-UBA3-NEDD8-ATP complex reveals the basis for selective ubiquitin-like protein activation by an E1. *Mol. Cell* 12, 1427–1437. doi: 10.1016/s1097-2765(03)00452-0
- Wang, D., Sun, H., Wei, J., Cen, B., and DuBois, R. N. (2017). CXCL1 is critical for premetastatic niche formation and metastasis in colorectal cancer. *Cancer Res.* 77, 3655–3665. doi: 10.1158/0008-5472.can-16-3199
- Wang, G., Lu, X., Dey, P., Deng, P., Wu, C. C., Jiang, S., et al. (2016). Targeting YAP-dependent MDSC infiltration impairs tumor progression. *Cancer Discov.* 6, 80–95. doi: 10.1158/2159-8290.cd-15-0224
- Wang, N., Liu, W., Zheng, Y., Wang, S., Yang, B., Li, M., et al. (2018). CXCL1 derived from tumor-associated macrophages promotes breast cancer metastasis via activating NF-kappaB/SOX4 signaling. *Cell Death Dis.* 9:880.
- Wang, S., Xian, J., Li, L., Jiang, Y., Liu, Y., Cai, L., et al. (2020). NEDD8-conjugating enzyme UBC12 as a novel therapeutic target in esophageal squamous cell carcinoma. *Signal Transduct. Target. Ther.* 5:123.
- Wolf, M. J., Hoos, A., Bauer, J., Boettcher, S., Knust, M., Weber, A., et al. (2012). Endothelial CCR2 signaling induced by colon carcinoma cells enables extravasation via the JAK2-Stat5 and p38MAPK pathway. *Cancer Cell.* 22, 91–105. doi: 10.1016/j.ccr.2012.05.023
- Xie, P., Yang, J. P., Cao, Y., Peng, L. X., Zheng, L. S., Sun, R., et al. (2017). Promoting tumorigenesis in nasopharyngeal carcinoma, NEDD8 serves as a potential theranostic target. *Cell Death Dis.* 8:e2834. doi: 10.1038/cddis.2017.195
- Xirodimas, D. P. (2008). Novel substrates and functions for the ubiquitin-like molecule NEDD8. *Biochem. Soc. Trans.* 36, 802–806. doi: 10.1042/bst0360802
- Yan, D., Kowal, J., Akkari, L., Schuhmacher, A. J., Huse, J. T., West, B. L., et al. (2017). Inhibition of colony stimulating factor-1 receptor abrogates microenvironment-mediated therapeutic resistance in gliomas. *Oncogene* 36, 6049–6058. doi: 10.1038/onc.2017.261
- Yang, C., Yu, H., Chen, R., Tao, K., Jian, L., Peng, M., et al. (2019). CXCL1 stimulates migration and invasion in ERnegative breast cancer cells via activation of the ERK/MMP2/9 signaling axis. *Int. J. Oncol.* 55, 684–696.
- Yu, J., Huang, W. L., Xu, Q. G., Zhang, L., Sun, S. H., Zhou, W. P., et al. (2018). Overactivated neddylation pathway in human hepatocellular carcinoma. *Cancer Med.* 7, 3363–3372. doi: 10.1002/cam4.1578
- Zhang, W. J., Wang, X. H., Gao, S. T., Chen, C., Xu, X. Y., Sun, Q., et al. (2018). Tumor-associated macrophages correlate with phenomenon of epithelial-mesenchymal transition and contribute to poor prognosis in triple-negative breast cancer patients. *J. Surg. Res.* 222, 93–101. doi: 10.1016/j.jss.2017.09.035
- Zhao, X., Qu, J., Sun, Y., Wang, J., Liu, X., Wang, F., et al. (2017). Prognostic significance of tumor-associated macrophages in breast cancer: a meta-analysis of the literature. *Oncotarget* 8, 30576–30586. doi: 10.18632/oncotarget.15736
- Zhao, Y., Morgan, M. A., and Sun, Y. (2014). Targeting neddylation pathways to inactivate cullin-RING ligases for anticancer therapy. *Antioxid. Redox Signal.* 21, 2383–2400. doi: 10.1089/ars.2013.5795
- Zhao, Y., and Sun, Y. (2013). Cullin-RING ligases as attractive anti-cancer targets. *Curr. Pharm. Des.* 19, 3215–3225. doi: 10.2174/13816128113199990300
- Zhou, L., and Jia, L. (2020). Targeting protein neddylation for cancer therapy. *Adv. Exp. Med. Biol.* 1217, 297–315. doi: 10.1007/978-981-15-1025-0\_18
- Zhou, L., Jiang, Y., Liu, X., Li, L., Yang, X., Dong, C., et al. (2019a). Promotion of tumor-associated macrophages infiltration by elevated neddylation pathway via NF-kappaB-CCL2 signaling in lung cancer. *Oncogene* 38, 5792–5804. doi: 10.1038/s41388-019-0840-4
- Zhou, L., Jiang, Y., Luo, Q., Li, L., and Jia, L. (2019b). Neddylation: a novel modulator of the tumor microenvironment. *Mol. Cancer* 18:77.
- Zhou, L., Zhang, W., Sun, Y., and Jia, L. (2018). Protein neddylation and its alterations in human cancers for targeted therapy. *Cell. Signal.* 44, 92–102. doi: 10.1016/j.cellsig.2018.01.009
- Zhou, W., Xu, J., Li, H., Xu, M., Chen, Z. J., Wei, W., et al. (2017). Neddylation E2 UBE2F promotes the survival of lung cancer cells by activating CRL5 to degrade NOXA via the K11 linkage. *Clin. Cancer Res.* 23, 1104–1116. doi: 10.1158/1078-0432.ccr-16-1585
- Zhu, Z., Sun, L., Hao, R., Jiang, H., Qian, F., and Ye, R. D. (2017). Nedd8 modification of Cullin-5 regulates lipopolysaccharide-induced acute lung injury. *Am. J. Physiol. Lung Cell. Mol. Physiol.* 313, L104–L114.
- Zhu, Z., Wang, L., Hao, R., Zhao, B., Sun, L., and Ye, R. D. (2016). Cutting edge: a Cullin-5-TRAF6 interaction promotes TRAF6 polyubiquitination and lipopolysaccharide signaling. *J. Immunol.* 197, 21–26. doi: 10.4049/jimmunol.1600447

**Conflict of Interest:** RMH was employed by company Anticancer Inc.

The remaining authors declare that the research was conducted in the absence of any commercial or financial relationships that could be construed as a potential conflict of interest.

Copyright © 2021 Jiang, Li, Liu, Hoffman and Jia. This is an open-access article distributed under the terms of the Creative Commons Attribution License (CC BY). The use, distribution or reproduction in other forums is permitted, provided the original author(s) and the copyright owner(s) are credited and that the original publication in this journal is cited, in accordance with accepted academic practice. No use, distribution or reproduction is permitted which does not comply with these terms.





# Development of an Individualized Ubiquitin Prognostic Signature for Clear Cell Renal Cell Carcinoma

Yue Wu<sup>1,2</sup>, Xi Zhang<sup>3</sup>, Xian Wei<sup>1,2</sup>, Huan Feng<sup>1,2</sup>, Bintao Hu<sup>1,2</sup>, Zhiyao Deng<sup>1,2</sup>, Bo Liu<sup>4</sup>, Yang Luan<sup>1,2</sup>, Yajun Ruan<sup>1,2</sup>, Xiaming Liu<sup>1,2</sup>, Zhuo Liu<sup>1,2</sup>, Jihong Liu<sup>1,2</sup> and Tao Wang<sup>1,2\*</sup>

<sup>1</sup> Department of Urology, Tongji Hospital, Tongji Medical College, Huazhong University of Science and Technology, Wuhan, China, <sup>2</sup> Institute of Urology, Tongji Hospital, Tongji Medical College, Huazhong University of Science and Technology, Wuhan, China, <sup>3</sup> School of Health Sciences, Wuhan University, Wuhan, China, <sup>4</sup> Department of Oncology, Tongji Hospital, Tongji Medical College, Huazhong University of Science and Technology, Wuhan, China

## OPEN ACCESS

### Edited by:

Cui Hua Liu,  
Institute of Microbiology, Chinese  
Academy of Sciences, China

### Reviewed by:

Michael Does,  
Hofstra University, United States  
Ting-Han Chang,  
National Yang Ming Chiao Tung  
University, Taiwan

### \*Correspondence:

Tao Wang  
twang@hust.edu.cn

### Specialty section:

This article was submitted to  
Cell Growth and Division,  
a section of the journal  
Frontiers in Cell and Developmental  
Biology

**Received:** 23 March 2021

**Accepted:** 02 June 2021

**Published:** 22 June 2021

### Citation:

Wu Y, Zhang X, Wei X, Feng H, Hu B, Deng Z, Liu B, Luan Y, Ruan Y, Liu X, Liu Z, Liu J and Wang T (2021) Development of an Individualized Ubiquitin Prognostic Signature for Clear Cell Renal Cell Carcinoma. *Front. Cell Dev. Biol.* 9:684643. doi: 10.3389/fcell.2021.684643

Clear cell renal cell carcinoma (ccRCC) is a common tumor type in genitourinary system and has a poor prognosis. Ubiquitin dependent modification systems have been reported in a variety of malignancies and have influenced tumor genesis and progression. However, the molecular characteristics and prognostic value of ubiquitin in ccRCC have not been systematically reported. In our study, 204 differentially expressed ubiquitin related genes (URGs) were identified from The Cancer Genome Atlas (TCGA) cohort, including 141 up-regulated and 63 down-regulated URGs. A total of seven prognostic related URGs (CDCA3, CHFR, CORO6, RNF175, TRIM72, VAV3, and WDR72) were identified by Cox regression analysis of differential URGs and used to construct a prognostic signature. Kaplan-Meier analysis confirmed that high-risk patients had a worse prognosis ( $P = 1.11\text{e-}16$ ), and the predicted area under the receiver operating characteristic (ROC) curves were 0.735 at 1 year, 0.702 at 3 years, and 0.744 at 5 years, showing good prediction accuracy. Stratified analysis showed that the URGs-based prognostic signature could be used to evaluate tumor progression in ccRCC. Further analysis confirmed that the signature is an independent prognostic factor related to the prognosis of ccRCC patients, which may help to reveal the molecular mechanism of ccRCC and provide potential diagnostic and prognostic markers for ccRCC.

**Keywords:** clear cell renal cell carcinoma, ubiquitin, prognostic signature, prognosis, bioinformatics

## INTRODUCTION

Renal cell carcinoma (RCC) is one of the most aggressive genitourinary tumors, accounting for about 4% of adult malignancies (Zhai et al., 2019). According to statistics, 76,080 new kidney cancer cases and 13,780 kidney cancer deaths are expected to occur in the United States in 2021 (Siegel et al., 2021). Clear cell renal cell carcinoma (ccRCC) is the most studied and common

**Abbreviations:** RCC, Renal cell carcinoma; CcRCC, Clear cell renal cell carcinoma; TCGA, The Cancer Genome Atlas; PTM, Post-translational modification; E1s, Ubiquitin-activating enzymes; E2s, Ubiquitin-conjugating enzymes; E3s, Ubiquitin protein ligases; UBD, Ubiquitin-binding domain-containing protein; ULDs, Ubiquitin-like domains; DUBs, deubiquitinases; URGs, Ubiquitin related genes; OS, Overall survival; FC, Fold change; FDR, False discovery rate; LASSO, Least absolute shrinkage and selection operator; ROC, Receiver operating characteristic; TFs, Transcription factors; GO, Gene ontology; KEGG, Kyoto Encyclopedia of Genes and Genomes; AUC, Area under the receiver operating characteristic curve; CIBERSORT, Cell type identification by estimating relative subsets of RNA transcripts; IHC, Immunohistochemical.

subtype of RCC, accounting for approximately 80% of all RCC (Escudier et al., 2019). CcRCC is a malignant and substantial tumor originating from proximal renal tubular epithelial cells, with high metastasis rate and poor prognosis. The 5-year survival rate for advanced ccRCCs is only 11.7% (Siegel et al., 2017). About 30% of patients with metastatic ccRCC at the time of initial diagnosis, and approximately 30% of patients relapse after complete removal of the primary tumor (Motzer et al., 2008; Nerich et al., 2014). Thus, a comprehensive understanding of the pathogenesis of ccRCC, identification of biomarkers, and development of effective early screening and diagnosis methods are of great significance for prognosis prediction and treatment of ccRCC.

Post-translational modification (PTM) is a covalent change that occurs during or after translation of almost all proteins. PTM induces covalent linkage between proteins and functional groups including phosphate, acetyl, methyl and ubiquitin through a variety of signaling pathways, thereby regulating the localization, stability, activity, interaction or folding of proteins, thus influencing various biological processes (Deribe et al., 2010; Chiang and Gack, 2017). Among PTM types, ubiquitin dependent modification system is one of the major PTM systems (Hershko and Ciechanover, 1998). Ubiquitin is a highly conserved protein containing 76 amino acids. Ubiquitin modified proteins are catalyzed by three enzyme cascades consisting of ubiquitin-activating enzymes (E1s), ubiquitin-conjugating enzymes (E2s), and ubiquitin protein ligases (E3s) (Pickart, 2001). In this process, the ubiquitin-binding domain-containing protein (UBD) (Husnjak and Dikic, 2012), proteins containing ubiquitin-like domains (ULDs) (Upadhyay and Hegde, 2003), and deubiquitinases (DUBs) (Nijman et al., 2005) play a negative regulatory role.

Studies have shown that dysregulation of the ubiquitin dependent modification system plays a key role in many diseases, including neurodegenerative diseases, autoimmune diseases, and malignancies (Seeler and Dejean, 2017; Rape, 2018). Lipkowitz and Weissman (2011) found that mutations or dysregulation of E3s expression are associated with poorer survival and prognosis in a variety of cancers. Another study reported that maternally expression gene 3 (Meg3) and miR-3163 may synergistically inhibit Skp2 translation in non-small cell lung cancer cells, thereby inhibiting cancer cell growth (Su et al., 2016). In the field of RCC, Zhang et al. (2020) found that the ubiquitin ligase KLHL2 inhibited the progression of RCC by promoting the degradation and ubiquitination of ARHGEF7 protein. Other studies have shown that low ubiquitin-specific protease 2 mRNA expression is associated with poor prognosis of ccRCC, which has prognostic and diagnostic value (Meng et al., 2020). However, most of the current functional studies have only focused on single genes, few studies have systematically explored the molecular characteristics and prognostic potential of ubiquitin related genes (URGs) in ccRCC using high-throughput sequencing expression profile datasets. Therefore, in this study, we systematically explored the molecular characteristics and prognostic potential of these URGs in ccRCC, and preliminarily revealed the complex biological functions and immune processes involved in these molecules as well as their regulatory networks.

## MATERIALS AND METHODS

### Data Download and Differential Expression URGs Analysis

Transcriptome data (read counts) containing 72 normal renal tissue samples and 539 ccRCC samples, together with corresponding clinical information, were downloaded from The Cancer Genome Atlas (TCGA)<sup>1</sup> database. Then, 27 E1s, 109 E2s, 1153 E3s, 164 DUBs, 396 UBDs, and 183 ULDs were collected from the iUUCD 2.0 database<sup>2</sup> (Gao et al., 2013), and 1,367 URGs were identified after duplication removal, and extracted 1,234 ccRCC-related URGs. Subsequently, the read counts data was preprocessed by “edgeR” package<sup>3</sup>, including deleting the genes whose average expression was less than 1 and normalizing the expression data with the trimmed mean of M-values algorithm.  $|\log_2 \text{fold change (FC)}| > 1.0$  and false discovery rate (FDR) < 0.05 were considered to be differentially expressed URGs. Additionally, the E-MTAB-1980 cohort was obtained from the ArrayExpress database<sup>4</sup> as an external validation cohort. The microarray data were background adjusted and normalized using robust multi-array analysis (RMA) method in “Affy” package.

### Construction and Assessment of URGs Associated Prognostic Signature

To screen out prognostic related URGs, we first determined the association between differentially expressed URG expression levels and overall survival (OS) in ccRCC patients by univariate Cox regression analysis, and significant URGs associated with OS was determined when *P*-value was less than 0.05. Next, the least absolute shrinkage and selection operator (LASSO) Cox regression analysis was performed on these preliminary screened URGs using the “glmnet” package to identify the valuable prognostic URGs. Finally, we further screened the URGs most associated with prognosis through multivariate Cox proportional hazards regression analysis. We then constructed a prognostic signature based on the  $\beta$  coefficients of multivariate Cox regression analysis and the expression values of corresponding URGs. The risk score was calculated according to the following formula:

$$\text{Risk score} = \sum_{i=1}^n \text{Exp}_i \beta_i,$$

in the above formula, Exp and  $\beta$  represent gene expression level and regression coefficient, respectively. Subsequently, Patients with ccRCC in the TCGA cohort were grouped according to the median risk score. Kaplan-Meier analysis was used to compare the difference in OS between high- and low-risk groups. Next, we constructed receiver operating characteristic (ROC) curves based on the “Survival ROC” package to explore the predictive power of the URGs-based risk signature. Moreover, we divided the whole TCGA cohort into two subsets as internal validation cohorts and the E-MTAB-1980 cohort as an external

<sup>1</sup><https://portal.gdc.cancer.gov/>

<sup>2</sup><http://iuucd.biocuckoo.org/index.php>

<sup>3</sup><http://www.bioconductor.org/packages/release/bioc/html/edgeR.html>

<sup>4</sup><https://www.ebi.ac.uk/arrayexpress/experiments/E-MTAB-1980/>

validation cohort to verify the prediction performance and stability of the URGs-based prognostic signature, respectively.

## Correlation Between Prognostic Signature, Prognostic URGs, and Clinical Characteristics

To explore the clinical value of the URGs-based prognostic signature, Kaplan-Meier analysis was conducted to investigate the differences in prognosis of ccRCC patients under different clinical characteristics stratification. We also compared the differences of risk score for different clinical characteristics to explore whether prognostic signature could assess the degree of tumor progression. Moreover, we stratified the expression levels of these URGs by different clinical characteristics and compared the differences in their expression levels to preliminarily reveal the possible roles of these URGs in ccRCC.

## Multidimensional Regulatory Network of Prognostic URGs and Functional Enrichment Analysis

We downloaded transcription factors (TFs) associated with tumorigenesis and progression from the Cistrome Project<sup>5</sup>, extracted ccRCC-related TFs and obtained differentially expressed TFs from the TCGA cohort. Then, we performed the co-expression of differentially expressed TFs and prognostic URGs to explore their regulatory relationship based on the criteria of  $|\text{Cor}| > 0.3$  and  $P < 0.001$ . Next, we performed gene ontology (GO) and Kyoto Encyclopedia of Genes and Genomes database (KEGG) function enrichment analysis on these differentially expressed URGs. The biological functions and molecular mechanisms of these URGs were revealed through GO annotation, including biological processes, cell components and molecular functions, and the key signal regulatory pathways of URGs were revealed through KEGG enrichment analysis. These analyses were performed using the “clusterProfiler”<sup>6</sup> package.

## Relationship Between Prognostic Signature and Degree of Immune Cell Infiltration

Since the ubiquitin dependent modification system is thought to profoundly influence the maturation of immune cells and shape the tumor microenvironment (Zhu et al., 2020), we evaluated the differences in the degree of immune cell infiltration between different subgroups based on the cell type identification by estimating relative subsets of RNA transcripts (CIBERSORT) algorithm. CIBERSORT is a deconvolution algorithm developed by Newman et al. (2015) that evaluates the relative abundance of immune cell infiltration in each patient based on data from 22 sets of genes associated with the infiltration of immune cells. The CIBERSORT algorithm was simulated 1,000 times, and the results were obtained according to  $P < 0.05$ .

## Evaluation of the Prognostic Significance of Different Clinical Characteristics in ccRCC Patients and Construction of a Nomogram

We then performed univariate and multivariate Cox regression analysis for each clinical characteristic and risk score to assess its clinical prognostic significance. Subsequently, we used the “rms” package to construct a nomogram combining different clinical characteristics and risk score to establish a quantitative prediction method for prognosis of ccRCC patients. Next, the calibration curves at different time points were plotted to evaluate the performance of the nomogram. Moreover, we further evaluated the predictive performance of the nomogram using the TCGA and E-MTAB-1980 cohorts.

## Immunohistochemical (IHC) Staining Analysis

To further verify the protein expression of these prognostic URGs, we used IHC staining assay to detect the expression levels of these genes in paraffin-embedded tissues of ccRCC and adjacent non-tumor renal tissues. The paraffin embedded tissue was stained in 5  $\mu\text{m}$  continuous sections. The specific procedures for paraffin section immunohistochemistry of kidney tissue are described above (Li et al., 2010). IHC assayed against CDCA3, CHFR, TRIM72, VAV3, and WDR72. Primary antibodies against CDCA3, CHFR, VAV3, and WDR72 were purchased from ABclonal (Wuhan, China). Primary antibodies against TRIM72 were purchased from Bioss (Beijing, China). All experiments were conducted independently for at least three times. The images were observed and obtained with the Panoramic SCAN (3DHISTECH, Hungary). Image Pro Plus software was used to analyze and quantify the IHC results.

## RESULTS

### Analysis of Differentially Expressed URGs in ccRCC

Since the molecular characteristics associated with ubiquitin and their prognostic potential in ccRCC are still unclear, we comprehensively explored the key role and clinical significance of URGs in ccRCC. **Figure 1** shows the research roadmap. We first obtained RNA sequencing data from the TCGA database containing 72 normal renal tissue samples and 539 ccRCC samples. Subsequently, according to the  $|\log_2 \text{FC}| > 1.0$  and  $\text{FDR} < 0.05$ , a total of 204 differentially expressed URGs were identified, of which 141 were up-regulated and 63 were down-regulated. The expression distribution of these URGs is shown in **Figures 2A,B**.

### Construction and Assessment of URGs-Based Prognostic Signature

For these differentially expressed URGs, we first identified 114 prognostic URGs by univariate Cox proportional hazards

<sup>5</sup> www.cistrome.org

<sup>6</sup> <http://www.bioconductor.org/packages/release/bioc/html/clusterProfiler.html>



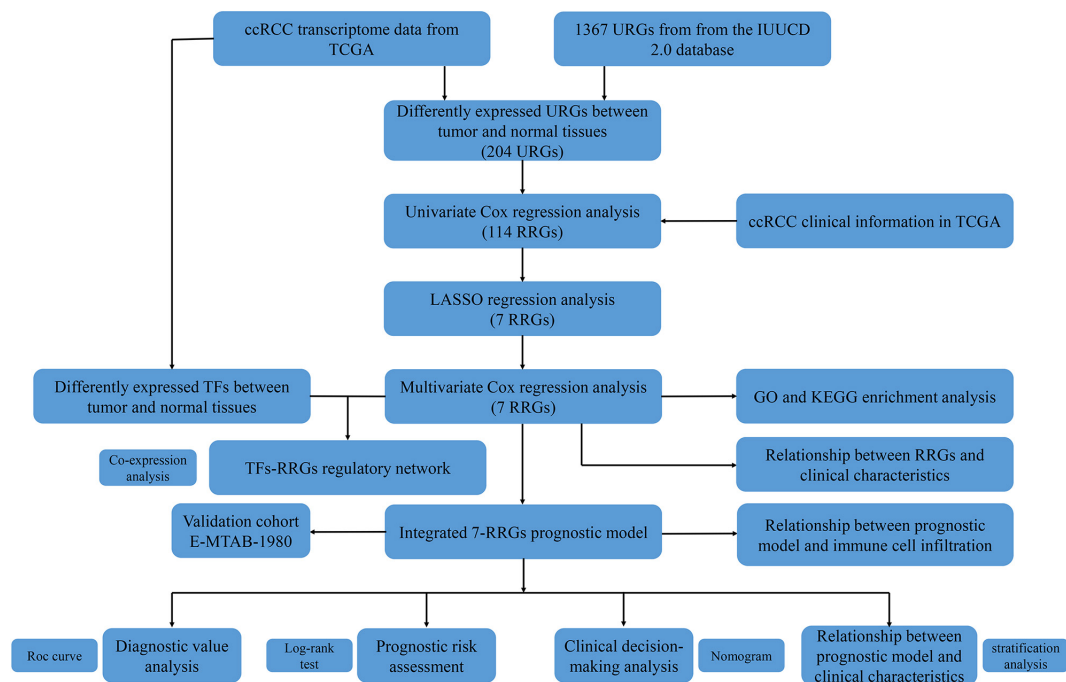


**FIGURE 1 |** Flowchart for developing an individualized ubiquitin-based prognostic signature for clear cell renal cell carcinoma (ccRCC). We developed the URGs-based prognostic signature using the TCGA cohort and validated it in the ArrayExpress cohort.

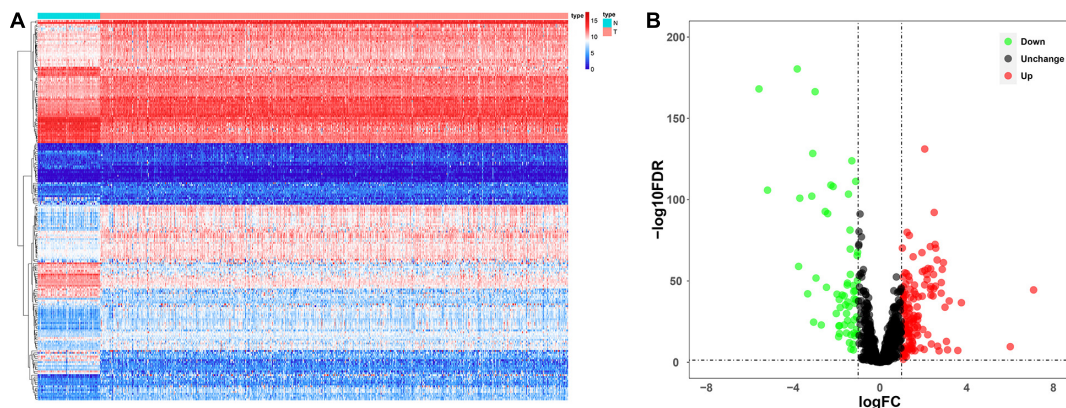


**FIGURE 2 |** Expression and distribution of differentially expressed URGs in ccRCC. (A) The differential expression of 204 ubiquitin related genes (URGs) in ccRCC tissue samples ( $n = 539$ ) compared with normal renal samples ( $n = 72$ ) is shown in the volcano plot. The red plot represented up-regulated URGs, the green plot represented down-regulated URGs; (B) the differential expression of 204 URGs in ccRCC tissue samples ( $n = 539$ ) compared with normal renal samples ( $n = 72$ ) is shown in the heatmap (the statistical method was multiple hypothesis testing).

regression analysis (Supplementary Table 1). Then, LASSO regression analysis further screened out seven URGs, including *CDCA3*, *CHFR*, *CORO6*, *RNF175*, *TRIM72*, *VAV3*, and *WDR72*. The trajectory changes of these independent variable coefficients are shown in Supplementary Figure 1A, and the Supplementary Figure 1B shows the model construction using cross validation. We then performed multivariate Cox proportional hazards regression analysis on these seven URGs and finally identified the seven URGs most associated with prognosis, including *CDCA3*, *CHFR*, *CORO6*, *RNF175*, *TRIM72*, *VAV3*, and *WDR72*.

Finally, we used the  $\beta$  coefficients of multivariate Cox proportional hazards regression analysis to establish a prognostic signature (Table 1), and multiplied these coefficients by the expression level of each URG to obtain the risk score. The risk score was calculated according to the following formula:

$$\text{Risk score} = (0.1726 \times \text{Exp } CDCA3) + (0.0788 \times \text{Exp } CHFR) + (0.0898 \times \text{Exp } CORO6) + (0.1389 \times \text{Exp } RNF175) + (0.0897 \times \text{Exp } TRIM72) + (-0.1586 \times \text{Exp } VAV3) + (-0.1202 \times \text{Exp } WDR72).$$



**TABLE 1** | Multivariate Cox regression analysis to identify prognosis-related URGs.

Gene	Coef	Exp(coef)	se(coef)	z	Pr(>  z )
CDCA3	0.1726	1.1884	0.1072	1.6106	0.1073
CHFR	0.0788	1.0820	0.2199	0.3583	0.7202
CORO6	0.0898	1.0939	0.0613	1.4648	0.1430
RNF175	0.1389	1.1490	0.0755	1.8398	0.0658
TRIM72	0.0897	1.0939	0.0543	1.6535	0.0982
VAV3	-0.1586	0.8533	0.0822	-1.9291	0.0537
WDR72	-0.1202	0.8868	0.0480	-2.5015	0.0124

Coef, coefficient. The statistical method was multiple hypothesis testing.

Patients with ccRCC in the TCGA cohort were grouped according to the median risk score. Survival analysis by Kaplan-Meier method showed that patients in the high-risk group had a shorter OS than those in the low-risk group ( $P = 1.11 \times 10^{-16}$ , **Figure 3A**), suggesting that the signature could accurately distinguish between ccRCC patients with poor prognosis. We then evaluated the predictive power and accuracy of the URGs-based risk signature according to ROC curve analysis,

and the predicted area under the ROC curves (AUC) were 0.735 at 1 year, 0.702 at 3 years, and 0.744 at 5 years (**Figure 3B**). The risk score and survival status distribution of each patient are shown in **Figure 3C**, suggesting that a higher risk score is associated with a higher mortality rate of ccRCC patients. **Figure 3D** shows the expression heatmap assessed by clinical characteristics and risk score. Additionally, we used the E-MTAB-1980 cohort as an external cohort to further evaluate whether the prognostic signature has similar predictive performance and accuracy in other ccRCC patient cohorts. Similarly, Survival analysis by Kaplan-Meier method showed a worse prognosis for patients in the high-risk group ( $P = 0.032$ , **Figure 3E**). The predicted AUCs were 0.725 at 1 year, 0.703 at 3 years, and 0.742 at 5 years (**Figure 3F**). The risk score and survival status distribution of each patient are shown in **Figure 3G**, and **Figure 3H** shows a heatmap of expression in the E-MTAB-1980 cohort, based on clinical characteristics and risk score. Moreover, to further verify the prognostic signature, we divided the TCGA cohort into two similar subsets (training,  $n = 270$ ; test,  $n = 269$ ) for signature

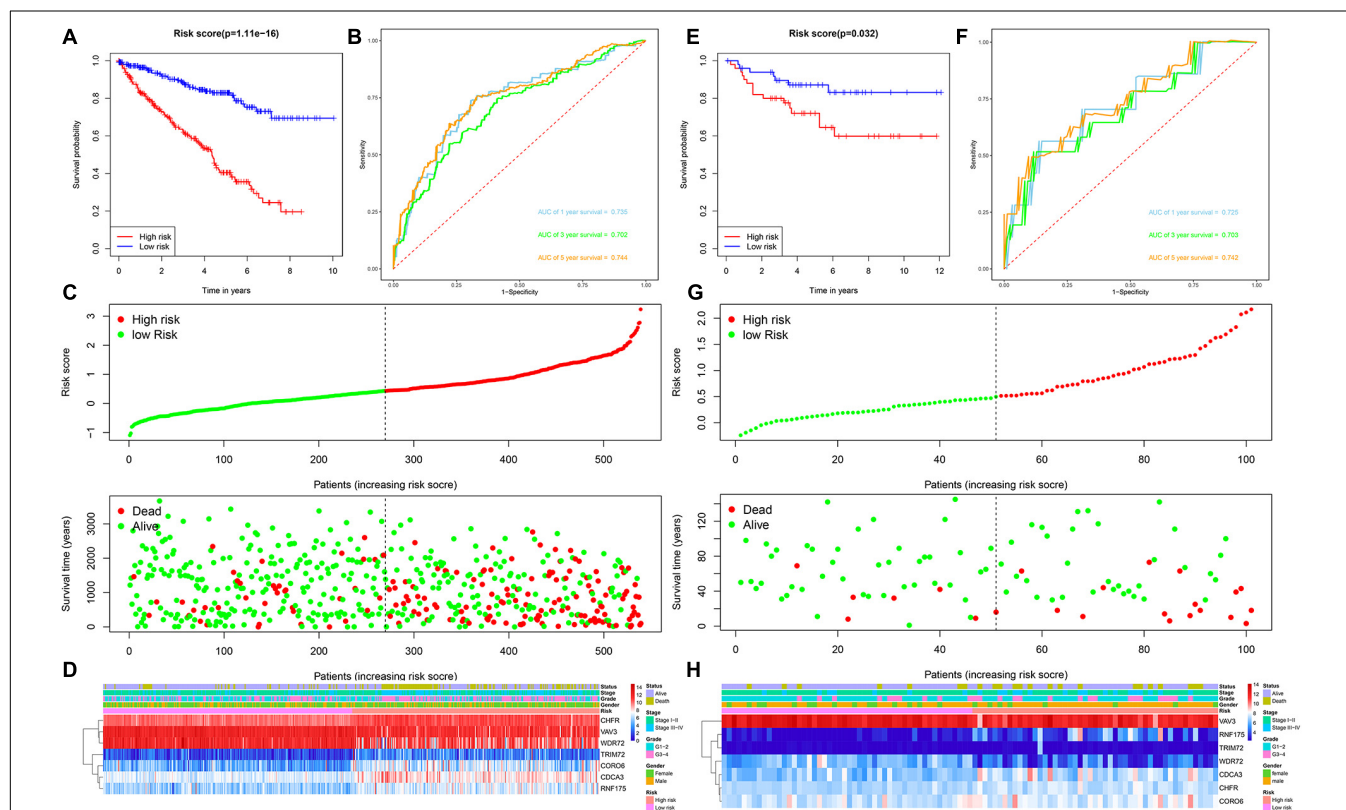
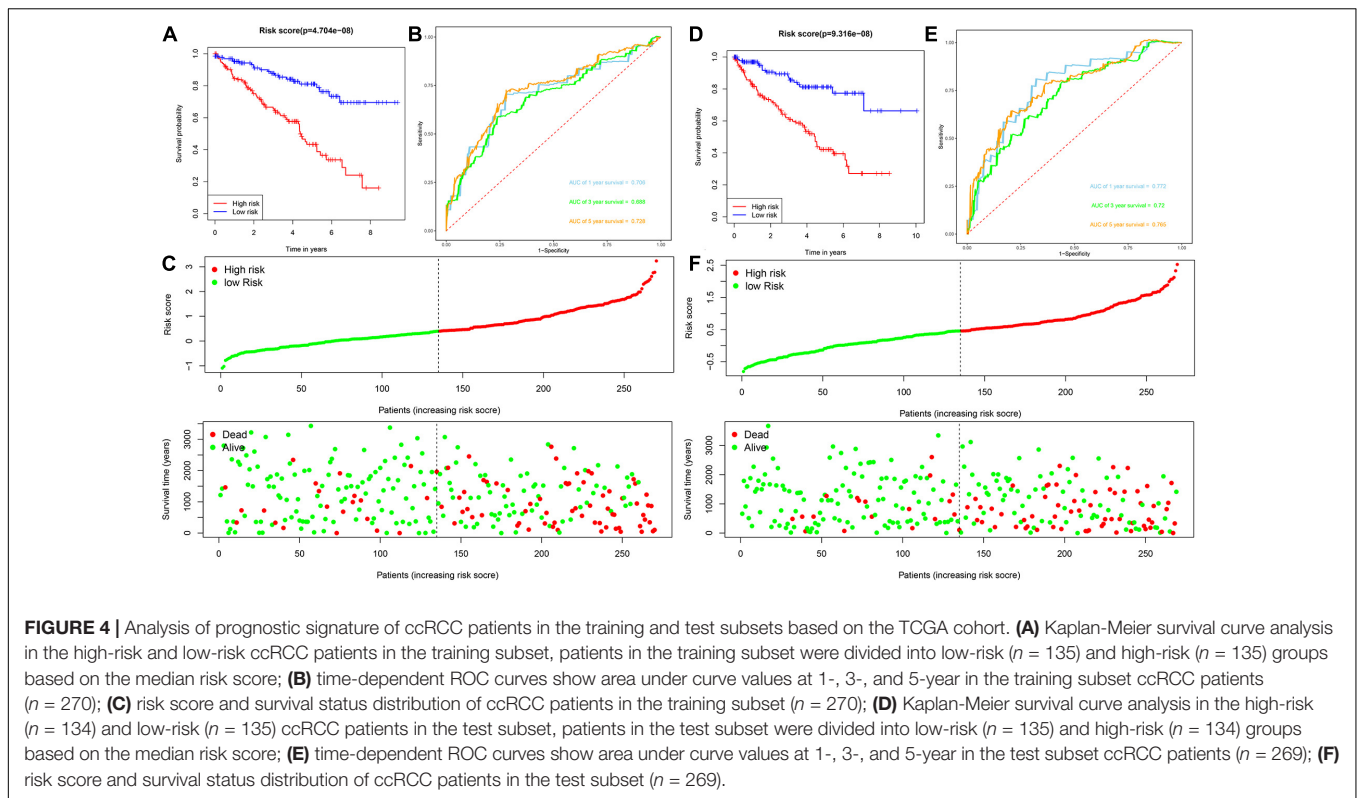


**FIGURE 3** | Prognostic signature analysis of ccRCC patients in the TCGA and E-MTAB-1980 cohorts. **(A)** Kaplan-Meier survival curve analysis in the high-risk and low-risk ccRCC patients in the TCGA cohort, patients in the entire TCGA cohort were divided into low-risk ( $n = 270$ ) and high-risk ( $n = 269$ ) groups based on the median risk score; **(B)** time-dependent ROC curves show area under curve values at 1-, 3-, and 5-year in the TCGA cohort ccRCC patients ( $n = 539$ ); **(C)** risk score and survival status distribution of ccRCC patients in the TCGA cohort ( $n = 539$ ); **(D)** heatmap of prognostic URGs expression under different parameters in the TCGA cohort ccRCC patients ( $n = 539$ ); **(E)** Kaplan-Meier survival curve analysis in the high-risk and low-risk ccRCC patients in the E-MTAB-1980 cohort ( $n = 101$ ), patients in the E-MTAB-1980 cohort were divided into low-risk ( $n = 51$ ) and high-risk ( $n = 50$ ) groups based on the median risk score; **(F)** time-dependent ROC curves show area under curve values at 1-, 3-, and 5-year in the E-MTAB-1980 cohort ccRCC patients ( $n = 101$ ); **(G)** risk score and survival status distribution of ccRCC patients in the E-MTAB-1980 cohort ( $n = 101$ ); **(H)** heatmap of prognostic URGs expression under different parameters in the E-MTAB-1980 cohort ccRCC patients ( $n = 101$ ) (the statistical method was a log-rank test for a single factor).



validation, respectively. In the training subset, survival analysis showed that patients in the high-risk group had a worse prognosis ( $P = 4.704\text{e-}08$ , **Figure 4A**). The predicted AUCs were 0.706 at 1 year, 0.688 at 3 years, and 0.728 at 5 years (**Figure 4B**). The risk score and survival status distribution of each patient are shown in **Figure 4C**. Analysis of the test subset shows similar results (**Figures 4D-F**). Therefore, we have a reason to believe that the URGs-based prognostic signature has good prediction performance and stability.

### Prognostic Significance of the Signature Under Different Clinical Characteristics Stratification

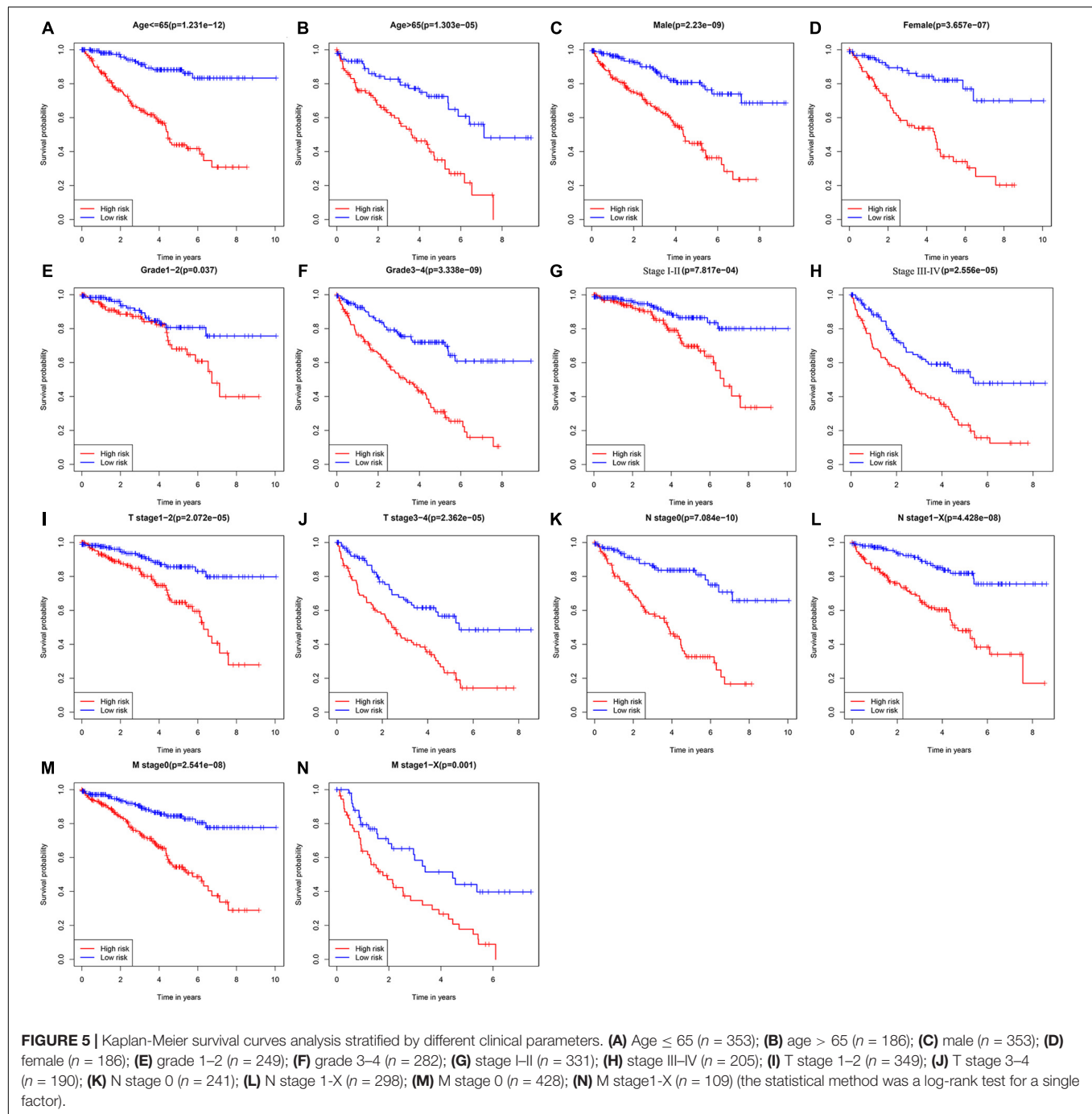
To explore the clinical value of the URGs-based prognostic signature, ccRCC patients in the TCGA cohort were stratified according to different clinical characteristics (including age, gender, tumor grade, tumor stage, T stage, N stage, and M stage). Survival analysis was performed by Kaplan-Meier method, and the results showed that the prognosis of patients in each high-risk group under different clinical parameter stratification was worse than that in the low-risk group (**Figure 5**), suggesting that our risk score can accurately identify ccRCC patients with poor prognosis under different clinical conditions. These results demonstrated that the seven URGs-based prognostic signature could be used to predict the prognosis of patients with ccRCC regardless of clinical parameters.

### Relationship Between URGs-Based Prognostic Signature and Different Clinical Characteristics

To explore whether prognostic signature could assess the degree of tumor progression, we compared the differences of risk score for different clinical characteristics. The results indicated that no significant differences were observed in risk scores between groups after stratification by age, gender, and N stage (**Figures 6A,B,F**). However, the risk score of tumor grade 3–4 was significantly higher than that of tumor grade 1–2 ( $P = 5.9\text{e-}13$ , **Figure 6C**), the risk score of tumor stage III–IV was significantly higher than that of tumor stage I–II ( $P = 6.6\text{e-}14$ , **Figure 6D**), the risk score of tumor T stage 3–4 was significantly higher than that of tumor T stage 1–2 ( $P = 2.5\text{e-}12$ , **Figure 6E**), and the risk score of tumor M stage 1–X was significantly higher than that of tumor M stage 0 ( $P = 3.8\text{e-}07$ , **Figure 6G**). These results suggested that prognostic signature can be used to assess the degree of progression of ccRCC tumors, and the higher the risk score, the higher the malignant degree of tumors.

### Assessment of the Association Between Prognostic URGs and Different Clinical Characteristics

In addition to the above analysis, we also preliminarily explored the possible roles of these seven URGs in ccRCC according to different clinical characteristics. We stratified the

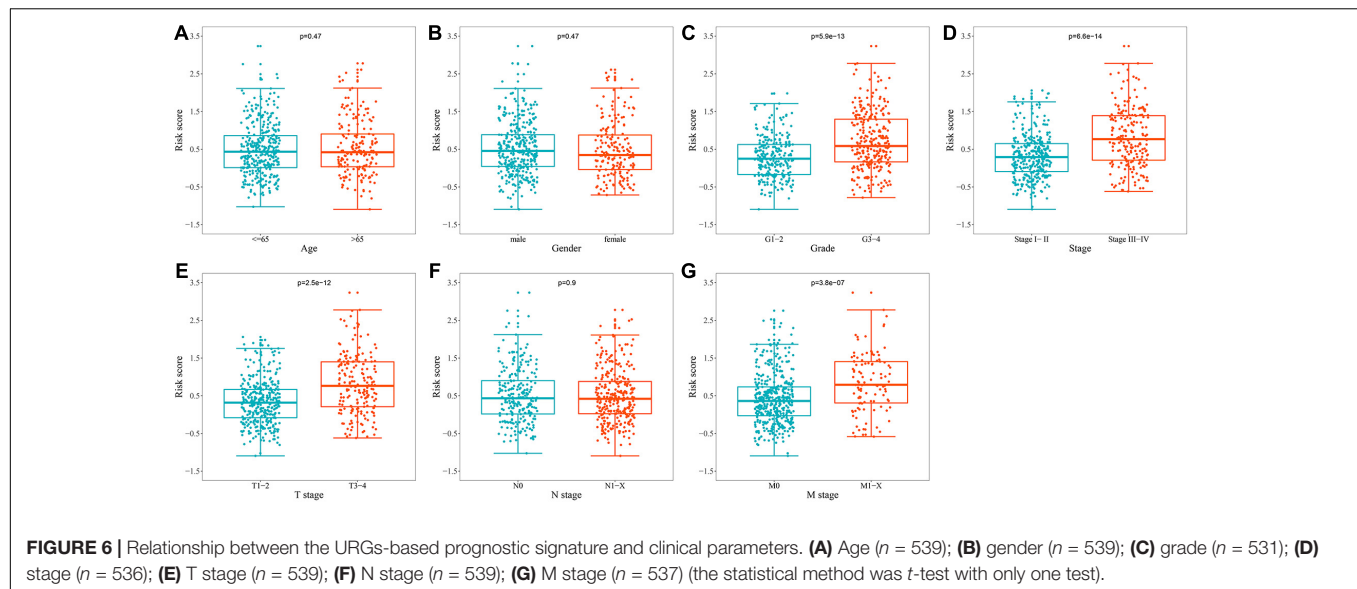


expression levels of these URGs based on different clinical variables, and then compared the differences in expression levels between the two groups. The results indicated that CDCA3, CHFR, CORO6, RNF175, TRIM72, VAV3, and WDR72 were significantly correlated with grade, stage, and T stage (Table 2); the correlation between CDCA3, CHFR, CORO6, RNF175, VAV3, and WDR72 and M stage was statistically significant (Table 2). However, no genes differed significantly with gender, or N stage (Table 2). These results suggested that these prognostic URGs may play an important

role in the tumor progression of ccRCC, which is worthy of further study.

## Multidimensional Regulatory Network of Prognostic URGs and Functional Enrichment Analysis

The ubiquitin-proteasome system plays an important regulatory role in the general transcription process, and through this role affects the function and activity of TFs. Cui et al. (2017) found



that hypoxia enhanced the stability and transcriptional activity of HIF-1 $\alpha$  through SENP1, thereby enhancing the stemness of hepatocellular carcinoma cells and hepatocarcinogenesis. Jin et al. (2017) found that FBW7 inhibits invasion of pancreatic cancer cells by inhibiting EZH2 activity and degrading EZH2. Therefore, it is worthwhile to reveal the regulatory networks of prognostic URGs and TFs in tumor genesis and progression. In our study, we downloaded 318 TFs from the Cistrome Project, extracted 314 ccRCC-related TFs based on the TCGA cohort, and finally obtained 66 differentially expressed TFs, including 46 up-regulated and 20 down-regulated TFs. The expression heatmap of these TFs is shown in **Figure 7A**. By co-expression analysis of differentially expressed TFs and prognostic URGs, a total of 54 TFs involved in regulation were identified. The regulatory network of the URGs-TFs is shown in **Figure 7B**, in which 10 TFs negatively regulated corresponding URGs and 44 TFs positively regulated them. The specific regulation relationship between them is shown in **Supplementary Table 2**.

In order to investigate the molecular functions and biological pathways of these differentially expressed URGs, the “clusterProfiler” package was used to perform GO and KEGG enrichment analysis on these URGs. Biological process analysis showed that these URGs were mainly concentrated in protein polyubiquitination, proteasomal protein catabolic process, proteasome-mediated ubiquitin-dependent protein catabolic process, post-translational protein modification, protein deubiquitination, I-kappaB kinase/NF-kappaB signaling, and regulation of protein ubiquitination (**Figure 7C**). Cellular component analysis showed that these URGs were mainly concentrated in ubiquitin ligase complex, cullin-RING ubiquitin ligase complex, and SCF ubiquitin ligase complex (**Figure 7C**). Molecular function analysis showed that these URGs were mainly concentrated in ubiquitin-protein transferase activity, ubiquitin-like protein transferase activity, ubiquitin protein ligase activity, phosphotyrosine residue binding, and superoxide-generating NADPH oxidase activity (**Figure 7C**). In terms of

KEGG analysis, these differentially expressed URGs were mainly concentrated in Ubiquitin mediated proteolysis, Fc gamma R-mediated phagocytosis, NOD-like receptor signaling pathway, and Osteoclast differentiation (**Figure 7D**).

### Evaluation of the Relationship Between the Prognostic Signature and the Degree of Immune Cell Infiltration

The degree of immune cell infiltration affects tumor progression and therapeutic effect. In this study, we evaluated the differences in immune cell infiltration between different subgroups based on the CIBERSORT algorithm. The results showed significant differences in the composition of the 22 immune cells in each sample in the TCGA cohort (**Figure 8A**). Specifically, the infiltration degree of plasma cells, T cells CD8, T cells CD4 memory resting, T cells CD4 memory activated, T cells follicular helper, T cells regulatory (Tregs), monocytes, macrophages M1, dendritic cells activated, mast cells resting, and eosinophils were significantly different between the high- and low-risk groups (**Figure 8B**), suggesting that there may be differences in immune status between the high- and low-risk groups. Correlation matrix results revealed that the T cells CD8 had the strongest positive correlation with T cells regulatory (Tregs), was also positively correlated with T cells follicular helper (**Figure 8C**).

### Evaluation of the Prognostic Significance of Different Clinical Characteristics in ccRCC Patients and Construction of a Nomogram

We first evaluated the prognostic value of different clinical characteristics in patients with ccRCC through univariate Cox proportional hazards regression analysis. The results showed that the age ( $P < 0.001$ ), tumor grade ( $P < 0.001$ ), tumor stage ( $P < 0.001$ ), primary tumor location ( $P < 0.001$ ), lymph node



**TABLE 2 |** The relationship between prognostic related ubiquitin genes and clinicopathologic parameters.

Gene		Gender (male/female)	Grade (G1–2/G3–4)	Stage (I–II/III–IV)	T stage (T1–T2/T3–T4)	N stage (N0/N1–X)	M stage (M0/M1–X)
N		353/186	249/282	331/205	349/190	241/298	428/109
CDCA3	<i>t</i> -value	1.687	NA*	NA*	NA*	0.519	NA*
	<i>P</i> -value	0.092	<0.001	<0.001	<0.001	0.604	<0.001
CHFR	<i>t</i> -value	0.073	NA*	5.967	5.670	0.139	4.574
	<i>P</i> -value	0.942	<0.001	<0.001	<0.001	0.890	<0.001
CORO6	<i>t</i> -value	1.650	3.427	3.504	3.454	1.014	4.538
	<i>P</i> -value	0.100	<0.001	<0.001	<0.001	0.311	<0.001
RNF175	<i>t</i> -value	1.331	3.750	4.174	4.112	0.050	2.502
	<i>P</i> -value	0.184	<0.001	<0.001	<0.001	0.960	0.013
TRIM72	<i>t</i> -value	NA*	2.168	2.548	2.048	NA*	NA*
	<i>P</i> -value	0.373	0.031	0.011	0.041	0.888	0.086
VAV3	<i>t</i> -value	NA*	NA*	NA*	NA*	0.815	NA*
	<i>P</i> -value	0.323	<0.001	<0.001	<0.001	0.416	<0.001
WDR72	<i>t</i> -value	1.774	NA*	NA*	NA*	0.289	NA*
	<i>P</i> -value	0.077	<0.001	<0.001	<0.001	0.773	<0.001

NA, not available. \*Non-parametric Mann-Whitney rank sum test. The statistical method was *t*-test or non-parametric Mann-Whitney rank sum test with only one test.

infiltration ( $P = 0.049$ ), distant metastasis ( $P < 0.001$ ), and risk score ( $P < 0.001$ ) of ccRCC patients were significantly correlated with OS (**Figure 9A**). However, multivariate Cox proportional hazards regression analysis revealed that age ( $P = 0.006$ ), tumor grade ( $P = 0.018$ ), tumor stage ( $P < 0.001$ ), primary tumor location ( $P = 0.030$ ), and risk score ( $P < 0.001$ ) affected OS as independent prognostic factors (**Figure 9B**).

Next, based on these seven prognostic URGs, we established a nomogram that could quantitatively predict the prognosis of patients with ccRCC (**Figure 9C**). Briefly, the points of each variable were mapped to the corresponding horizontal line, then the total points of each patient were calculated and normalized to a distribution of 0–100. This allows us to estimate 1-, 3-, and 5-year survival rates for ccRCC patients based on the prognosis axis and total point axis, which can be used as a reference for clinical decision-making. The results of the calibration curve at different time points showed that there is a strong consistency between the predicted value of the nomogram and the actual value (**Figures 9D–F**). Additionally, we further evaluated the clinical applicability and validity of the nomogram using the TCGA and E-MTAB-1980 cohorts. Survival analysis using Kaplan-Meier method showed that nomogram can accurately identify ccRCC patients with low survival probability in the TCGA and E-MTAB-1980 cohorts ( $P < 0.001$  and  $P = 0.002$ , **Figures 9G,I**). Based on the nomogram, in the TCGA cohort, the predicted AUCs were 0.856 at 1 year, 0.806 at 3 years, and 0.781 at 5 years (**Figure 9H**), and in the E-MTAB-1980 dataset, the predicted AUCs were 0.893 at 1 year, 0.868 at 3 years, and 0.855 at 5 years (**Figure 9J**), indicating that the nomogram had good predictive power and accuracy.

## IHC Staining Analysis

IHC assay was used to preliminarily verify the protein expression levels of these URGs between normal kidney tissues and ccRCC tissues. The results revealed that CDCA3 ( $P < 0.001$ ), VAV3

( $P = 0.034$ ), and WDR72 ( $P = 0.033$ ) were low expressed in ccRCC tissues compared with normal renal tissues. However, the CHFR ( $P = 0.018$ ) were high expressed in ccRCC tissues compared with normal renal tissues (**Figure 10**). All the results of IHC analysis were shown in **Supplementary Table 3**.

## DISCUSSION

Ubiquitin modification is a PTM of proteins in pathophysiological processes that plays a regulatory role in complex biological processes, including protein-protein interactions, protein activation, and substrate activation or inactivation (Pickart and Eddins, 2004). Abnormalities in the ubiquitin-modifying system are responsible for a variety of diseases, including neurodegenerative diseases, autoimmune diseases, and tumors. Abnormal expression of E3S and DUBS has been found to affect human malignancies by regulating the activity of tumor-associated proteins (Love et al., 2013; Paul et al., 2017). However, only a small number of ubiquitin molecules have been thoroughly studied, and most of the research has focused on the function of individual genes. Few studies have systematically explored the molecular characteristics and prognostic potential of URGs using expression profile datasets. In our study, we identified 204 differentially expressed URGs, including 141 up-regulated URGs and 63 down-regulated URGs. The biological functions and molecular mechanisms of these URGs were systematically analyzed by using bioinformatics techniques. A total of seven prognostic related URGs were identified by Cox regression analysis of differential URGs and used to construct a prognostic signature. We also analyzed the correlation between prognostic signature, prognostic URGs and clinical characteristics. Additionally, we further revealed the regulatory network of URGs-TFs and the relationship between prognostic signature and immune cell infiltration.

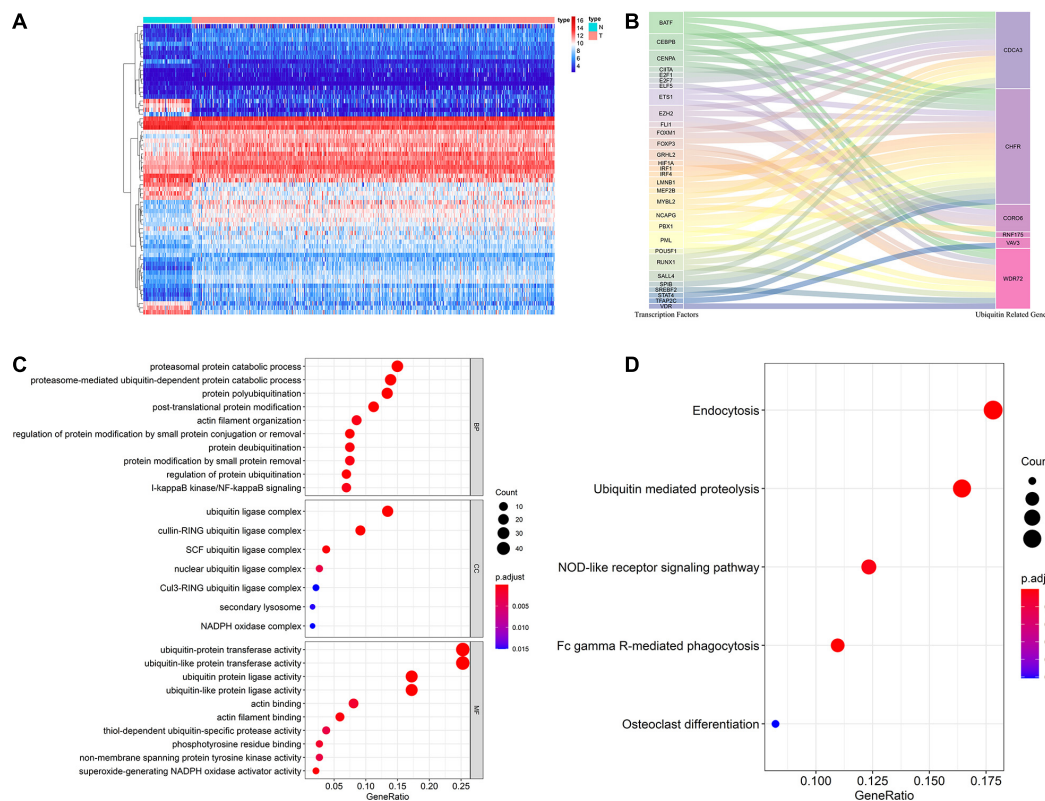


**FIGURE 7 |** Multidimensional regulatory network of prognostic URGs and functional enrichment analysis. **(A)** The differential expression of 66 TFs in ccRCC tissue samples ( $n = 539$ ) compared with normal renal samples ( $n = 72$ ) is shown in the heatmap; **(B)** Sankey plot of URGs-TFs regulatory networks; **(C)** GO enrichment analysis of the differentially expressed URGs; **(D)** KEGG enrichment analysis of the differentially expressed URGs (the statistical method was multiple hypothesis testing).

Through the Cox proportional hazards regression analysis of URGs, we screened out a total of seven URGs including *CDCA3*, *CHFR*, *CORO6*, *RNF175*, *TRIM72*, *VAV3*, and *WDR72*. *CDCA3* is a major regulator of mitosis and cell cycle. *CDCA3* overexpression has been reported to promote the G1/S phase transformation and promote the proliferation of colorectal cancer cells by activating the NF- $\kappa$ B/cyclin D1 signaling pathway (Zhang et al., 2018). Liu et al. (2020) found that in RCC, the long non-coding RNA *SNHG12* promoted tumor progression and sunitinib resistance by upregulating *CDCA3*. *CHFR* plays an important role in cell cycle regulation. Numerous studies have shown that the *CHFR* gene is significantly silenced or mutated by promoter methylation in many cancer types including non-small cell lung cancer (Mizuno et al., 2002) and esophageal cancer (Shibata et al., 2002). Yang et al. (2019) found that *CHFR* promoted the invasion of gastric cancer cells by inducing epithelial to mesenchymal transformation in a HDAC1-dependent manner. Coronin-6, a gene product of *CORO6*, is a member of the coronin family and has been shown to play a role in cell movement, vesicle transport, and cell division (Roadcap et al., 2008). Studies have shown that *CORO6* is a potential tumor suppressor in renal cancer (Morris et al., 2011). Kiely et al. (2020) found that low *CORO6*

expression was associated with poorer overall breast cancer survival. *RNF175* and *RNF213* share their E3 ubiquitin ligase activity and play an important role in protein post-translational ubiquitination modification (Kaneko et al., 2016). *TRIM72* is a member of the tripartite motif family. Studies suggest that *TRIM72* ubiquitin ligase activity may be associated with insulin resistance and metabolic syndrome, a well-known risk factor for colon cancer (Liu et al., 2018). Fernández-Aceñero et al. (2020) found that immunohistochemical expression of *TRIM72* could predict colorectal cancer recurrence. *VAV3* is a member of the guanine nucleotide exchange factor family and is involved in many important pathological processes, including tumorigenesis and cell transformation. Studies have shown that *VAV3* expression is increased in a variety of cancers and can promote gastric cancer cell metastasis (Aguilar et al., 2014; Xie et al., 2019). The *WDR72* gene encodes proteins that promote the formation of heterotrimeric or multiprotein complexes. WDR proteins may act as molecular adapters for substrate recognition and regulate a variety of biological processes through ubiquitin-independent proteolysis. Mares et al. (2013) found that *WDR72* can be used as a biomarker for predicting low- and moderate-risk recurrence of non-muscularly invasive bladder cancer. These results suggested that these URGs play important roles in a variety

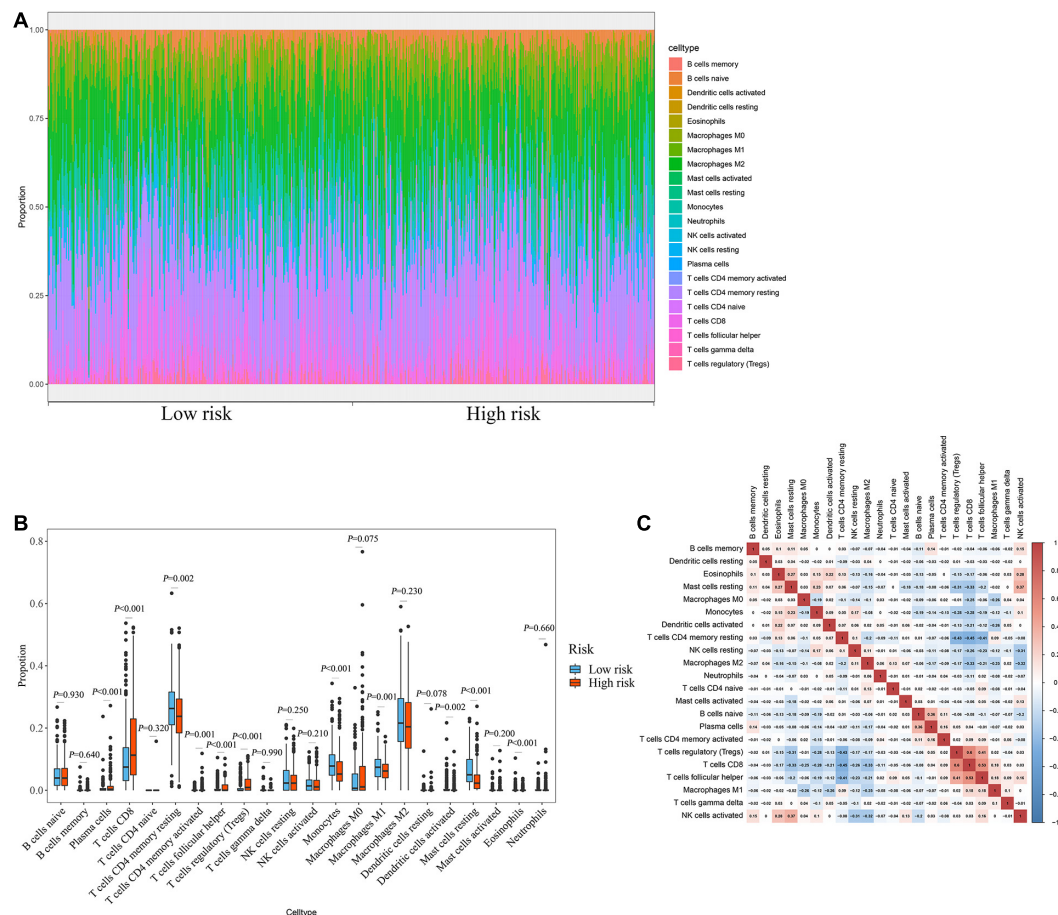


**FIGURE 8 |** Relationship between prognostic signature and immune cell infiltration. **(A)** Stacked bar chart of the distribution of 22 immune cells in each ccRCC sample of the TCGA cohort ( $n = 539$ ). **(B)** Box plot of immune cell infiltrates in ccRCC patients at high- ( $n = 269$ ) and low-risk ( $n = 270$ ). **(C)** Immune cell proportional correlation matrix (the statistical method was  $t$ -test).

of tumors and may be involved in the occurrence and development of ccRCC. However, further experiments *in vitro* and *in vivo* are needed to explore the exact molecular mechanisms of these URGs.

Subsequently, we developed a URGs-based prognostic signature for OS. Survival analysis by Kaplan-Meier method showed that patients in the high-risk group had a shorter OS than those in the low-risk group. ROC curve analysis showed that the URGs-based prognostic signature could better screen ccRCC patients with poor prognosis. Further analysis showed that the prognosis of patients in each high-risk group under different clinical parameter stratification was worse than that in the low-risk group. Moreover, we also found that the prognostic signature can be used to assess the degree of progression of ccRCC tumors. These results suggested that this prognostic signature has a good ability to distinguish the degree of malignancy and prognosis of ccRCC patients.

Moreover, we explored the URGs-TFs regulatory network based on the TCGA cohort, and co-expression analysis revealed a regulatory network consisting of 6 prognostic URGs and 54 differentially expressed TFs. The function and activity of

these TFs may be affected, thereby regulating the occurrence and progression of tumors, which is worthy of further study. Subsequent GO and KEGG enrichment analysis indicated that these differentially expressed URGs were mainly concentrated in protein polyubiquitination, proteasomal protein catabolic process, proteasome-mediated ubiquitin-dependent protein catabolic process, post-translational protein modification, protein deubiquitination, regulation of protein ubiquitination, and ubiquitin mediated proteolysis. Ubiquitination has a wide range of cellular functions, including proteolytic and non-proteolytic effects, such as proteasomal degradation of proteins, internalization and down-regulation of receptors, assembly of multi-protein complexes, inflammatory signaling, autophagy, DNA repair, and regulation of enzyme activity (Grabbe et al., 2011). Thus, dysregulation of ubiquitination can have a wide range of effects. It may cause abnormal activation or deactivation ways (such as those involved in tumor formation, or cell metabolism), inappropriate or inadequate protein complex assembly (such as occurred in the process of regulating inflammation or DNA repair), or the accumulation of misfolded proteins (in neurodegenerative diseases during

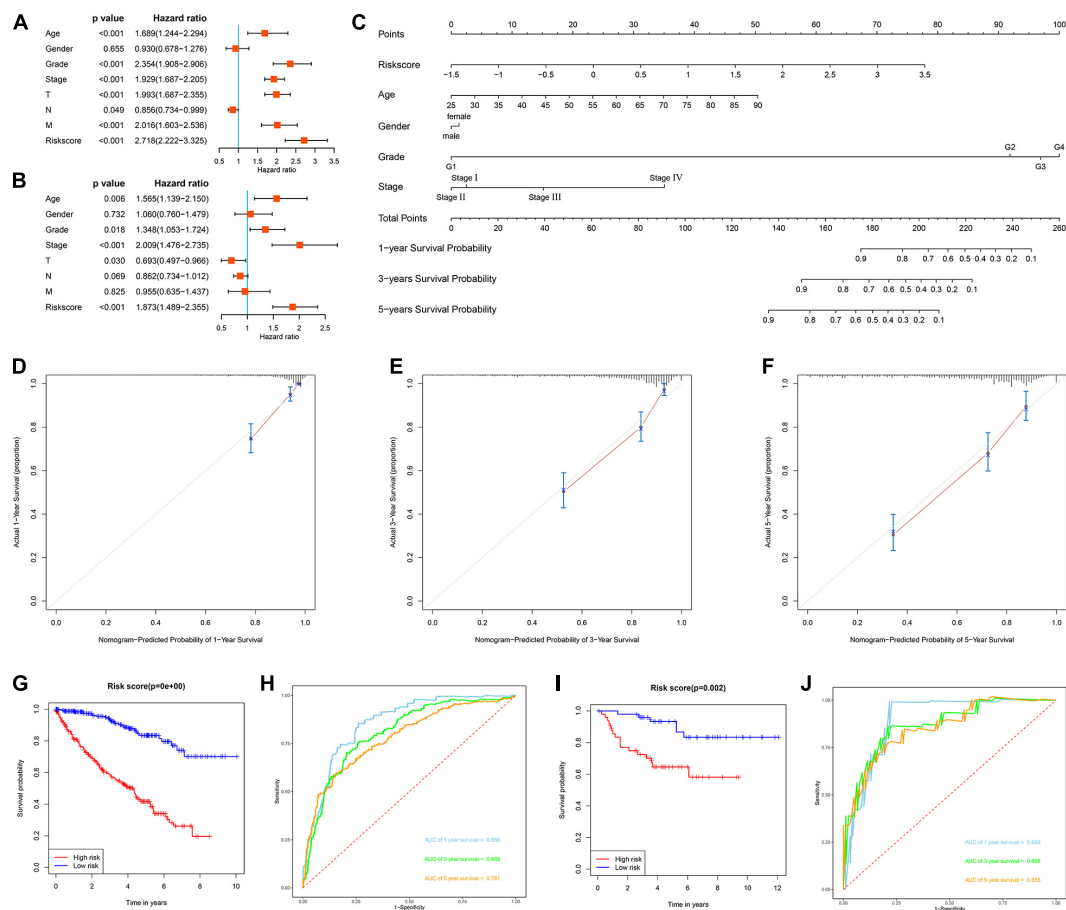


**FIGURE 9 |** Evaluation of the prognostic significance of different clinical characteristics in ccRCC patients and construction of a nomogram. **(A)** Univariate Cox regression analyses in the TCGA cohort ccRCC patients ( $n = 539$ ); **(B)** multivariate Cox regression analyses in the TCGA cohort ccRCC patients ( $n = 526$ ); **(C)** the nomogram for predicting the 1-, 3-, and 5-year OS of ccRCC patients ( $n = 526$ ); **(D)** the calibration curve of the nomogram for predicting 1-year OS of ccRCC patients; **(E)** the calibration curve of the nomogram for predicting 3-year OS of ccRCC patients; **(F)** the calibration curve of the nomogram for predicting 5-year OS of ccRCC patients; **(G)** Kaplan-Meier survival curve analysis in the TCGA cohort based the nomogram ( $n = 526$ ); **(H)** ROC curve analysis shows 1, 3, and 5-year OS and the corresponding AUC values for ccRCC patients from the TCGA cohort based the nomogram ( $n = 526$ ); **(I)** Kaplan-Meier survival curve analysis in the E-MTAB-1980 cohort based the nomogram ( $n = 99$ ); **(J)** ROC curve analysis shows 1, 3, and 5-year OS and the corresponding AUC values for ccRCC patients from the E-MTAB-1980 cohort based the nomogram ( $n = 99$ ) (the statistical method was a log-rank test for a single factor).

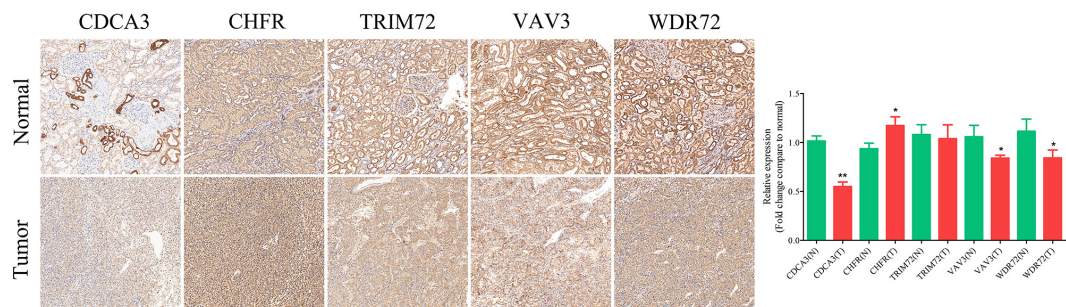


**FIGURE 10 |** Validation of the expression of the prognostic URGs in ccRCC and normal renal tissues by immunohistochemical staining analysis. The expressions of CDCA3, CHFR, TRIM72, VAV3, and WDR72 in ccRCC tissues and adjacent non-tumor renal tissues were detected by immunohistochemical staining (magnification 100 $\times$ ). Quantification of immunohistochemical staining for CDCA3, CHFR, TRIM72, VAV3, and WDR72 by Image Pro Plus software. \* $P < 0.05$  vs. normal group, \*\* $P < 0.01$  vs. normal group.



endoplasmic reticulum or in the cytoplasm) (Hoeller and Dikic, 2009; Popovic et al., 2014). Additionally, ubiquitination also regulates T cell development, activation, and differentiation, thereby mediating and maintaining effective adaptive immune responses and immune tolerance. Dysregulated events of ubiquitination are associated with immune disorders including autoimmune diseases and inflammatory diseases (Hu and Sun, 2016). Further studies found significant differences in the degree of immune cell infiltration between the high-risk and low-risk groups according to the prognostic signature. These results suggested that ubiquitination and its dysregulation may affect the occurrence and development of tumors through a variety of pathways.

Overall, this study provides a new insight into the tumorigenesis and progression of ccRCC from the perspective of ubiquitin. These seven URGs-based prognostic signature has a better effect on the prediction of survival in ccRCC patients. In addition, URGs-based prognostic signature show important biological functions and clinical value, suggesting that they may be used in adjuvant clinical therapy. However, our study also has some limitations. First of all, the construction and validation of this signature is based on retrospective analysis, and prospective clinical cohort validation is also required. Secondly, different platforms may lead to differences in patients due to their heterogeneity. Finally, the specific functions and molecular mechanisms of these prognostic URGs in ccRCC are still unclear, and this study may also omit some URGs that have significant influence on disease progression but are rarely expressed, which require follow-up attention and further experimental exploration.

## CONCLUSION

In summary, through multiple bioinformatics analyses, we systematically explored the molecular characteristics and prognostic value of URGs in ccRCC based on the high-throughput sequencing expression profile datasets, and preliminarily revealed the complex biological functions and immune processes involved in these molecules and their regulatory networks. These URGs may be involved in the occurrence, development, invasion, and metastasis of ccRCC. We also constructed a prognostic signature that could independently

predict prognosis in ccRCC patients. Our results will help to reveal the pathogenesis of ccRCC and develop new biomarkers, and provide certain guiding significance for clinical decision-making.

## DATA AVAILABILITY STATEMENT

The data and materials can be obtained by contacting the corresponding author.

## ETHICS STATEMENT

The studies involving human tissues samples were reviewed and approved by the Research Ethics Committee of Tongji Hospital, Tongji Medical College, Huazhong University of Science and Technology, and complied with the Declaration of Helsinki. All patients were aware of the present study and signed an informed consent agreement.

## AUTHOR CONTRIBUTIONS

YW designed the study and performed the data analysis. XZ carried out the immunohistochemical experiments, performed the data analysis, and revised the manuscript. XW, HF, BH, ZD, and BL performed the data analysis. YL, YR, XL, ZL, and JL performed the data analysis and revised the manuscript. TW designed the study and revised the manuscript. All authors read and approved the final manuscript.

## FUNDING

This work was supported by a grant from the National Natural Science Foundation of China (No. 81874165).

## SUPPLEMENTARY MATERIAL

The Supplementary Material for this article can be found online at: <https://www.frontiersin.org/articles/10.3389/fcell.2021.684643/full#supplementary-material>

## REFERENCES

- Aguilar, H., Urruticoechea, A., Halonen, P., Kiyotani, K., Mushiroda, T., Barril, X., et al. (2014). VAV3 mediates resistance to breast cancer endocrine therapy. *Br. Cancer Res.* 16:R53. doi: 10.1186/bcr3664
- Chiang, C., and Gack, M. U. (2017). Post-translational control of intracellular pathogen sensing pathways. *Trends Immunol.* 38, 39–52. doi: 10.1016/j.it.2016.10.008
- Cui, C. P., Wong, C. C., Kai, A. K., Ho, D. W., Lau, E. Y., Tsui, Y. M., et al. (2017). SENP1 promotes hypoxia-induced cancer stemness by HIF-1 $\alpha$  deSUMOylation and SENP1/HIF-1 $\alpha$  positive feedback loop. *Gut* 66, 2149–2159. doi: 10.1136/gutjnl-2016-313264
- Deribe, Y. L., Pawson, T., and Dikic, I. (2010). Post-translational modifications in signal integration. *Nat. Struct. Mol. Biol.* 17, 666–666. doi: 10.1038/nsmb.1842
- Escudier, B., Porta, C., Schmidinger, M., Rioux-Leclercq, N., Bex, A., Khoo, V., et al. (2019). Renal cell carcinoma: ESMO clinical practice guidelines for diagnosis, treatment and follow-up†. *Ann. Oncol.* 30, 706–707. doi: 10.1093/annonc/mdz056
- Fernández-Aceñero, M. J., Cruz, M., Sastre-Varela, J., Casal, J. I., Nieto, M., Del Puerto-Nevado, L., et al. (2020). TRIM72 immunohistochemical expression can predict relapse in colorectal carcinoma. *Pathol. Oncol. Res.* 26, 861–868. doi: 10.1007/s12253-019-00629-w
- Gao, T., Liu, Z., Wang, Y., Cheng, H., Yang, Q., Guo, A., et al. (2013). UUCD: a family-based database of ubiquitin and ubiquitin-like conjugation. *Nucleic Acids Res.* 41, D445–D451. doi: 10.1093/nar/gks1103

- Grabbe, C., Husnjak, K., and Dikic, I. (2011). The spatial and temporal organization of ubiquitin networks. *Nat. Rev. Mol. Cell. Biol.* 12, 295–307. doi: 10.1038/nrm3099
- Hershko, A., and Ciechanover, A. (1998). The ubiquitin system. *Annu. Rev. Biochem.* 67, 425–479. doi: 10.1146/annurev.biochem.67.1.425
- Hoeller, D., and Dikic, I. (2009). Targeting the ubiquitin system in cancer therapy. *Nature* 458, 438–444. doi: 10.1038/nature07960
- Hu, H., and Sun, S. C. (2016). Ubiquitin signaling in immune responses. *Cell. Res.* 26, 457–483. doi: 10.1038/cr.2016.40
- Husnjak, K., and Dikic, I. (2012). Ubiquitin-binding proteins: decoders of ubiquitin-mediated cellular functions. *Annu. Rev. Biochem.* 81, 291–293. doi: 10.1146/annurev-biochem-051810-094654
- Jin, X., Yang, C., Fan, P., Xiao, J., Zhang, W., Zhan, S., et al. (2017). CDK5/FBW7-dependent ubiquitination and degradation of EZH2 inhibits pancreatic cancer cell migration and invasion. *J. Biol. Chem.* 292, 6269–6280. doi: 10.1074/jbc.M116.764407
- Kaneko, M., Iwase, I., Yamasaki, Y., Takai, T., Wu, Y., Kanemoto, S., et al. (2016). Genome-wide identification and gene expression profiling of ubiquitin ligases for endoplasmic reticulum protein degradation. *Sci. Rep.* 6:309. doi: 10.1038/srep30955
- Kiely, M., Tse, L. A., Koka, H., Wang, D., Lee, P., Wang, F., et al. (2020). Age-related DNA methylation in paired normal and tumour breast tissue in Chinese breast cancer patients. *Epigenetics* 16, 677–691. doi: 10.1080/15592294.2020.1819661
- Li, Y., McLaren, M. C., and McMartin, K. E. (2010). Involvement of urinary proteins in the rat strain difference in sensitivity to ethylene glycol-induced renal toxicity. *Am. J. Physiol. Renal. Physiol.* 299, F605–F606. doi: 10.1152/ajprenal.00419.2009
- Lipkowitz, S., and Weissman, A. M. (2011). RINGs of good and evil: RING finger ubiquitin ligases at the crossroads of tumour suppression and oncogenesis. *Nat. Rev. Cancer* 11, 629–643. doi: 10.1038/nrc3120
- Liu, L., Wong, C. C., Gong, B., and Yu, J. (2018). Functional significance and therapeutic implication of ring-type E3 ligases in colorectal cancer. *Oncogene* 37, 148–159. doi: 10.1038/onc.2017.313
- Liu, Y., Cheng, G., Huang, Z., Bao, L., Liu, J., Wang, C., et al. (2020). Long noncoding RNA SNHG12 promotes tumour progression and sunitinib resistance by upregulating CDCA3 in renal cell carcinoma. *Cell Death Dis.* 11:5. doi: 10.1038/s41419-020-2713-8
- Love, I. M., Shi, D., and Grossman, S. R. (2013). p53 Ubiquitination and proteasomal degradation. *Methods Mol. Biol.* 962, 63–73. doi: 10.1007/978-1-62703-236-0\_5
- Mares, J., Szakacsova, M., Soukup, V., Duskova, J., Horinek, A., and Babjuk, M. (2013). Prediction of recurrence in low and intermediate risk non-muscle invasive bladder cancer by real-time quantitative PCR analysis: cDNA microarray results. *Neoplasma* 60, 295–301. doi: 10.4149/neo\_2013\_0391
- Meng, X., Xiong, Z., Xiao, W., Yuan, C., Wang, C., Huang, Y., et al. (2020). Downregulation of ubiquitin-specific protease 2 possesses prognostic and diagnostic value and promotes the clear cell renal cell carcinoma progression. *Ann. Transl. Med.* 8:319. doi: 10.21037/atm.2020.02.141
- Mizuno, K., Osada, H., Konishi, H., Tatematsu, Y., Yatabe, Y., Mitsudomi, T., et al. (2002). Aberrant hypermethylation of the CHFR prophase checkpoint gene in human lung cancers. *Oncogene* 21, 2328–2333. doi: 10.1038/sj.onc.1205402
- Morris, M. R., Ricketts, C. J., Gentle, D., McDonald, F., Carli, N., Khalili, H., et al. (2011). Genome-wide methylation analysis identifies epigenetically inactivated candidate tumour suppressor genes in renal cell carcinoma. *Oncogene* 30, 1390–1401. doi: 10.1038/onc.2010.525
- Motzer, R. J., Bukowski, R. M., Figlin, R. A., Hutson, T. E., Michaelson, M. D., Kim, S. T., et al. (2008). Prognostic nomogram for sunitinib in patients with metastatic renal cell carcinoma. *Cancer* 113, 1552–1558. doi: 10.1002/cncr.23776
- Nerich, V., Hugues, M., Paillard, M. J., Borowski, L., Nai, T., Stein, U., et al. (2014). Clinical impact of targeted therapies in patients with metastatic clear-cell renal cell carcinoma. *Onco. Targets Ther.* 7, 365–374. doi: 10.2147/OTT.S56370
- Newman, A. M., Liu, C. L., Green, M. R., Gentles, A. J., Feng, W., Xu, Y., et al. (2015). Robust enumeration of cell subsets from tissue expression profiles. *Nat. Methods* 12, 453–454. doi: 10.1038/nmeth.3337
- Nijman, S. M., Luna-Vargas, M. P., Velds, A., Brummelkamp, T. R., Dirac, A. M., Sixma, T. K., et al. (2005). A genomic and functional inventory of deubiquitinating enzymes. *Cell* 123, 773–777. doi: 10.1016/j.cell.2005.11.007
- Paul, I., Batth, T. S., Iglesias-Gato, D., Al-Araimi, A., Al-Haddabi, I., Alkharusi, A., et al. (2017). The ubiquitin ligase Cullin5SOCS2 regulates NDR1/STK38 stability and NF- $\kappa$ B transactivation. *Sci. Rep.* 7:428. doi: 10.1038/srep42800
- Pickart, C. M. (2001). Mechanisms underlying ubiquitination. *Annu. Rev. Biochem.* 70, 503–505. doi: 10.1146/annurev.biochem.70.1.503
- Pickart, C. M., and Eddins, M. J. (2004). Ubiquitin: structures, functions, mechanisms. *Biochim. Biophys. Acta* 1695, 55–72. doi: 10.1016/j.bbamer.2004.09.019
- Popovic, D., Vucic, D., and Dikic, I. (2014). Ubiquitination in disease pathogenesis and treatment. *Nat. Med.* 20, 1242–1253. doi: 10.1038/nm.3739
- Rape, M. (2018). Ubiquitylation at the crossroads of development and disease. *Nat. Rev. Mol. Cell. Biol.* 19, 59–70. doi: 10.1038/nrm.2017.83
- Roadcap, D. W., Clemen, C. S., and Bear, J. E. (2008). The role of mammalian coronins in development and disease. *Subcell. Biochem.* 48, 124–135. doi: 10.1007/978-0-387-09595-0\_12
- Seeler, J. S., and Dejean, A. (2017). SUMO and the robustness of cancer. *Nat. Rev. Cancer* 17, 184–197. doi: 10.1038/nrc.2016.143
- Shibata, Y., Haruki, N., Kuwabara, Y., Ishiguro, H., Shinoda, N., Sato, A., et al. (2002). Chfr expression is downregulated by CpG island hypermethylation in esophageal cancer. *Carcinogenesis* 23, 1695–1699. doi: 10.1093/carcin/23.10.1695
- Siegel, R. L., Miller, K. D., and Jemal, A. (2017). Cancer statistics, 2021. *CA Cancer J. Clin.* 67, 7–33. doi: 10.3322/caac.21387
- Siegel, R. L., Miller, K. D., Fuchs, H. E., and Jemal, A. (2021). Cancer statistics, 2021. *CA Cancer J. Clin.* 71, 7–33. doi: 10.3322/caac.21654
- Su, L., Han, D., Wu, J., and Huo, X. (2016). Skp2 regulates non-small cell lung cancer cell growth by Meg3 and miR-31. *Tumour. Biol.* 37, 3925–3939. doi: 10.1007/s13277-015-4151-2
- Upadhyay, S. C., and Hegde, A. N. (2003). A potential proteasome-interacting motif within the ubiquitin-like domain of parkin and other proteins. *Trends Biochem. Sci.* 28, 280–282. doi: 10.1016/S0968-0004(03)00092-6
- Xie, M., Ma, T., Xue, J., Ma, H., Sun, M., Zhang, Z., et al. (2019). The long intergenic non-protein coding RNA 707 promotes proliferation and metastasis of gastric cancer by interacting with mRNA stabilizing protein HuR. *Cancer Lett.* 443, 67–79. doi: 10.1016/j.canlet.2018.11.032
- Yang, S., He, F., Dai, M., Pan, J., Wang, J., and Ye, B. (2019). CHFR promotes the migration of human gastric cancer cells by inducing epithelial-to-mesenchymal transition in a HDAC1-dependent manner. *Onco. Targets Ther.* 12, 1075–1084. doi: 10.2147/OTT.S191016
- Zhai, W., Zhu, R., Ma, J., Gong, D., Zhang, H., Zhang, J., et al. (2019). A positive feed-forward loop between LncRNA-URRCC and EGFL7/P-AKT/FOXO3 signaling promotes proliferation and metastasis of clear cell renal cell carcinoma. *Mol. Cancer* 18:81. doi: 10.1186/s12943-019-0998-y
- Zhang, E., Dong, X., Chen, S., Shao, J., Zhang, P., Wang, Y., et al. (2020). Ubiquitin ligase KLHL2 promotes the degradation and ubiquitination of ARHGEF7 protein to suppress renal cell carcinoma progression. *Am. J. Cancer Res.* 10, 3345–3357.
- Zhang, W., Lu, Y., Li, X., Zhang, J., Zheng, L., Zhang, W., et al. (2018). CDCA3 promotes cell proliferation by activating the NF- $\kappa$ B/cyclin D1 signaling pathway in colorectal cancer. *Biochem. Biophys. Res. Commun.* 500, 196–203. doi: 10.1016/j.bbrc.2018.04.034
- Zhu, B., Zhu, L., Xia, L., Xiong, Y., Yin, Q., and Rui, K. (2020). Roles of ubiquitination and deubiquitination in regulating dendritic cell maturation and function. *Front. Immunol.* 11:5866. doi: 10.3389/fimmu.2020.586613

**Conflict of Interest:** The authors declare that the research was conducted in the absence of any commercial or financial relationships that could be construed as a potential conflict of interest.

Copyright © 2021 Wu, Zhang, Wei, Feng, Hu, Deng, Liu, Luan, Ruan, Liu, Liu, Liu and Wang. This is an open-access article distributed under the terms of the Creative Commons Attribution License (CC BY). The use, distribution or reproduction in other forums is permitted, provided the original author(s) and the copyright owner(s) are credited and that the original publication in this journal is cited, in accordance with accepted academic practice. No use, distribution or reproduction is permitted which does not comply with these terms.



# Global Screening of LUBAC and OTULIN Interacting Proteins by Human Proteome Microarray

Lijie Zhou<sup>1,2†</sup>, Yingwei Ge<sup>2†</sup>, Yesheng Fu<sup>2</sup>, Bo Wu<sup>2</sup>, Yong Zhang<sup>2</sup>, Lei Li<sup>2</sup>, Chun-Ping Cui<sup>2</sup>, Siying Wang<sup>1\*</sup> and Lingqiang Zhang<sup>2\*</sup>

<sup>1</sup> Department of Physiopathology, Anhui Medical University, Hefei, China, <sup>2</sup> State Key Laboratory of Proteomics, National Center for Protein Sciences (Beijing), Beijing Institute of Lifeomics, Beijing, China

## OPEN ACCESS

### Edited by:

Helen He Zhu,  
School of Medicine, Shanghai Jiao  
Tong University, China

### Reviewed by:

Li Li,  
Shanghai Jiao Tong University, China  
Xiangming Hu,  
Fujian Medical University, China

### \*Correspondence:

Siying Wang  
sywang@ahmu.edu.cn  
Lingqiang Zhang  
zhanglq@nic.bmi.ac.cn

<sup>†</sup> These authors have contributed  
equally to this work

### Specialty section:

This article was submitted to  
Cell Growth and Division,  
a section of the journal  
Frontiers in Cell and Developmental  
Biology

**Received:** 26 March 2021

**Accepted:** 13 May 2021

**Published:** 28 June 2021

### Citation:

Zhou LJ, Ge YW, Fu YS, Wu B,  
Zhang Y, Li L, Cui C-P, Wang SY and  
Zhang LQ (2021) Global Screening  
of LUBAC and OTULIN Interacting  
Proteins by Human Proteome  
Microarray.  
Front. Cell Dev. Biol. 9:686395.  
doi: 10.3389/fcell.2021.686395

Linear ubiquitination is a reversible posttranslational modification, which plays key roles in multiple biological processes. Linear ubiquitin chain assembly complex (LUBAC) catalyzes linear ubiquitination, while the deubiquitinase OTULIN (OTU deubiquitinase with linear linkage specificity, FAM105B) exclusively cleaves the linear ubiquitin chains. However, our understanding of linear ubiquitination is restricted to a few substrates and pathways. Here we used a human proteome microarray to detect the interacting proteins of LUBAC and OTULIN by systematically screening up to 20,000 proteins. We identified many potential interacting proteins of LUBAC and OTULIN, which may function as regulators or substrates of linear ubiquitination. Interestingly, our results also hint that linear ubiquitination may have broad functions in diverse pathways. In addition, we recognized lymphocyte activation gene-3 (LAG3, CD223), a transmembrane receptor that negatively regulates lymphocyte functions as a novel substrate of linear ubiquitination in the adaptive immunity pathway. In conclusion, our results provide searchable, accessible data for the interacting proteins of LUBAC and OTULIN, which broaden our understanding of linear ubiquitination.

**Keywords:** human proteome microarray, LUBAC, OTULIN, linear ubiquitination, LAG3

## INTRODUCTION

Ubiquitination is a reversible posttranslational modification and plays crucial roles in the regulation of various cellular pathways, such as the cell cycle, DNA damage repair, immune signaling, and diverse signal transduction (Komander and Rape, 2012; Swatek and Komander, 2016). Ubiquitination is an enzymatic cascade catalyzed by ubiquitin-activating enzyme E1, ubiquitin-conjugating enzyme E2, and ubiquitin ligase E3. Moreover, the substrates can be modified by mono-ubiquitination or poly-ubiquitination at lysine or non-lysine residues, such as serine, threonine, and cysteine (Cadwell, 2005; Shimizu et al., 2010; Swatek and Komander, 2016; Wang et al., 2017; Pao et al., 2018). Poly-ubiquitination occurs by diverse ubiquitin chain linkage *via* the formation of isopeptide bonds at the seven lysine sites of proximal ubiquitin. In addition, the first methionine (M1) of ubiquitin can also be modified by linking to another ubiquitin molecule *via* a peptide bond named linear ubiquitination or M1 ubiquitination (Kirisako et al., 2006; Spit et al., 2019).

Linear ubiquitination is a distinct linkage type of poly-ubiquitination, as the formation and erasure are catalyzed by unique enzymes named linear ubiquitin chain assembly complex (LUBAC)

and OTULIN, respectively (Kirisako et al., 2006; Keusekotten et al., 2013). LUBAC is an enzyme complex of 600 kDa and contains three members: HOIP (RNF31), HOIL-1L (RBCK1), and SHARPIN (SIPL1) (Kirisako et al., 2006; Gerlach et al., 2011; Ikeda et al., 2011; Tokunaga et al., 2011). HOIP and HOIL-1 are both RING-in-between-RING (RBR) E3 ligases (Eisenhaber et al., 2007), but only HOIP catalyzes peptide bond formation between ubiquitin molecules *via* the RBR-LDD (linear ubiquitin chain determining domain) domain (Smit et al., 2012). HOIP alone has negligible catalysis activity. The UBL (ubiquitin-like) domain of HOIL-1L and SHARPIN directly binds to the UBA (ubiquitin-associated domain) of HOIP, which greatly boosts the activity of HOIP and promotes the formation of linear ubiquitin chains (Yagi et al., 2012; Fujita et al., 2018). OTULIN is a member of ovarian tumor (OTU) deubiquitinases. It is broadly accepted that OTULIN has exclusive cleavage activity towards linear ubiquitin chains, and OTULIN restricts LUBAC functions in an enzyme activity-dependent manner (Heger et al., 2018).

Linear ubiquitination, formed by LUBAC, is involved in canonical nuclear factor- $\kappa$ B (NF- $\kappa$ B) activation and the TNFR1 signaling complex (TNF-RSC) (Haas et al., 2009; Iwai and Tokunaga, 2009; Tokunaga et al., 2009; Niu et al., 2011). Deficiencies in *Hoip* (Peltzer et al., 2014), *Hoil-1l* (Peltzer et al., 2018), and *Sharpin* in mice have remarkable phenotypes in inflammation and immunity (HogenEsch et al., 1993; Seymour et al., 2007; Gerlach et al., 2011; Ikeda et al., 2011; Tokunaga et al., 2011). However, to make things complicated, *Otulin*<sup>C129A/C129A</sup> knock-in mice are embryonically lethal, and the TNF signal pathway is disordered (Heger et al., 2018). Further evidence indicates that OTULIN is also indispensable for LUBAC to function correctly (Elliott et al., 2014; Schaeffer et al., 2014). In addition, HOIL-1L catalyzes mono-ubiquitination at multiple LUBAC sites and attenuates LUBAC functions (Fuseya et al., 2020). Consequently, LUBAC regulation and linear ubiquitination are complicated and merit further study.

To date, limited numbers of substrates and regulators of linear ubiquitination have been reported. Tandem ubiquitin-binding entities (TUBEs) are useful tools to pull down ubiquitin chains, but they are limited in their affinity and specificity (Hjerpe et al., 2009). The accessible linear ubiquitin antibodies are not workable for immunoprecipitation and mass spectrometry. Internally tagged ubiquitin without lysine was constructed to pull down linear ubiquitin, which recognized several new substrates in TNF pathways (Kliza et al., 2017). However, this exogenous ubiquitin mutation may enrich unexpected substrates beyond physiological background levels. Owing to the low abundance of linear ubiquitin chains in cells, the present methods that rely on mass spectrometry cannot easily distinguish authentic substrates from background noise.

To further understand the novel functions of linear ubiquitination, we used a human proteome microarray (Sjöberg et al., 2016) to identify new interacting proteins of LUBAC and OTULIN. Using relatively strict criteria, we identified 330 potential interactors of LUBAC and 376 potential interactors of OTULIN, of which 260 were shared. We selected proteins for validation, and the results confirmed that the system was stable and reliable. Furthermore, we confirmed that lymphocyte

activation gene-3 (LAG3, CD223) is a new substrate of linear ubiquitination, which may provide new ideas to understand the novel function of linear ubiquitination in T cell immunity.

## MATERIALS AND METHODS

### Protein Expression and Purification

OTULIN cDNA was cloned into the pET28a vector with an N-terminal 6xHis tag. After transforming into BL21 (DE3) strain and selecting on LB agar plates supplemented with 50  $\mu$ g/ml kanamycin, a single clone was picked and cultured in LB medium supplemented with 50  $\mu$ g/ml kanamycin until the OD<sub>600</sub> reached 0.6. The expression of OTULIN was induced with 0.4 mM isopropyl  $\beta$ -D-1-thiogalactopyranoside (IPTG) at 20°C for 10 h before harvesting.

The HOIP expression vector was constructed using the pCDH-CMV vector with an N-terminal 6xHis tag, and transfection was performed using polyethylenimine for transient expression in HEK 293T cells. Cells were harvested 48 h after transfection.

To purify the His-tagged proteins, cells were resuspended and lysed in buffer containing 20 mM sodium phosphate, pH 8.0, 300 mM NaCl, 20 mM imidazole, and 0.5% Triton X-100. Lysozyme (20  $\mu$ g/ml) and PMSF (0.5 mM) were added to the bacterial cell lysates. A protease inhibitor cocktail (Topsience, China) was added to the HEK 293T cell lysates. After sonication, the cell lysates were centrifuged at 15,000g for 15 min, and the insoluble pellet was discarded. The supernatant was incubated with His-tag Purification Resin (Beyotime, China) for the duration indicated by the manufacturer, and the resin was washed with lysis buffer five times to remove the uncoupled proteins. The His-tagged proteins were eluted with lysis buffer containing 200 mM imidazole, pH 7.5, and were dialyzed against phosphate-buffered saline (PBS; 20 mM sodium phosphate, pH 7.5, 150 mM NaCl). Protein purity was validated by Coomassie brilliant blue staining.

### Cell Culture

HEK 293T cell lines were cultured in Dulbecco's modified Eagle's medium high glucose (Hyclone, United States) supplemented with 10% fetal bovine serum (Gemini Bio, United States). All the culture media were supplemented with 100 U/ml penicillin and 0.1 mg/ml streptomycin. Cells were cultured at 37°C with 5% CO<sub>2</sub>.

### Plasmids and DNA Transfection

cDNAs for human HOIP, HOIL-1L, and OTULIN were amplified by reverse transcription from HEK 293T cells and inserted into the pFlag-CMV2 vector. Non-tagged ubiquitin, Myc-HOIP, and Myc-HOIP-CS (C699S/C702S/C871S/C874S) were constructed using Gibson assembly methods. LAG3 cDNA was gifted from Dr. Xiaoming Yang (State Key Laboratory of Proteomics, Beijing), and the mammalian expression vectors and the LAG3 mutations were constructed by PCR and Gibson assembly into pCMV-Myc and pCDNA3.1-Myc-His A.



cDNAs for ABI1, ABI2, SIRT3, SIRT5, DDX6, and WWP2 were amplified from human spleen cDNA and inserted into the pCMV-Myc vector.

Transfection was performed using polyethylenimine according to the standard protocol and cultured before harvesting for experiments.

## Co-immunoprecipitation

Cells were lysed in buffer containing 50 mM Tris-HCl, pH 7.4, 150 mM NaCl, 5 mM EDTA, and 1% Triton X-100 with protease inhibitor cocktail on ice before sonicating for 1 min. The lysates were centrifuged at 12,000g for 10 min, and the supernatants were transferred to 1.5-ml EP tubes and precleared with protein A/G agarose (Santa Cruz Biotechnology, United States) for 30 min at 4°C. Next, the lysates were incubated with specific antibodies for at least 1 h and then sequentially incubated with protein A/G agarose on a rotor at 4°C overnight. The agarose beads were washed four times with lysis buffer before boiling in Laemmli sample buffer, and the proteins were analyzed by immunoblotting.

## Immunoprecipitation, Linear Ubiquitination Assay, and Immunoblotting

Cells were lysed in buffer containing 50 mM Tris-HCl, pH 7.4, 150 mM NaCl, 5 mM EDTA, 0.5% sodium deoxycholate, and 1% Triton X-100 with protease inhibitor cocktail on ice. To detect linear ubiquitination, sodium dodecyl sulfate (SDS, 0.5%) was added to the cell lysates, which were then heated at 90°C for 5 min. The lysates were sonicated for 1 min, diluted to 0.1% SDS, and precleared for 30 min before incubating with the antibody and protein A/G agarose on a rotor at 4°C overnight. After washing four times with lysis buffer, Laemmli sample buffer was added, and the samples were boiled for 8 min. The samples were separated by SDS-PAGE and transferred onto a nitrocellulose membrane. The membranes were blocked in 5% non-fat milk for 1 h at room temperature and incubated with the following antibodies: anti-DDDDK tag (MBL, Japan), anti-Myc tag (MBL, Japan), anti-HA tag (MBL, Japan), anti-HIS tag (Biodragon, China), and anti-linear ubiquitin (Lifesensors, clone LUB9, United States). After incubation, the membrane was washed with 0.1% Tween-20 (TBST) buffer and incubated with a secondary antibody (Jackson, United States) or light-chain-specific secondary antibody (Abbkine, China) for 1 h at room temperature. After an additional wash with TBST, the membranes were incubated with enhanced chemiluminescence substrates (Thermo Fisher Scientific, United States) and developed in the darkroom.

## Immunofluorescence

HEK 293T cells were cultured in a 35-mm dish with a glass bottom and transfected with Flag-HOIP, Flag-OTULIN, and Myc-LAG3. The cells were washed with cold PBS 48 h after transfection and fixed with 4% paraformaldehyde for 15 min, permeabilized by 0.5% Triton X-100 for 20 min, and then blocked with 2% BSA for 30 min at room temperature. The cells

were incubated with anti-DYKDDDDK antibody (Cell Signal Technology, United States) and anti-Myc antibody in 0.5% BSA at 4°C overnight. After incubation, the cells were washed four times with PBS containing 0.05% Tween-20 (PBST) for 20 min and then incubated with DAPI (Cell Signal Technology, United States) and Alexa Fluor 594 goat anti-rabbit IgG (Invitrogen, United States) or Alexa Fluor 488 goat anti-mouse IgG (Invitrogen, United States). Confocal images were visualized on a Nikon A1R confocal microscope.

## Human Proteome Microarray

We performed the human proteome microarray assays according to the HuProt User Guide (Figure 1A). The recombinant OTULIN and LUBAC proteins were labeled with biotin (Full Moon Biosystems, United States). Briefly, the microarrays were blocked with blocking buffer (PBS, 5% BSA, 0.1% Tween-20) and incubated with 5 µg/5 ml biotin-labeled protein sample for 1 h at room temperature with gentle shaking. The microarrays were washed four times with PBST and then incubated with 0.1% Cy5-streptavidin solution for 20 min at room temperature. After four PBST washes and three ddH<sub>2</sub>O washes, the desiccated microarrays were scanned with a GenePix 4000B (Axon Instruments, United States) at 635 nm. The data were extracted using GenePix Pro version 6.0 (Axon Instruments, United States).

## Protein Microarray Data Analysis

Data normalization was performed according to the HuProt User Guide.

$I$  is the intensity of spot-normalized fluorescence signal at 635 nm, and  $M$  is the median of  $I$  of all spots across each microarray. The Z-score was calculated according to standard deviation (SD) as the standardized value of each spot [ $Z\text{-score} = (I - M)/SD$ ].

When  $I_{mean}$  was the mean value of each protein spot,  $I_{Mean\_Ratio}$  was the ratio of each spot and was used to filter the false and the positive spots in the negative control microarray (BSA).

The criteria used to filter the positive spots were  $Z\text{-score} \geq 3$  and  $I_{Mean\_Ratio} \geq 1.4$ , which were stringent, resulting in only almost 1.5% of proteins being isolated from the microarray.

## RESULTS

### Screening of LUBAC and OTULIN Interacting Proteins by Human Proteome Microarray

To identify LUBAC and OTULIN interacting proteins *via* the ProtoArray Human Proteome Microarray, we first purified HOIP and OTULIN proteins *in vitro*. OTULIN expresses as a soluble protein in *Escherichia coli*, but the purification of HOIP is troublesome in prokaryotic expression systems. Using HEK 293T cells as the protein expression system, HIS-tagged HOIP and the LUBAC subunit HOIL-1 were successfully purified from the

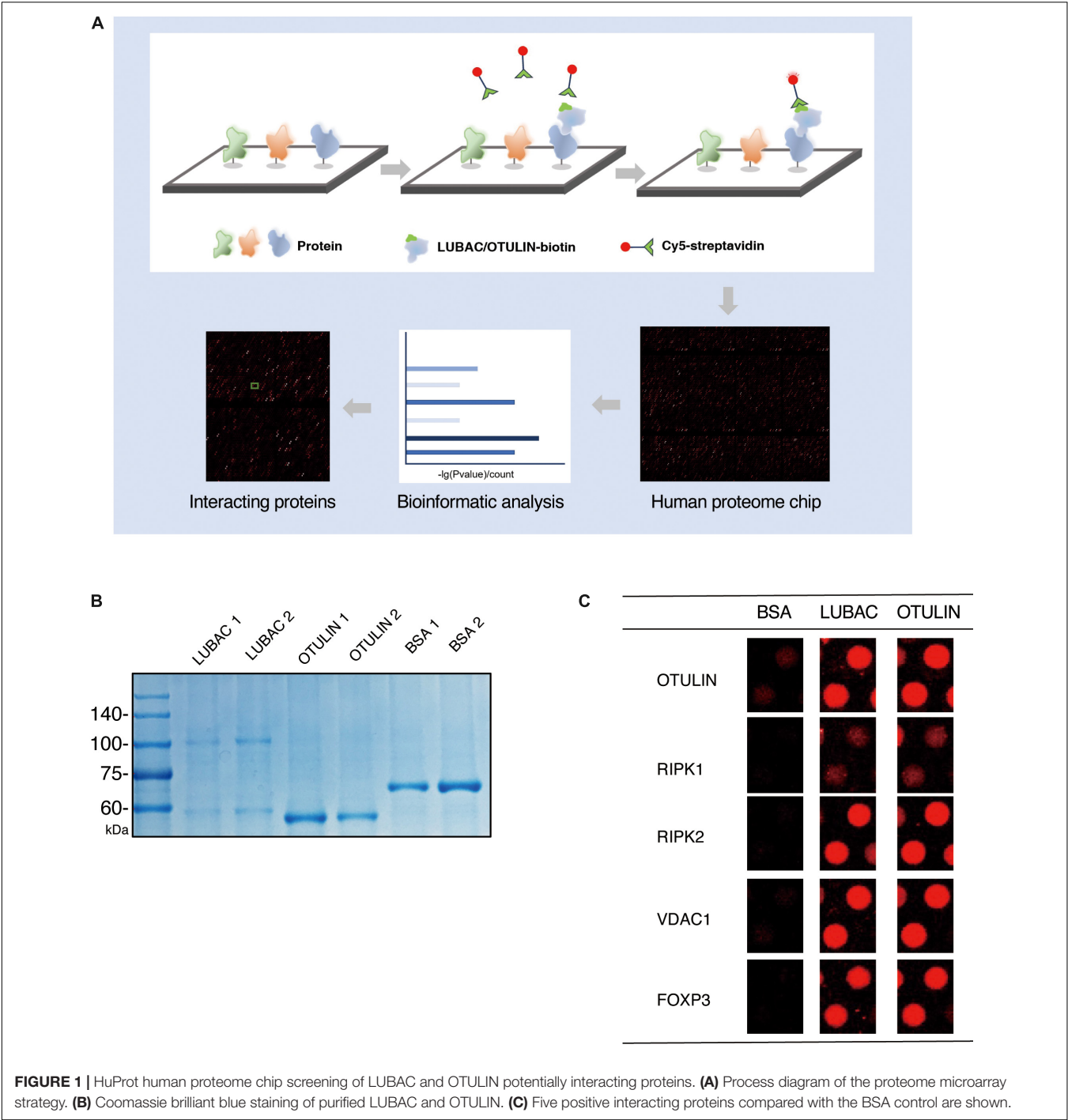


**FIGURE 1 |** HuProt human proteome chip screening of LUBAC and OTULIN potentially interacting proteins. **(A)** Process diagram of the proteome microarray strategy. **(B)** Coomassie brilliant blue staining of purified LUBAC and OTULIN. **(C)** Five positive interacting proteins compared with the BSA control are shown.

soluble cell lysate. Protein purity was confirmed by Coomassie brilliant blue staining (**Figure 1B**).

Using BSA as a negative control, the purified LUBAC and OTULIN proteins were labeled with biotin and then incubated with the proteome microarray (**Supplementary Figure S1**). Cy5-streptavidin was used to conjugate the biotin-labeled proteins, which directly interacted with the proteins in the microarray. After screening with the GenePix 4200B fluorescence microarray

scanner, GenePix Pro version 6.0 was used to analyze the fluorescence signal. To validate the reliability of this assay, the spots of several proteins reported to interact with LUBAC or OTULIN (RIPK1, RIPK2, FOXP3, VDAC1, and OTULIN) were picked (Haas et al., 2009; Fiil et al., 2013; Elliott et al., 2014; Schaeffer et al., 2014; Kliza et al., 2017; Zhu et al., 2018). As shown in **Figure 1C**, these spots showed strong signals compared to the BSA control. These results validated the effectiveness of the

human proteome microarray screening to detect the interactors of LUBAC and OTULIN.

## Verification of LUBAC and OTULIN Potential Interacting Proteins

To narrow the number of spots filtered from the microarrays, we used the criteria  $Z\text{-score} \geq 3$  and  $I_{\text{Mean\_Ratio}} \geq 1.4$ . These criteria were relatively stringent, and only 330 proteins for LUBAC and 376 proteins for OTULIN were identified from the 20,000 proteins in the microarray. Interestingly, 260 of these proteins were co-interactors of LUBAC and OTULIN (Table 1, Figure 2A and Supplementary Tables S1–S3). A heat map was drawn to rank and visualize the co-interactors using the pheatmap package in R (Figure 2B). To visualize the potential interactors, these proteins are shown in the scatter plot and distributed with  $I_{\text{Mean\_Ratio}}$  as well as  $Z\text{-score\_mean}$  (Figure 2C). We constructed expression vectors for several of the top-ranked proteins with Myc tags, and a co-immunoprecipitation (Co-IP) assay confirmed that SIRT5 and DDX6 interact with LUBAC and OTULIN (Figures 2D,E). ABI1 and ABI2 interact with HOIP, but not OTULIN (Figures 2F,G). SIRT3 and WWP2 did not interact with either HOIP or OTULIN (Figures 2H,I). These results also suggest that, although the protein microarray data appear reliable, they are a mixed bag and merit further validation.

## Bioinformatics Analysis of the Potential LUBAC and OTULIN Interacting Proteins

To gain further insight into the novel functions of LUBAC and OTULIN, we performed Gene Ontology (GO) enrichment analysis and pathway analysis with the shared interactors (Gene Ontology Consortium, 2004). We performed these analysis using the Database for Annotation, Visualization, and Integrated Discovery (Dennis et al., 2003).

Currently, our understanding of linear ubiquitination is mainly limited to inflammatory and immune signaling pathways. However, these pathways were not enriched in the top positions in our data. As shown in Figure 3A, the bar plot ranked the GO enrichment results in biology process (BP), cellular component (CC), and molecular function (MF). The results of the BP analysis showed that the potential interactors of LUBAC and OTULIN were enriched mainly in various metabolic processes and RNA processing. These results indicated that linear ubiquitination may have additional functions in the regulation of pre-translation level of proteins. For MF, the candidates were mostly classified into two groups: binding, including nucleic acid binding and nucleotide binding, and oxidoreductase activity. For CC, the candidates were enriched in the cytoplasm, membrane, and nucleus. These data showed that linear ubiquitination is involved in broad cellular biological processes, molecular functions, and interactions with proteins in different subcellular locations. To better visualize the GO enrichment results, we used the BiNGO plugin in Cytoscape to rebuild the enrichment results (Shannon et al., 2003; Maere et al., 2005). As shown in Figure 3B, the biology process is mainly clustered in metabolism, especially amino acid metabolism and catabolic process. The visualization of CC and MF is shown in Supplementary Figures S2B,C.

To further understand the signaling pathways of the LUBAC- and OTULIN-interacting proteins, we performed Kyoto Encyclopedia of Genes and Genomes pathway analysis (Kanehisa and Goto, 2000; Kanehisa, 2002), and the results were visualized by bubble chart in R. The interactors were predominantly enriched in 11 pathways, of which the top five were biosynthesis of amino acids, metabolic pathways, biosynthesis of antibiotics, RNA degradation, and carbon metabolism (Figure 3C).

Previously, our understanding of linear ubiquitination is subjected to immunity and inflammation, yet the ongoing research have uncovered the new functions in mitosis (Wu et al., 2019), viral infection (Zuo et al., 2020), protein quality control (Well et al., 2019), and regulation in diverse pathways. These data indicated that LUBAC, OTULIN, or linear ubiquitination may have broad functions beyond the present indications, which merit further exploration.

## LAG3 Harbors Linear Ubiquitination Mediated by HOIP

Previous evidence indicates that linear ubiquitination regulates T cell-mediated immunity, but the mechanism has been poorly elucidated (Ikeda, 2015; Shimizu et al., 2015). LAG3, an inhibitory lymphocyte receptor, was shown to be a potential interactor of LUBAC and OTULIN by our data. LAG3 is a type I transmembrane protein expressed on activated T cells and natural killer (NK) cells, consisting of four extracellular Ig-like domains (D1–D4) and several conserved motifs in the cytoplasmic segment (Triebel et al., 1990; Workman et al., 2002; Macon-Lemaître and Triebel, 2005; Andrews et al., 2017; Zhang et al., 2017; Wang et al., 2019). The conserved cytoplasmic segment is indispensable for the inhibitory function of LAG3, but the downstream regulators and effectors have not been clearly described.

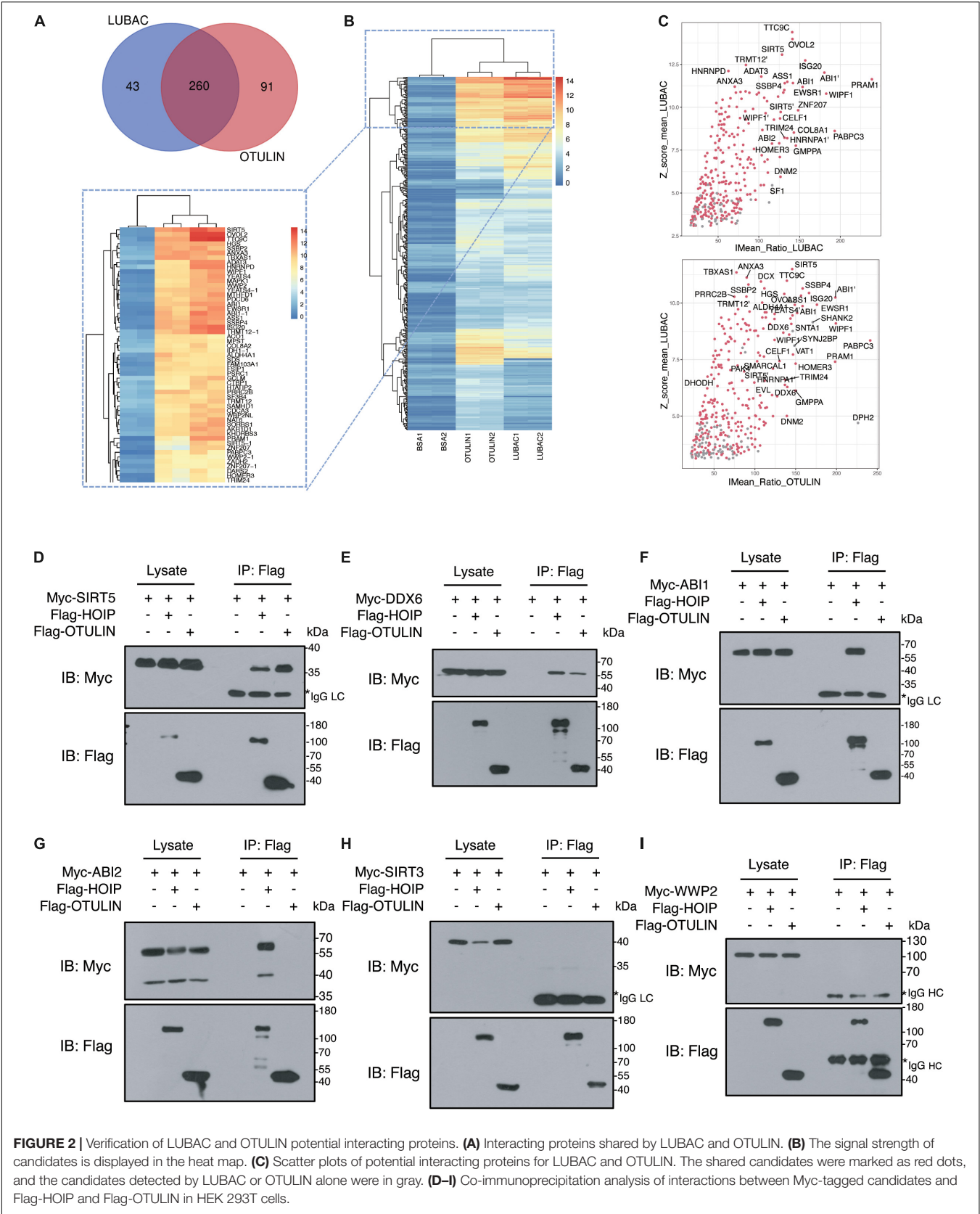
In our study, LAG3 was identified as a potential LUBAC and OTULIN interactor by comparing the signals with the negative BSA control (Figure 4A). To confirm the association of LAG3 with HOIP/OTULIN, exogenous co-immunoprecipitation and immunofluorescence assays were performed, which revealed that LAG3 interacts with HOIP/OTULIN in the cell (Figures 4B,C). Next, we sought to detect the linear ubiquitination of LAG3. Exogenous ubiquitination assays showed that HOIP coupled with HOIL-1L ubiquitinated LAG3, while the catalytically inactive HOIP mutant (HOIP-CS) did not ubiquitinate LAG3 (Figure 4D). In addition, overexpression of OTULIN greatly decreased the linear ubiquitination of LAG3 (Figure 4E).

LAG3 consists of five lysine residues, of which three are conserved (K356, K366, and K498). K498 is the only lysine residue in the cytoplasmic segment, and the KIEELE motif (498–503) is crucial for the inhibitory function of LAG3 (Workman et al., 2002). However, the K498R, 3KR (K356R/K366R/K498R), and LAG3-K0 mutations showed only a slight decline in linear ubiquitination (Figures 5A,B). Ubiquitination can be catalyzed at non-lysine residues, such as serine, threonine, or cysteine (Cadwell, 2005; McDowell and Philpott, 2013; Pao et al., 2018), and HOIL-1 can catalyze the formation of oxyester bonds between ubiquitin and serine or

**TABLE 1 |** The list of interacting proteins shared by LUBAC and OTULIN.

Protein	Protein (continued)	Protein (continued)	Protein (continued)	Protein (continued)
A1CF	CSTF2T	IGHG1	PAK4	SMARCE1
ABCA8	CTBP1	IGKC	PCBP4	SMPD1
ABI1	CTBP2	IRF2BP1	PDCD6	SOHLH2
ABI2	CUTA	IRF2BP2	PFKP	SORBS1
ACO1	CYB5R1	Irx5	PNKP	SORBS3
ACOT7	DARS2	ISCU	POGZ	SORD
ACSL6	DCX	ISG20	POP7	SOX6
ADAMTSL4	DDX6	ITPKB	PPP1R13L	SPATC1
ADAT3	DECR2	IVD	PRAM1	SPRR4
AKAP8	DHODH	KCNAB1	PRR30	SR1A
AKR1C3	DLG3	KCNAB2	PRR35	SRRT
AKR1D1	DNAL1	KDM1A	PRRC2B	SRXN1
ALDH16A1	DNM2	KHDRBS1	PSMB4	SSBP1
ALDH4A1	DOK1	KHDRBS3	PSRC1	SSBP2
ALKBH2	DTX2	KIF23	PTK2	SSBP4
ALKBH3	ECI2	KLHDC9	PUF60	STARD7
AMBRA1	EIF4G3	LAG3	PXK	STAU2
AMOTL2	EIF4H	LARS2	PYCR2	SULT1B1
ANGPTL2	ELAVL1	LNP	PYCRL	SULT1C2
ANXA3	ELAVL2	LOC105372481	QARS	TAF6
APTX	ELAVL4	LONP1	QKI	TAF9B
ARPC1B	ELN	LOR	RAB2B	TBXAS1
ARPC3	ENAH	MAGEB1	RAB5A	TCF7L1
ASS1	EVL	MAPK1	RAB5C	TIA1
ATIC	EWSR1	MAPK3	RALY	TK1
BAG6	F2	MBNL3	RBM12	TLE3
BC014212	FAAH2	MBP	RBM3	TMEM116
BC035666	FAM103A1	MCCC2	RBM42	TRIM24
BC047522.1	FAM120B	MCM7	RBM46	TRMT12
BCAR3	FAM49B	MIF	RBMS1	TRMT2A
BCS1L	FAM81A	MISP	RBMS2	TST
BLVRB	FKBP1A	MPST	RPL30	TTC9
BPHL	FOXP4	MSI2	RPLP0	TTC9C
C11orf1	FSCB	MTHFD1	RPP25	TTL1
C17orf82	FSIP1	NABP1	RTCA	TUFM
C1orf74	FUBP1	NAT6	RXRA	UNG
C1orf94	GAPDH	NCOA3	SAMD4B	VASP
C21orf59	GBGT1	NECAP2	SAMHD1	VAT1
C9orf9	GCLM	NFYC	SATB1	WBP2NL
CBLN4	GMPPA	NG_006966.3	SCEL	WIPF1
CCNB1IP1	GPT2	NME2	SDS	WWP2
CDCA3	GSTZ1	NTPCR	SF3B4	XAGE3
CELF1	GTF2B	NUDT16L1	SGK494	XDH
COASY	HCFC2	NUDT6	SH3GLB2	XPNPEP3
COL8A1	HGS	NUMBL	SHMT1	XRN2
COL8A2	HNRNPA1	NUPL2	SIRT3	YAP1
CPT1A	HNRNPC	ODAM	SIRT5	YEATS4
CRY2	HNRNPD	OLA1	SKIL	ZADH2
CRYZ	HOMER3	OPHN1	SLC25A16	ZFYVE1
CSNK1G1	HSPD1	OVOL2	SLC30A6	ZNF207
CSRP1	HTATIP2	PABPC3	SLFN5	ZNF385A
CSRP3	IDH1	PABPC4	SMARCA1	ZNF385B





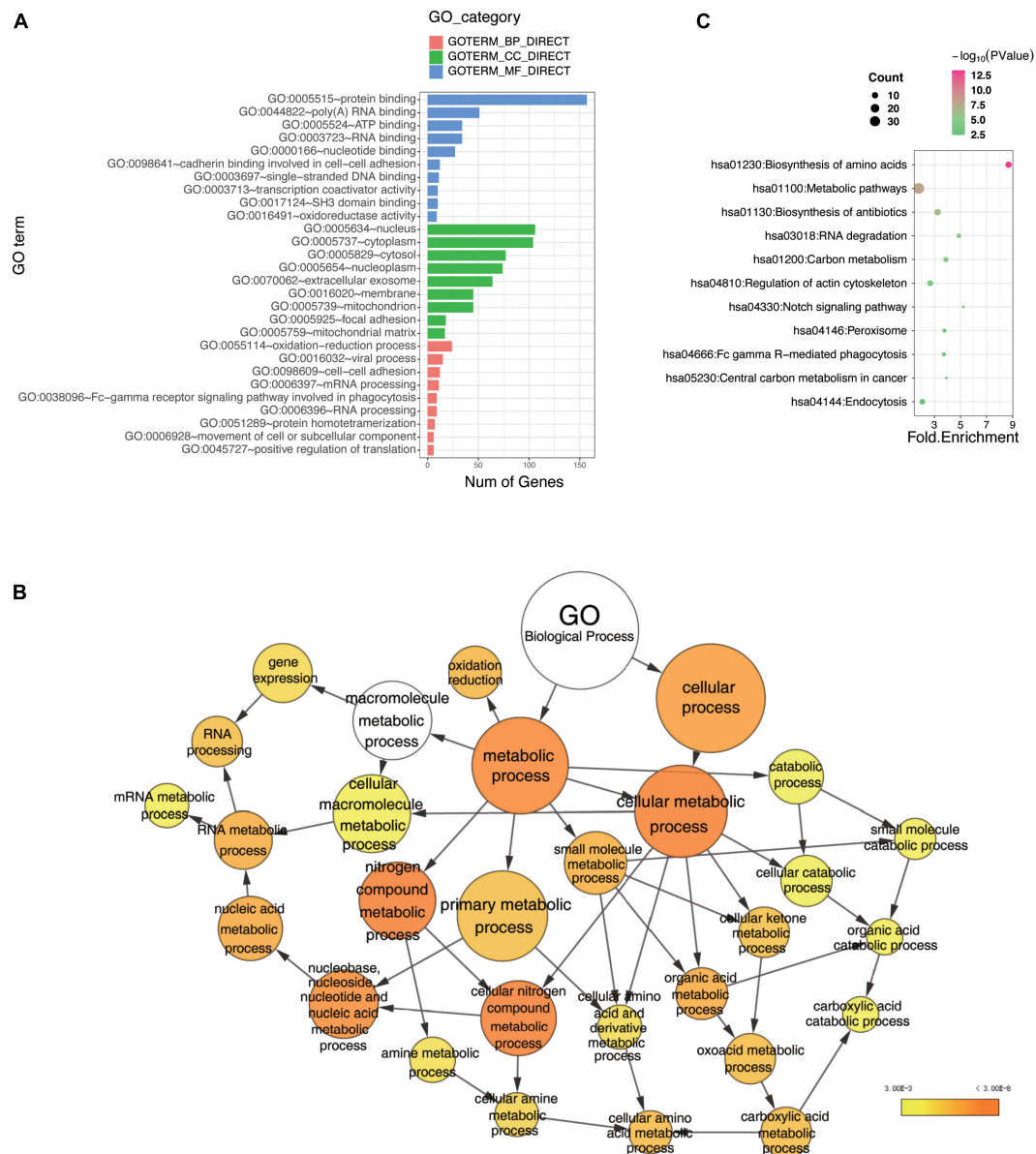
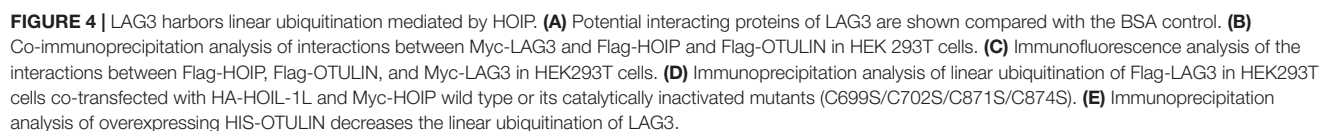


**FIGURE 3 |** Bioinformatics analysis of the LUBAC and OTULIN potential interacting proteins. **(A)** Gene Ontology (GO) analysis showed the enrichment of potential interacting proteins of LUBAC and OTULIN in terms of GO categories BP, MF, and CC. Clustering based on information provided by Database for Annotation, Visualization, and Integrated Discovery database and visualized by bar plot in R. **(B)** GO analysis showed the enrichment of potential interacting proteins in terms of GO categories BP. The node size represents the gene number in the category, while the color change from yellow to orange indicates the change in  $P$ -value from large to small values for the corresponding category. Categorizations are based on information using the BiNGO plugin in Cytoscape. **(C)** Enriched pathways of potential interacting proteins analyzed by Kyoto Encyclopedia of Genes and Genomes. The node size represents the gene number in the corresponding pathway, while the color change from red to green indicates the change in  $P$ -value from large to small values for the corresponding pathway. These results were visualized by bubble chart in R.

threonine in substrates (Kellsall et al., 2019; Fuseya et al., 2020). LAG3 contains two conserved serine residues (S484 and S497) in the intracytoplasmic tail, and previous results have indicated that phosphorylation is not involved in the inhibitory function of LAG3 (Bae et al., 2014). The ubiquitination assay showed that LAG3-K0-S484A and LAG3-K0-S497A mutations displayed obviously reduced linear ubiquitination compared with

the K0 mutation (**Figure 5B**). Furthermore, exogenous co-immunoprecipitation and immunofluorescence assays confirmed that LAG3 mutations (K0, K0-S484A, and K0-S497A) still interact with HOIP in the cell, and the mutations had not altered the cellular localization of LAG-3 (**Figures 5C,D**). K498 of the KIEELE motif is indispensable for the negative functions of LAG3, and S497 is adjacent to the KIEELE motif. Our results



The ubiquitin ligase complex LUBAC, composed of HOIP, HOIL-1L, and SHARPIN, generates linear (M1)-linked polyubiquitin chains. The deubiquitinase OTULIN specifically disassembles linear ubiquitin chains. Currently, linear ubiquitination is known to regulate TNF-RSC and NF- $\kappa$ B signaling pathways to maintain inflammation and immune homeostasis, but our understanding of linear ubiquitination is limited. Our results showed that LUBAC and OTULIN have a broad landscape of interacting proteins, hinting that linear

Linear ubiquitination is an important posttranslational modification that is involved in multiple biological processes.

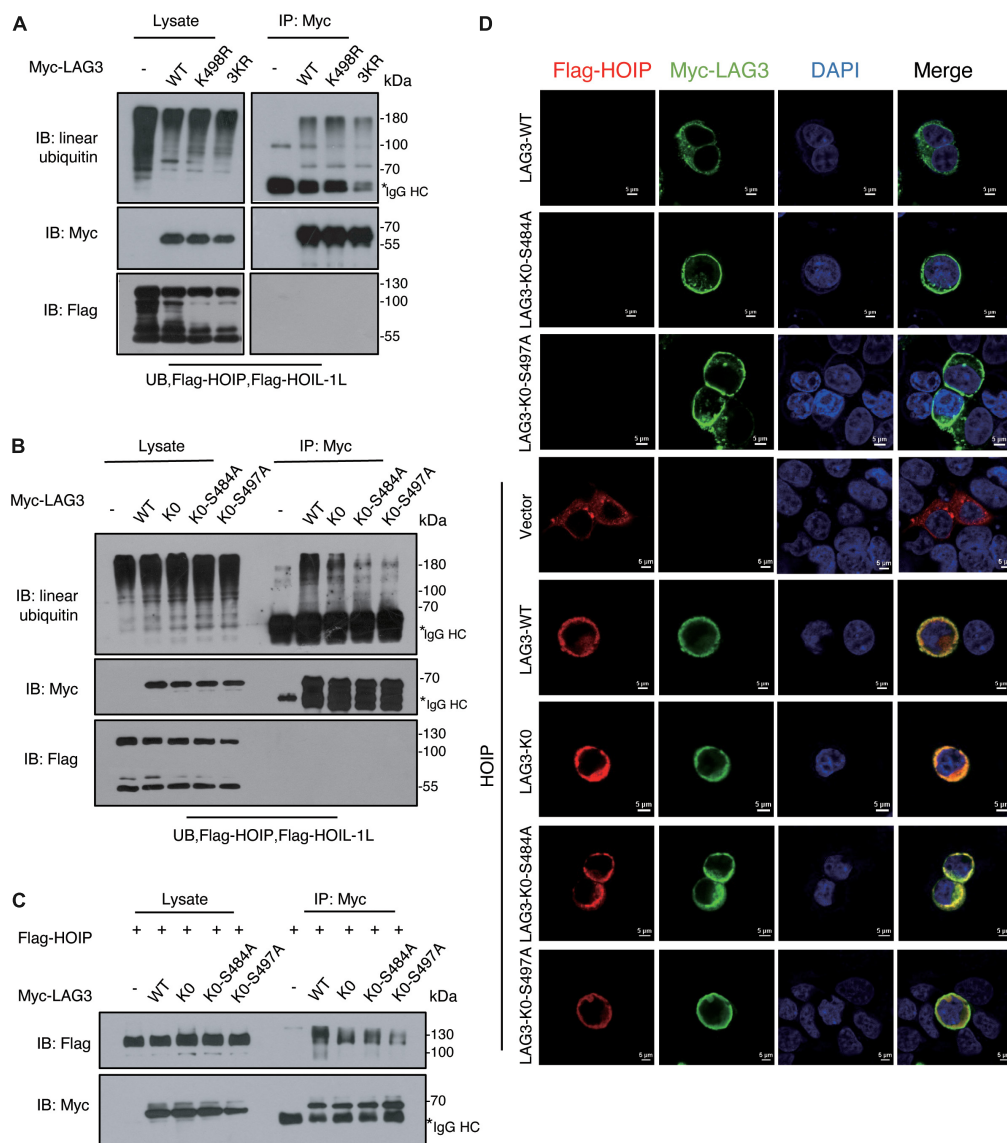


**FIGURE 5 |** LAG3 can be linear-ubiquitinated at multiple sites by LUBAC. **(A)** Immunoprecipitation analysis of LAG3 ubiquitination in HEK293T cells co-transfected with Myc-LAG3 wild type or its mutants K498R and 3KR (3KR = K356R, K357R, and K398R). **(B)** Immunoprecipitation analysis of LAG3 ubiquitination in HEK293T cells co-transfected with Flag-LAG3 wild type, KO, KO-S484A, and KO-S497A (KO = K21R/K297R/K356R/K366R/K498R). **(C)** Immunofluorescence analysis for the cellular location of LAG3 wild type and mutations, the interaction between Flag-HOIP and Myc-LAG3 wild type, and mutations in HEK293T cells. **(D)** Co-immunoprecipitation analysis of interactions between Myc-LAG3 wild type, mutations, and Flag-HOIP in HEK293T cells.

ubiquitination has additional functions beyond our present understanding.

The interactors of LUBAC and OTULIN were detected in the absence of a cellular model, circumventing the effects of the TNF and NF- $\kappa$ B signaling pathways in the cellular background. However, *in vitro* high-throughput microarray screening may be helpful to find new substrates and regulators of linear ubiquitination. Inevitably, the *in vitro* microarray assay neglects the subcellular location of the proteins, which has added to the false-positive ratio.

Using relatively stringent criteria, we identified 330 potential interacting proteins of LUBAC and 376 potential interacting

proteins of OTULIN, of which 260 were shared. We used co-immunoprecipitation to verify the interaction of these potential interacting proteins with HOIP and OTULIN. These results indicated that our protein microarray data were reliable, and the positive rate was satisfactory.

Bioinformatics analysis revealed that the candidate proteins were enriched in several novel pathways, such as metabolic pathways, RNA processing, and biosynthesis processing. These results also indicate new functions of linear ubiquitination for exploration.

Furthermore, we verified that LAG3 is a new substrate of linear ubiquitination mediated by LUBAC. LAG3 is



a transmembrane protein expressed on activated T cells and NK cells. LAG3 consists of conserved motifs in the cytoplasmic domain, which possesses two potential serine phosphorylation sites, “KIEELE” motif and “EP” repetitive motif. Interestingly, the LAG3 cytoplasmic motif does not have immunoreceptor tyrosine-based inhibition motifs or immunoreceptor tyrosine-based switch motifs, which are phosphorylation motifs found in many receptors that recruit tyrosine phosphatases to limit TCR signaling (Unkeless and Jin, 1997). Studies in recent years have suggested that LAG3 may have different regulatory mechanisms beyond phosphorylation. Our results suggest that the conserved KIEELE motif and the serine sites in the LAG3 intracellular segment can be ubiquitinated by LUBAC, indicating that ubiquitination, not phosphorylation, may be responsible for the inhibitory functions of LAG3. In addition, the role of linear ubiquitination in adaptive immunity has been poorly elucidated (Ikeda, 2015). The negative regulatory role of LAG3 in the T cell signaling pathway explains the phenotypes in the *Hoip*<sup>ΔCd4</sup>, *Hoil*<sup>ΔCd4</sup>, and *Cpdm* mice, which have a substantial reduction in the number of T cells and defective development and function of T cells (Park et al., 2016; Teh et al., 2016).

In summary, we have performed a global protein interaction screening of LUBAC and OTULIN using the human proteome microarray. Our results have broadened the LUBAC and OTULIN interactome and may serve as a valuable resource to explore new functions of linear ubiquitination.

## DATA AVAILABILITY STATEMENT

All the data that support the conclusions are presented in this paper. The raw data for the human proteome microarray are provided in **Supplementary Table 4**.

## AUTHOR CONTRIBUTIONS

LqZ and SW designed the research. LjZ and YG performed the research and wrote the manuscript. C-PC contributed to results

analysis and discussion. YF, BW, LL, and YZ contributed new reagents and to the discussion. All authors contributed to the article and approved the submitted version.

## FUNDING

This work was supported by the National Key Research and Development Project of China (2017YFA0505602) and the Project of State Key Laboratory of Proteomics (SKLP-K202001).

## ACKNOWLEDGMENTS

We thank Ms. Ping Wu from the Imaging Facility of the National Center for Protein Sciences Beijing for her assistance with microscopy imaging. We are also thankful to Huaying Bio (Shanghai) for providing the chips technical support.

## SUPPLEMENTARY MATERIAL

The Supplementary Material for this article can be found online at: <https://www.frontiersin.org/articles/10.3389/fcell.2021.686395/full#supplementary-material>

**Supplementary Figure 1** | The whole chip picture of BSA (A), HIS-LUBAC (B), and HIS-OTULIN (C).

**Supplementary Figure 2** | Gene Ontology (GO) analysis showed the enrichment of potential interacting proteins in terms of GO categories molecular function (A) and cellular component (B). The node size represents the gene number in the category, while the color change from yellow to orange indicates the change in *P*-value from large to small values for the corresponding category. The categorizations are based on information using the BINGO plugin in Cytoscape.

**Supplementary Table 1** | Detailed list of potential interacting proteins shared by LUBAC and OTULIN.

**Supplementary Table 2** | Detailed list of potential interacting proteins of LUBAC.

**Supplementary Table 3** | Detailed list of potential interacting proteins of OTULIN.

**Supplementary Table 4** | Raw data for human proteome microarray.

## REFERENCES

- Andrews, L. P., Marciscano, A. E., Drake, C. G., and Vignali, D. A. A. (2017). LAG3 (CD223) as a cancer immunotherapy target. *Immunol. Rev.* 276, 80–96. doi: 10.1111/imr.12519
- Bae, J., Lee, S. J., Park, C.-G., Lee, Y. S., and Chun, T. (2014). Trafficking of LAG-3 to the surface on activated T cells via its cytoplasmic domain and protein kinase c signaling. *J. Immunol.* 193, 3101–3112. doi: 10.4049/jimmunol.1401025
- Cadwell, K. (2005). Ubiquitination on nonlysine residues by a viral E3 ubiquitin ligase. *Science* 309, 127–130. doi: 10.1126/science.1110340
- Dennis, G., Sherman, B. T., Hosack, D. A., Yang, J., Gao, W., Lane, H. C., et al. (2003). DAVID: database for annotation, visualization, and integrated discovery. *Genome Biol.* 4:3.
- Eisenhaber, B., Chumak, N., Eisenhaber, F., and Hauser, M.-T. (2007). The ring between ring fingers (RBR) protein family. *Genome Biol.* 8:209. doi: 10.1186/gb-2007-8-3-209
- Elliott, P. R., Nielsen, S. V., Marco-Casanova, P., Fiil, B. K., Keusekotten, K., Mailand, N., et al. (2014). Molecular basis and regulation of OTULIN-LUBAC interaction. *Mol. Cell* 54, 335–348. doi: 10.1016/j.molcel.2014.03.018
- Fiil, B. K., Damgaard, R. B., Wagner, S. A., Keusekotten, K., Fritsch, M., Bekker-Jensen, S., et al. (2013). OTULIN restricts Met1-linked ubiquitination to control innate immune signaling. *Mol. Cell* 50, 818–830. doi: 10.1016/j.molcel.2013.06.004
- Fujita, H., Tokunaga, A., Shimizu, S., Whiting, A. L., Aguilar-Alonso, F., Takagi, K., et al. (2018). Cooperative domain formation by homologous motifs in HOIL-1L and SHARPIN plays a crucial role in LUBAC stabilization. *Cell Rep.* 23, 1192–1204. doi: 10.1016/j.celrep.2018.03.112
- Fuseya, Y., Fujita, H., Kim, M., Ohtake, F., Nishide, A., Sasaki, K., et al. (2020). The HOIL-1L ligase modulates immune signalling and cell death via monoubiquitination of LUBAC. *Nat. Cell Biol.* 22, 663–673. doi: 10.1038/s41556-020-0517-9
- Gene Ontology Consortium (2004). The Gene Ontology (GO) database and informatics resource. *Nucleic Acids Res.* 32, D258–D261. doi: 10.1093/nar/gkh036
- Gerlach, B., Cordier, S. M., Schmukle, A. C., Emmerich, C. H., Rieser, E., Haas, T. L., et al. (2011). Linear ubiquitination prevents inflammation and regulates immune signalling. *Nature* 471, 591–596. doi: 10.1038/nature09816

- Haas, T. L., Emmerich, C. H., Gerlach, B., Schmukle, A. C., Cordier, S. M., Rieser, E., et al. (2009). Recruitment of the linear ubiquitin chain assembly complex stabilizes the TNF-R1 signaling complex and is required for TNF-mediated gene induction. *Mol. Cell* 36, 831–844. doi: 10.1016/j.molcel.2009.10.013
- Heger, K., Wickliffe, K. E., Ndoja, A., Zhang, J., Murthy, A., Dugger, D. L., et al. (2018). OTULIN limits cell death and inflammation by deubiquitinating LUBAC. *Nature* 559, 120–124. doi: 10.1038/s41586-018-0256-2
- Hjerpe, R., Aillet, F., Lopitz-Otsoa, F., Lang, V., England, P., and Rodriguez, M. S. (2009). Efficient protection and isolation of ubiquitylated proteins using tandem ubiquitin-binding entities. *EMBO Rep.* 10, 1250–1258. doi: 10.1038/embor.2009.192
- Hogenesch, H., Gijbels, M. J., Offerman, E., van Hooft, J., van Bekkum, D. W., and Zurcher, C. (1993). A spontaneous mutation characterized by chronic proliferative dermatitis in C57BL mice. *Am. J. Pathol.* 143, 972–982.
- Ikedo, F. (2015). Linear ubiquitination signals in adaptive immune responses. *Immunol. Rev.* 266, 222–236. doi: 10.1111/imr.12300
- Ikedo, F., Deribe, Y. L., Skånland, S. S., Stieglitz, B., Grabbe, C., Franz-Wachtel, M., et al. (2011). SHARPIN forms a linear ubiquitin ligase complex regulating NF- $\kappa$ B activity and apoptosis. *Nature* 471, 637–641. doi: 10.1038/nature09814
- Iwai, K., and Tokunaga, F. (2009). Linear polyubiquitination: a new regulator of NF- $\kappa$ B activation. *EMBO Rep.* 10, 706–713. doi: 10.1038/embor.2009.144
- Kanehisa, M. (2002). The KEGG database. *Novartis Found Symp* 247, 91–101; discussion 101–103, 119–128, 244–252.
- Kanehisa, M., and Goto, S. (2000). KEGG: kyoto encyclopedia of genes and genomes. *Nucleic Acids Res.* 28, 27–30. doi: 10.1093/nar/28.1.27
- Kelsall, I. R., Zhang, J., Knebel, A., Arthur, J. S. C., and Cohen, P. (2019). The E3 ligase HOIL-1 C ester bond formation between ubiquitin and components of the Myddosome in mammalian cells. *Proc. Natl. Acad. Sci. U.S.A.* 116, 13293–13298. doi: 10.1073/pnas.1905873116
- Keusekotten, K., Elliott, P. R., Glöckner, L., Fiil, B. K., Damgaard, R. B., Kulathu, Y., et al. (2013). OTULIN antagonizes LUBAC signaling by specifically hydrolyzing Met1-linked polyubiquitin. *Cell* 153, 1312–1326. doi: 10.1016/j.cell.2013.05.014
- Kirisako, T., Kamei, K., Murata, S., Kato, M., Fukumoto, H., Kanie, M., et al. (2006). A ubiquitin ligase complex assembles linear polyubiquitin chains. *EMBO J.* 25, 4877–4887. doi: 10.1038/sj.emboj.7601360
- Kliza, K., Taumer, C., Pinzuti, I., Franz-Wachtel, M., Kunzelmann, S., Stieglitz, B., et al. (2017). Internally tagged ubiquitin: a tool to identify linear polyubiquitin-modified proteins by mass spectrometry. *Nat. Methods* 14, 504–512. doi: 10.1038/nmeth.4228
- Komander, D., and Rape, M. (2012). The ubiquitin code. *Annu. Rev. Biochem.* 81, 203–229. doi: 10.1146/annurev-biochem-060310-170328
- Macon-Lemaître, L., and Triebel, F. (2005). The negative regulatory function of the lymphocyte-activation gene-3 co-receptor (CD223) on human T cells. *Immunology* 115, 170–178. doi: 10.1111/j.1365-2567.2005.02145.x
- Maere, S., Heymans, K., and Kuiper, M. (2005). BiNGO: a Cytoscape plugin to assess overrepresentation of Gene Ontology categories in biological networks. *Bioinformatics* 21, 3448–3449. doi: 10.1093/bioinformatics/bti551
- McDowell, G. S., and Philpott, A. (2013). Non-canonical ubiquitylation: mechanisms and consequences. *Int. J. Biochem. Cell Biol.* 45, 1833–1842. doi: 10.1016/j.biocel.2013.05.026
- Niu, J., Shi, Y., Iwai, K., and Wu, Z.-H. (2011). LUBAC regulates NF- $\kappa$ B activation upon genotoxic stress by promoting linear ubiquitination of NEMO: NEMO linear ubiquitination upon genotoxic stress. *EMBO J.* 30, 3741–3753. doi: 10.1038/emboj.2011.264
- Pao, K.-C., Wood, N. T., Knebel, A., Rafie, K., Stanley, M., Mabbitt, P. D., et al. (2018). Activity-based E3 ligase profiling uncovers an E3 ligase with esterification activity. *Nature* 556, 381–385. doi: 10.1038/s41586-018-0026-1
- Park, Y., Jin, H., Lopez, J., Lee, J., Liao, L., Elly, C., et al. (2016). SHARPIN controls regulatory T cells by negatively modulating the T cell antigen receptor complex. *Nat. Immunol.* 17, 286–296. doi: 10.1038/ni.3352
- Peltzer, N., Darding, M., Montinaro, A., Draber, P., Draberova, H., Kupka, S., et al. (2018). LUBAC is essential for embryogenesis by preventing cell death and enabling haematopoiesis. *Nature* 557, 112–117. doi: 10.1038/s41586-018-0064-8
- Peltzer, N., Rieser, E., Taraborrelli, L., Draber, P., Darding, M., Pernaute, B., et al. (2014). HOIP deficiency causes embryonic lethality by aberrant TNFR1-mediated endothelial cell death. *Cell Rep.* 9, 153–165. doi: 10.1016/j.celrep.2014.08.066
- Schaeffer, V., Akutsu, M., Olma, M. H., Gomes, L. C., Kawasaki, M., and Dikic, I. (2014). Binding of OTULIN to the PUB domain of HOIP Controls NF- $\kappa$ B signaling. *Mol. Cell* 54, 349–361. doi: 10.1016/j.molcel.2014.03.016
- Seymour, R. E., Hasham, M. G., Cox, G. A., Shultz, L. D., Hogenesch, H., Roopenian, D. C., et al. (2007). Spontaneous mutations in the mouse Sharpin gene result in multiorgan inflammation, immune system dysregulation and dermatitis. *Genes Immun.* 8, 416–421. doi: 10.1038/sj.gene.6364403
- Shannon, P., Markiel, A., Ozier, O., Baliga, N. S., Wang, J. T., Ramage, D., et al. (2003). Cytoscape: a software environment for integrated models of biomolecular interaction networks. *Genome Res.* 13, 2498–2504. doi: 10.1101/gr.1239303
- Shimizu, Y., Okuda-Shimizu, Y., and Hendershot, L. M. (2010). Ubiquitylation of an ERAD substrate occurs on multiple types of amino acids. *Mol. Cell* 40, 917–926. doi: 10.1016/j.molcel.2010.11.033
- Shimizu, Y., Taraborrelli, L., and Walczak, H. (2015). Linear ubiquitination in immunity. *Immunol. Rev.* 266, 190–207. doi: 10.1111/imr.12309
- Sjöberg, R., Mattsson, C., Andersson, E., Hellström, C., Uhlen, M., Schwenk, J. M., et al. (2016). Exploration of high-density protein microarrays for antibody validation and autoimmunity profiling. *N. Biotechnol.* 33, 582–592. doi: 10.1016/j.nbt.2015.09.002
- Smit, J. J., Monteferrario, D., Noordermeer, S. M., van Dijk, W. J., van der Reijden, B. A., and Sixma, T. K. (2012). The E3 ligase HOIP specifies linear ubiquitin chain assembly through its RING-IBR-RING domain and the unique LDD extension: HOIP RBR-LDD module specifies linear ubiquitin chains. *EMBO J.* 31, 3833–3844. doi: 10.1038/emboj.2012.217
- Spit, M., Rieser, E., and Walczak, H. (2019). Linear ubiquitination at a glance. *J. Cell Sci.* 132:jcs.208512. doi: 10.1242/jcs.208512
- Swatek, K. N., and Komander, D. (2016). Ubiquitin modifications. *Cell Res.* 26, 399–422. doi: 10.1038/cr.2016.39
- Teh, C. E., Lalaoui, N., Jain, R., Policheni, A. N., Heinlein, M., Alvarez-Diaz, S., et al. (2016). Linear ubiquitin chain assembly complex coordinates late thymic T-cell differentiation and regulatory T-cell homeostasis. *Nat. Commun.* 7:13353. doi: 10.1038/ncomms13353
- Tokunaga, F., Nakagawa, T., Nakahara, M., Saeki, Y., Taniguchi, M., Sakata, S., et al. (2011). SHARPIN is a component of the NF- $\kappa$ B-activating linear ubiquitin chain assembly complex. *Nature* 471, 633–636. doi: 10.1038/nature09815
- Tokunaga, F., Sakata, S., Saeki, Y., Satomi, Y., Kirisako, T., Kamei, K., et al. (2009). Involvement of linear polyubiquitylation of NEMO in NF- $\kappa$ B activation. *Nat. Cell Biol.* 11, 123–132. doi: 10.1038/ncb1821
- Triebel, F., Jitsukawa, S., Baixeras, E., Roman-Roman, S., Genevée, C., Viegas-Pequignot, E., et al. (1990). LAG-3, a novel lymphocyte activation gene closely related to CD4. *J. Exp. Med.* 171, 1393–1405. doi: 10.1084/jem.171.5.1393
- Unkles, J. C., and Jin, J. (1997). Inhibitory receptors, ITIM sequences and phosphatases. *Curr. Opin. Immunol.* 9, 338–343. doi: 10.1016/s0952-7915(97)80079-9
- Wang, J., Sanmamed, M. F., Datar, I., Su, T. T., Ji, L., Sun, J., et al. (2019). Fibrinogen-like protein 1 is a major immune inhibitory ligand of LAG-3. *Cell* 176, 334.e–347.e. doi: 10.1016/j.cell.2018.11.010 334-347.e12,
- Wang, Y.-J., Bian, Y., Luo, J., Lu, M., Xiong, Y., Guo, S.-Y., et al. (2017). Cholesterol and fatty acids regulate cysteine ubiquitylation of ACAT2 through competitive oxidation. *Nat. Cell Biol.* 19, 808–819. doi: 10.1038/ncb3551
- Well, E. M., Bader, V., Patra, M., Sánchez-Vicente, A., Meschede, J., Furthmann, N., et al. (2019). A protein quality control pathway regulated by linear ubiquitination. *EMBO J.* 38:e100730. doi: 10.15252/emboj.2018100730
- Workman, C. J., Dugger, K. J., and Vignali, D. A. A. (2002). Cutting edge: molecular analysis of the negative regulatory function of lymphocyte activation gene-3. *J. Immunol.* 169, 5392–5395. doi: 10.4049/jimmunol.169.10.5392
- Wu, M., Chang, Y., Hu, H., Mu, R., Zhang, Y., Qin, X., et al. (2019). LUBAC controls chromosome alignment by targeting CENP-E to attached kinetochores. *Nat. Commun.* 10:273. doi: 10.1038/s41467-018-08043-7
- Yagi, H., Ishimoto, K., Hiromoto, T., Fujita, H., Mizushima, T., Uekusa, Y., et al. (2012). A non-canonical UBA–UBL interaction forms the linear-ubiquitin-chain assembly complex. *EMBO Rep.* 13, 462–468. doi: 10.1038/embor.2012.24

- Zhang, Q., Chikina, M., Szymczak-Workman, A. L., Horne, W., Kolls, J. K., Vignali, K. M., et al. (2017). LAG3 limits regulatory T cell proliferation and function in autoimmune diabetes. *Sci. Immunol.* 2:eah4569. doi: 10.1126/sciimmunol.aah4569
- Zhu, F., Yi, G., Liu, X., Zhu, F., Zhao, A., Wang, A., et al. (2018). Ring finger protein 31-mediated atypical ubiquitination stabilizes forkhead box P3 and thereby stimulates regulatory T-cell function. *J. Biol. Chem.* 293, 20099–20111. doi: 10.1074/jbc.RA118.005802
- Zuo, Y., Feng, Q., Jin, L., Huang, F., Miao, Y., Liu, J., et al. (2020). Regulation of the linear ubiquitination of STAT1 controls antiviral interferon signaling. *Nat. Commun.* 11:1146. doi: 10.1038/s41467-020-14948-z

**Conflict of Interest:** The authors declare that the research was conducted in the absence of any commercial or financial relationships that could be construed as a potential conflict of interest.

Copyright © 2021 Zhou, Ge, Fu, Wu, Zhang, Li, Cui, Wang and Zhang. This is an open-access article distributed under the terms of the Creative Commons Attribution License (CC BY). The use, distribution or reproduction in other forums is permitted, provided the original author(s) and the copyright owner(s) are credited and that the original publication in this journal is cited, in accordance with accepted academic practice. No use, distribution or reproduction is permitted which does not comply with these terms.



# Ubiquitination-Dependent Regulation of Small GTPases in Membrane Trafficking: From Cell Biology to Human Diseases

Zehui Lei<sup>1,2†</sup>, Jing Wang<sup>1†</sup>, Lingqiang Zhang<sup>3\*</sup> and Cui Hua Liu<sup>1,2\*</sup>

<sup>1</sup> CAS Key Laboratory of Pathogenic Microbiology and Immunology, Institute of Microbiology, Center for Biosafety Mega-Science, Chinese Academy of Sciences, Beijing, China, <sup>2</sup> Savaid Medical School, University of Chinese Academy of Sciences, Beijing, China, <sup>3</sup> State Key Laboratory of Proteomics, Beijing Proteome Research Center, National Center for Protein Sciences (Beijing), Beijing Institute of Lifeomics, Beijing, China

## OPEN ACCESS

### Edited by:

Hongmin Qin,  
Texas A&M University, United States

### Reviewed by:

Christopher Stroupe,  
Stroupe.net, United States  
Yusong Guo,  
Hong Kong University of Science  
and Technology, Hong Kong

### \*Correspondence:

Cui Hua Liu  
liucuihua@im.ac.cn  
Lingqiang Zhang  
zhanglq@nic.bmi.ac.cn

<sup>†</sup> These authors have contributed  
equally to this work

### Specialty section:

This article was submitted to  
Cell Growth and Division,  
a section of the journal  
Frontiers in Cell and Developmental  
Biology

**Received:** 30 March 2021

**Accepted:** 09 June 2021

**Published:** 01 July 2021

### Citation:

Lei Z, Wang J, Zhang L and  
Liu CH (2021)  
Ubiquitination-Dependent Regulation  
of Small GTPases in Membrane  
Trafficking: From Cell Biology  
to Human Diseases.  
Front. Cell Dev. Biol. 9:688352.  
doi: 10.3389/fcell.2021.688352

Membrane trafficking is critical for cellular homeostasis, which is mainly carried out by small GTPases, a class of proteins functioning in vesicle budding, transport, tethering and fusion processes. The accurate and organized membrane trafficking relies on the proper regulation of small GTPases, which involves the conversion between GTP- and GDP-bound small GTPases mediated by guanine nucleotide exchange factors (GEFs) and GTPase-activating proteins (GAPs). Emerging evidence indicates that post-translational modifications (PTMs) of small GTPases, especially ubiquitination, play an important role in the spatio-temporal regulation of small GTPases, and the dysregulation of small GTPase ubiquitination can result in multiple human diseases. In this review, we introduce small GTPases-mediated membrane trafficking pathways and the biological processes of ubiquitination-dependent regulation of small GTPases, including the regulation of small GTPase stability, activity and localization. We then discuss the dysregulation of small GTPase ubiquitination and the associated human membrane trafficking-related diseases, focusing on the neurological diseases and infections. An in-depth understanding of the molecular mechanisms by which ubiquitination regulates small GTPases can provide novel insights into the membrane trafficking process, which knowledge is valuable for the development of more effective and specific therapeutics for membrane trafficking-related human diseases.

**Keywords:** small GTPase, ubiquitination, membrane trafficking, neurological diseases, infections

## INTRODUCTION

Membrane trafficking along with the endocytic, exocytic and autophagic pathways ensures the flow of membranes and cargoes (which contain proteins, nutrients or other molecules) between different compartments within cells, and thus plays a critical role in cellular homeostasis. These complex membrane trafficking events are mostly regulated by small GTPases, which are divided into five families: Ras sarcoma (Ras), Ras homologous (Rho), Ras-like proteins in brain (Rab), ADP-ribosylation factor (Arf), and Ras-like nuclear (Ran) proteins (Wennerberg et al., 2005). The Rab family comprises approximately 60 members that are localized on distinct membranes



(Wandinger-Ness and Zerial, 2014), and these proteins are the master modulators of membrane trafficking pathways (Pfeffer, 2017). The Arf and Arf-like (Arl) families also play a critical role in membrane trafficking along with the endocytic and exocytic pathways (Gillingham and Munro, 2007; Donaldson and Jackson, 2011; Yu and Lee, 2017; Kjos et al., 2018). Moreover, recent studies have demonstrated that the Rho as well as Ras families are also involved in membrane trafficking-related processes. For instance, Rho GTPases are required for the endocytic and exocytic pathways (Olayioye et al., 2019), while Ras GTPases mainly function in exocytic and autophagic pathways (Simicek et al., 2013; Nishida-Fukuda, 2019).

The basis of small GTPases to exert their functions is the conversion between GDP- and GTP-bound forms catalyzed by guanine nucleotide exchange factors (GEFs) and GTPase-activating proteins (GAPs) (Stenmark, 2009). Generally, GTP-bound form is considered to be the active state of GTPase, which can recruit specific effectors to regulate cellular activities, while GDP-bound form is the inactive state of GTPase that is usually restricted in the cytosol till being activated. Furthermore, increasing studies have shed light on the role of post-translational modifications (PTMs), mainly including phosphorylation, ubiquitination and prenylation, in the regulation of small GTPases (Ahearn et al., 2011; Hodge and Ridley, 2016; Shinde and Maddika, 2018). Among these modifications, ubiquitination is a highly conserved multistep enzymatic process catalyzed by ubiquitin-activating enzymes (E1s), ubiquitin-conjugating enzymes (E2s), and ubiquitin-ligase enzymes (E3s) sequentially, ultimately resulting in the attachment of single ubiquitin or multiple ubiquitin chains to target proteins. Ubiquitination is a critical signal to determine the stability, activity and localization of substrates, and thus is essential for regulating physiological functions of the substrates (Foot et al., 2017). Consistently, ubiquitination is critical for the spatio-temporal regulation of small GTPases, and this ubiquitination-dependent modulation is correlated with multiple human diseases (Qiu et al., 2016; Escamilla et al., 2017).

Here, we first provide an overview of small GTPases involved in membrane trafficking pathways. Then, we introduce the current knowledge on ubiquitination-dependent regulation of small GTPases. We also discuss human diseases associated with the dysregulation of small GTPase ubiquitination with a focus on neurological and infectious diseases. A better understanding of the ubiquitination-mediated regulation of small GTPases and its specific effects on membrane trafficking-related diseases will provide new insights into the therapeutics for these diseases.

## SMALL GTPASES IN MEMBRANE TRAFFICKING PATHWAYS

Membrane trafficking-mediated protein and membrane transport ensures the proceeding of endocytic, exocytic and autophagic pathways. Small GTPases, including Rab, Arf, Rho, and Ras families, play crucial roles in the membrane trafficking along with these pathways (Figure 1).

## Small GTPases in Endocytic Pathway

Small GTPases control the orderly proceeding of the trafficking steps involved in the endocytic pathway, which involves the following four steps: formation of endocytic vesicles via membrane internalization, trafficking of endocytic vesicles to early endosomes, trafficking of early endosomes to lysosomes, as well as trafficking of endosomes to the recycling compartments (Elkin et al., 2016).

### Membrane Internalization Step

Small GTPases are involved in the three modes of membrane internalization, including phagocytosis, pinocytosis and receptor-mediated endocytosis. Phagocytosis and pinocytosis are actin-dependent endocytic pathways and are mainly mediated by Rho as well as Rab GTPases, which have been summarized in elegant reviews (Hall, 2012; Egami, 2016). In addition, Ras can promote the translocation of vacuolar ATPase (V-ATPase) from intracellular membranes to the plasma membrane, followed by the stimulation of membrane ruffling and the occurrence of pinocytosis (Ramirez et al., 2019).

Clathrin-mediated endocytosis (CME) and clathrin-independent endocytosis (CIE) are routes of receptor-mediated endocytosis, and are mainly modulated by Rab and Arf GTPases, respectively. Specifically, Rab5 promotes the CME of transferrin receptor (TfR) (Stenmark et al., 1994), while Rab15 reduces the rate of TfR internalization, which may be caused by the decreased vesicle budding from the plasma membrane (Zuk and Elferink, 1999). Rab14 mediates the CME of the urea transporter A1 (UT-A1) (Su et al., 2013), and Rab5, Rab7, and Rab11 are required for virus intake through CME pathway (Shi et al., 2016; Liu et al., 2017). Additionally, the small GTPase Arf6, which is located at the cell surface in an active state to promote phospholipid metabolism, is the main modulator of CIE process (D'Souza-Schorey and Chavrier, 2006). Furthermore, Rab35 is involved in the communication and coordination between CME and CIE. The inhibition of CME shifts the sorting of CIE cargo proteins to lysosomes for degradation, and Rab35 can rescue the altered trafficking by recruiting the Arf6 GAP protein ACAP2 [Arf GAP, with Coil, ankyrin (ANK) repeat, pleckstrin homology (PH) domain protein 2] to inactivate Arf6 (Kobayashi and Fukuda, 2012; Dutta and Donaldson, 2015).

### Trafficking of Endocytic Vesicles to Early Endosomes

Upon internalization, the endocytic vesicles are transported to fuse with early endosomes, and are then sorted to decide their final fates (Huotari and Helenius, 2011). Since Rab5 and Rab23 are localized on both plasma membrane and early endosomes, they can mediate the trafficking of components between these two compartments by recruiting numerous effector proteins (Evans et al., 2003; Wandinger-Ness and Zerial, 2014). Besides Rab GTPases, Rho GTPases (such as RhoB, RhoD, and Rac1) that are located on the early endosomes, are also reported to be involved in cargoes transport to early endosomes (Olayioye et al., 2019). The identification of Rho effectors at the specific sites will

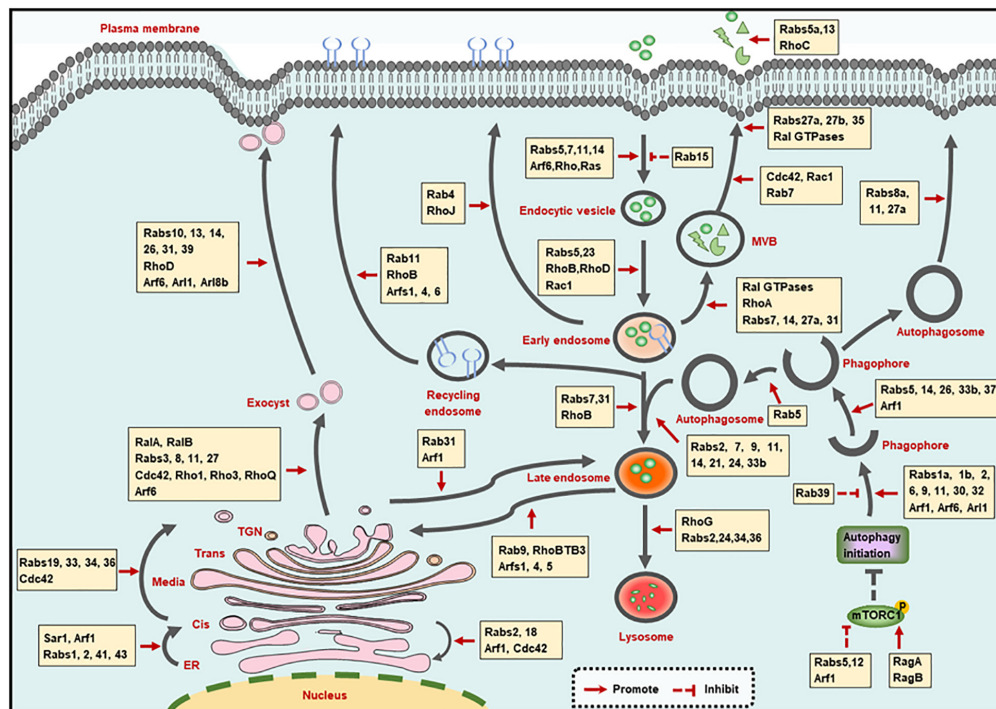


**FIGURE 1 |** Small GTPases in membrane trafficking pathways. The illustration shows the main intracellular membrane trafficking pathways including endocytic, exocytic, and autophagic pathways regulated by small GTPases. TGN: trans-Golgi network; ER, endoplasmic reticulum; MVB, multivesicular bodies.

extend our knowledge regarding the function of Rho GTPases in trafficking of endocytic vesicles to early endosomes.

## Trafficking of Early Endosomes to Lysosomes

The trafficking of early endosomes to lysosomes is tightly regulated by the transition of Rab5-to-Rab7 and Rab7-to-Arl8b. For the transition of early to late endosomes, Rab5 can recruit the Mon1/Ccz1 protein complex to promote Rab7 activation. Meanwhile, Rab5 GEF was removed by the Mon1/Ccz1 complex, resulting in the transition of Rab5-positive early endosome to Rab7-positive late endosomes (Poteryaev et al., 2010; Langemeyer et al., 2020). Consecutively, Rab7 is inactivated by Arl8b effector SKIP and is then removed from hybrid Rab7/Arl8b endosomes, leading to an ordered Rab7-to-Arl8b handover, followed by the fusion of late endosomes with lysosomes (Jongsma et al., 2020). Moreover, some other GTPases also participate in the early endosome to lysosomal transport. Rab31 and RhoB are required for the transition of early to late endosomes (Huang et al., 2007; Chua and Tang, 2014). Rab2 (Lund et al., 2018), Rab24 (Amaya et al., 2016), Rab34 (Wang and Hong, 2002), Rab36 (Chen et al., 2010), and RhoG (Vignal et al., 2001) are involved in the fusion of late endosomes with lysosomes.

Additionally, during the maturation process from early to late endosomes, multivesicular bodies (MVBs) are generated and then fused with plasma membrane for secretion, leading to the formation of exosomes. Various of small GTPases have been implicated in exosome biogenesis and secretion. Specifically,

Ras-related (Ral) proteins (Hyenne et al., 2015), Rab7, Rab27a (Dorayappan et al., 2018), and RhoA (Li et al., 2012) contribute to the formation of MVBs; Rab31 drives MVB formation but suppresses their degradation simultaneously (Wei et al., 2021); Rab14 positively modulates the MVB diameter and number (Maziveyi et al., 2019). Additionally, Cdc42 and Rac1 promote MVB maturation (Kajimoto et al., 2018); and Rab7 mediates the transportation of MVBs (Sun et al., 2020). Moreover, Rab27a, 27b (Ostrowski et al., 2010), Rab35 (Hsu et al., 2010), and Ral GTPases (Pathak and Dermardirossian, 2013) function in the attachment of MVBs to the plasma membrane. Finally, Rab5a (Gorji-Bahri et al., 2021), Rab13 (Hinger et al., 2020), and RhoC (Hu et al., 2020) promote the secretion of exosomes.

## Trafficking of Endosomes to the Recycling Compartments

Endocytic vesicles from early endosomes and late endosomes can also be recycled to the plasma membrane and the trans-Golgi network (TGN), respectively. Basically, endocytic vesicles sorting from early endosomes can be recycled back to the plasma membrane by a fast or a slow route. Rab4 and Rab11 are the major regulators of the fast- and slow- recycling pathways, respectively (Wandinger-Ness and Zerial, 2014). Moreover, RhoB and RhoJ in Rho family GTPases, as well as Arf1, Arf4, and Arf6 in Arf family GTPases, are also involved in the recycling pathway from endosomes to the plasma membrane (de Toledo et al., 2003; Huang et al., 2011; Kondo et al., 2012; Grossmann et al., 2019). Significantly, the recycling pathways mediated

by multiple GTPases are often crossing with each other. For instance, the Rab-to-Arf and Arf-to-Rab regulatory cascades have been reported. On the one hand, Rab10 recruits its effector CNT-1 (homolog of ACAP1/2 in *Caenorhabditis elegans*), which is also the GAP of Arf6, to suppress Arf6 activity, leading to the inhibition of membrane bending and membrane fission (Shi et al., 2012). On the other hand, the activated Arf6 can interact with the Rab35 GAP TBC1D10 to decrease Rab35 activity (Chesneau et al., 2012). These cascades ensure the ordered proceeding of complicated trafficking pathways.

Besides recycling to the plasma membrane, vesicles can also be sent to the TGN via the retrograde trafficking pathway from late endosomes. Rab9 that is located on the TGN and late endosomes mediates the recycling of mannose-6-phosphate receptors (MPRs) from late endosomes to TGN (Riederer et al., 1994; Kucera et al., 2016). And through interacting with Rab9, the atypical Rho GTPase family member RhoBTB3 is also involved in the retrograde trafficking pathway (Espinosa et al., 2009). Additionally, Arf, and Arl proteins, encompassing Arf1, Arf4, and Arl5, also contribute to endosome-to-TGN trafficking by recruiting different effectors (Nakai et al., 2013; Rosa-Ferreira et al., 2015).

## Small GTPases in Exocytic Pathway

The exocytic pathway involves the transporting between a series of membrane bound organelles, mainly including the transport from endoplasmic reticulum (ER) to Golgi, the transport within Golgi, the transport from Golgi to the cell surface, as well as transport from Golgi to the endocytic compartment. This dynamic and organized process transfers the synthesized proteins or other molecules into the cell surface or lysosomes in a small GTPase-dependent manner (Beraud-Dufour and Balch, 2002; Wu and Guo, 2015).

## ER-to-Golgi Transport

Upon being synthesized at the ER, proteins or other molecules need to exit from the ER and are then transferred to ER-Golgi intermediate compartment (ERGIC) and Golgi for further selection and transportation. The coat protein complex II (COPII) vesicles contribute to the ER exit, and small GTPase secretion-associated Ras-related 1 (Sar1) is required for the assembly of COPII vesicles (Nakano and Muramatsu, 1989). The assembled vesicles are then transported to ERGIC or Golgi. During this process, Rab1 cooperates with the tethering factors, and soluble NSF attachment protein receptor (SNARE) to promote the COPII vesicles transport to and fuse with Golgi (Allan et al., 2000; Moyer et al., 2001). Rabs2, 41, and 43 are also needed for rapid ER-to-Golgi trafficking (Dejgaard et al., 2008; Brandizzi and Barlowe, 2013; Liu et al., 2013; Li et al., 2017). Moreover, Arf1, which is primarily localized to the Golgi complex, is involved in the translocation of stimulator of interferon genes (STING) and soluble VEGFR-1 from ER to ERGIC or Golgi (Jung et al., 2012; Gui et al., 2019).

Once COPII vesicles are transported to Golgi, ER receptors and other ER proteins carrying a Lys-Asp-Glu-Leu (KDEL) motif are returned back to the ER through the COPI-mediated retrograde transport. This process is largely regulated by Arf1,

since the recruitment of COPI is relied on the activated Arf1 (Serafini et al., 1991). Rab2, Rab18, and Cdc42 are also the modulators of the trafficking from Golgi to ER (Luna et al., 2002; Dejgaard et al., 2008; Brandizzi and Barlowe, 2013). It is worth mentioning that Rab2 and Arf1 mediate the bi-directional ER-Golgi trafficking, which may be achieved by recruiting different effectors at the specific stage.

## Intra-Golgi Transport

The Golgi complex is composed of cis-, medial-, trans-cisternal, and the TGN. After entering the Golgi, proteins or other molecules are transported from the cis face to the TGN (intra-Golgi transport), and are then sorted to determine their final destination (Boncompain and Weigel, 2018). Rab19, Rab33, Rab34, and Rab36 are localized to the distinct compartments of Golgi, and may be involved in the anterograde transport of intra-Golgi, while Rab6 is a key determinant of retrograde trafficking in Golgi (Galea and Simpson, 2015). Of note, Rho family GTPase Cdc42 can modulate bi-directional Golgi transport by targeting the dual functions of COPI vesicles, and this effect is controlled by environmental cues (Park et al., 2015). Actually, the mechanisms behind intra-Golgi transport remain poorly understood.

## Golgi-to-Cell Surface Transport

The transportation of TGN to cell surface is directed by exocyst, which is a multimeric complex that associates with the TGN and the plasma membrane. The assembly of the exocyst complex is mainly regulated by RalA and RalB. In addition, Rab (Rabs3, 8, 11, and 27), Rho (Cdc42, Rho1, Rho3, and RhoQ) and Arf (Arf6) family proteins can also interact with exocyst subunits to modulate its function (Wu and Guo, 2015; Nishida-Fukuda, 2019). Then the vesicles are secreted with the coordination of Arf6 (Lawrence and Birnbaum, 2003; Pelletan et al., 2015). Moreover, Rab10, Rab13, Rab14, Rab26, Rab31, and Rab39 in Rab family GTPases (Bhuin and Roy, 2014; Galea and Simpson, 2015), and RhoD in Rho family GTPases (Olayioye et al., 2019), as well as Arl1, Arl8b in Arl family GTPases (Tuli et al., 2013; Yu and Lee, 2017), are also required for the trafficking of TGN to cell surface.

## Golgi-to-Endocytic Compartment Transport

Endocytic compartments (endosomes or lysosomes) are another destination for vesicles from TGN, since the proteins such as MPR and lysosomal associated membrane protein (LAMP) function in late endosomes or lysosomes (Boncompain and Weigel, 2018). The MPR transport from TGN to endocytic pathway is regulated by Arf1 GTPase (Waguri et al., 2003). And Rab31 is another GTPase that thought to play a role in TGN-to-endosome trafficking, as evidenced by the colocalization of Rab31 with TGN and endosomes, also by the involvement of Rab31-containing vesicular organelles in TGN-to-endosome transports (Rodriguez-Gabin et al., 2001).

## Small GTPases in Autophagic Pathway

Autophagy is an evolutionary conserved process that eliminates defunct proteins and organelles to maintain cellular homeostasis.



This pathway comprises the processes for autophagosome formation and maturation, as well as protein secretion mediated by autophagy (exophagy), and is achieved by small GTPase-mediated dynamic membrane trafficking and membrane interaction (Soreng et al., 2018).

## Autophagosome Formation Step

The autophagosome is formed by the following ordered steps: initiation of autophagy, formation of the phagophore, expansion, and elongation of the phagophore membrane, ultimate closure of phagophore to become an autophagosome (Soreng et al., 2018). These processes are largely exerted by the autophagy-related (ATG) proteins [reviewed in (Yu et al., 2018)], and are also regulated by multiple small GTPases. For the initiation of autophagy, Rab5 and Arf1 remove mammalian/mechanistic target of rapamycin complex 1 (mTORC1) from lysosomes to the cytosol, thus inhibiting mTORC1 activity and promoting autophagy initiation (Li et al., 2010). Rab12-mediated trafficking promotes the degradation of mTORC1 activator, then stimulates the autophagy induction as well (Matsui and Fukuda, 2013). While other small GTPases including Ras-related GTP-binding protein A and B (RagA and RagB) suppress the autophagy initiation by delivering mTORC1 to a location where it can be activated (Sancak et al., 2008). The phagophore is formed with membranes that from membranous organelles (Nakatogawa, 2020). This process is mediated by Arf1 (Gui et al., 2019), Arf6 (Moreau et al., 2012), Rab1a,1b (Zoppino et al., 2010; Lipatova et al., 2012; Mochizuki et al., 2013), Rab2 (Ding et al., 2019), Rab6 (Yang and Rosenwald, 2016), Rab9 (Nishida et al., 2009; Saito et al., 2019), Rab11 (Longatti et al., 2012; Puri et al., 2018), Rab30 (Nakajima et al., 2019), Rab32 (Hirota and Tanaka, 2009), and Arl1 (Yang and Rosenwald, 2016), while Rab39 functions as a negative regulator of this process (Seto et al., 2013). Then the phagophore membrane expands and elongates with the assistance of Arf1 (van der Vaart et al., 2010), Rab5 (Dou et al., 2013), Rab14 (Mauvezin et al., 2016), Rab26 (Binotti et al., 2015), Rab33b (Itoh et al., 2008), and Rab37 (Sheng et al., 2018). Finally, Rab5 promotes the phagophore closure catalyzed by endosomal sorting complex required for transport (ESCRT) through recruiting ESCRT subunit Snf7 to Atg17-decorated open phagophores (Zhou et al., 2019).

## Autophagosome Maturation Step

The autophagosome maturation process mainly refers to the fusion between autophagosomes with endosomes (early and late endosomes) and lysosomes, while the distribution of lysosomes and the delivery of lysosomal proteins or hydrolases are membrane trafficking events that can also affect the maturation of autophagosomes, and all these processes are controlled by small GTPases. Because the process for autophagosome maturation is quite similar to the endosome maturation in endocytic pathway, thus it is not surprising that small GTPases functioning in endosome maturation also regulate the maturation of autophagosomes. Additionally, the autophagosome-endosome/lysosome fusion step largely relies on Rab7 (Stroupe, 2018), but also requires Rab2 (Ding et al., 2019), Rab9 (Nozawa et al., 2012; Szatmari et al., 2014), Rab11

(Szatmari et al., 2014), Rab14 (Mauvezin et al., 2016), Rab21 (Jean et al., 2015), Rab24 (Amaya et al., 2016), and Rab33b (Itoh et al., 2008). Moreover, the lysosomal transport toward cell periphery is mainly determined by Arl8b (Korolchuk et al., 2011; Adnan et al., 2020). And the delivery of lysosomal membrane protein to lysosomes is dependent on Rab2 (Lund et al., 2018), while Rab6 selectively promotes the delivery of hydrolases, but not other lysosomal proteins, such as V-ATPase subunits or LAMP (Ayala et al., 2018).

## Exophagy Step

Emerging evidence demonstrates that a plethora of factors (mainly the leaderless proteins that lack an ER-signal peptide) are secreted in an autophagy-dependent manner, and this process is exophagy (Abrahamsen and Stenmark, 2010; Cavalli and Cenci, 2020). A study revealed that interferon (IFN)- $\gamma$ -induced exophagy of annexin A2 (ANXA2) is dependent on Rab8a, Rab11, and Rab27a (Chen et al., 2017). Another study reported that IL-1 $\beta$  secretion caused by autophagy induction is relied on Rab8a (Dupont et al., 2011). Since these GTPases (Rab8a, Rab11, and Rab27a) are also involved in other membrane trafficking process such as exocytic pathway, the findings that these GTPases modulate the exophagic pathway implicate a cooperation between exophagy with other membrane trafficking pathways. In addition, the role of other small GTPases in exophagy and the underlying mechanisms of these GTPases require further investigation.

## REGULATION OF SMALL GTPASES BY UBIQUITINATION

As mentioned above, small GTPases play an important role in multiple membrane trafficking processes, thus the modulation of these GTPases is the key determinant for exerting their functions. Studies have reported that small GTPase stability, activity, and localization can be regulated by ubiquitination (Table 1).

### Ubiquitination Regulates Small GTPase Stability

As two major protein degradation pathways, the ubiquitin-proteasome system (UPS) and autophagy are critical for the maintenance of protein homeostasis in cells, and they recognize ubiquitin as a degradation signal (Pohl and Dikic, 2019). The UPS mainly recognizes K48-linked polyubiquitin chains conjugated on single and short-lived proteins and targets them to proteasome for degradation, while autophagy sequesters K63- and K48-linked polyubiquitin chains associated long-lived proteins to autophagosomes and ultimately fuse with lysosomes for degradation. The modulation of small GTPases by ubiquitination plays an important role in membrane trafficking processes, and the proteolysis of them mostly relies on the UPS.

The most well-studied GTPase that is degraded by the UPS is RhoA. Specifically, RhoA can be polyubiquitin-modified by the SMAD-specific E3 ubiquitin protein ligase 1 (Smurf1) on lysine (Lys) 6 and Lys7 residues, thus resulting in the degradation of RhoA (Wang et al., 2003; Tian et al., 2011). Cullin3-BACURD



**TABLE 1 |** E3s and DUBs regulating small GTPase stability, activity, or localization.

Small GTPases	Ubiquitination site (s)	E3s	DUBs	References
<b>E3s and DUBs regulating small GTPase stability</b>				
RhoA	Lys6, 7	Smurf1		Wang et al., 2003; Tian et al., 2011
GDP-RhoA		Cullin3-BACURD		Chen et al., 2009
Total RhoA, GTP-RhoA		Fbxw7		Li J. et al., 2016
Total RhoA, GTP-RhoA, and GDP-RhoA	Lys135	SCF		Wei et al., 2013
GTP-RhoA			OTUB1	Edelmann et al., 2010
RhoB	Lys6, 7	Smurf1		Wang et al., 2014
RhoB	Lys162, 181	Cullin3-Rbx1		Xu et al., 2015; Kovacevic et al., 2018
Rac1	Lys147	XIAP, cIAP1		Oberoi et al., 2012
GTP-Rac1		HACE1		Torrino et al., 2011; Daugaard et al., 2013
Rac1	Lys166	SCF <sup>FBXL19</sup>		Zhao et al., 2013
Rac3	Lys166	SCF <sup>FBXL19</sup>		Dong et al., 2014
Cdc42	Lys166	XIAP		Murali et al., 2017
Rab35				Villarroel-Campos et al., 2016
GDP-Rab8				Takahashi et al., 2019
Rab27a				Song et al., 2019
Arl4c and Arf6		Cullin5		Han et al., 2020
<b>E3s and DUBs regulating small GTPase activity</b>				
Rab5	Lys140, 165			Shin et al., 2017
Rab7	Lys38	Parkin		Song et al., 2016
Rab7	Lys191		USP32	Sapmaz et al., 2019
Rab11a	Lys145	HACE1- $\beta$ 2AR		Lachance et al., 2014
<b>E3s and DUBs regulating small GTPase localization</b>				
Rab7	Lys191		USP32	Sapmaz et al., 2019
Rab7	Lys38	Parkin		Song et al., 2016
RhoB	Lys162, 181	Cullin3-Rbx1		Kovacevic et al., 2018
GTP-RhoA, GTP-Rac1, and GTP-Cdc42			USP17	de la Vega et al., 2011
RalA and RalB				Neyraud et al., 2012

ubiquitin ligase complex selectively interacts with GDP-bound RhoA, rather than GTP-bound or nucleotide free RhoA, to mediate its ubiquitination and proteasomal degradation (Chen et al., 2009). Different from the Cullin3-BACURD ubiquitin ligase, F-box and WD repeat domain-containing7 (Fbxw7) E3 ubiquitin ligase complex mediates the ubiquitination and degradation of the total RhoA and the active GTP-RhoA (Li H. et al., 2016). Additionally, Skp1-Cullin1-F-box (SCF) E3 ligase catalyzes the ubiquitination of the total, active and inactive forms of RhoA on Lys135 and then promotes the degradation of RhoA, which is dependent on the phosphorylation of RhoA by Erk2 (Wei et al., 2013). On the contrary, the ubiquitination modification of RhoA can be removed by deubiquitinating enzymes (DUBs). For instance, during *Yersinia* infection, otubain 1 (OTUB1) can disassemble the Lys48-linked polyubiquitin chains from GTP-RhoA to maintain its stability (Edelmann et al., 2010).

Additionally, the stability of other Rho GTPases encompassing RhoB, Rac1, Cdc42 and atypical Rho GTPases, is also controlled by the UPS. RhoB is polyubiquitinated for proteasomal degradation mainly by two E3 ligases. Smurf1 promotes RhoB degradation by conjugating ubiquitin on its Lys6 and Lys7 residues (Wang et al., 2014), while Cullin3-Rbx1 E3 ligase complex transfers K63 polyubiquitin chain to Lys162 and Lys181

of RhoB to promote its lysosomal localization and degradation via a proteasomal as well as a lysosomal pathway (Xu et al., 2015; Kovacevic et al., 2018). Moreover, inhibitors of apoptosis proteins (IAPs), including X-linked IAP (XIAP), and cellular IAP1 (c-IAP1), usually target Rac1 to catalyze its polyubiquitination on Lys147 site and then promote its degradation (Oberoi et al., 2012). Meanwhile, HECT domain and Ankyrin repeat containing E3 ubiquitin-protein ligase (HACE1) preferentially binds to the active form of Rac1 (GTP-Rac1) for its degradation (Torrino et al., 2011; Daugaard et al., 2013). The stability of Rac1 and Rac3 are also regulated by SCF<sup>FBXL19</sup> complex that transfers polyubiquitin chains to Lys166 residue of phosphorylated Rac1 or Rac3 to promote their proteasomal degradation (Zhao et al., 2013; Dong et al., 2014). And the Lys166 residue of Cdc42 can also be conjugated with polyubiquitin chains by XIAP, and this modification provide a signal for its proteasomal degradation (Murali et al., 2017).

Among the Rab GTPases, Rab35 is the first protein reported to be degraded by the UPS, which is controlled by p53-related protein kinase (PRPK) and microtubule associated protein 1B (MAP1B) (Villarroel-Campos et al., 2016). Rab8 can also be targeted by the UPS, but only GDP-Rab8a is rapidly degraded with the assistance of BAG6 (BAT3/Scythe), while GTP-Rab8a is highly stable (Takahashi et al., 2019). The accumulated

GDP-bound Rab proteins tend to form aggregates in the cytoplasm due to the exposure of hydrophobic groups, so the clearance mechanism of inactive GDP-Rab proteins is critical for maintaining cellular homeostasis. However, the specific E3 ubiquitin ligase of GDP-Rab8a is not identified. As BAG6 can associate with E3s including RNF126 and gp78 (Xu et al., 2013; Rodrigo-Brenni et al., 2014), it is possible Rab8a may be a substrate of BAG6-associated ubiquitin ligase. Another recent study demonstrates that the kidney and brain protein (KIBRA) can interact with Rab27a, and then prevents the ubiquitination-mediated degradation of Rab27a (Song et al., 2019). In addition, the stability of Arf GTPases has also been reported to be regulated by UPS. An example is that the protein levels of Arl4c and Arf6 are downregulated in the presence of Cullin5 E3 ligase (Han et al., 2020). Since UPS can mediate the degradation of specific GTP-bound, GDP-bound or total GTPases, it is reasonable that the activity of GTPases is altered accompanied by the degradation of these proteins.

## Ubiquitination Regulates Small GTPase Activity

The conversion between GDP- and GTP-bound GTPases is the key determinant in exerting their functions. Upon being formed, GTP-bound GTPases can recruit specific effectors

to regulate cellular activities. Based on this, ubiquitination may regulate small GTPase activity through two modes, including the exchange of GDP- and GTP-bound GTPases, and the recruitment of effectors. And this ubiquitination-mediated regulatory functions have been demonstrated in several Rab GTPases.

The early endosome marker Rab5, a key member of the Rab family, is crucial in endocytosis and membrane transport. Rab5 could be monoubiquitinated on three residues, including Lys116, Lys140, and Lys165, among which, the monoubiquitination on Lys140 and Lys165, but not Lys116, suppresses the activity of Rab5. Specifically, monoubiquitination on Lys140 impairs the interaction between Rab5 and its downstream effectors such as Rabaptin 5 and early endosome antigen 1 (EEA1), and Lys165 monoubiquitylation hinders GEF-mediated guanine nucleotide conversion, thereby leading to the blockade of endocytic pathway (Figures 2A,B; Shin et al., 2017). It is worth mentioning that the ubiquitination site is critical to determine small GTPase activity.

Rab7 activity is also regulated by its ubiquitination. The dimerubiquitination on the Lys191 residue of Rab7 blocks its interaction with RILP, thus inhibiting Rab7-mediated late endosome motility and the perinuclear localization of the late compartment. In turn, the DUB enzyme ubiquitin-specific protease 32 (USP32) removes the ubiquitin chains from Lys191,

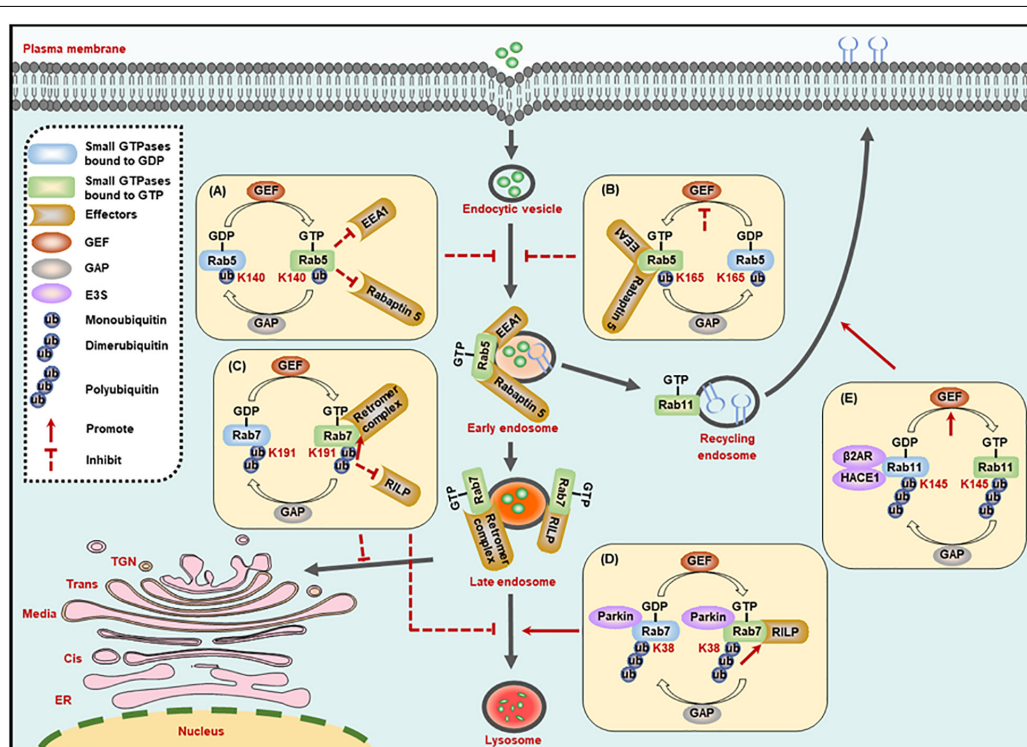


**FIGURE 2 |** Ubiquitination regulates the activity of small GTPases in the membrane trafficking processes. (A,B) The monoubiquitination of Rab5 inhibits its interaction with effectors (A), or its exchange of GDP- to GTP-bound form (B), to suppress the formation of Rab5-positive early endosomes. (C) The dimerubiquitination of Rab7 inhibits its interaction with RILP to suppress the motility of late endosomes to lysosomes, while promoting its affinity to retromer complex to suppress the recycling from late endosomes to TGN. (D) The polyubiquitination of Rab7 promotes its interaction with RILP to enhance the motility of late endosomes to lysosomes. (E) The polyubiquitination of Rab11 promotes its exchange of GDP- to GTP-bound form to enhance the receptor recycling to cell membrane. GEF, guanine nucleotide exchange factor; GAP, GTPase-activating protein; K, Lysine (Lys).

and then restores the late endosome motility and the perinuclear localization of the late compartment mediated by Rab7 (Sapmaz et al., 2019). Most importantly, the ubiquitination of Rab7 on Lys191 residue can also inhibit the recycling from late endosomes to TGN by enhancing the interplay between Rab7 and the retromer complex and thus stabilize the retromer complex on endosomes (Figure 2C; Sapmaz et al., 2019). In addition, polyubiquitinated Rab7 on the Lys38 residue by the E3 ligase Parkin exhibits stronger affinity for its effector RILP, and the high affinity improves the activity and membrane localization of Rab7 (Figure 2D; Song et al., 2016).

Another example regarding ubiquitination-dependent regulation of small GTPase activity is Rab11a, which mediates the receptor recycling, and its activity is regulated by ubiquitination catalyzed by HACE1 and a scaffold  $\beta$ 2AR. The HACE1- $\beta$ 2AR complex-catalyzed Rab11a ubiquitination on Lys145 destroys the interaction between  $\beta$ 2AR and GDP-bound Rab11a, and then releases Rab11a to combine GTP and thus promotes its activation (Figure 2E). But the mechanism that ubiquitination of Rab11a leads to its activation needs further determination. In addition, co-expression of HACE1 and  $\beta$ 2AR also potentiates the ubiquitination of Rab6a and Rab8a. Considering the functional connection of Rab6a, Rab8a, and Rab11a in intracellular transport, whether the ubiquitination of these three proteins will affect each other remains to be defined (Lachance et al., 2014).

## Ubiquitination Regulates Small GTPase Localization

Small GTPases are usually localized on the cytosol in their inactive GDP-bound form. Accompanied with the conversion between GDP- and GTP-bound forms, GTPases are transferred from the cytosol to specific membranes to recruit effectors for functioning (Stenmark, 2009). Thus, the ubiquitination-dependent regulation of small GTPase activity may also plays important roles in modulating their localizations. For example, ubiquitination of Rab7 on Lys191 residue blocks late endosome motility and the perinuclear localization of the late compartment, and this modification also facilitates the membrane localization of Rab7, as evidenced by the increased membrane-to-cytosol ratio (Sapmaz et al., 2019). Another study indicates that Parkin catalyzes the ubiquitination of Rab7 to enhance its binding affinity for RILP, and thus ultimately promoting the membrane localization of Rab7 (Song et al., 2016).

Moreover, the localization of Rho and Ras family GTPases is also modulated by ubiquitination. For instance, the ubiquitination of RhoB on Lys162 and Lys181 can direct RhoB to lysosome for degradation (Kovacevic et al., 2018). And the ubiquitin-specific protease 17 (USP17) is required for the membrane localization of active Rho GTPases, including RhoA, Rac1, and Cdc42, while the underlying molecular mechanism is still unclear (de la Vega et al., 2011). Furthermore, the ubiquitination of Ras GTPases (including RalA and RalB) can provide a signal for their localization. Specifically, ubiquitination directs RalA transport to plasma membrane, while deubiquitination of RalA occurs in lipid raft microdomains and promotes raft endocytosis (Neyraud et al., 2012). Up to now,

the role and the underlying molecular mechanism by which ubiquitylation regulate the location of the small GTPases remain obscure and warrant further investigation.

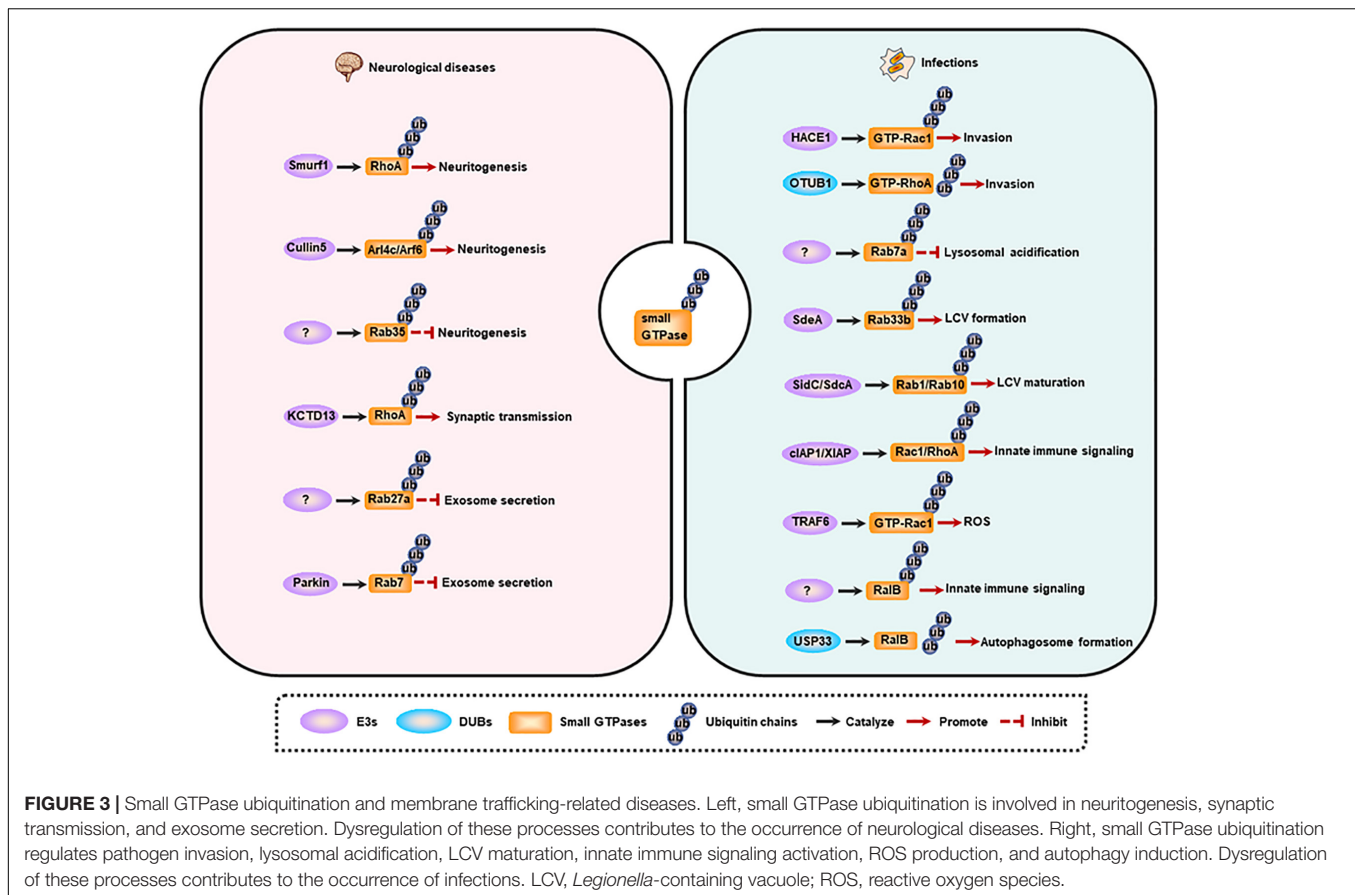
## DYSREGULATION OF SMALL GTPASE UBIQUITINATION IN MEMBRANE TRAFFICKING-RELATED DISEASES

Membrane trafficking is the key determinant for cellular activities, including neurodevelopment and host immune response against pathogens. The trafficking is a complex, dynamic, but an ordered process, which is mainly controlled by small GTPases' spatiotemporal alterations that potentially dependent on ubiquitination (as described above). Consequently, the dysregulation of small GTPase ubiquitination will cause multiple human membrane trafficking-related diseases, and here we focus on the neurological and infectious diseases (Figure 3).

### Dysregulation of Small GTPase Ubiquitination in Neurological Diseases

The nervous system is the commander of multitude biogenic activities, and neurodevelopment is critical for this ability. The entire neurodevelopmental process, including neurogenesis, neuritogenesis, synaptogenesis, differentiation, synaptic plasticity, synaptic transmission, and aggregate secretion, depends on the membrane trafficking, and is regulated by small GTPases [reviewed in (Qu et al., 2019)]. Emerging evidence shows that small GTPase ubiquitination is a more precise mechanism for modulating neurodevelopment at the specific stage. Moreover, the alteration of this protein modification accounts for many neurological disorders.

Neuritogenesis has been reported to be regulated by small GTPase ubiquitination. Neuritogenesis is inhibited by RhoA, and Smurf1 can interact with RhoA and mediate its ubiquitination and degradation, thus enhancing neurite outgrowth (Bryan et al., 2005; Deglincerti et al., 2015). Some other small GTPases including Arl4c and its effector Arf6 are also negative regulators of neuritogenesis (particularly dendritogenesis), and are ubiquitinated and degraded by Cullin-5 under physiological conditions. Furthermore, depletion of Cullin-5 causes the formation of V-shaped dendrites that usually appears in neurodegenerative models or in the brains of Alzheimer's disease (AD) patients (Han et al., 2020). However, Rab35 favors axon elongation in rat primary neurons, and this process is controlled by the proteolysis of Rab35 in a UPS-dependent manner (Villarreal-Campos et al., 2016). Additionally, synaptic transmission is also modulated by small GTPase ubiquitination. RhoA can prevent synaptic transmission, and deletion of its E3 ligase KCTD13 results in accumulated RhoA, which in turn reduces functional synapse number and synaptic transmission. Consistently, treatment with RhoA inhibitor rhosin can reverse the reduced synaptic transmission in *Kctd13*-deleted mice, implicating that RhoA is a potential therapeutic target for neuropsychiatric disorders (Escamilla et al., 2017).



The abnormal aggregation of misfolded proteins is the pathological character of neurodegenerative diseases, and these proteins can be delivered to non-effected regions by exosomes, thus promoting the progression of the disease (Jan et al., 2017). The secretion of exosomes in neural cells is another process that is controlled by small GTPase ubiquitination. Evidence indicates that KIBRA and Rab27a are predominantly expressed in the brain, and KIBRA-mediated inhibition of Rab27a ubiquitination and degradation promotes the secretion of exosomes, suggesting that decreased Rab27a ubiquitination may be involved in the initiation and progression of neurodegenerative diseases (Song et al., 2019). Another study shows that Parkin mediates the ubiquitination of Rab7, and then promotes its affinity for RILP, eventually directing Rab7 to the retromer pathway. While the deregulation of Rab7 ubiquitination in Parkin-deficient cells results in the impairment of the retromer function, but leading to the increased secretion of exosomes, a phenomenon observed in Parkinson disease (PD). These findings raise a possibility that increasing Rab7 ubiquitination may be a potential therapeutic strategy for PD (Song et al., 2016).

## Dysregulation of Small GTPase Ubiquitination in Infections

Membrane trafficking is vital for host immune response against pathogens. Based on this, trafficking events, such as

phagocytosis and the following phagosome maturation, together with autophagy, can be prevented, or hijacked by pathogens (especially intracellular pathogens) to benefit their survival (Inoue et al., 2018; Chai et al., 2020). Moreover, increasing studies have demonstrated that the ubiquitin system is another sensitive target of many bacterial pathogens (Li J. et al., 2016). As small GTPases are the main modulators in membrane trafficking, the ubiquitination of these proteins has also been reported to be manipulated by pathogenic microorganisms.

The invasion into host cells is fundamental for intracellular pathogens to establish an infection, and Rho family GTPases are crucial for this process (Visvikis et al., 2011). Targeting Rho GTPases to regulate their ubiquitination is the strategy of pathogens for entering the host cells. Specifically, effectors or toxins produced by pathogenic microorganisms interfere with the ubiquitination of Rho GTPases. For instance, cytotoxic necrotizing factor-1 (CNF1) from *Escherichia coli* can induce the activation of Rac1, and then promotes the HACE1-mediated ubiquitination and degradation of GTP-bound Rac1, leading to an increased invasion of pathogens toward endothelial cell monolayer (Torrino et al., 2011). While prior to *Yersinia* infection, wild-type OTUB1 catalyzes the deubiquitination of active-form RhoA to stabilize the protein, and then enhances the cellular susceptibility to invasion. However, once virulence factor *Yersinia* serine/threonine kinase A (YpkA) is secreted into the infected cells, it can interact with phosphorylated OTUB1 as



well as GDP-bound RhoA to block active RhoA formation, and ultimately preventing further bacterial uptake. And the limiting invasion efficiency of bacteria may contribute to a decreased intracellular killing mediated by host immune defense (Edelmann et al., 2010). Additionally, a ubiquitinome study of *Salmonella*-infected epithelial cells has revealed that the ubiquitination level of Cdc42 and RhoG is upregulated, whereas Rac1 ubiquitination is decreased, at early-stage of infection. These effects may benefit the invasion of the pathogen. However, the exact functional output of these modifications and the E3s as well as DUBs of these proteins need further research in the future (Fiskin et al., 2016).

To replicate in the cell, pathogenic microorganisms can manipulate the host's membrane trafficking pathways to avoid degradation and to shape a replication-permissive niche, such as *Salmonella*-containing vacuoles (SCV) for *Salmonella enterica*, and *Legionella*-containing vacuole (LCV) for *Legionella pneumophila* (*L. pneumophila*). Upon *Salmonella* infection, Rab7a is highly ubiquitinated by an unknown E3 ligase, which may contribute to the inhibition of lysosomal acidification and the subsequent degradation (Fiskin et al., 2016). Furthermore, effectors released by *L. pneumophila* have evolved ubiquitinating enzyme activities to mediate the ubiquitination of host proteins directly. During infection, effector protein SdeA secreted by *L. pneumophila* can promote the ubiquitination of ER-associated protein Rab33b, leading to an increased intracellular bacterial replication by facilitating LCV formation (Qiu et al., 2016). Rab10 can be recruited to the LCV and then be ubiquitinated by SidC/SdcA to promote LCV maturation (Jeng et al., 2019). Rab1, a GTPase that is localized on the LCV, can also be ubiquitinated in a SidC/SdcA-dependent manner and then play key roles in LCV maturation (Horenkamp et al., 2014).

Other host immune responses related to small GTPase ubiquitination can also be manipulated by pathogens. For example, CNF1-induced ubiquitination-mediated proteasomal degradation of activated Rho proteins limits the production of inflammatory proteins and immunomodulators, thus attenuating host cell immune responses (Munro et al., 2004). Another example is that VopS from *Vibrio parahaemolyticus* hinders the interaction of Rho GTPases (Rac1 and RhoA) with their E3 ligases (cIAP1 and XIAP), may causing a suppression to host immune response such as collapse of the actin cytoskeleton, inactivation of NF- $\kappa$ B, Erk and JNK pathways (Woolery et al., 2014). Additionally, in response to pathogen infection, E3 ubiquitin ligase TRAF6 selectively interacts with inactive Rac1T17N. Once the GDP-dissociation inhibitor (GDI) is dissociated from Rac1, this will promote the charging of GTP on Rac1. Under this condition, TRAF6 can further catalyze K63-linked polyubiquitination of GTP-Rac1, eventually inducing the recruitment of mitochondria to phagosome and the subsequently formation of ROS in macrophages for pathogen killing (Geng et al., 2015). And RalB ubiquitination is critical for its binding to exocyst complex component 2 (EXOC2) and the triggered innate immune signaling, while deubiquitination of RalB mediated by ubiquitin-specific protease 33 (USP33) facilitates the assembly of the RalB-Exocyst complex component 84 (EXO84)-beclin-1 complex to drive autophagosome formation (Simicek et al., 2013). These studies suggest that the ubiquitination of small GTPases is involved in multiple steps of pathogen infections.

## CONCLUSION

Membrane trafficking is tightly regulated to maintain cellular homeostasis, and defects in the regulatory machinery of this process leads to human diseases. This review discusses the modulation of membrane trafficking pathways by small GTPases, and the regulation of small GTPases by ubiquitination as well as the associated human diseases (focusing on the neurological diseases and infections). Three key points are extracted from this review: first, there is a crosstalk between different regulatory pathways, which may lead to synergistic or antagonistic effects; second, the regulatory function of ubiquitination on small GTPases is not singular due to the interactions among GTPase stability, activity and localization; third, the ubiquitination levels of small GTPases may be altered during the progression of diseases, especially the infections, as pathogens can manipulate host immune response to benefit their intracellular survival through multiple strategies. Moreover, emerging ubiquitinome studies have revealed that ubiquitination of small GTPases is a prominent characteristic of multiple human diseases (Fiskin et al., 2016; Jeng et al., 2019). Additionally, the ubiquitination site is critical to decide small GTPase activities (Shin et al., 2017). Therefore, identifying the ubiquitination sites and their output functions during the progression of diseases will provide new insights into novel therapeutics for these diseases. Furthermore, several other important issues also warrant further study to provide clearer and more comprehensive picture for disease treatment. For instance, what are the E3s and DUBs of small GTPases? If E3 or DUBs are effectors from pathogens, whether they regulate host protein substrates and their functions by novel mechanisms different from their host counterparts? Moreover, various types of atypical ubiquitination have been revealed, and what are their regulatory roles on small GTPases and membrane trafficking, and whether there is a crosstalk between different ubiquitination modifications? Thus, there are many exciting questions waiting to be clarified, and a more in-depth understanding of the molecular mechanisms by which ubiquitination regulates small GTPases and the membrane trafficking process can provide new insights and novel targets for the development of more effective and specific therapeutics for membrane trafficking-related human diseases.

## AUTHOR CONTRIBUTIONS

All authors listed have made a substantial, direct and intellectual contribution to the work, and approved it for publication.

## FUNDING

This work was supported by the National Natural Science Foundation of China (81825014, 31830003, and 82022041), the Strategic Priority Research Program of the Chinese Academy of Sciences (XDB29020000), the National Key Research and Development Program of China (2017YFA0505900), and the Youth Innovation Promotion Association CAS (20181118).

## REFERENCES

- Abrahamsen, H., and Stenmark, H. (2010). Protein secretion: unconventional exit by exophagy. *Curr. Biol.* 20, R415–R418. doi: 10.1016/j.cub.2010.03.011
- Adnan, G., Rubikaite, A., Khan, M., Reber, M., Suetterlin, P., Hindges, R., et al. (2020). The GTPase Arl8B plays a principle role in the positioning of interstitial axon branches by spatially controlling autophagosome and lysosome location. *J. Neurosci.* 40, 8103–8118. doi: 10.1523/JNEUROSCI.1759-19.2020
- Ahearn, I. M., Haigis, K., Bar-Sagi, D., and Philips, M. R. (2011). Regulating the regulator: post-translational modification of RAS. *Nat. Rev. Mol. Cell Biol.* 13, 39–51. doi: 10.1038/nrm3255
- Allan, B. B., Moyer, B. D., and Balch, W. E. (2000). Rab1 recruitment of p115 into a cis-SNARE complex: programming budding COPII vesicles for fusion. *Science* 289, 444–448. doi: 10.1126/science.289.5478.444
- Amaya, C., Militello, R. D., Calligaris, S. D., and Colombo, M. I. (2016). Rab24 interacts with the Rab7/Rab interacting lysosomal protein complex to regulate endosomal degradation. *Traffic* 17, 1181–1196. doi: 10.1111/tra.12431
- Ayala, C. I., Kim, J., and Neufeld, T. P. (2018). Rab6 promotes insulin receptor and cathepsin trafficking to regulate autophagy induction and activity in *Drosophila*. *J. Cell Sci.* 131:jcs.216127. doi: 10.1242/jcs.216127
- Beraud-Dufour, S., and Balch, W. (2002). A journey through the exocytic pathway. *J. Cell Sci.* 115(Pt 9), 1779–1780.
- Bhuin, T., and Roy, J. K. (2014). Rab proteins: the key regulators of intracellular vesicle transport. *Exp. Cell Res.* 328, 1–19. doi: 10.1016/j.yexcr.2014.07.027
- Binotti, B., Pavlos, N. J., Riedel, D., Wenzel, D., Vorbruggen, G., Schalk, A. M., et al. (2015). The GTPase Rab26 links synaptic vesicles to the autophagy pathway. *Elife* 4:e05597. doi: 10.7554/eLife.05597
- Boncompain, G., and Weigel, A. V. (2018). Transport and sorting in the Golgi complex: multiple mechanisms sort diverse cargo. *Curr. Opin. Cell Biol.* 50, 94–101. doi: 10.1016/j.cub.2018.03.002
- Brandizzi, F., and Barlowe, C. (2013). Organization of the ER-Golgi interface for membrane traffic control. *Nat. Rev. Mol. Cell Biol.* 14, 382–392. doi: 10.1038/nrm3588
- Bryan, B., Cai, Y., Wrighton, K., Wu, G., Feng, X. H., and Liu, M. (2005). Ubiquitination of RhoA by Smurf1 promotes neurite outgrowth. *FEBS Lett.* 579, 1015–1019. doi: 10.1016/j.febslet.2004.12.074
- Cavalli, G., and Cenci, S. (2020). Autophagy and protein secretion. *J. Mol. Biol.* 432, 2525–2545. doi: 10.1016/j.jmb.2020.01.015
- Chai, Q., Wang, L., Liu, C. H., and Ge, B. (2020). New insights into the evasion of host innate immunity by *Mycobacterium tuberculosis*. *Cell. Mol. Immunol.* 17, 901–913. doi: 10.1038/s41423-020-0502-z
- Chen, L., Hu, J., Yun, Y., and Wang, T. (2010). Rab36 regulates the spatial distribution of late endosomes and lysosomes through a similar mechanism to Rab34. *Mol. Membr. Biol.* 27, 23–30. doi: 10.3109/09687680903417470
- Chen, Y., Yang, Z., Meng, M., Zhao, Y., Dong, N., Yan, H., et al. (2009). Cullin mediates degradation of RhoA through evolutionarily conserved BTB adaptors to control actin cytoskeleton structure and cell movement. *Mol. Cell* 35, 841–855. doi: 10.1016/j.molcel.2009.09.004
- Chen, Y. D., Fang, Y. T., Cheng, Y. L., Lin, C. F., Hsu, L. J., Wang, S. Y., et al. (2017). Exophagy of annexin A2 via RAB11, RAB8A and RAB27A in IFN- $\gamma$ -stimulated lung epithelial cells. *Sci. Rep.* 7:5676. doi: 10.1038/s41598-017-06076-4
- Chesneau, L., Dambournet, D., Machicoane, M., Kouranti, I., Fukuda, M., Goud, B., et al. (2012). An ARF6/Rab35 GTPase cascade for endocytic recycling and successful cytokinesis. *Curr. Biol.* 22, 147–153. doi: 10.1016/j.cub.2011.11.058
- Chua, C. E., and Tang, B. L. (2014). Engagement of the small GTPase Rab31 protein and its effector, early endosome antigen 1, is important for trafficking of the ligand-bound epidermal growth factor receptor from the early to the late endosome. *J. Biol. Chem.* 289, 12375–12389. doi: 10.1074/jbc.M114.548321
- Daugaard, M., Nitsch, R., Razaghi, B., McDonald, L., Jarrar, A., Torrino, S., et al. (2013). Hsc1 controls ROS generation of vertebrate Rac1-dependent NADPH oxidase complexes. *Nat. Commun.* 4:2180. doi: 10.1038/ncomms3180
- de la Vega, M., Kelvin, A. A., Dunican, D. J., McFarlane, C., Burrows, J. F., Jaworski, J., et al. (2011). The deubiquitinating enzyme USP17 is essential for GTPase subcellular localization and cell motility. *Nat. Commun.* 2:259. doi: 10.1038/ncomms1243
- de Toledo, M., Senic-Matuglia, F., Salamero, J., Uze, G., Comunale, F., Fort, P., et al. (2003). The GTP/GDP cycling of rho GTPase TCL is an essential regulator of the early endocytic pathway. *Mol. Biol. Cell* 14, 4846–4856. doi: 10.1091/mbc.e03-04-0254
- Degincerti, A., Liu, Y., Colak, D., Hengst, U., Xu, G., and Jaffrey, S. R. (2015). Coupled local translation and degradation regulate growth cone collapse. *Nat. Commun.* 6:6888. doi: 10.1038/ncomms7888
- Dejgaard, S. Y., Murshid, A., Erman, A., Kizilay, O., Verbich, D., Lodge, R., et al. (2008). Rab18 and Rab43 have key roles in ER-Golgi trafficking. *J. Cell Sci.* 121(Pt 16), 2768–2781. doi: 10.1242/jcs.021808
- Ding, X., Jiang, X., Tian, R., Zhao, P., Li, L., Wang, X., et al. (2019). RAB2 regulates the formation of autophagosome and autolysosome in mammalian cells. *Autophagy* 15, 1774–1786. doi: 10.1080/15548627.2019.1596478
- Donaldson, J. G., and Jackson, C. L. (2011). ARF family G proteins and their regulators: roles in membrane transport, development and disease. *Nat. Rev. Mol. Cell Biol.* 12, 362–375. doi: 10.1038/nrm3117
- Dong, S., Zhao, J., Wei, J., Bowser, R. K., Khoo, A., Liu, Z., et al. (2014). F-box protein complex FBXL19 regulates TGF $\beta$ 1-induced E-cadherin down-regulation by mediating Rac3 ubiquitination and degradation. *Mol. Cancer* 13:76. doi: 10.1186/1476-4598-13-76
- Dorayappan, K. D. P., Wanner, R., Wallbillich, J. J., Saini, U., Zingarelli, R., Suarez, A. A., et al. (2018). Hypoxia-induced exosomes contribute to a more aggressive and chemoresistant ovarian cancer phenotype: a novel mechanism linking STAT3/Rab proteins. *Oncogene* 37, 3806–3821. doi: 10.1038/s41388-018-0189-0
- Dou, Z., Pan, J. A., Dbouk, H. A., Ballou, L. M., DeLeon, J. L., Fan, Y., et al. (2013). Class IA PI3K p110 $\beta$  subunit promotes autophagy through Rab5 small GTPase in response to growth factor limitation. *Mol. Cell* 50, 29–42. doi: 10.1016/j.molcel.2013.01.022
- D'Souza-Schorey, C., and Chavrier, P. (2006). ARF proteins: roles in membrane traffic and beyond. *Nat. Rev. Mol. Cell Biol.* 7, 347–358. doi: 10.1038/nrm1910
- Dupont, N., Jiang, S., Pilli, M., Ornatowski, W., Bhattacharya, D., and Deretic, V. (2011). Autophagy-based unconventional secretory pathway for extracellular delivery of IL-1 $\beta$ . *EMBO J.* 30, 4701–4711. doi: 10.1038/emboj.2011.398
- Dutta, D., and Donaldson, J. G. (2015). Sorting of clathrin-independent cargo proteins depends on rab35 delivered by clathrin-mediated endocytosis. *Traffic* 16, 994–1009. doi: 10.1111/tra.12302
- Edelmann, M. J., Kramer, H. B., Altun, M., and Kessler, B. M. (2010). Post-translational modification of the deubiquitinating enzyme otubain 1 modulates active RhoA levels and susceptibility to *Yersinia* invasion. *FEBS J.* 277, 2515–2530. doi: 10.1111/j.1742-4658.2010.07665.x
- Egami, Y. (2016). Molecular imaging analysis of Rab GTPases in the regulation of phagocytosis and macropinocytosis. *Anat. Sci. Int.* 91, 35–42. doi: 10.1007/s12565-015-0313-y
- Elkin, S. R., Lakoduk, A. M., and Schmid, S. L. (2016). Endocytic pathways and endosomal trafficking: a primer. *Wien. Med. Wochenschr.* 166, 196–204. doi: 10.1007/s10354-016-0432-7
- Escamilla, C. O., Filonova, I., Walker, A. K., Xuan, Z. X., Holehonnur, R., Espinosa, F., et al. (2017). Kctd13 deletion reduces synaptic transmission via increased RhoA. *Nature* 551, 227–231. doi: 10.1038/nature24470
- Espinosa, E. J., Calero, M., Sridevi, K., and Pfeffer, S. R. (2009). RhoBTB3: a Rho GTPase-family ATPase required for endosome to Golgi transport. *Cell* 137, 938–948. doi: 10.1016/j.cell.2009.03.043
- Evans, T. M., Ferguson, C., Wainwright, B. J., Parton, R. G., and Wicking, C. (2003). Rab23, a negative regulator of hedgehog signaling, localizes to the plasma membrane and the endocytic pathway. *Traffic* 4, 869–884. doi: 10.1046/j.1600-0854.2003.00141.x
- Fiskin, E., Bionda, T., Dikic, I., and Behrends, C. (2016). Global analysis of host and bacterial ubiquitinome in response to *Salmonella* typhimurium infection. *Mol. Cell* 62, 967–981. doi: 10.1016/j.molcel.2016.04.015
- Foot, N., Henshall, T., and Kumar, S. (2017). Ubiquitination and the regulation of membrane proteins. *Physiol. Rev.* 97, 253–281. doi: 10.1152/physrev.00012.2016
- Galea, G., and Simpson, J. C. (2015). High-content analysis of Rab protein function at the ER-Golgi interface. *Bioarchitecture* 5, 44–53. doi: 10.1080/19490992.2015.1102826
- Geng, J., Sun, X., Wang, P., Zhang, S., Wang, X., Wu, H., et al. (2015). Kinases Mst1 and Mst2 positively regulate phagocytic induction of reactive oxygen species and bactericidal activity. *Nat. Immunol.* 16, 1142–1152. doi: 10.1038/ni.3268

- Gillingham, A. K., and Munro, S. (2007). The small G proteins of the Arf family and their regulators. *Annu. Rev. Cell Dev. Biol.* 23, 579–611. doi: 10.1146/annurev.cellbio.23.090506.123209
- Gorji-Bahri, G., Moghimi, H. R., and Hashemi, A. (2021). RAB5A is associated with genes involved in exosome secretion: integration of bioinformatics analysis and experimental validation. *J. Cell Biochem.* 122, 425–441. doi: 10.1002/jcb.29871
- Grossmann, A. H., Zhao, H., Jenkins, N., Zhu, W., Richards, J. R., Yoo, J. H., et al. (2019). The small GTPase ARF6 regulates protein trafficking to control cellular function during development and in disease. *Small GTPases* 10, 1–12. doi: 10.1080/21541248.2016.1259710
- Gui, X., Yang, H., Li, T., Tan, X., Shi, P., Li, M., et al. (2019). Autophagy induction via STING trafficking is a primordial function of the cGAS pathway. *Nature* 567, 262–266. doi: 10.1038/s41586-019-1006-9
- Hall, A. (2012). Rho family GTPases. *Biochem. Soc. Trans.* 40, 1378–1382. doi: 10.1042/BST20120103
- Han, J. S., Hino, K., Li, W., Reyes, R. V., Canales, C. P., Miltner, A. M., et al. (2020). CRL5-dependent regulation of the small GTPases ARL4C and ARF6 controls hippocampal morphogenesis. *Proc. Natl. Acad. Sci. U. S. A.* 117, 23073–23084. doi: 10.1073/pnas.2002749117
- Hinger, S. A., Abner, J. J., Franklin, J. L., Jeppesen, D. K., Coffey, R. J., and Patton, J. G. (2020). Rab13 regulates sEV secretion in mutant KRAS colorectal cancer cells. *Sci. Rep.* 10:15804. doi: 10.1038/s41598-020-72503-8
- Hirota, Y., and Tanaka, Y. (2009). A small GTPase, human Rab32, is required for the formation of autophagic vacuoles under basal conditions. *Cell. Mol. Life Sci.* 66, 2913–2932. doi: 10.1007/s00018-009-0080-9
- Hodge, R. G., and Ridley, A. J. (2016). Regulating Rho GTPases and their regulators. *Nat. Rev. Mol. Cell Biol.* 17, 496–510. doi: 10.1038/nrm.2016.67
- Horenkamp, F. A., Mukherjee, S., Alix, E., Schauder, C. M., Hubber, A. M., Roy, C. R., et al. (2014). *Legionella pneumophila* subversion of host vesicular transport by SidC effector proteins. *Traffic* 15, 488–499. doi: 10.1111/tra.12158
- Hsu, C., Morohashi, Y., Yoshimura, S., Manrique-Hoyos, N., Jung, S., Lauterbach, M. A., et al. (2010). Regulation of exosome secretion by Rab35 and its GTPase-activating proteins TBC1D10A-C. *J. Cell Biol.* 189, 223–232. doi: 10.1083/jcb.200911018
- Hu, S. Q., Zhang, Q. C., Meng, Q. B., Hu, A. N., Zou, J. P., and Li, X. L. (2020). Autophagy regulates exosome secretion in rat nucleus pulposus cells via the RhoC/ROCK2 pathway. *Exp. Cell Res.* 395:112239. doi: 10.1016/j.yexcr.2020.112239
- Huang, M., Duhadaway, J. B., Prendergast, G. C., and Laury-Kleintop, L. D. (2007). RhoB regulates PDGFR-beta trafficking and signaling in vascular smooth muscle cells. *Arterioscler. Thromb. Vasc. Biol.* 27, 2597–2605. doi: 10.1161/ATVBAHA.107.154211
- Huang, M., Satchell, L., Duhadaway, J. B., Prendergast, G. C., and Laury-Kleintop, L. D. (2011). RhoB links PDGF signaling to cell migration by coordinating activation and localization of Cdc42 and Rac. *J. Cell Biochem.* 112, 1572–1584. doi: 10.1002/jcb.23069
- Huotari, J., and Helenius, A. (2011). Endosome maturation. *EMBO J.* 30, 3481–3500. doi: 10.1038/emboj.2011.286
- Hyenne, V., Apaydin, A., Rodriguez, D., Spiegelhalter, C., Hoff-Yoessle, S., Diem, M., et al. (2015). RAL-1 controls multivesicular body biogenesis and exosome secretion. *J. Cell Biol.* 211, 27–37. doi: 10.1083/jcb.201504136
- Inoue, J., Ninomiya, M., Shimosegawa, T., and McNiven, M. A. (2018). Cellular membrane trafficking machineries used by the hepatitis viruses. *Hepatology* 68, 751–762. doi: 10.1002/hep.29785
- Itoh, T., Fujita, N., Kanno, E., Yamamoto, A., Yoshimori, T., and Fukuda, M. (2008). Golgi-resident small GTPase Rab33B interacts with Atg16L and modulates autophagosome formation. *Mol. Biol. Cell* 19, 2916–2925. doi: 10.1091/mbc.E07-12-1231
- Jan, A. T., Malik, M. A., Rahman, S., Yeo, H. R., Lee, E. J., Abdullah, T. S., et al. (2017). Perspective insights of exosomes in neurodegenerative diseases: a critical appraisal. *Front. Aging Neurosci.* 9:317. doi: 10.3389/fnagi.2017.00317
- Jean, S., Cox, S., Nassari, S., and Kiger, A. A. (2015). Starvation-induced MTMR13 and RAB21 activity regulates VAMP8 to promote autophagosome-lysosome fusion. *EMBO Rep.* 16, 297–311. doi: 10.15252/embr.201439464
- Jeng, E. E., Bhadkamkar, V., Ibe, N. U., Gause, H., Jiang, L., Chan, J., et al. (2019). Systematic identification of host cell regulators of *Legionella pneumophila* pathogenesis using a genome-wide CRISPR screen. *Cell Host Microbe* 26, 551–563.e6. doi: 10.1016/j.chom.2019.08.017
- Jongsma, M. L., Bakker, J., Cabukusta, B., Liv, N., van Elsland, D., Fermie, J., et al. (2020). SKIP-HOPS recruits TBC1D15 for a Rab7-to-Arl8b identity switch to control late endosome transport. *EMBO J.* 39:e102301. doi: 10.15252/emboj.2019102301
- Jung, J. J., Tiwari, A., Inamdar, S. M., Thomas, C. P., Goel, A., and Choudhury, A. (2012). Secretion of soluble vascular endothelial growth factor receptor 1 (sVEGFR1/sFlt1) requires Arf1, Arf6, and Rab11 GTPases. *PLoS One* 7:e44572. doi: 10.1371/journal.pone.0044572
- Kajimoto, T., Mohamed, N. N. I., Badawy, S. M. M., Matovelo, S. A., Hirase, M., Nakamura, S., et al. (2018). Involvement of Gbetagamma subunits of Gi protein coupled with S1P receptor on multivesicular endosomes in F-actin formation and cargo sorting into exosomes. *J. Biol. Chem.* 293, 245–253. doi: 10.1074/jbc.M117.808733
- Kjos, I., Vestre, K., Guadagno, N. A., Borg Distefano, M., and Progidia, C. (2018). Rab and Arf proteins at the crossroad between membrane transport and cytoskeleton dynamics. *Biochim. Biophys. Acta Mol. Cell Res.* 1865, 1397–1409. doi: 10.1016/j.bbamcr.2018.07.009
- Kobayashi, H., and Fukuda, M. (2012). Rab35 regulates Arf6 activity through centaurin-beta2 (ACAP2) during neurite outgrowth. *J. Cell Sci.* 125(Pt 9), 2235–2243. doi: 10.1242/jcs.098657
- Kondo, Y., Hanai, A., Nakai, W., Katoh, Y., Nakayama, K., and Shin, H. W. (2012). ARF1 and ARF3 are required for the integrity of recycling endosomes and the recycling pathway. *Cell Struct. Funct.* 37, 141–154. doi: 10.1247/csf.12015
- Korolchuk, V. I., Saiki, S., Lichtenberg, M., Siddiqi, F. H., Roberts, E. A., Imarisio, S., et al. (2011). Lysosomal positioning coordinates cellular nutrient responses. *Nat. Cell Biol.* 13, 453–460. doi: 10.1038/ncb2204
- Kovacevic, I., Sakaue, T., Majolee, J., Pronk, M. C., Maekawa, M., Geerts, D., et al. (2018). The Cullin-3-Rbx1-KCTD10 complex controls endothelial barrier function via K63 ubiquitination of RhoB. *J. Cell Biol.* 217, 1015–1032. doi: 10.1083/jcb.201606055
- Kucera, A., Borg Distefano, M., Berg-Larsen, A., Skjeldal, F., Repnik, U., Bakke, O., et al. (2016). Spatiotemporal resolution of Rab9 and CI-MPR dynamics in the endocytic pathway. *Traffic* 17, 211–229. doi: 10.1111/tra.12357
- Lachance, V., Degrandmaison, J., Marois, S., Robitaille, M., Genier, S., Nadeau, S., et al. (2014). Ubiquitylation and activation of a Rab GTPase is promoted by a beta(2)AR-HACE1 complex. *J. Cell Sci.* 127(Pt 1), 111–123. doi: 10.1242/jcs.132944
- Langemeyer, L., Borchers, A. C., Herrmann, E., Fullbrunn, N., Han, Y., Perz, A., et al. (2020). A conserved and regulated mechanism drives endosomal Rab transition. *Elife* 9:e56090. doi: 10.7554/eLife.56090
- Lawrence, J. T., and Birnbaum, M. J. (2003). ADP-ribosylation factor 6 regulates insulin secretion through plasma membrane phosphatidylinositol 4,5-bisphosphate. *Proc. Natl. Acad. Sci. U. S. A.* 100, 13320–13325. doi: 10.1073/pnas.2232129100
- Li, B., Antonyak, M. A., Zhang, J., and Cerione, R. A. (2012). RhoA triggers a specific signaling pathway that generates transforming microvesicles in cancer cells. *Oncogene* 31, 4740–4749. doi: 10.1038/onc.2011.636
- Li, C., Wei, Z., Fan, Y., Huang, W., Su, Y., Li, H., et al. (2017). The GTPase Rab43 controls the anterograde ER-golgi trafficking and sorting of GPCRs. *Cell Rep.* 21, 1089–1101. doi: 10.1016/j.celrep.2017.10.011
- Li, H., Wang, Z., Zhang, W., Qian, K., Xu, W., and Zhang, S. (2016). Fbxw7 regulates tumor apoptosis, growth arrest and the epithelial-to-mesenchymal transition in part through the RhoA signaling pathway in gastric cancer. *Cancer Lett.* 370, 39–55. doi: 10.1016/j.canlet.2015.10.006
- Li, J., Chai, Q. Y., and Liu, C. H. (2016). The ubiquitin system: a critical regulator of innate immunity and pathogen-host interactions. *Cell Mol. Immunol.* 13, 560–576. doi: 10.1038/cmi.2016.40
- Li, L., Kim, E., Yuan, H., Inoki, K., Goraksha-Hicks, P., Schiesher, R. L., et al. (2010). Regulation of mTORC1 by the Rab and Arf GTPases. *J. Biol. Chem.* 285, 19705–19709. doi: 10.1074/jbc.C110.102483
- Lipatova, Z., Belogortseva, N., Zhang, X. Q., Kim, J., Taussig, D., and Segev, N. (2012). Regulation of selective autophagy onset by a Ypt/Rab GTPase module. *Proc. Natl. Acad. Sci. U. S. A.* 109, 6981–6986. doi: 10.1073/pnas.1121299109
- Liu, C. C., Zhang, Y. N., Li, Z. Y., Hou, J. X., Zhou, J., Kan, L., et al. (2017). Rab5 and Rab11 are required for clathrin-dependent endocytosis of Japanese encephalitis virus in BHK-21 cells. *J. Virol.* 91, e01113–e01117. doi: 10.1128/JVI.01113-17



- Liu, S., Hunt, L., and Storrie, B. (2013). Rab41 is a novel regulator of Golgi apparatus organization that is needed for ER-to-Golgi trafficking and cell growth. *PLoS One* 8:e71886. doi: 10.1371/journal.pone.0071886
- Longatti, A., Lamb, C. A., Razi, M., Yoshimura, S., Barr, F. A., and Tooze, S. A. (2012). TBC1D14 regulates autophagosome formation via Rab11- and ULK1-positive recycling endosomes. *J. Cell Biol.* 197, 659–675. doi: 10.1083/jcb.201111079
- Luna, A., Matas, O. B., Martinez-Menarguez, J. A., Mato, E., Duran, J. M., Ballesta, J., et al. (2002). Regulation of protein transport from the Golgi complex to the endoplasmic reticulum by CDC42 and N-WASP. *Mol. Biol. Cell* 13, 866–879. doi: 10.1091/mbc.01-12-0579
- Lund, V. K., Madsen, K. L., and Kjaerulf, O. (2018). Drosophila Rab2 controls endosome-lysosome fusion and LAMP delivery to late endosomes. *Autophagy* 14, 1520–1542. doi: 10.1080/15548627.2018.1458170
- Matsui, T., and Fukuda, M. (2013). Rab12 regulates mTORC1 activity and autophagy through controlling the degradation of amino-acid transporter PAT4. *EMBO Rep.* 14, 450–457. doi: 10.1038/embor.2013.32
- Mauvezin, C., Neisch, A. L., Ayala, C. I., Kim, J., Beltrame, A., Braden, C. R., et al. (2016). Coordination of autophagosome-lysosome fusion and transport by a Klp98A-Rab14 complex in Drosophila. *J. Cell Sci.* 129, 971–982. doi: 10.1242/jcs.175224
- Maziveyi, M., Dong, S., Baranwal, S., Mehrnezhad, A., Rathinam, R., Huckaba, T. M., et al. (2019). Exosomes from nischarin-expressing cells reduce breast cancer cell motility and tumor growth. *Cancer Res.* 79, 2152–2166. doi: 10.1158/0008-5472.CAN-18-0842
- Mochizuki, Y., Ohashi, R., Kawamura, T., Iwanari, H., Kodama, T., Naito, M., et al. (2013). Phosphatidylinositol 3-phosphatase myotubularin-related protein 6 (MTMR6) is regulated by small GTPase Rab1B in the early secretory and autophagic pathways. *J. Biol. Chem.* 288, 1009–1021. doi: 10.1074/jbc.M112.395087
- Moreau, K., Ravikumar, B., Puri, C., and Rubinsztein, D. C. (2012). Arf6 promotes autophagosome formation via effects on phosphatidylinositol 4,5-bisphosphate and phospholipase D. *J. Cell Biol.* 196, 483–496. doi: 10.1083/jcb.201110114
- Moyer, B. D., Allan, B. B., and Balch, W. E. (2001). Rab1 interaction with a GM130 effector complex regulates COPII vesicle cis-Golgi tethering. *Traffic* 2, 268–276. doi: 10.1034/j.1600-0854.2001.10007.x
- Munro, P., Flatau, G., Doye, A., Boyer, L., Oregioni, O., Mege, J. L., et al. (2004). Activation and proteasomal degradation of rho GTPases by cytotoxic necrotizing factor-1 elicit a controlled inflammatory response. *J. Biol. Chem.* 279, 35849–35857. doi: 10.1074/jbc.M401580200
- Murali, A., Shin, J., Yurugi, H., Krishnan, A., Akutsu, M., Carpy, A., et al. (2017). Ubiquitin-dependent regulation of Cdc42 by XIAP. *Cell Death Dis.* 8:e2900. doi: 10.1038/cddis.2017.305
- Nakai, W., Kondo, Y., Saitoh, A., Naito, T., Nakayama, K., and Shin, H. W. (2013). ARF1 and ARF4 regulate recycling endosomal morphology and retrograde transport from endosomes to the Golgi apparatus. *Mol. Biol. Cell* 24, 2570–2581. doi: 10.1091/mbc.E13-04-0197
- Nakajima, K., Nozawa, T., Minowa-Nozawa, A., Toh, H., Yamada, S., Aikawa, C., et al. (2019). RAB30 regulates PI4KB (phosphatidylinositol 4-kinase beta)-dependent autophagy against group A Streptococcus. *Autophagy* 15, 466–477. doi: 10.1080/15548627.2018.1532260
- Nakano, A., and Muramatsu, M. (1989). A novel GTP-binding protein, Sar1p, is involved in transport from the endoplasmic reticulum to the Golgi apparatus. *J. Cell Biol.* 109(6 Pt 1), 2677–2691. doi: 10.1083/jcb.109.6.2677
- Nakatogawa, H. (2020). Mechanisms governing autophagosome biogenesis. *Nat. Rev. Mol. Cell Biol.* 21, 439–458. doi: 10.1038/s41580-020-0241-0
- Neyraud, V., Aushev, V. N., Hatzoglou, A., Meunier, B., Cascone, I., and Camonis, J. (2012). RalA and RalB proteins are ubiquitinated GTPases, and ubiquitinated RalA increases lipid raft exposure at the plasma membrane. *J. Biol. Chem.* 287, 29397–29405. doi: 10.1074/jbc.M112.357764
- Nishida, Y., Arakawa, S., Fujitani, K., Yamaguchi, H., Mizuta, T., Kanaseki, T., et al. (2009). Discovery of Atg5/Atg7-independent alternative macroautophagy. *Nature* 461, 654–658. doi: 10.1038/nature08455
- Nishida-Fukuda, H. (2019). The exocyst: dynamic machine or static tethering complex? *Bioessays* 41:e1900056. doi: 10.1002/bies.201900056
- Nozawa, T., Aikawa, C., Goda, A., Maruyama, F., Hamada, S., and Nakagawa, I. (2012). The small GTPases Rab9A and Rab23 function at distinct steps in autophagy during Group A Streptococcus infection. *Cell Microbiol.* 14, 1149–1165. doi: 10.1111/j.1462-5822.2012.01792.x
- Obero, T. K., Dogan, T., Hocking, J. C., Scholz, R. P., Mooz, J., Anderson, C. L., et al. (2012). IAPs regulate the plasticity of cell migration by directly targeting Rac1 for degradation. *EMBO J.* 31, 14–28. doi: 10.1038/emboj.2011.423
- Olayioye, M. A., Noll, B., and Hauser, A. (2019). Spatiotemporal control of intracellular membrane trafficking by Rho GTPases. *Cells* 8:1478. doi: 10.3390/cells8121478
- Ostrowski, M., Carmo, N. B., Krumeich, S., Fanget, I., Raposo, G., Savina, A., et al. (2010). Rab27a and Rab27b control different steps of the exosome secretion pathway. *Nat. Cell Biol.* 12, su11–su13. doi: 10.1038/ncb2000
- Park, S. Y., Yang, J. S., Schmider, A. B., Soberman, R. J., and Hsu, V. W. (2015). Coordinated regulation of bidirectional COPI transport at the Golgi by CDC42. *Nature* 521, 529–532. doi: 10.1038/nature14457
- Pathak, R., and Dermardirossian, C. (2013). GEF-H1: orchestrating the interplay between cytoskeleton and vesicle trafficking. *Small GTPases* 4, 174–179. doi: 10.4161/sgtp.24616
- Pelletan, L. E., Suhaiman, L., Vaquer, C. C., Bustos, M. A., De Blas, G. A., Vitale, N., et al. (2015). ADP ribosylation factor 6 (ARF6) promotes acrosomal exocytosis by modulating lipid turnover and Rab3A activation. *J. Biol. Chem.* 290, 9823–9841. doi: 10.1074/jbc.M114.629006
- Pfeffer, S. R. (2017). Rab GTPases: master regulators that establish the secretory and endocytic pathways. *Mol. Biol. Cell* 28, 712–715. doi: 10.1091/mbc.E16-10-0737
- Pohl, C., and Dikic, I. (2019). Cellular quality control by the ubiquitin-proteasome system and autophagy. *Science* 366, 818–822. doi: 10.1126/science.aax3769
- Poteryaev, D., Datta, S., Ackema, K., Zerial, M., and Spang, A. (2010). Identification of the switch in early-to-late endosome transition. *Cell* 141, 497–508. doi: 10.1016/j.cell.2010.03.011
- Puri, C., Vicinanza, M., Ashkenazi, A., Gratian, M. J., Zhang, Q., Bento, C. F., et al. (2018). The RAB11A-positive compartment is a primary platform for autophagosome assembly mediated by WIP1 recognition of PI3P-RAB11A. *Dev. Cell* 45, 114–131.e8. doi: 10.1016/j.devcel.2018.03.008
- Qiu, J., Sheedlo, M. J., Yu, K., Tan, Y., Nakayasu, E. S., Das, C., et al. (2016). Ubiquitination independent of E1 and E2 enzymes by bacterial effectors. *Nature* 533, 120–124. doi: 10.1038/nature17657
- Qu, L., Pan, C., He, S. M., Lang, B., Gao, G. D., Wang, X. L., et al. (2019). The ras superfamily of Small GTPases in non-neoplastic cerebral diseases. *Front. Mol. Neurosci.* 12:121. doi: 10.3389/fnmol.2019.00121
- Ramirez, C., Hauser, A. D., Vucic, E. A., and Bar-Sagi, D. (2019). Plasma membrane V-ATPase controls oncogenic RAS-induced macropinocytosis. *Nature* 576, 477–481. doi: 10.1038/s41586-019-1831-x
- Riederer, M. A., Soldati, T., Shapiro, A. D., Lin, J., and Pfeffer, S. R. (1994). Lysosome biogenesis requires Rab9 function and receptor recycling from endosomes to the trans-Golgi network. *J. Cell Biol.* 125, 573–582. doi: 10.1083/jcb.125.3.573
- Rodrigo-Brenni, M. C., Gutierrez, E., and Hegde, R. S. (2014). Cytosolic quality control of mislocalized proteins requires RNF126 recruitment to Bag6. *Mol. Cell* 55, 227–237. doi: 10.1016/j.molcel.2014.05.025
- Rodriguez-Gabin, A. G., Cammer, M., Almazan, G., Charron, M., and Larocca, J. N. (2001). Role of rRAB22b, an oligodendrocyte protein, in regulation of transport of vesicles from trans Golgi to endocytic compartments. *J. Neurosci. Res.* 66, 1149–1160. doi: 10.1002/jnr.1253
- Rosa-Ferreira, C., Christis, C., Torres, I. L., and Munro, S. (2015). The small G protein Arl5 contributes to endosome-to-Golgi traffic by aiding the recruitment of the GARP complex to the Golgi. *Biol. Open* 4, 474–481. doi: 10.1242/bio.201410975
- Saito, T., Nah, J., Oka, S. I., Mukai, R., Monden, Y., Maejima, Y., et al. (2019). An alternative mitophagy pathway mediated by Rab9 protects the heart against ischemia. *J. Clin. Invest.* 129, 802–819. doi: 10.1172/JCI122035
- Sancak, Y., Peterson, T. R., Shaul, Y. D., Lindquist, R. A., Thoreen, C. C., Bar-Peled, L., et al. (2008). The Rag GTPases bind raptor and mediate amino acid signaling to mTORC1. *Science* 320, 1496–1501. doi: 10.1126/science.1157535
- Sapmaz, A., Berlin, I., Bos, E., Wijdeven, R. H., Janssen, H., Konietzny, R., et al. (2019). USP32 regulates late endosomal transport and recycling through deubiquitination of Rab7. *Nat. Commun.* 10:1454. doi: 10.1038/s41467-019-09437-x



- Serafini, T., Orci, L., Amherdt, M., Brunner, M., Kahn, R. A., and Rothman, J. E. (1991). ADP-ribosylation factor is a subunit of the coat of Golgi-derived COP-coated vesicles: a novel role for a GTP-binding protein. *Cell* 67, 239–253. doi: 10.1016/0092-8674(91)90176-y
- Seto, S., Sugaya, K., Tsujimura, K., Nagata, T., Horii, T., and Koide, Y. (2013). Rab39a interacts with phosphatidylinositol 3-kinase and negatively regulates autophagy induced by lipopolysaccharide stimulation in macrophages. *PLoS One* 8:e83324. doi: 10.1371/journal.pone.0083324
- Sheng, Y., Song, Y., Li, Z., Wang, Y., Lin, H., Cheng, H., et al. (2018). RAB37 interacts directly with ATG5 and promotes autophagosome formation via regulating ATG5-12-16 complex assembly. *Cell Death Differ.* 25, 918–934. doi: 10.1038/s41418-017-0023-1
- Shi, A., Liu, O., Koenig, S., Banerjee, R., Chen, C. C., Eimer, S., et al. (2012). RAB-10-GTPase-mediated regulation of endosomal phosphatidylinositol-4,5-bisphosphate. *Proc. Natl. Acad. Sci. U. S. A.* 109, E2306–E2315. doi: 10.1073/pnas.1205278109
- Shi, B. J., Liu, C. C., Zhou, J., Wang, S. Q., Gao, Z. C., Zhang, X. M., et al. (2016). Entry of classical swine fever virus into PK-15 cells via a pH-, Dynamin-, and cholesterol-dependent, clathrin-mediated endocytic pathway that requires Rab5 and Rab7. *J. Virol.* 90, 9194–9208. doi: 10.1128/JVI.00688-16
- Shin, D., Na, W., Lee, J. H., Kim, G., Baek, J., Park, S. H., et al. (2017). Site-specific monoubiquitination downregulates Rab5 by disrupting effector binding and guanine nucleotide conversion. *Elife* 6:e29154. doi: 10.7554/eLife.29154
- Shinde, S. R., and Maddika, S. (2018). Post translational modifications of Rab GTPases. *Small GTPases* 9, 49–56. doi: 10.1080/21541248.2017.1299270
- Simicek, M., Lievens, S., Laga, M., Guzenko, D., Aushev, V. N., Kaleb, P., et al. (2013). The deubiquitylase USP33 discriminates between RALB functions in autophagy and innate immune response. *Nat. Cell Biol.* 15, 1220–1230. doi: 10.1038/ncb2847
- Song, L., Tang, S., Han, X., Jiang, Z., Dong, L., Liu, C., et al. (2019). KIBRA controls exosome secretion via inhibiting the proteasomal degradation of Rab27a. *Nat. Commun.* 10:1639. doi: 10.1038/s41467-019-09720-x
- Song, P., Trajkovic, K., Tsunemi, T., and Krainc, D. (2016). Parkin modulates endosomal organization and function of the endo-lysosomal pathway. *J. Neurosci.* 36, 2425–2437. doi: 10.1523/JNEUROSCI.2569-15.2016
- Soreng, K., Neufeld, T. P., and Simonsen, A. (2018). Membrane trafficking in autophagy. *Int. Rev. Cell Mol. Biol.* 336, 1–92. doi: 10.1016/bs.ircmb.2017.07.001
- Stenmark, H. (2009). Rab GTPases as coordinators of vesicle traffic. *Nat. Rev. Mol. Cell Biol.* 10, 513–525. doi: 10.1038/nrm2728
- Stenmark, H., Parton, R. G., Steele-Mortimer, O., Lutcke, A., Gruenberg, J., and Zerial, M. (1994). Inhibition of rab5 GTPase activity stimulates membrane fusion in endocytosis. *EMBO J.* 13, 1287–1296.
- Stroupe, C. (2018). This is the end: regulation of Rab7 nucleotide binding in endolysosomal trafficking and autophagy. *Front. Cell Dev. Biol.* 6:129. doi: 10.3389/fcell.2018.00129
- Su, H., Liu, B., Frohlich, O., Ma, H., Sands, J. M., and Chen, G. (2013). Small GTPase Rab14 down-regulates UT-A1 urea transport activity through enhanced clathrin-dependent endocytosis. *FASEB J.* 27, 4100–4107. doi: 10.1096/fj.13-229294
- Sun, C., Wang, P., Dong, W., Liu, H., Sun, J., and Zhao, L. (2020). LncRNA PVT1 promotes exosome secretion through YKT6, RAB7, and VAMP3 in pancreatic cancer. *Aging (Albany NY)* 12, 10427–10440. doi: 10.18632/aging.103268
- Szatmari, Z., Kis, V., Lippai, M., Hegedus, K., Farago, T., Lorincz, P., et al. (2014). Rab11 facilitates cross-talk between autophagy and endosomal pathway through regulation of Hook localization. *Mol. Biol. Cell* 25, 522–531. doi: 10.1091/mbc.E13-10-0574
- Takahashi, T., Minami, S., Tsuchiya, Y., Tajima, K., Sakai, N., Suga, K., et al. (2019). Cytoplasmic control of Rab family small GTPases through BAG6. *EMBO Rep.* 20:e46794. doi: 10.15252/embr.201846794
- Tian, M., Bai, C., Lin, Q., Lin, H., Liu, M., Ding, F., et al. (2011). Binding of RhoA by the C2 domain of E3 ligase Smurf1 is essential for Smurf1-regulated RhoA ubiquitination and cell protrusive activity. *FEBS Lett.* 585, 2199–2204. doi: 10.1016/j.febslet.2011.06.016
- Torrino, S., Visvikis, O., Doye, A., Boyer, L., Stefani, C., Munro, P., et al. (2011). The E3 ubiquitin-ligase HACE1 catalyzes the ubiquitylation of active Rac1. *Dev. Cell* 21, 959–965. doi: 10.1016/j.devcel.2011.08.015
- Tuli, A., Thiery, J., James, A. M., Michelet, X., Sharma, M., Garg, S., et al. (2013). Arf-like GTPase Arl8b regulates lytic granule polarization and natural killer cell-mediated cytotoxicity. *Mol. Biol. Cell* 24, 3721–3735. doi: 10.1091/mbc.E13-05-0259
- van der Vaart, A., Griffith, J., and Reggiori, F. (2010). Exit from the Golgi is required for the expansion of the autophagosomal phagophore in yeast *Saccharomyces cerevisiae*. *Mol. Biol. Cell* 21, 2270–2284. doi: 10.1091/mbc.E09-04-0345
- Vignal, E., Blangy, A., Martin, M., Gauthier-Rouviere, C., and Fort, P. (2001). Kinectin is a key effector of RhoG microtubule-dependent cellular activity. *Mol. Cell Biol.* 21, 8022–8034. doi: 10.1128/MCB.21.23.8022-8034.2001
- Villarroel-Campos, D., Henriquez, D. R., Bodaleo, F. J., Oguchi, M. E., Bronfman, F. C., Fukuda, M., et al. (2016). Rab35 functions in axon elongation are regulated by P53-related protein kinase in a mechanism that involves Rab35 protein degradation and the microtubule-associated protein 1B. *J. Neurosci.* 36, 7298–7313. doi: 10.1523/JNEUROSCI.4064-15.2016
- Visvikis, O., Boyer, L., Torrino, S., Doye, A., Lemonnier, M., Lores, P., et al. (2011). *Escherichia coli* producing CNF1 toxin hijacks Tollip to trigger Rac1-dependent cell invasion. *Traffic* 12, 579–590. doi: 10.1111/j.1600-0854.2011.01174.x
- Waguri, S., Dewitte, F., Le Borgne, R., Rouille, Y., Uchiyama, Y., Dubremetz, J. F., et al. (2003). Visualization of TGN to endosome trafficking through fluorescently labeled MPR and AP-1 in living cells. *Mol. Biol. Cell* 14, 142–155. doi: 10.1091/mbc.e02-06-0338
- Wandinger-Ness, A., and Zerial, M. (2014). Rab proteins and the compartmentalization of the endosomal system. *Cold Spring Harb. Perspect. Biol.* 6:a022616. doi: 10.1101/cshperspect.a022616
- Wang, H. R., Zhang, Y., Ozdamar, B., Ogunjimi, A. A., Alexandrova, E., Thomsen, G. H., et al. (2003). Regulation of cell polarity and protrusion formation by targeting RhoA for degradation. *Science* 302, 1775–1779. doi: 10.1126/science.1090772
- Wang, M., Guo, L., Wu, Q., Zeng, T., Lin, Q., Qiao, Y., et al. (2014). ATR/Chk1/Smurf1 pathway determines cell fate after DNA damage by controlling RhoB abundance. *Nat. Commun.* 5:4901. doi: 10.1038/ncomms5901
- Wang, T., and Hong, W. (2002). Interorganellar regulation of lysosome positioning by the Golgi apparatus through Rab34 interaction with Rab-interacting lysosomal protein. *Mol. Biol. Cell* 13, 4317–4332. doi: 10.1091/mbc.e02-05-0280
- Wei, D., Zhan, W., Gao, Y., Huang, L., Gong, R., Wang, W., et al. (2021). RAB31 marks and controls an ESCRT-independent exosome pathway. *Cell Res.* 31, 157–177. doi: 10.1038/s41422-020-00409-1
- Wei, J., Mialki, R. K., Dong, S., Khoo, A., Mallampalli, R. K., Zhao, Y., et al. (2013). A new mechanism of RhoA ubiquitination and degradation: roles of SCF(FBLX19) E3 ligase and Erk2. *Biochim. Biophys. Acta* 1833, 2757–2764. doi: 10.1016/j.bbamcr.2013.07.005
- Wennerberg, K., Rossman, K. L., and Der, C. J. (2005). The Ras superfamily at a glance. *J. Cell Sci.* 118(Pt 5), 843–846. doi: 10.1242/jcs.01660
- Woolery, A. R., Yu, X., LaBaer, J., and Orth, K. (2014). AMPylation of Rho GTPases subverts multiple host signaling processes. *J. Biol. Chem.* 289, 32977–32988. doi: 10.1074/jbc.M114.601310
- Wu, B., and Guo, W. (2015). The exocyst at a glance. *J. Cell Sci.* 128, 2957–2964. doi: 10.1242/jcs.156398
- Xu, J., Li, L., Yu, G., Ying, W., Gao, Q., Zhang, W., et al. (2015). The neddylation-cullin 2-RBX1 E3 ligase axis targets tumor suppressor RhoB for degradation in liver cancer. *Mol. Cell Proteomics* 14, 499–509. doi: 10.1074/mcp.M114.045211
- Xu, Y., Liu, Y., Lee, J. G., and Ye, Y. (2013). A ubiquitin-like domain recruits an oligomeric chaperone to a retrotranslocation complex in endoplasmic reticulum-associated degradation. *J. Biol. Chem.* 288, 18068–18076. doi: 10.1074/jbc.M112.449199
- Yang, S., and Rosenwald, A. G. (2016). Autophagy in *Saccharomyces cerevisiae* requires the monomeric GTP-binding proteins, Arl1 and Ypt6. *Autophagy* 12, 1721–1737. doi: 10.1080/15548627.2016.1196316
- Yu, C. J., and Lee, F. J. (2017). Multiple activities of Arl1 GTPase in the trans-Golgi network. *J. Cell Sci.* 130, 1691–1699. doi: 10.1242/jcs.201319
- Yu, L., Chen, Y., and Tooze, S. A. (2018). Autophagy pathway: cellular and molecular mechanisms. *Autophagy* 14, 207–215. doi: 10.1080/15548627.2017.1378838
- Zhao, J., Mialki, R. K., Wei, J., Coon, T. A., Zou, C., Chen, B. B., et al. (2013). SCF E3 ligase F-box protein complex SCF(FBLX19) regulates cell migration by mediating Rac1 ubiquitination and degradation. *FASEB J.* 27, 2611–2619. doi: 10.1096/fj.12-223099

- Zhou, F., Wu, Z., Zhao, M., Murtazina, R., Cai, J., Zhang, A., et al. (2019). Rab5-dependent autophagosome closure by ESCRT. *J. Cell Biol.* 218, 1908–1927. doi: 10.1083/jcb.201811173
- Zoppino, F. C., Militello, R. D., Slavin, I., Alvarez, C., and Colombo, M. I. (2010). Autophagosome formation depends on the small GTPase Rab1 and functional ER exit sites. *Traffic* 11, 1246–1261. doi: 10.1111/j.1600-0854.2010.01086.x
- Zuk, P. A., and Elferink, L. A. (1999). Rab15 mediates an early endocytic event in Chinese hamster ovary cells. *J. Biol. Chem.* 274, 22303–22312. doi: 10.1074/jbc.274.32.22303

**Conflict of Interest:** The authors declare that the research was conducted in the absence of any commercial or financial relationships that could be construed as a potential conflict of interest.

Copyright © 2021 Lei, Wang, Zhang and Liu. This is an open-access article distributed under the terms of the Creative Commons Attribution License (CC BY). The use, distribution or reproduction in other forums is permitted, provided the original author(s) and the copyright owner(s) are credited and that the original publication in this journal is cited, in accordance with accepted academic practice. No use, distribution or reproduction is permitted which does not comply with these terms.



# Light-Controllable PROTACs for Temporospatial Control of Protein Degradation

Jing Liu<sup>†</sup>, Yunhua Peng<sup>†</sup> and Wenyi Wei<sup>\*</sup>

Department of Pathology, Beth Israel Deaconess Medical Center, Harvard Medical School, Boston, MA, United States

## OPEN ACCESS

### Edited by:

Yu Rao,  
Tsinghua University, China

### Reviewed by:

Tae Ho Lee,  
Fujian Medical University, China  
Catherine Lindon,  
University of Cambridge,  
United Kingdom

### \*Correspondence:

Wenwei Wei  
wwwei2@bidmc.harvard.edu

<sup>†</sup>These authors have contributed  
equally to this work

### Specialty section:

This article was submitted to  
Cell Growth and Division,  
a section of the journal  
Frontiers in Cell and Developmental  
Biology

**Received:** 08 March 2021

**Accepted:** 14 June 2021

**Published:** 19 July 2021

### Citation:

Liu J, Peng Y and Wei W (2021)  
Light-Controllable PROTACs  
for Temporospatial Control of Protein  
Degradation.  
Front. Cell Dev. Biol. 9:678077.  
doi: 10.3389/fcell.2021.678077

PROteolysis-TArgeting Chimeras (PROTACs) is an emerging and promising approach to target intracellular proteins for ubiquitination-mediated degradation, including those so-called undruggable protein targets, such as transcriptional factors and scaffold proteins. To date, plenty of PROTACs have been developed to degrade various disease-relevant proteins, such as estrogen receptor (ER), androgen receptor (AR), RTK, and CDKs. However, the on-target off-tissue and off-target effect is one of the major limitation that prevents the usage of PROTACs in clinic. To this end, we and several other groups have recently developed light-controllable PROTACs, as the representative for the third generation controllable PROTACs, by using either photo-caging or photo-switch approaches. In this review, we summarize the emerging light-controllable PROTACs and the prospective for other potential ways to achieve temporospatial control of PROTACs.

**Keywords:** ubiquitin, E3 ligase, PROTAC, tumorigenesis, light controllable

## INTRODUCTION

The ubiquitin-proteasome system (UPS) governs the degradation and turnover of protein, thus playing critical functions in many cellular processes including protein quality control, cell cycle progression, and cell signaling transduction (Komander and Rape, 2012; Pohl and Dikic, 2019). Catalyzed by the ubiquitin-activating enzyme (E1), the ubiquitin is transferred onto the ubiquitin-conjugating enzyme (E2), and eventually transferred onto protein target by the E3 ubiquitin ligase. The selectivity of the ubiquitination process on a protein substrate primarily relies on its recognition by a E3 ubiquitin ligase (Pickart, 2001; Bernassola et al., 2008; Zhou et al., 2013), through a short sequence motif on the protein substrate, known as degron (Mészáros et al., 2017; Kumar et al., 2020). For instance, the SCF<sup>β-TrCP</sup> E3 ligase recognizes the phospho-degron of DpSGXXpS/pT (X represents any amino acid, and p represents phosphorylation modification), and the von Hippel-Lindau (VHL) E3 ligase binds to substrates with the proline-hydroxyl-degron of LAP-OH (P-OH represents the hydroxylation on the proline). Based on the growing understanding about biological function of E3 ligase and UPS, PROteolysis TArgeting Chimera (PROTAC) emerges as a new pharmaceutical approach since 2001 (Sakamoto et al., 2001). By hijacking the endogenous UPS to specifically degrade proteins of interest (POI), PROTACs are theoretically capable of targeting any proteins in cells (Sakamoto, 2010; Neklesa et al., 2017; Churcher, 2018; Guo et al., 2019; Paiva and Crews, 2019). Of the three functional moieties in the PROTAC molecule, the E3 ligase-ligand is designed for recruiting endogenous E3 ubiquitin ligase, and the warhead part (or called target-recruiting ligand) determines the specificity of protein targets, while the linker region between them should be optimized to achieve best efficiency and specificity to degrade individual substrate, in a case-by-case manner (Figure 1; Flanagan and Neklesa, 2019; Pettersson and Crews, 2019).

The first generation of PROTACs take advantage of degron-derived peptides, such as phospho-peptides (Sakamoto et al., 2001, 2003) or hydroxyl-peptides (Schneekloth et al., 2004; Zhang et al., 2004; Rodriguez-Gonzalez et al., 2008), to recruit the endogenous  $\beta$ -TrCP or VHL E3 ubiquitin ligases, respectively. These peptide-based PROTACs have relatively high molecule weight, which limits their permeability into cells and their function as a *bona fide* drug. Moreover, peptide is unstable, and could only be injected into target cells, making them not practical in clinic. Recently, a modified version of peptide-based PROTAC, TD-PROTAC (Jiang et al., 2018), has been developed with better stability and cell-permeability, making it capable of degrading ER $\alpha$  *in vitro* and *in vivo*.

Besides these degron-derived peptides, small molecule inhibitors or binding partners have been developed for several E3 ligase, such as auxin for TIR E3 ligase (Dharmasiri et al., 2005), nutlin for mouse double minute 2 homolog (MDM2) E3 ligase (Vassilev et al., 2004). Based on these specific binding ligands of E3 ligases, the second generation small molecule PROTACs have been developed. In 2008, the first nutlin-based small molecule PROTAC has been developed to target androgen receptor (AR) for degradation in prostate cancer cells (Schneekloth et al., 2008). A recent study has shown that compared with VHL-based PROTACs, MDM2-based PROTACs might offer a synergistic anti-proliferative activity to cancer cells (Hines et al., 2019), in part due to the degradation of target protein bromodomain-containing protein 4 (BRD4), as well as the stabilization and accumulation of the tumor suppressor p53, a well-characterized endo-substrate of MDM2 (Chene, 2003). Several antagonists of cellular inhibitor of apoptosis protein 1 (cIAP1) E3 ligase, including bestatin (Sato et al., 2008), methyl bestatin (MeBS) (Sekine et al., 2008), MV1 (Varfolomeev et al., 2007) and LCL161 (Yang et al., 2016) have been reported to bind with cIAP1 and to promote its auto-ubiquitination and degradation. These small molecule antagonists have also been used in targeted protein degradation (TPD), also known as Specific and Non-genetic IAP-dependent Protein ERaser (SNIPER), to degrade many protein targets such as AR (Shibata et al., 2018), BCL-ABL (Demizu et al., 2016; Shibata et al., 2017; Shimokawa et al., 2017), BRDs (Ohoka et al., 2017b, 2019), Bruton's tyrosine kinase (BTK) (Tinworth et al., 2019), cellular retinoic acid-binding protein 2 (CRABP2) (Okuhira et al., 2017), estrogen receptor (ER) (Okuhira et al., 2013), and transforming acidic coiled-coil containing protein 3 (TACC3) (Ohoka et al., 2014, 2017a).

In 2010, pomalidomide and its analogs immunomodulatory imide drugs (IMiDs) have been defined as molecule glues to bind with the endogenous cereblon (CRBN) E3 ligase (Ito et al., 2010; Fischer et al., 2014), subsequently causing the proteasomal degradation of several neo-substrates, including IKZFs (Kronke et al., 2014; Lu et al., 2014), CK1 $\alpha$  (Kronke et al., 2015), GSPT1 (Matyskiela et al., 2016), SALL4 (Donovan et al., 2018), p63 (Asatsuma-Okumura et al., 2019) and ARID2 (Yamamoto et al., 2020). In 2015, IMiDs as ligands of the CRBN E3 ligase have been firstly used to develop CRBN-based PROTACs for the degradation of BRD4 and FKBP12 (Winter et al., 2015), and to date CRBN-based PROTACs have been applied to more than 30 different protein targets, for the treatment of cancer and

inflammation disease (**Supplementary Table 1**; Mullard, 2021), among which ARV-110 (Neklesa et al., 2018) (NCT03888612) and ARV471 (Flanagan et al., 2019) (NCT04072952) are in Phase I/II clinical trials for the treatment of prostate cancer (Petrylak et al., 2020) and breast cancer (BRCA), respectively. In 2012, the small molecule VHL ligand (VHL ligand 1) has been developed to specifically interact with VHL without an inhibitory effect to the tumor suppressive function of the VHL E3 ligase (Buckley et al., 2012a,b; Galdeano et al., 2014). Furthermore, several other modified VHL ligands have been developed, including the 1, 3-fluoro-4-hydroxyprolines and methyl-VHL ligand 1 (Testa et al., 2018). Using these small molecule VHL ligands, dozens small molecule VHL-based PROTACs have been developed to target intracellular proteins, including AR (Salami et al., 2018; Han et al., 2019) and ER (Hu et al., 2019; Kargbo, 2019; **Supplementary Table 1**).

Compared with small molecule inhibitors, PROTACs have several advantages. First, unlike typical reversible enzymatic inhibitors, active center or allosteric site of protein targets is not necessary for PROTACs, making it possible to target those so-called undruggable proteins. Second, PROTACs function in a catalytic manner, and the drug could be recycled after the protein target being degraded, making it more potent than small molecule inhibitors. However, the catalytic feature of PROTACs might also introduce potential higher toxicity to cells in part due to the off-tissue on-target effects and off-target effects (Raina et al., 2016; Moreau et al., 2020), which is one of the major limitation for their application in practice. For example, thalidomide has been approved in 1950s for treating morning sickness in pregnant women in Europe, which caused a tragedy that affects thousands of children with severe birth defects (Rehman et al., 2011). Until recent, the teratogenic effects is defined for CRBN-mediated degradation of p63 (Asatsuma-Okumura et al., 2019) and SALL4 (Donovan et al., 2018). Besides, more and more CRBN neo-substrates of IMiDs have been reported, including IKZFs (Kronke et al., 2014; Lu et al., 2014), CK1 $\alpha$  (Kronke et al., 2015), GSPT1 (Matyskiela et al., 2016), ARID2 (Yamamoto et al., 2020), RNF166 (You et al., 2020), ZNF827, and ZFP91 (Zorba et al., 2018). Furthermore, the subcutaneous injection of BRD4 degrader ARV-771 in xenograft tumor mice causes noticeable skin discoloration (Raina et al., 2016), which is consistent with the phenotype of *Brd4* depleted mice (Bolden et al., 2014). Thus, next generation of PROTACs should at least have the property to distinguish target versus non-target tissues/cells to alleviate its toxicity issue.

## THE THIRD GENERATION PROTACS WITH TARGETING DELIVERY AND/OR CONTROLLABLE ACTIVATION

One way to achieve targeted degradation of protein is to specifically deliver PROTACs into cancer cells, by taking advantage of the receptors expressed on the membrane of cancer cells, but not of normal cells. Recently, the antibody drug-conjugate (ADC) approach has been adopted for delivering



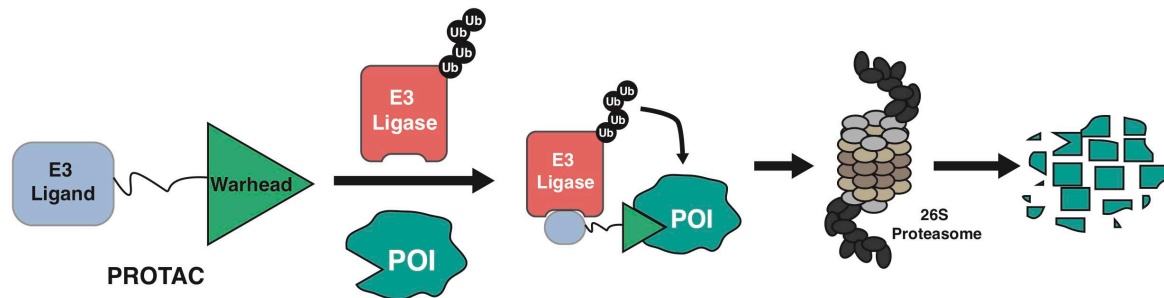


**FIGURE 1** | A schematic diagram for the action model of PROTAC. PROTAC recruits endogenous E3 ligase to ubiquitinate protein of interests (POIs), thus promoting the subsequent degradation of POI by the 26S proteasome.

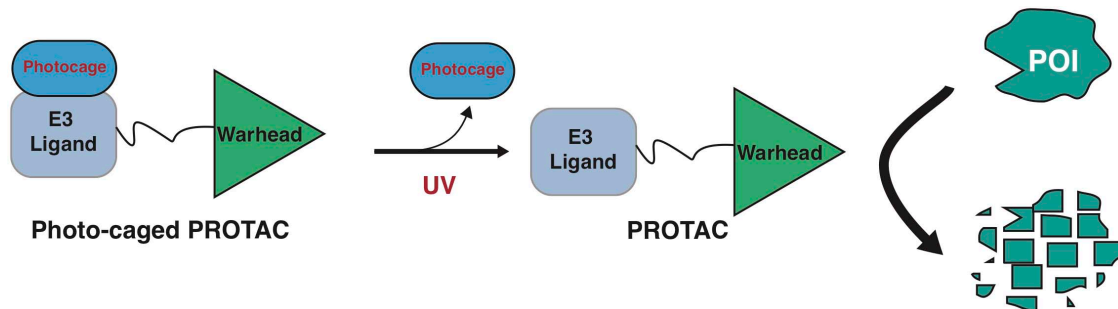


**FIGURE 2** | A schematic diagram for action model of photo-caged-PROTAC under control of UV illumination. The photo-caged-PROTAC is inert at beginning and activated by UV illumination, which leads to the release of the photocage group, thus enabling the degradation of POI in a controllable manner.

PROTACs into cancer cells that expressing cancer-specific membrane-anchored receptors, such as HER2 (Dragovich et al., 2020, 2021a,b; Maneiro et al., 2020; Pillow et al., 2020). A major disadvantage of antibody-conjugated PROTAC is its relatively high molecule weight and weak stability. Thus, we have recently developed a small molecule version of targeting delivery platform for PROTACs, namely folate-PROTAC (Liu et al., 2021), by conjugating a folate group on the hydroxyl group of VHL ligand, to specific deliver PROTACs into cancer cells that express relatively high levels of folate receptor  $\alpha$  (FOLR1) (Scaranti et al., 2020). Moreover, PROTACs that recruits cancer-specific E3 ligase might provide a way to achieve cancer-selective action of PROTACs (Nalawansa and Crews, 2020). For example, VHL-based PROTAC for BCL-xL is more tolerable than BCL-xL inhibitor ATB263, in part due to the relatively low expression of VHL in platelets than in cancer cells, thus reducing potential on-target toxicity (Khan et al., 2019). Several cancer specific or tissue specific E3 ligases have been recently identified (Schapira et al., 2019), however, none of these E3 ligase has ready-to-use small molecule binders yet, which prevents its further clinical development.

Another approach to achieve controllable protein degradation is to use an extraneous cellular signaling for the activation of PROTAC, such as by phosphoPROTACs (Hines et al., 2013). After stimulated with either nerve growth factor (NGF) or neuregulin, the two prototype phosphoPROTACs degraded fibroblast growth factor receptor substrate 2 $\alpha$  (FRS2 $\alpha$ ) or PI3K, respectively (Hines et al., 2013). The phosphoPROTACs

provide an option for controllable-PROTACs, but it still lacks tissue/cell specificity as these extraneous cues largely rely on universal receptors that are expressed in all cells regardless of normal or tumor cells. Recently, we and several other laboratories have independently developed light-controllable PROTACs, using either photo-cage or photo-switch approaches, which are widely used in photodynamic therapy (PDT) (Betha et al., 1999; Moore et al., 2009; Agostinis et al., 2011; Shafirstein et al., 2016). Here, we summarize these light-controllable PROTACs and discuss for the advantages and limits for their applications in clinic.

## PHOTO-CAGE ENABLES CONTROLLABLE PROTAC ACTIVATION TO DEGRADE PROTEINS IN TARGETING CELLS

### Photo-Cage and Photo-Cage Chemical Group

Photo-cage groups, also known as photoremovable protecting groups, provide a standard approach to spatially and temporally control the release of chemicals in cells. To date, several types of photo-cage groups have been develop for the purpose of controlled release of organic molecules (Klan et al., 2013). However, only a few types of photo-cage groups are available for caging small molecule drugs, in part due to the strict release

condition in water solution rather than other organic solution, such as methanol or ethanol (Klan et al., 2013). In the past few years, the development in biorthogonal chemistry prompts several photolabile groups for caging cellular molecules such as neurotransmitters, secondary messengers, and amino acids (Bardhan and Deiters, 2019), making it a powerful tool in biological studies. Taking advantage of these photo-cage groups, we and other groups have recently developed photo-caged PROTACs, which enable controllable activation of PROTACs in target cells (Xue et al., 2019; Liu et al., 2020; Naro et al., 2020; Figure 2).

## Photo-Cage Approach for CRBN-Based PROTACs

Further investigations on the crystal structure of CRBN and phthalimide complex indicate that the glutarimide NH in phthalimide is critical for its binding with CRBN, particularly for the backbone carbonyl of the His380 residual (Petzold et al., 2016; Sievers et al., 2018; Matyskiela et al., 2020). Caging of glutarimide NH with methyl or other groups completely abolish the ability of pomalidomide to bind with the CRBN E3 ligase, and methyl-PROTACs are usually used as negative controls during the designation of PROTACs (Bondeson et al., 2018; Zhang et al., 2018). There are several photo-caged CRBN-based PROTACs that have been reported, including opto-PROTAC (Liu et al., 2020), pc-PROTAC (Xue et al., 2019), and others (Naro et al., 2020; Figure 3).

By incorporated a reversible photo-cage group, nitroveratryloxycarbonyl (NVOC) on the glutarimide NH of pomalidomide, opto-pomalidomide is inert and loss the capability in degrading IKZFs in cells (Liu et al., 2020), thus might be suitable to be applied to any other CRBN-based PROTACs. Two prototype opto-PROTACs, opto-dBET1 and opto-dALK, are inert and could be activated only after illuminated with UVA ( $\lambda = 365$  nm) to degrade BRDs and ALK-fusion proteins, respectively (Liu et al., 2020). From another independent report, by using a similar photo-cage approach with NVOC, two pc-PROTACs prototypes, pc-PROTAC1 and pc-PROTAC3, degrade BRD4 and BTK, respectively, only after UVA illumination (Xue et al., 2019). Furthermore, by using a zebrafish model, they have validated the capability of pc-PROTAC1 in degrading endogenous BRDs under the control of UVA ( $\lambda = 365$  nm) *in vivo* (Xue et al., 2019). Moreover, another photo-cage group, 6-nitropiperonyloxymethyl (NPOM) has also been used to cage the glutarimide NH in dBET1, and the resulting photo-caged PROTAC could degrade BRD4 after being illuminated with UVA ( $\lambda = 402$  nm) (Naro et al., 2020). These studies together indicate that photo-cage on the glutarimide NH group could likely be an universal way for developing light-controllable PROTACs, and might be easily applied to other CRBN-based PROTACs in future studies.

## Photo-Cage Approaches for VHL-Based PROTACs

Apart from CRBN-based PROTACs, VHL-based PROTACs represent another major class of second-generation small

molecule PROTACs, and the photo-cage approach has also been used in VHL-based PROTACs (Figure 4). In a recent study, a photocleavable 4,5-dimethoxy-2-nitrobenzyl (DMNB) group has been incorporated onto the hydroxyl group of VHL ligand 1, and a prototype caged-PROTAC could degrade BRD4 after irradiation with UVA ( $\lambda = 365$  nm) (Kounde et al., 2020). In another independent study, the photo-cage group diethylamino coumarin (DEACM) has been used to cage the VHL ligand in VHL-based PROTAC against ERR $\alpha$ , and the resulting caged-PROTAC is inert and regains the ability to degrade ERR $\alpha$  after activated by UVA ( $\lambda = 360$  nm) (Naro et al., 2020). Given that the incorporation of photo-cage groups only affects the binding between PROTACs and the VHL E3 ligase, but not the protein substrate, those reported photo-cage methods could also be applied to other VHL-based PROTACs.

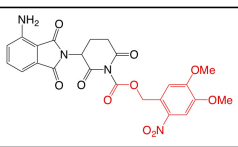
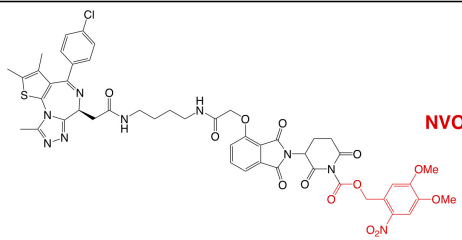
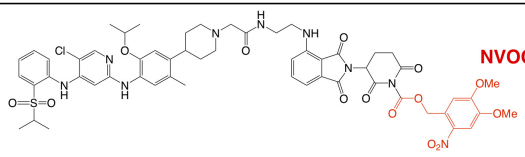
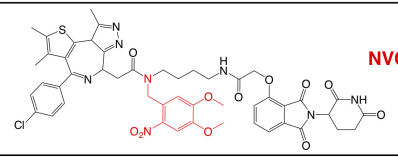
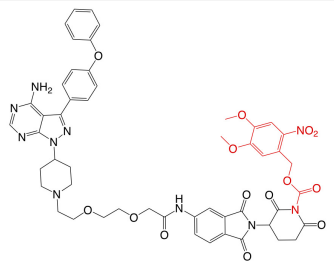
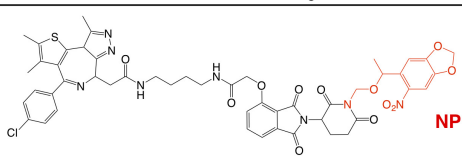
## PHOTO-SWITCH PROVIDE A REVERSIBLE ON/OFF SHIFT FOR PROTAC TO DEGRADE INTRACELLULAR PROTEINS IN TARGET CELLS

### Photo-Switchable Chemical Group in Biology

After entering target tissues/cells, focal UVA illumination leads to the release of activated PROTACs to be functional (Xue et al., 2019; Kounde et al., 2020; Liu et al., 2020; Naro et al., 2020). Activated PROTACs constantly degrade protein targets, and the degradation process will not stop before the clearance of PROTAC molecules. Thus, theoretically it should be better to add another OFF switch to inactivate the PROTACs, and the photo-switch provides a practical way. To this end, by taking advantage of the light-switchable azobenzene group or its analogs, several photo-switch PROTACs have been developed, including PHOTACs (Reynders et al., 2020), Azo-PROTACs (Jin et al., 2020) and photoPROTACs (Pfaff et al., 2019; Figures 5, 6).

### Photo-Switch PROTACs

Recently, several groups have utilized the photoswitch approach, i.e., azobenzene, to achieve photochemical isomerization of PROTAC molecules, and those photo-switch PROTACs could be reversibly turned on and off with light of different wave lengths (Reynders et al., 2020). By incorporating an azobenzene group in the linker region of pomalidomide-derived PROTACs, a type of light-inducible PROTACs, namely PHOTACs have developed. The two prototype PHOTACs remain in a *trans* inactive form in visible light ( $\lambda = 525$  nm), and could be switched on with UVA illumination ( $\lambda = 390$  nm), which leads to the conformation change to a *cis* active form, thus becoming capable of degrading BRDs and FKBP12, respectively. Furthermore, these PHOTACs could be turned off by visible light ( $\lambda = 525$  nm), where PHOTACs return to the *trans* inactive form (Reynders et al., 2020). Furthermore, a similar photoswitchable azobenzene-based approach has been adopted in CRBN-based PROTACs to develop Azo-PROTACs. The prototype Azo-PROTAC could be switch

Photo-caged PROTACs	Structure	Ref.
opto-pomalidomide	 NVOC	Liu et al., 2020
opto-dBET1	 NVOC	Liu et al., 2020
opto-dALK	 NVOC	Liu et al., 2020
pc-PROTAC1	 NVOC	Xue et al., 2019
pc-PROTAC3	 NVOC	Xue et al., 2019
NPOM-PROTAC	 NPOM	Naro et al., 2020

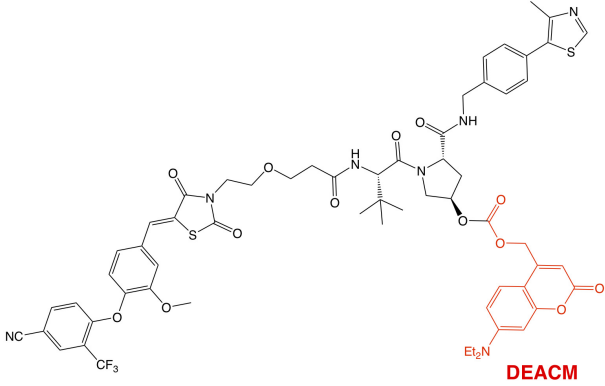
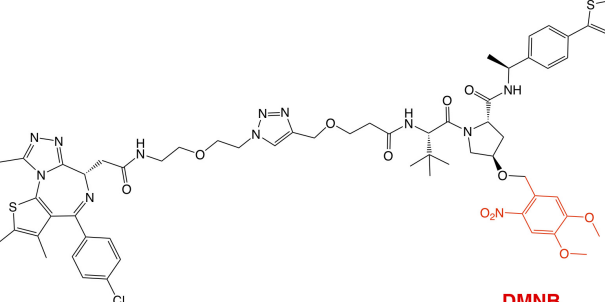
**FIGURE 3 |** Summary of photo-caged CRBN-based PROTACs. The photo-cage groups are marked in red. NVOC, nitroveratryloxycarbonyl; NPOM, 6-nitropiperonyloxymethyl.

between the *trans* active (ON) and the *cis* inactive (OFF) forms with either visible light or UV-C illumination, to ensure the light-controlled degradation of BCR-ABL fusion and ABL proteins in myelogenous leukemia K562 cells (Jin et al., 2020). Similarly, photo-switch could also be applied to VHL-based PROTAC. In another independent study, by using a similar photo-switch method to VHL-based PROTAC, photoPROTACs adopt the ortho-F4-azobenzene in the linker region between VHL ligand and warhead moiety against protein target (Pfaff et al., 2019). In contrast with PHOTACs, photoPROTACs remains as *cis* inactive form at beginning, and could be activated by UVA ( $\lambda = 415$  nm) to change into a *trans* active form. Further illuminated by visible light ( $\lambda = 530$  nm) could turn off the photoPROTAC,

and the prototype photoPROTAC-1 could be switched on and off to degrade BRDs in cells in a light-controllable manner (Pfaff et al., 2019).

## LIMITATIONS OF LIGHT-CONTROLLABLE PROTACS AND PERSPECTIVE

The potential on-target off-tissue effects and off-target effects limit the application of PROTACs in clinic. These third-generation controllable PROTACs using light to activate or inactivate the PROTAC provide another layer of regulation

Photo-caged PROTACs	Structure	Ref.
DEACM-caged ERR $\alpha$ PROTAC 2		Kounde et al., 2020
DMNB-caged BRDs PROTAC 3		Naro et al., 2020

**FIGURE 4 |** Summary of photo-caged VHL-based PROTACs. Photo-cage groups are marked in red. The photo-cage groups are in red. DMNB, 4,5-dimethoxy-2-nitrobenzyl; DEACM, diethylamino coumarin.

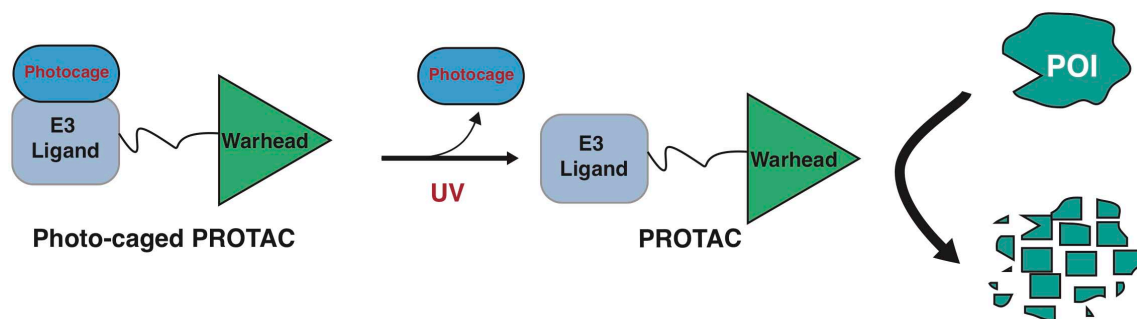


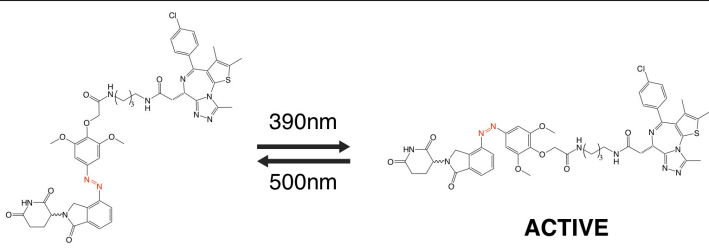
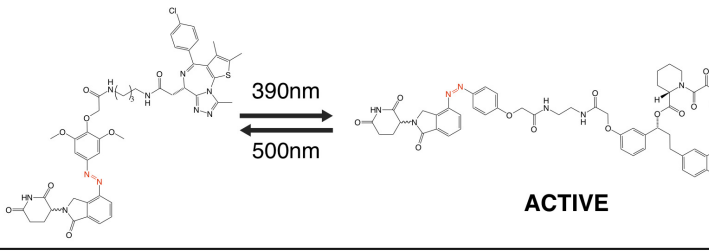
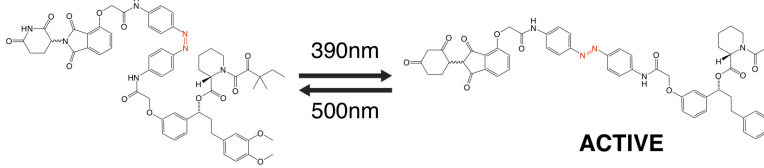
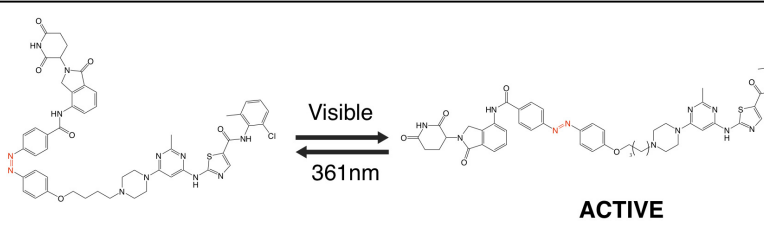
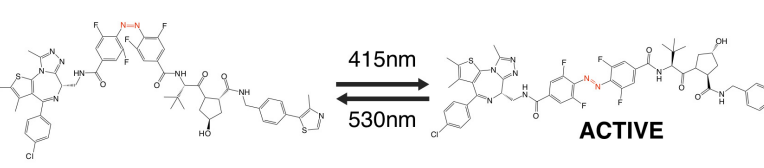
**FIGURE 5 |** A schematic diagram for action model of photo-switch-PROTAC. The photo-switch PROTACs can be switched on and off by illumination with different wavelengths of light, which leads to the switch between the *cis* and *trans* forms of the photo-switch-PROTAC.

on PROTACs, making it more practicable and controllable. However, those light-controllable PROTACs also have some disadvantages.

Notably, UVA light is used to activate or inactivate these light-controllable PROTACs, however, UVA light might trigger damage to DNA (Mouret et al., 2006; Cadet and Douki, 2011), especially when used in patients. Compared with UVB with shorter wavelength that causes DNA damage by triggering pyrimidine dimerization, UVA is less genotoxic (de Gruijl, 2002). However, UVA radiation is still thought to induce oxidant stress and DNA damage, which causes skin aging and possible

skin cancers, including the deadly form of melanomas (de Gruijl, 2002). Moreover, UV light (used in both photo-caged PROTACs and photo-switch PROTACs) and visible light (used in photo-switch PROTACs) have limited penetration ability, thus making those light-controllable PROTACs only suitable for several types of cancer that can be accessed easily by light, such as skin cancer or leukemia. To overcome such disadvantages, further efforts should be focused on adopting other light sources rather than UV light to trigger the photo-cage or photo-switch process. To this end, visible light or near-infrared light has longer wavelength and less energy than UV to trigger



Photo-switch PROTACs	Structure	Ref.
<b>PHOTAC-I-3</b>	 <p>390nm 500nm</p> <p><b>ACTIVE</b></p>	<b>Reynders et al., 2020</b>
<b>PHOTAC-II-5</b>	 <p>390nm 500nm</p> <p><b>ACTIVE</b></p>	<b>Reynders et al., 2020</b>
<b>PHOTAC-II-6</b>	 <p>390nm 500nm</p> <p><b>ACTIVE</b></p>	<b>Reynders et al., 2020</b>
<b>Azo-PROTAC-4C</b>	 <p>Visible 361nm</p> <p><b>ACTIVE</b></p>	<b>Jin et al., 2020</b>
<b>photoPROTAC-1</b>	 <p>415nm 530nm</p> <p><b>ACTIVE</b></p>	<b>Pfaff et al., 2019</b>

**FIGURE 6 |** Summary of photo-switch PROTACs.

potential DNA damage (Mouret et al., 2006; Cadet and Douki, 2011), making them more suitable to be the cage group on PROTACs. More importantly, several photo-cage group with red and near-infrared light sensitivity have been developed recently (Vorobev and Moskalensky, 2020), including N-NO (Nakagawa, 2016) and benzoquinone-based photocage (Chen and Steinmetz, 2006; Wang and Kalow, 2018; Alabugin, 2019). Furthermore, other endogenous cues in cancers such as those cancer-specific antigens or receptors should be also useful for targeting delivery of PROTAC to cancer cells, thus eliminating possible toxic issue to normal tissues/cells (Liu et al., 2019; Saw and Song, 2019).

Another potential disadvantage of light-controllable PROTACs is due to their permeability. Compared with small molecule drug which is usually less than 500 Da, according to the Lipinski's rule of five (Lipinski et al., 2001), standard PROTACs are usually more than 600 Da and these light-controllable PROTACs are usually near 1,000 Da. The relatively large molecule weight might compromise the pharmacokinetic and pharmacodynamic parameters of light-controllable PROTACs. To date, in most *in vivo* study, PROTACs are administrated by Raina et al. (2016); Ohoka et al. (2017b), Sun B. et al. (2018), intraperitoneally (Winter et al., 2015; Zhou et al., 2018; Gao et al., 2020) or intravenously (Mares et al., 2020) injection. Thus, it

still warrants further in-depth investigation on optimization the pharmaceutical properties of PROTAC to make it possible for orally administered.

Finally, in clinic, there is lack of clear boundary between tumor tissues and adjunct normal tissues, making it hard to only activate these light-controllable PROTACs at the tumor tissues/cells. An alternative approach for controllable action of PROTACs in cancer cells could be taking advantage of cancer-specific receptors or transporters, such as HER2 and FOLR1 (Scaranti et al., 2020) for the guided delivery of PROTACs into cancer, but not normal cells. To this end, other types of third generation PROTACs, including antibody-conjugated PROTACs (Dragovich et al., 2020, 2021a,b; Maneiro et al., 2020; Pillow et al., 2020) and folate-PROTAC (Liu et al., 2021), have been recently developed, which specifically deliver PROTAC to cancer cells, thus avoiding potential toxicity to normal cells. Compared with the light-controllable PROTACs, folate-PROTAC (Liu et al., 2021) have relatively higher molecule weight of over 1,000 Da, and antibody-conjugated PROTACs (Dragovich et al., 2020, 2021a,b; Maneiro et al., 2020; Pillow et al., 2020) are macromolecule drug that could only be administrated by injection. Taken together, further studies are needed to make these third generation PROTACs (light-controllable PROTACs, antibody-conjugated PROTACs and folate-PROTAC) more practical in clinic.

## REFERENCES

- Adhikari, B., Bozilovic, J., Diebold, M., Schwarz, J. D., Hofstetter, J., Schroder, M., et al. (2020). PROTAC-mediated degradation reveals a non-catalytic function of AURORA-A kinase. *Nat. Chem. Biol.* 16, 1179–1188. doi: 10.1038/s41589-020-00652-y
- Agostinis, P., Berg, K., Cengel, K. A., Foster, T. H., Girotti, A. W., Gollnick, S. O., et al. (2011). Photodynamic therapy of cancer: an update. *CA Cancer J. Clin.* 61, 250–281. doi: 10.3322/caac.20114
- Alabugin, A. (2019). Near-IR photochemistry for biology: exploiting the optical window of tissue. *Photochem. Photobiol.* 95, 722–732. doi: 10.1111/php.13068
- An, Z., Lv, W., Su, S., Wu, W., and Rao, Y. (2019). Developing potent PROTACs tools for selective degradation of HDAC6 protein. *Protein Cell* 10, 606–609. doi: 10.1007/s13238-018-0602-z
- Asatsuma-Okumura, T., Ando, H., De Simone, M., Yamamoto, J., Sato, T., Shimizu, N., et al. (2019). p63 is a cereblon substrate involved in thalidomide teratogenicity. *Nat. Chem. Biol.* 15, 1077–1084. doi: 10.1038/s41589-019-0366-7
- Bai, L., Zhou, H., Xu, R., Zhao, Y., Chinnaswamy, K., McEachern, D., et al. (2019). A potent and selective small-molecule degrader of STAT3 achieves complete tumor regression In Vivo. *Cancer Cell* 36, 498.e17–511.e17. doi: 10.1016/j.ccell.2019.10.002
- Bardhan, A., and Deiters, A. (2019). Development of photolabile protecting groups and their application to the photochemical control of cell signaling. *Curr. Opin. Struct. Biol.* 57, 164–175. doi: 10.1016/j.sbi.2019.03.028
- Bassi, Z. I., Fillmore, M. C., Miah, A. H., Chapman, T. D., Maller, C., Roberts, E. J., et al. (2018). Modulating PCAF/GCN5 immune cell function through a PROTAC approach. *ACS Chem. Biol.* 13, 2862–2867. doi: 10.1021/acscchembio.8b00705
- Bernassola, F., Karin, M., Ciechanover, A., and Melino, G. (2008). The HECT family of E3 ubiquitin ligases: multiple players in cancer development. *Cancer Cell* 14, 10–21. doi: 10.1016/j.ccr.2008.06.001
- Bethea, D., Fullmer, B., Syed, S., Seltzer, G., Tiano, J., Rischko, C., et al. (1999). Psoralen photobiology and photochemotherapy: 50 years of science and medicine. *J. Dermatol. Sci.* 19, 78–88. doi: 10.1016/S0923-1811(98)00064-4
- Bian, J., Ren, J., Li, Y., Wang, J., Xu, X., Feng, Y., et al. (2018). Discovery of Wogonin-based PROTACs against CDK9 and capable of achieving antitumor activity. *Bioorg. Chem.* 81, 373–381. doi: 10.1016/j.bioorg.2018.08.028

## AUTHOR CONTRIBUTIONS

All authors listed have made a substantial, direct and intellectual contribution to the work, and approved it for publication.

## FUNDING

This work was supported in part by funding from NIH (R01CA200651 and R35CA253027 to WW).

## ACKNOWLEDGMENTS

We apologize for not citing all relevant reports owing to space limitations.

## SUPPLEMENTARY MATERIAL

The Supplementary Material for this article can be found online at: <https://www.frontiersin.org/articles/10.3389/fcell.2021.678077/full#supplementary-material>

- Bolden, J. E., Tasdemir, N., Dow, L. E., van Es, J. H., Wilkinson, J. E., Zhao, Z., et al. (2014). Inducible in vivo silencing of Brd4 identifies potential toxicities of sustained BET protein inhibition. *Cell Rep.* 8, 1919–1929. doi: 10.1016/j.celrep.2014.08.025
- Bond, M. J., Chu, L., Nalawansa, D. A., Li, K., and Crews, C. M. (2020). Targeted degradation of oncogenic KRAS(G12C) by VHL-Recruiting PROTACs. *ACS Cent. Sci.* 6, 1367–1375. doi: 10.1021/acscentsci.0c00411
- Bondeson, D. P., Smith, B. E., Burslem, G. M., Buhimschi, A. D., Hines, J., Jaime-Figueroa, S., et al. (2018). Lessons in PROTAC design from selective degradation with a promiscuous warhead. *Cell Chem. Biol.* 25, 78.e5–87.e5. doi: 10.1016/j.chembiol.2017.09.010
- Brand, M., Jiang, B., Bauer, S., Donovan, K. A., Liang, Y., Wang, E. S., et al. (2019). Homolog-Selective degradation as a strategy to probe the function of CDK6 in AML. *Cell Chem. Biol.* 26, 300.e9–306.e9. doi: 10.1016/j.chembiol.2018.11.006
- Buckley, D. L., Gustafson, J. L., Van Molle, I., Roth, A. G., Tae, H. S., Gareiss, P. C., et al. (2012a). Small-molecule inhibitors of the interaction between the E3 ligase VHL and HIF1alpha. *Angew. Chem. Int. Ed. Engl.* 51, 11463–11467. doi: 10.1002/anie.201206231
- Buckley, D. L., Van Molle, I., Gareiss, P. C., Tae, H. S., Michel, J., Noblin, D. J., et al. (2012b). Targeting the von Hippel-Lindau E3 ubiquitin ligase using small molecules to disrupt the VHL/HIF-1alpha interaction. *J. Am. Chem. Soc.* 134, 4465–4468. doi: 10.1021/ja209924v
- Burslem, G. M., Schultz, A. R., Bondeson, D. P., Eide, C. A., Savage Stevens, S. L., Druker, B. J., et al. (2019). Targeting BCR-ABL1 in chronic myeloid leukemia by PROTAC-Mediated targeted protein degradation. *Cancer Res.* 79, 4744–4753. doi: 10.1158/0008-5472.CAN-19-1236
- Burslem, G. M., Smith, B. E., Lai, A. C., Jaime-Figueroa, S., McQuaid, D. C., Bondeson, D. P., et al. (2018). The advantages of targeted protein degradation over inhibition: an RTK case study. *Cell Chem. Biol.* 25, 67.e3–77.e3. doi: 10.1016/j.chembiol.2017.09.009
- Cadet, J., and Douki, T. (2011). Oxidatively generated damage to DNA by UVA radiation in cells and human skin. *J. Invest. Dermatol.* 131, 1005–1007. doi: 10.1038/jid.2011.51
- Chen, H., Chen, F., Pei, S., and Gou, S. (2019). Pomalidomide hybrids act as proteolysis targeting chimeras: synthesis, anticancer activity and B-Raf degradation. *Bioorg. Chem.* 87, 191–199. doi: 10.1016/j.bioorg.2019.03.035
- Chen, Y., and Steinmetz, M. G. (2006). Photoactivation of amino-substituted 1,4-benzoquinones for release of carboxylate and phenolate leaving groups

- using visible light. *J. Org. Chem.* 71, 6053–6060. doi: 10.1021/jo060790g
- Chene, P. (2003). Inhibiting the p53-MDM2 interaction: an important target for cancer therapy. *Nat. Rev. Cancer* 3, 102–109. doi: 10.1038/nrc991
- Cheng, M., Yu, X., Lu, K., Xie, L., Wang, L., Meng, F., et al. (2020). Discovery of potent and selective Epidermal Growth Factor Receptor (EGFR) bifunctional small-molecule degraders. *J. Med. Chem.* 63, 1216–1232. doi: 10.1021/acs.jmedchem.9b01566
- Chi, J. J., Li, H., Zhou, Z., Izquierdo-Ferrer, J., Xue, Y., Wavelet, C. M., et al. (2019). A novel strategy to block mitotic progression for targeted therapy. *EBioMedicine* 49, 40–54. doi: 10.1016/j.ebiom.2019.10.013
- Churcher, I. (2018). Protac-induced protein degradation in drug discovery: breaking the rules or just making new ones? *J. Med. Chem.* 61, 444–452. doi: 10.1021/acs.jmedchem.7b01272
- Cromm, P. M., Samarasinghe, K. T. G., Hines, J., and Crews, C. M. (2018). Addressing kinase-independent functions of fak via PROTAC-Mediated degradation. *J. Am. Chem. Soc.* 140, 17019–17026. doi: 10.1021/jacs.8b08008
- De Dominicis, M., Porazzi, P., Xiao, Y., Chao, A., Tang, H. Y., Kumar, G., et al. (2020). Selective inhibition of Ph-positive ALL cell growth through kinase-dependent and -independent effects by CDK6-specific PROTACs. *Blood* 135, 1560–1573. doi: 10.1182/blood.2019003604
- de Gruijil, F. R. (2002). Photocarcinogenesis: UVA vs. UVB radiation. *Skin Pharmacol. Appl. Skin Physiol.* 15, 316–320. doi: 10.1159/000064535
- Demizu, Y., Shibata, N., Hattori, T., Ohoka, N., Motoi, H., Misawa, T., et al. (2016). Development of BCR-ABL degradation inducers via the conjugation of an imatinib derivative and a cIAP1 ligand. *Bioorg. Med. Chem. Lett.* 26, 4865–4869. doi: 10.1016/j.bmcl.2016.09.041
- Dharmasiri, N., Dharmasiri, S., and Estelle, M. (2005). The F-box protein TIR1 is an auxin receptor. *Nature* 435, 441–445. doi: 10.1038/nature03543
- Donovan, K. A., An, J., Nowak, R. P., Yuan, J. C., Fink, E. C., Berry, B. C., et al. (2018). Thalidomide promotes degradation of SALL4, a transcription factor implicated in Duane Radial Ray syndrome. *eLife* 7:e38430. doi: 10.7554/eLife.38430
- Dragovich, P. S., Adhikari, P., Blake, R. A., Blaquiére, N., Chen, J., Cheng, Y. X., et al. (2020). Antibody-mediated delivery of chimeric protein degraders which target estrogen receptor alpha (ERalpha). *Bioorg. Med. Chem. Lett.* 30:126907. doi: 10.1016/j.bmcl.2019.126907
- Dragovich, P. S., Pillow, T. H., Blake, R. A., Sadowsky, J. D., Adaligil, E., Adhikari, P., et al. (2021a). Antibody-mediated delivery of chimeric BRD4 Degraders. Part 1: exploration of antibody linker, payload loading, and payload molecular properties. *J. Med. Chem.* 64, 2534–2575. doi: 10.1021/acs.jmedchem.0c01845
- Dragovich, P. S., Pillow, T. H., Blake, R. A., Sadowsky, J. D., Adaligil, E., Adhikari, P., et al. (2021b). Antibody-mediated delivery of chimeric BRD4 Degraders. Part 2: improvement of in vitro antiproliferation activity and in vivo antitumor efficacy. *J. Med. Chem.* 64, 2576–2607. doi: 10.1021/acs.jmedchem.0c01846
- Farnaby, W., Koegl, M., Roy, M. J., Whitworth, C., Diers, E., Trainor, N., et al. (2019). BAF complex vulnerabilities in cancer demonstrated via structure-based PROTAC design. *Nat. Chem. Biol.* 15, 672–680. doi: 10.1038/s41589-019-0294-6
- Fischer, E. S., Bohm, K., Lydeard, J. R., Yang, H., Stadler, M. B., Cavadini, S., et al. (2014). Structure of the DDB1-CRBN E3 ubiquitin ligase in complex with thalidomide. *Nature* 512, 49–53. doi: 10.1038/nature13527
- Flanagan, J. J., and Neklesa, T. K. (2019). Targeting nuclear receptors with PROTAC degraders. *Mol. Cell Endocrinol.* 493:110452. doi: 10.1016/j.mce.2019.110452
- Flanagan, J. J., Qian, Y., Gough, S. M., Andreoli, M., Bookbinder, M., Cadelina, G., et al. (2019). Abstract P5-04-18: ARV-471, an oral estrogen receptor PROTAC degrader for breast cancer. *Cancer Res.* 81(4 Suppl.), S17–S32.
- Galdeano, C., Gadd, M. S., Soares, P., Scaffidi, S., Van Molle, I., Birced, I., et al. (2014). Structure-guided design and optimization of small molecules targeting the protein-protein interaction between the von Hippel-Lindau (VHL) E3 ubiquitin ligase and the hypoxia inducible factor (HIF) alpha subunit with in vitro nanomolar affinities. *J. Med. Chem.* 57, 8657–8663. doi: 10.1021/jm5011258
- Gao, H., Zheng, C., Du, J., Wu, Y., Sun, Y., Han, C., et al. (2020). FAK-targeting PROTAC as a chemical tool for the investigation of non-enzymatic FAK function in mice. *Protein Cell* 11, 534–539. doi: 10.1007/s13238-020-00732-8
- Gechijian, L. N., Buckley, D. L., Lawlor, M. A., Reyes, J. M., Paulk, J., Ott, C. J., et al. (2018). Functional TRIM24 degrader via conjugation of ineffectual bromodomain and VHL ligands. *Nat. Chem. Biol.* 14, 405–412. doi: 10.1038/s41589-018-0010-y
- Guo, J., Liu, J., and Wei, W. (2019). Degrading proteins in animals: “PROTAC”tion goes in vivo. *Cell Res.* 29, 179–180. doi: 10.1038/s41422-019-0144-9
- Han, X., Wang, C., Qin, C., Xiang, W., Fernandez-Salas, E., Yang, C. Y., et al. (2019). Discovery of ARD-69 as a highly potent proteolysis targeting chimera (PROTAC) degrader of androgen receptor (AR) for the treatment of prostate cancer. *J. Med. Chem.* 62, 941–964. doi: 10.1021/acs.jmedchem.8b01631
- Han, X. R., Chen, L., Wei, Y., Yu, W., Chen, Y., Zhang, C., et al. (2020). Discovery of Selective Small Molecule Degradors of BRAF-V600E. *J. Med. Chem.* 63, 4069–4080. doi: 10.1021/acs.jmedchem.9b02083
- He, Y., Zhang, X., Chang, J., Kim, H. N., Zhang, P., Wang, Y., et al. (2020). Using proteolysis-targeting chimera technology to reduce navitoclax platelet toxicity and improve its senolytic activity. *Nat. Commun.* 11:1996. doi: 10.1038/s41467-020-15838-0
- Hines, J., Gough, J. D., Corson, T. W., and Crews, C. M. (2013). Posttranslational protein knockdown coupled to receptor tyrosine kinase activation with phosphoPROTACs. *Proc. Natl. Acad. Sci. U.S.A.* 110, 8942–8947. doi: 10.1073/pnas.1217206110
- Hines, J., Lartigue, S., Dong, H., Qian, Y., and Crews, C. M. (2019). MDM2-Recruiting PROTAC offers superior, synergistic antiproliferative activity via simultaneous degradation of BRD4 and stabilization of p53. *Cancer Res.* 79, 251–262. doi: 10.1158/0008-5472.CAN-18-2918
- Hu, J., Hu, B., Wang, M., Xu, F., Miao, B., Yang, C. Y., et al. (2019). Discovery of ERD-308 as a highly potent proteolysis targeting chimera (PROTAC) degrader of estrogen receptor (ER). *J. Med. Chem.* 62, 1420–1442. doi: 10.1021/acs.jmedchem.8b01572
- Huang, H. T., Dobrovolsky, D., Paulk, J., Yang, G., Weisberg, E. L., Doctor, Z. M., et al. (2018). A chemoproteomic approach to query the degradable kinome using a multi-kinase degrader. *Cell Chem. Biol.* 25, 88.e6–99.e6. doi: 10.1016/j.chembiol.2017.10.005
- Ito, T., Ando, H., Suzuki, T., Ogura, T., Hotta, K., Imamura, Y., et al. (2010). Identification of a primary target of thalidomide teratogenicity. *Science* 327, 1345–1350. doi: 10.1126/science.1177319
- Jang, J., To, C., De Clercq, D. J. H., Park, E., Ponthier, C. M., Shin, B. H., et al. (2020). Mutant-selective allosteric EGFR degraders are effective against a broad range of drug-resistant mutations. *Angew. Chem. Int. Ed. Engl.* 59, 14481–14489. doi: 10.1002/anie.202003500
- Jiang, B., Wang, E. S., Donovan, K. A., Liang, Y., Fischer, E. S., Zhang, T., et al. (2019). Development of dual and selective degraders of cyclin-dependent Kinases 4 and 6. *Angew. Chem. Int. Ed. Engl.* 58, 6321–6326. doi: 10.1002/anie.201901336
- Jiang, Y., Deng, Q., Zhao, H., Xie, M., Chen, L., Yin, F., et al. (2018). Development of stabilized peptide-based PROTACs against estrogen receptor alpha. *ACS Chem. Biol.* 13, 628–635. doi: 10.1021/acschembio.7b00985
- Jin, Y. H., Lu, M. C., Wang, Y., Shan, W. X., Wang, X. Y., You, Q. D., et al. (2020). Azo-PROTAC: novel light-controlled small-molecule tool for protein knockdown. *J. Med. Chem.* 63, 4644–4654. doi: 10.1021/acs.jmedchem.9b02058
- Kang, C. H., Lee, D. H., Lee, C. O., Ha, J. Du, Park, C. H., and Hwang, J. Y. (2018). Induced protein degradation of anaplastic lymphoma kinase (ALK) by proteolysis targeting chimera (PROTAC). *Biochem. Biophys. Res. Commun.* 505, 542–547. doi: 10.1016/j.bbrc.2018.09.169
- Kargbo, R. B. (2019). PROTAC-mediated degradation of estrogen receptor in the treatment of cancer. *ACS Med. Chem. Lett.* 10, 1367–1369. doi: 10.1021/acsmedchemlett.9b00397
- Khan, S., Zhang, X., Lv, D., Zhang, Q., He, Y., Zhang, P., et al. (2019). A selective BCL-XL PROTAC degrader achieves safe and potent antitumor activity. *Nat. Med.* 25, 1938–1947. doi: 10.1038/s41591-019-0668-z
- Klan, P., Solomek, T., Bochet, C. G., Blanc, A., Givens, R., Rubina, M., et al. (2013). Photoremovable protecting groups in chemistry and biology: reaction mechanisms and efficacy. *Chem. Rev.* 113, 119–191. doi: 10.1021/cr300177k
- Komander, D., and Rape, M. (2012). The ubiquitin code. *Annu. Rev. Biochem.* 81, 203–229. doi: 10.1146/annurev-biochem-060310-170328
- Kounde, C. S., Shchepinova, M. M., Saunders, C. N., Muelbaier, M., Rackham, M. D., Harling, J. D., et al. (2020). A caged E3 ligase ligand for PROTAC-mediated protein degradation with light. *Chem. Commun.* 56, 5532–5535. doi: 10.1039/d0cc00523a
- Kronke, J., Fink, E. C., Hollenbach, P. W., MacBeth, K. J., Hurst, S. N., Udeshi, N. D., et al. (2015). Lenalidomide induces ubiquitination and degradation of CK1alpha in del(5q) MDS. *Nature* 523, 183–188. doi: 10.1038/nature14610

- Kronke, J., Udeshi, N. D., Narla, A., Grauman, P., Hurst, S. N., McConkey, M., et al. (2014). Lenalidomide causes selective degradation of IKZF1 and IKZF3 in multiple myeloma cells. *Science* 343, 301–305. doi: 10.1126/science.1244851
- Kumar, M., Gouw, M., Michael, S., Samano-Sanchez, H., Pancer, R., Glavina, J., et al. (2020). ELM-the eukaryotic linear motif resource in 2020. *Nucleic Acids Res.* 48, D296–D306. doi: 10.1093/nar/gkz1030
- Lai, A. C., Toure, M., Hellerschmied, D., Salami, J., Jaime-Figueroa, S., Ko, E., et al. (2016). Modular PROTAC design for the degradation of oncogenic BCR-ABL. *Angew. Chem. Int. Ed. Engl.* 55, 807–810. doi: 10.1002/anie.201507634
- Li, M. X., Yang, Y., Zhao, Q., Wu, Y., Song, L., Yang, H., et al. (2020). Degradation versus inhibition: development of proteolysis-targeting chimeras for overcoming statin-induced compensatory upregulation of 3-Hydroxy-3-methylglutaryl coenzyme a reductase. *J. Med. Chem.* 63, 4908–4928. doi: 10.1021/acs.jmedchem.0c00339
- Li, W., Gao, C., Zhao, L., Yuan, Z., Chen, Y., and Jiang, Y. (2018). Phthalimide conjugations for the degradation of oncogenic PI3K. *Eur. J. Med. Chem.* 151, 237–247. doi: 10.1016/j.ejmech.2018.03.066
- Li, Y., Yang, J., Aguilar, A., McEachern, D., Przybranowski, S., Liu, L., et al. (2019). Discovery of MD-224 as a first-in-class, highly potent, and efficacious proteolysis targeting chimera murine double Minute 2 degrader capable of achieving complete and durable tumor regression. *J. Med. Chem.* 62, 448–466. doi: 10.1021/acs.jmedchem.8b00909
- Li, Z., Pinch, B. J., Olson, C. M., Donovan, K. A., Nowak, R. P., Mills, C. E., et al. (2020). Development and characterization of a weel kinase degrader. *Cell Chem. Biol.* 27, 57.e9–65.e9. doi: 10.1016/j.chembiol.2019.10.013
- Lipinski, C. A., Lombardo, F., Dominy, B. W., and Feeney, P. J. (2001). Experimental and computational approaches to estimate solubility and permeability in drug discovery and development settings. *Adv. Drug Deliv. Rev.* 46, 3–26. doi: 10.1016/s0169-409x(00)00129-0
- Liu, J., Chen, H., Liu, Y., Shen, Y., Meng, F., Kaniskan, H. U., et al. (2021). Cancer selective target degradation by folate-caged PROTACs. *J. Am. Chem. Soc.* 143, 7380–7387. doi: 10.1021/jacs.1c00451
- Liu, J., Chen, H., Ma, L., He, Z., Wang, D., Liu, Y., et al. (2020). Light-induced control of protein destruction by opto-PROTAC. *Sci. Adv.* 6:eay5154. doi: 10.1126/sciadv.aay5154
- Liu, J., Lai, H., Xiong, Z., Chen, B., and Chen, T. (2019). Functionalization and cancer-targeting design of ruthenium complexes for precise cancer therapy. *Chem. Commun.* 55, 9904–9914. doi: 10.1039/c9cc04098f
- Lu, G., Middleton, R. E., Sun, H., Naniong, M., Ott, C. J., Mitsiades, C. S., et al. (2014). The myeloma drug lenalidomide promotes the cereblon-dependent destruction of Ikaros proteins. *Science* 343, 305–309. doi: 10.1126/science.1244917
- Lu, J., Qian, Y., Altieri, M., Dong, H., Wang, J., Raina, K., et al. (2015). Hijacking the E3 ubiquitin ligase cereblon to efficiently target BRD4. *Chem. Biol.* 22, 755–763. doi: 10.1016/j.chembiol.2015.05.009
- Maneiro, M. A., Forte, N., Shchepinova, M. M., Kounde, C. S., Chudasama, V., Baker, J. R., et al. (2020). Antibody-PROTAC conjugates enable HER2-dependent targeted protein degradation of BRD4. *ACS Chem. Biol.* 15, 1306–1312. doi: 10.1021/acscchembio.0c00285
- Mares, A., Miah, A. H. I., Smith, E. D., Rackham, M., Thawani, A. R., Cryan, J., et al. (2020). Extended pharmacodynamic responses observed upon PROTAC-mediated degradation of RIPK2. *Commun. Biol.* 3:140. doi: 10.1038/s42003-020-0868-6
- Matyskiela, M. E., Clayton, T., Zheng, X., Mayne, C., Tran, E., Carpenter, A., et al. (2020). Crystal structure of the SALL4-pomalidomide-cereblon-DDB1 complex. *Nat. Struct. Mol. Biol.* 27, 319–322. doi: 10.1038/s41594-020-0405-9
- Matyskiela, M. E., Lu, G., Ito, T., Pagarigan, B., Lu, C. C., Miller, K., et al. (2016). A novel cereblon modulator recruits GSPT1 to the CRL4(CRBN) ubiquitin ligase. *Nature* 535, 252–257. doi: 10.1038/nature18611
- McCoull, W., Cheung, T., Anderson, E., Barton, P., Burgess, J., Byth, K., et al. (2018). Development of a Novel B-Cell Lymphoma 6 (BCL6) PROTAC to provide insight into small molecule targeting of BCL6. *ACS Chem. Biol.* 13, 3131–3141. doi: 10.1021/acscchembio.8b00698
- Mészáros, B., Kumar, M., Gibson, T. J., Uyar, B., and Dosztányi, Z. (2017). Degrons in cancer. *Sci. Signal.* 10:eak9982. doi: 10.1126/scisignal.aak9982
- Moore, C. M., Pendse, D., and Emberton, M. (2009). Photodynamic therapy for prostate cancer—a review of current status and future promise. *Nat. Clin. Pract. Urol.* 6, 18–30. doi: 10.1038/ncpuro1274
- Moreau, K., Coen, M., Zhang, A. X., Pachl, F., Castaldi, M. P., Dahl, G., et al. (2020). Proteolysis-targeting chimeras in drug development: a safety perspective. *Br. J. Pharmacol.* 177, 1709–1718. doi: 10.1111/bph.15014
- Mouret, S., Baudouin, C., Charveron, M., Favier, A., Cadet, J., and Douki, T. (2006). Cyclobutane pyrimidine dimers are predominant DNA lesions in whole human skin exposed to UVA radiation. *Proc. Natl. Acad. Sci. U.S.A.* 103, 13765–13770. doi: 10.1073/pnas.0604213103
- Mullard, A. (2021). Targeted protein degraders crowd into the clinic. *Nat. Rev. Drug Discov.* 20, 247–250. doi: 10.1038/d41573-021-00052-4
- Nakagawa, H. (2016). Photocontrol of NO, H<sub>2</sub>S, and HNO release in biological systems by using specific caged compounds. *Chem. Pharm. Bull.* 64, 1249–1255. doi: 10.1248/cpb.c16-00403
- Nalawansha, D. A., and Crews, C. M. (2020). PROTACs: an emerging therapeutic modality in precision medicine. *Cell Chem. Biol.* 27, 998–1014. doi: 10.1016/j.chembiol.2020.07.020
- Naro, Y., Darrah, K., and Deiters, A. (2020). Optical control of small molecule-induced protein degradation. *J. Am. Chem. Soc.* 142, 2193–2197. doi: 10.1021/jacs.9b12718
- Neklesa, T., Snyder, L. B., Willard, R. R., Vitale, N., Raina, K., Pizzano, J., et al. (2018). Abstract 5236: ARV-110: An androgen receptor PROTAC degrader for prostate cancer. *Cancer Res.* 78(13 Suppl.), 5236–5236.
- Neklesa, T. K., Winkler, J. D., and Crews, C. M. (2017). Targeted protein degradation by PROTACs. *Pharmacol. Ther.* 174, 138–144. doi: 10.1016/j.pharmthera.2017.02.027
- Nunes, J., McGonagle, G. A., Eden, J., Kiritharan, G., Touzet, M., Lewell, X., et al. (2019). Targeting IRAK4 for Degradation with PROTACs. *ACS Med. Chem. Lett.* 10, 1081–1085. doi: 10.1021/acscmedchemlett.9b00219
- Ohoka, N., Nagai, K., Hattori, T., Okuhira, K., Shibata, N., Cho, N., et al. (2014). Cancer cell death induced by novel small molecules degrading the TACC3 protein via the ubiquitin-proteasome pathway. *Cell Death Dis.* 5:e1513. doi: 10.1038/cddis.2014.471
- Ohoka, N., Nagai, K., Shibata, N., Hattori, T., Nara, H., Cho, N., et al. (2017a). SNIPER(TACC3) induces cytoplasmic vacuolization and sensitizes cancer cells to Bortezomib. *Cancer Sci.* 108, 1032–1041. doi: 10.1111/cas.13198
- Ohoka, N., Okuhira, K., Ito, M., Nagai, K., Shibata, N., Hattori, T., et al. (2017b). In vivo knockdown of pathogenic proteins via specific and nongenetic inhibitor of apoptosis protein (IAP)-dependent protein erasers (SNIPERs). *J. Biol. Chem.* 292, 4556–4570. doi: 10.1074/jbc.M116.768853
- Ohoka, N., Ujikawa, O., Shimokawa, K., Sameshima, T., Shibata, N., Hattori, T., et al. (2019). Different degradation mechanisms of inhibitor of apoptosis proteins (IAPs) by the specific and nongenetic IAP-dependent protein eraser (SNIPER). *Chem. Pharm. Bull.* 67, 203–209. doi: 10.1248/cpb.c18-00567
- Okuhira, K., Demizu, Y., Hattori, T., Ohoka, N., Shibata, N., Nishimaki-Mogami, T., et al. (2013). Development of hybrid small molecules that induce degradation of estrogen receptor- $\alpha$  and necrotic cell death in breast cancer cells. *Cancer Sci.* 104, 1492–1498. doi: 10.1111/cas.12272
- Okuhira, K., Shoda, T., Omura, R., Ohoka, N., Hattori, T., Shibata, N., et al. (2017). Targeted degradation of proteins localized in subcellular compartments by hybrid small molecules. *Mol. Pharmacol.* 91, 159–166. doi: 10.1124/mol.116.105569
- Paiva, S. L., and Crews, C. M. (2019). Targeted protein degradation: elements of PROTAC design. *Curr. Opin. Chem. Biol.* 50, 111–119. doi: 10.1016/j.cbpa.2019.02.022
- Peng, L., Zhang, Z., Lei, C., Li, S., Ren, X., Chang, Y., et al. (2019). Identification of new small-molecule inducers of estrogen-related receptor  $\alpha$  (ERR $\alpha$ ) degradation. *ACS Med. Chem. Lett.* 10, 767–772. doi: 10.1021/acscmedchemlett.9b00025
- Petrylak, P. D., Gao, X., Vogelzang, J. N., Garfield, H. M., Taylor, I., Moore, D. M., et al. (2020). First-in-human phase I study of ARV-110, an androgen receptor (AR) PROTAC degrader in patients (pts) with metastatic castrate-resistant prostate cancer (mCRPC) following enzalutamide (ENZ) and/or abiraterone (ABI). *J. Clin. Oncol.* 38, 3500–3500. doi: 10.1200/JCO.2020.38.15\_suppl.3500
- Pettersson, M., and Crews, C. M. (2019). PROTeolysis TARgeting chimeras (PROTACs) - Past, present and future. *Drug Discov. Today Technol.* 31, 15–27. doi: 10.1016/j.ddtec.2019.01.002
- Petzold, G., Fischer, E. S., and Thoma, N. H. (2016). Structural basis of lenalidomide-induced CK1 $\alpha$  degradation by the CRL4(CRBN) ubiquitin ligase. *Nature* 532, 127–130. doi: 10.1038/nature16979



- Pfaff, P., Samarasinghe, K. T. G., Crews, C. M., and Carreira, E. M. (2019). Reversible spatiotemporal control of induced protein degradation by bistable PhotoPROTACs. *ACS Cent. Sci.* 5, 1682–1690. doi: 10.1021/acscentsci.9b00713
- Pickart, C. M. (2001). Mechanisms underlying ubiquitination. *Annu. Rev. Biochem.* 70, 503–533. doi: 10.1146/annurev.biochem.70.1.503
- Pillow, T. H., Adhikari, P., Blake, R. A., Chen, J., Del Rosario, G., Deshmukh, G., et al. (2020). Antibody conjugation of a chimeric BET degrader enables in vivo activity. *ChemMedChem* 15, 17–25. doi: 10.1002/cmdc.201900497
- Pohl, C., and Dikic, I. (2019). Cellular quality control by the ubiquitin-proteasome system and autophagy. *Science* 366, 818–822. doi: 10.1126/science.aax3769
- Potjewyd, F., Turner, A. W., Beri, J., Rectenwald, J. M., Norris-Drouin, J. L., Cholenky, S. H., et al. (2020). Degradation of polycomb repressive complex 2 with an EED-Targeted bivalent chemical degrader. *Cell Chem. Biol.* 27, 47.e15–56.e15. doi: 10.1016/j.chembiol.2019.11.006
- Powell, C. E., Gao, Y., Tan, L., Donovan, K. A., Nowak, R. P., Loehr, A., et al. (2018). Chemically induced degradation of anaplastic lymphoma kinase (ALK). *J. Med. Chem.* 61, 4249–4255. doi: 10.1021/acs.jmedchem.7b01655
- Raina, K., Lu, J., Qian, Y., Altieri, M., Gordon, D., Rossi, A. M., et al. (2016). PROTAC-induced BET protein degradation as a therapy for castration-resistant prostate cancer. *Proc. Natl. Acad. Sci. U.S.A.* 113, 7124–7129. doi: 10.1073/pnas.1521738113
- Rana, S., Bendjennat, M., Kour, S., King, H. M., Kizhake, S., Zahid, M., et al. (2019). Selective degradation of CDK6 by a palbociclib based PROTAC. *Bioorg. Med. Chem. Lett.* 29, 1375–1379. doi: 10.1016/j.bmcl.2019.03.035
- Rehman, W., Arfons, L. M., and Lazarus, H. M. (2011). The rise, fall and subsequent triumph of thalidomide: lessons learned in drug development. *Ther. Adv. Hematol.* 2, 291–308. doi: 10.1177/2040620711413165
- Reynders, M., Matsuura, B. S., Berouti, M., Simoneschi, D., Marzio, A., Pagano, M., et al. (2020). PHOTACs enable optical control of protein degradation. *Sci. Adv.* 6:eay5064. doi: 10.1126/sciadv.aay5064
- Robb, C. M., Contreras, J. I., Kour, S., Taylor, M. A., Abid, M., Sonawane, Y. A., et al. (2017). Chemically induced degradation of CDK9 by a proteolysis targeting chimera (PROTAC). *Chem. Commun.* 53, 7577–7580. doi: 10.1039/c7cc03879h
- Rodriguez-Gonzalez, A., Cyrus, K., Salcius, M., Kim, K., Crews, C. M., Deshaies, R. J., et al. (2008). Targeting steroid hormone receptors for ubiquitination and degradation in breast and prostate cancer. *Oncogene* 27, 7201–7211. doi: 10.1038/onc.2008.320
- Sakamoto, K. M. (2010). Protacs for treatment of cancer. *Pediatr. Res.* 67, 505–508. doi: 10.1203/PDR.0b013e3181d35017
- Sakamoto, K. M., Kim, K. B., Kumagai, A., Mercurio, F., Crews, C. M., and Deshaies, R. J. (2001). Protacs: chimeric molecules that target proteins to the Skp1-Cullin-F box complex for ubiquitination and degradation. *Proc. Natl. Acad. Sci. U.S.A.* 98, 8554–8559. doi: 10.1073/pnas.141230798
- Sakamoto, K. M., Kim, K. B., Verma, R., Ransick, A., Stein, B., Crews, C. M., et al. (2003). Development of Protacs to target cancer-promoting proteins for ubiquitination and degradation. *Mol. Cell Proteomics* 2, 1350–1358. doi: 10.1074/mcp.T300009-MCP200
- Salami, J., Alabi, S., Willard, R. R., Vitale, N. J., Wang, J., Dong, H., et al. (2018). Androgen receptor degradation by the proteolysis-targeting chimera ARCC-4 outperforms enzalutamide in cellular models of prostate cancer drug resistance. *Commun. Biol.* 1:100. doi: 10.1038/s42003-018-0105-8
- Sato, S., Aoyama, H., Miyachi, H., Naito, M., and Hashimoto, Y. (2008). Demonstration of direct binding of cIAP1 degradation-promoting bestatin analogs to BIR3 domain: synthesis and application of fluorescent bestatin ester analogs. *Bioorg. Med. Chem. Lett.* 18, 3354–3358. doi: 10.1016/j.bmcl.2008.04.031
- Saw, P. E., and Song, E. W. (2019). Phage display screening of therapeutic peptide for cancer targeting and therapy. *Protein Cell* 10, 787–807. doi: 10.1007/s13238-019-0639-7
- Scaranti, M., Cojocar, E., Banerjee, S., and Banerji, U. (2020). Exploiting the folate receptor alpha in oncology. *Nat. Rev. Clin. Oncol.* 17, 349–359. doi: 10.1038/s41571-020-0339-5
- Schapiro, M., Calabrese, M. F., Bullock, A. N., and Crews, C. M. (2019). Targeted protein degradation: expanding the toolbox. *Nat. Rev. Drug Discov.* 18, 949–963. doi: 10.1038/s41573-019-0047-y
- Schiedel, M., Herp, D., Hammelmann, S., Swyter, S., Lehotzky, A., Robaa, D., et al. (2018). Chemically induced degradation of sirtuin 2 (Sirt2) by a proteolysis targeting chimera (PROTAC) based on sirtuin rearranging ligands (SirReals). *J. Med. Chem.* 61, 482–491. doi: 10.1021/acs.jmedchem.6b01872
- Schneekloth, A. R., Pucheault, M., Tae, H. S., and Crews, C. M. (2008). Targeted intracellular protein degradation induced by a small molecule: en route to chemical proteomics. *Bioorg. Med. Chem. Lett.* 18, 5904–5908. doi: 10.1016/j.bmcl.2008.07.114
- Schneekloth, J. S. Jr., Fonseca, F. N., Koldobskiy, M., Mandal, A., Deshaies, R., Sakamoto, K., et al. (2004). Chemical genetic control of protein levels: selective in vivo targeted degradation. *J. Am. Chem. Soc.* 126, 3748–3754. doi: 10.1021/ja309025z
- Sekine, K., Takubo, K., Kikuchi, R., Nishimoto, M., Kitagawa, M., Abe, F., et al. (2008). Small molecules destabilize cIAP1 by activating auto-ubiquitylation. *J. Biol. Chem.* 283, 8961–8968. doi: 10.1074/jbc.M709525200
- Shafirstein, G., Battoo, A., Harris, K., Baumann, H., Gollnick, S. O., Lindenmann, J., et al. (2016). Photodynamic therapy of non-small cell lung cancer. narrative review and future directions. *Ann. Am. Thorac. Soc.* 13, 265–275. doi: 10.1513/AnnalsATS.201509-650FR
- Shibata, N., Miyamoto, N., Nagai, K., Shimokawa, K., Sameshima, T., Ohoka, N., et al. (2017). Development of protein degradation inducers of oncogenic BCR-ABL protein by conjugation of ABL kinase inhibitors and IAP ligands. *Cancer Sci.* 108, 1657–1666. doi: 10.1111/cas.13284
- Shibata, N., Nagai, K., Morita, Y., Ujikawa, O., Ohoka, N., Hattori, T., et al. (2018). Development of protein degradation inducers of androgen receptor by conjugation of androgen receptor ligands and inhibitor of apoptosis protein ligands. *J. Med. Chem.* 61, 543–575. doi: 10.1021/acs.jmedchem.7b00168
- Shimokawa, K., Shibata, N., Sameshima, T., Miyamoto, N., Ujikawa, O., Nara, H., et al. (2017). Targeting the allosteric site of oncoprotein BCR-ABL as an alternative strategy for effective target protein degradation. *ACS Med. Chem. Lett.* 8, 1042–1047. doi: 10.1021/acsmedchemlett.7b00247
- Sievers, Q. L., Petzold, G., Bunker, R. D., Renneville, A., Slabicki, M., Liddicoat, B. J., et al. (2018). Defining the human C2H2 zinc finger degrome targeted by thalidomide analogs through CRBN. *Science* 362:eaat0572. doi: 10.1126/science.aat0572
- Smalley, J. P., Adams, G. E., Millard, C. J., Song, Y., Norris, J. K. S., Schwabe, J. W. R., et al. (2020). PROTAC-mediated degradation of class I histone deacetylase enzymes in corepressor complexes. *Chem. Commun.* 56, 4476–4479. doi: 10.1039/d0cc01485k
- Smith, B. E., Wang, S. L., Jaime-Figueroa, S., Harbin, A., Wang, J., Hamman, B. D., et al. (2019). Differential PROTAC substrate specificity dictated by orientation of recruited E3 ligase. *Nat. Commun.* 10:131. doi: 10.1038/s41467-018-08027-7
- Su, S., Yang, Z., Gao, H., Yang, H., Zhu, S., An, Z., et al. (2019). Potent and preferential degradation of CDK6 via proteolysis targeting chimera degraders. *J. Med. Chem.* 62, 7575–7582. doi: 10.1021/acs.jmedchem.9b00871
- Sun, B., Fiskus, W., Qian, Y., Rajapakse, K., Raina, K., Coleman, K. G., et al. (2018). BET protein proteolysis targeting chimera (PROTAC) exerts potent lethal activity against mantle cell lymphoma cells. *Leukemia* 32, 343–352. doi: 10.1038/leu.2017.207
- Sun, N., Ren, C., Kong, Y., Zhong, H., Chen, J., Li, Y., et al. (2020). Development of a Brigatinib degrader (SIAIS117) as a potential treatment for ALK positive cancer resistance. *Eur. J. Med. Chem.* 193:112190. doi: 10.1016/j.ejmech.2020.112190
- Sun, Y., Ding, N., Song, Y., Yang, Z., Liu, W., Zhu, J., et al. (2019). Degradation of Bruton's tyrosine kinase mutants by PROTACs for potential treatment of ibrutinib-resistant non-Hodgkin lymphomas. *Leukemia* 33, 2105–2110. doi: 10.1038/s41375-019-0440-x
- Sun, Y., Zhao, X., Ding, N., Gao, H., Wu, Y., Yang, Y., et al. (2018). PROTAC-induced BTK degradation as a novel therapy for mutated BTK C481S induced ibrutinib-resistant B-cell malignancies. *Cell Res.* 28, 779–781. doi: 10.1038/s41422-018-0055-1
- Teng, M., Jiang, J., He, Z., Kwiatkowski, N. P., Donovan, K. A., Mills, C. E., et al. (2020). Development of CDK2 and CDK5 dual degrader TMX-2172. *Angew. Chem. Int. Ed. Engl.* 59, 13865–13870. doi: 10.1002/anie.202004087
- Testa, A., Lucas, X., Castro, G. V., Chan, K. H., Wright, J. E., Runcie, A. C., et al. (2018). 3-Fluoro-4-hydroxyprolines: synthesis, conformational analysis, and stereoselective recognition by the VHL E3 Ubiquitin ligase for targeted protein degradation. *J. Am. Chem. Soc.* 140, 9299–9313. doi: 10.1021/jacs.8b05807
- Tinworth, C. P., Lithgow, H., Dittus, L., Bassi, Z. I., Hughes, S. E., Muelbauer, M., et al. (2019). PROTAC-mediated degradation of bruton's tyrosine kinase is inhibited by covalent binding. *ACS Chem. Biol.* 14, 342–347. doi: 10.1021/acscchembio.8b01094
- Tovell, H., Testa, A., Zhou, H., Shpiro, N., Crafter, C., Ciulli, A., et al. (2019). Design and characterization of SGK3-PROTAC1, an isoform specific SGK3 Kinase

- PROTAC Degradation. *ACS Chem. Biol.* 14, 2024–2034. doi: 10.1021/acscchembio.9b00505
- Varfolomeev, E., Blankenship, J. W., Wayson, S. M., Fedorova, A. V., Kayagaki, N., Garg, P., et al. (2007). IAP antagonists induce autoubiquitination of c-IAPs, NF-kappaB activation, and TNFalpha-dependent apoptosis. *Cell* 131, 669–681. doi: 10.1016/j.cell.2007.10.030
- Vassilev, L. T., Vu, B. T., Graves, B., Carvajal, D., Podlaski, F., Filipovic, Z., et al. (2004). In vivo activation of the p53 pathway by small-molecule antagonists of MDM2. *Science* 303, 844–848. doi: 10.1126/science.1092472
- Vollmer, S., Cunoosamy, D., Lv, H., Feng, H., Li, X., Nan, Z., et al. (2020). Design, synthesis, and biological evaluation of MEK PROTACs. *J. Med. Chem.* 63, 157–162. doi: 10.1021/acs.jmedchem.9b00810
- Vorobev, A. Y., and Moskalensky, A. E. (2020). Long-wavelength photoremovable protecting groups: on the way to in vivo application. *Comput. Struct. Biotechnol. J.* 18, 27–34. doi: 10.1016/j.csbj.2019.11.007
- Wang, L., Shao, X., Zhong, T., Wu, Y., Xu, A., Sun, X., et al. (2021). Discovery of a first-in-class CDK2 selective degrader for AML differentiation therapy. *Nat. Chem. Biol.* 17, 567–575. doi: 10.1038/s41589-021-00742-5
- Wang, M., Lu, J., Yang, C. Y., and Wang, S. (2020). Discovery of SHP2-D26 as a first, potent, and effective PROTAC Degradation of SHP2 Protein. *J. Med. Chem.* 63, 7510–7528. doi: 10.1021/acs.jmedchem.0c00471
- Wang, S., Han, L., Han, J., Li, P., Ding, Q., Zhang, Q. J., et al. (2019). Uncoupling of PARP1 trapping and inhibition using selective PARP1 degradation. *Nat. Chem. Biol.* 15, 1223–1231. doi: 10.1038/s41589-019-0379-2
- Wang, X., Feng, S., Fan, J., Li, X., Wen, Q., and Luo, N. (2016). New strategy for renal fibrosis: targeting Smad3 proteins for ubiquitination and degradation. *Biochem. Pharmacol.* 116, 200–209. doi: 10.1016/j.bcp.2016.07.017
- Wang, X., and Kalow, J. A. (2018). Rapid aqueous photocaging by red light. *Org. Lett.* 20, 1716–1719. doi: 10.1021/acs.orglett.8b00100
- Wang, Z., He, N., Guo, Z., Niu, C., Song, T., Guo, Y., et al. (2019). Proteolysis targeting chimeras for the selective degradation of Mcl-1/Bcl-2 derived from nonselective target binding ligands. *J. Med. Chem.* 62, 8152–8163. doi: 10.1021/acs.jmedchem.9b00919
- Wei, J., Hu, J., Wang, L., Xie, L., Jin, M. S., Chen, X., et al. (2019). Discovery of a first-in-class mitogen-activated protein kinase kinase 1/2 degrader. *J. Med. Chem.* 62, 10897–10911. doi: 10.1021/acs.jmedchem.9b01528
- Winter, G. E., Buckley, D. L., Paultk, J., Roberts, J. M., Souza, A., Dhe-Paganon, S., et al. (2015). DRUG DEVELOPMENT. Phthalimide conjugation as a strategy for in vivo target protein degradation. *Science* 348, 1376–1381. doi: 10.1126/science.aab1433
- Winter, G. E., Mayer, A., Buckley, D. L., Erb, M. A., Roderick, J. E., Vittori, S., et al. (2017). BET bromodomain proteins function as master transcription elongation factors independent of CDK9 recruitment. *Mol. Cell* 67, 5.e19–18.e19. doi: 10.1016/j.molcel.2017.06.004
- Wu, H., Yang, K., Zhang, Z., Leisten, E. D., Li, Z., Xie, H., et al. (2019). Development of multifunctional histone deacetylase 6 degraders with potent antimyeloma activity. *J. Med. Chem.* 62, 7042–7057. doi: 10.1021/acs.jmedchem.9b00516
- Wurz, R. P., and Cee, V. J. (2019). Targeted degradation of MDM2 as a new approach to improve the efficacy of MDM2-p53 inhibitors. *J. Med. Chem.* 62, 445–447. doi: 10.1021/acs.jmedchem.8b01945
- Xue, G., Wang, K., Zhou, D., Zhong, H., and Pan, Z. (2019). Light-induced protein degradation with photocage PROTACs. *J. Am. Chem. Soc.* 141, 18370–18374. doi: 10.1021/jacs.9b06422
- Yamamoto, J., Suwa, T., Murase, Y., Tateno, S., Mizutome, H., Asatsuma-Okumura, T., et al. (2020). ARID2 is a pomalidomide-dependent CRL4(CRBN) substrate in multiple myeloma cells. *Nat. Chem. Biol.* 16, 1208–1217. doi: 10.1038/s41589-020-0645-3
- Yang, C., Wang, H., Zhang, B., Chen, Y., Zhang, Y., Sun, X., et al. (2016). LCL161 increases paclitaxel-induced apoptosis by degrading cIAP1 and cIAP2 in NSCLC. *J. Exp. Clin. Cancer Res.* 35:158. doi: 10.1186/s13046-016-0435-7
- Yang, K., Song, Y., Xie, H., Wu, H., Wu, Y. T., Leisten, E. D., et al. (2018). Development of the first small molecule histone deacetylase 6 (HDAC6) degraders. *Bioorg. Med. Chem. Lett.* 28, 2493–2497. doi: 10.1016/j.bmcl.2018.05.057
- Yang, K., Wu, H., Zhang, Z., Leisten, E. D., Nie, X., Liu, B., et al. (2020). Development of selective histone deacetylase 6 (HDAC6) degraders recruiting von hippel-lindau (VHL) E3 ubiquitin ligase. *ACS Med. Chem. Lett.* 11, 575–581. doi: 10.1021/acsmchemlett.0c00046
- You, I., Erickson, E. C., Donovan, K. A., Eleuteri, N. A., Fischer, E. S., Gray, N. S., et al. (2020). Discovery of an AKT degrader with prolonged inhibition of downstream signaling. *Cell Chem. Biol.* 27, 66.e7–73.e7. doi: 10.1016/j.chembiol.2019.11.014
- Zengerle, M., Chan, K. H., and Ciulli, A. (2015). Selective small molecule induced degradation of the BET bromodomain protein BRD4. *ACS Chem. Biol.* 10, 1770–1777. doi: 10.1021/acscchembio.5b00216
- Zhang, C., Han, X. R., Yang, X., Jiang, B., Liu, J., Xiong, Y., et al. (2018). Proteolysis targeting chimeras (PROTACs) of Anaplastic Lymphoma Kinase (ALK). *Eur. J. Med. Chem.* 151, 304–314. doi: 10.1016/j.ejmech.2018.03.071
- Zhang, D., Baek, S. H., Ho, A., Lee, H., Jeong, Y. S., and Kim, K. (2004). Targeted degradation of proteins by small molecules: a novel tool for functional proteomics. *Comb. Chem. High Throughput Screen* 7, 689–697. doi: 10.2174/1386207043328364
- Zhang, H., Zhao, H. Y., Xi, X. X., Liu, Y. J., Xin, M., Mao, S., et al. (2020a). Discovery of potent epidermal growth factor receptor (EGFR) degraders by proteolysis targeting chimera (PROTAC). *Eur. J. Med. Chem.* 189:112061. doi: 10.1016/j.ejmech.2020.112061
- Zhang, X., Thummuri, D., Liu, X., Hu, W., Zhang, P., Khan, S., et al. (2020b). Discovery of PROTAC BCL-XL degraders as potent anticancer agents with low on-target platelet toxicity. *Eur. J. Med. Chem.* 192:112186. doi: 10.1016/j.ejmech.2020.112186
- Zhang, X., Xu, F., Tong, L., Zhang, T., Xie, H., Lu, X., et al. (2020b). Design and synthesis of selective degraders of EGFR(L858R/T790M) mutant. *Eur. J. Med. Chem.* 192:112199. doi: 10.1016/j.ejmech.2020.112199
- Zhao, B., and Burgess, K. (2019). PROTACs suppression of CDK4/6, crucial kinases for cell cycle regulation in cancer. *Chem. Commun.* 55, 2704–2707. doi: 10.1039/c9cc00163h
- Zhao, Q., Lan, T., Su, S., and Rao, Y. (2019). Induction of apoptosis in MDA-MB-231 breast cancer cells by a PARP1-targeting PROTAC small molecule. *Chem. Commun.* 55, 369–372. doi: 10.1039/c8cc07813k
- Zhao, Q., Ren, C., Liu, L., Chen, J., Shao, Y., Sun, N., et al. (2019). Discovery of SIAIS178 as an effective BCR-ABL degrader by recruiting von hippel-lindau (VHL) E3 ubiquitin ligase. *J. Med. Chem.* 62, 9281–9298. doi: 10.1021/acs.jmedchem.9b01264
- Zhou, B., Hu, J., Xu, F., Chen, Z., Bai, L., Fernandez-Salas, E., et al. (2018). Discovery of a small-molecule degrader of bromodomain and extra-terminal (BET) proteins with picomolar cellular potencies and capable of achieving tumor regression. *J. Med. Chem.* 61, 462–481. doi: 10.1021/acs.jmedchem.6b01816
- Zhou, F., Chen, L., Cao, C., Yu, J., Luo, X., Zhou, P., et al. (2020). Development of selective mono or dual PROTAC degrader probe of CDK isoforms. *Eur. J. Med. Chem.* 187:111952. doi: 10.1016/j.ejmech.2019.111952
- Zhou, H., Bai, L., Xu, R., Zhao, Y., Chen, J., McEachern, D., et al. (2019). Structure-based discovery of SD-36 as a potent, selective, and efficacious PROTAC degrader of STAT3 Protein. *J. Med. Chem.* 62, 11280–11300. doi: 10.1021/acs.jmedchem.9b01530
- Zhou, W., Wei, W., and Sun, Y. (2013). Genetically engineered mouse models for functional studies of SKP1-CUL1-F-box-protein (SCF) E3 ubiquitin ligases. *Cell Res.* 23, 599–619. doi: 10.1038/cr.2013.44
- Zoppi, V., Hughes, S. J., Maniaci, C., Testa, A., Gmaschitz, T., Wieshofer, C., et al. (2019). Iterative design and optimization of initially inactive proteolysis targeting chimeras (PROTACs) Identify VZ185 as a potent, fast, and selective von hippel-lindau (VHL) based dual degrader probe of BRD9 and BRD7. *J. Med. Chem.* 62, 699–726. doi: 10.1021/acs.jmedchem.8b01413
- Zorba, A., Nguyen, C., Xu, Y., Starr, J., Borzilleri, K., Smith, J., et al. (2018). Delineating the role of cooperativity in the design of potent PROTACs for BTK. *Proc. Natl. Acad. Sci. U.S.A.* 115, E7285–E7292. doi: 10.1073/pnas.1803662115

**Conflict of Interest:** WW is a co-founder and consultant for the ReKindle Therapeutics.

The remaining authors declare that the research was conducted in the absence of any commercial or financial relationships that could be construed as a potential conflict of interest.

Copyright © 2021 Liu, Peng and Wei. This is an open-access article distributed under the terms of the Creative Commons Attribution License (CC BY). The use, distribution or reproduction in other forums is permitted, provided the original author(s) and the copyright owner(s) are credited and that the original publication in this journal is cited, in accordance with accepted academic practice. No use, distribution or reproduction is permitted which does not comply with these terms.



# Regulation of Ferroptosis Pathway by Ubiquitination

Xinbo Wang<sup>†</sup>, Yanjin Wang<sup>†</sup>, Zan Li<sup>†</sup>, Jieling Qin and Ping Wang\*

Tongji University Cancer Center, Shanghai Tenth People's Hospital, School of Medicine, Tongji University, Shanghai, China

## OPEN ACCESS

### Edited by:

Lingqiang Zhang,  
National Center for Protein Sciences  
Shanghai, China

### Reviewed by:

Ejaz Ahmad,  
University of Michigan, United States  
Yuanjun Shen,  
University of California, Davis,  
United States

### \*Correspondence:

Ping Wang  
wangp@tongji.edu.cn

<sup>†</sup>These authors have contributed  
equally to this work

### Specialty section:

This article was submitted to  
Cell Growth and Division,  
a section of the journal  
Frontiers in Cell and Developmental  
Biology

**Received:** 23 April 2021

**Accepted:** 19 July 2021

**Published:** 13 August 2021

### Citation:

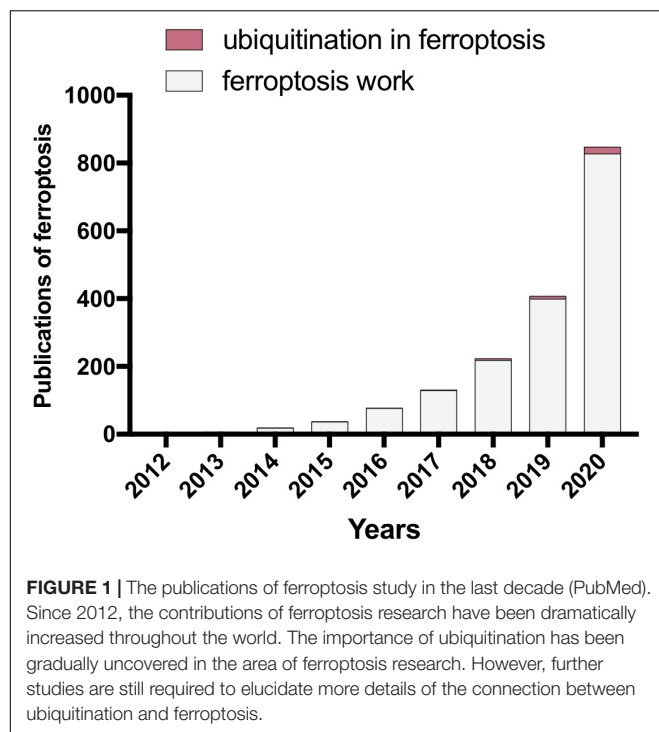
Wang X, Wang Y, Li Z, Qin J and  
Wang P (2021) Regulation  
of Ferroptosis Pathway by  
Ubiquitination.  
Front. Cell Dev. Biol. 9:699304.  
doi: 10.3389/fcell.2021.699304

Ferroptosis is an iron-dependent form of programmed cell death, which plays crucial roles in tumorigenesis, ischemia-reperfusion injury and various human degenerative diseases. Ferroptosis is characterized by aberrant iron and lipid metabolisms. Mechanistically, excess of catalytic iron is capable of triggering lipid peroxidation followed by Fenton reaction to induce ferroptosis. The induction of ferroptosis can be inhibited by sufficient glutathione (GSH) synthesis via system Xc<sup>-</sup> transporter-mediated cystine uptake. Therefore, induction of ferroptosis by inhibition of cystine uptake or dampening of GSH synthesis has been considered as a novel strategy for cancer therapy, while reversal of ferroptotic effect is able to delay progression of diverse disorders, such as cardiopathy, steatohepatitis, and acute kidney injury. The ubiquitin (Ub)-proteasome pathway (UPP) dominates the majority of intracellular protein degradation by coupling Ub molecules to the lysine residues of protein substrate, which is subsequently recognized by the 26S proteasome for degradation. Ubiquitination is crucially involved in a variety of physiological and pathological processes. Modulation of ubiquitination system has been exhibited to be a potential strategy for cancer treatment. Currently, more and more emerged evidence has demonstrated that ubiquitous modification is involved in ferroptosis and dominates the vulnerability to ferroptosis in multiple types of cancer. In this review, we will summarize the current findings of ferroptosis surrounding the viewpoint of ubiquitination regulation. Furthermore, we also highlight the potential effect of ubiquitination modulation on the perspective of ferroptosis-targeted cancer therapy.

**Keywords:** ferroptosis, ubiquitination, lipid peroxidation, cell metabolism, cancer therapy

## INTRODUCTION

All living organisms have been refined by the natural selection during the evolution. A sophisticated and unique reproduction system has been evolved in various species to ensure a sustained anagenesis (Bedoui et al., 2020; Rothlin et al., 2020; Koren and Fuchs, 2021). Cell suicide, namely, programmed cell death, includes apoptosis (Taylor et al., 2008), necroptosis (Zong and Thompson, 2006), ferroptosis (Green, 2019), and pyroptosis (Nagata, 2018). Ferroptosis, which is a novel type of programmed cell death, is characterized by a dysregulated iron metabolism and accumulation of lipid peroxides (Stockwell et al., 2017). Ferroptosis differs from other types of cell death such as apoptosis and necrosis. It features the alteration of mitochondria and aberrant accumulation of excessive iron as well as loss of cysteine-glutathione-GPX4 axis, a major cellular antioxidant system (Tang D. et al., 2021). While catalytic iron is indispensably involved in cell growth of all



organisms, it ensures the essential function of vital enzymes encompassing oxygen transport, ATP generation, and DNA synthesis (Silva and Faustino, 2015). However, excessive iron can also impede cells by induction of Fenton reaction, leading to various DNA damages and even cell death (Eid et al., 2017). Therefore, maintaining an appropriate labile iron is critical for cell viability. Cells ongoing ferroptosis, however, show a dysregulated iron metabolism displaying ceaseless iron intake and retention. Eventually, a mass of catalytic iron assembled in the cytosol and other organelles contributes to lipid peroxidation, which will lead to ferroptosis (Conrad and Proneth, 2020). Although the research contribution of ferroptosis has been more and more fruitful, the involvement of post-translational regulation in ferroptosis has been largely unknown yet.

In living cells, the ubiquitin (Ub)-proteasome pathway (UPP) dominates the majority of intracellular protein degradation by coupling Ub molecules to the lysine residues of protein substrate, which is subsequently recognized by the 26S proteasome for degradation (Lu et al., 2021). Dysregulated ubiquitination has been implicated in neurological diseases and tumorigenesis (Bard et al., 2018; Lu et al., 2021). Recently, emerged evidence has emphasized the crucial roles of ubiquitination in ferroptosis regulation. Although the regulation of ubiquitous pathway in cells ongoing ferroptosis remains elusive, the crosstalk between ubiquitous modulation and ferroptosis has captured the more and more imagination of researchers (Figure 1). Herein, we summarize the progression of ubiquitination regulation in ferroptosis in recent years. Furthermore, we look into the distance to the development trend of ferroptosis in the clinical application of cancer therapy by targeting ubiquitous regulation.

## THE HALLMARKS OF FERROPTOSIS

Although the increased iron supply and accelerated lipid production satisfy the demand of cancer cells to boost cancer cell division and spreading, excessive iron will greatly accelerate lipid peroxidation, which consequently gives rise to higher vulnerability to ferroptosis. Apart from other types of cell death, ferroptosis appears to show an iron-addiction phenotype accompanied by a lipid peroxidation phenomenon. Herein, we will discuss the recent findings related to ferroptosis surrounding these points.

## Alteration of Iron Metabolism

Iron is one of the most abundant elements on Earth and indispensably involved in cell growth of all organisms. It ensures the essential function of vital enzymes encompassing oxygen transport, ATP generation, and DNA synthesis (Sheftel et al., 2012). Iron possesses unpaired electrons, exhibiting a wide range of oxidation states that contribute to its versatile participant in redox reactions (Barton et al., 2019), which endow iron with crucial roles in maintaining biological activities, such as cell division, metabolism, and growth (Torti et al., 2018). Therefore, maintaining an appropriate labile iron is critical for cell viability. Cells ongoing ferroptosis, however, show a dysregulated iron metabolism displaying ceaseless iron intake and retention. Briefly, intracellular iron acquisition is predominantly mediated by transferrin receptor 1 (TFRC) that engages in uptake of transferrin-bound Fe (III) and cooperates with clathrin-mediated endocytosis (Kawabata, 2019). Then the absorbed iron is released into acidic endosomes where the Fe (III) is reduced to Fe (II) status by the ferriductase enzyme STEAP3 (Ohgami et al., 2005). Then, Fe (II) is released from endosome to cytosol by divalent metal transporter 1 (DMT1), which is also involved in Fe (II) and other ions such as cadmium ( $\text{Ca}^{2+}$ ), copper ( $\text{Cu}^{2+}$ ), and zinc ( $\text{Zn}^{2+}$ ) uptake across the plasma membrane (Illing et al., 2012). Iron storage is primarily conducted by ferritin protein complex, which comprises heavy chain (FTH) and light chain (FTL) protecting cells against reactive oxygen species (ROS) (Vidal et al., 2008; Zhang et al., 2009). Ferroportin (FPN1), the only known iron exporter, enables iron exporting across the plasma membrane (Ward and Kaplan, 2012). The catalytic iron transiently assembled in the cytosol constitutes a labile-iron pool (LIP) serving as a crossroad of intracellular iron trafficking (Kakhlon and Cabantchik, 2002; Figure 2).

Iron addiction, which is commonly existing in most malignancies, has been revealed as a potential risk of ferroptosis (Basuli et al., 2017; Li et al., 2019). The rapid consumption of iron fulfills the needs of aggressive behaviors including higher proliferation, metastasis, and invasion in tumors (Hann et al., 1988). Furthermore, the enrichment of catalytic iron in tumor cells can be further enhanced by hypoxia. The increased levels of iron transporters (TFRC and DMT1) and iron regulatory protein 2 (IRP2) have been uncovered in response to activation of HIF-1 accompanied by stabilization of iron-storage proteins (FTL/H) (Hanson et al., 1999; Tacchini et al., 1999; Qian et al., 2011; Huang et al., 2014; Li et al., 2019). These evidence suggests that iron addiction is favored by cancer cells. However, it may



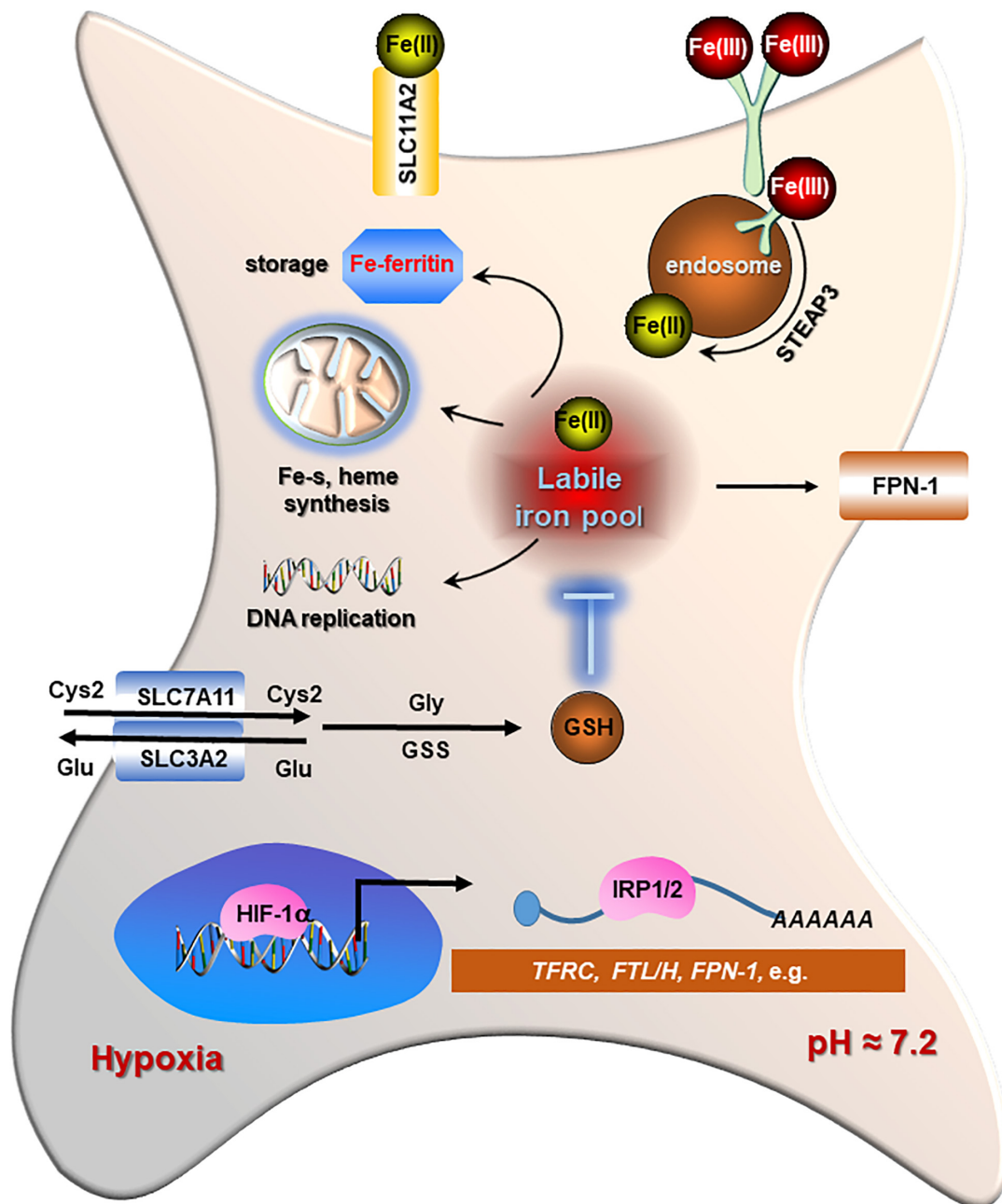


**FIGURE 2 |** The regulations of iron metabolism and redox homeostasis in cancer cells. Cancer cells display higher iron transporting, storage, and bioavailability as well as increased levels of glutathione (GSH) and GPX4 for detoxification in contrast to normal cells. Iron regulatory proteins (IRP1/2) play a central role in maintaining an adequate iron homeostasis in cancer cells by regulating the stability of each mRNA differentially [increasing for transferrin receptor 1 (TFRC) and SLC11A2, while decreasing for light chain (FTL)/H protecting cells]. The classical marker of hypoxia, HIF-1 $\alpha$ , also supports the stabilization of TFRC, IRP1/2, as well as FTL/H to promote both iron absorption and availability in cancer cells.

also potentially render malignancies to be highly vulnerable to iron-induced cytotoxicity contributing to ferroptosis.

### Lipid Peroxidation in Ferroptosis

The catalytic radicals induced by excessive iron will attack electrons from the lipids localized in the plasma and organelle membranes (Chen et al., 2021a; Yan et al., 2021). Lipid

peroxidation can be caused by either non-enzymatic iron-catalyzed form or enzymatic generation of signals (Conrad and Pratt, 2019). Acyl-CoA synthetase long-chain family member 4 (ACSL4) dominates the catalyzing reaction, which converts arachidonoyl (AA) or adrenoyl (AdA) into AA or AdA acyl-CoA derivatives (AA-CoA or AdA-CoA). Both AA-CoA and AdA-CoA will be esterified by lysophosphatidylcholine acyltransferase

3 (LPCTA3) to produce phosphati-dylethanolamines (AA-PE and AdA-PE). Subsequently, AA-PE and AdA-PE will be oxidized by 15-lipoxygenase (ALOX15), which is iron-containing dioxygenase that catalyzes the hydrogen abstraction of polyunsaturated fatty acid (PUFA) to generate lipid hydroperoxides and induce ferroptosis (Mashima and Okuyama, 2015). Importantly, iron also exerts roles in oxidative cleaving of 15-hydroperoxy-AA-PE (HOO-AA-PE), which is able to react with protein targets to induce plasma membrane disruption (Mashima and Okuyama, 2015; **Figure 3**).

## Main Regulators of Ferroptosis

In the recent decade, a great number of efforts have been contributed to the progression of ferroptosis work. Thereby, we summarize the key findings related to ferroptosis since 2012 (**Figure 4**). Moreover, we emphasize the studies about ubiquitination modification in ferroptosis according to the recent findings.

Dixon et al. (2012) (Brent R. Stockwell Lab) have proposed that erastin, a small-molecule compound, can efficiently kill cancer cells by induction of iron-dependent cell death, named ferroptosis. Apparently, this type of cell death is morphologically and biochemically distinct from other types of cell death (Stockwell et al., 2017). Mechanistically, erastin inhibits cystine uptake via the cystine/glutamate  $Xc^-$  antiporter, which has been found overexpressed in many types of cancer. Disruption of cysteine-GSH-GPX4 remarkably triggers ferroptosis in cancer cells. Solute carrier family 7 member 11 (SLC7A11), one of the components constituting  $Xc^-$  antiporter, is transcriptionally regulated by nuclear factor, erythroid 2-like 2 (NRF2) and ATF3/4 (Ye et al., 2014; Ogiwara et al., 2019), indicating the key role of cystine metabolism and redox balance in ferroptosis (Chu et al., 2019; Zhang Y. et al., 2021).

Additionally, further investigation has indicated that this type of cell death is accompanied by induction of lipid peroxidation and aberrant morphology of the mitochondria. Moreover, iron chelator also shows effective inhibitory effect on erastin-induced cell lethality (Chen P.H. et al., 2021; Zeng et al., 2021). Besides, ferrostatin-1, a specific lipid ROS scavenger, has been found to be a potent inhibitor of ferroptosis in cancer cells, which is hereafter widely used in ferroptosis research (Lee et al., 2020; Hong et al., 2021). As  $Xc^-$  antiporter is an essential factor dictating ferroptosis susceptibility (Lang et al., 2019), its corresponding ubiquitination regulators [E3 ubiquitin ligases and deubiquitylating enzymes (DUBs)] are supposed to be theoretically important for ferroptosis regulation.

In parallel with SLC7A11, selenium-containing GPX4 is another key protein with a potent role in blocking ferroptosis. Yang et al. (2014) have discovered that GPX4 is the target of ferroptosis inducing compounds RSL3 and ML162, thus, revealing GPX4 as an essential protector against ferroptosis. In this study, the authors have also identified that *PTGS2*, a gene encoding cyclooxygenase-2 (COX-2), was the utmost expression gene in response to RSL3 treatment (Wu et al., 2019; Li et al., 2020; Yi et al., 2020). It should be noted that degradation of GPX4 has been revealed in cells ongoing ferroptosis, which is irrespective of GPX4 activity inhibition (Chen et al., 2021b),

suggesting that ubiquitination modification of GPX4 degradation is supposed to be existing.

Inactivation of the p53 has been found in many types of cancer (Hafner et al., 2019; Levine, 2020). p53 has been considered as a potent tumor suppressor due to multiple roles in cell cycle arrest, DNA damage, apoptosis, and senescence (Kakhlon and Cabantchik, 2002; Jiang et al., 2015; Boutelle and Attardi, 2021). Unexpectedly, it has been reported that p53 inhibits cystine uptake and sensitizes cells to ferroptosis by repressing the expression of SLC7A11 (Jiang et al., 2015), thus, uncovering a novel role of p53 in ferroptosis. Notably, p53 is tightly regulated by both E3 ubiquitin ligases (MDM2, TRIM69, UBE2T, RBCK1, COP1, and CHIP) and DUBs (USP7, USP3, USP11, USP15, USP49, OTUD1, and OTUD5), suggesting a crosslinking between ubiquitination and p53-mediated ferroptosis (Liu Y. et al., 2019).

Nutrient availability dictates the cell survival and proliferation rate, especially in tumor cells (Hoxhaj and Manning, 2020; Sukjoi et al., 2021). Long-time deprivation of amino acids, glucose, or growth factors are able to result in cell death, which is considered as a passive death process (Tummers and Green, 2017; Hayes et al., 2020). It has been indicated that ferroptosis is associated with serum supplement upon amino acid starvation. Both iron carrier protein transferrin and amino acid glutamine have been demonstrated as ferroptosis inducers (Gao et al., 2015). Moreover, a crosstalk among different types of cell death has been well demonstrated (Nikolietopoulou et al., 2013; Kasprowska-Liśkiewicz, 2017; Frank and Vince, 2019; Snyder and Oberst, 2021). In addition, Gao et al. (2016) have found that ferroptosis is an autophagic cell death process due to the degradation of iron storage protein ferritin (FTH1) mediated by nuclear receptor coactivator 4 (NCOA4), referred to as ferritinophagy. Consequently, the resultant ferrous iron liberated from the breakdown of ferritin amplifies the labile iron pool in cytosol and results in a large accumulation of ROS, eventually triggering lipid peroxidation and ferroptosis (Gao et al., 2016; Hou et al., 2016). Since ubiquitination has been shown to largely participate in amino acid metabolism and autophagy regulation (Kwon and Ciechanover, 2017; Harper et al., 2018; Senft et al., 2018), thus, we propose that ubiquitination is potentially closely related to the ferroptosis process. Additionally, whether ubiquitination occurs in iron-related protein, such as TFRC and FTH1, needs further investigation.

Lipid peroxidation is a hallmark of ferroptosis (Zou et al., 2020a), and PUFA biosynthesis dictates ferroptosis sensitivity (Yang and Stockwell, 2016; Wu et al., 2020). Doll et al. (2017) have uncovered acyl-CoA synthetase long-chain family member 4 (ACSL4) as a crucial player in ferroptosis execution. Moreover, the ACSL4 expression is indicative of ferroptosis confirmed by several studies (Doll et al., 2017; Bersuker et al., 2019; Zou et al., 2020a,b). ACSL4 is responsible for the esterification of CoA to long-chain PUFAs, a key step involved in ferroptosis (Doll et al., 2017). Arachidonic acid has been indicated to promote ACSL4 ubiquitination and proteasomal degradation (Kan et al., 2014). Further investigation found that p115, the vesicular trafficking protein, may be involved in regulation of ACSL4 degradation. However, the specific E3 ubiquitin ligases and DUBs for ACSL4

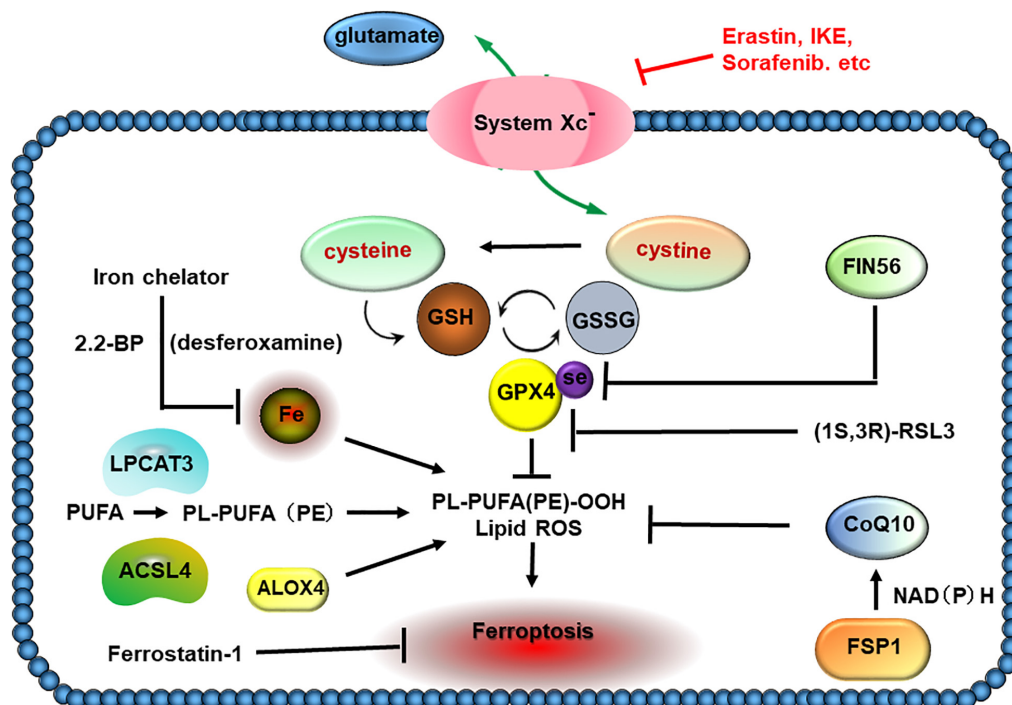


**FIGURE 3 |** Lipid peroxidation in ferroptosis. The increased absorption of cysteine in tumor cells is utilized to build up the cysteine–glutathione (GSH)–GPX4 axis, which plays a crucial role in detoxifying cellular oxidants and evading ferroptosis. Acyl-CoA synthetase long-chain family member 4 (ACSL4) associates with lysophosphatidylcholine acyltransferase 3 (LPCAT3) to incorporate polyunsaturated fatty acids (PUFAs) into PL-PUFA (PE), which shows higher susceptibility to peroxidation and ferroptosis. The catalytic iron inside cells appears to be the source of Fenton chemistry, which creates hydroxyl and peroxy radicals capturing hydrogen atoms from PUFAs and triggering peroxidation of PL-PUFA. FSP1, a novel finding of ferroptosis suppressor, protects cells against ferroptosis by catalyzing the regeneration of CoQ10 using NAD(P)H. FIN56 induces ferroptosis by promoting the GPX4 degradation and lowering the CoQ10 amount.

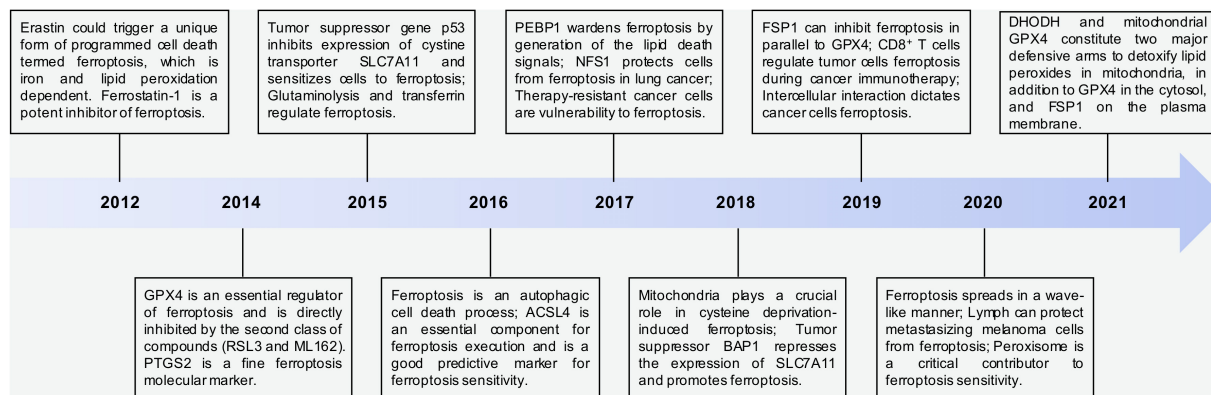


**FIGURE 4 |** The key points in discovery and research history of ferroptosis. Time line of key findings in ferroptosis research. Ferroptosis was firstly defined in 2012. In this decade, a great number of efforts have contributed to the progression of ferroptosis work. Overall, DHODH and mitochondrial GPX4 are two major defensive arms to detoxify lipid peroxides in the mitochondria, in addition to FSP1 on the plasma membrane and GPX4 in the cytosol.

remained to be elucidated (Sen et al., 2020). The oxygenation of PUFAs by ALOX15 has been found involved in ferroptosis execution (Li et al., 2018). Wenzel et al. have discovered that phosphatidylethanolamine-binding protein 1 (PEBP1), a scaffold protein inhibitor of protein kinase cascades, complexes with ALOX15 and changes its substrate competence to generate hydroperoxy-PE to promote ferroptosis (Wenzel et al., 2017).

Further studies are needed to elucidate whether there are some post-translational modifications on ALOX15 and PEBP1 to affect ferroptosis sensitivity.

As mentioned above, ferroptosis is featured by dramatic morphological changes of mitochondria, including mitochondrial fragmentation and cristae enlargement (Del Re et al., 2019; Bock and Tait, 2020), whereas the underlying



mechanism is largely unknown for a long time. Some studies have shown that the mitochondria play a crucial role in cysteine deprivation-induced ferroptosis. Mechanistically, the mitochondrial tricarboxylic acid (TCA) cycle and electron transport chain can promote cysteine deprivation-induced ferroptosis by serving as the major source for cellular lipid peroxide production (Gao et al., 2019). It will be interesting to demonstrate whether ubiquitination is involved in mitochondrial alteration in cells ongoing ferroptosis, as the clearance of dysfunctional mitochondria (known as mitophagy) requires Parkin, the E3 ubiquitin ligase that promotes ubiquitination of mitochondrial proteins (Ashrafi and Schwarz, 2013; Pickrell and Youle, 2015; Ravanelli et al., 2020; Song et al., 2021a).

GPX4 is regarded as an effective suppressor of ferroptosis. However, some cancer cells that expressed a low level of GPX4 strongly confers resistance to ferroptosis, suggesting that additional ferroptosis suppressors are supposed to be existing. By using synthetic lethal CRISPR–Cas9 (clustered regularly interspaced short palindromic repeats–Cas9) screening and an overexpression cloning approach, Bersuker et al. (2019) and Doll et al. (2019) have identified apoptosis-inducing factor mitochondria-associated 2 (AIFM2, also known as FSP1) as a key component of CoQ antioxidant system that acts in parallel with the canonical GPX4 pathway. The FSP1–CoQ10–NADPH pathway exists as a stand-alone parallel system, which coordinates GPX4 and GSH to suppress phospholipid peroxidation and ferroptosis. Notably, FSP1 has been shown to be highly ubiquitinated (Hornbeck et al., 2015), suggesting ubiquitination modification and corresponding E3 ligases or DUBs regulating FSP1 may play vital roles in dictating ferroptosis sensitivity.

Cancer immunotherapy can enhance the effector function of CD8<sup>+</sup> T cells in the tumor microenvironment. It is traditionally considered that CD8<sup>+</sup> T cells enable tumor cell apoptosis. Unexpectedly, Wang W. et al. (2019) have found that immunotherapy-activated CD8<sup>+</sup> T cells can enhance lipid peroxidation in tumor cells, which contributes to the antitumor efficacy of immunotherapy. Mechanistically, interferon gamma (IFN $\gamma$ ) released from CD8<sup>+</sup> T cells enables the reduced expression of SLC7A11. Ionizing radiation (IR) induces substantial tumor cell death and is, thus, widely used in cancer treatment. Similarly, it has been showed that IR promotes ferroptosis in cancer cells (Lang et al., 2019), which is associated with elevation of ACSL4 expression, resulting in amplified lipid peroxidation (Lei et al., 2020). Therefore, ubiquitination of both antiporter system Xc<sup>−</sup> and ACSL4 may influence ferroptosis and may be an effective strategy for immune- and radiotherapies.

Ferroptosis occurs not only in cell-autonomous mechanism; cell density has been revealed to impact on ferroptosis susceptibility via the Hippo signaling pathway signaling axis. In epithelial cells, E-cadherin enables the inhibitory effect on ferroptosis by activating the intracellular Merlin (NF2) and Hippo signaling pathway. Antagonizing this signaling axis allows the transcriptional coactivator yes-associated protein (YAP) to promote ferroptosis by upregulating expression levels of both ACSL4 and TFRC (Wu et al., 2019). Consistently, another study has found that s-phase kinase-associated protein 2 (SKP2), an E3

ubiquitin ligase, is a direct target of YAP-regulating ferroptosis (Yang et al., 2021). PDZ-binding motif (TAZ) is also considered as a regulator of ferroptosis in renal and ovarian cancer cells (Yang et al., 2019c). More recently, it has been suggested that ferroptosis signal appears to be spread through cell populations in a wave-like manner, resulting in a distinct spatiotemporal pattern of cell death (Riegman et al., 2020). Ubiquitination is potentially essential for cell interaction-mediated ferroptosis since it plays an important role in the Hippo pathway. For example,  $\beta$ -TrCP is the well-known E3 ligase of YAP/TAZ, which promotes the reduction of YAP/TAZ, while E3 ligase ITCH targets LATS1/2 for degradation. It will be interesting to explore the potential roles of these E3 ubiquitin ligases in regulating ferroptosis (Kim and Jho, 2018; Deng et al., 2020).

The reason why cancer cells are always carried in the lymphatic system prior to circulation in the blood is largely unknown. A recent study has found that melanoma cells in lymph can experience less oxidative stress and induce more metastasis foci than those in blood due to higher levels of GSH and oleic acid, which attenuate oxidative stress and ferroptosis. Moreover, oleic acid protects melanoma cells against ferroptosis in an ACSL3-dependent manner and increases the capacity to form metastatic tumors (Ubellacker et al., 2020). Thus, ubiquitination may also regulate ferroptosis during metastasis of cancer cells by regulating ACSL3 stability and oleic acid metabolism.

## UBIQUITINATION REGULATION IN FERROPTOSIS

Ubiquitination is a crucial step consisting of vast cellular processes, such as cell proliferation, differentiation, and death (Lu et al., 2021). Protein ubiquitination is mediated by a cascade of reactions carried out by E1 (ubiquitin-activating enzymes), E2 (ubiquitin-conjugating enzyme), and E3 (ubiquitin ligases) coordinately (Lu et al., 2021). Similarly to other post-translational modifications, ubiquitination is also reversible, termed as deubiquitination, which is conducted by DUBs (Harrigan et al., 2018; Sun et al., 2020). Dysregulated ubiquitination contributes to carcinogenesis as well as other diseases. Currently, accumulated evidence has emphasized that ubiquitination is pivotally involved in ferroptosis (Harrigan et al., 2018; Rape, 2018; **Figure 5** and **Table 1**). At present, however, the role of ubiquitination still remains as a tip of the iceberg of ferroptosis.

### Ubiquitination of SLC7A11

System Xc<sup>−</sup> is a disulfide-linked heterodimer composed of SLC7A11 and SLC3A2 subunits. SLC7A11 predominately confers ferroptosis-resistance and is highly expressed in many cancers (Koppula et al., 2020). SLC7A11 is indispensably involved in cystine-uptake, which is required for GSH formation (Koppula et al., 2020). Although many studies have focused on transcriptional regulation of SLC7A11, whether the post-translational modifications occur on SLC7A11 (especially ubiquitination) remains largely unknown. Liu et al. have revealed that OTU deubiquitinase ubiquitin aldehyde-binding 1 (OTUB1) physically binds SLC7A11, promoting its deubiquitination



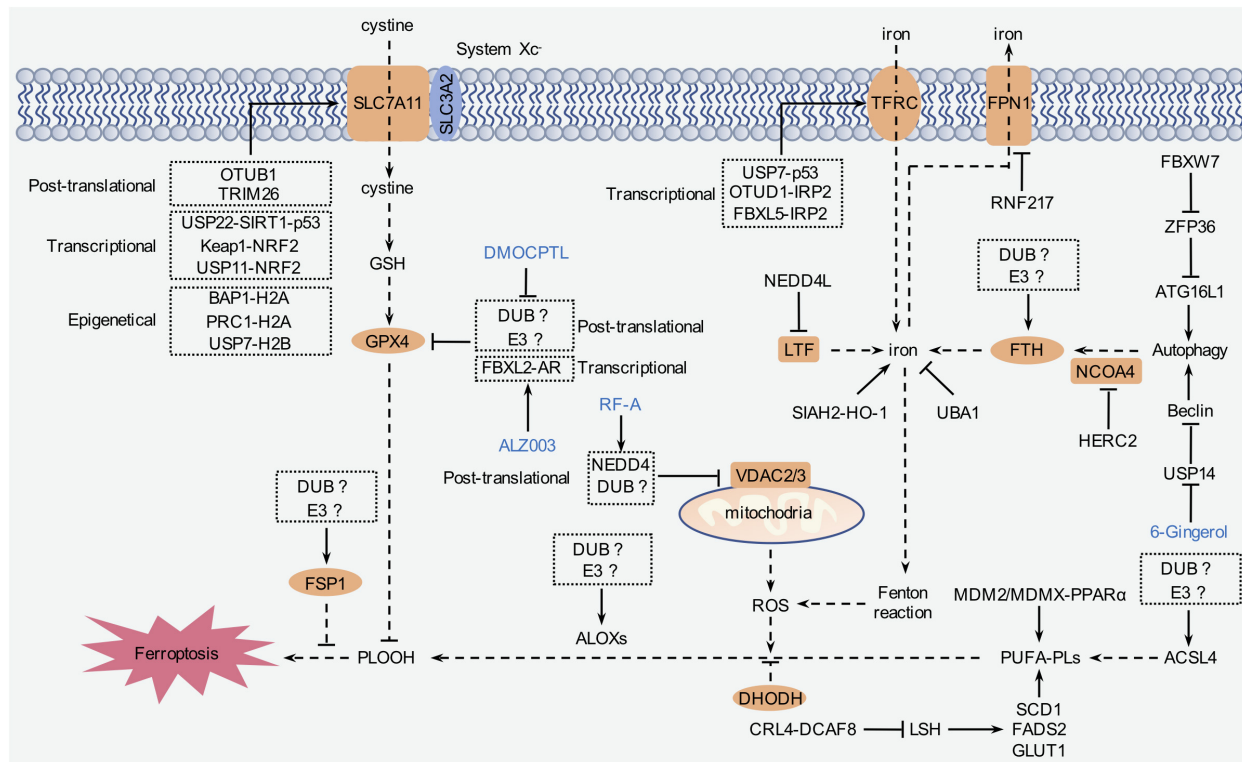


**FIGURE 5 |** The regulation mechanism of ferroptosis by ubiquitination. Ferroptosis is tightly relevant to amino acid, iron, and lipid metabolism. Intracellular labile iron is capable of triggering lipid peroxidation to induce ferroptosis. System Xc<sup>-</sup> transporter-mediated cystine uptake, which, in concert with GPX4, can reduce the cytotoxic lipid peroxides and inhibit ferroptosis. In addition, FSP1 and DHODH inhibit ferroptosis independent of GPX4. Modulation of these pathways by ubiquitination contributes to ferroptosis regulation.

to stabilize SLC7A11 protein (Liu T. et al., 2019). Genomic depletion of *OTUB1* gene dramatically downregulates SLC7A11 expression and sensitizes cancer cells to ferroptosis. Indeed, OTUB1 is frequently overexpressed in multiple types of cancer, and OTUB1 deficiency abolishes xenograft growth in mice, which can be rescued by SLC7A11 overexpression. It has been reported that CD44, a cancer stem cell marker, positively regulates OTUB1-SLC7A11 pathway and promotes SLC7A11 protein stability for tumor growth (Liu T. et al., 2019). Moreover, endogenous hydrogen sulfides regulate SLC7A11 stability through persulfidation of OTUB-C91 in colon cancer cells (Chen S. et al., 2021). A recent study has displayed that tripartite motif-containing protein 26 (TRIM26) interacts with SLC7A11 and mediates its ubiquitination. In addition, TRIM26 overexpression promotes ferroptosis in hepatic stellate cells (HSCs) and suppresses CCl<sub>4</sub>-induced liver fibrosis (Zhu et al., 2021).

The tumor suppressor gene BRCA1-associated protein 1 (BAP1) encodes a nuclear DUB to reduce histone 2A ubiquitination (H2A-ub) on chromatin (Louie and Kurzrock, 2020). Zhang et al. (2018) have uncovered that BAP1 decreases H2A-ub occupancy on the SLC7A11 promoter to repress SLC7A11 expression and cystine uptake in a deubiquitinating-dependent manner, causing an elevation of lipid peroxidation and ferroptosis. Moreover, polycomb repressive complex 1 (PRC1)

is a well-known E3 ubiquitin ligase of H2A-ub. A previous study has reported that PRC1 can enhance H2A-ub binding on SLC7A11 promoter, and PRC1 deficiency increases the protein level of SLC7A11, suggesting that the dynamic regulation of H2A ubiquitination importantly impacts on SLC7A11 expression (Zhang et al., 2019a).

A recent research has exhibited that p53 has a role in repressing SLC7A11 expression (Jiang et al., 2015). Notably, only p53 homozygous-deficient cells, but not the classical acetylation-defective mutant, show an increase in SLC7A11 expression. As a result of de-repression of SLC7A11, cystine uptake is dramatically increased accompanied by ferroptosis resistance. Meanwhile, SLC7A11 can be recognized by H2B-ub (mono-ubiquitination of histone H2B) via targeting lysine 120 (Wang Y. et al., 2019). The level of H2B-ub is decreased in cells ongoing ferroptosis. Loss of H2B-ub significantly enhances vulnerability of cells to ferroptosis. It should be noted that p53 has been shown to promote the translocation of USP7 inward in the nucleus, which has a role in de-ubiquitinating H2B. As a result of repressed SLC7A11 expression, the ferroptosis will be promoted (Wang Y. et al., 2019).

Ferroptosis is also involved in myocardial ischemia-reperfusion (MI/R) injury (Wu et al., 2021). Ma et al. (2020) have revealed an increase in p53 protein level, but downregulations of USP22, SLC7A11, and SIRT1 in response

to MI/R injury. In this study, the authors have uncovered that deubiquitination and stabilization of SIRT1 by USP22 can repress transcriptional activity of p53, which leads to SLC7A11 upregulation and ferroptosis resistance. The expression of USP22 shows a protective effect against MI/R injury through SIRT1/p53/SLC7A11 axis *in vivo*. All these studies highlight the essential role of ubiquitination effect on the expression of SLC7A11 and ferroptosis inhibition.

## Ubiquitination of GPX4

GPX4 is an essential selenoprotein reducing phospholipid hydroperoxide and plays a key role in defending cells against lipid peroxidation (Friedmann Angeli and Conrad, 2018; Forcina and Dixon, 2019) and ferroptosis (Hassannia et al., 2019). Inhibition of GPX4 by a synthesized small molecule induces cell lethality and lipid peroxidation (Yang et al., 2014; Gaschler et al., 2018). However, whether a modification of GPX4 at the post-translational level exists is still largely unknown. Androgen receptor (AR) is a steroid hormone receptor overexpressed in several types of cancer (Narayanan, 2020) and is inversely correlated with survival rate (Chen et al., 2020). Chen et al. (2020) has revealed that ALZ003, an FDA-approved curcumin analog drug, induces AR degradation via FBXL2-mediated ubiquitination. Notably, AR expression is also important for redox homeostasis. Moreover, either AR knockdown or ALZ003 treatment dramatically increases the level of lipid ROS followed by a decrease in the protein level of GPX4 in glioblastoma cells.

The natural product parthenolide (PTL) has attracted much attention due to its anticancer effect (Sztiller-Sikorska and Czyz, 2020). However, the clinical application of PTL remains to be investigated because of low oral bioavailability and poor solubility (Araújo et al., 2020). A derivative of PTL, DMOCPTL, has been designed with an improvement of solubility. DMOCPTL is capable of repressing the growth of triple negative breast cancer (TNBC) cells. Lipid ROS and iron level are significantly increased upon DMOCPTL treatment in TNBC, while the GPX4 protein level is reduced. Mechanistically, DMOCPTL can bind to GPX4 and promote its ubiquitination in TNBC cells. DMOCPTL effectively inhibits breast tumor growth and prolongs survival rate in mice (Ding et al., 2021). Palladium pyridine complex (PdPT), a broad-spectrum DUB (including USP7, USP10, USP14, USP15, USP25, and UCHL5) inhibitor, can also cause GPX4 protein degradation in non-small cell lung cancer cells (Yang L. et al., 2020). As mentioned above, we propose that ubiquitination modification of GPX4 drives the vulnerability to ferroptosis. However, the specific E3 ubiquitin ligases and DUBs for GPX4 remain to be identified.

## Ubiquitination of Voltage-Dependent Anion Channel2/3

Voltage-dependent anion channels (VDACs) are located at the outer membrane of the mitochondrion allowing shuttling of metabolites and ions between the mitochondrion and cytosol (Fang and Maldonado, 2018). Erastin can target VDAC2/3 in addition to SLC7A11 and causes VDAC2/3 degradation.

**TABLE 1 |** Ferroptosis regulation by E3s and deubiquitylating enzymes (DUBs).

Targets	Levels	E3s	DUBs	Biological functions	References
SLC7A11	Post-translation	TRIM26		Degrading SLC7A11; promoting ferroptosis	Zhu et al., 2021
			OTUB1	Stabilizing SLC7A11; suppressing ferroptosis	Liu T. et al., 2019; Chen S. et al., 2021
	Transcription		USP22	Increasing SLC7A11 expression; suppressing ferroptosis	Ma et al., 2020
	Epigenetic		BAP1	Suppressing SLC7A11 expression; promoting ferroptosis	Zhang et al., 2018
			PRC1	Suppressing SLC7A11 expression; promoting ferroptosis	Zhang et al., 2019a
		USP7	Suppressing SLC7A11 expression; promoting ferroptosis	Wang Y. et al., 2019	
GPX4	Post-translation	Unknown		Degrading GPX4; promoting ferroptosis	Yang L. et al., 2020; Ding et al., 2021
	Transcription	FBXL2		Suppressing GPX4 expression; promoting ferroptosis	Chen et al., 2020
VDAC2/3	Post-translation	NEDD4		Degrading VDAC2/3; suppressing ferroptosis	Yang Y. et al., 2020
NRF2	Post-translation		USP11	Stabilizing NRF2; suppressing ferroptosis	Meng et al., 2021
		KEAP1		Degrading NRF2; promoting ferroptosis	Kansanen et al., 2013
NCOA4	Post-translation	HERC2		Degrading NCOA4; suppressing ferroptosis	Mancias et al., 2015
Beclin1	Post-translation		USP14	Deubiquitylating Beclin1; suppressing ferroptosis	Tsai et al., 2020
ATG16L1	Transcription	FBXW7		Promoting ATG16L1 expression; promoting ferroptosis	Zhang et al., 2020
TFRC	Transcription		USP7	Promoting TFRC expression; Promoting ferroptosis	Tang L.J. et al., 2021
FPN1	Post-translation	RNF217		Degrading FPN1;promoting ferroptosis	De Domenico et al., 2007; Jiang et al., 2021
IRP2	Post-translation	FBXL5		Degrading IRP2; suppressing ferroptosis	Dixon et al., 2012
			OTUD1	Stabilizing IRP2; promoting ferroptosis	Song et al., 2021b
LTF	Post-translation	NEDD4L		Degrading LTF; suppressing ferroptosis	Wang et al., 2020b
LSH	Post-translation	CRL4- DCAF8		Degrading LSH; promoting ferroptosis	Huang et al., 2020
HO-1	Post-translation	SIAH2		Degrading HO-1; suppressing ferroptosis	Chillappagari et al., 2020
	Transcription	SIAH2		Suppressing HO-1 expression; suppressing ferroptosis	Chillappagari et al., 2020

E3 ubiquitin ligases and DUBs are pivotally involved in ferroptosis through targeting multiple substrates, including solute carrier family 7 member 11 (SLC7A11), voltage-dependent anion channels (VDAC2/3), nuclear factor, erythroid 2-like 2 (NRF2), and iron regulatory protein 2 (IRP2).

Yang Y. et al. (2020) have reported that treatment of erastin is able to elevate the expression of neural precursor cell-expressed developmentally downregulated protein 4 (NEDD4), which is an E3 ubiquitin ligase. Genomic deletion of *NEDD4* increases expression level of VDAC2/3 and enhances ferroptosis susceptibility. Additionally, natural metabolite biflavonoids extracted from plants are regarded as promising anticancer drugs in breast cancer treatment. The C-3'-C-6'' type of biflavonoids robustaflavone A (RF-A) extracted from *Selaginella trichoclada* has been shown to decrease cell viability of breast cancer and diminish the NEDD4 expression. Eventually, VDAC2 is stabilized accompanied by lipid peroxidation and ferroptosis (Xie et al., 2021).

## Ubiquitination of Nuclear Factor, Erythroid 2-Like 2

The transcription factor NRF2 plays a vital role in ferroptosis and cancer progression (Dodson et al., 2019). It has been widely reported that E3 ligase KEAP1 promotes NRF2 ubiquitination (Kansanen et al., 2013), whereas the deubiquitination mechanism of NRF2 remains largely elusive. Meng et al. (2021) have identified USP11, which can work as a DUB of NRF2. A stabilized NRF2 protein has been revealed to be attributed to USP11-modified deubiquitination. Functionally, USP11 deficiency contributes to the induction of ferroptosis, which can be rescued by NRF2 expression. USP11 is highly expressed in lung cancer patients and correlates to poorer prognosis. These studies demonstrate that DUBs play a pivotal role in the modulation of ferroptosis by regulating ubiquitination of ferroptosis-related proteins.

## Ubiquitination in Autophagy

Autophagy-mediated ferritin degradation (ferritinophagy) is an essential step involved in ferroptosis (Gao et al., 2016). NCOA4 is a selective cargo receptor for the autophagic turnover of ferritin, a process critical for regulation of intracellular iron bioavailability. The arginine residues in FTH1 and a C-terminal element in NCOA4 are essential for ferritin degradation in autophagosomes. Moreover, NCOA4 stability is under the control of the ubiquitin proteasome system in addition to autophagy. Ubiquitin-dependent NCOA4 turnover is accelerated by excessive iron, which is associated with HECT domain and RCC1-like domain 2 (HERC2) ubiquitin ligase (Mancias et al., 2015). HERC2 only binds to NCOA4 when the iron level is increased, which leads to NCOA4 degradation by the proteasome. When the concentration of iron becomes lower, the interaction between HERC2 and NCOA4 does not take place. Therefore, an increase in the protein level of NCOA4 will promote ferritinophagy, which subsequently enlarges labile iron pool and induces ferroptosis in the cells. Furthermore, autophagy-related proteins are not only essential for autophagy induction but also are involved in erastin-induced ferroptosis (Zhou et al., 2020). ATG7 plays a central role in both autophagy-specific UBL systems (Hong et al., 2011) and ferroptosis (Hou et al., 2016). ATG7 can work as an E1 enzyme for ubiquitin-like proteins (UBL), such as ATG8 and ATG12. ATG7 enables ATG12

and ATG8 targeting their molecules by binding to them and motivating their transfer to an E2 enzyme (Kaiser et al., 2013).

In addition, Beclin1 and 6-Gingerol have been shown to regulate autophagy and ferroptosis mediated by USP14, which can be suppressed by 6-Gingerol. Mechanistically, USP14 affects autophagy through deubiquitination of Beclin1. Moreover, administration of 6-Gingerol represses tumor growth followed by increased intracellular iron level and ferroptosis. Thus, 6-Gingerol may be utilized as a therapeutic agent to promote ferroptosis in lung cancer treatment (Tsai et al., 2020).

Hepatic stellate cell (HSC) plays an important role in liver fibrosis. Targeting HSCs is considered a potent approach for liver fibrosis alleviation (Tsuchida and Friedman, 2017). However, overexpression of RNA-binding protein ZFP36 (also known as TTP) shows resistance to ferroptosis in HSCs (Zhang et al., 2020). Zhang et al. (2020) have showed that ZFP36 inhibits autophagy by destabilizing autophagy-related 16-like 1 (ATG16L1) mRNA, which is required for autophagy induction. A decrease in stability of ATG16L1 mRNA abolishes ferritinophagy-associated ferroptosis. In addition, other studies also reveal that erastin can promote ZFP36 degradation via the E3 ubiquitin ligase FBXW7. FBXW7 is able to identify ZFP36 through the consensus degron (SFSGGLPS). Due to the fact that effective therapy for liver fibrosis has not been approved yet, thus far, ferroptosis may be utilized as a novel approach to overcome liver fibrosis.

## Ubiquitination in Iron Metabolism

TFRC is a major iron importer and takes the responsibility of ferric iron uptake (Yan et al., 2020). Moreover, increased intracellular iron has been regarded as a surrogate marker of ferroptosis (Yu et al., 2019). Tang L.J. et al. (2021) have found evidence of ubiquitination effect compromised in TFRC expression, which is enhanced by USP7-mediated p53 stabilization. The small molecular inhibitor targeting USP7 decreases ferroptosis. Therefore, the USP7/53/TFRC axis appears to be a potential target for myocardial I/R injury therapy. FPN1 is the sole iron exporter existing on the plasma membrane. It has been displayed that FPN1 is able to be phosphorylated and ubiquitinated (De Domenico et al., 2007); however, the corresponding E3 ubiquitin ligases and DUBs remain largely unknown. A recent study has shown that RNF217 mediates the ubiquitination and subsequent degradation of FPN1 (Jiang et al., 2021).

Iron regulatory protein 2 (IRP2) plays a central role in iron metabolism. FBXL5 has been identified as the E3 ubiquitin ligase targeting on IRP2 for its degradation (Vashisht et al., 2009). Importantly, FBXL5 silencing stimulates an increase in hepatocellular iron level and embryonic lethality (Moroishi et al., 2011) as well as ferroptosis (Dixon et al., 2012). It has been also reported that OTUD1 promotes TFRC-mediated iron transport through deubiquitinating of IRP2 irrespective of iron concentration, eventually leading to ferroptosis (Song et al., 2021b).

Wang et al. (2020b) have screened 571 ubiquitin-related genes, which are potentially related to ferroptosis regulation. The E3 ligase NEDD4 like E3 ubiquitin protein ligase (NEDD4L), a novel ferroptosis suppressor in human pancreatic cancer cells, has been



found with a role in regulating iron metabolism by targeting iron-binding transport protein lactotransferrin (LTF).

Ubiquitin-like modifier-activating enzyme 1 (UBA1) is a potential marker for hepatocellular carcinoma (HCC) prognosis since its expression positively correlates with survival rate. Inhibition of UBA1 reduces proliferation, migration, and invasion in HCC cells. Moreover, both iron concentration and malondialdehyde (MDA) levels are elevated in response to UBA1 suppression. The expression of UBA1 has been found related to NRF2 as well as the downstream targets like heme oxygenase-1 (HO-1), NAD(P)H quinone dehydrogenase 1 (NQO1), and FTH1, which are associated with iron metabolism regulation. These findings suggest that UBA1 may play a vital role in ferroptosis (Shan et al., 2020).

Epigenetic factor lymphoid-specific helicase (LSH) is a member of SNF2 family chromatin remodeling ATPases (Baumann et al., 2020; Ni et al., 2020). The expression of LSH is essential for an adequate maintenance of genomic stability (Ni et al., 2020). Dysregulation of LSH has been exhibited in various malignancies (Liu and Tao, 2016; Yang et al., 2019a,b; He et al., 2020) as well as chronological aging (Zhou et al., 2009). Intriguingly, LSH also inhibits ferroptosis by sequestering labile iron and limits the generation of lipid ROS (Jiang et al., 2017). Moreover, LSH has been uncovered to be associated with WD40-repeat protein 76 (WDR76) to inhibit ferroptosis by activating lipid metabolism-associated genes, including glucose transporter 1 (GLUT1), ferroptosis-related gene stearoyl-CoA desaturase 1 (SCD1), and fatty acid desaturase 2 (FADS2) (Jiang et al., 2017). It has been reported that erastin induces LSH destabilization, and CRL4-DCAF8 synergizes with WDR76 to control the protein levels of LSH (Huang et al., 2020). E3 ligase CRL4-DCAF8 mediates polyubiquitination and proteasomal degradation of LSH, and WDR76 antagonizes DCAF8-targeted LSH proteolysis through competitive inhibition of the holo-CRL4-DCAF8-LSH complex assembly (Huang et al., 2020).

Heme oxygenase-1 (HO-1) catalyzes the oxidative cleavage of heme to biliverdin, iron, and carbon monoxide. The role of HO-1 in erastin-induced ferroptosis has been investigated (Chillappagari et al., 2020). A recent study has identified seven *in absentia* homologs (SIAH2) as crucial E3 ubiquitin ligases to control HO-1 protein stability. Controversially, SIAH2 can also downregulate transcriptional expression of HO-1, which depends on the transcription factor NRF2 (Chillappagari et al., 2020). Thus, SIAH2 can govern the expression level of HO-1 by a dual mechanism.

## Ubiquitination in Lipid Metabolism

Generation of lipid peroxides determines the sensitivity of ferroptosis. Thus, lipogenesis has been considered as a potent strategy to defend against ferroptosis in cancer cells. E3 ubiquitin ligases MDM2 and MDMX are well-known negative regulators of p53. It has been reported that MDM2 and MDMX can promote ferroptosis via PPAR $\alpha$ -mediated lipid remodeling irrespective of p53 activity. Additionally, MDM2 or MDMX depletion can also lead to increased levels of FSP1 and CoQ10, which are potent suppressors of ferroptosis (Venkatesh et al., 2020).

## Ubiquitination in Hippo Pathway

YAP and TAZ are the main downstream factors regulated by NF2. Activation of YAP enhances expression of iron transporter, TFRC (Wu et al., 2019), followed by increased level of intracellular iron and ferroptosis induction in mesothelioma cells. YAP also promotes ferroptosis via different targets such as ACSL4. Interestingly, TAZ, but not YAP, appears to specifically sensitize renal cell carcinoma cell lines to ferroptosis via regulation of epithelial membrane protein 1 (EMP1), suggesting a context-dependent role of YAP/TAZ in ferroptosis (Yang et al., 2019c). The E3 ubiquitin ligase FBXW7 has been regarded as a tumor suppressor. A recent study has shown that FBXW7 targets YAP for degradation (Tu et al., 2014). However, FBXW7 can induce ferroptosis by targeting RNA-binding protein ZFP36/TTP (Zhang et al., 2020). These studies indicate that FBXW7 plays a crucial role in ferroptosis regulation. However, further studies are necessary to address more details under different contexts.  $\beta$ -transducin repeat-containing E3 ubiquitin protein ligase ( $\beta$ TrCP) targets YAP and TAZ for degradation by the SCF ubiquitin ligase complex. Recently, deletion of  $\beta$ TrCP has been shown to inhibit erastin-induced ferroptosis in lung cancer cells (Zhang X. et al., 2021). However, the mechanisms remain to be further elucidated yet.

## TARGETING UBIQUITINATION FOR FERROPTOSIS IN CANCER THERAPY

Multiple studies have revealed that induction of ferroptosis is a promising approach in cancer therapy (Cramer et al., 2017; Zhang et al., 2019b; Badgley et al., 2020; Chen et al., 2021a; Koren and Fuchs, 2021). However, most synthetic ferroptosis inducers appear to be unsuitable for clinical application, thus far, due to the poor solubility and *Ki* value *in vivo* (Shen et al., 2018; Gautheron et al., 2020). Besides, an adequate druggable candidate involved in ferroptosis has not been uncovered yet (Dang et al., 2017). As accumulated evidence has shown that ubiquitination plays a vital role in ferroptosis, targeting the ubiquitin system will be an alternative strategy to further realize the role of ferroptosis in cancer and other diseases. Notably, the FDA-approved 20S proteasome inhibitors bortezomib and carfilzomib have been used for the treatment of hematological malignancies (Farshi et al., 2015; Nunes and Annunziata, 2017; Chari et al., 2019). Inhibition of the proteasome by bortezomib has been validated for targeting the UPS in cancer therapy (Crawford and Irvine, 2013; Ettari et al., 2018); however, the acquired resistance to bortezomib always occurred in clinical settings. Palladium pyridine complex (PdPT) targeting upstream components of the proteasome has been investigated to enhance the anticancer effect of bortezomib by targeting GPX4 degradation and induce both ferroptosis and apoptosis (Yang L. et al., 2020). Carfilzomib is a second-generation proteasome inhibitor approved by the FDA. Interestingly, iron has been shown to improve carfilzomib efficacy in MM cells suggesting that a combination of iron supplementation and ferroptosis induction may represent a novel strategy to overcome resistance to carfilzomib (Bordini et al., 2020). The selenoprotein thioredoxin reductase 1 (TXNRD1)



plays a vital role in protecting tumor cells against oxidative stress. Modulation of ferroptosis sensitivity by TXNRD1 has been addressed in pancreatic cancer cells (Cai et al., 2020). It should be noted that lenalidomide, which has been shown to interact with the ubiquitin E3 ligase cereblon, has been approved for medical use since 2005. Lenalidomide is capable of inhibiting TXNRD1 that leads to an accumulation of cytotoxic  $H_2O_2$  levels, suggesting that lenalidomide may have roles in ferroptosis regulation (Sebastian et al., 2017).

Targeted protein ubiquitination and subsequent degradation using the Proteolysis Targeting Chimeras (PROTACs) have emerged as a novel therapeutic technology in drug discovery (Paiva and Crews, 2019). In 2019, PROTAC ARV-110, which targets the androgen receptor (AR) for degradation in prostate cancer, has been approved by the FDA for phase I clinical trials (Neklesa et al., 2017; Pettersson and Crews, 2019; Schapira et al., 2019; Ding et al., 2020; Poh, 2020; Wang et al., 2020a). Development of novel therapies by targeting the ubiquitin system (DUBs/E3s inhibitors or PROTACs) on ferroptosis-related proteins may facilitate the clinical application of ferroptosis in the future (Popovic et al., 2014; Liu J. et al., 2021; Zhou and Sun, 2021).

## CONCLUSION AND PERSPECTIVE—NEXT DECADES

Although emerging evidence has pointed out the potential role of ubiquitination in ferroptosis, the details of the mechanism remain to be elucidated. Identification of specific enzymes involved in ubiquitination of ferroptosis will solidify the understanding of the role of ferroptosis in cancers as well as in other disorders. Still, the specific E3 ubiquitin ligases for targeting GPX4, FSP1, and other essential proteins in ferroptosis are still unknown. Whole genome-wide or sub-pool of E3/DUBs library CRISPR-cas9 screening approach will be of great help to identify key ubiquitination regulators in ferroptosis. Thus far, most ferroptosis-related research predominantly focuses on cultured cells and xenograft models in nude mice; however, the precise regulations of ferroptosis in physiological and pathological conditions are unclear. Elucidation of the relationship between ubiquitination and ferroptosis will provide novel insights into cancer therapy.

SLC7A11 overexpresses in most types of cancer and is regulated by multiple transcriptional factors (Ye et al., 2014; Jiang et al., 2015; Zhang et al., 2018; Ogiwara et al., 2019).

However, whether post-translational modification, especially ubiquitination, contributing to this overexpression (in addition to OTUB1 and TRIM26) is unclear. Mass spectrometry (MS) data shows that SLC7A11 can be highly ubiquitinated at multiple sites (PhosphoSitePlus) (Hornbeck et al., 2015), emphasizing the importance of E3 ubiquitin ligase in SLC7A11-mediated ferroptosis resistance. GPX4 holds the core fortress in ferroptosis. GPX4 is a selenoprotein, which contains selenocysteine, a non-canonical amino acid coded by the termination codon (UGA). A selenocysteine insertion sequence (SECIS) of the selenoprotein mRNA is necessary for the translation of UGA to Sec, via a series of precise protein collaborations (Driscoll and Copeland, 2003). CRL2 ubiquitin ligase, a member of the cullin-RING ligase (CRL) superfamily, specifically eliminates truncated proteins produced by failed UGA/Sec decoding, controlling selenoprotein quality (Lin et al., 2015). A recent study has revealed that peroxisome proliferator-activated receptor  $\gamma$  (PPAR $\gamma$ ) can act as an E3 ubiquitin ligase, mediating ubiquitination and degradation of selenoproteins (SelS and SelK) (Lee et al., 2019). Notably, rapamycin, an mTOR inhibitor, induces GPX4 protein degradation at high doses in human pancreatic cancer cell lines (Liu Y. et al., 2021). However, the mechanism of GPX4 degradation is still unclear, especially that the specific E3 ligase and DUB remain to be identified. This may be achieved by identifying E3/DUB interaction partners of these substrates via MS strategy or Bioplex database<sup>1</sup> in addition to E3/DUB prediction tools such as UbiBrowser.<sup>2</sup>

## AUTHOR CONTRIBUTIONS

XW, YW, and ZL wrote the manuscript. JQ and PW edited the manuscript. All authors contributed to the article and approved the submitted version.

## FUNDING

This work was supported by the National Natural Science Foundation of China (31920103007, 31830053, and 31900525), Shanghai International Science and Technology Cooperation Fund Project (18410722000), and China Postdoctoral Science Foundation (2019M650090 and 2019T120353).

<sup>1</sup><https://bioplex.hms.harvard.edu>

<sup>2</sup><http://ubibrowser.ncpsb.org.cn/ubibrowser/>

## REFERENCES

- Araújo, T. G., Vecchi, L., Lima, P., Ferreira, E. A. I., Campos, M., Brandão, D. C., et al. (2020). Parthenolide and its analogues: a new potential strategy for the treatment of triple-negative breast tumors. *Curr. Med. Chem.* 27, 6628–6642. doi: 10.2174/0929867326666190816230121
- Ashrafi, G., and Schwarz, T. L. (2013). The pathways of mitophagy for quality control and clearance of mitochondria. *Cell Death Differ.* 20, 31–42.
- Badgley, M. A., Kremer, D. M., Maurer, H. C., DelGiorno, K. E., Lee, H. J., Purohit, V., et al. (2020). Cysteine depletion induces pancreatic tumor ferroptosis in mice. *Science* 368, 85–89. doi: 10.1126/science.aaw9872
- Bard, J. A. M., Goodall, E. A., Greene, E. R., Jonsson, E., Dong, K. C., and Martin, A. (2018). Structure and function of the 26S proteasome. *Annu. Rev. Biochem.* 87, 697–724.
- Barton, J. K., Silva, R. M. B., and O'Brien, E. (2019). Redox chemistry in the genome: emergence of the [4Fe4S] cofactor in repair and replication. *Annu. Rev. Biochem.* 88, 163–190. doi: 10.1146/annurev-biochem-013118-110644
- Basuli, D., Tesfay, L., Deng, Z., Paul, B., Yamamoto, Y., Ning, G., et al. (2017). Iron addiction: a novel therapeutic target in ovarian cancer. *Oncogene* 36, 4089–4099. doi: 10.1038/onc.2017.11
- Baumann, C., Ma, W., Wang, X., Kandasamy, M. K., Viveiros, M. M., and De La Fuente, R. (2020). Helicase LSH/Hells regulates kinetochore function, histone

- H3/Thr3 phosphorylation and centromere transcription during oocyte meiosis. *Nat. Commun.* 11:4486.
- Bedoui, S., Herold, M. J., and Strasser, A. (2020). Emerging connectivity of programmed cell death pathways and its physiological implications. *Nat. Rev. Mol. Cell Biol.* 21, 678–695. doi: 10.1038/s41580-020-0270-8
- Bersuker, K., Hendricks, J. M., Li, Z., Magtanong, L., Ford, B., Tang, P. H., et al. (2019). The CoQ oxidoreductase FSP1 acts parallel to GPX4 to inhibit ferroptosis. *Nature* 575, 688–692. doi: 10.1038/s41586-019-1705-2
- Bock, F. J., and Tait, S. W. G. (2020). Mitochondria as multifaceted regulators of cell death. *Nat. Rev. Mol. Cell Biol.* 21, 85–100. doi: 10.1038/s41580-019-0173-8
- Bordini, J., Morisi, F., Cerruti, F., Cascio, P., Camaschella, C., Ghia, P., et al. (2020). Iron causes lipid oxidation and inhibits proteasome function in multiple myeloma cells: a proof of concept for novel combination therapies. *Cancers (Basel)* 12:970. doi: 10.3390/cancers12040970
- Boutelle, A. M., and Attardi, L. D. (2021). p53 and tumor suppression: it takes a network. *Trends Cell Biol.* 31, 298–310. doi: 10.1016/j.tcb.2020.12.011
- Cai, L. L., Ruberto, R. A., Ryan, M., Eaton, J. K., Schreiber, S., and Viswanathan, V. S. (2020). Modulation of ferroptosis sensitivity by TXNRD1 in pancreatic cancer cells. *bioRxiv* [preprint] doi: 10.1101/2020.06.25.165647
- Chari, A., Martinez-Lopez, J., Mateos, M. V., Bladé, J., Benboubker, L., Oriol, A., et al. (2019). Daratumumab plus carfilzomib and dexamethasone in patients with relapsed or refractory multiple myeloma. *Blood* 134, 421–431.
- Chen, P. H., Wu, J., Xu, Y., Ding, C. C., Mestre, A. A., Lin, C. C., et al. (2021). Zinc transporter ZIP7 is a novel determinant of ferroptosis. *Cell Death Dis.* 12:198.
- Chen, S., Bu, D., Zhu, J., Yue, T., Guo, S., Wang, X., et al. (2021). Endogenous hydrogen sulfide regulates xCT stability through persulfidation of OTUB1 at cysteine 91 in colon cancer cells. *Neoplasia* 23, 461–472. doi: 10.1016/j.neo.2021.03.009
- Chen, T. C., Chuang, J. Y., Ko, C. Y., Kao, T. J., Yang, P. Y., Yu, C. H., et al. (2020). AR ubiquitination induced by the curcumin analog suppresses growth of temozolomide-resistant glioblastoma through disrupting GPX4-Mediated redox homeostasis. *Redox Biol.* 30:101413. doi: 10.1016/j.redox.2019.101413
- Chen, X., Kang, R., Kroemer, G., and Tang, D. (2021a). Broadening horizons: the role of ferroptosis in cancer. *Nat. Rev. Clin. Oncol.* 18, 280–296. doi: 10.1038/s41571-020-00462-0
- Chen, X., Yu, C., Kang, R., Kroemer, G., and Tang, D. (2021b). Cellular degradation systems in ferroptosis. *Cell Death Differ.* 28, 1135–1148. doi: 10.1038/s41418-020-00728-1
- Chillappagari, S., Belapurkar, R., Möller, A., Molenda, N., Kracht, M., Rohrbach, S., et al. (2020). SIAH2-mediated and organ-specific restriction of HO-1 expression by a dual mechanism. *Sci. Rep.* 10:2268.
- Chu, B., Kon, N., Chen, D., Li, T., Liu, T., Jiang, L., et al. (2019). ALOX12 is required for p53-mediated tumour suppression through a distinct ferroptosis pathway. *Nat. Cell Biol.* 21, 579–591. doi: 10.1038/s41556-019-0305-6
- Conrad, M., and Pratt, D. A. (2019). The chemical basis of ferroptosis. *Nat. Chem. Biol.* 15, 1137–1147. doi: 10.1038/s41589-019-0408-1
- Conrad, M., and Proneth, B. (2020). Selenium: tracing another essential element of ferroptotic cell death. *Cell Chem. Biol.* 27, 409–419. doi: 10.1016/j.chembiol.2020.03.012
- Cramer, S. L., Saha, A., Liu, J., Tadi, S., Tiziani, S., Yan, W., et al. (2017). Systemic depletion of L-cyst(e)ine with cyst(e)inase increases reactive oxygen species and suppresses tumor growth. *Nat. Med.* 23, 120–127. doi: 10.1038/nm.4232
- Crawford, L. J., and Irvine, A. E. (2013). Targeting the ubiquitin proteasome system in haematological malignancies. *Blood Rev.* 27, 297–304. doi: 10.1016/j.blre.2013.10.002
- Dang, C. V., Reddy, E. P., Shokat, K. M., and Soucek, L. (2017). Drugging the 'undruggable' cancer targets. *Nat. Rev. Cancer* 17, 502–508. doi: 10.1038/nrc.2017.36
- De Domenico, I., Ward, D. M., Langelier, C., Vaughn, M. B., Nemeth, E., Sundquist, W. I., et al. (2007). The molecular mechanism of hepcidin-mediated ferroportin down-regulation. *Mol. Biol. Cell* 18, 2569–2578. doi: 10.1091/mbc.e07-01-0060
- Del Re, D. P., Amgala, D., Linkermann, A., Liu, Q., and Kitis, R. N. (2019). Fundamental mechanisms of regulated cell death and implications for heart disease. *Physiol. Rev.* 99, 1765–1817. doi: 10.1152/physrev.00022.2018
- Deng, L., Meng, T., Chen, L., Wei, W., and Wang, P. (2020). The role of ubiquitination in tumorigenesis and targeted drug discovery. *Signal Transduct. Target. Ther.* 5:11.
- Ding, Y., Chen, X., Liu, C., Ge, W., Wang, Q., Hao, X., et al. (2021). Identification of a small molecule as inducer of ferroptosis and apoptosis through ubiquitination of GPX4 in triple negative breast cancer cells. *J. Hematol. Oncol.* 14:19.
- Ding, Y., Fei, Y., and Lu, B. (2020). Emerging new concepts of degrader technologies. *Trends Pharmacol. Sci.* 41, 464–474. doi: 10.1016/j.tips.2020.04.005
- Dixon, S. J., Lemberg, K. M., Lamprecht, M. R., Skouta, R., Zaitsev, E. M., Gleason, C. E., et al. (2012). Ferroptosis: an iron-dependent form of nonapoptotic cell death. *Cell* 149, 1060–1072. doi: 10.1016/j.cell.2012.03.042
- Dodson, M., Castro-Portuguez, R., and Zhang, D. D. (2019). NRF2 plays a critical role in mitigating lipid peroxidation and ferroptosis. *Redox Biol.* 23:101107. doi: 10.1016/j.redox.2019.101107
- Doll, S., Freitas, F. P., Shah, R., Aldrovandi, M., da Silva, M. C., Ingold, I., et al. (2019). FSP1 is a glutathione-independent ferroptosis suppressor. *Nature* 575, 693–698. doi: 10.1038/s41586-019-1707-0
- Doll, S., Proneth, B., Tyurina, Y. Y., Panzilius, E., Kobayashi, S., Ingold, I., et al. (2017). ACSL4 dictates ferroptosis sensitivity by shaping cellular lipid composition. *Nat. Chem. Biol.* 13, 91–98.
- Driscoll, D. M., and Copeland, P. R. (2003). Mechanism and regulation of selenoprotein synthesis. *Annu. Rev. Nutr.* 23, 17–40. doi: 10.1016/b0-12-443710-9/00616-5
- Eid, R., Arab, N. T., and Greenwood, M. T. (2017). Iron mediated toxicity and programmed cell death: a review and a re-examination of existing paradigms. *Biochim. Biophys. Acta Mol. Cell Res.* 1864, 399–430. doi: 10.1016/j.bbamer.2016.12.002
- Ettari, R., Zappalà, M., Grasso, S., Musolino, C., Innao, V., and Allegra, A. (2018). Immunoproteasome-selective and non-selective inhibitors: a promising approach for the treatment of multiple myeloma. *Pharmacol. Ther.* 182, 176–192. doi: 10.1016/j.pharmthera.2017.09.001
- Fang, D., and Maldonado, E. N. (2018). VDAC regulation: a mitochondrial target to stop cell proliferation. *Adv. Cancer Res.* 138, 41–69. doi: 10.1016/bs.acr.2018.02.002
- Farshi, P., Deshmukh, R. R., Nwankwo, J. O., Arkwright, R. T., Cvek, B., Liu, J., et al. (2015). Deubiquitinases (DUBs) and DUB inhibitors: a patent review. *Expert Opin. Ther. Pat.* 25, 1191–1208. doi: 10.1517/13543776.2015.1056737
- Forcina, G. C., and Dixon, S. J. (2019). GPX4 at the crossroads of lipid homeostasis and ferroptosis. *Proteomics* 19:e1800311.
- Frank, D., and Vince, J. E. (2019). Pyroptosis versus necroptosis: similarities, differences, and crosstalk. *Cell Death Differ.* 26, 99–114. doi: 10.1038/s41418-018-0212-6
- Friedmann Angeli, J. P., and Conrad, M. (2018). Selenium and GPX4, a vital symbiosis. *Free Radic. Biol. Med.* 127, 153–159. doi: 10.1016/j.freeradbiomed.2018.03.001
- Gao, M., Monian, P., Pan, Q., Zhang, W., Xiang, J., and Jiang, X. (2016). Ferroptosis is an autophagic cell death process. *Cell Res.* 26, 1021–1032. doi: 10.1038/cr.2016.95
- Gao, M., Monian, P., Quadri, N., Ramasamy, R., and Jiang, X. (2015). Glutaminolysis and transferrin regulate ferroptosis. *Mol. Cell* 59, 298–308. doi: 10.1016/j.molcel.2015.06.011
- Gao, M., Yi, J., Zhu, J., Minikes, A. M., Monian, P., Thompson, C. B., et al. (2019). Role of mitochondria in ferroptosis. *Mol. Cell* 73, 354–363.e3.
- Gaschler, M. M., Andia, A. A., Liu, H., Csuka, J. M., Hurlocker, B., Vaiana, C. A., et al. (2018). FINO(2) initiates ferroptosis through GPX4 inactivation and iron oxidation. *Nat. Chem. Biol.* 14, 507–515. doi: 10.1038/s41589-018-0031-6
- Gautheron, J., Gores, G. J., and Rodrigues, C. M. P. (2020). Lytic cell death in metabolic liver disease. *J. Hepatol.* 73, 394–408. doi: 10.1016/j.jhep.2020.04.001
- Green, D. R. (2019). The coming decade of cell death research: five riddles. *Cell* 177, 1094–1107. doi: 10.1016/j.cell.2019.04.024
- Hafner, A., Bulyk, M. L., Jambhekar, A., and Lahav, G. (2019). The multiple mechanisms that regulate p53 activity and cell fate. *Nat. Rev. Mol. Cell Biol.* 20, 199–210. doi: 10.1038/s41580-019-0110-x
- Hann, H. W., Stahlhut, M. W., and Blumberg, B. S. (1988). Iron nutrition and tumor growth: decreased tumor growth in iron-deficient mice. *Cancer Res.* 48, 4168–4170.
- Hanson, E. S., Foot, L. M., and Leibold, E. A. (1999). Hypoxia post-translationally activates iron-regulatory protein 2. *J. Biol. Chem.* 274, 5047–5052. doi: 10.1074/jbc.274.8.5047
- Harper, J. W., Ordureau, A., and Heo, J. M. (2018). Building and decoding ubiquitin chains for mitophagy. *Nat. Rev. Mol. Cell Biol.* 19, 93–108. doi: 10.1038/nrm.2017.129
- Harrigan, J. A., Jacq, X., Martin, N. M., and Jackson, S. P. (2018). Deubiquitylating enzymes and drug discovery: emerging opportunities. *Nat. Rev. Drug Discov.* 17, 57–78. doi: 10.1038/nrd.2017.152

- Hassannia, B., Vandenabeele, P., and Vanden Berghe, T. (2019). Targeting ferroptosis to iron out cancer. *Cancer Cell* 35, 830–849. doi: 10.1016/j.ccell.2019.04.002
- Hayes, J. D., Dinkova-Kostova, A. T., and Tew, K. D. (2020). Oxidative stress in cancer. *Cancer Cell* 38, 167–197.
- He, Y., Ren, J., Xu, X., Ni, K., Schwader, A., Finney, R., et al. (2020). Lsh/HELLS is required for B lymphocyte development and immunoglobulin class switch recombination. *Proc. Natl. Acad. Sci. U.S.A.* 117, 20100–20108. doi: 10.1073/pnas.2004112117
- Hong, S. B., Kim, B. W., Lee, K. E., Kim, S. W., Jeon, H., Kim, J., et al. (2011). Insights into noncanonical E1 enzyme activation from the structure of autophagic E1 Atg7 with Atg8. *Nat. Struct. Mol. Biol.* 18, 1323–1330. doi: 10.1038/nsmb.2165
- Hong, X., Roh, W., Sullivan, R. J., Wong, K. H. K., Wittner, B. S., Guo, H., et al. (2021). The lipogenic regulator SREBP2 induces transferrin in circulating melanoma cells and suppresses ferroptosis. *Cancer Discov.* 11, 678–695. doi: 10.1158/2159-8290.cd-19-1500
- Hornbeck, P. V., Zhang, B., Murray, B., Kornhauser, J. M., Latham, V., and Skrzypek, E. (2015). PhosphoSitePlus, 2014: mutations, PTMs and recalibrations. *Nucleic Acids Res.* 43, D512–D520.
- Hou, W., Xie, Y., Song, X., Sun, X., Lotze, M. T., Zeh, H. J. III, et al. (2016). Autophagy promotes ferroptosis by degradation of ferritin. *Autophagy* 12, 1425–1428. doi: 10.1080/15548627.2016.1187366
- Hoxhaj, G., and Manning, B. D. (2020). The PI3K-AKT network at the interface of oncogenic signalling and cancer metabolism. *Nat. Rev. Cancer* 20, 74–88. doi: 10.1038/s41568-019-0216-7
- Huang, B. W., Miyazawa, M., and Tsuji, Y. (2014). Distinct regulatory mechanisms of the human ferritin gene by hypoxia and hypoxia mimetic cobalt chloride at the transcriptional and post-transcriptional levels. *Cell. Signal.* 26, 2702–2709. doi: 10.1016/j.cellsig.2014.08.018
- Huang, D., Li, Q., Sun, X., Sun, X., Tang, Y., Qu, Y., et al. (2020). CRL4(DCAF8) dependent opposing stability control over the chromatin remodeler LSH orchestrates epigenetic dynamics in ferroptosis. *Cell Death Differ.* 28, 1593–1609. doi: 10.1038/s41418-020-00689-5
- Illing, A. C., Shawki, A., Cunningham, C. L., and Mackenzie, B. (2012). Substrate profile and metal-ion selectivity of human divalent metal-ion transporter-1. *J. Biol. Chem.* 287, 30485–30496. doi: 10.1074/jbc.m112.364208
- Jiang, L., Kon, N., Li, T., Wang, S.-J., Su, T., Hibshoosh, H., et al. (2015). Ferroptosis as a p53-mediated activity during tumour suppression. *Nature* 520, 57–62. doi: 10.1038/nature14344
- Jiang, L., Wang, J., Wang, K., Wang, H., Wu, Q., Yang, C., et al. (2021). RNF217 regulates iron homeostasis through its E3 ubiquitin ligase activity by modulating ferroportin degradation. *Blood* doi: 10.1182/blood.202008986 [Epub ahead of print].
- Jiang, Y., Mao, C., Yang, R., Yan, B., Shi, Y., Liu, X., et al. (2017). EGLN1-c-Myc induced lymphoid-specific helicase inhibits ferroptosis through lipid metabolic gene expression changes. *Theranostics* 7, 3293–3305. doi: 10.7150/thno.19988
- Kaiser, S. E., Qiu, Y., Coats, J. E., Mao, K., Klionsky, D. J., and Schulman, B. A. (2013). Structures of Atg7-Atg3 and Atg7-Atg10 reveal noncanonical mechanisms of E2 recruitment by the autophagy E1. *Autophagy* 9, 778–780. doi: 10.4161/auto.23644
- Kakhlon, O., and Cabantchik, Z. I. (2002). The labile iron pool: characterization, measurement, and participation in cellular processes(1). *Free Radic. Biol. Med.* 33, 1037–1046. doi: 10.1016/s0891-5849(02)01006-7
- Kan, C. F., Singh, A. B., Stafforini, D. M., Azhar, S., and Liu, J. (2014). Arachidonic acid downregulates acyl-CoA synthetase 4 expression by promoting its ubiquitination and proteasomal degradation. *J. Lipid Res.* 55, 1657–1667. doi: 10.1194/jlr.m045971
- Kansanen, E., Kuosmanen, S. M., Leinonen, H., and Levonen, A. L. (2013). The Keap1-Nrf2 pathway: mechanisms of activation and dysregulation in cancer. *Redox Biol.* 1, 45–49. doi: 10.1016/j.redox.2012.10.001
- Kasprowska-Liśkiewicz, D. (2017). The cell on the edge of life and death: crosstalk between autophagy and apoptosis. *Postepy Hig. Med. Dosw.* 71, 825–841.
- Kawabata, H. (2019). Transferrin and transferrin receptors update. *Free Radic. Biol. Med.* 133, 46–54. doi: 10.1016/j.freeradbiomed.2018.06.037
- Kim, Y., and Jho, E. H. (2018). Regulation of the Hippo signaling pathway by ubiquitin modification. *BMB Rep.* 51, 143–150. doi: 10.5483/bmbrep.2018.51.3.017
- Koppula, P., Zhuang, L., and Gan, B. (2020). Cystine transporter SLC7A11/xCT in cancer: ferroptosis, nutrient dependency, and cancer therapy. *Protein Cell* 12, 599–620. doi: 10.1007/s13238-020-00789-5
- Koren, E., and Fuchs, Y. (2021). Modes of regulated cell death in cancer. *Cancer Discov.* 11, 245–265. doi: 10.1158/2159-8290.cd-20-0789
- Kwon, Y. T., and Ciechanover, A. (2017). The ubiquitin code in the ubiquitin-proteasome system and autophagy. *Trends Biochem. Sci.* 42, 873–886. doi: 10.1016/j.tibs.2017.09.002
- Lang, X., Green, M. D., Wang, W., Yu, J., Choi, J. E., Jiang, L., et al. (2019). Radiotherapy and immunotherapy promote tumoral lipid oxidation and ferroptosis via synergistic repression of SLC7A11. *Cancer Discov.* 9, 1673–1685. doi: 10.1158/2159-8290.cd-19-0338
- Lee, H., Zandkarimi, F., Zhang, Y., Meena, J. K., Kim, J., Zhuang, L., et al. (2020). Energy-stress-mediated AMPK activation inhibits ferroptosis. *Nat. Cell Biol.* 22, 225–234. doi: 10.1038/s41556-020-0461-8
- Lee, J. H., Jang, J. K., Ko, K. Y., Jin, Y., Ham, M., Kang, H., et al. (2019). Degradation of selenoprotein S and selenoprotein K through PPAR $\gamma$ -mediated ubiquitination is required for adipocyte differentiation. *Cell Death Differ.* 26, 1007–1023. doi: 10.1038/s41418-018-0180-x
- Lei, G., Zhang, Y., Koppula, P., Liu, X., Zhang, J., Lin, S. H., et al. (2020). The role of ferroptosis in ionizing radiation-induced cell death and tumor suppression. *Cell Res.* 30, 146–162. doi: 10.1038/s41422-019-0263-3
- Levine, A. J. (2020). p53: 800 million years of evolution and 40 years of discovery. *Nat. Rev. Cancer* 20, 471–480. doi: 10.1038/s41568-020-0262-1
- Li, N., Wang, W., Zhou, H., Wu, Q., Duan, M., Liu, C., et al. (2020). Ferritinophagy-mediated ferroptosis is involved in sepsis-induced cardiac injury. *Free Radic. Biol. Med.* 160, 303–318. doi: 10.1016/j.freeradbiomed.2020.08.009
- Li, Q. Q., Li, Q., Jia, J. N., Liu, Z. Q., Zhou, H. H., and Mao, X. Y. (2018). 12/15 lipoxygenase: a crucial enzyme in diverse types of cell death. *Neurochem. Int.* 118, 34–41. doi: 10.1016/j.neuint.2018.04.002
- Li, Z., Jiang, L., Chew, S. H., Hirayama, T., Sekido, Y., and Toyokuni, S. (2019). Carbonic anhydrase 9 confers resistance to ferroptosis/apoptosis in malignant mesothelioma under hypoxia. *Redox Biol.* 26:101297. doi: 10.1016/j.redox.2019.101297
- Lin, H. C., Ho, S. C., Chen, Y. Y., Khoo, K. H., Hsu, P. H., and Yen, H. C. (2015). CRL2 aids elimination of truncated selenoproteins produced by failed UGA/Sec decoding. *Science* 349, 91–95. doi: 10.1126/science.aab0515
- Liu, J., Cheng, Y., Zheng, M., Yuan, B., Wang, Z., Li, X., et al. (2021). Targeting the ubiquitination/deubiquitination process to regulate immune checkpoint pathways. *Signal Transduct. Target. Ther.* 6:28.
- Liu, S., and Tao, Y. G. (2016). Chromatin remodeling factor LSH affects fumarate hydratase as a cancer driver. *Chin. J. Cancer* 35:72.
- Liu, T., Jiang, L., Tavana, O., and Gu, W. (2019). The Deubiquitylase OTUB1 Mediates Ferroptosis via Stabilization of SLC7A11. *Cancer Res.* 79, 1913–1924. doi: 10.1158/0008-5472.can-18-3037
- Liu, Y., Tavana, O., and Gu, W. (2019). p53 modifications: exquisite decorations of the powerful guardian. *J. Mol. Cell Biol.* 11, 564–577. doi: 10.1093/jmcb/mjz060
- Liu, Y., Wang, Y., Liu, J., Kang, R., and Tang, D. (2021). Interplay between MTOR and GPX4 signaling modulates autophagy-dependent ferroptotic cancer cell death. *Cancer Gene Ther.* 28, 55–63. doi: 10.1038/s41417-020-0182-y
- Louie, B. H., and Kurzrock, R. (2020). BAP1: not just a BRCA1-associated protein. *Cancer Treat. Rev.* 90:102091. doi: 10.1016/j.ctrv.2020.102091
- Lu, G., Wang, L., Zhou, J., Liu, W., and Shen, H. M. (2021). A destiny for degradation: interplay between Cullin-RING E3 ligases and autophagy. *Trends Cell Biol.* 31, 432–444. doi: 10.1016/j.tcb.2021.01.005
- Ma, S., Sun, L., Wu, W., Wu, J., Sun, Z., and Ren, J. (2020). USP22 protects against myocardial ischemia-reperfusion injury via the SIRT1-p53/SLC7A11-Dependent inhibition of ferroptosis-induced cardiomyocyte death. *Front. Physiol.* 11:551318. doi: 10.3389/fphys.2020.551318
- Mancias, J. D., Pontano Vaitea, L., Nissim, S., Biancur, D. E., Kim, A. J., Wang, X., et al. (2015). Ferritinophagy via NCOA4 is required for erythropoiesis and is regulated by iron dependent HERC2-mediated proteolysis. *Elife* 4:e10308.
- Mashima, R., and Okuyama, T. (2015). The role of lipoxygenases in pathophysiology; new insights and future perspectives. *Redox Biol.* 6, 297–310. doi: 10.1016/j.redox.2015.08.006
- Meng, C., Zhan, J., Chen, D., Shao, G., Zhang, H., Gu, W., et al. (2021). The deubiquitinase USP11 regulates cell proliferation and ferroptotic cell death via stabilization of NRF2 USP11 deubiquitinates and stabilizes NRF2. *Oncogene* 40, 1706–1720. doi: 10.1038/s41388-021-01660-5



- Moroishi, T., Nishiyama, M., Takeda, Y., Iwai, K., and Nakayama, K. I. (2011). The FBXL5-IRP2 axis is integral to control of iron metabolism in vivo. *Cell Metab.* 14, 339–351. doi: 10.1016/j.cmet.2011.07.011
- Nagata, S. (2018). Apoptosis and clearance of apoptotic cells. *Annu. Rev. Immunol.* 36, 489–517. doi: 10.1146/annurev-immunol-042617-053010
- Narayanan, R. (2020). Therapeutic targeting of the androgen receptor (AR) and AR variants in prostate cancer. *Asian J. Urol.* 7, 271–283. doi: 10.1016/j.ajur.2020.03.002
- Neklesa, T. K., Winkler, J. D., and Crews, C. M. (2017). Targeted protein degradation by PROTACs. *Pharmacol. Ther.* 174, 138–144. doi: 10.1016/j.pharmthera.2017.02.027
- Ni, K., Ren, J., Xu, X., He, Y., Finney, R., Braun, S. M. G., et al. (2020). LSH mediates gene repression through macroH2A deposition. *Nat. Commun.* 11:5647.
- Nikolopoulou, V., Markaki, M., Palikaras, K., and Tavernarakis, N. (2013). Crosstalk between apoptosis, necrosis and autophagy. *Biochim. Biophys. Acta* 1833, 3448–3459. doi: 10.1016/j.bbamer.2013.06.001
- Nunes, A. T., and Annunziata, C. M. (2017). Proteasome inhibitors: structure and function. *Semin. Oncol.* 44, 377–380. doi: 10.1053/j.seminoncol.2018.01.004
- Ogiwara, H., Takahashi, K., Sasaki, M., Kuroda, T., Yoshida, H., Watanabe, R., et al. (2019). Targeting the vulnerability of glutathione metabolism in ARID1A-deficient cancers. *Cancer Cell* 35, 177–190.e8.
- Ohgami, R. S., Campagna, D. R., Greer, E. L., Antiochos, B., McDonald, A., Chen, J., et al. (2005). Identification of a ferriredutase required for efficient transferrin-dependent iron uptake in erythroid cells. *Nat. Genet.* 37, 1264–1269. doi: 10.1038/ng1658
- Paiva, S. L., and Crews, C. M. (2019). Targeted protein degradation: elements of PROTAC design. *Curr. Opin. Chem. Biol.* 50, 111–119. doi: 10.1016/j.cbpa.2019.02.022
- Pettersson, M., and Crews, C. M. (2019). PROteolysis TARgeting Chimeras (PROTACs) - Past, present and future. *Drug Discov. Today Technol.* 31, 15–27. doi: 10.1016/j.ddtec.2019.01.002
- Pickrell, A. M., and Youle, R. J. (2015). The roles of PINK1, parkin, and mitochondrial fidelity in Parkinson's disease. *Neuron* 85, 257–273. doi: 10.1016/j.neuron.2014.12.007
- Poh, A. (2020). Proof-of-Concept with PROTACs in prostate cancer. *Cancer Discov.* 10:1084.
- Popovic, D., Vucic, D., and Dikic, I. (2014). Ubiquitination in disease pathogenesis and treatment. *Nat. Med.* 20, 1242–1253. doi: 10.1038/nm.3739
- Qian, Z. M., Wu, X. M., Fan, M., Yang, L., Du, F., Yung, W. H., et al. (2011). Divalent metal transporter 1 is a hypoxia-inducible gene. *J. Cell. Physiol.* 226, 1596–1603. doi: 10.1002/jcp.22485
- Rape, M. (2018). Ubiquitylation at the crossroads of development and disease. *Nat. Rev. Mol. Cell Biol.* 19, 59–70. doi: 10.1038/nrm.2017.83
- Ravanelli, S., den Brave, F., and Hoppe, T. (2020). Mitochondrial quality control governed by ubiquitin. *Front. Cell Dev. Biol.* 8:270. doi: 10.3389/fcell.2020.00270
- Riegman, M., Sagie, L., Galed, C., Levin, T., Steinberg, N., Dixon, S. J., et al. (2020). Ferroptosis occurs through an osmotic mechanism and propagates independently of cell rupture. *Nat. Cell Biol.* 22, 1042–1048. doi: 10.1038/s41556-020-0565-1
- Rothlin, C. V., Hille, T. D., and Ghosh, S. (2020). Determining the effector response to cell death. *Nat. Rev. Immunol.* 21, 292–304.
- Schapira, M., Calabrese, M. F., Bullock, A. N., and Crews, C. M. (2019). Targeted protein degradation: expanding the toolbox. *Nat. Rev. Drug Discov.* 18, 949–963. doi: 10.1038/s41573-019-0047-y
- Sebastian, S., Zhu, Y. X., Braggio, E., Shi, C. X., Panchabhai, S. C., Van Wier, S. A., et al. (2017). Multiple myeloma cells' capacity to decompose H(2)O(2) determines lenalidomide sensitivity. *Blood* 129, 991–1007. doi: 10.1182/blood-2016-09-738872
- Sen, P., Kan, C. F. K., Singh, A. B., Rius, M., Kraemer, F. B., Sztul, E., et al. (2020). Identification of p115 as a novel ACSL4 interacting protein and its role in regulating ACSL4 degradation. *J. Proteomics* 229:103926. doi: 10.1016/j.jprot.2020.103926
- Senft, D., Qi, J., and Ronai, Z. A. (2018). Ubiquitin ligases in oncogenic transformation and cancer therapy. *Nat. Rev. Cancer* 18, 69–88. doi: 10.1038/nrc.2017.105
- Shan, Y., Yang, G., Huang, H., Zhou, Y., Hu, X., Lu, Q., et al. (2020). Ubiquitin-Like modifier activating enzyme 1 as a novel diagnostic and prognostic indicator that correlates with ferroptosis and the malignant phenotypes of liver cancer cells. *Front. Oncol.* 10:592413. doi: 10.3389/fonc.2020.592413
- Sheftel, A. D., Mason, A. B., and Ponka, P. (2012). The long history of iron in the Universe and in health and disease. *Biochim. Biophys. Acta* 1820, 161–187. doi: 10.1016/j.bbagen.2011.08.002
- Shen, Z., Song, J., Yung, B. C., Zhou, Z., Wu, A., and Chen, X. (2018). Emerging strategies of cancer therapy based on ferroptosis. *Adv. Mater.* 30:e1704007.
- Silva, B., and Faustino, P. (2015). An overview of molecular basis of iron metabolism regulation and the associated pathologies. *Biochim. Biophys. Acta* 1852, 1347–1359. doi: 10.1016/j.bbadis.2015.03.011
- Snyder, A. G., and Oberst, A. (2021). The antisocial network: cross talk between cell death programs in host defense. *Annu. Rev. Immunol.* 39, 77–101. doi: 10.1146/annurev-immunol-112019-072301
- Song, J., Herrmann, J. M., and Becker, T. (2021a). Quality control of the mitochondrial proteome. *Nat. Rev. Mol. Cell Biol.* 22, 54–70. doi: 10.1038/s41580-020-00300-2
- Song, J., Liu, T., Yin, Y., Zhao, W., Lin, Z., Yin, Y., et al. (2021b). The deubiquitinase OTUD1 enhances iron transport and potentiates host antitumor immunity. *EMBO Rep.* 22:e51162.
- Stockwell, B. R., Friedmann Angeli, J. P., Bayir, H., Bush, A. I., Conrad, M., Dixon, S. J., et al. (2017). Ferroptosis: a regulated cell death nexus linking metabolism, redox biology, and disease. *Cell* 171, 273–285. doi: 10.1016/j.cell.2017.09.021
- Sukjoi, W., Ngamkham, J., Attwood, P. V., and Jitrapakdee, S. (2021). Targeting cancer metabolism and current anti-cancer drugs. *Adv. Exp. Med. Biol.* 1286, 15–48. doi: 10.1097/00001813-199512006-00003
- Sun, T., Liu, Z., and Yang, Q. (2020). The role of ubiquitination and deubiquitination in cancer metabolism. *Mol. Cancer* 19:146.
- Sztiller-Sikorska, M., and Czyz, M. (2020). Parthenolide as cooperating agent for anti-cancer treatment of various malignancies. *Pharmaceuticals (Basel)* 13:194. doi: 10.3390/ph13080194
- Tacchini, L., Bianchi, L., Bernelli-Zazzera, A., and Cairo, G. (1999). Transferrin receptor induction by hypoxia. HIF-1-mediated transcriptional activation and cell-specific post-transcriptional regulation. *J. Biol. Chem.* 274, 24142–24146.
- Tang, D., Chen, X., Kang, R., and Kroemer, G. (2021). Ferroptosis: molecular mechanisms and health implications. *Cell Res.* 31, 107–125. doi: 10.1038/s41422-020-00441-1
- Tang, L. J., Zhou, Y. J., Xiong, X. M., Li, N. S., Zhang, J. J., Luo, X. J., et al. (2021). Ubiquitin-specific protease 7 promotes ferroptosis via activation of the p53/TfR1 pathway in the rat hearts after ischemia/reperfusion. *Free Radic. Biol. Med.* 162, 339–352. doi: 10.1016/j.freeradbiomed.2020.10.307
- Taylor, R. C., Cullen, S. P., and Martin, S. J. (2008). Apoptosis: controlled demolition at the cellular level. *Nat. Rev. Mol. Cell Biol.* 9, 231–241. doi: 10.1038/nrm2312
- Torti, S. V., Manz, D. H., Paul, B. T., Blanchette-Farra, N., and Torti, F. M. (2018). Iron and cancer. *Annu. Rev. Nutr.* 38, 97–125.
- Tsai, Y., Xia, C., and Sun, Z. (2020). The inhibitory effect of 6-gingerol on ubiquitin-specific peptidase 14 enhances autophagy-dependent ferroptosis and anti-tumor in vivo and in vitro. *Front. Pharmacol.* 11:598555. doi: 10.3389/fphar.2020.598555
- Tsuchida, T., and Friedman, S. L. (2017). Mechanisms of hepatic stellate cell activation. *Nat. Rev. Gastroenterol. Hepatol.* 14, 397–411.
- Tu, K., Yang, W., Li, C., Zheng, X., Lu, Z., Guo, C., et al. (2014). Fbxw7 is an independent prognostic marker and induces apoptosis and growth arrest by regulating YAP abundance in hepatocellular carcinoma. *Mol. Cancer* 13:110. doi: 10.1186/1476-4598-13-110
- Tummers, B., and Green, D. R. (2017). Caspase-8: regulating life and death. *Immunol. Rev.* 277, 76–89. doi: 10.1111/imr.12541
- Ubellacker, J. M., Tasdogan, A., Ramesh, V., Shen, B., Mitchell, E. C., Martin-Sandoval, M. S., et al. (2020). Lymph protects metastasizing melanoma cells from ferroptosis. *Nature* 585, 113–118. doi: 10.1038/s41586-020-2623-z
- Vashisht, A. A., Zumbrennen, K. B., Huang, X., Powers, D. N., Durazo, A., Sun, D., et al. (2009). Control of iron homeostasis by an iron-regulated ubiquitin ligase. *Science* 326, 718–721. doi: 10.1126/science.1176333
- Venkatesh, D., O'Brien, N. A., Zandkarimi, F., Tong, D. R., Stokes, M. E., Dunn, D. E., et al. (2020). MDM2 and MDMX promote ferroptosis by PPAR $\alpha$ -mediated lipid remodeling. *Genes Dev.* 34, 526–543. doi: 10.1101/gad.334219.119
- Vidal, R., Miravalle, L., Gao, X., Barbeito, A. G., Baraibar, M. A., Hekmatyar, S. K., et al. (2008). Expression of a mutant form of the ferritin light chain gene induces neurodegeneration and iron overload in transgenic mice. *J. Neurosci.* 28, 60–67. doi: 10.1523/jneurosci.3962-07.2008



- Wang, W., Green, M., Choi, J. E., Gijon, M., Kennedy, P. D., Johnson, J. K., et al. (2019). CD8(+) T cells regulate tumour ferroptosis during cancer immunotherapy. *Nature* 569, 270–274. doi: 10.1038/s41586-019-1170-y
- Wang, Y., Jiang, X., Feng, F., Liu, W., and Sun, H. (2020a). Degradation of proteins by PROTACs and other strategies. *Acta Pharm. Sin. B* 10, 207–238. doi: 10.1016/j.apsb.2019.08.001
- Wang, Y., Liu, Y., Liu, J., Kang, R., and Tang, D. (2020b). NEDD4L-mediated LTF protein degradation limits ferroptosis. *Biochem. Biophys. Res. Commun.* 531, 581–587. doi: 10.1016/j.bbrc.2020.07.032
- Wang, Y., Yang, L., Zhang, X., Cui, W., Liu, Y., Sun, Q. R., et al. (2019). Epigenetic regulation of ferroptosis by H2B monoubiquitination and p53. *EMBO Rep.* 20:e47563.
- Ward, D. M., and Kaplan, J. (2012). Ferroportin-mediated iron transport: expression and regulation. *Biochim. Biophys. Acta* 1823, 1426–1433. doi: 10.1016/j.bbamcr.2012.03.004
- Wenzel, S. E., Tyurina, Y. Y., Zhao, J., St Croix, C. M., Dar, H. H., Mao, G., et al. (2017). PEBP1 wards ferroptosis by enabling lipoxygenase generation of lipid death signals. *Cell* 171, 628–641.e26.
- Wu, J., Minikes, A. M., Gao, M., Bian, H., Li, Y., Stockwell, B. R., et al. (2019). Intercellular interaction dictates cancer cell ferroptosis via NF2-YAP signalling. *Nature* 572, 402–406. doi: 10.1038/s41586-019-1426-6
- Wu, X., Li, Y., Zhang, S., and Zhou, X. (2021). Ferroptosis as a novel therapeutic target for cardiovascular disease. *Theranostics* 11, 3052–3059. doi: 10.7150/thno.54113
- Wu, Y., Zhang, S., Gong, X., Tam, S., Xiao, D., Liu, S., et al. (2020). The epigenetic regulators and metabolic changes in ferroptosis-associated cancer progression. *Mol. Cancer* 19:39.
- Xie, Y., Zhou, X., Li, J., Yao, X. C., Liu, W. L., Kang, F. H., et al. (2021). Identification of a new natural biflavonoids against breast cancer cells induced ferroptosis via the mitochondrial pathway. *Bioorg. Chem.* 109:104744.
- Yan, H. F., Tuo, Q. Z., Yin, Q. Z., and Lei, P. (2020). The pathological role of ferroptosis in ischemia/reperfusion-related injury. *Zool. Res.* 41, 220–230. doi: 10.24272/j.issn.2095-8137.2020.042
- Yan, H. F., Zou, T., Tuo, Q. Z., Xu, S., Li, H., Belaidi, A. A., et al. (2021). Ferroptosis: mechanisms and links with diseases. *Signal Transduct. Target. Ther.* 6:49.
- Yang, L., Chen, X., Yang, Q., Chen, J., Huang, Q., Yao, L., et al. (2020). Broad spectrum deubiquitinase inhibition induces both apoptosis and ferroptosis in cancer cells. *Front. Oncol.* 10:949. doi: 10.3389/fonc.2020.00949
- Yang, R., Liu, N., Chen, L., Jiang, Y., Shi, Y., Mao, C., et al. (2019a). GIAT4RA functions as a tumor suppressor in non-small cell lung cancer by counteracting Uchl3-mediated deubiquitination of LSH. *Oncogene* 38, 7133–7145. doi: 10.1038/s41388-019-0909-0
- Yang, R., Liu, N., Chen, L., Jiang, Y., Shi, Y., Mao, C., et al. (2019b). LSH interacts with and stabilizes GINS4 transcript that promotes tumorigenesis in non-small cell lung cancer. *J. Exp. Clin. Cancer Res.* 38:280.
- Yang, W. H., Ding, C. C., Sun, T., Rupprecht, G., Lin, C. C., Hsu, D., et al. (2019c). The hippo pathway effector TAZ regulates ferroptosis in renal cell carcinoma. *Cell Rep.* 28, 501–2508.e4.
- Yang, W. H., Lin, C. C., Wu, J., Chao, P. Y., Chen, K., Chen, P. H., et al. (2021). The hippo pathway effector YAP promotes ferroptosis via the E3 ligase SKP2. *Mol. Cancer Res.* 19, 1005–1014. doi: 10.1158/1541-7786.mcr-20-0534
- Yang, W. S., and Stockwell, B. R. (2016). Ferroptosis: death by lipid peroxidation. *Trends Cell Biol.* 26, 165–176. doi: 10.1016/j.tcb.2015.10.014
- Yang, W. S., SriRamaratnam, R., Welsch, M. E., Shimada, K., Skouta, R., Viswanathan, V. S., et al. (2014). Regulation of ferroptotic cancer cell death by GPX4. *Cell* 156, 317–331. doi: 10.1016/j.cell.2013.12.010
- Yang, Y., Luo, M., Zhang, K., Zhang, J., Gao, T., Connell, D. O., et al. (2020). Nedd4 ubiquitylates VDAC2/3 to suppress erastin-induced ferroptosis in melanoma. *Nat. Commun.* 11:433.
- Ye, P., Mimura, J., Okada, T., Sato, H., Liu, T., Maruyama, A., et al. (2014). Nrf2- and ATF4-dependent upregulation of xCT modulates the sensitivity of T24 bladder carcinoma cells to proteasome inhibition. *Mol. Cell. Biol.* 34, 3421–3434. doi: 10.1128/mcb.00221-14
- Yi, J., Zhu, J., Wu, J., Thompson, C. B., and Jiang, X. (2020). Oncogenic activation of PI3K-AKT-mTOR signaling suppresses ferroptosis via SREBP-mediated lipogenesis. *Proc. Natl. Acad. Sci. U.S.A.* 117, 31189–31197. doi: 10.1073/pnas.2017152117
- Yu, H., Yang, C., Jian, L., Guo, S., Chen, R., Li, K., et al. (2019). Sulfasalazine-induced ferroptosis in breast cancer cells is reduced by the inhibitory effect of estrogen receptor on the transferrin receptor. *Oncol. Rep.* 42, 826–838.
- Zeng, X., An, H., Yu, F., Wang, K., Zheng, L., Zhou, W., et al. (2021). Benefits of iron chelators in the treatment of Parkinson's disease. *Neurochem. Res.* 46, 1239–1251. doi: 10.1007/s11064-021-03262-9
- Zhang, K. H., Tian, H. Y., Gao, X., Lei, W. W., Hu, Y., Wang, D. M., et al. (2009). Ferritin heavy chain-mediated iron homeostasis and subsequent increased reactive oxygen species production are essential for epithelial-mesenchymal transition. *Cancer Res.* 69, 5340–5348. doi: 10.1158/0008-5472.can-09-0112
- Zhang, X., Yu, K., Ma, L., Qian, Z., Tian, X., Miao, Y., et al. (2021). Endogenous glutamate determines ferroptosis sensitivity via ADCY10-dependent YAP suppression in lung adenocarcinoma. *Theranostics* 11, 5650–5674. doi: 10.7150/thno.55482
- Zhang, Y., Koppula, P., and Gan, B. (2019a). Regulation of H2A ubiquitination and SLC7A11 expression by BAP1 and PRC1. *Cell Cycle* 18, 773–783. doi: 10.1080/15384101.2019.1597506
- Zhang, Y., Shi, J., Liu, X., Feng, L., Gong, Z., Koppula, P., et al. (2018). BAP1 links metabolic regulation of ferroptosis to tumour suppression. *Nat. Cell Biol.* 20, 1181–1192. doi: 10.1038/s41556-018-0178-0
- Zhang, Y., Swanda, R. V., Nie, L., Liu, X., Wang, C., Lee, H., et al. (2021). mTORC1 couples cyst(e)ine availability with GPX4 protein synthesis and ferroptosis regulation. *Nat. Commun.* 12:1589.
- Zhang, Y., Tan, H., Daniels, J. D., Zandkarimi, F., Liu, H., Brown, L. M., et al. (2019b). Imidazole ketone erastin induces ferroptosis and slows tumor growth in a mouse lymphoma model. *Cell Chem. Biol.* 26, 623–633.e9.
- Zhang, Z., Guo, M., Li, Y., Shen, M., Kong, D., Shao, J., et al. (2020). RNA-binding protein ZFP36/TTP protects against ferroptosis by regulating autophagy signaling pathway in hepatic stellate cells. *Autophagy* 16, 1482–1505. doi: 10.1080/15548627.2019.1687985
- Zhou, B., Liu, J., Kang, R., Klionsky, D. J., Kroemer, G., and Tang, D. (2020). Ferroptosis is a type of autophagy-dependent cell death. *Semin. Cancer Biol.* 66, 89–100. doi: 10.1016/j.semcancer.2019.03.002
- Zhou, R., Han, L., Li, G., and Tong, T. (2009). Senescence delay and repression of p16INK4a by Lsh via recruitment of histone deacetylases in human diploid fibroblasts. *Nucleic Acids Res.* 37, 5183–5196. doi: 10.1093/nar/gkp533
- Zhou, X., and Sun, S. C. (2021). Targeting ubiquitin signaling for cancer immunotherapy. *Signal Transduct. Target. Ther.* 6:16.
- Zhu, Y., Zhang, C., Huang, M., Lin, J., Fan, X., and Ni, T. (2021). TRIM26 induces ferroptosis to inhibit hepatic stellate cell activation and mitigate liver fibrosis through mediating SLC7A11 ubiquitination. *Front. Cell Dev. Biol.* 9:644901. doi: 10.3389/fcell.2021.644901
- Zong, W. X., and Thompson, C. B. (2006). Necrotic death as a cell fate. *Genes Dev.* 20, 1–15. doi: 10.1101/gad.1376506
- Zou, Y., Henry, W. S., Ricq, E. L., Graham, E. T., Phadnis, V. V., Maretich, P., et al. (2020a). Plasticity of ether lipids promotes ferroptosis susceptibility and evasion. *Nature* 585, 603–608. doi: 10.1038/s41586-020-2732-8
- Zou, Y., Li, H., Graham, E. T., Deik, A. A., Eaton, J. K., Wang, W., et al. (2020b). Cytochrome P450 oxidoreductase contributes to phospholipid peroxidation in ferroptosis. *Nat. Chem. Biol.* 16, 302–309. doi: 10.1038/s41589-020-0472-6

**Conflict of Interest:** The authors declare that the research was conducted in the absence of any commercial or financial relationships that could be construed as a potential conflict of interest.

**Publisher's Note:** All claims expressed in this article are solely those of the authors and do not necessarily represent those of their affiliated organizations, or those of the publisher, the editors and the reviewers. Any product that may be evaluated in this article, or claim that may be made by its manufacturer, is not guaranteed or endorsed by the publisher.

Copyright © 2021 Wang, Wang, Li, Qin and Wang. This is an open-access article distributed under the terms of the Creative Commons Attribution License (CC BY). The use, distribution or reproduction in other forums is permitted, provided the original author(s) and the copyright owner(s) are credited and that the original publication in this journal is cited, in accordance with accepted academic practice. No use, distribution or reproduction is permitted which does not comply with these terms.



# Functions and Molecular Mechanisms of Deltex Family Ubiquitin E3 Ligases in Development and Disease

Lidong Wang<sup>1</sup>, Xiaodan Sun<sup>2</sup>, Jingni He<sup>1</sup> and Zhen Liu<sup>1\*</sup>

<sup>1</sup> Department of General Surgery, Shengjing Hospital of China Medical University, Shenyang, China, <sup>2</sup> Postdoctoral Research Workstation, Jilin Cancer Hospital, Changchun, China

## OPEN ACCESS

### Edited by:

Lixin Wan,  
Moffitt Cancer Center, United States

### Reviewed by:

Mark A. Nakasone,  
University of Glasgow,  
United Kingdom  
Ariz Mohammad,  
Washington University in St. Louis,  
United States

### \*Correspondence:

Zhen Liu  
liuzhen1973@aliyun.com

### Specialty section:

This article was submitted to  
Cell Growth and Division,  
a section of the journal  
Frontiers in Cell and Developmental  
Biology

**Received:** 08 May 2021

**Accepted:** 05 August 2021

**Published:** 25 August 2021

### Citation:

Wang L, Sun X, He J and Liu Z  
(2021) Functions and Molecular  
Mechanisms of Deltex Family  
Ubiquitin E3 Ligases in Development  
and Disease.  
*Front. Cell Dev. Biol.* 9:706997.  
doi: 10.3389/fcell.2021.706997

Ubiquitination is a posttranslational modification of proteins that significantly affects protein stability and function. The specificity of substrate recognition is determined by ubiquitin E3 ligase during ubiquitination. Human Deltex (DTX) protein family, which functions as ubiquitin E3 ligases, comprises five members, namely, DTX1, DTX2, DTX3, DTX3L, and DTX4. The characteristics and functional diversity of the DTX family proteins have attracted significant attention over the last decade. DTX proteins have several physiological and pathological roles and are closely associated with cell signal transduction, growth, differentiation, and apoptosis, as well as the occurrence and development of various tumors. Although they have been extensively studied in various species, data on structural features, biological functions, and potential mechanisms of action of the DTX family proteins remain limited. In this review, recent research progress on each member of the DTX family is summarized, providing insights into future research directions and potential strategies in disease diagnosis and therapy.

**Keywords:** Deltex family proteins, ubiquitination, ubiquitin E3 ligase, ubiquitin code, protein homeostasis, post-translational modification

## INTRODUCTION

Intracellular protein homeostasis, i.e., proteostasis, is influenced by the dynamic equilibrium between protein synthesis, localization, maintenance, and degradation, all of which are regulated by protein-protein interaction networks (Zhong et al., 2019). Dysregulated proteostasis is associated with cellular dysfunction and can lead to disease onset, including neurodegeneration (Kaushik and Cuervo, 2015) and cancer (Dai and Sampson, 2016). Ubiquitination is a prominent and highly conserved post-translational modification (PTM) of proteins, during which ubiquitin (Ub) molecules are attached to a target protein. A majority of intracellular proteins are modified by ubiquitination (Amm et al., 2014). Several Ub signals are recognized by proteasomes, thereby serving as a regulatory mechanism for protein degradation, affecting nearly all aspects of cellular processes (Chowdhury and Enenkel, 2015; Hanna et al., 2019; Sakai et al., 2020; Fhu and Ali, 2021; Goetzke et al., 2021; Qu et al., 2021; Zou and Lin, 2021). Ubiquitin signaling is strictly regulated

by a multistep cascade reaction consisting of three enzyme groups. Initially, energy from adenosine triphosphate (ATP) hydrolysis is used by the ubiquitin-activating enzyme (E1) to generate a high energy thioester bond between the C-terminus of Ub and a catalytic cysteine residue of the active site in E1. Next, Ub is transferred from E1 to a cysteine residue in the active site of the ubiquitin-conjugating enzyme (E2), forming a similar thioester bond to that of E1. Finally, ubiquitin ligase (E3) catalyzes the covalent attachment of Ub to lysine residues of the substrate protein (Thapa et al., 2020). E2 and/or E3 enzymes are also associated with the elongation of Ub chains (Dikic et al., 2009). Ub contains 76-amino acids with seven lysine residues (Lys6, 11, 27, 29, 33, 48, and 63) and a methionine residue (Met1), all of which can be ubiquitinated and attached to numerous linkage types of Ub chains via an isopeptide bond (Ikeda and Dikic, 2008). Ub ends with a diglycine motif, which is critical for attachment to substrate proteins (Hanna et al., 2019). Monoubiquitination is the attachment of a single Ub molecule to a single Lys of the target protein, which regulates several aspects of protein function, including subcellular localization and protein-protein interaction, in both normal and disease states (Sewduth et al., 2020). Conversely, polyubiquitin (polyUb) chains can be formed on a single Lys by attachment of multiple Ub molecules through internal Ub–Ub linkages (Akutsu et al., 2016); hence, the different types of polyUb chains depend on the Lys for the Ub linkage (Komander and Rape, 2012). In homotypic polyUb chains, a total of eight different chain types can be formed; meanwhile, heterotypic polyUb chains comprise mixed and branched types, containing two or more linkages (Pickart and Fushman, 2004; Kliza and Husnjak, 2020). Among these polyUb chains, Lys48-linked polyUb chains are primarily involved in protein degradation by proteasomes, whereas Lys63-linked polyUb chains are more associated with non-degradative processes, such as vesicular trafficking (Trempe, 2011; Matyskiela and Martin, 2013). Lys63-linked polyUb chain also influences the induction of autophagy, a lysosome mediated protein degradation process (Chen et al., 2019). The linear homotypic polyUb chains are Met1-linked and assembled by a multi-subunit complex referred to as linear Ub chain assembly complex (LUBAC) (Kirisako et al., 2006). Several signaling cascades, such as tumor necrosis factor (TNF) and nuclear factor kappa-light-chain-enhancer of activated B cells (NF- $\kappa$ B), which are involved in immune and inflammatory diseases, are regulated by linear Ub chains (Rittinger and Ikeda, 2017).

More than 600 E3 ligases have been identified in humans. Based on their characteristic catalytic domains and the mechanisms underlying Ub transfer to target proteins, E3s are divided into three major types, namely, the homologous to the E6-AP carboxyl terminus (HECT) family, Really Interesting New Gene (RING) family, and RING-in-between-RING (RBR) family (Morreale and Walden, 2016). Among these types, there are approximately 300 predicted RING E3s, making it the most abundant type of E3s (Li et al., 2008). The typical RING E3s contain a zinc-binding RING domain and function as monomers, homodimers, or heterodimers (Morreale and Walden, 2016). RING E3s typically function as a scaffold to recruit E2 in close proximity to substrate, thereby promoting direct transfer of Ub

(Zheng and Shabek, 2017). Both monomeric and homodimeric U-box E3s belong to the RING type, despite the lack of zinc ions in its modified RING motif (Hatakeyama and Nakayama, 2003). The ubiquitination of HECT and RBR E3s involves a two-step reaction: (1) the transfer of Ub to the catalytic cysteine residue on E3s, and (2) the transfer of Ub from E3 to the target protein (Cotton and Lechtenberg, 2020; Wang et al., 2020b). Numerous E2s can function with a single E3 resulting in various outcomes, confirming that E2 significantly influences the outcomes of ubiquitination (Wenzel et al., 2011; Stewart et al., 2016). Over the last decade, research interest in DTX family E3s has increased, and considerable efforts have been made to study this family of RING type E3 ligases. The current available data suggest that the DTX family members are closely involved in cell growth, differentiation, apoptosis, intracellular signal transduction, as well as several diseases, including cancer. However, our knowledge of their substrates, biological and pathological functions, and exact molecular mechanisms is limited. In this review, we aim to provide a comprehensive view on characteristic structural features, functions and associated molecular mechanisms of DTX family proteins. Moreover, we highlight some perspectives for future investigations. The improved understanding of the impacts of DTX family proteins on development and disease may pave the way for their potential clinical applications as diagnostic and prognostic targets.

## STRUCTURAL FEATURES OF DTX FAMILY IN DIFFERENT SPECIES

*Drosophila Melanogaster* is one of the most popular experimental animal models due to its relatively short life cycle, easy maintenance, and high homology to the human genome (Singh and Irvine, 2012). The *Drosophila* genome contains four sets of chromosomes, thus making it easy to use for genetic manipulation in research (Taormina et al., 2019). *Drosophila*'s sole *Deltex* gene is located on chromosome X and has four exons and three introns. The murine homologs (*MDTX* genes) contain four additional exons and introns, compared to *Drosophila Deltex* (Pampeno et al., 2001). In mammals, the encoded DTX family proteins comprise five members, namely DTX1, DTX2, DTX3, DTX3L, and DTX4 (Kishi et al., 2001; Takeyama et al., 2003; Chatrin et al., 2020). Compared with the amino acid sequences of *Drosophila Deltex* (Dx) protein, seven additional amino acids (amino acids 145–151) are found in MDTXs, and 82 additional amino acids occur in the N-terminal sequences of human DTXs (Pampeno et al., 2001). Furthermore, the vertebrate DTX proteins lack the polyglutamine sequences (amino acids 250–302 and 488–513) (Pampeno et al., 2001). The diverse amino acid sequences in different species may indicate some evolutionary characteristics of DTX family proteins. However, the biological relevance of these amino acid sequence variations of DTX family proteins are yet to be fully understood.

Deltex has three distinct domains (I, II, and III) from the N- to C-terminus. The N-terminal domain I of Dx comprises two WWE motifs, both of which bind to the ankyrin repeat sequences of Notch (Zweifel et al., 2005). The N-termini of

human DTX1, DTX2, and DTX4 share homology with that of Dx. However, DTX3 cannot interact with Notch due to the truncated sequences in the N-terminus (Takeyama et al., 2003). Moreover, the N-terminus of DTX3L differs from the remaining DTX family members and contains both nuclear localization and export signals (Takeyama et al., 2003). Poly-adenosine diphosphate (ADP)-ribosylation (PARylation) is a PTM process by which ADP-ribose (ADPr) units, from nicotinamide adenine dinucleotide (NAD<sup>+</sup>), are added to targeted residues (Glu, Asp, Lys, Arg, or Ser) of a protein (Zhang et al., 2013; Martello et al., 2016). The WWE motifs of the DTX family proteins attach to complexes via recognizing *iso*-ADPr, the minimal subunit of PAR polymer, with a characteristic glycosidic bond (Aravind, 2001; He et al., 2012; Wang et al., 2012). Domain II of Dx contains a proline-rich motif, which is the binding site of the SH3 domain, that primarily regulates the interaction with other proteins, such as growth factor receptor-binding protein 2 (Grb2) (Matsuno et al., 1998). Lacking the proline-rich motif negatively reverses the Dx regulation of Notch signaling pathway (Matsuno et al., 2002). The C-terminal structures of *Drosophila* Dx, MDTXs, and human DTXs are highly evolutionarily conserved according to their amino acid sequence and crystal structure alignment (Kishi et al., 2001; Takeyama et al., 2003; Chatrin et al., 2020). The high sequence conservation across species suggests that DTX family proteins are likely to function in a similar manner, including binding to NAD<sup>+</sup> (Chatrin et al., 2020). The C-terminus of Dx contains a RING-H2 domain with E3 ligase activity (Takeyama et al., 2003). In the integral steps of Dx regulated signaling pathway, the formation of homo-multimeric Dx is mediated by the RING-H2 domain (Matsuno et al., 2002). The RING-H2 domain of the DTX family adopts a novel circular fold with eight conserved cysteine and histidine residues, which is different from other RINGs (Miyamoto et al., 2019), whereas DTX3 and DTX3L contain a RING-HC structure with a single histidine (Takeyama et al., 2003). The Deltex C-terminal (DTC) domain, a relatively conserved novel fold and a close neighbor to the RING domain, has been reported in DTX family (Obiero et al., 2012). The functions of the DTC domain are poorly understood. The domain structures and sequence alignments of Dx and DTX family proteins are illustrated in **Figure 1**.

## FUNCTIONS AND ASSOCIATED MOLECULAR MECHANISMS OF THE DTX FAMILY

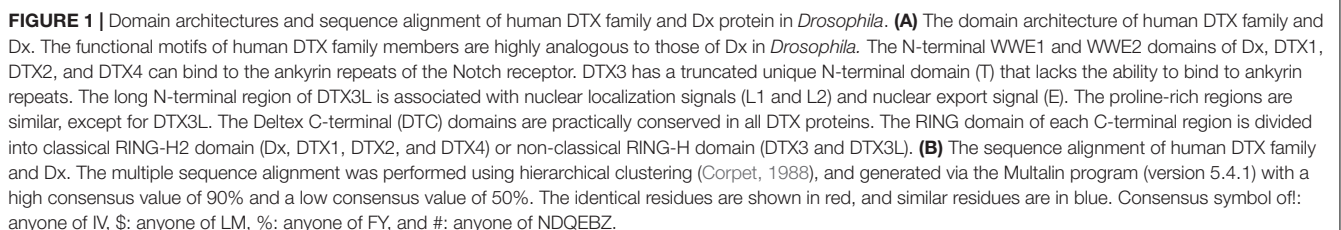
### Dx

The domain features of Dx influence its association with the Notch signaling pathway, one of the pivotal regulators of cell fate (Liang et al., 2019). The direct interactions between the cytoplasmic protein Dx and transmembrane receptor Notch have been previously demonstrated (Diederich et al., 1994). Upon Notch receptor activation, the intracellular domain of Notch receptors (NICD) is released, which translocates into the nucleus where it triggers the expression of the downstream genes (Kovall et al., 2017; Bray and Gomez-Lamarca, 2018).

Dx interacts with the Notch receptor via the non-canonical signaling pathway in *Drosophila* (Hori et al., 2012). The established molecular mechanisms of Dx protein are illustrated in **Figure 2**. Dx overexpression induces morphological and phenotypic changes in *Drosophila*'s eyes, wings, and bristles, consistent with phenotypic changes induced by activation of NICD. Moreover, phenotypic changes caused by Dx inhibition could be partially rescued by an extra copy of Notch (Gorman and Girton, 1992). The classical Notch signaling pathway is activated prior to the Notch receptor entry into the multivesicular body, whereas Dx-mediated Notch signaling transduction is activated in a different manner (Yamada et al., 2011). It is established that endogenous Dx is necessary to: (1) assist Notch transport more efficiently from the plasma membrane into the endocytic vesicles, and (2) retain Notch on the surface of the late endosome, which prevents Notch trafficking to lysosomes for degradation (Yamada et al., 2011). Dx promotes the endocytosis and intracellular transport of Notch based on the activities of homotypic fusion and vacuole protein sorting (HOPS) and adaptor protein-3 (AP-3) complexes, which are regulated by Rab5 and Rab7 GTPases (Wilkin et al., 2008). Moreover, some evolutionarily conserved key transmembrane proteins, such as Crumbs, rely on Dx to modify the localization and trafficking of the Notch receptor (Nemetschke and Knust, 2016). In stellate cells, an expressional decrease or functional inhibition of Rab11 can lead to the accumulation of Notch receptors in early and late endosomes, thus activating Dx mediated non-canonical Notch signaling pathway (Choubey et al., 2020). During regulation of the endocytic trafficking of Notch, domains I and III of Dx are essential for stabilizing Notch in the late endosome (Hori et al., 2005).

Deltex has been shown to positively regulate the Notch signaling pathway (Xu and Artavanis-Tsakonas, 1990; Gorman and Girton, 1992). The interaction between Dx and Notch ankyrin repeats also interferes with the retention of the Suppressor of Hairless [Su(H)] in the cytoplasm and facilitates its translocation into the nucleus (Matsuno et al., 1995). In addition, Dx can solely promote monoubiquitination of the Notch receptor and triggers intracellular activation of Notch independent of canonical ligands (Hori et al., 2011). Neural precursor cell expressed developmentally down-regulated 4 (Nedd4), which contains a calcium/lipid-binding domain (C2 domain), two conserved tryptophan residues (WW domains), and a HECT domain, belongs to a family of HECT E3s (Kumar et al., 1992; Bork and Sudol, 1994; Boase and Kumar, 2015). The C2 domain in Nedd4 family is involved in protein-protein interactions and relocates target proteins to phospholipid membranes (Morrione et al., 1999; Plant et al., 2000; Dunn et al., 2004). The WW domains interact with phospho-serine/threonine residues of substrates (Sudol et al., 1995), while the HECT domain attaches activated Ub via an intermediate thioester bond, and catalyzes the attachment of Ub and a lysine on the substrate protein (Rotin and Kumar, 2009). Nedd4 suppresses the internalization and activation of Notch receptor by directly antagonizing Dx, further suggesting Dx as a positive modulator of the Notch signaling pathway (Sakata et al., 2004).





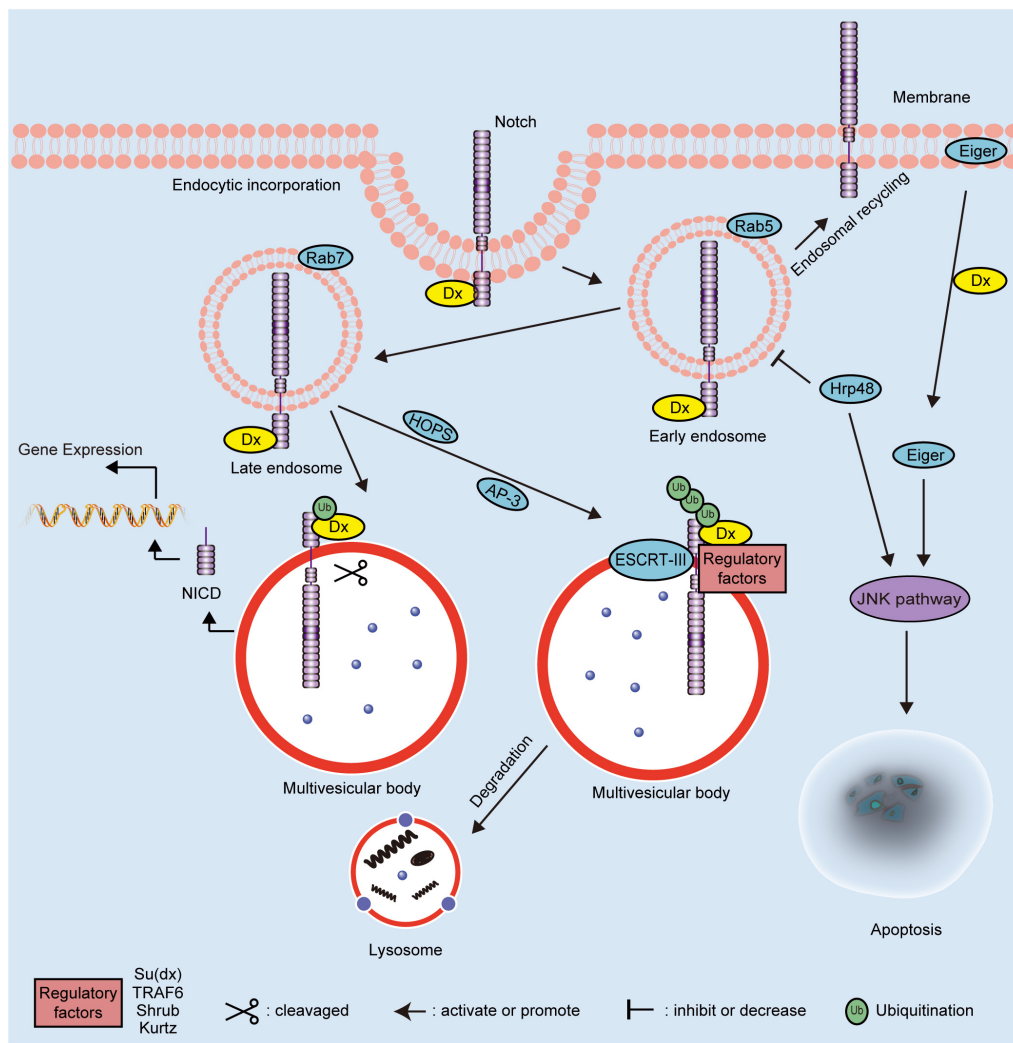


**FIGURE 2 |** Schematic diagram showing the molecular mechanisms of Dx in *Drosophila*. The regulation mechanisms of Dx on the Notch signaling pathway depend on the ubiquitination pattern of the Notch receptor. Dx activates the endocytosis of Notch independent on the canonical ligands. The endosomal maturation is initiated by the HOPS complex and converted from Rab5 to Rab7. Interaction with the AP-3 complex promotes Notch targeting to the late-endosomal and lysosomal vesicle membranes. Dx functions as a positive modulator of the Notch signaling pathway when the Notch receptor is monoubiquitinated. The extracellular domain of monoubiquitinated Notch is removed and degraded following cleavage. Then, the NICD of Notch is released to activate the downstream gene expression. However, Dx acts as a negative regulator of the Notch signaling pathway when Notch is polyubiquitinated by Dx and regulatory factors, including Su(dx), TRAF6, Shrub, and Kurtz. The polyubiquitinated Notch is transferred into multivesicular body via ESCRT-III and degraded via the endosome/lysosome pathway. Dx also influences the JNK signaling pathway to induce apoptosis via interacting with Hrp48 or Eiger. NICD, intracellular domain; Dx, Deltex; TRAF6, tumor necrosis factor receptor associated factor 6; AP-3, adaptor protein-3; HOPS, homotypic fusion and vacuole protein sorting; ESCRT-III, endosomal sorting complex required for transport-III; Hrp48, heterogeneous nuclear ribonucleoprotein 48; JNK, Jun N-terminal Kinase; Su(dx), Suppressor of Deltex; Ub, ubiquitin.

Interestingly, when interacting with additional proteins, such as Suppressor of deltex [Su(dx)] and Kurtz, Dx plays a negative regulatory role in the Notch signaling pathway. Su(dx), which belongs to the Nedd4 family E3, is a negative regulator of Notch (Mazaleyrat et al., 2003). Under normal circumstances, the WW domains and a linker region act synergistically to maintain Su(dx) in an autoinhibitory inactive state. Upon activation, Su(dx) induces the ubiquitination and degradation of Notch, while co-expression of Su(dx) and Dx blocks the activation of Notch signaling induced by Dx alone (Wilkin et al., 2008; Yao et al., 2018). Kurtz is the only homolog of non-visual beta-arrestin in

*Drosophila* (Roman et al., 2000). Based on the results of yeast two-hybrid analysis, a region between amino acids 10 and 251 in Kurtz interacts with Dx, which leads to the polyubiquitination and degradation of Notch, thereby negatively regulating the Notch signaling pathway (Mukherjee et al., 2005). With the assistance of the core element, Shrub, of the endosomal sorting complex required for transport-III (ESCRT-III), the poly-ubiquitination of Notch is increased. Shrub and Dx shift the delivery of Notch receptor to multivesicular bodies, ultimately promoting the endosomal/lysosomal degradation of Notch (Hori et al., 2011). In addition, the proteins encoded by the *maheshvara*

and *TNF receptor-associated factor 6* (TRAF6) are co-expressed with Dx to inhibit the Notch signaling pathway (Mishra et al., 2014; Surabhi et al., 2015). Therefore, the ubiquitination status (mono- or poly-ubiquitination) of Notch, mediated by Dx alone or in combination with any other possible interacting proteins, is correlated with the mechanisms underlying the effects of Dx on the downstream regulation pattern of Notch signaling pathway positively or negatively.

During homeostasis, cells integrate the activities of multiple pathways and turn on the interaction crosstalk, such as that between the Notch and c-Jun N-terminal kinase (JNK) signaling pathways (Ammeux et al., 2016). The synergistic interaction of heterogeneous nuclear ribonucleoprotein 48 (Hrp48) and Dx negatively regulates the Notch signaling pathway by inhibiting the transport of Notch from the cell membrane to the cytoplasm (Dutta et al., 2017). Additionally, The combinatorial expression of Hrp48 and Dx induces apoptotic cell death via the activation of the JNK signaling pathway (Dutta et al., 2019); similarly, Eda-like cell death trigger (Eiger) induces apoptosis by triggering JNK signal pathway (Igaki and Miura, 2014). Dx triggers the transport of Eiger from the cell membrane to cytoplasm and modulates its activity to induce the JNK signal pathway (Dutta et al., 2018). The cooperation of Dx and TRAF6 also mediates the Eiger-independent JNK activation, which is also regulated by the endocytic pathway component Rab7 (Sharma et al., 2021). Taken together, Dx has been shown to play a significant role in morphology and development of *Drosophila*, mainly by regulating JNK and non-canonical Notch signaling pathways. The understanding of the functions and molecular mechanisms of Dx in *Drosophila* establishes a quantitative framework for deeper research into mammalian DTX family proteins.

## MDTX Family of Proteins

Since conducting medical research on humans is restricted due to ethical issues and various other limiting factors, the laboratory mouse, *Mus musculus*, is one of the most commonly used mammals for studying human disease (Lloyd et al., 2016; Gurumurthy and Lloyd, 2019). The high genetic and physiological conservation are key advantages for mice as a suitable research animal model (Justice and Dhillon, 2016). The MDTX family of proteins have a high degree of similarity with Dx and their human homologs. In adult mice, the expression of MDTX1, MDTX3, and MDTX4 are prominently observed in the brain and testis, while MDTX2 is strongly expressed in the testis (Kishi et al., 2001; Storck et al., 2005). MDTX proteins inhibit the activity of a mammalian transcription factor E47 alone, rather than the E47-VP16 complex. In addition, overexpression of MDTX2 suppresses the expression of myogenic transcriptional factor *myogenin* and the frequency of muscle cell differentiation (Kishi et al., 2001). MDTX proteins can negatively regulate the Notch signaling pathway of T cells (Lehar and Bevan, 2006).

In the sections that follow, the functions and associated molecular mechanisms of human DTX family proteins are summarized and reviewed. The related signaling pathways and interactions of DTX family proteins in cell development and in carcinomas are shown in **Figures 3, 4**, respectively. An overview of DTX family proteins during the developmental process of

different cell types is listed in **Table 1**, while **Table 2** summarizes the altered levels, functions, and mechanisms of DTX family proteins in different cancer types.

## DTX1

The human *DTX1* is located on chromosome 12 (12q24.13) and its 67.4 kDa coded protein contains 620 amino acids. DTX1 is 26% identical and 40% similar to Dx based on Needleman-Wunsch alignment of two protein sequences (Altschul et al., 1997). As for cellular location, it is located both in the cytoplasm and in the nucleus (Ordentlich et al., 1998; Yamamoto et al., 2001). The functions of DTX1 are determined by numerous factors. For example, during early development of thymocytes, a positive feedback loop has been reported between DTX1 upregulation and the activation of Notch signaling (Deftos et al., 1998). Meanwhile, a negative feedback between DTX1 and Notch is regulated by *HES1*, a downstream target gene of Notch, which directly binds to the promoter of *DTX1* and inhibits its transcription (Zhang et al., 2010). Atrophin-1-interacting protein 4 (AIP4) is another inhibitor of DTX1, which interacts with the proline-rich motif of DTX1 and mediates its degradation, primarily via K29-linked polyubiquitination and the lysosomal pathway (Chastagner et al., 2006). DTX1 was thought to directly bind to Notch and regulate its ubiquitination status, however, more recently, the regulation was found to be indirect (Zheng and Conner, 2018). The lipid kinase phosphatidylinositol-5-phosphate 4-kinase  $\gamma$  (PI5P4K $\gamma$ ), as a substrate of DTX1, promotes Notch receptor internalization and localization in the tubulovesicular compartment via a Rab4a-dependent pathway, thus, preventing Notch receptor's endosomal recycling back to the membrane and negatively regulating the Notch signaling pathway (Zheng and Conner, 2018).

DTX1 plays an essential role in cell differentiation. During avian development, DTX1 regulates the formation of the cranial neural crest via the Notch1 pathway (Endo et al., 2003). F3/contactin and its homolog NB-3 interact with Notch, thereby releasing the NICD via the non-canonical Notch pathway, and form a complex with DTX1 to mediate myelin-related protein expression in the nucleus (Hu et al., 2003; Cui et al., 2004). The neuron-specific transmembrane protein Delta/Notch-like epidermal growth factor-related receptor (DNER) mediates the interaction between neurons and glial cells via the DTX1 dependent Notch signaling pathway and promotes the morphological differentiation of Bergmann glial cells (Eiraku et al., 2005). DTX1, expressed in the nucleus of neural progenitor cells, directly interacts with the transcription activator p300, forming a complex that inhibits the transcriptional activity of *mammalian achaete-scute homolog 1* (*MASH1*), thereby restricting cell differentiation (Yamamoto et al., 2001). During differentiation of smooth muscle cells, DTX1 inhibits the proliferation of bone marrow mesenchymal stem cells and promotes their differentiation into smooth muscle cells by overexpressing smooth muscle myosin heavy chains (MyHCs) (Wang et al., 2018). DTX1 also effectively inhibits the formation of granulation tissue in the tunica albuginea, which is a treatment strategy used against closed penile fracture (Guo et al., 2018). During the development of lymphocytes, DTX1 induces



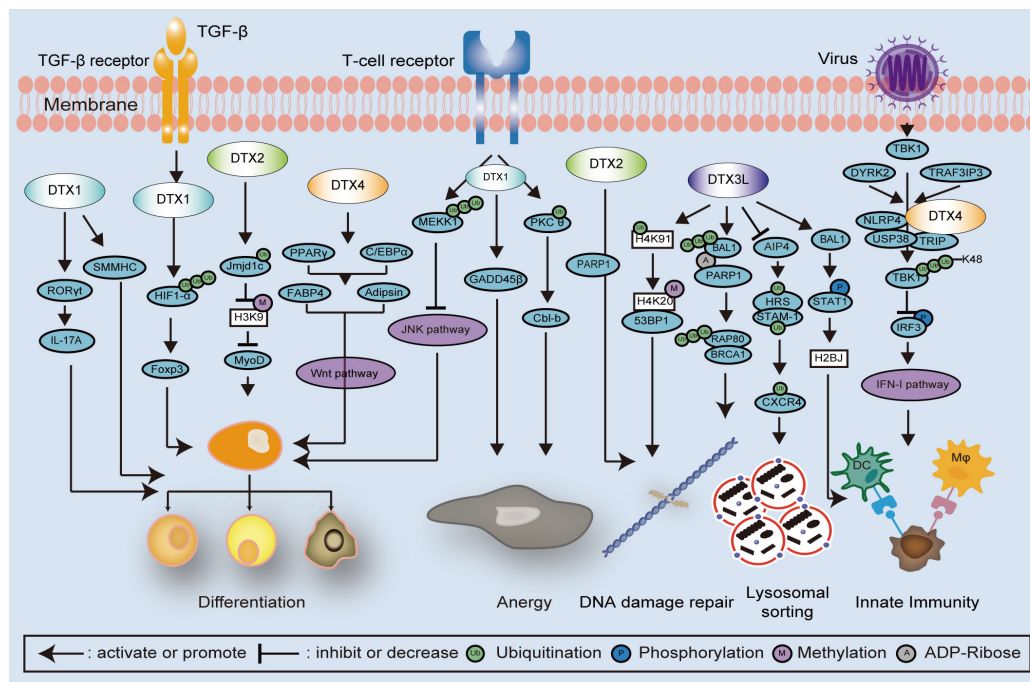


**FIGURE 3 |** Schematic diagram showing DTX family related signaling pathways and interactions in cell development. DTX family proteins regulate cell differentiation via several mechanisms and signaling pathways, such as poly-ubiquitination of HIF1- $\alpha$  and MEKK1, monoubiquitination of Jmjd1c, methylation of histones, and JNK and Wnt signaling pathways. In the regulation of cell anergy, the T cell receptor is activated and monoubiquitination of PKC $\theta$  is induced by DTX1, following the alteration of GADD45 $\beta$  and Cbl-b expression. In the regulation of DNA damage repair, DTX3L promotes the polyubiquitination of the RAP80-BRCA1 complex, monoubiquitination of histones, and STAT1 phosphorylation. The combination of DTX2 and PARP1 is also involved with the regulation of DNA damage repair. Upon viral infection, TBK1 is phosphorylated thereby activating the IFN-I pathway. The DTX4, NLRP4, USP38, and TRIP complex inhibits the IFN-I pathway via enhancing polyubiquitination of TBK1, which is also associated with DYRK2 and TRAF3IP3. STAT1, signal transducer and activator of transcription 1; PARP1, Poly (ADP-Ribose) Polymerase 1; HIF1- $\alpha$ , hypoxia inducible factor 1 subunit alpha; MEKK1, mitogen activated protein kinase/ERK kinase 1; Jmjd1c, Jumonji domain containing 1c; JNK, Jun N-terminal Kinase; PKC $\theta$ , protein kinase C $\theta$ ; GADD45 $\beta$ , growth arrest and DNA damage inducible 45 beta; Cbl-b, Casitas B-lineage lymphoma-b; RAP80, receptor associated protein 80; BRCA1, Breast Cancer 1; TBK1, TANK binding kinase 1; NLRP4, nod-like receptor (NLR) family pyrin domain containing 4; USP38, Ub-specific protease 38; TRIP, TRAF-interacting protein; IFN-I, interferon type I; DYRK2, dual-specificity tyrosine-(Y)-phosphorylation-regulated kinase 2; TRAF3IP3, TNF receptor associated factor 3 interacting protein 3.

lymphoid progenitor cells to differentiate into B cells, and is consistently involved in the differentiation of germinal-center B cells (Izon et al., 2002; Gupta-Rossi et al., 2003). During differentiation of marginal-zone B cells, DTX1 is overexpressed and restrains Notch2 expression (Saito et al., 2003). In addition, DTX1 inhibits the differentiation of hematopoietic stem cells into T cells (Yun and Bevan, 2003). T-lineage cells differentiate from multipotent progenitors, which exhibit different CD4 and CD8 phenotypes (Wu, 2006). During the early stages of T-cell development, the transcriptional level of *DTX1* is increased by the transcription factor GATA-binding factor 3 (GATA3); *DTX1* interferes with T-cell differentiation by regulating the Notch signaling pathway (Wang et al., 2009). The HeLa E box-binding (HEB) protein is often heterodimeric with E2A in thymocytes (Sawada and Littman, 1993). During maturation of CD4 and CD8 double-positive T cells, DTX1 competes with p300 for binding to the E2A/HEB protein complex, thereby enhancing the resistance of cells to glucocorticoid (GC)-induced apoptosis (Jang et al., 2006). DTX1 specifically promotes the degradation of the mitogen-activated protein kinase (MAPK)/ERK kinase 1 (MEKK1) via ubiquitination to inhibit T-cell activation

(Liu and Lai, 2005). In addition to regulating the maturation of T cells, DTX1 also plays vital roles in the T-cell anergy process. DTX1 promotes the degradation of hypoxia-inducible factor-1 $\alpha$  (HIF-1 $\alpha$ ) to maintain the expression of the transcription factor Forkhead box protein P3 (Foxp3), which is essential for sustaining the effector activities of regulatory T cells (Hsiao et al., 2015). Retinoic acid-related orphan receptor  $\gamma$  t (ROR $\gamma$ t) is a transcription factor that is necessary for the differentiation of Th17 cells, CD4<sup>+</sup> T helper lymphocytes that secrete interleukin (IL)-17A and IL-17F (Lee et al., 2020). When CD4<sup>+</sup> T cells are stimulated by IL-6 and transforming growth factor- $\beta$  (TGF- $\beta$ ), DTX1 promotes their differentiation into Th17 cells by enhancing the DNA-binding ability of ROR $\gamma$ t in the nucleus and the production of the corresponding cytokines (Tang et al., 2020). The Casitas B-lineage lymphoma (Cbl) family is a RING type of E3 ligases, which acts as a negative regulator of immune activation (Liu and Gu, 2002). The mammalian Cbl family contains three homologs, namely c-Cbl, Cbl-b, and Cbl-c (Jafari et al., 2021). During the T-cell anergy process, DTX1 acts as a Notch-independent regulator, which induces the degradation of protein kinase C- $\theta$  (PKC- $\theta$ ) by promoting



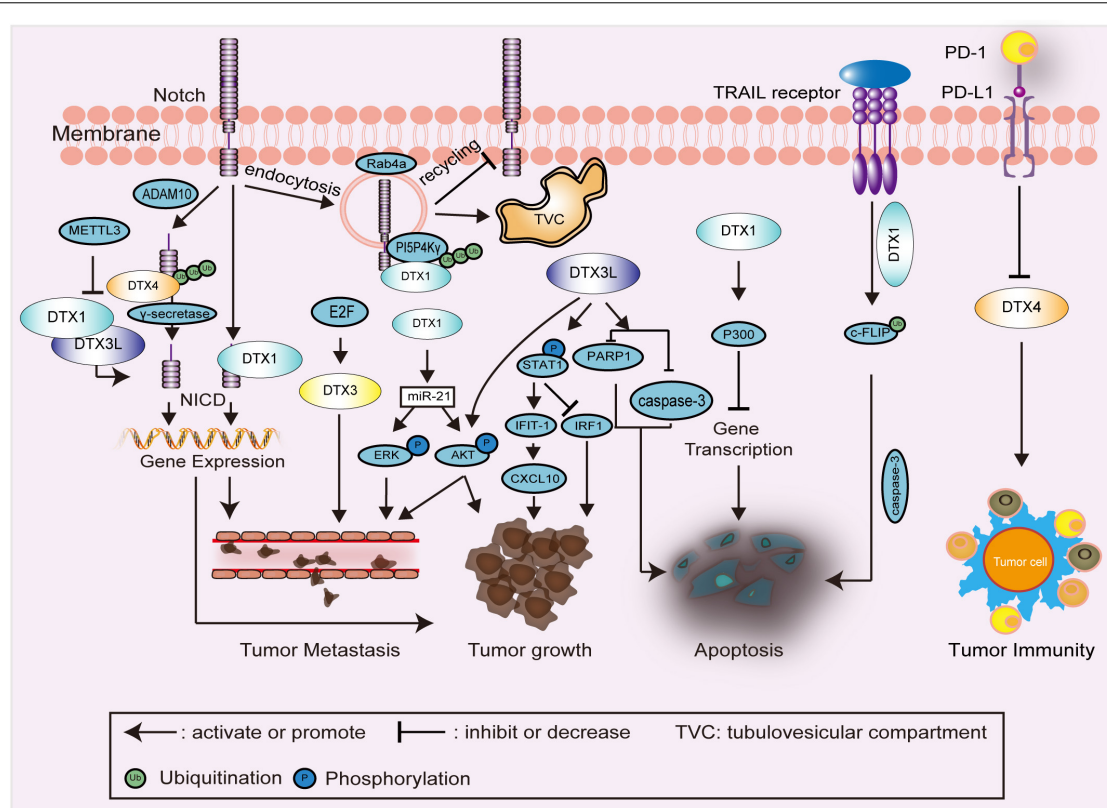


**FIGURE 4 |** Schematic diagram showing DTX family related signaling pathways and interactions in carcinomas. In the regulation of Notch endocytosis, ubiquitination of PI5P4Ky, as a substrate of DTX1, promotes the endocytosis and maintaining of TVC, thereby restraining the recycling of Notch to the cell membrane. DTX family proteins, such as DTX1, DTX3L, and DTX4, are primarily involved in the regulation of the Notch signaling pathway and expression of downstream genes to affect tumor growth, and metastasis. In the regulation of tumor growth and metastasis, DTX1 and DTX3L also enhance the phosphorylation of downstream proteins, such as STAT1, AKT, and ERK. In the regulation of apoptosis, ubiquitination of c-FLIP by DTX1 stimulates TRAIL-induced cell death. The combination of P300 and DTX1 inhibits the expression of multiple genes, which is also associated with apoptosis. The expression of caspase-3 and PARP1 is decreased by DTX3L to inhibit apoptosis. In the regulation of tumor immunity, the expression of DTX4 is negatively regulated by PD-L1. NICD, intracellular domain of Notch receptor; PI5P4Ky, phosphatidylinositol-5-phosphate 4-kinase  $\gamma$ ; TVC, tubulovesicular compartment; STAT1, signal transducer and activator of transcription 1; c-FLIP, cellular FADD-like interleukin-1 $\beta$  converting enzyme inhibitory protein; TRAIL, TNF-related apoptosis-inducing ligand; PARP1, poly (ADP-Ribose) polymerase 1; PD-L1, programmed death ligand 1; METTL3, methyltransferase-like 3; ADAM10, a disintegrin and metalloproteinase 10; IFIT-1, interferon (IFN)-induced protein with tetratricopeptide repeats 1; IRF-1, IFN regulatory factor-1; CXCL10, Chemokine (C-X-C motif) ligand (CXCL)10.

its mono-ubiquitination and the endosome/lysosome pathway. Thus, the protein stability of Cbl-b increases to attenuate T-cell activation and promote anergy (Hsu et al., 2014). Upon induction by nuclear factor of activated T cells (NFAT), DTX1 regulates the expression of other anergy-associated molecules such as growth arrest and DNA-damage-inducible 45 beta (GADD45 $\beta$ ) during the T-cell anergy process (Hsiao et al., 2009).

DTX1 also plays a pivotal role in tumorigenesis, invasion, and metastasis of several cancers. Overexpression of DTX1 increases the clonal ability, growth potential, and invasiveness of glioblastoma cells. Patients with low expression of DTX1 have a longer survival and a better prognosis of glioblastoma. DTX1 triggers a specific transcription process, including microRNA-21 and antiapoptotic *Mcl-1*, which are involved in the activation of the AKT and ERK pathways (Huber et al., 2013). In addition, induction of DNER by the histone deacetylase inhibitor trichostatin A (TSA) has been shown to reduce the tumorigenicity and cell differentiation of glioblastoma-derived

neurosphere lines via the DTX1-mediated non-canonical Notch signaling pathway (Sun et al., 2009). Furthermore, DTX1 plays a tumor-suppressive role and is negatively associated with gastric cancer progression. In gastric cancer cells, DTX1 primarily promotes the degradation of cellular FADD-like IL-1 $\beta$ -converting enzyme-inhibitory protein (c-FLIP) in the lysosomal pathway and enhances TNF-related apoptosis-inducing ligand (TRAIL)-induced cell death (Hsu et al., 2018). Missense or nonsilent *DTX1* mutations have been reported in splenic marginal zone lymphomas and in Chinese patients with primary and recurrent diffuse large B-cell lymphomas (DLBCLs) (Rossi et al., 2012; de Miranda et al., 2014; Green et al., 2015). Almost all these mutations occur in the WWE domains of *DTX1* and impair its function as a negative Notch regulator, thereby promoting the development of DLBCLs (Meriranta et al., 2017). Mutations in the promoter region of *DTX1* were detected during early non-small-cell lung cancer (NSCLC); both overall survival (OS) and disease-free survival (DFS) rates were higher in patients

**TABLE 1** | Overview of studies with described functions and mechanisms of DTX family members during the development of different cell types.

Year	DTXs	Cell type	Results and findings
2002	DTX1	B cells	DTX1 antagonizes Notch1 signal pathway to induce the differentiation of lymphoid progenitor cells to B cells (Izon et al., 2002)
2003	DTX1	B cells	DTX1 is likely involved in the germinal center B cell differentiation (Gupta-Rossi et al., 2003)
2003	DTX1	B cells	DTX1 restrains Notch2 expression in the differentiation of marginal zone B cells (Saito et al., 2003)
1998	DTX1	T cells	Relative higher DTX1 expression and activated Notch signal pathway are detected in double negative and CD4 <sup>+</sup> and CD8 <sup>+</sup> single positive thymocytes, while both lower DTX1 expression and inactivated Notch signal pathway are detected in double positive thymocytes (Deftos et al., 1998)
2003	DTX1	T cells	DTX1 blocks hematopoietic stem cells to T lineage commitment, but not involved in early thymocyte development (Yun and Bevan, 2003)
2005	DTX1	T cells	DTX1 ubiquitinated MEKK1 and promotes its degradation to suppress the activation of T cells (Liu and Lai, 2005)
2006	DTX1	T cells	DTX1 competed with the binding of p300 to E2A/HEB protein, increasing survival of double positive thymocytes from the glucocorticoid-induced apoptosis (Jang et al., 2006)
2009	DTX1	T cells	DTX1 regulates the expression of anergy associated molecules, suppresses T cell activation, and participates in calcium-NFAT signal pathway to enhance T cell anergy (Hsiao et al., 2009)
2009	DTX1 DTX4	T cells	The combination of <i>DTX1</i> and <i>DTX4</i> , regulated by GATA3 in transcriptional level, interferes with Notch signal pathway during the early stage of T cell development (Wang et al., 2009)
2014	DTX1	T cells	DTX1 attenuates T cell activation and promotes the generation of T cell anergy by mono-ubiquitinating protein kinase C- $\theta$ , redirecting the localization of protein kinase C- $\theta$ and stabilizing Cbl-b (Hsu et al., 2014)
2015	DTX1	T cells	DTX1 degrades HIF-1 $\alpha$ and enhances Foxp3 expression to maintain the stability of regulatory T cells (Hsiao et al., 2015)
2018	DTX4	T cells	The gene expression of <i>DTX4</i> is regulated by hsa_circ_0045272 to regulate apoptosis and interleukin-2 secretion of T cells in patients with systemic lupus erythematosus (Li et al., 2018)
2020	DTX1	T cells	DTX1 promoted the differentiation of CD4 <sup>+</sup> T cells into T helper 17 cells by enhancing the DNA binding ability of ROR $\gamma$ t (Tang et al., 2020)
2020	DTX3L	Mononuclear cells	DTX3L advances phosphorylation of STAT1 and increases expression of CXCL10 to promote the infiltration of mononuclear cells (Tian et al., 2020)
2020	DTX4	Myeloid cells	DTX4 is regulated by TRAF3IP3 to decrease virus-triggered IFN-I production in myeloid cells (Deng et al., 2020)
2001	DTX1	Neural progenitor cells	DTX1 binds with transcription activator p300 and inhibits the activity of <i>MASH1</i> to restrain the differentiation of neural progenitor cells (Yamamoto et al., 2001)
2003	DTX1	Oligodendrocyte	F3/contactin initiates DTX1 dependent Notch signaling pathway to promote oligodendrocyte maturation and myelination (Hu et al., 2003)
2004	DTX1	Oligodendrocyte	NB-3, a member of the F3/contactin family, triggers Notch signal pathway via DTX1 to promote oligodendrocyte generation (Cui et al., 2004)
2005	DTX1	Bergmann glia	DNER mediated DTX1 dependent Notch signal to stimulate the morphological differentiation of Bergmann glial cells (Eiraku et al., 2005)
2018	DTX1	Muscle cells	DTX1 promotes the differentiation of smooth muscle cells by overexpressing the smooth muscle myosin heavy chain (MyHC) (Wang et al., 2018)
2018	DTX1	Muscle cells	DTX1 positively regulates the differentiation into smooth muscle cells to inhibit granulation tissue formation effectively for the treatment of closed penile fracture (Guo et al., 2018)
2017	DTX2	Muscle cells	DTX2 inhibits myogenic differentiation by suppressing the methylation of histone 3 of myogenic regulatory factor <i>MyoD</i> (Luo et al., 2017)
2020	DTX3L	Fibroblast like synoviocytes	DTX3L induces fibroblast like synoviocytes to produce inflammatory cytokines through STAT1 signal pathway (Hong et al., 2020)
2020	DTX1 DTX3L	Endothelial cells	The heterodimerization of DTX3L and DTX1 inhibits Notch signal pathway and ultimately restrains the angiogenesis of endothelial cells (Wang et al., 2020a)
2017	DTX4	Renal cells	The mRNA expression change of <i>DTX4</i> is regulated by microRNA let-7a and involved in the fibrotic processes of instructive nephropathy (Papadopoulos et al., 2017)
2017	DTX4	Preadipocytes	DTX4 upregulates the number of lipid granules, the expression of fat forming transcription factors, and adipogenic marker genes to increase differentiation of preadipocytes (Wang et al., 2017)
2017	DTX4	Hepatic cells	The DNA promoter methylation decrease of <i>DTX4</i> activates the differentiation of hepatic stellate cells (Schumacher et al., 2017)
2018	DTX4	Hepatic cells	DTX4 mediates IFN-I signal to influence HBV sustenance and maintenance of HBsAg in chronic hepatitis B (Kim et al., 2018)

with mutations than in those without mutations, suggesting that *DTX1* mutations were beneficial for the survival and prognosis of patients with early NSCLC (Lee et al., 2019). In contrast, patients

with small cell lung cancer (SCLC) carrying *DTX1* mutations showed a worse response to chemotherapy and a lower OS rate, suggesting that mutations in the same gene may play opposite

**TABLE 2 |** Overview of studies with described altered levels, functions, and mechanisms of DTX family members in different cancer types.

Year	DTXs	Cancer type	Expression	Results and findings
2012	DTX1	Splenic marginal zone lymphoma	Gene mutation	The mutation in WWE1 and proline-rich domains of <i>DTX1</i> occurs in splenic marginal zone lymphoma (Rossi et al., 2012)
2006	DTX3L	Diffuse large B-cell lymphoma	Up regulated	<i>DTX3L</i> is overexpressed in diffuse large B-cell lymphoma cells and shares the same bidirectional interferon-responsive promoter with <i>BAL1</i> (Juszczynski et al., 2006)
2013	DTX3L	Diffuse large B-cell lymphoma	Up regulated	<i>DTX3L</i> regulates the early Ub chain formation, RAP80 and BRCA1 recruitment to DNA damage sites in diffuse large B-cell lymphoma cells (Yan et al., 2013)
2014	DTX1	Diffuse large B-cell lymphoma	Gene mutation	<i>DTX1</i> mutations impair the inhibitory effects of Notch signal pathway in diffuse large B-cell lymphomas (de Miranda et al., 2014)
2017	DTX1	Diffuse large B-cell lymphoma	Gene mutation	<i>DTX1</i> with gene mutations plays tumor promoting roles in diffuse large B-cell lymphomas (Meriranta et al., 2017)
2017	DTX3L	Myeloma	Up regulated	<i>DTX3L</i> increases proliferation, adhesion, and chemo-resistance of myeloma cells, by blocking caspase-3 and PARP1 expression and inhibiting apoptosis (Shen et al., 2017)
2009	DTX1	Glioma	Up regulated	TSA increases the expression of DNER and <i>DTX1</i> to abrogate growth and differentiation of glioblastoma derived neurospheres (Sun et al., 2009)
2013	DTX1	Glioma	Up regulated	<i>DTX1</i> promotes the proliferation and invasiveness of glioblastoma cells and correlates with prognosis by activating the AKT and ERK pathways (Huber et al., 2013)
2017	DTX3L	Glioma	Up regulated	<i>DTX3L</i> is highly expressed in gliomas, relating to the malignant degree and the prognosis of patients (Xu et al., 2017)
2010	DTX1	Osteosarcoma	Down regulated	<i>DTX1</i> inhibits invasiveness of osteosarcoma cells and negatively regulates Notch1 signaling (Zhang et al., 2010)
2018	DTX1	Gastric cancer	Down regulated	<i>DTX1</i> decreases c-FLIP expression in lysosome dependent pathway and increases TRAIL-induced apoptosis in gastric cancer (Hsu et al., 2018)
2020	DTX3	esophageal carcinoma	Down regulated	<i>DTX3</i> ubiquitinates Notch2 to suppress the proliferation and migration of esophageal carcinoma cells (Ding et al., 2020)
2011	DTX3 DTX4	Hepatocellular carcinoma	Up regulated	The E2F family transcription factors E2F1 and E2F3 binds directly to the proximal promoter regions of <i>DTX3</i> and <i>DTX4</i> to increase the levels of transcription in hepatocellular carcinoma cells (Viatour et al., 2011)
2010	DTX4	Colorectal cancer	Down regulated	<i>DTX4</i> is altered by a 1.6-fold change following treatment with Pomalidomide in colorectal cancer cells (Liu et al., 2010).
2019	DTX1	Non-small cell lung cancer	Gene mutation	The overall survival rate and disease-free survival rate of non-small cell lung cancer patients with <i>DTX1</i> gene mutation are both higher than those without <i>DTX1</i> mutation (Lee et al., 2019)
2020	DTX1	Small cell lung cancer	Gene mutation	The lower overall survival rate and worse response to chemotherapy are appeared in small cell lung cancer patients with <i>DTX1</i> gene mutation (Yoo et al., 2020)
2014	DTX3	Luminal subtype breast cancer	Up regulated	<i>DTX3</i> is essential for cell proliferation and uniquely amplified in highly proliferative luminal breast tumors (Gatza et al., 2014)
2020	DTX3	Triple-negative breast cancer	Down regulated	<i>DTX3</i> mRNA is degraded and its inhibitory effects on Notch4 is weaken, which promotes the metastasis of triple-negative breast cancer cells (Liu et al., 2020)
2020	DTX3L	Breast cancer	Up regulated	<i>DTX3L</i> is higher in breast cancers, especially in triple-negative breast cancer. <i>DTX3L</i> functions as a negative regulator of ATRA induced growth inhibition of breast cancer cells (Bolis et al., 2020)
2014	DTX3L	Prostate cancer	Up regulated	The overexpression of <i>DTX3L</i> enhances proliferation, metastasis, and chemo-resistance of prostate cancer cells by repressing the transcription of <i>IRF-1</i> and influencing phosphorylation of STAT1 (Bachmann et al., 2014)
2015	DTX3L	Melanoma	Up regulated	<i>DTX3L</i> regulates FAK/PI3K/AKT signal pathway to strengthen the invasion and metastasis of melanoma (Thang et al., 2015)
2016	DTX4	Melanoma	Up regulated	<i>DTX4</i> is highly expressed as a Notch4 signaling pathway molecule in melanoma cancer stem like cells (Lin et al., 2016)
2016	DTX4	Nasopharyngeal carcinoma	Up regulated	The expression of <i>DTX4</i> is higher in nasopharyngeal carcinoma cells (Liu et al., 2016)
2020	DTX4	Soft tissue sarcoma	Down regulated	The expression of <i>DTX4</i> in soft tissue sarcoma is regulated by IDO1 inhibitor combined with PD-L1 blockers (Nafia et al., 2020)

roles in different subtypes of malignant tumors in the same organ. The specific mechanisms underlying these mutations remain to be determined (Yoo et al., 2020).

## DTX2

Human *DTX2*, located on chromosome 7 (7q11.23), encodes a 67.2 kDa intranuclear protein with 622 amino acids. *DTX2* is

26% identical and 38% similar to Dx following the comparison of the two protein sequences. PAR polymerase 1 (PARP1), activated by DNA damage, promotes PAR chain formation on many target proteins, including DTX2 (Jungmichel et al., 2013; Gupte et al., 2017; Ray Chaudhuri and Nussenzweig, 2017). The catalytic DTX2 is then recruited to promote ubiquitination of its targets at DNA damage sites. It was recently reported that the DTC domain of DTX2, not the WWE domains, played an essential role in binding PARylated substrate proteins and facilitated ubiquitination of substrate proteins by the RING domain (Ahmed et al., 2020). As the sequences of DTC domains are very similar in DTX family of proteins, almost all members, theoretically, can attach to PARylated proteins. Data from proteomics show that each DTX family protein has a specific protein interaction network (Ahmed et al., 2020). The results also suggest that 2,087 peptides, corresponding to 1,035 proteins, could be ubiquitinated by DTX2. In addition, only DTX2 showed a strong correlation with 71 DNA damage repair proteins. This diversity is partly attributed to the different cellular localization of DTX family proteins (Ahmed et al., 2020). The effects of DTX2 on cell differentiation have been demonstrated. Upon *DTX2* knock-out, skeletal muscle stem cells undergo early myogenic differentiation and accelerated regeneration in response to injury. In this process, DTX2 changes the methylation status of H3K9 in the distal regulatory region of the *MyoD* promoter and directly inhibits demethylase activity of Jumonji domain-containing 1C (JMJD1C) by monoubiquitination to reduce *MyoD* expression (Luo et al., 2017).

## DTX3

Human *DTX3* is located on chromosome 12 (12q13.3). The 38.0 kDa *DTX3* protein has 347 amino acids and is primarily expressed in the nucleus. *DTX3* is only 16% identical and 24% similar to Dx. The roles of *DTX3* in tumor development have been extensively investigated. For example, a knockout of three retinoblastoma family genes in the liver of adult mice induced the development of liver tumors, similar to human hepatocellular carcinoma. In this model, the overexpression of *DTX3* was activated by the E2F family transcription factors E2F1 and E2F3 (Viatour et al., 2011). In ductal breast cancer, the amplification of *DTX3* is correlated with high proliferation of tumor cells and a poor prognosis (Gatza et al., 2014). Meanwhile, the expression of *DTX3* in esophageal cancer tissue and cell lines is abnormally downregulated. *DTX3* inhibits the proliferation and tumorigenicity of esophageal cancer cells and promotes the ubiquitination and degradation of Notch2 (Ding et al., 2020). Furthermore, *DTX3* acts as a tumor suppressor gene in triple-negative breast cancer and is expressed at a low level, which hinders its ubiquitination and degradation ability toward Notch4 and its ability to effectively inhibit triple-negative breast cancer metastasis (Liu et al., 2020).

## DTX3L

Human *DTX3L*, also known as B-lymphoma and B-aggressive lymphoma (BAL)-associated protein (BBAP), is located on chromosome 3 (3q21.1). The 83.6 kDa *DTX3L* protein has 740 amino acids. Protein sequence comparison results showed that

*DTX3L* is 21% identical and 36% similar to Dx. *MDTX3L* is highly expressed in multiple organs and tissues, such as the thymus, hypothalamus, anterior pituitary gland, olfactory bulb, nose, mouth, urogenital sinus, and rectum (Hakme et al., 2008). *DTX3L* was originally identified as a binding partner of BAL1 (PARP9/ARTD9), which is an oncogenic factor in DLBCL with a prominent immune/inflammatory infiltrate (Juszczynski et al., 2006). Both *DTX3L* and *BAL1* are located on chromosome 3q21 in a head-to-head orientation and share the same bidirectional interferon (IFN)-responsive promoter (Juszczynski et al., 2006). The PARylation of protein is abundant at DNA lesion sites and critical for participating in the DNA damage repair pathways (Wei and Yu, 2016; Liu et al., 2017). PARP9 alone, without enzymatic activity, is unable to enzymatically active the PARylation of target proteins (Vyas et al., 2014). The presence of the *DTX3L*/PARP9 heterodimer, shuttling between the nucleus and cytoplasm and targeting proteins within the nucleosome, brings about the possibility that their functions are coupled in some way (Juszczynski et al., 2006). The heterodimer of *DTX3L*/PARP9 displays the PARylation activity, which requires E1, E2, and ATP, by cleaving NAD<sup>+</sup> and generating ADPr. Ub is observed to be mono-ADP-ribosylated with the ADPr, which produced from *DTX3L*/PARP9 reaction. The ADP-ribosylated modification of Ub occurs on C-terminal Gly<sup>76</sup>, which is an important residue for the formation of polyUb chain. As a result, ADP-ribosylation of Ub strongly reduce polyUb formation while has no obvious effect on monoubiquitination of target proteins (Yang et al., 2017). Recently, it is unexpectedly found that the ADP-ribosylation of Ub happens independent of PARP9. *DTX3L* alone can transfer ADPr directly to Ub. The DTC and RING domains, when together, are the minimum fragments required of the DTX family proteins for catalyzing ADP-ribosylation of Ub. In ADP-ribosylation of Ub, the DTC domain accommodates NAD<sup>+</sup> while the RING domain is responsible for recruiting E2~Ub; conformational arrangement of these two domains is essential (Chatrin et al., 2020). *DTX3L* catalyzes the monoubiquitination of histone H4K91 and promotes the binding of methylated histone H4K20 to 53BP1 during DNA damage response (Yan et al., 2009). Breast Cancer 1 (BRCA1) protein is a RING type of E3 ligase, consisting of C-terminal BRCT motifs and a N-terminal RING domain, and plays a key role during checkpoint modulation and DNA damage repair (Scully and Livingston, 2000; Xu et al., 2001; Yarden et al., 2002; Zhang et al., 2004; Zhuang et al., 2006). BRCA1 interacts with different adaptor proteins, including receptor-associated protein 80 (RAP80), and forms complexes with distinct functions for DNA repair (Kim et al., 2007; Sobhian et al., 2007; Yan et al., 2007). The early Ub chain formation and the recruitment of RAP80 and BRCA1 to DNA damage sites are dependent on the colocalization of PARP1, BAL1, and *DTX3L* (Yan et al., 2013). In addition, *DTX3L* directly interacts with AIP4 and limits the ubiquitination of ESCRT-0 subunits, hepatocyte growth factor receptor tyrosine kinase substrate (HRS), and signal transducing adaptor molecule (STAM), which regulate the maintenance of ESCRT-0 on early endosomes to sort ubiquitinated chemokine (C-X-C motif) receptor 4 (CXCR4) for lysosomal degradation (Holleman and Marchese, 2014).



Several studies have shown that the expression of DTX3L is associated with inflammatory diseases. For instance, during viral infection, the PARP9/DTX3L complex targets histone H2B $\gamma$  by interacting with signal transducer and activator of transcription 1 (STAT1) (Zhang et al., 2015). Meanwhile, in rheumatoid arthritis, DTX3L induces fibroblast-like synoviocytes (FLS) to produce inflammatory cytokines via the STAT1 signal transduction pathway (Hong et al., 2020). A low level of RNA N<sup>6</sup>-methyladenosine methyltransferase methyltransferase-like 3 (METTL3) has been reported in tissues of cerebral arteriovenous malformations. METTL3 modulates the mRNA stability of DTX3L and inhibits the heterodimerization of DTX3L and DTX1. It consequently promotes the downstream gene expression of the Notch signaling pathway and ultimately accelerates the angiogenesis of endothelial cells (Wang et al., 2020a). In primary Sjogren's syndrome, the DTX3L/BAL1 complex enhances the phosphorylation of STAT1 to upregulate IFN-induced protein with tetratricopeptide repeats 1 (IFIT-1) and increases the expression of chemokine (C-X-C motif) ligand 10 (CXCL10), thereby promoting the infiltration of mononuclear cells (Tian et al., 2020).

The overexpression of DTX3L in multiple carcinomas has been previously investigated. In lymphoma, the high expression level of DTX3L contributes to the resistance to DNA-damaging chemotherapeutic agents (Yan et al., 2013). The overexpression of DTX3L and BAL1 promotes the phosphorylation of STAT1 and represses the transcription of *IFN regulatory factor-1* (*IRF-1*), thus enhancing the proliferation, metastasis, and chemoresistance of prostate cancer cells (Bachmann et al., 2014). DTX3L is also highly expressed in gliomas, and its expression level correlates with the degree of malignancy and the overall prognosis (Xu et al., 2017). The regulatory mechanism underlying the invasion and metastasis of melanoma by DTX3L involves the focal adhesion kinase (FAK)/PI3K/AKT signal transduction, but not the MEK/ERK pathway (Thang et al., 2015). The expression of DTX3L is regulated by FAK and gradually increases during proliferation of myeloma cells, which results in cell cycle arrest at the G1 phase and promotes the adhesion of myeloma cells to fibronectin or bone marrow stromal cells (Shen et al., 2017). Meanwhile, inhibition of DTX3L expression has been shown to enhance the sensitivity to chemotherapy and increase the expression of caspase-3 and PARP1 in multiple myeloma cell lines, thus promoting apoptosis (Shen et al., 2017). Furthermore, DTX3L expression is higher in triple-negative breast cancer cells than in estrogen receptor (ER) positive and human epidermal growth factor receptor 2 (HER2) positive breast cancers, and is a part of the negative feedback loop controlling all-trans retinoic acid (ATRA)-dependent inhibition of breast cancer cell growth (Bolis et al., 2020).

## DTX4

DTX4, as the last discovered member of the DTX family, is located on chromosome 11 (11q12.1). The 67.4 kDa DTX4 protein with 619 amino acids is primarily expressed in the cytoplasm, and is 27% identical and 39% similar to Dx. DTX4 is closely involved in the Notch signaling pathway. After Notch1 is ubiquitinated by DTX4 on the cell surface, ligand-expressing

cells internalize the extracellular domain of Notch1. At the same time, Notch1 receptor-expressing cells internalize the complex of Notch1 and DTX4 in a process referred to as bilateral endocytosis (Chastagner et al., 2017). A disintegrin and metalloproteinase 10 (ADAM10) generates a cleavage product of Notch, necessary for the NICD formation. Blocking endocytosis of Notch1 and DTX4 reduces the colocalization of Notch1 and ADAM10 and the formation of the NICD, which suggests that DTX4 ubiquitinates Notch1 prior to the cleavage by ADAM10 (Chastagner et al., 2017).

In addition to Notch signaling, DTX4 is also involved in IFN-I signaling pathway in innate immunity. In virus-infected cells, IRF-3 is phosphorylated by TANK-binding kinase 1 (TBK1), thereby activating the IFN-I signaling pathway. The Ub-specific protease 38 (USP38), TRAF-interacting protein (TRIP), Nod-like receptor (NLR) family pyrin domain containing 4 (NLRP4), and DTX4 complex polyubiquitinates TBK1, thereby degrading it to limit the virus-induced IFN-I signaling pathway (Cui et al., 2012). Some interacting proteins, such as TNF receptor-associated factor 3-interacting protein 3 (TRAF3IP3) and dual-specificity tyrosine-(Y)-phosphorylation regulated kinase 2 (DYRK2), are also essential for the NLRP4/DTX4 complex to promote TBK1 degradation via Lys48-linked ubiquitination (An et al., 2015; Deng et al., 2020). In chronic hepatitis B, the reduction of DTX4 expression partially mediates the IFN-I signaling pathway to increase the sustenance of hepatitis B virus (HBV) and maintenance of hepatitis B surface antigen (HBsAg) in the serum (Kim et al., 2018).

DNA promoter methylation negatively correlates with gene expression. With the decrease in its DNA promoter methylation, DTX4 expression is promoted during the activation of hepatic stellate cells (Schumacher et al., 2017). In systemic lupus erythematosus, the mRNA expression of DTX4 is partially modulated by circular RNA hsa\_circ\_0045272 and is associated with early apoptosis of Jurkat cells (Li et al., 2018). DTX4 is also involved in fibrotic processes in obstructive nephropathy, and its mRNA levels are regulated by microRNA let-7a (Papadopoulos et al., 2017).

DTX4 plays vital roles in cell differentiation. The elevated expression of DTX4, together with DTX1, has been shown to contribute to their inhibitory effects on Notch signaling pathway. As a result, T-cell commitment and developmental progression are impeded (Wang et al., 2009). During preadipocyte differentiation, the expression of DTX4 protein gradually increases. Then, the artificially reduced expression of DTX4 is found to decrease the number of lipid granules, along with the decreased expression of CCAAT enhancer-binding protein alpha (C/EBP $\alpha$ ) and peroxisome proliferator-activated receptor gamma (PPAR $\gamma$ ). Moreover, downregulation of DTX4 reduces the expression of adipogenic marker genes *fatty acid-binding protein 4* (*FABP4*) and *adipsin*, which arrest mitosis and inhibit expression of Wnt signaling genes, such as *Wnt6* and *Wnt10b* (Wang et al., 2017).

DTX4 is associated with the development and metastasis of several carcinomas, such as hepatocellular carcinoma (Viatour et al., 2011), colorectal cancer (Liu et al., 2010), and melanoma (Lin et al., 2016). Comparison of the interaction networks

between microRNAs and target genes in nasopharyngeal carcinoma samples showed that *DTX4*, regulated by several microRNAs, was substantially upregulated, which illustrates the promotional roles of *DTX4* in the occurrence and development of nasopharyngeal carcinoma (Liu et al., 2016). Indoleamine 2,3 dioxygenase (IDO1), the rate-limiting enzyme of the kynurenine pathway, and programmed cell death 1 ligand 1 (PD-L1) are potential immunotherapeutic targets against soft tissue sarcoma. The expression of *DTX4* increases upon the inhibition of both IDO1 and PD-L1, which suggests the potential controlling function of *DTX4* in immunotherapy of heterogeneous malignant mesenchymal neoplasms (Nafia et al., 2020).

## CONCLUSION

DTX family E3 ligases are highly evolutionarily conserved and essential during protein ubiquitination, yet differ from each other with various functions in the expressed tissues. DTX1, expressed in both cytoplasm and nucleus, has the highest homology with D<sub>x</sub> of *Drosophila*. The structure, function, and mechanism of DTX1 remains a hot topic in research. DTX1 activates multiple signaling cascades to regulate cell development, while dysregulated DTX1 expression induces numerous human diseases, including malignant conditions. Several substrate proteins of DTX1 have already been identified, for example, PI5P4K $\gamma$ , c-FLIP, and PKC- $\theta$ . The cellular localizations of DTX2, DTX3, and DTX3L are primarily in the nucleus, indicating that the functions and mechanisms of these three DTX proteins are associated with transcriptional regulation and DNA damage repair. The mechanism of DTX2 involves PARylation. The N-termini of DTX3 and DTX3L are disparate from those of other DTX proteins, while the current available data on DTX3 are limited. DTX3L and PARP9 heterodimer targets proteins within the nucleosome. DTX4 is the last discovered member and primarily expressed in the cytoplasm and is involved in human innate immune by regulating IFN-I signaling pathway. Owing to the complexity of multiple E2 and substrate proteins, the function and mechanism of DTX family proteins remain nebulous. Further research can provide deeper insights into ubiquitination. Current data suggest DTX proteins as potential diagnostic and therapeutic targets for carcinomas and other diseases.

## FUTURE PERSPECTIVES

It is well accepted that the protein structure determines function. In the future, with the help of AlphaFold, an artificial intelligent system to predict the 3-D structure of a protein accurately, the structural features, molecular mechanisms, and potential drug targets of DTX family proteins will be no longer mysterious

(Jumper et al., 2021). The DTX family proteins have a great significance in both physiology and pathology, hence further research is warranted to elucidate the mechanisms underlying their function and influence, such as: (1) What other substrate proteins are directly ubiquitinated by DTX family proteins? The fundamental function of DTX family proteins is the ubiquitination of substrate proteins. Although some have been identified, many substrate proteins of DTX family have yet to be fully characterized. Binding specificity of substrate proteins, to a certain extent, determines the exact molecular mechanism and downstream signaling pathway. Further investigation will provide a better understanding of functional roles of individual DTX proteins. (2) What results in the aberrant expression of DTX family proteins in carcinoma and other diseases? Genetic mutation and transcriptional dysregulation are associated with the over- or down- expression of DTX family proteins under pathological conditions. However, the exact mechanisms remain to be determined. (3) What is the relationship between other E3s and DTX family proteins? Several other E3s, for instance, AIP4, Nedd4, and BRCA1, play different roles in enhancement or inhibition of the ubiquitination by DTX family proteins. Both extracellular stimuli and intracellular conditions influence the combination of other E3s with DTX proteins, which are extremely complicated and require in depth investigation. It is of great importance to identify the association between other E3s and DTX proteins, which will provide insights into translational medicine of DTX proteins.

## AUTHOR CONTRIBUTIONS

LW and ZL conceived and designed the review. LW wrote the manuscript. LW, XS, and JH revised the manuscript. All authors contributed to the article and approved the submitted version.

## FUNDING

This work was supported by the National Natural Science Foundation of China (Grant Number: 81672644), Young Scholar Support Program 2018 of China Medical University (Grant Number: QGZD2018061), and 345 Talent Project of Shengjing Hospital of China Medical University (50A).

## ACKNOWLEDGMENTS

We would like to thank Yang Fan (Shengjing Hospital of China Medical University) for her critical reading of the manuscript. We apologize to those scientists whose outstanding works are not cited here due to limited space.

## REFERENCES

- Ahmed, S. F., Buetow, L., Gabrielsen, M., Lilla, S., Chatrin, C., Sibbet, G. J., et al. (2020). DELTEX2 C-terminal domain recognizes and recruits ADP-ribosylated proteins for ubiquitination. *Sci. Adv.* 6:eabc0629. doi: 10.1126/sciadv.abc0629
- Akutsu, M., Dikic, I., and Bremm, A. (2016). Ubiquitin chain diversity at a glance. *J. Cell. Sci.* 129, 875–880. doi: 10.1242/jcs.183954
- Altschul, S. F., Madden, T. L., Schaffer, A. A., Zhang, J., Zhang, Z., Miller, W., et al. (1997). Gapped BLAST and PSI-BLAST: a new generation of protein database search programs. *Nucleic Acids Res.* 25, 3389–3402. doi: 10.1093/nar/25.17.3389

- Amm, I., Sommer, T., and Wolf, D. H. (2014). Protein quality control and elimination of protein waste: the role of the ubiquitin-proteasome system. *Biochim. Biophys. Acta* 1843, 182–196. doi: 10.1016/j.bbamcr.2013.06.031
- Ammeux, N., Housden, B. E., Georgiadis, A., Hu, Y., and Perrimon, N. (2016). Mapping signaling pathway cross-talk in *Drosophila* cells. *Proc. Natl. Acad. Sci. U S A* 113, 9940–9945. doi: 10.1073/pnas.1610432113
- An, T., Li, S., Pan, W., Tien, P., Zhong, B., Shu, H. B., et al. (2015). DYRK2 Negatively Regulates Type I Interferon Induction by Promoting TBK1 Degradation via Ser527 Phosphorylation. *PLoS Pathog.* 11:e1005179. doi: 10.1371/journal.ppat.1005179
- Aravind, L. (2001). The WWE domain: a common interaction module in protein ubiquitination and ADP ribosylation. *Trends Biochem. Sci.* 26, 273–275. doi: 10.1016/s0968-0004(01)01787-x
- Bachmann, S. B., Frommel, S. C., Camicia, R., Winkler, H. C., Santoro, R., and Hassa, P. O. (2014). DTX3L and ARTD9 inhibit IRF1 expression and mediate in cooperation with ARTD8 survival and proliferation of metastatic prostate cancer cells. *Mol. Cancer* 13:125. doi: 10.1186/1476-4598-13-125
- Boase, N. A., and Kumar, S. (2015). NEDD4: The founding member of a family of ubiquitin-protein ligases. *Gene* 557, 113–122. doi: 10.1016/j.gene.2014.12.020
- Bolis, M., Paroni, G., Fratelli, M., Vallerger, A., Guarrera, L., Zanetti, A., et al. (2020). All-trans retinoic acid stimulates viral mimicry, interferon responses and antigen presentation in breast-cancer cells. *Cancers (Basel)* 12:1169. doi: 10.3390/cancers12051169
- Bork, P., and Sudol, M. (1994). The WW domain: a signalling site in dystrophin? *Trends Biochem. Sci.* 19, 531–533. doi: 10.1016/0968-0004(94)90053-1
- Bray, S. J., and Gomez-Lamarca, M. (2018). Notch after cleavage. *Curr. Opin. Cell. Biol.* 51, 103–109. doi: 10.1016/j.cceb.2017.12.008
- Chastagner, P., Israel, A., and Brou, C. (2006). Itch/AIP4 mediates Deltex degradation through the formation of K29-linked polyubiquitin chains. *EMBO Rep.* 7, 1147–1153. doi: 10.1038/sj.embor.7400822
- Chastagner, P., Rubinstein, E., and Brou, C. (2017). Ligand-activated Notch undergoes DTX4-mediated ubiquitylation and bilateral endocytosis before ADAM10 processing. *Sci. Signal.* 10:eaa92989. doi: 10.1126/scisignal.aag2989
- Chatrin, C., Gabrielsen, M., Buetow, L., Nakasone, M. A., Ahmed, S. F., Sumpton, D., et al. (2020). Structural insights into ADP-ribosylation of ubiquitin by Deltex family E3 ubiquitin ligases. *Sci. Adv.* 6:eabc0418. doi: 10.1126/sciadv.abc0418
- Chen, R. H., Chen, Y. H., and Huang, T. Y. (2019). Ubiquitin-mediated regulation of autophagy. *J. Biomed. Sci.* 26:80. doi: 10.1186/s12929-019-0569-y
- Choubey, P. K., Nandy, N., Pandey, A., and Roy, J. K. (2020). Rab11 plays a key role in stellate cell differentiation via non-canonical Notch pathway in Malpighian tubules of *Drosophila melanogaster*. *Dev. Biol.* 461, 19–30. doi: 10.1016/j.ydbio.2020.01.002
- Chowdhury, M., and Enenkel, C. (2015). Intracellular dynamics of the ubiquitin-proteasome-system. *F1000Res* 4:367. doi: 10.12688/f1000research.6835.2
- Corpet, F. (1988). Multiple sequence alignment with hierarchical clustering. *Nucleic Acids Res.* 16, 10881–10890. doi: 10.1093/nar/16.22.10881
- Cotton, T. R., and Lechtenberg, B. C. (2020). Chain reactions: molecular mechanisms of RBR ubiquitin ligases. *Biochem. Soc. Trans.* 48, 1737–1750. doi: 10.1042/BST20200237
- Cui, J., Li, Y., Zhu, L., Liu, D., Songyang, Z., Wang, H. Y., et al. (2012). NLRP4 negatively regulates type I interferon signaling by targeting the kinase TBK1 for degradation via the ubiquitin ligase DTX4. *Nat. Immunol.* 13, 387–395. doi: 10.1038/ni.12239
- Cui, X. Y., Hu, Q. D., Tekaya, M., Shimoda, Y., Ang, B. T., Nie, D. Y., et al. (2004). NB-3/Notch1 pathway via Deltex1 promotes neural progenitor cell differentiation into oligodendrocytes. *J. Biol. Chem.* 279, 25858–25865. doi: 10.1074/jbc.M313505200
- Dai, C., and Sampson, S. B. (2016). HSF1: guardian of proteostasis in cancer. *Trends Cell. Biol.* 26, 17–28. doi: 10.1016/j.tcb.2015.10.011
- de Miranda, N. F., Georgiou, K., Chen, L., Wu, C., Gao, Z., Zaravinos, A., et al. (2014). Exome sequencing reveals novel mutation targets in diffuse large B-cell lymphomas derived from Chinese patients. *Blood* 124, 2544–2553. doi: 10.1182/blood-2013-12-546309
- Deftos, M. L., He, Y. W., Ojala, E. W., and Bevan, M. J. (1998). Correlating notch signaling with thymocyte maturation. *Immunity* 9, 777–786. doi: 10.1016/s1074-7613(00)80643-3
- Deng, M., Tam, J. W., Wang, L., Liang, K., Li, S., Zhang, L., et al. (2020). TRAF3IP3 negatively regulates cytosolic RNA induced anti-viral signaling by promoting TBK1 K48 ubiquitination. *Nat. Commun.* 11:2193. doi: 10.1038/s41467-020-16014-0
- Diederich, R. J., Matsuno, K., Hing, H., and Artavanis-Tsakonas, S. (1994). Cytosolic interaction between deltex and Notch ankyrin repeats implicates deltex in the Notch signaling pathway. *Development* 120, 473–481. doi: 10.1242/dev.120.3.473
- Dikic, I., Wakatsuki, S., and Walters, K. J. (2009). Ubiquitin-binding domains - from structures to functions. *Nat. Rev. Mol. Cell. Biol.* 10, 659–671. doi: 10.1038/nrm2767
- Ding, X. Y., Hu, H. Y., Huang, K. N., Wei, R. Q., Min, J., Qi, C., et al. (2020). Ubiquitination of NOTCH2 by DTX3 suppresses the proliferation and migration of human esophageal carcinoma. *Cancer Sci.* 111, 489–501. doi: 10.1111/cas.14288
- Dunn, R., Klos, D. A., Adler, A. S., and Hicke, L. (2004). The C2 domain of the Rsp5 ubiquitin ligase binds membrane phosphoinositides and directs ubiquitination of endosomal cargo. *J. Cell. Biol.* 165, 135–144. doi: 10.1083/jcb.200309026
- Dutta, D., Mutsuddi, M., and Mukherjee, A. (2019). Synergistic interaction of Deltex and Hrp48 leads to JNK activation. *Cell Biol Int* 43, 350–357. doi: 10.1002/cbin.11089
- Dutta, D., Paul, M. S., Singh, A., Mutsuddi, M., and Mukherjee, A. (2017). Regulation of notch signaling by the heterogeneous nuclear ribonucleoprotein Hrp48 and deltex in *Drosophila melanogaster*. *Genetics* 206, 905–918. doi: 10.1534/genetics.116.198879
- Dutta, D., Singh, A., Paul, M. S., Sharma, V., Mutsuddi, M., and Mukherjee, A. (2018). Deltex interacts with Eiger and consequently influences the cell death in *Drosophila melanogaster*. *Cell. Signal.* 49, 17–29. doi: 10.1016/j.cellsig.2018.05.003
- Eiraku, M., Tohgo, A., Ono, K., Kaneko, M., Fujishima, K., Hirano, T., et al. (2005). DNER acts as a neuron-specific Notch ligand during Bergmann glial development. *Nat. Neurosci.* 8, 873–880. doi: 10.1038/nn1492
- Endo, Y., Osumi, N., and Wakamatsu, Y. (2003). Deltex/Dtx mediates NOTCH signaling in regulation of Bmp4 expression in cranial neural crest formation during avian development. *Dev. Growth Differ.* 45, 241–248. doi: 10.1046/j.1524-4725.2003.693.x
- Fhu, C. W., and Ali, A. (2021). Dysregulation of the ubiquitin proteasome system in human malignancies: A window for therapeutic intervention. *Cancers (Basel)* 13:1513. doi: 10.3390/cancers13071513
- Gatza, M. L., Silva, G. O., Parker, J. S., Fan, C., and Perou, C. M. (2014). An integrated genomics approach identifies drivers of proliferation in luminal-subtype human breast cancer. *Nat. Genet.* 46, 1051–1059. doi: 10.1038/ng.3073
- Goetzke, C. C., Ebstein, F., and Kallinich, T. (2021). Role of proteasomes in inflammation. *J. Clin. Med.* 10:1783. doi: 10.3390/jcm10081783
- Gorman, M. J., and Gorton, J. R. (1992). A genetic analysis of deltex and its interaction with the Notch locus in *Drosophila melanogaster*. *Genetics* 131, 99–112. doi: 10.1093/genetics/131.1.99
- Green, M. R., Kihira, S., Liu, C. L., Nair, R. V., Salari, R., Gentles, A. J., et al. (2015). Mutations in early follicular lymphoma progenitors are associated with suppressed antigen presentation. *Proc. Natl. Acad. Sci. U S A* 112, E1116–E1125. doi: 10.1073/pnas.1501199112
- Guo, R., Li, Q., Yang, F., Hu, X., Jiao, J., Guo, Y., et al. (2018). In vivo MR imaging of dual MRI reporter genes and Deltex-1 gene-modified human mesenchymal stem cells in the treatment of closed penile fracture. *Mol. Imaging Biol.* 20, 417–427. doi: 10.1007/s11307-017-1128-0
- Gupta-Rossi, N., Storck, S., Griebel, P. J., Reynaud, C. A., Weill, J. C., and Dahan, A. (2003). Specific over-expression of deltex and a new Kelch-like protein in human germinal center B cells. *Mol. Immunol.* 39, 791–799. doi: 10.1016/s0161-5890(03)00002-6
- Gupte, R., Liu, Z., and Kraus, W. L. (2017). PARPs and ADP-ribosylation: recent advances linking molecular functions to biological outcomes. *Genes Dev.* 31, 101–126. doi: 10.1101/gad.291518.116
- Gurumurthy, C. B., and Lloyd, K. C. K. (2019). Generating mouse models for biomedical research: technological advances. *Dis. Model. Mech.* 12:dmm029462. doi: 10.1242/dmm.029462
- Hakme, A., Huber, A., Dolle, P., and Schreiber, V. (2008). The macroPARP genes Parp-9 and Parp-14 are developmentally and differentially regulated in mouse tissues. *Dev. Dyn.* 237, 209–215. doi: 10.1002/dvdy.21399



- Hanna, J., Guerra-Moreno, A., Ang, J., and Micoogullari, Y. (2019). Protein degradation and the pathologic basis of disease. *Am. J. Pathol.* 189, 94–103. doi: 10.1016/j.ajpath.2018.09.004
- Hatakeyama, S., and Nakayama, K. I. (2003). U-box proteins as a new family of ubiquitin ligases. *Biochem. Biophys. Res. Commun.* 302, 635–645. doi: 10.1016/s0006-291x(03)00245-6
- He, F., Tsuda, K., Takahashi, M., Kuwasako, K., Terada, T., Shirouzu, M., et al. (2012). Structural insight into the interaction of ADP-ribose with the PARP WWE domains. *FEBS Lett.* 586, 3858–3864. doi: 10.1016/j.febslet.2012.09.009
- Holleman, J., and Marchese, A. (2014). The ubiquitin ligase deltex-3l regulates endosomal sorting of the G protein-coupled receptor CXCR4. *Mol. Biol. Cell.* 25, 1892–1904. doi: 10.1091/mbc.E13-10-0612
- Hong, R., Wang, Y., Dong, H., and Geng, R. (2020). DTX3L/ARTD9 contributes to inflammation of fibroblast-like synoviocytes by increasing STAT1 translocation. *Tissue Cell.* 64:101339. doi: 10.1016/j.tice.2020.101339
- Hori, K., Fuwa, T. J., Seki, T., and Matsuno, K. (2005). Genetic regions that interact with loss- and gain-of-function phenotypes of deltex implicate novel genes in *Drosophila* Notch signaling. *Mol. Genet. Genom.* 272, 627–638. doi: 10.1007/s00438-004-1098-1
- Hori, K., Sen, A., Kirchhausen, T., and Artavanis-Tsakonas, S. (2011). Synergy between the ESCRT-III complex and Deltex defines a ligand-independent Notch signal. *J. Cell. Biol.* 195, 1005–1015. doi: 10.1083/jcb.201104146
- Hori, K., Sen, A., Kirchhausen, T., and Artavanis-Tsakonas, S. (2012). Regulation of ligand-independent Notch signal through intracellular trafficking. *Commun. Integr. Biol.* 5, 374–376. doi: 10.4161/cib.19995
- Hsiao, H. W., Hsu, T. S., Liu, W. H., Hsieh, W. C., Chou, T. F., Wu, Y. J., et al. (2015). Deltex1 antagonizes HIF-1 $\alpha$  and sustains the stability of regulatory T cells in vivo. *Nat. Commun.* 6:6353. doi: 10.1038/ncomms7353
- Hsiao, H. W., Liu, W. H., Wang, C. J., Lo, Y. H., Wu, Y. H., Jiang, S. T., et al. (2009). Deltex1 is a target of the transcription factor NFAT that promotes T cell anergy. *Immunity* 31, 72–83. doi: 10.1016/j.immuni.2009.04.017
- Hsu, T. S., Hsiao, H. W., Wu, P. J., Liu, W. H., and Lai, M. Z. (2014). Deltex1 promotes protein kinase C $\theta$  degradation and sustains Casitas B-lineage lymphoma expression. *J. Immunol.* 193, 1672–1680. doi: 10.4049/jimmunol.1301416
- Hsu, T. S., Mo, S. T., Hsu, P. N., and Lai, M. Z. (2018). c-FLIP is a target of the E3 ligase deltex1 in gastric cancer. *Cell. Death Dis.* 9:135. doi: 10.1038/s41419-017-0165-6
- Hu, Q. D., Ang, B. T., Karsak, M., Hu, W. P., Cui, X. Y., Duka, T., et al. (2003). F3/contactin acts as a functional ligand for Notch during oligodendrocyte maturation. *Cell* 115, 163–175. doi: 10.1016/s0092-8674(03)00810-9
- Huber, R. M., Rajski, M., Sivasankaran, B., Moncayo, G., Hemmings, B. A., and Merlo, A. (2013). Deltex-1 activates mitotic signaling and proliferation and increases the clonogenic and invasive potential of U373 and LN18 glioblastoma cells and correlates with patient survival. *PLoS One* 8:e57793. doi: 10.1371/journal.pone.0057793
- Igaki, T., and Miura, M. (2014). The *Drosophila* TNF ortholog Eiger: emerging physiological roles and evolution of the TNF system. *Semin. Immunol.* 26, 267–274. doi: 10.1016/j.smim.2014.05.003
- Ikeda, F., and Dikic, I. (2008). Atypical ubiquitin chains: new molecular signals. 'Protein Modifications: Beyond the Usual Suspects' review series. *EMBO Rep.* 9, 536–542. doi: 10.1038/embor.2008.93
- Izon, D. J., Aster, J. C., He, Y., Weng, A., Karnell, F. G., Patriub, V., et al. (2002). Deltex1 redirects lymphoid progenitors to the B cell lineage by antagonizing Notch1. *Immunity* 16, 231–243. doi: 10.1016/s1074-7613(02)00271-6
- Jafari, D., Mousavi, M. J., Keshavarz Shahbaz, S., Jafarzadeh, L., Tahmasebi, S., Spoor, J., et al. (2021). E3 ubiquitin ligase Casitas B lineage lymphoma-b and its potential therapeutic implications for immunotherapy. *Clin. Exp. Immunol.* 204, 14–31. doi: 10.1111/cei.13560
- Jang, J., Choi, Y. I., Choi, J., Lee, K. Y., Chung, H., Jeon, S. H., et al. (2006). Notch1 confers thymocytes a resistance to GC-induced apoptosis through Deltex1 by blocking the recruitment of p300 to the SRG3 promoter. *Cell. Death Differ.* 13, 1495–1505. doi: 10.1038/sj.cdd.4401827
- Jumper, J., Evans, R., Pritzel, A., Green, T., Figurnov, M., Ronneberger, O., et al. (2021). Highly accurate protein structure prediction with AlphaFold. *Nature* 2021:e3819–2. doi: 10.1038/s41586-021-03819-2
- Jungmichel, S., Rosenthal, F., Altmeyer, M., Lukas, J., Hottiger, M. O., and Nielsen, M. L. (2013). Proteome-wide identification of poly(ADP-Ribosyl)ation targets in different genotoxic stress responses. *Mol. Cell.* 52, 272–285. doi: 10.1016/j.molcel.2013.08.026
- Justice, M. J., and Dhillon, P. (2016). Using the mouse to model human disease: increasing validity and reproducibility. *Dis. Model. Mech.* 9, 101–103. doi: 10.1242/dmm.024547
- Juszczynski, P., Kutok, J. L., Li, C., Mitra, J., Aguiar, R. C., and Shipp, M. A. (2006). BAL1 and BBAP are regulated by a gamma interferon-responsive bidirectional promoter and are overexpressed in diffuse large B-cell lymphomas with a prominent inflammatory infiltrate. *Mol. Cell. Biol.* 26, 5348–5359. doi: 10.1128/MCB.02351-05
- Kaushik, S., and Cuervo, A. M. (2015). Proteostasis and aging. *Nat. Med.* 21, 1406–1415. doi: 10.1038/nm.4001
- Kim, H., Chen, J., and Yu, X. (2007). Ubiquitin-binding protein RAP80 mediates BRCA1-dependent DNA damage response. *Science* 316, 1202–1205. doi: 10.1126/science.1139621
- Kim, T. H., Lee, E. J., Choi, J. H., Yim, S. Y., Lee, S., Kang, J., et al. (2018). Identification of novel susceptibility loci associated with hepatitis B surface antigen seroclearance in chronic hepatitis B. *PLoS One* 13:e0199094. doi: 10.1371/journal.pone.0199094
- Kirisako, T., Kamei, K., Murata, S., Kato, M., Fukumoto, H., Kanie, M., et al. (2006). A ubiquitin ligase complex assembles linear polyubiquitin chains. *EMBO J.* 25, 4877–4887. doi: 10.1038/sj.emboj.7601360
- Kishi, N., Tang, Z., Maeda, Y., Hirai, A., Mo, R., Ito, M., et al. (2001). Murine homologs of deltex define a novel gene family involved in vertebrate Notch signaling and neurogenesis. *Int. J. Dev. Neurosci.* 19, 21–35. doi: 10.1016/s0736-5748(00)00071-x
- Kliza, K., and Husnjak, K. (2020). Resolving the complexity of ubiquitin networks. *Front. Mol. Biosci.* 7:21. doi: 10.3389/fmolb.2020.00021
- Komander, D., and Rape, M. (2012). The ubiquitin code. *Annu. Rev. Biochem.* 81, 203–229. doi: 10.1146/annurev-biochem-060310-170328
- Kovall, R. A., Gebelein, B., Sprinzak, D., and Kopan, R. (2017). The canonical notch signaling pathway: structural and biochemical insights into shape, sugar, and force. *Dev. Cell.* 41, 228–241. doi: 10.1016/j.devcel.2017.04.001
- Kumar, S., Tomooka, Y., and Noda, M. (1992). Identification of a set of genes with developmentally down-regulated expression in the mouse brain. *Biochem. Biophys. Res. Commun.* 185, 1155–1161. doi: 10.1016/0006-291x(92)91747-e
- Lee, J. H., Shin, K. M., Lee, S. Y., Hong, M. J., Choi, J. E., Kang, H. G., et al. (2019). Genetic variant of notch regulator DTX1 predicts survival after lung cancer surgery. *Ann. Surg. Oncol.* 26, 3756–3764. doi: 10.1245/s10434-019-07614-2
- Lee, J. Y., Hall, J. A., Kroehling, L., Wu, L., Najar, T., Nguyen, H. H., et al. (2020). Serum Amyloid A proteins induce pathogenic Th17 cells and promote inflammatory disease. *Cell* 180, 79–91. doi: 10.1016/j.cell.2019.11.026
- Lehar, S. M., and Bevan, M. J. (2006). T cells develop normally in the absence of both Deltex1 and Deltex2. *Mol. Cell. Biol.* 26, 7358–7371. doi: 10.1128/MCB.00149-06
- Li, L. J., Zhu, Z. W., Zhao, W., Tao, S. S., Li, B. Z., Xu, S. Z., et al. (2018). Circular RNA expression profile and potential function of hsa\_circ\_0045272 in systemic lupus erythematosus. *Immunology* 155, 137–149. doi: 10.1111/imm.12940
- Li, W., Bengtson, M. H., Ulbrich, A., Matsuda, A., Reddy, V. A., Orth, A., et al. (2008). Genome-wide and functional annotation of human E3 ubiquitin ligases identifies MULAN, a mitochondrial E3 that regulates the organelle's dynamics and signaling. *PLoS One* 3:e1487. doi: 10.1371/journal.pone.0001487
- Liang, S. J., Li, X. G., and Wang, X. Q. (2019). Notch signaling in mammalian intestinal stem cells: determining cell fate and maintaining homeostasis. *Curr. Stem Cell. Res. Ther.* 14, 583–590. doi: 10.2174/1574888X14666190429143734
- Lin, X., Sun, B., Zhu, D., Zhao, X., Sun, R., Zhang, Y., et al. (2016). Notch4+ cancer stem-like cells promote the metastatic and invasive ability of melanoma. *Cancer Sci.* 107, 1079–1091. doi: 10.1111/cas.12978
- Liu, C., Vyas, A., Kassab, M. A., Singh, A. K., and Yu, X. (2017). The role of poly ADP-ribosylation in the first wave of DNA damage response. *Nucleic Acids Res.* 45, 8129–8141. doi: 10.1093/nar/gkx565
- Liu, J., Li, H., Mao, A., Lu, J., Liu, W., Qie, J., et al. (2020). DCAF13 promotes triple-negative breast cancer metastasis by mediating DTX3 mRNA degradation. *Cell Cycle* 19, 3622–3631. doi: 10.1080/15384101.2020.1859196
- Liu, M., Zhu, K., Qian, X., and Li, W. (2016). Identification of miRNA/mRNA-negative regulation pairs in nasopharyngeal carcinoma. *Med. Sci. Monit.* 22, 2215–2234. doi: 10.12659/msm.896047



- Liu, W. H., and Lai, M. Z. (2005). Deltex regulates T-cell activation by targeted degradation of active MEKK1. *Mol. Cell. Biol.* 25, 1367–1378. doi: 10.1128/MCB.25.4.1367-1378.2005
- Liu, W. M., Laux, H., Henry, J. Y., Bolton, T. B., Dalglish, A. G., and Galustian, C. (2010). A microarray study of altered gene expression in colorectal cancer cells after treatment with immunomodulatory drugs: differences in action in vivo and in vitro. *Mol. Biol. Rep.* 37, 1801–1814. doi: 10.1007/s11033-009-9614-3
- Liu, Y. C., and Gu, H. (2002). Cbl and Cbl-b in T-cell regulation. *Trends Immunol.* 23, 140–143. doi: 10.1016/s1471-4906(01)02157-3
- Lloyd, K. C., Robinson, P. N., and MacRae, C. A. (2016). Animal-based studies will be essential for precision medicine. *Sci. Transl. Med.* 8:352ed12. doi: 10.1126/scitranslmed.aaf5474
- Luo, D., de Morree, A., Boutet, S., Quach, N., Natu, V., Rustagi, A., et al. (2017). Deltex2 represses MyoD expression and inhibits myogenic differentiation by acting as a negative regulator of Jmjd1c. *Proc. Natl. Acad. Sci. U S A.* 114, E3071–E3080. doi: 10.1073/pnas.1613592114
- Martello, R., Leutert, M., Jungmichel, S., Bilan, V., Larsen, S. C., Young, C., et al. (2016). Proteome-wide identification of the endogenous ADP-ribosylome of mammalian cells and tissue. *Nat. Commun.* 7:12917. doi: 10.1038/ncomms12917
- Matsuno, K., Diederich, R. J., Go, M. J., Blaumueller, C. M., and Artavanis-Tsakonas, S. (1995). Deltex acts as a positive regulator of Notch signaling through interactions with the Notch ankyrin repeats. *Development* 121, 2633–2644. doi: 10.1242/dev.121.8.2633
- Matsuno, K., Eastman, D., Mitsiades, T., Quinn, A. M., Carcanci, M. L., Ordentlich, P., et al. (1998). Human deltex is a conserved regulator of Notch signalling. *Nat. Genet.* 19, 74–78. doi: 10.1038/ng0598-74
- Matsuno, K., Ito, M., Hori, K., Miyashita, F., Suzuki, S., Kishi, N., et al. (2002). Involvement of a proline-rich motif and RING-H2 finger of Deltex in the regulation of Notch signaling. *Development* 129, 1049–1059. doi: 10.1242/dev.129.4.1049
- Matyskiela, M. E., and Martin, A. (2013). Design principles of a universal protein degradation machine. *J. Mol. Biol.* 425, 199–213. doi: 10.1016/j.jmb.2012.11.001
- Mazaleyrat, S. L., Fostier, M., Wilkin, M. B., Aslam, H., Evans, D. A., Cornell, M., et al. (2003). Down-regulation of Notch target gene expression by Suppressor of deltex. *Dev. Biol.* 255, 363–372. doi: 10.1016/s0012-1606(02)00086-6
- Meriranta, L., Pasanen, A., Louhimo, R., Cervera, A., Alkods, A., Autio, M., et al. (2017). Deltex-1 mutations predict poor survival in diffuse large B-cell lymphoma. *Haematologica* 102, e195–e198. doi: 10.3324/haematol.2016.157495
- Mishra, A. K., Sachan, N., Mutsuddi, M., and Mukherjee, A. (2014). TRAF6 is a novel regulator of Notch signaling in *Drosophila melanogaster*. *Cell Signal.* 26, 3016–3026. doi: 10.1016/j.cellsig.2014.09.016
- Miyamoto, K., Fujiwara, Y., and Saito, K. (2019). Zinc finger domain of the human DTX protein adopts a unique RING fold. *Protein Sci.* 28, 1151–1156. doi: 10.1002/pro.3610
- Morreale, F. E., and Walden, H. (2016). Types of ubiquitin ligases. *Cell* 165, 248–248. doi: 10.1016/j.cell.2016.03.003
- Morrione, A., Plant, P., Valentinis, B., Staub, O., Kumar, S., Rotin, D., et al. (1999). mGrb10 interacts with Nedd4. *J. Biol. Chem.* 274, 24094–24099. doi: 10.1074/jbc.274.34.24094
- Mukherjee, A., Veraksa, A., Bauer, A., Rosse, C., Camonis, J., and Artavanis-Tsakonas, S. (2005). Regulation of Notch signalling by non-visual beta-arrestin. *Nat. Cell. Biol.* 7, 1191–1201. doi: 10.1038/ncb1327
- Nafia, I., Toulmonde, M., Bortolotto, D., Chaibi, A., Bodet, D., Rey, C., et al. (2020). IDO targeting in sarcoma: biological and clinical implications. *Front. Immunol.* 11:274. doi: 10.3389/fimmu.2020.00274
- Nemetschke, L., and Knust, E. (2016). *Drosophila* Crumbs prevents ectopic Notch activation in developing wings by inhibiting ligand-independent endocytosis. *Development* 143, 4543–4553. doi: 10.1242/dev.141762
- Obiero, J., Walker, J. R., and Dhe-Paganon, S. (2012). Fold of the conserved DTC domain in Deltex proteins. *Proteins* 80, 1495–1499. doi: 10.1002/prot.24054
- Ordentlich, P., Lin, A., Shen, C. P., Blaumueller, C., Matsuno, K., Artavanis-Tsakonas, S., et al. (1998). Notch inhibition of E47 supports the existence of a novel signaling pathway. *Mol. Cell. Biol.* 18, 2230–2239. doi: 10.1128/MCB.18.4.2230
- Pampeno, C. L., Vallerie, A. M., Choi, J., Meruelo, N. C., and Meruelo, D. (2001). Genomic analysis and localization of murine Deltex, a modulator of notch activity, to mouse chromosome 5 and its human homolog to chromosome 12. *DNA Cell Biol.* 20, 141–148. doi: 10.1089/104454901300068960
- Papadopoulos, T., Casemayou, A., Neau, E., Breuil, B., Caubet, C., Calise, D., et al. (2017). Systems biology combining human- and animal-data miRNA and mRNA data identifies new targets in ureteropelvic junction obstruction. *BMC Syst. Biol.* 11:31. doi: 10.1186/s12918-017-0411-7
- Pickart, C. M., and Fushman, D. (2004). Polyubiquitin chains: polymeric protein signals. *Curr. Opin. Chem. Biol.* 8, 610–616. doi: 10.1016/j.cbpa.2004.09.009
- Plant, P. J., Lafont, F., Lecat, S., Verkade, P., Simons, K., and Rotin, D. (2000). Apical membrane targeting of Nedd4 is mediated by an association of its C2 domain with annexin XIIIb. *J. Cell. Biol.* 149, 1473–1484. doi: 10.1083/jcb.149.7.1473
- Qu, J., Zou, T., and Lin, Z. (2021). The roles of the ubiquitin-proteasome system in the endoplasmic reticulum stress pathway. *Int. J. Mol. Sci.* 22:1526. doi: 10.3390/ijms22041526
- Ray Chaudhuri, A., and Nussenzweig, A. (2017). The multifaceted roles of PARP1 in DNA repair and chromatin remodelling. *Nat. Rev. Mol. Cell. Biol.* 18, 610–621. doi: 10.1038/nrm.2017.53
- Rittinger, K., and Ikeda, F. (2017). Linear ubiquitin chains: enzymes, mechanisms and biology. *Open Biol.* 7:170026. doi: 10.1098/rsob.170026
- Roman, G., He, J., and Davis, R. L. (2000). kurtz, a novel nonvisual arrestin, is an essential neural gene in *Drosophila*. *Genetics* 155, 1281–1295. doi: 10.1093/genetics/155.3.1281
- Rossi, D., Trifonov, V., Fangazio, M., Bruscaggin, A., Rasi, S., Spina, V., et al. (2012). The coding genome of splenic marginal zone lymphoma: activation of NOTCH2 and other pathways regulating marginal zone development. *J. Exp. Med.* 209, 1537–1551. doi: 10.1084/jem.20120904
- Rotin, D., and Kumar, S. (2009). Physiological functions of the HECT family of ubiquitin ligases. *Nat. Rev. Mol. Cell. Biol.* 10, 398–409. doi: 10.1038/nrm2690
- Saito, T., Chiba, S., Ichikawa, M., Kunisato, A., Asai, T., Shimizu, K., et al. (2003). Notch2 is preferentially expressed in mature B cells and indispensable for marginal zone B lineage development. *Immunity* 18, 675–685. doi: 10.1016/s1074-7613(03)00111-0
- Sakai, W., Yuasa-Sunagawa, M., Kusakabe, M., Kishimoto, A., Matsui, T., Kaneko, Y., et al. (2020). Functional impacts of the ubiquitin-proteasome system on DNA damage recognition in global genome nucleotide excision repair. *Sci. Rep.* 10:19704. doi: 10.1038/s41598-020-76898-2
- Sakata, T., Sakaguchi, H., Tsuda, L., Higashitani, A., Aigaki, T., Matsuno, K., et al. (2004). *Drosophila* Nedd4 regulates endocytosis of notch and suppresses its ligand-independent activation. *Curr. Biol.* 14, 2228–2236. doi: 10.1016/j.cub.2004.12.028
- Sawada, S., and Littman, D. R. (1993). A heterodimer of HEB and an E12-related protein interacts with the CD4 enhancer and regulates its activity in T-cell lines. *Mol. Cell. Biol.* 13, 5620–5628. doi: 10.1128/mcb.13.9.5620-5628.1993
- Schumacher, E. C., Gotze, S., Kordes, C., Benes, V., and Haussinger, D. (2017). Combined methylome and transcriptome analysis during rat hepatic stellate cell activation. *Stem Cells Dev.* 26, 1759–1770. doi: 10.1089/scd.2017.0128
- Scully, R., and Livingston, D. M. (2000). In search of the tumour-suppressor functions of BRCA1 and BRCA2. *Nature* 408, 429–432. doi: 10.1038/35044000
- Sewduth, R. N., Baietti, M. F., and Sablina, A. A. (2020). Cracking the monoubiquitin code of genetic diseases. *Int. J. Mol. Sci.* 21:3036. doi: 10.3390/ijms21093036
- Sharma, V., Mutsuddi, M., and Mukherjee, A. (2021). Deltex cooperates with TRAF6 to promote apoptosis and cell migration through Eiger-independent JNK activation in *Drosophila*. *Cell. Biol. Int.* 45, 686–700. doi: 10.1002/cbin.11521
- Shen, Y., Sun, Y., Zhang, L., and Liu, H. (2017). Effects of DTX3L on the cell proliferation, adhesion, and drug resistance of multiple myeloma cells. *Tumour. Biol.* 39:1010428317703941. doi: 10.1177/1010428317703941
- Singh, A., and Irvine, K. D. (2012). *Drosophila* as a model for understanding development and disease. *Dev. Dyn.* 241, 1–2. doi: 10.1002/dvdy.23712
- Sobhian, B., Shao, G., Lilli, D. R., Culhane, A. C., Moreau, L. A., Xia, B., et al. (2007). RAP80 targets BRCA1 to specific ubiquitin structures at DNA damage sites. *Science* 316, 1198–1202. doi: 10.1126/science.1139516
- Stewart, M. D., Ritterhoff, T., Klevit, R. E., and Brzovic, P. S. (2016). E2 enzymes: more than just middle men. *Cell. Res.* 26, 423–440. doi: 10.1038/cr.2016.35

- Storck, S., Delbos, F., Stadler, N., Thirion-Delalande, C., Bernex, F., Verthuy, C., et al. (2005). Normal immune system development in mice lacking the Deltex-1 RING finger domain. *Mol. Cell. Biol.* 25, 1437–1445. doi: 10.1128/MCB.25.4.1437-1445.2005
- Sudol, M., Chen, H. I., Bougeret, C., Einbond, A., and Bork, P. (1995). Characterization of a novel protein-binding module—the WW domain. *FEBS Lett.* 369, 67–71. doi: 10.1016/0014-5793(95)00550-s
- Sun, P., Xia, S., Lal, B., Eberhart, C. G., Quinones-Hinojosa, A., Maciaczyk, J., et al. (2009). DNER, an epigenetically modulated gene, regulates glioblastoma-derived neurosphere cell differentiation and tumor propagation. *Stem Cells* 27, 1473–1486. doi: 10.1002/stem.89
- Surabhi, S., Tripathi, B. K., Maurya, B., Bhaskar, P. K., Mukherjee, A., and Mutsuddi, M. (2015). Regulation of notch signaling by an evolutionary conserved DEAD Box RNA helicase, maheshvara in *Drosophila melanogaster*. *Genetics* 201, 1071–1085. doi: 10.1534/genetics.115.181214
- Takeyama, K., Aguiar, R. C., Gu, L., He, C., Freeman, G. J., Kutok, J. L., et al. (2003). The BAL-binding protein BBAP and related Deltex family members exhibit ubiquitin-protein isopeptide ligase activity. *J. Biol. Chem.* 278, 21930–21937. doi: 10.1074/jbc.M301157200
- Tang, Z., Wang, Y., Xing, R., Zeng, S., Di, J., and Xing, F. (2020). Deltex-1 is indispensable for the IL-6 and TGF-beta treatment-triggered differentiation of Th17 cells. *Cell. Immunol.* 356:104176. doi: 10.1016/j.cellimm.2020.104176
- Taormina, G., Ferrante, F., Vieni, S., Grassi, N., Russo, A., and Mirisola, M. G. (2019). Longevity: Lesson from Model Organisms. *Genes (Basel)* 10:518. doi: 10.3390/genes10070518
- Thang, N. D., Yajima, I., Kumasaka, M. Y., Iida, M., Suzuki, T., and Kato, M. (2015). Deltex-3-like (DTX3L) stimulates metastasis of melanoma through FAK/PI3K/AKT but not MEK/ERK pathway. *Oncotarget* 6, 14290–14299. doi: 10.18632/oncotarget.3742
- Thapa, P., Shanmugam, N., and Pokrzywa, W. (2020). Ubiquitin signaling regulates RNA biogenesis, processing, and metabolism. *Bioessays* 42:e1900171. doi: 10.1002/bies.201900171
- Tian, Q., Zhao, H., Ling, H., Sun, L., Xiao, C., Yin, G., et al. (2020). Poly(ADP-Ribose) polymerase enhances infiltration of mononuclear cells in primary Sjogren's syndrome through interferon-induced protein with tetratricopeptide repeats 1-mediated up-regulation of CXCL10. *Arthritis Rheumatol.* 72, 1003–1012. doi: 10.1002/art.41195
- Trempe, J. F. (2011). Reading the ubiquitin postal code. *Curr. Opin. Struct. Biol.* 21, 792–801. doi: 10.1016/j.sbi.2011.09.009
- Viatour, P., Ehmer, U., Saddic, L. A., Dorrell, C., Andersen, J. B., Lin, C., et al. (2011). Notch signaling inhibits hepatocellular carcinoma following inactivation of the RB pathway. *J. Exp. Med.* 208, 1963–1976. doi: 10.1084/jem.20110198
- Vyas, S., Matic, I., Uchima, L., Rood, J., Zaja, R., Hay, R. T., et al. (2014). Family-wide analysis of poly(ADP-ribose) polymerase activity. *Nat. Commun.* 5:4426. doi: 10.1038/ncomms5426
- Wang, H. C., Perry, S. S., and Sun, X. H. (2009). Id1 attenuates Notch signaling and impairs T-cell commitment by elevating Deltex1 expression. *Mol. Cell. Biol.* 29, 4640–4652. doi: 10.1128/MCB.00119-09
- Wang, L. J., Xue, Y., Huo, R., Yan, Z., Xu, H., Li, H., et al. (2020a). N6-methyladenosine methyltransferase METTL3 affects the phenotype of cerebral arteriovenous malformation via modulating Notch signaling pathway. *J. Biomed. Sci.* 27:62. doi: 10.1186/s12929-020-00655-w
- Wang, Y., Argiles-Castillo, D., Kane, E. I., Zhou, A., and Spratt, D. E. (2020b). HECT E3 ubiquitin ligases - emerging insights into their biological roles and disease relevance. *J. Cell. Sci.* 133:jcs228072. doi: 10.1242/jcs.228072
- Wang, Y., Yang, B. P., Chi, Y. G., Liu, L. B., and Lei, L. (2018). Effect of Deltex-1 on proliferation and differentiation of bone marrow mesenchymal stem cells into smooth muscle cells. *Eur. Rev. Med. Pharmacol. Sci.* 22, 3627–3634. doi: 10.26355/eurrev\_201806\_15239
- Wang, Z., Dai, Z., Pan, Y., Wu, S., Li, Z., and Zuo, C. (2017). E3 ubiquitin ligase DTX4 is required for adipogenic differentiation in 3T3-L1 preadipocytes cell line. *Biochem. Biophys. Res. Commun.* 492, 419–424. doi: 10.1016/j.bbrc.2017.08.083
- Wang, Z., Michaud, G. A., Cheng, Z., Zhang, Y., Hinds, T. R., Fan, E., et al. (2012). Recognition of the iso-ADP-ribose moiety in poly(ADP-ribose) by WWE domains suggests a general mechanism for poly(ADP-ribosyl)ation-dependent ubiquitination. *Genes Dev.* 26, 235–240. doi: 10.1101/gad.182618.111
- Wei, H., and Yu, X. (2016). Functions of PARylation in DNA damage repair pathways. *Genom. Proteom. Bioinform.* 14, 131–139. doi: 10.1016/j.gpb.2016.05.001
- Wenzel, D. M., Stoll, K. E., and Klevit, R. E. (2011). E2s: structurally economical and functionally replete. *Biochem. J.* 433, 31–42. doi: 10.1042/BJ20100985
- Wilkin, M., Tongngok, P., Gensch, N., Clemence, S., Motoki, M., Yamada, K., et al. (2008). *Drosophila* HOPS and AP-3 complex genes are required for a Deltex-regulated activation of notch in the endosomal trafficking pathway. *Dev. Cell.* 15, 762–772. doi: 10.1016/j.devcel.2008.09.002
- Wu, L. (2006). T lineage progenitors: the earliest steps en route to T lymphocytes. *Curr. Opin. Immunol.* 18, 121–126. doi: 10.1016/j.coi.2006.01.006
- Xu, B., Kim, S., and Kastan, M. B. (2001). Involvement of Brca1 in S-phase and G(2)-phase checkpoints after ionizing irradiation. *Mol. Cell. Biol.* 21, 3445–3450. doi: 10.1128/MCB.21.10.3445-3450.2001
- Xu, P., Tao, X., Zhao, C., Huang, Q., Chang, H., Ban, N., et al. (2017). DTX3L is upregulated in glioma and is associated with glioma progression. *Int. J. Mol. Med.* 40, 491–498. doi: 10.3892/ijmm.2017.3023
- Xu, T., and Artavanis-Tsakonas, S. (1990). Deltex, a locus interacting with the neurogenic genes, Notch, Delta and mastermind in *Drosophila melanogaster*. *Genetics* 126, 665–677. doi: 10.1093/genetics/126.3.665
- Yamada, K., Fuwa, T. J., Ayukawa, T., Tanaka, T., Nakamura, A., Wilkin, M. B., et al. (2011). Roles of *Drosophila* Deltex in Notch receptor endocytic trafficking and activation. *Genes Cell.* 16, 261–272. doi: 10.1111/j.1365-2443.2011.01488.x
- Yamamoto, N., Yamamoto, S., Inagaki, F., Kawaichi, M., Fukamizu, A., Kishi, N., et al. (2001). Role of Deltex-1 as a transcriptional regulator downstream of the Notch receptor. *J. Biol. Chem.* 276, 45031–45040. doi: 10.1074/jbc.M105245200
- Yan, J., Kim, Y. S., Yang, X. P., Li, L. P., Liao, G., Xia, F., et al. (2007). The ubiquitin-interacting motif containing protein RAP80 interacts with BRCA1 and functions in DNA damage repair response. *Cancer Res.* 67, 6647–6656. doi: 10.1158/0008-5472.CAN-07-0924
- Yan, Q., Dutt, S., Xu, R., Graves, K., Juszczynski, P., Manis, J. P., et al. (2009). BBAP monoubiquitylates histone H4 at lysine 91 and selectively modulates the DNA damage response. *Mol. Cell.* 36, 110–120. doi: 10.1016/j.molcel.2009.08.019
- Yan, Q., Xu, R., Zhu, L., Cheng, X., Wang, Z., Manis, J., et al. (2013). BAL1 and its partner E3 ligase, BBAP, link Poly(ADP-ribose) activation, ubiquitylation, and double-strand DNA repair independent of ATM, MDC1, and RNF8. *Mol. Cell. Biol.* 33, 845–857. doi: 10.1128/MCB.00990-12
- Yang, C. S., Jividen, K., Spencer, A., Dworak, N., Ni, L., Oostdyk, L. T., et al. (2017). Ubiquitin modification by the E3 Ligase/ADP-Ribosyltransferase Dtx3L/Parp9. *Mol. Cell.* 66, 503–516. doi: 10.1016/j.molcel.2017.04.028
- Yao, W., Shan, Z., Gu, A., Fu, M., Shi, Z., and Wen, W. (2018). WW domain-mediated regulation and activation of E3 ubiquitin ligase Suppressor of Deltex. *J. Biol. Chem.* 293, 16697–16708. doi: 10.1074/jbc.RA118.003781
- Yarden, R. I., Pardo-Reoyo, S., Sgagias, M., Cowan, K. H., and Brody, L. C. (2002). BRCA1 regulates the G2/M checkpoint by activating Chk1 kinase upon DNA damage. *Nat. Genet.* 30, 285–289. doi: 10.1038/ng837
- Yoo, S. S., Lee, J. H., Hong, M. J., Choi, J. E., Kang, H. G., Do, S. K., et al. (2020). Effect of genetic variation in Notch regulator DTX1 on SCLC prognosis compared with the effect on NSCLC prognosis. *Thorac. Cancer* 11, 2698–2703. doi: 10.1111/1759-7714.13566
- Yun, T. J., and Bevan, M. J. (2003). Notch-regulated ankyrin-repeat protein inhibits Notch1 signaling: multiple Notch1 signaling pathways involved in T cell development. *J. Immunol.* 170, 5834–5841. doi: 10.4049/jimmunol.170.12.5834
- Zhang, J., Willers, H., Feng, Z., Ghosh, J. C., Kim, S., Weaver, D. T., et al. (2004). Chk2 phosphorylation of BRCA1 regulates DNA double-strand break repair. *Mol. Cell. Biol.* 24, 708–718. doi: 10.1128/MCB.24.2.708-718.2004
- Zhang, P., Yang, Y., Nolo, R., Zweidler-McKay, P. A., and Hughes, D. P. (2010). Regulation of NOTCH signaling by reciprocal inhibition of HES1 and Deltex 1 and its role in osteosarcoma invasiveness. *Oncogene* 29, 2916–2926. doi: 10.1038/nc.2010.62
- Zhang, Y., Mao, D., Roswit, W. T., Jin, X., Patel, A. C., Patel, D. A., et al. (2015). PARP9-DTX3L ubiquitin ligase targets host histone H2BJ and viral 3C protease to enhance interferon signaling and control viral infection. *Nat. Immunol.* 16, 1215–1227. doi: 10.1038/ni.3279

- Zhang, Y., Wang, J., Ding, M., and Yu, Y. (2013). Site-specific characterization of the Asp- and Glu-ADP-ribosylated proteome. *Nat. Methods* 10, 981–984. doi: 10.1038/nmeth.2603
- Zheng, L., and Conner, S. D. (2018). PI5P4Kgamma functions in DTX1-mediated Notch signaling. *Proc. Natl. Acad. Sci. U S A.* 115, E1983–E1990. doi: 10.1073/pnas.1712142115
- Zheng, N., and Shabek, N. (2017). Ubiquitin ligases: structure, function, and regulation. *Annu. Rev. Biochem.* 86, 129–157. doi: 10.1146/annurev-biochem-060815-014922
- Zhong, M., Lee, G. M., Sijbesma, E., Ottmann, C., and Arkin, M. R. (2019). Modulating protein-protein interaction networks in protein homeostasis. *Curr. Opin. Chem. Biol.* 50, 55–65. doi: 10.1016/j.cbpa.2019.02.012
- Zhuang, J., Zhang, J., Willers, H., Wang, H., Chung, J. H., van Gent, D. C., et al. (2006). Checkpoint kinase 2-mediated phosphorylation of BRCA1 regulates the fidelity of nonhomologous end-joining. *Cancer Res.* 66, 1401–1408. doi: 10.1158/0008-5472.CAN-05-3278
- Zou, T., and Lin, Z. (2021). The involvement of ubiquitination machinery in cell cycle regulation and cancer progression. *Int. J. Mol. Sci.* 22:5754. doi: 10.3390/ijms22115754
- Zweifel, M. E., Leahy, D. J., and Barrick, D. (2005). Structure and Notch receptor binding of the tandem WWE domain of Deltex. *Structure* 13, 1599–1611. doi: 10.1016/j.str.2005.07.015
- Conflict of Interest:** The authors declare that the research was conducted in the absence of any commercial or financial relationships that could be construed as a potential conflict of interest.
- Publisher's Note:** All claims expressed in this article are solely those of the authors and do not necessarily represent those of their affiliated organizations, or those of the publisher, the editors and the reviewers. Any product that may be evaluated in this article, or claim that may be made by its manufacturer, is not guaranteed or endorsed by the publisher.
- Copyright © 2021 Wang, Sun, He and Liu. This is an open-access article distributed under the terms of the Creative Commons Attribution License (CC BY). The use, distribution or reproduction in other forums is permitted, provided the original author(s) and the copyright owner(s) are credited and that the original publication in this journal is cited, in accordance with accepted academic practice. No use, distribution or reproduction is permitted which does not comply with these terms.



# Tumor Suppressor FBXW7 and Its Regulation of DNA Damage Response and Repair

Huiyin Lan<sup>1,2</sup> and Yi Sun<sup>3,4\*</sup>

<sup>1</sup> Department of Thoracic Radiation Oncology, Zhejiang Cancer Hospital, Cancer Hospital of University of Chinese Academy of Sciences, Hangzhou, China, <sup>2</sup> Institute of Cancer and Basic Medicine, Chinese Academy of Sciences, Hangzhou, China, <sup>3</sup> Cancer Institute of the Second Affiliated Hospital, Institute of Translational Medicine, Zhejiang University School of Medicine, Hangzhou, China, <sup>4</sup> Cancer Center, Zhejiang University, Hangzhou, China

## OPEN ACCESS

### Edited by:

Daming Gao,  
Shanghai Institute of Biochemistry  
and Cell Biology, Chinese Academy  
of Sciences (CAS), China

### Reviewed by:

Xiangpeng Dai,  
Jilin University, China  
Mathew J. K. Jones,  
University of Queensland, Australia

### \*Correspondence:

Yi Sun  
yisun@zju.edu.cn

### Specialty section:

This article was submitted to  
Cell Growth and Division,  
a section of the journal  
Frontiers in Cell and Developmental  
Biology

**Received:** 01 August 2021

**Accepted:** 05 October 2021

**Published:** 25 October 2021

### Citation:

Lan H and Sun Y (2021) Tumor  
Suppressor FBXW7 and Its  
Regulation of DNA Damage  
Response and Repair.  
Front. Cell Dev. Biol. 9:751574.  
doi: 10.3389/fcell.2021.751574

The proper DNA damage response (DDR) and repair are the central molecular mechanisms for the maintenance of cellular homeostasis and genomic integrity. The abnormality in this process is frequently observed in human cancers, and is an important contributing factor to cancer development. FBXW7 is an F-box protein serving as the substrate recognition component of SCF (SKP1-CUL1-F-box protein) E3 ubiquitin ligase. By selectively targeting many oncoproteins for proteasome-mediated degradation, FBXW7 acts as a typical tumor suppressor. Recent studies have demonstrated that FBXW7 also plays critical roles in the process of DDR and repair. In this review, we first briefly introduce the processes of protein ubiquitylation by SCF<sup>FBXW7</sup> and DDR/repair, then provide an overview of the molecular characteristics of FBXW7. We next discuss how FBXW7 regulates the process of DDR and repair, and its translational implication. Finally, we propose few future perspectives to further elucidate the role of FBXW7 in regulation of a variety of biological processes and tumorigenesis, and to design a number of approaches for FBXW7 reactivation in a subset of human cancers for potential anticancer therapy.

**Keywords:** cancer, DDR, DNA repair, FBXW7, ubiquitylation

## INTRODUCTION

### Protein Ubiquitylation and SCF E3 Ligase With FBXW7 as a Substrate Receptor

Ubiquitylation is a typical post-translational modification, that couples with proteasome, designated as ubiquitin-proteasome system (UPS), as the key proteolytic mechanism in eukaryotes for timely degradation of cellular proteins (Hershko et al., 2000). In general, the UPS-mediated protein degradation includes two steps: (1) covalent attachment of the small peptide ubiquitin to a substrate, a process called ubiquitylation; (2) delivery of ubiquitylated substrates into 26S proteasome for degradation. Ubiquitylation is a well-defined three-step enzymatic cascade catalyzed sequentially by the ubiquitin-activating enzymes (E1s), ubiquitin-conjugating enzymes (E2s), and ubiquitin ligases (E3s) (Ciechanover, 1998). Crucially, E3s determine the substrate specificity through selectively recognizing and directly binding with substrate proteins doomed for ubiquitylation and subsequent degradation.



Among the estimated >600 human E3 ubiquitin ligases, SCF (SKP1-CUL1-F-box protein) is the best studied member of CRL (Cullin-RING-Ligase) family of E3 enzymes. The SCF is a multi-component E3, consisting of a scaffold cullin-1, an adaptor SKP1, a E2 binding RING-domain protein (RBX1/RBX2), and a substrate-receptor F-box protein (Zhao and Sun, 2013; **Figure 1A**). Although mammalian genome contains 69 F-box proteins (Jin et al., 2004), only three, namely FBXW7,  $\beta$ -TrCP, and SKP2 are well defined and characterized (Skaar et al., 2014). Among these three, FBXW7 is a typical tumor suppressor that promotes the ubiquitylation and degradation of many cellular oncoproteins, and is frequently mutated and inactivated in many human cancers (Welcker and Clurman, 2008; Wang et al., 2012; **Figure 2**).

## General Introduction of DNA Damage Response and Repair

Mammalian cells are constantly exposed to external and internal insults, such as ionizing radiation (IR), ultraviolet (UV) light, reactive oxygen species (ROS), and many cellular metabolites. These insults typically cause genomic DNA damage in the forms of single strand breaks (SSBs), double strand breaks (DSBs) or replication fork stagnation, and the other types. Among them, DSBs is the most toxic form of DNA damage (Finn et al., 2012).

Upon DSB, a typical DDR is triggered in a cell in an attempt to repair damaged DNA to maintain the genomic integrity. Specifically, three phosphoinositide 3-kinases: ATM (ataxia telangiectasia mutated), ATR (ATM-and RAD3-related), and DNA-PK (DNA-dependent protein kinase) are first recruited into the damage sites and activated via auto-phosphorylation. They then phosphorylate H2AX into  $\gamma$ H2AX, which directly binds with MDC1 (mediator of DNA damage checkpoint 1), and recruits the MRN (MRE11-RAD50-NBS1) protein complex to accumulate within the damage sites. The MRN complex acts as an amplifier of DDR signals by enhancing the activity of ATM (Sancar et al., 2004), whereas  $\gamma$ -H2AX is a key mediator for recruitment and retention of high concentration of DNA damage repair enzymes, such as 53BP1, RAD51, and BRCA1 in the vicinity of damaged sites (Nakamura et al., 2010). Following the expansion of DDR signals, two DNA damage repair machineries, namely homologous recombination (HR) and non-homologous end joining (NHEJ), are triggered rapidly and executed to repair the damaged DNA. The failure in DDR and repair is the cause of genomic instability, leading to cell death (if the damage is severe), or various gene mutations to trigger tumorigenesis (Srivastava and Raghavan, 2015).

During the process of DNA damage response and repair, the chromatin and repairing factors are regulated by a spectrum of post-translational modifications including phosphorylation, acetylation, methylation, and ubiquitylation (Wurtele and Verreault, 2006; Van and Santos, 2018). In particular, FBXW7, a receptor protein of SCF E3 ubiquitin ligase, has been recently shown to play fundamental roles in DDR and repair, which is the focus of this review.

## MOLECULAR CHARACTERIZATION OF FBXW7

### Isoforms and Subcellular Localizations

The human *FBXW7* gene is localized at chromosome 4q32, a region deleted in 30% of cancers, and encodes three different isoforms (FBXW7 $\alpha$ ,  $\beta$ , and  $\gamma$ ), derived from alternative splicing of the same transcript (Davis et al., 2014). These three isoforms share 10 common exons, encoding three conserved functional domains: (1) the DD dimerization domain, (2) F-box domain to recruit other SCF components, essential for its E3 ligase activity, and (3) substrate recognizing WD40 domain (Hao et al., 2007; **Figure 1B**). Three isoforms vary at the N-terminus and have different subcellular locations with FBXW7 $\alpha$  in the nucleoplasm, FBXW7 $\beta$  in the cytoplasm, and FBXW7 $\gamma$  in the nucleolus (Davis et al., 2014). FBXW7 $\alpha$  is functionally the most dominant isoform, which is ubiquitously expressed in most human tissues; FBXW7 $\beta$  expression is mainly found in brain and testis, whereas FBXW7 $\gamma$  is poorly understood and expressed mainly in muscles (Spruck et al., 2002; Matsumoto et al., 2006).

### Dimerization

Dimerization is a common phenomenon and key regulatory modality for FBXW7 (Tang et al., 2007; Welcker and Clurman, 2007; Welcker et al., 2013), as well as for other F-box proteins, such as  $\beta$ -TrCP (Suzuki et al., 2000) and SKP2 (Inuzuka et al., 2012). The FBXW7 dimerization is mediated by the DD domain which enhances its catalytic efficiency for substrate degradation with two possible underlying mechanisms (Tang et al., 2007; Welcker et al., 2013): (1) Dimerization enhances the binding affinity between FBXW7 and substrates. Specifically, the dimer form of SCF<sup>FBXW7</sup> provides spatial variability for accommodating diverse acceptor lysine geometries in both substrates and ubiquitin chain; and (2) The dimer-orthologs may provide suboptimal and independent recognition sites for substrates, serving as a complementary “buffer” against deleterious mutations in the WD40 domain (Welcker et al., 2013). Furthermore, under overexpressed conditions, FBXW7 could form the stable dimeric form by preventing autoubiquitylation of the monomeric form (Min et al., 2012; Lan et al., 2019). However, a contradictory study showed that while endogenous monomers and dimers are equally stable, the exogenous FBXW7 monomers appears to be more stable than that of dimers (Welcker et al., 2013). Exact reason for this discrepancy is unclear. The authors used wild-type FBXW7 monomer coupled with ubiquitylation-dead FBXW7 $\Delta$ F monomer and proposed that *trans*-autoubiquitylation may be a major destabilization mechanism. Another possibility is that FBXW7 overexpression may trigger a limiting factor, such as a deubiquitylating enzyme, to block FBXW7 degradation (Welcker et al., 2013).

Recently, we and the others found that FBXW7 dimerization was regulated by several FBXW7-interacting proteins. For example, the prolyl isomerase PIN1 interacts with FBXW7 to prevent its dimerization in a phosphorylation-dependent manner (Min et al., 2012), whereas LSD1 directly binds to FBXW7 to

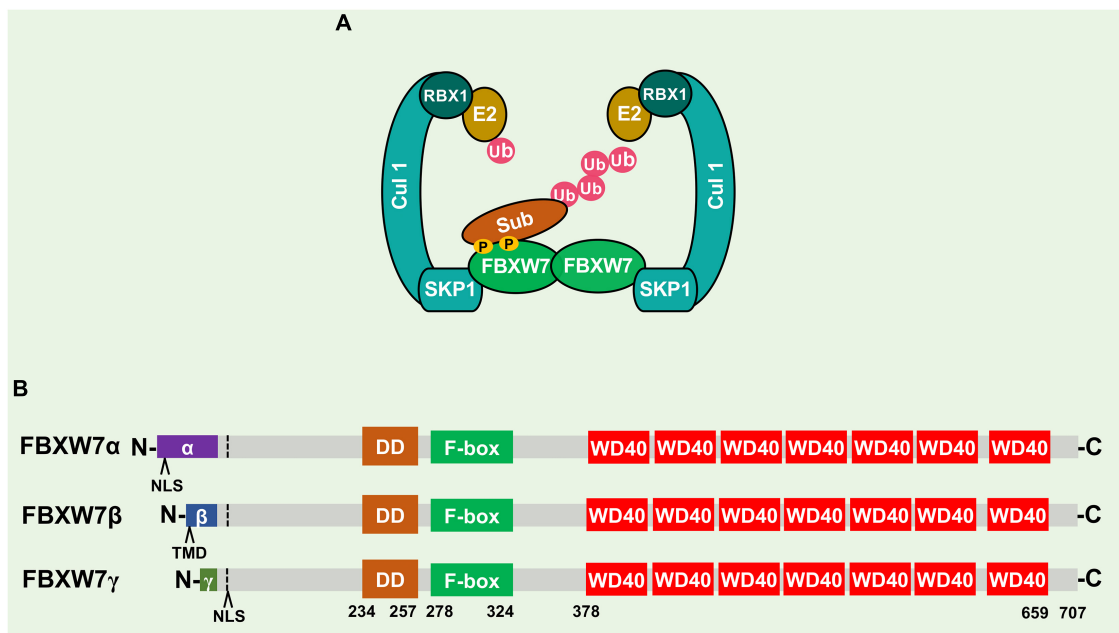


**FIGURE 1 |** Schematics of SCF, FBXW7, and FBXW7 isoforms. **(A)** SCF<sup>FBXW7</sup> consists of a scaffold cullin-1 (CUL-1), an adaptor SKP1, a RING-domain protein (RBX1/RBX2), and a substrate-receptor F-box protein (FBXW7). Shown is SCF<sup>FBXW7</sup> complex in FBXW7 dimerization format for ubiquitylation of a substrate. **(B)** Three FBXW7 isoforms ( $\alpha$ ,  $\beta$ , and  $\gamma$ ) with domain alignment. NLS, nuclear localization signal; TMD, transmembrane domain; DD, dimerization domain.

disrupt FBXW7 dimerization, leading to its self-ubiquitylation (Lan et al., 2019).

## Phosphorylation

FBXW7 was also regulated by phosphorylation which also affects its stability. One study showed that extracellular signal-regulated kinase (ERK) directly interacted with and phosphorylated FBXW7 at Thr<sup>205</sup>, which promoted FBXW7 ubiquitylation in a PIN-1 dependent manner in pancreatic cancer cells, although exactly how ERK-mediated FBXW7 phosphorylation triggers FBXW7 ubiquitylation remains elusive (Ji et al., 2015). Nevertheless, the study revealed a new mechanism by which the Kras-MAPK signal promotes pancreatic tumorigenesis via promoting degradation of tumor suppressor FBXW7. Another study showed that PLK1 phosphorylates FBXW7 at Ser<sup>58</sup> and Thr<sup>284</sup> to promote FBXW7 self-ubiquitylation, leading to stabilization of FBXW7 substrate N-MYC, which in turn transactivates PLK1, thus establishing a positive feed-forward loop that enhance MYC-regulated oncogenic programs (Xiao et al., 2016). On the contrary, two studies showed that FBXW7 phosphorylation at Ser<sup>227</sup> by either serum and glucocorticoid-regulated kinase 1 (SGK1) or phosphoinositide 3-kinase (PI3K), respectively, switched the catalytic activity of FBXW7 toward its substrates instead of targeting itself for self-ubiquitylation (Mo et al., 2011; Schulein et al., 2011). Thus, FBXW7 phosphorylation appears to play critical role in FBXW7 stability in the manner dependent of the kinases and their phosphorylation sites. In addition, protein kinase (PK) C mediated FBXW7 phosphorylation at Ser<sup>8</sup>/Ser<sup>10</sup> was reported to be involved in the nuclear localization of FBXW7 $\alpha$  (Durgan and Parker, 2010).

## Mutations in Human Cancers

Consistent with its role as a tumor suppressor, FBXW7 is the most frequently mutated gene among all the genes encoding F-box proteins in human cancers. We performed the meta-analyses of the cBioPortal Database<sup>1</sup> and found an overall FBXW7 somatic mutation rate of 3.23% in human cancers (1,497 cases out of 46,305 tested), though different cancer types exhibit different mutational spectra (**Figure 2A**). The cancer with the highest mutational frequency is endometrial cancer (20.5%), followed by colorectal cancer (15.7%), cervical cancer (13.6), and esophagogastric adenocarcinoma (10.7%). Significantly, most of the FBXW7 mutations are single nucleotide change, resulting in single amino acid substitutions, within the WD40 domains responsible for substrate binding. As such, the mutations of these key residues often disrupt FBXW7 binding with its oncogenic substrates. **Figure 2B** showed three mutation hotspots R465, R479, and R505 (Welcker and Clurman, 2008; Davis et al., 2014), representing as much as 27.3% of cases (408/1497) found in all FBXW7 mutations, along with other mutation sites detected in more than 15 cases in all human cancers, including R224, R278, R367, G423, R441, Y545, S582, R658, R668, and R689.

## Known FBXW7 Substrates

FBXW7 is well-known for its tumor suppressor function against cancer development by targeting a variety of oncoproteins for proteasomal degradation. A majority of FBXW7 substrates identified and characterized to date were summarized in

<sup>1</sup><https://www.cbioportal.org/>

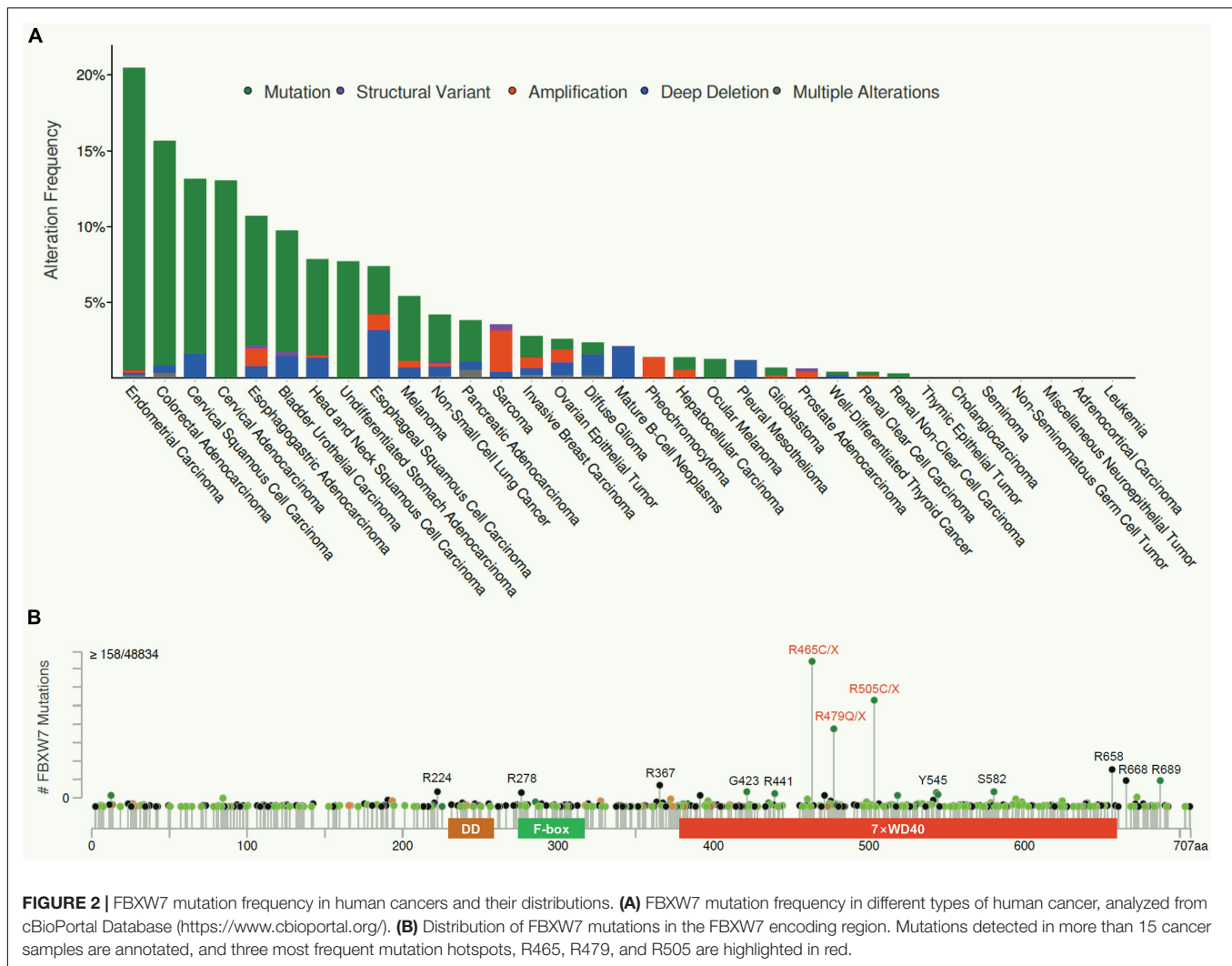


**Table 1.** Almost all substrates contain a evolutionarily conserved phosphorylation motif, designated as CDC4 phospho-degron (CPD), of which substrate phosphorylation is a prerequisite event for FBXW7 binding and subsequent ubiquitylation (Nash et al., 2001). Among all FBXW7 substrates, most of them are well-known oncoproteins, which play the key roles in regulation of cell growth, apoptosis, differentiation and cell migration among the others (Wang et al., 2012). Some of these oncogenic substrates, such as c-MYC, NOTCH 1, MCL-1, Cyclin E, and c-JUN, likely play a driver role in FBXW7-associated cancers (Fryer et al., 2004; Wei et al., 2005; Welcker and Clurman, 2008; Davis et al., 2014). Taking c-MYC as an example, the studies using both *in vitro* and *in vivo* models showed that c-MYC is a classic substrate of FBXW7. Specifically, FBXW7-mediated c-MYC degradation relies on prior CPD phosphorylation of C-MYC at Thr<sup>58</sup> and Ser<sup>62</sup> by GSK3 and MAPK, respectively (Welcker et al., 2004; Yada et al., 2004). It is, therefore, not surprising that the point mutations on Thr<sup>58</sup> and Ser<sup>62</sup> were found on c-Myc in a variety of human cancers, thus avoiding FBXW7 degradation and being selected with growth

advantage (Bahram et al., 2000). Moreover, in several *fbxw7* KO mouse models, c-Myc was remarkably accumulated to accelerate tumorigenesis and promote tumor growth (Yada et al., 2004; Onoyama et al., 2007).

In addition to these classical substrates targeted by FBXW7 for ubiquitylation and degradation, several non-canonical substrates were also targeted by FBXW7, but not for degradation (Lan and Sun, 2019). For instance, FBXW7 mediated K63-linked polyubiquitylation of XRCC4 to facilitate the NHEJ repair (Zhang et al., 2016); whereas polyubiquitylation of  $\gamma$ -catenin via K63-linkage by FBXW7 led to enhanced suppression of cell proliferation and G2/M cell cycle transition (Li et al., 2018). Most recently, we found that LSD1 acts as a FBXW7 pseudo-substrate, not being ubiquitylated by FBXW7, but triggering FBXW7 self-ubiquitylation and degradation via disrupting FBXW7 dimerization (Lan et al., 2019). Likewise, EBNA1-binding protein 2 (Ebp2) was also shown to behave as a pseudo-substrate, which directly binds with FBXW7 $\gamma$  in the canonical CPD-dependent manner, not for its degradation, but facilitating the nucleolar localization of FBXW7 $\gamma$  (Welcker et al., 2011).

**TABLE 1 |** Summary of FBXW7 substrates.

Substrates	Functions/Pathways	Kinase(s)	References
Aurora A	Protein kinase	GSK3	Kwon et al., 2012
Aurora B	Protein kinase	–	Teng et al., 2012
BLM	DNA helicase	GSK3, CDK2	Kharat et al., 2016
B-Raf	Protein kinase	ERK	de la Cova and Greenwald, 2012
Brg1	Transcription factor	CK1	Huang et al., 2018
C/EBP $\alpha$	Transcription factor	–	Bengoechea-Alonso and Ericsson, 2010a
C/EBP $\delta$	Transcription factor	GSK3	Balamurugan et al., 2013
CCDC6	ATM substrate	–	Zhao et al., 2012
c-JUN	Transcription factor	GSK3	Nateri et al., 2004; Wei et al., 2005
c-MYB	Transcription factor	GSK3, NLK	Kanei-Ishii et al., 2008; Kitagawa et al., 2009
c-MYC	Transcription factor	GSK3, MAPK	Welcker et al., 2004; Yada et al., 2004
CREB3L1/2	Transcription factor	–	Yumimoto et al., 2013
Cyclin E	Cyclin protein, Cell cycle	CDK2, GSK3	Koepp et al., 2001; Moberg et al., 2001; Strohmaier et al., 2001
DEK	Chromatin regulator	GSK3	Babaei-Jadidi et al., 2011
ERG	TMPRSS2-ERG fusion protein	GSK3, WEE1	Hong et al., 2020
FAAP20	Subunit of FA core complex	GSK3	Wang et al., 2016
Fetuin-A	Alpha-2-HS-glycoprotein	–	Zhao et al., 2018
GCSF-R	Cytokine receptor	GSK3	Lochab et al., 2013
GR $\alpha$	Transcription factor	GSK3	Malyukova et al., 2013
HIF1 $\alpha$	Transcription factor	GSK3	Cassavaugh et al., 2011
Jun B	Transcription factor	GSK3	Perez-Benavente et al., 2011
KLF13	Transcription factor	GSK3	Kim et al., 2012
KLF2	Transcription factor	GSK3	Wang et al., 2013
KLF5	Transcription factor	GSK3	Zhao et al., 2010
MCL-1	Bcl2 family protein	GSK3	Inuzuka et al., 2011b; Wertz et al., 2011
MED13/13L	Component of mediator complex	–	Davis et al., 2013
mTOR	Protein kinase	–	Mao et al., 2008
NF1	Ras GTPase regulator	–	Tan et al., 2011
Notch1	Transcription factor	CDK8	Fryer et al., 2004
Nrf1	Transcription factor	GSK3	Biswas et al., 2011
p100	Transcription factor	GSK3	Arabi et al., 2012; Busino et al., 2012; Fukushima et al., 2012
p53	Transcription factor	GSK3, ATM	Galindo-Moreno et al., 2019; Tripathi et al., 2019; Cui et al., 2020
p63	Transcription factor	GSK3	Galli et al., 2010
PDC-1 $\alpha$	Nuclear receptor co-activator	GSK3, p38	Olson et al., 2008
PLK1	Serine/threonine kinase	GSK3	Giraldez et al., 2014
Presenilin	Protease	–	Wu et al., 1998
PU.1	Transcription factor	GSK3	Mishra et al., 2021
RCAN1	Calcineurin A binding protein	–	Lee et al., 2012
REV-ERB $\alpha$	Nuclear receptor	CDK1	Zhao et al., 2016
RIG-1	RNA helicase	–	Wang et al., 2017
SHOC2	RAS activator	MAPK	Xie et al., 2019
SOX9	Transcription factor	GSK3	Hong et al., 2016; Suryo Rahmanto et al., 2016
SRC-3	Nuclear receptor co-activator	GSK3	Wu et al., 2007
SREBP1	Transcription factor	GSK3	Sundqvist et al., 2005
TG1F1	Transcription factor	–	Bengoechea-Alonso and Ericsson, 2010b
Topo II $\alpha$	Topoisomerase	GSK3, CK2	Chen et al., 2011
TPP1	Telomere protection protein 1	GSK3	Wang et al., 2020
XRCC4	DNA repair protein	DNA-PKcs	Zhang et al., 2016
ZNF322A	Transcription factor	CK1, GSK3	Liao et al., 2017
$\gamma$ -Catenin	Transcription factor	–	Li et al., 2018
$\Delta$ Np63 $\alpha$	Transcription factor	GSK3	Galli et al., 2010



## THE ROLE OF FBXW7 IN DNA DAMAGE RESPONSE

By targeting a wide array of protein substrates for ubiquitylation and degradation, FBXW7 was involved in regulatory networks of various biological processes such as cell cycle progression, cell differentiation, apoptosis, and autophagy (Welcker and Clurman, 2008; Davis et al., 2014). However, knowledge on whether and how FBXW7 regulates DNA damage response (DDR) and repair is rather limited. An early study showed that genetic inactivation of *hCDC4* (encoding FBXW7) in karyotype stable colorectal cancer cells resulted in nuclear atypia, such as micronuclei and lobulated or elongated nuclei, as well as chromosomal instability, as evidenced by increased multipolar spindles and euploidy in a manner dependent of cyclin E accumulation (Rajagopalan et al., 2004). However, no rescue experiment nor detailed underlying mechanism was provided to demonstrate whether cyclin E is indeed playing a causal role. Nevertheless, this study did implicate that FBXW7 is likely involved in the maintenance of the genomic integrity. Another *in vivo* study showed that *Fbxw7* is a p53-dependent haploinsufficiency tumor suppressor, and *Fbxw7*<sup>±</sup> mice are much more susceptible to radiation-induced tumorigenesis (Mao et al., 2004). A recent study also showed that *Fbxw7*<sup>±</sup> mice have an increased the risk of developing gastric cancer induced by chemical carcinogen N-methyl-N-nitrosourea

(MNU), which is dependent of the accumulation of DNA damage and c-Myc oncoprotein (Jiang et al., 2017).

Recently, more studies showed that FBXW7 is indeed involved in DDR. Upon DNA damage, FBXW7 was found to promote the ubiquitylation and degradation of several key DDR regulatory proteins, including p53 (Galindo-Moreno et al., 2019; Tripathi et al., 2019; Cui et al., 2020), polo-like kinase 1 (PLK1; Strebhardt, 2010), SOX9 (Hong et al., 2016), and bloom (BLM) helicase (Kharat et al., 2016) among others, which is described below (Figures 3A–D).

### Negative Feedback Loop Between FBXW7 and p53

p53 is the best-known tumor suppressor in human cancer, acting as a transcription factor to regulate a wide range of cellular processes, including growth arrest, apoptosis, senescence, DDR, and DNA repair (Vogelstein et al., 2000). The abundance and activity of p53 were fine-tuned by multiple cellular signals and post-translational modifications. In response to DNA damage and other cellular stresses, p53 level is usually increased due to enhanced protein stabilization, mainly resulting from disruption of Mdm2 binding and Mdm2-mediated degradation (Wade et al., 2013). An early study reported that FBXW7 expression was transcriptionally induced upon p53 accumulation after DNA damage stress, thus demonstrating FBXW7 as a *bona fide*

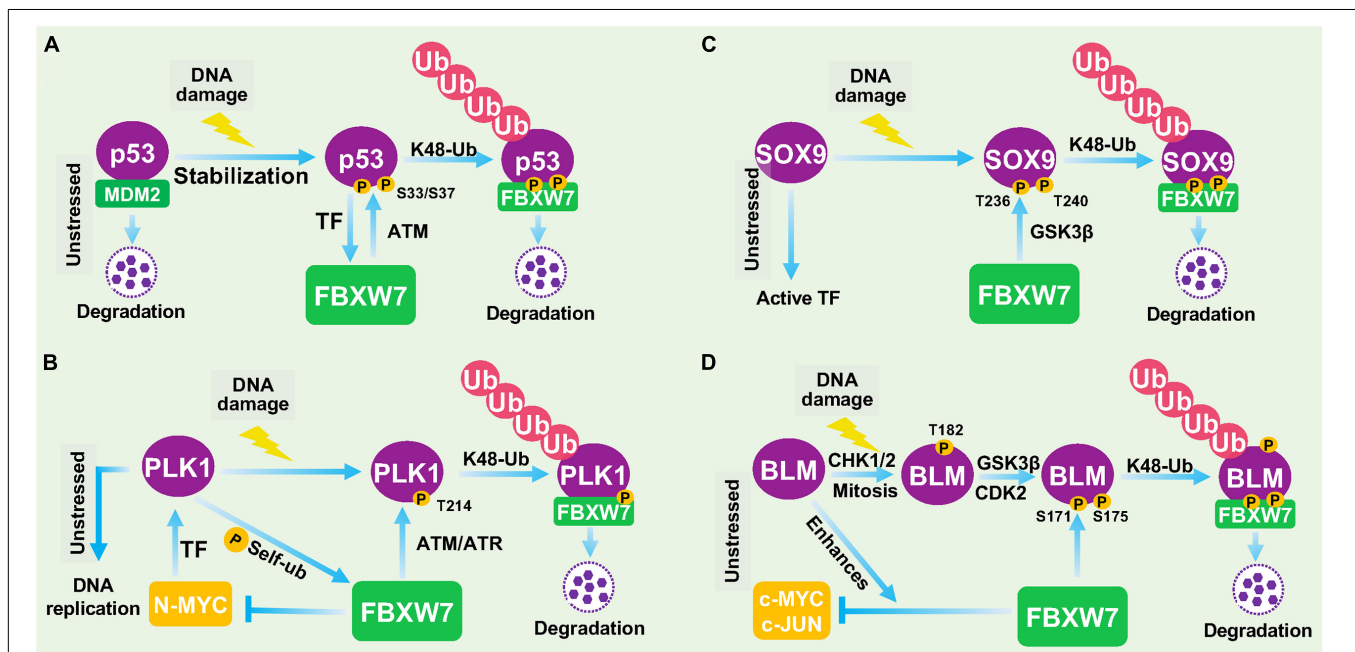


**FIGURE 3 |** FBXW7 in DNA damage responses. **(A)** Negative feedback loop between FBXW7 and p53. Under unstressed condition, p53 level is low due to targeted degradation by MDM2 E3 ligase. Upon DNA damage, p53 protein is accumulated to transcriptionally induce FBXW7 expression; the induced FBXW7 then promotes p53 ubiquitylation and degradation after ATM-mediated p53 phosphorylation at Ser<sup>33/37</sup> residues (Cui et al., 2020). **(B)** PLK1 degradation by FBXW7 upon DDR. Under unstressed condition, PLK1 was transcriptionally induced by N-MYC. PLK also phosphorylates FBXW7 to trigger its self-ubiquitylation and cause N-MYC accumulation. Upon DNA damage, ATM/ATR phosphorylates PLK1 at Thr<sup>214</sup>, which facilitated FBXW7 binding and subsequent ubiquitylation and degradation. **(C)** FBXW7 degrades SOX9 upon DDR. Under unstressed condition, SOX9 acts as a transcription factor. Upon DNA damage, SOX9 was phosphorylated at Thr<sup>236/240</sup> by GSK3β, which facilitated FBXW7 binding and subsequent ubiquitylation and degradation. **(D)** FBXW7 degrades BLM upon DDR. Upon DNA damage, BLM was sequentially phosphorylated at Thr<sup>182</sup> by CHK1/2, and at Thr<sup>171</sup> and Ser<sup>175</sup> by GSK3β/CDK2, which facilitated FBXW7 binding and subsequent ubiquitylation and degradation. TF, Transcription factor.

transcriptional target of p53 using cell culture models (Kimura et al., 2003). A subsequent study using a mouse model confirmed that *Fbxw7* is indeed a p53-dependent, haploinsufficient tumor suppressor gene (Mao et al., 2004). Very interestingly, three recent studies showed that p53 is also subject to post-translational regulation by FBXW7 for targeted degradation in response to DNA damage in multiple human cancer cell lines (Galindo-Moreno et al., 2019; Tripathi et al., 2019; Cui et al., 2020), thus demonstrating FBXW7 participation in DDR to protect cancer cells from DNA damage-induced cell cycle arrest and apoptosis. Collectively, it is apparent that a negative feedback loop exists between FBXW7 and p53. In response to DNA damage, p53 protein is accumulated to transcriptionally induce FBXW7 expression; the induced FBXW7 then promotes p53 degradation to keep the p53 level in check as a mechanism of self-defense (**Figure 3A**). Given both FBXW7 and p53 are frequently mutated in many types of human cancers, we performed a bioinformatics analysis on TCGA databases and found interestingly that mutations of p53 and FBXW7 in human cancers are co-occurrence (Zehir et al., 2017), suggesting that this p53-FBXW7 negative feedback loop may have a biological implication.

### FBXW7 Degrades PLK1 in Response to DNA Damage

PLK1 is a serine/threonine-protein kinase that performs important biological functions mainly in the late G2/M phase of cell cycle, including centrosome maturation, spindle assembly and sister chromatid separation (Strebhardt, 2010). PLK1 was also shown to promote DNA replication by regulating pre-replicative complexes (pre-RCs) loading of mini-chromosome maintenance (MCM) 2/6 (Yoo et al., 2004; Tsvetkov and Stern, 2005). In response to UV-induced DNA damage, PLK1 was degraded by FBXW7 in cells arrested at G1- and S-phase, thus blocking the formation of pre-RCs to prevent the improper progression of cell cycle and avoid the proliferation of cells carrying damaged DNA (Giraldez et al., 2014). Thus, by degrading PLK1 to temporarily halt cell cycle progression, FBXW7 acts as a gate-keeper to ensure genome stability (Giraldez et al., 2014; **Figure 3B**).

### FBXW7 Degrades SOX9 in Response to DNA Damage

SOX9 is a member of the high-mobility group (HMG)-box class of transcription factors, and plays a key role in chondrocytes differentiation and skeletal development (Adam et al., 2015). It was reported that under the DNA damage induced by UV irradiation or genotoxic chemotherapeutic agents, SOX9 was actively degraded in various cancer types and even in normal epithelial cells. Mechanistic study revealed that FBXW7 is the E3 ubiquitin ligase mediating SOX9 degradation in a manner dependent on prior phosphorylation by GSK3 $\beta$  (Hong et al., 2016; **Figure 3C**). However, how FBXW7-mediated SOX9 degradation contributes to overall DDR remains elusive. Furthermore, SOX9 protein was also targeted by FBXW7 for proteasomal degradation in medulloblastoma cells even under

normal unstressed conditions (Suryo Rahmanto et al., 2016), suggesting that FBXW7-mediated SOX9 degradation might be in a cell and context dependent event, and not specific to DDR.

### FBXW7 Degrades Bloom Helicase in Response to DNA Damage

BLM is an ATP-dependent DNA helicase that unwinds single- and double-stranded DNA. Once stalled DNA replication or DNA damage occurs, BLM is recruited to participate in fixing the genomic error (Chu and Hickson, 2009). The interaction between BLM and FBXW7 has been previously reported to enhance FBXW7-mediated c-MYC degradation (Chandra et al., 2013). A more recent study showed that the protein levels of BLM is dynamically fluctuant during cell cycle progression with the interphase cells having a higher level than the mitotic cells. Further mechanistic studies revealed that FBXW7 promoted the K48-linked polyubiquitylation of BLM in a manner dependent on GSK3 $\beta$  and CDK2-mediated prior phosphorylation of BLM at Thr<sup>171</sup> and Ser<sup>175</sup> (Kharat et al., 2016). The authors further found that FBXW7-promoted BLM degradation is a mitosis-specific event requiring prior phosphorylation at Thr<sup>182</sup> by CHK1/CHK2 (**Figure 3D**). Given that CHK1/CHK2 activation is a common signal during DDR, FBXW7-mediated BLM degradation triggered by CHK1/CHK2 is likely involved in the process of DDR, although detailed underlying mechanism remains elusive.

Furthermore, we recently found that FBXW7 was recruited to the DSB sites by poly(ADP-ribose) (PAR) (Zhang Q. et al., 2019) and maintained at DNA damage sites in a ATM-dependent manner upon laser irradiation to facilitate the non-homolog end-joining (NHEJ) repair (Zhang et al., 2016) (see below). The others reported that FBXW7 binds to telomere protection protein 1 (TPP1) and promotes its polyubiquitylation at multi-sites for enhanced degradation, which triggers telomere uncapping and DNA damage response and affects senescence and fibrosis of pulmonary epithelial stem cell (Wang et al., 2020). Upon DNA damage stress in prostate cancer (PCa) cells, *TMPRSS2-ERG* gene fusion product was degraded by FBXW7 in a manner dependent of GSK3 $\beta$  and WEE1 kinases. Blockage of such degradation promoted genotoxic therapy-resistant growth of fusion-positive PCa cells both *in vitro* and *in vivo* (Hong et al., 2020). In nasopharyngeal carcinoma cells, fructose-1,6-bisphosphatase 1 (FBP1) was found to suppress the autoubiquitylation of FBXW7 to restrained mTOR-glycolysis signals and promote radiation-induced apoptosis and DNA damage (Zhang et al., 2021). FBXW7 also cooperated with MDM2 following DDR, to regulate the levels of the pro-proliferative  $\Delta$ Np63 $\alpha$  protein, resulting in cell proliferation (Galli et al., 2010). Finally, in addition to p53, other transcription factors known to be FBXW7 substrates were also reported to be involved in DDR. For example, HIF-1 was involved in  $\gamma$ H2AX accumulation by tumor hypoxia (Wrann et al., 2013), whereas KLF5 plays a significant role in the DNA damage response by regulating the phosphorylation of CHK1/2 (Zhang H. et al., 2019). Taken together, it appears that FBXW7 is indeed implicated in DDR that likely contribute to its role in the maintenance of genome integrity, mainly by targeted

ubiquitylation and degradation of key regulatory proteins, such as p53, PLK1, and BLM.

## THE ROLE OF FBXW7 IN DNA DAMAGE REPAIR

The DDR and repairs are two sequential events which are essential for the maintenance of genomic stability. The DNA attack by different external and internal insults produces a variety of DNA lesion modalities, mainly including simple base modification, base mismatches, bulky DNA adducts, inter-strand and intra-strand crosslinks (ICLs), SSBs and DSBs, which trigger different types of DDRs and repair processes to fix these damages (Roos et al., 2016). For example, base mismatches are repaired by mismatch repair machinery (MMR), ICLs are repaired by NER, HR, and Fanconi Anaemia (FA) repair pathways, whereas DSBs are mainly repaired by NHEJ or HR (Roos et al., 2016). So far, FBXW7 was found to regulate FA and NHEJ pathways by targeting Fanconi anemia core complex-associated protein (FAAP) 20 (Wang et al., 2016, 2019) and XRCC4 (Zhang et al., 2016), respectively (Figure 4).

### In Regulation of Fanconi Anemia Pathway

The Fanconi Anemia (FA) pathway is a DNA repair process responsible for resolving ICLs (Roos et al., 2016). Germ-line mutations of key FA genes caused inherited FA disorders with cancer predisposition. The key step of FA pathway to initiate the repair process is the monoubiquitylation of FANCD2, mediated by FA core complex containing a scaffold protein FANCA.

FANCA has a binding partner, FAAP20, which is required for its stability (Leung et al., 2012). It was reported that FBXW7 promoted the polyubiquitylation of FAAP20 in a manner dependent on GSK3 $\beta$ -mediated prior phosphorylation at Ser<sup>113</sup> in response to DNA damage. Thus, by modulating the levels of FAAP20 and subsequent stability of FANCA, FBXW7 acts as an upstream regulator of FA pathway and its repair process (Wang et al., 2016).

### In Regulation of Non-homologous End Joining Repair

Recently, we reported that in response to DSB DNA damage, ATM is activated to remain FBXW7 at the damage sites and then trigger NHEJ, but not HR, repair (Zhang et al., 2016). Specifically, ionizing radiation caused DNA damage that activates both DNA-PKcs and ATM. On the one hand, DNA-PKcs phosphorylates XRCC4, a key regulator of NHEJ on damaged site, and on the other hand, PAR and ATM recruit FBXW7 to the DSBs sites, where FBXW7 promotes polyubiquitylation of phosphorylated XRCC4 via the K63 linkage. Polyubiquitylated XRCC4 was not delivered to proteasome for degradation, rather to build up a platform that facilitated the recruitment of Ku70/80 heterodimer to promote NHEJ repair (Zhang et al., 2016; Zhang Q. et al., 2019). Thus, FBXW7 is actively involved in processes of DNA damage repair by FA and NHEJ.

Furthermore, it is worth noting that c-MYC, as a typical substrate of FBXW7, was also reported to function in DNA damage repair. Specifically, it was reported that c-MYC suppresses DSB accumulation in a manner strictly dependent of Polymerase Associated Factor 1 complex (Endres et al., 2021). Another study reported that c-MYC directly interacts with Ku70

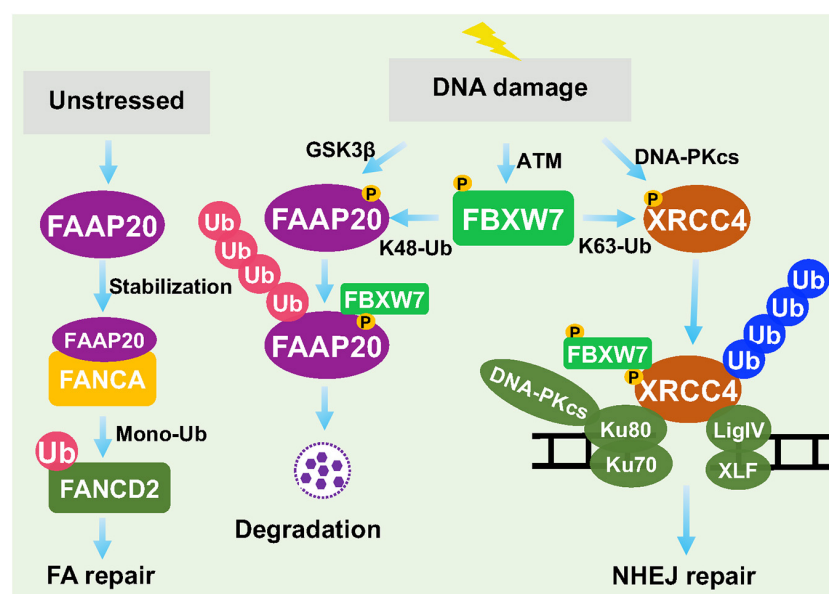


**FIGURE 4 |** FBXW7 in regulation of DNA repair. Under unstressed condition, FAAP20 binds FANCA to facilitate mono-ubiquitylation of FANCD2. Upon DDR, FAAP20 was phosphorylated by GSK3 $\beta$  to facilitate FBXW7 binding and ubiquitylation. On the other hand, DNA-PKcs phosphorylates XRCC4, whereas ATM phosphorylates FBXW7. At the damage site, FBXW7 promoted XRCC4 polyubiquitylation via the K63 linkage to facilitate recruitment of Ku70/Ku80 for NHEJ repair.

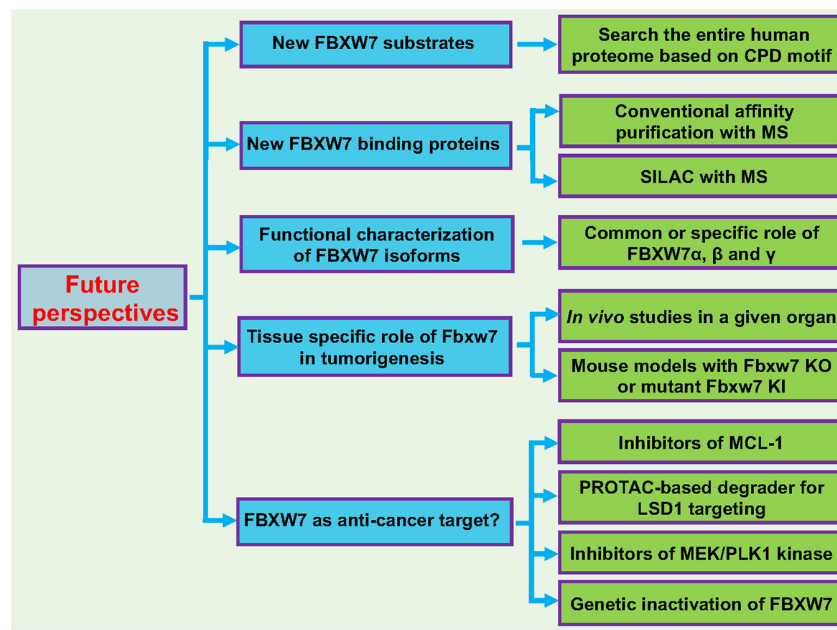


**FIGURE 5 |** Future perspectives. Five future directions are proposed to further broaden our understanding of FBXW7 functions: (1) Identification and characterization of new FBXW7 substrates; (2) Identification and characterization of FBXW7 binding proteins; (3) Functional characterization of FBXW7 isoforms ( $\alpha$ ,  $\beta$ , and  $\gamma$ ); (4) Tissue specific role of Fbxw7 in tumorigenesis using mouse cKO or KI models; (5) Target human cancers by reactivating FBXW7. See text for details.

protein through its Myc box II (MBII) domain to block DSB repair and V(D)J recombination, which probably occur through inhibition of the NHEJ pathway (Li et al., 2012). Given the fact that FBXW7 has a variety of substrates, it is likely that some of these substrates may regulate DNA damage repair in an indirect manner, if not in a direct manner, which is, however, out of scope of this focused review.

## CONCLUSION AND FUTURE PERSPECTIVES

In the past two decades, the FBXW7-related studies were mainly focused on identification and characterization of its substrates. To date, more than 40 proteins have been identified, and most of them are transcription factors that regulate a broad range of biological processes. By timely modulating ubiquitylation and degradation of these substrates, FBXW7 acts as a central regulator of key biological processes and various cellular signal pathways. However, the knowledge on the role of FBXW7 in DDR and repair is rather limited, though the involvement of FBXW7 in genomic stability was implicated almost two decades ago. In this review, we summarized current available data and concluded that FBXW7 is indeed actively involved in DDR and repair processes by acting as an E3 ligase to promote ubiquitylation of (a) key DDR regulatory proteins for degradation or (b) key repair proteins for facilitating repair process (Figures 3, 4).

Here, we propose few future studies on FBXW7 to further elucidate the role of FBXW7 in a variety of biological processes (Figure 5).

### Identification and Characterization of Additional FBXW7 Substrates Which May or May Not Be Involved in DNA Damage Response and Repair Processes

Given that FBXW7 binding motif, also known as CDC4 phosphodegron (CPD), on a substrate has been well-defined, the quick and easy way to identify new putative FBXW7 substrate candidates is to search the entire human proteome for CPD motif or its modified version with mimicking negative charged residues within the CPD motif, followed by detailed characterization of candidates as the *bona fide* FBXW7 substrates. FBXW7 functions will be further extended, based upon the known functions of these newly identified substrates in a given signaling pathway.

### Identification and Characterization of FBXW7 Binding Proteins That Regulate FBXW7 Functions

Conventional affinity purification coupled with Mass-Spectrometry (MS) or stable isotope labeling by amino acids in cell culture (SILAC) with the MS-based quantitative proteomics (Ong and Mann, 2006) can be used to identify FBXW7 binding proteins under unstressed physiological condition or after a given stress of interest. The identified binding proteins can also be FBXW7 substrates or merely FBXW7 binding proteins not subjected to FBXW-mediated ubiquitylation. FBXW7 may have novel functions independent of its E3 ligase activity, which can be identified and defined through the characterization of these binding partners.



## Functional Characterization of FBXW7 Isoforms

The majority of current studies have been focused upon FBXW7 $\alpha$  localized in the nucleus. No detailed functional characterization of other isoforms, particularly FBXW7 $\gamma$  localized in the nucleolus. It is unclear whether other SCF components are localized in nucleolus and if not, FBXW7 $\gamma$  may not act as an active E3 ligase. It will be interesting to define the role of this isoform, particularly in response to ribosomal stress that is mainly triggered in nucleolus (Golomb et al., 2014), a subcellular organelle which also plays a role in maintenance of genome stability (Lindstrom et al., 2018).

## Tissue Specific Role of Fbxw7 in Tumorigenesis

In human cancer cells, FBXW7 is frequently inactivated via point mutations, allele deletion, promoter methylation, and induced self-ubiquitylation (Welcker and Clurman, 2008; Wang et al., 2012; Lan and Sun, 2019). It is very likely that cancer cells with FBXW7 inactivation have growth advantage and were selected during tumorigenesis. However, these correlation-based studies did not validate whether FBXW7 truly plays a causal role in organ-specific tumorigenesis. Thus, for *in vivo* validation of the role of FBXW7 in tumorigenesis in a given organ, the mouse models with tissue-specific *Fbxw7* KO or mutant *Fbxw7* KI should be generated, particularly in those tissues with high frequency of FBXW7 alterations (Figure 2A). A detailed characterization of these genetically modified mouse models will reveal whether FBXW7 indeed plays a driver role or merely co-operate with other dominant oncogenes (such as Kras activation) or tumor suppressors (such as loss of p53 or Pten) in compound mouse models in a particular organ.

## FBXW7 as a Potential Anti-cancer Target?

FBXW7 is a tumor suppressor and FBXW7 itself certainly cannot be served as a direct anti-cancer target. However, few correlation studies have shown an association of FBXW7 expression with chemotherapeutic sensitivity. For example, loss of FBXW7 was associated with increased sensitivity of lung cancer cells to histone deacetylase (HDAC) inhibitor, MS-275 (Yokobori et al., 2014), and tumor cell lines harboring deletions or mutations in FBXW7 are particularly sensitive to rapamycin treatment (Mao et al., 2008). Given the fact that pro-survival protein MCL-1 is a substrate of FBXW7, it is not surprised that T-cell acute lymphoblastic leukemia cell lines with defective FBXW7 have increased levels of MCL1 and are particularly resistance to BCL2 antagonist ABT-737 in a manner dependent of MCL1 (Inuzuka et al., 2011a). Furthermore, FBXW7 loss conferred resistance to anti-tubulin agents and promoted chemotherapeutic-induced polyploidy due to MCL1 accumulation (Wertz et al., 2011). These studies together suggest that loss-of-function FBXW7 mutations indeed impact chemotherapy sensitivity, although it is mainly due to accumulation of its anti-apoptotic substrates, not directly related to its DNA repair function. Nevertheless,

small molecule inhibitors of MCL1, currently under clinical development (Hird and Tron, 2019; Negi and Murphy, 2021), are certainly a proper choice to target human cancers with FBXW7 mutations.

On the other hand, the upstream regulators of FBXW7 also provide sound strategies for potential FBXW7-based translational application in cancer treatment. Specifically, several oncoproteins have been shown to trigger FBXW7 self-ubiquitylation and targeting these oncoproteins would, in theory, stabilize FBXW7 to execute its tumor suppressor function.

The first case is LSD1 (lysine-specific demethylase-1), an enzyme overexpressed in many human cancers with correlation of poor patient survival (Kooistra and Helin, 2012), which has been validated as an attractive cancer target with extensive drug discovery efforts (Fu et al., 2017). We recently found that LSD1 is a pseudo FBXW7 substrate, which binds with FBXW7 in the classical CPD-dependent manner. Instead of being ubiquitylated by FBXW7 for proteasomal degradation, LSD1-FBXW7 binding inhibited FBXW7 dimerization, leading to FBXW7 self-ubiquitylation and subsequent degradation via proteasome and lysosome systems in a manner independent of its demethylase activity (Lan et al., 2019; Gu et al., 2020). Currently, several LSD1 demethylase inhibitors have been in the Phase I/IIa clinical trials (Hosseini and Minucci, 2017). Future drug discovery effort could be directed to screen for small molecules that specifically bind to LSD1, not necessary to inhibit its demethylase activity, followed by discovery of PROTAC-based degrader (Gu et al., 2018) for LSD1 targeting. This type of LSD1 specific PROTAC drugs should have broad applications for the treatment of human cancers harboring a wild type FBXW7 with LSD1 overexpression by reactivating FBXW7, as well as for potential immunotherapy in combination with PD-L1 blockade (Sheng et al., 2018).

The second example is the ERK kinase that has been shown to phosphorylate FBXW7, leading to its destabilization in a manner dependent of PIN-1 (Ji et al., 2015). The inhibitors of MEK, an ERK upstream kinase, have also been in a number of Phase II/III clinical trials (Kim and Giaccone, 2018). The third case is the PLK kinase that has also been shown to phosphorylate FBXW7 to promote its self-ubiquitylation (Xiao et al., 2016). Again, several PLK inhibitors were also under clinic development (Janning and Fiedler, 2014). These inhibitors may have new applications in the treatment of human cancers with activated MAPK or PLK1 signals by reactivating FBXW7. Finally, in a subset of human cancers with developed resistance to chemo- and radiotherapies, but harboring wild-type p53, inactivation of FBXW7 via genetic approaches may reactivate p53 to overcome the resistance (Cui et al., 2020).

## AUTHOR CONTRIBUTIONS

HL wrote the first draft of the manuscript. YS revised and finalized the manuscript. Both authors contributed to the article and approved the submitted version.

## FUNDING

This work was supported by the National Key R&D Program of China (2016YFA0501800 to YS), National Natural Science Foundation of China (82102947 to HL), and National Natural Science Foundation of China (81630076 to YS).

## REFERENCES

- Adam, R. C., Yang, H., Rockowitz, S., Larsen, S. B., Nikolova, M., Oristian, D. S., et al. (2015). Pioneer factors govern super-enhancer dynamics in stem cell plasticity and lineage choice. *Nature* 521:366. doi: 10.1038/nature14289
- Arabi, A., Ullah, K., Branca, R. M. M., Johansson, J., Bandarra, D., Haneklaus, M., et al. (2012). Proteomic screen reveals Fbw7 as a modulator of the NF-kappa B pathway. *Nat. Commun.* 3:976. doi: 10.1038/ncomms1975
- Babaei-Jadidi, R., Li, N. N., Saadeddin, A., Spencer-Dene, B., Jandke, A., Muhammad, B., et al. (2011). FBXW7 influences murine intestinal homeostasis and cancer, targeting Notch, Jun, and DEK for degradation. *J. Exp. Med.* 208, 295–312. doi: 10.1084/jem.20100830
- Bahram, F., von der Lehr, N., Cetinkaya, C., and Larsson, L. G. (2000). c-Myc hot spot mutations in lymphomas result in inefficient ubiquitination and decreased proteasome-mediated turnover. *Blood* 95, 2104–2110.
- Balamurugan, K., Sharan, S., Klarmann, K. D., Zhang, Y., Coppola, V., Summers, G. H., et al. (2013). FBXW7 alpha attenuates inflammatory signalling by downregulating C/EBP delta and its target gene Tlr4. *Nat. Commun.* 4:1662. doi: 10.1038/ncomms2677
- Bengoechea-Alonso, M. T., and Ericsson, J. (2010a). The ubiquitin ligase Fbxw7 controls adipocyte differentiation by targeting C/EBP alpha for degradation. *Proc. Natl. Acad. Sci. U.S.A.* 107, 11817–11822. doi: 10.1073/pnas.0913367107
- Bengoechea-Alonso, M. T., and Ericsson, J. (2010b). Tumor suppressor Fbxw7 regulates TGF beta signaling by targeting TGF1 for degradation. *Oncogene* 29, 5322–5328. doi: 10.1038/nc.2010.278
- Biswas, M., Phan, D., Watanabe, M., and Chan, J. Y. (2011). The Fbw7 tumor suppressor regulates nuclear factor E2-related factor 1 transcription factor turnover through proteasome-mediated proteolysis. *J. Biol. Chem.* 286, 39282–39289. doi: 10.1074/jbc.M111.253807
- Busino, L., Millman, S. E., Scotto, L., Kyratsous, C. A., Basrur, V., O'Connor, O., et al. (2012). Fbxw7 alpha- and GSK3-mediated degradation of p100 is a pro-survival mechanism in multiple myeloma. *Nat. Cell Biol.* 14:375. doi: 10.1038/ncb2463
- Cassavaugh, J. M., Hale, S. A., Wellman, T. L., Howe, A. K., Wong, C., and Lounsbury, K. M. (2011). Negative regulation of HIF-1 alpha by an FBW7-mediated degradation pathway during hypoxia. *J. Cell Biochem.* 112, 3882–3890. doi: 10.1002/jcb.23321
- Chandra, S., Priyadarshini, R., Madhavan, V., Tikoo, S., Hussain, M., Mudgal, R., et al. (2013). Enhancement of c-Myc degradation by BLM helicase leads to delayed tumor initiation. *J. Cell Sci.* 126(Pt 16), 3782–3795. doi: 10.1242/jcs.124719
- Chen, M. C., Chen, C. H., Chuang, H. C., Kulp, S. K., Teng, C. M., and Chen, C. S. (2011). Novel mechanism by which histone deacetylase inhibitors facilitate topoisomerase II alpha degradation in hepatocellular carcinoma cells. *Hepatology* 53, 148–159. doi: 10.1002/hep.23964
- Chu, W. K., and Hickson, I. D. (2009). RecQ helicases: multifunctional genome caretakers. *Nat. Rev. Cancer* 9, 644–654.
- Ciechanover, A. (1998). The ubiquitin-proteasome pathway: on protein death and cell life. *EMBO J.* 17, 7151–7160.
- Cui, D., Xiong, X., Shu, J., Dai, X., Sun, Y., and Zhao, Y. (2020). FBXW7 confers radiation survival by targeting p53 for degradation. *Cell Rep.* 30, 497–509.e4. doi: 10.1016/j.celrep.2019.12.032
- Davis, M. A., Larimore, E. A., Fissel, B. M., Swanger, J., Taatjes, D. J., and Clurman, B. E. (2013). The SCF-Fbw7 ubiquitin ligase degrades MED13 and MED13L and regulates CDK8 module association with Mediator. *Gene Dev.* 27, 151–156. doi: 10.1101/gad.207720.112
- Davis, R. J., Welcker, M., and Clurman, B. E. (2014). Tumor suppression by the Fbw7 ubiquitin ligase: mechanisms and opportunities. *Cancer Cell* 26, 455–464. doi: 10.1016/j.ccell.2014.09.013
- de la Cova, C., and Greenwald, I. (2012). SEL-10/Fbw7-dependent negative feedback regulation of LIN-45/Braf signaling in *C. elegans* via a conserved phosphodegron. *Gene Dev.* 26, 2524–2535. doi: 10.1101/gad.203703.112
- Durgan, J., and Parker, P. J. (2010). Regulation of the tumour suppressor Fbw7 alpha by PKC-dependent phosphorylation and cancer-associated mutations. *Biochem. J.* 432, 77–87. doi: 10.1042/BJ20100799
- Endres, T., Solvie, D., Heidelberger, J. B., Andrioletti, V., Baluapuri, A., Ade, C. P., et al. (2021). Ubiquitylation of MYC couples transcription elongation with double-strand break repair at active promoters. *Mol. Cell* 81, 830–844.e13. doi: 10.1016/j.molcel.2020.12.035
- Finn, K., Lowndes, N. F., and Grenon, M. (2012). Eukaryotic DNA damage checkpoint activation in response to double-strand breaks. *Cell Mol. Life Sci.* 69, 1447–1473.
- Fryer, C. J., White, J. B., and Jones, K. A. (2004). Mastermind recruits CycC: CDK8 to phosphorylate the notch ICD and coordinate activation with turnover. *Mol. Cell* 16, 509–520. doi: 10.1016/j.molcel.2004.10.014
- Fu, X., Zhang, P., and Yu, B. (2017). Advances toward LSD1 inhibitors for cancer therapy. *Future Med. Chem.* 9, 1227–1242.
- Fukushima, H., Matsumoto, A., Inuzuka, H., Zhai, B., Lau, A. W., Wan, L. X., et al. (2012). SCFFbw7 modulates the NF kappa B signaling pathway by targeting NF kappa B2 for ubiquitination and destruction. *Cell Rep.* 1, 434–443. doi: 10.1016/j.celrep.2012.04.002
- Galindo-Moreno, M., Giraldez, S., Limon-Mortes, M. C., Belmonte-Fernandez, A., Reed, S. I., Saez, C., et al. (2019). SCF(FBXW7)-mediated degradation of p53 promotes cell recovery after UV-induced DNA damage. *FASEB J.* 33, 11420–11430. doi: 10.1096/fj.201900885R
- Galli, F., Rossi, M., D'Alessandra, Y., De Simone, M., Lopardo, T., Haupt, Y., et al. (2010). MDM2 and Fbw7 cooperate to induce p63 protein degradation following DNA damage and cell differentiation. *J. Cell. Sci.* 123, 2423–2433. doi: 10.1242/jcs.061010
- Giraldez, S., Herrero-Ruiz, J., Mora-Santos, M., Japon, M. A., Tortolero, M., and Romero, F. (2014). SCF(FBXW7alpha) modulates the intra-S-phase DNA-damage checkpoint by regulating Polo like kinase-1 stability. *Oncotarget* 5, 4370–4383. doi: 10.18632/oncotarget.2021
- Golomb, L., Volarevic, S., and Oren, M. (2014). p53 and ribosome biogenesis stress: the essentials. *FEBS Lett.* 588, 2571–2579.
- Gu, F., Lin, Y., Wang, Z., Wu, X., Ye, Z., Wang, Y., et al. (2020). Biological roles of LSD1 beyond its demethylase activity. *Cell Mol. Life Sci.* 77, 3341–3350.
- Gu, S., Cui, D., Chen, X., Xiong, X., and Zhao, Y. (2018). PROTACs: an emerging targeting technique for protein degradation in drug discovery. *Bioessays* 40:e1700247.
- Hao, B., Oehlmann, S., Sowa, M. E., Harper, J. W., and Pavletich, N. P. (2007). Structure of a Fbw7-Skp1-cyclin E complex: multisite-phosphorylated substrate recognition by SCF ubiquitin ligases. *Mol. Cell.* 26, 131–143. doi: 10.1016/j.molcel.2007.02.022
- Hershko, A., Ciechanover, A., and Varshavsky, A. (2000). Basic medical research award. the ubiquitin system. *Nat. Med.* 6, 1073–1081.
- Hird, A. W., and Tron, A. E. (2019). Recent advances in the development of Mcl-1 inhibitors for cancer therapy. *Pharmacol. Ther.* 198, 59–67.
- Hong, X., Liu, W., Song, R., Shah, J. J., Feng, X., Tsang, C. K., et al. (2016). SOX9 is targeted for proteasomal degradation by the E3 ligase FBW7 in response to DNA damage. *Nucleic Acids Res.* 44, 8855–8869. doi: 10.1093/nar/gkw748
- Hong, Z., Zhang, W., Ding, D. L., Huang, Z. L., Yan, Y. Q., Cao, W., et al. (2020). DNA damage promotes TMPRSS2-ERG oncoprotein destruction and prostate cancer suppression via signaling converged by GSK3 beta and WEE1. *Mol. Cell* 79:1008. doi: 10.1016/j.molcel.2020.07.028
- Hosseini, A., and Minucci, S. (2017). A comprehensive review of lysine-specific demethylase 1 and its roles in cancer. *Epigenomics* 9, 1123–1142.

## ACKNOWLEDGMENTS

We would like to thank Haomin Li at the Children's Hospital of Zhejiang University School of Medicine for his bioinformatics analysis on association of mutations of p53 and FBXW7 in human cancers.

- Huang, L. Y., Zhao, J. J., Chen, H., Wan, L. X., Inuzuka, H., Guo, J. P., et al. (2018). SCFFBW7-mediated degradation of Brg1 suppresses gastric cancer metastasis. *Nat. Commun.* 9:3569. doi: 10.1038/s41467-018-06038-y
- Inuzuka, H., Gao, D., Finley, L. W., Yang, W., Wan, L., Fukushima, H., et al. (2012). Acetylation-dependent regulation of Skp2 function. *Cell* 150, 179–193.
- Inuzuka, H., Shaik, S., Onoyama, I., Gao, D., Tseng, A., Maser, R. S., et al. (2011a). SCF(FBW7) regulates cellular apoptosis by targeting MCL1 for ubiquitylation and destruction. *Nature* 471, 104–109. doi: 10.1038/nature09732
- Inuzuka, H., Shaik, S., Onoyama, I., Gao, D. M., Tseng, A., Maser, R. S., et al. (2011b). SCFFBW7 regulates cellular apoptosis by targeting MCL1 for ubiquitylation and destruction. *Nature* 471, 104–U28.
- Janning, M., and Fiedler, W. (2014). Volasertib for the treatment of acute myeloid leukemia: a review of preclinical and clinical development. *Future Oncol.* 10, 1157–1165.
- Ji, S., Qin, Y., Shi, S., Liu, X., Hu, H., Zhou, H., et al. (2015). ERK kinase phosphorylates and destabilizes the tumor suppressor FBW7 in pancreatic cancer. *Cell Res.* 25, 561–573. doi: 10.1038/cr.2015.30
- Jiang, Y. N., Qi, X. M., Liu, X. Y., Zhang, J., Ji, J., Zhu, Z. G., et al. (2017). Fbxw7 haploinsufficiency loses its protection against DNA damage and accelerates MNU-induced gastric carcinogenesis. *Oncotarget* 8, 33444–33456. doi: 10.18632/oncotarget.16800
- Jin, J., Cardozo, T., Lovering, R. C., Elledge, S. J., Pagano, M., and Harper, J. W. (2004). Systematic analysis and nomenclature of mammalian F-box proteins. *Genes Dev.* 18, 2573–2580. doi: 10.1101/gad.1255304
- Kaneishi, C., Nomura, T., Takagi, T., Watanabe, N., Nakayama, K. I., and Ishii, S. (2008). Fbxw7 Acts as an E3 ubiquitin ligase that targets c-Myb for Nemo-like Kinase (NLK)-induced degradation. *J. Biol. Chem.* 283, 30540–30548. doi: 10.1074/jbc.M804340200
- Kharat, S. S., Tripathi, V., Damodaran, A. P., Priyadarshini, R., Chandra, S., Tikoo, S., et al. (2016). Mitotic phosphorylation of Bloom helicase at Thr182 is required for its proteasomal degradation and maintenance of chromosomal stability. *Oncogene* 35, 1025–1038. doi: 10.1038/ncr.2015.157
- Kim, C., and Giaccone, G. (2018). MEK inhibitors under development for treatment of non-small-cell lung cancer. *Expert Opin. Investig. Drugs* 27, 17–30.
- Kim, D. S., Zhang, W., Millman, S. E., Hwang, B. J., Kwon, S. J., Clayberger, C., et al. (2012). Fbw7 gamma-mediated degradation of KLF13 prevents RANTES expression in resting human but not murine T lymphocytes. *Blood* 120, 1658–1667. doi: 10.1182/blood-2012-03-415968
- Kimura, T., Gotoh, M., Nakamura, Y., and Arakawa, H. (2003). hCDC4b, a regulator of cyclin E, as a direct transcriptional target of p53. *Cancer Sci.* 94, 431–436. doi: 10.1111/j.1349-7006.2003.tb01460.x
- Kitagawa, K., Hiramatsu, Y., Uchida, C., Isobe, T., Hattori, T., Oda, T., et al. (2009). Fbw7 promotes ubiquitin-dependent degradation of c-Myb: involvement of GSK3-mediated phosphorylation of Thr-572 in mouse c-Myb. *Oncogene* 28, 2393–2405. doi: 10.1038/ncr.2009.111
- Koepp, D. M., Schaefer, L. K., Ye, X., Keyomarsi, K., Chu, C., Harper, J. W., et al. (2001). Phosphorylation-dependent ubiquitination of cyclin E by the SCFFbw7 ubiquitin ligase. *Science* 294, 173–177.
- Kooistra, S. M., and Helin, K. (2012). Molecular mechanisms and potential functions of histone demethylases. *Nat. Rev. Mol. Cell Biol.* 13, 297–311.
- Kwon, Y. W., Kim, I. J., Wu, D., Lu, J., Stock, W. A., Liu, Y. Y., et al. (2012). Pten regulates aurora-A and cooperates with Fbxw7 in modulating radiation-induced tumor development. *Mol. Cancer Res.* 10, 834–844. doi: 10.1158/1541-7786.MCR-12-0025
- Lan, H., Tan, M., Zhang, Q., Yang, F., Wang, S., Li, H., et al. (2019). LSD1 destabilizes FBXW7 and abrogates FBXW7 functions independent of its demethylase activity. *Proc. Natl. Acad. Sci. U.S.A.* 116, 12311–12320.
- Lan, H. Y., and Sun, Y. (2019). FBXW7 E3 ubiquitin ligase: degrading, not degrading, or being degraded. *Protein Cell* 10, 861–863.
- Lee, J. W., Kang, H. S., Lee, J. Y., Lee, E. J., Rhim, H., Yoon, J. H., et al. (2012). The transcription factor STAT2 enhances proteasomal degradation of RCAN1 through the ubiquitin E3 ligase FBW7. *Biochem. Biophys. Res. Commun.* 420, 404–410. doi: 10.1016/j.bbrc.2012.03.007
- Leung, J. W., Wang, Y., Fong, K. W., Huen, M. S., Li, L., and Chen, J. (2012). Fanconi anemia (FA) binding protein FAAP20 stabilizes FA complementation group A (FANCA) and participates in interstrand cross-link repair. *Proc. Natl. Acad. Sci. U.S.A.* 109, 4491–4496. doi: 10.1073/pnas.1118720109
- Li, Y., Hu, K., Xiao, X., Wu, W., Yan, H., Chen, H., et al. (2018). FBW7 suppresses cell proliferation and G2/M cell cycle transition via promoting gamma-catenin K63-linked ubiquitylation. *Biochem. Biophys. Res. Commun.* 497, 473–479. doi: 10.1016/j.bbrc.2018.01.192
- Li, Z., Owonikoko, T. K., Sun, S. Y., Ramalingam, S. S., Doetsch, P. W., Xiao, Z. Q., et al. (2012). c-Myc suppression of DNA double-strand break repair. *Neoplasia* 14, 1190–1202.
- Liao, S. Y., Chiang, C. W., Hsu, C. H., Chen, Y. T., Jen, J., Juan, H. F., et al. (2017). CK1 delta/GSK3 beta/FBXW7 alpha axis promotes degradation of the ZNF322A oncoprotein to suppress lung cancer progression. *Oncogene* 36, 5722–5733. doi: 10.1038/ncr.2017.168
- Lindstrom, M. S., Jurada, D., Bursac, S., Orsolic, I., Bartek, J., and Volarevic, S. (2018). Nucleolus as an emerging hub in maintenance of genome stability and cancer pathogenesis. *Oncogene* 37, 2351–2366. doi: 10.1038/s41388-017-0121-z
- Lochab, S., Pal, P., Kapoor, I., Kanaujiya, J. K., Sanyal, S., Behre, G., et al. (2013). E3 ubiquitin ligase Fbw7 negatively regulates granulocytic differentiation by targeting G-CSFR for degradation. *Biochim. Biophys. Acta.* 1833, 2639–2652. doi: 10.1016/j.bbamcr.2013.06.018
- Malyukova, A., Brown, S., Papa, R., O'Brien, R., Giles, J., Trahair, T. N., et al. (2013). FBXW7 regulates glucocorticoid response in T-cell acute lymphoblastic leukaemia by targeting the glucocorticoid receptor for degradation. *Leukemia* 27, 1053–1062. doi: 10.1038/leu.2012.361
- Mao, J. H., Kim, I. J., Wu, D., Climent, J., Kang, H. C., DelRosario, R., et al. (2008). FBXW7 targets mTOR for degradation and cooperates with PTEN in tumor suppression. *Science* 321, 1499–1502. doi: 10.1126/science.1162981
- Mao, J. H., Perez-Losada, J., Wu, D., Delrosario, R., Tsunematsu, R., Nakayama, K. I., et al. (2004). Fbxw7/Cdc4 is a p53-dependent, haploinsufficient tumour suppressor gene. *Nature* 432, 775–779. doi: 10.1038/nature03155
- Matsumoto, A., Onoyama, I., and Nakayama, K. I. (2006). Expression of mouse Fbxw7 isoforms is regulated in a cell cycle- or p53-dependent manner. *Biochem. Biophys. Res. Commun.* 350, 114–119.
- Min, S. H., Lau, A. W., Lee, T. H., Inuzuka, H., Wei, S., Huang, P., et al. (2012). Negative regulation of the stability and tumor suppressor function of Fbw7 by the Pin1 prolyl isomerase. *Mol. Cell.* 46, 771–783. doi: 10.1016/j.molcel.2012.04.012
- Mishra, M., Thacker, G., Sharma, A., Singh, A. K., Upadhyay, V., Sanyal, S., et al. (2021). FBW7 inhibits myeloid differentiation in acute myeloid leukemia via GSK3-dependent ubiquitination of PU.1. *Mol. Cancer Res.* 19, 261–273. doi: 10.1158/1541-7786.MCR-20-0268
- Mo, J. S., Ann, E. J., Yoon, J. H., Jung, J., Choi, Y. H., Kim, H. Y., et al. (2011). Serum- and glucocorticoid-inducible kinase 1 (SGK1) controls Notch1 signaling by downregulation of protein stability through Fbw7 ubiquitin ligase. *J. Cell Sci.* 124(Pt 1), 100–112. doi: 10.1242/jcs.073924
- Moberg, K. H., Bell, D. W., Wahrer, D. C. R., Haber, D. A., and Hariharan, I. K. (2001). Archipelago regulates cyclin E levels in *Drosophila* and is mutated in human cancer cell lines. *Nature* 413, 311–316. doi: 10.1038/35095068
- Nakamura, A. J., Rao, V. A., Pommier, Y., and Bonner, W. M. (2010). The complexity of phosphorylated H2AX foci formation and DNA repair assembly at DNA double-strand breaks. *Cell Cycle* 9, 389–397.
- Nash, P., Tang, X. J., Orlicky, S., Chen, Q. H., Gertler, F. B., Mendenhall, M. D., et al. (2001). Multisite phosphorylation of a CDK inhibitor sets a threshold for the onset of DNA replication. *Nature* 414, 514–521. doi: 10.1038/35107009
- Nateri, A. S., Riera-Sans, L., Da Costa, C., and Behrens, A. (2004). The ubiquitin ligase SCFFbw7 antagonizes apoptotic JNK signaling. *Science* 303, 1374–1378. doi: 10.1126/science.1092880
- Negi, A., and Murphy, P. V. (2021). Development of Mcl-1 inhibitors for cancer therapy. *Eur. J. Med. Chem.* 210:113038.
- Olson, B. L., Hock, M. B., Ekholm-Reed, S., Wohlschlegel, J. A., Dev, K. K., Kralli, A., et al. (2008). SCFCdc4 acts antagonistically to the PGC-1 alpha transcriptional coactivator by targeting it for ubiquitin-mediated proteolysis. *Gene Dev.* 22, 252–264. doi: 10.1101/gad.1624208
- Ong, S. E., and Mann, M. (2006). A practical recipe for stable isotope labeling by amino acids in cell culture (SILAC). *Nat. Protoc.* 1, 2650–2660. doi: 10.1038/nprot.2006.427



- Onoyama, I., Tsunematsu, R., Matsumoto, A., Kimura, T., de Alboran, I. M., Nakayama, K., et al. (2007). Conditional inactivation of Fbxw7 impairs cell-cycle exit during T cell differentiation and results in lymphomatogenesis. *J. Exp. Med.* 204, 2875–2888. doi: 10.1084/jem.20062299
- Perez-Benavente, B., Garcia, J. L., Rodriguez, M. S., de Mora, J. F., and Farras, R. (2011). GSK3-SCFFbw7 targets junB for degradation in G2 to preserve chromatid cohesion. *FEBS J.* 278, 473–474. doi: 10.1038/ncr.2012.235
- Rajagopalan, H., Jallepalli, P. V., Rago, C., Velculescu, V. E., Kinzler, K. W., Vogelstein, B., et al. (2004). Inactivation of hCDC4 can cause chromosomal instability. *Nature* 428, 77–81.
- Roos, W. P., Thomas, A. D., and Kaina, B. (2016). DNA damage and the balance between survival and death in cancer biology. *Nat. Rev. Cancer* 16, 20–33.
- Sancar, A., Lindsey-Boltz, L. A., Unsal-Kacmaz, K., and Linn, S. (2004). Molecular mechanisms of mammalian DNA repair and the DNA damage checkpoints. *Annu. Rev. Biochem.* 73, 39–85.
- Schulein, C., Eilers, M., and Popov, N. (2011). PI3K-dependent phosphorylation of Fbw7 modulates substrate degradation and activity. *FEBS Lett.* 585, 2151–2157. doi: 10.1016/j.febslet.2011.05.036
- Sheng, W., LaFleur, M. W., Nguyen, T. H., Chen, S., Chakravarty, A., Conway, J. R., et al. (2018). LSD1 ablation stimulates anti-tumor immunity and enables checkpoint blockade. *Cell* 174, 549–563.e19. doi: 10.1016/j.cell.2018.05.052
- Skaar, J. R., Pagan, J. K., and Pagano, M. (2014). SCF ubiquitin ligase-targeted therapies. *Nat. Rev. Drug Discov.* 13, 889–903. doi: 10.1038/nrd4432
- Spruck, C. H., Strohmaier, H., Sangfelt, O., Muller, H. M., Hubalek, M., Muller-Holzner, E., et al. (2002). hCDC4 gene mutations in endometrial cancer. *Cancer Res.* 62, 4535–4539.
- Srivastava, M., and Raghavan, S. C. (2015). DNA double-strand break repair inhibitors as cancer therapeutics. *Chem. Biol.* 22, 17–29.
- Strebhardt, K. (2010). Multifaceted polo-like kinases: drug targets and antitargets for cancer therapy. *Nat. Rev. Drug Discov.* 9, 643–U24. doi: 10.1038/nrd3184
- Strohmaier, H., Spruck, C. H., Kaiser, P., Won, K. A., Sangfelt, O., and Reed, S. I. (2001). Human F-box protein hCdc4 targets cyclin E for proteolysis and is mutated in a breast cancer cell line. *Nature* 413, 316–322. doi: 10.1038/35095076
- Sundqvist, A., Bengoechea-Alonso, M. T., Ye, X., Lukiyanchuk, V., Jin, J. P., Harper, J. W., et al. (2005). Control of lipid metabolism by phosphorylation-dependent degradation of the SREBP family of transcription factors by SCFFbw7. *Cell Metab.* 1, 379–391. doi: 10.1016/j.cmet.2005.04.010
- Surjo Rahmanto, A., Savov, V., Brunner, A., Bolin, S., Weishaupt, H., Malyukova, A., et al. (2016). FBW7 suppression leads to SOX9 stabilization and increased malignancy in medulloblastoma. *EMBO J.* 35, 2192–2212. doi: 10.15252/embj.201693889
- Suzuki, H., Chiba, T., Suzuki, T., Fujita, T., Ikenoue, T., Omata, M., et al. (2000). Homodimer of two F-box proteins betaTrCP1 or betaTrCP2 binds to IkkappaBalpha for signal-dependent ubiquitination. *J. Biol. Chem.* 275, 2877–2884.
- Tan, M. J., Zhao, Y. C., Kim, S. J., Liu, M., Jia, L. J., Saunders, T. L., et al. (2011). SAG/RBX2/ROC2 E3 ubiquitin ligase is essential for vascular and neural development by targeting NF1 for degradation. *Dev. Cell* 21, 1062–1076. doi: 10.1016/j.devcel.2011.09.014
- Tang, X., Orlicky, S., Lin, Z., Willems, A., Neculai, D., Ceccarelli, D., et al. (2007). Suprafacial orientation of the SCFCdc4 dimer accommodates multiple geometries for substrate ubiquitination. *Cell* 129, 1165–1176. doi: 10.1016/j.cell.2007.04.042
- Teng, C. L., Hsieh, Y. C., Phan, L., Shin, J., Gully, C., Velazquez-Torres, G., et al. (2012). FBXW7 is involved in Aurora B degradation. *Cell Cycle* 11, 4059–4068. doi: 10.4161/cc.22381
- Tripathi, V., Kaur, E., Kharat, S. S., Hussain, M., Damodaran, A. P., Kulshrestha, S., et al. (2019). Abrogation of FBW7 alpha-dependent p53 degradation enhances p53's function as a tumor suppressor. *J. Biol. Chem.* 294, 13224–13232. doi: 10.1074/jbc.AC119.008483
- Tsvetkov, L., and Stern, D. F. (2005). Interaction of chromatin-associated Plk1 and Mcm7. *J. Biol. Chem.* 280, 11943–11947. doi: 10.1074/jbc.M413514200
- Van, H. T., and Santos, M. A. (2018). Histone modifications and the DNA double-strand break response. *Cell Cycle* 17, 2399–2410.
- Vogelstein, B., Lane, D., and Levine, A. J. (2000). Surfing the p53 network. *Nature* 408, 307–310.
- Wade, M., Li, Y. C., and Wahl, G. M. (2013). MDM2, MDMX and p53 in oncogenesis and cancer therapy. *Nat. Rev. Cancer* 13, 83–96.
- Wang, J. M., Chan, B., Tong, M., Paung, Y. T., Jo, U., Martin, D., et al. (2019). Prolyl isomerization of FAAP20 catalyzed by PIN1 regulates the Fanconi anemia pathway. *PLoS Genet.* 15:e1007983. doi: 10.1371/journal.pgen.1007983
- Wang, J. M., Jo, U., Joo, S. Y., and Kim, H. (2016). FBW7 regulates DNA interstrand cross-link repair by modulating FAAP20 degradation. *Oncotarget.* 7, 35724–35740. doi: 10.18632/oncotarget.9595
- Wang, L. H., Chen, R. P., Li, G., Wang, Z. G., Liu, J., Liang, Y., et al. (2020). FBW7 mediates senescence and pulmonary fibrosis through telomere uncapping. *Cell Metab.* 32:860. doi: 10.1016/j.cmet.2020.10.004
- Wang, Q. Q., Song, Y. J., Xue, Y., and Yu, H. (2017). E3 ligase FBXW7 is critical for RIG-I stabilization during antiviral responses. *Nat. Commun.* 8:14654. doi: 10.1038/ncomms14654
- Wang, R., Wang, Y., Liu, N., Ren, C. G., Jiang, C., Zhang, K., et al. (2013). FBW7 regulates endothelial functions by targeting KLF2 for ubiquitination and degradation. *Cell Res.* 23, 803–819. doi: 10.1038/cr.2013.42
- Wang, Z., Inuzuka, H., Zhong, J., Wan, L., Fukushima, H., Sarkar, F. H., et al. (2012). Tumor suppressor functions of FBW7 in cancer development and progression. *FEBS Lett.* 586, 1409–1418.
- Wei, W., Jin, J., Schlisio, S., Harper, J. W., and Kaelin, W. G. Jr. (2005). The v-Jun point mutation allows c-Jun to escape GSK3-dependent recognition and destruction by the Fbw7 ubiquitin ligase. *Cancer Cell* 8, 25–33. doi: 10.1016/j.ccr.2005.06.005
- Welcker, M., and Clurman, B. E. (2007). Fbw7/hCDC4 dimerization regulates its substrate interactions. *Cell Div.* 2:7. doi: 10.1186/1747-1028-2-7
- Welcker, M., and Clurman, B. E. (2008). FBW7 ubiquitin ligase: a tumour suppressor at the crossroads of cell division, growth and differentiation. *Nat. Rev. Cancer* 8, 83–93. doi: 10.1038/nrc2290
- Welcker, M., Larimore, E. A., Frappier, L., and Clurman, B. E. (2011). Nucleolar targeting of the fbw7 ubiquitin ligase by a pseudosubstrate and glycogen synthase kinase 3. *Mol. Cell Biol.* 31, 1214–1224. doi: 10.1128/MCB.01347-10
- Welcker, M., Larimore, E. A., Swanger, J., Bengoechea-Alonso, M. T., Grim, J. E., Ericsson, J., et al. (2013). Fbw7 dimerization determines the specificity and robustness of substrate degradation. *Genes Dev.* 27, 2531–2536. doi: 10.1101/gad.229195.113
- Welcker, M., Orian, A., Jin, J. P., Grim, J. A., Harper, J. W., Eisenman, R. N., et al. (2004). The Fbw7 tumor suppressor regulates glycogen synthase kinase 3 phosphorylation-dependent c-Myc protein degradation. *Proc. Natl. Acad. Sci. U.S.A.* 101, 9085–9090. doi: 10.1073/pnas.0402770101
- Wertz, I. E., Kusam, S., Lam, C., Okamoto, T., Sandoval, W., Anderson, D. J., et al. (2011). Sensitivity to antitubulin chemotherapeutics is regulated by MCL1 and FBW7. *Nature* 471, 110–114. doi: 10.1038/nature09779
- Wrann, S., Kaufmann, M. R., Wirthner, R., Stiehl, D. P., and Wenger, R. H. (2013). HIF mediated and DNA damage independent histone H2AX phosphorylation in chronic hypoxia. *Biol. Chem.* 394, 519–528. doi: 10.1515/hsz-2012-0311
- Wu, G. Y., Hubbard, E. J. A., Kitajewski, J. K., and Greenwald, I. (1998). Evidence for functional and physical association between *Caenorhabditis elegans* SEL-10, a Cdc4p-related protein, and SEL-12 presenilin. *Proc. Natl. Acad. Sci. U.S.A.* 95, 15787–15791. doi: 10.1073/pnas.95.26.15787
- Wu, R. C., Feng, Q., Lonard, D. M., and O'Malley, B. W. (2007). SRC-3 coactivator functional lifetime is regulated by a phospho-dependent ubiquitin time clock. *Cell* 129, 1125–1140. doi: 10.1016/j.cell.2007.04.039
- Wurtele, H., and Verreault, A. (2006). Histone post-translational modifications and the response to DNA double-strand breaks. *Curr. Opin. Cell Biol.* 18, 137–144.
- Xiao, D., Yue, M., Su, H., Ren, P., Jiang, J., Li, F., et al. (2016). Polo-like kinase-1 regulates Myc stabilization and activates a feedforward circuit promoting tumor cell survival. *Mol. Cell* 64, 493–506. doi: 10.1016/j.molcel.2016.09.016
- Xie, C. M., Tan, M., Lin, X. T., Wu, D., Jiang, Y., Tan, Y., et al. (2019). The FBXW7-SHOC2-raptor axis controls the cross-talks between the RAS-ERK and mTORC1 signaling pathways. *Cell Rep.* 26, 3037–3050.e4. doi: 10.1016/j.celrep.2019.02.052
- Yada, M., Hatakeyama, S., Kamura, T., Nishiyama, M., Tsunematsu, R., Imaki, H., et al. (2004). Phosphorylation-dependent degradation of c-Myc is mediated by the F-box protein Fbw7. *EMBO J.* 23, 2116–2125. doi: 10.1038/sj.emboj.7600217



- Yokobori, T., Yokoyama, Y., Mogi, A., Endoh, H., Altan, B., Kosaka, T., et al. (2014). FBXW7 mediates chemotherapeutic sensitivity and prognosis in NSCLCs. *Mol. Cancer Res.* 12, 32–37. doi: 10.1158/1541-7786.MCR-13-0341
- Yoo, H. Y., Kumagai, A., Shevchenko, A., Shevchenko, A., and Dunphy, W. G. (2004). Adaptation of a DNA replication checkpoint response depends upon inactivation of Claspin by the Polo-like kinase. *Cell* 117, 575–588. doi: 10.1016/s0092-8674(04)00417-9
- Yumimoto, K., Matsumoto, M., Onoyama, I., Imaizumi, K., and Nakayama, K. I. (2013). F-box and WD repeat domain-containing-7 (Fbxw7) protein targets endoplasmic reticulum-anchored osteogenic and chondrogenic transcriptional factors for degradation. *J. Biol. Chem.* 288, 28488–28502. doi: 10.1074/jbc.M113.465179
- Zehir, A., Benayed, R., Shah, R. H., Syed, A., Middha, S., Kim, H. R., et al. (2017). Mutational landscape of metastatic cancer revealed from prospective clinical sequencing of 10,000 patients. *Nat. Med.* 23, 703–713.
- Zhang, H., Shao, F., Guo, W., Gao, Y., and He, J. (2019). Knockdown of KLF5 promotes cisplatin-induced cell apoptosis via regulating DNA damage checkpoint proteins in non-small cell lung cancer. *Thorac. Cancer* 10, 1069–1077. doi: 10.1111/1759-7714.13046
- Zhang, P., Shao, Y., Quan, F., Liu, L., and Yang, J. (2021). FBP1 enhances the radiosensitivity by suppressing glycolysis via the FBXW7/mTOR axis in nasopharyngeal carcinoma cells. *Life Sci.* 283:119840. doi: 10.1016/j.lfs.2021.119840
- Zhang, Q., Karnak, D., Tan, M., Lawrence, T. S., Morgan, M. A., and Sun, Y. (2016). FBXW7 facilitates nonhomologous end-joining via K63-linked polyubiquitylation of XRCC4. *Mol. Cell* 61, 419–433. doi: 10.1016/j.molcel.2015.12.010
- Zhang, Q., Mady, A. S. A., Ma, Y. Y., Ryan, C., Lawrence, T. S., Nikolovska-Coleska, Z., et al. (2019). The WD40 domain of FBXW7 is a poly(ADP-ribose)-binding domain that mediates the early DNA damage response. *Nucleic Acids Res.* 47, 4039–4053. doi: 10.1093/nar/gkz058
- Zhao, D., Zheng, H. Q., Zhou, Z. M., and Chen, C. S. (2010). The Fbw7 tumor suppressor targets KLF5 for ubiquitin-mediated degradation and suppresses breast cell proliferation. *Cancer Res.* 70, 4728–4738. doi: 10.1158/0008-5472.CAN-10-0040
- Zhao, J. G., Tang, J., Men, W. F., and Ren, K. M. (2012). FBXW7-mediated degradation of CCDC6 is impaired by ATM during DNA damage response in lung cancer cells. *FEBS Lett.* 586, 4257–4263. doi: 10.1016/j.febslet.2012.10.029
- Zhao, J. J., Xiong, X. L., Li, Y., Liu, X., Wang, T., Zhang, H., et al. (2018). Hepatic F-box protein FBXW7 maintains glucose homeostasis through degradation of fetuin-A. *Diabetes* 67, 818–830. doi: 10.2337/db17-1348
- Zhao, X., Hirota, T., Han, X., Cho, H., Chong, L. W., Lamia, K., et al. (2016). Circadian amplitude regulation via FBXW7-targeted REV-ERB alpha degradation. *Cell* 165, 1644–1657. doi: 10.1016/j.cell.2016.05.012
- Zhao, Y. C., and Sun, Y. (2013). Cullin-RING ligases as attractive anti-cancer targets. *Curr. Pharm. Des.* 19, 3215–3225.

**Conflict of Interest:** The authors declare that the research was conducted in the absence of any commercial or financial relationships that could be construed as a potential conflict of interest.

**Publisher's Note:** All claims expressed in this article are solely those of the authors and do not necessarily represent those of their affiliated organizations, or those of the publisher, the editors and the reviewers. Any product that may be evaluated in this article, or claim that may be made by its manufacturer, is not guaranteed or endorsed by the publisher.

Copyright © 2021 Lan and Sun. This is an open-access article distributed under the terms of the Creative Commons Attribution License (CC BY). The use, distribution or reproduction in other forums is permitted, provided the original author(s) and the copyright owner(s) are credited and that the original publication in this journal is cited, in accordance with accepted academic practice. No use, distribution or reproduction is permitted which does not comply with these terms.

# Advantages of publishing in Frontiers



## OPEN ACCESS

Articles are free to read  
for greatest visibility  
and readership



## FAST PUBLICATION

Around 90 days  
from submission  
to decision



## HIGH QUALITY PEER-REVIEW

Rigorous, collaborative,  
and constructive  
peer-review



## TRANSPARENT PEER-REVIEW

Editors and reviewers  
acknowledged by name  
on published articles

## Frontiers

Avenue du Tribunal-Fédéral 34  
1005 Lausanne | Switzerland

Visit us: [www.frontiersin.org](http://www.frontiersin.org)

Contact us: [frontiersin.org/about/contact](http://frontiersin.org/about/contact)



## REPRODUCIBILITY OF RESEARCH

Support open data  
and methods to enhance  
research reproducibility



## DIGITAL PUBLISHING

Articles designed  
for optimal readership  
across devices



## FOLLOW US

@frontiersin



## IMPACT METRICS

Advanced article metrics  
track visibility across  
digital media



## EXTENSIVE PROMOTION

Marketing  
and promotion  
of impactful research



## LOOP RESEARCH NETWORK

Our network  
increases your  
article's readership